INSIGHTS IN ANTIMICROBIALS, RESISTANCE & CHEMOTHERAPY: 2021

EDITED BY: Rustam Aminov
PUBLISHED IN: Frontiers in Microbiology

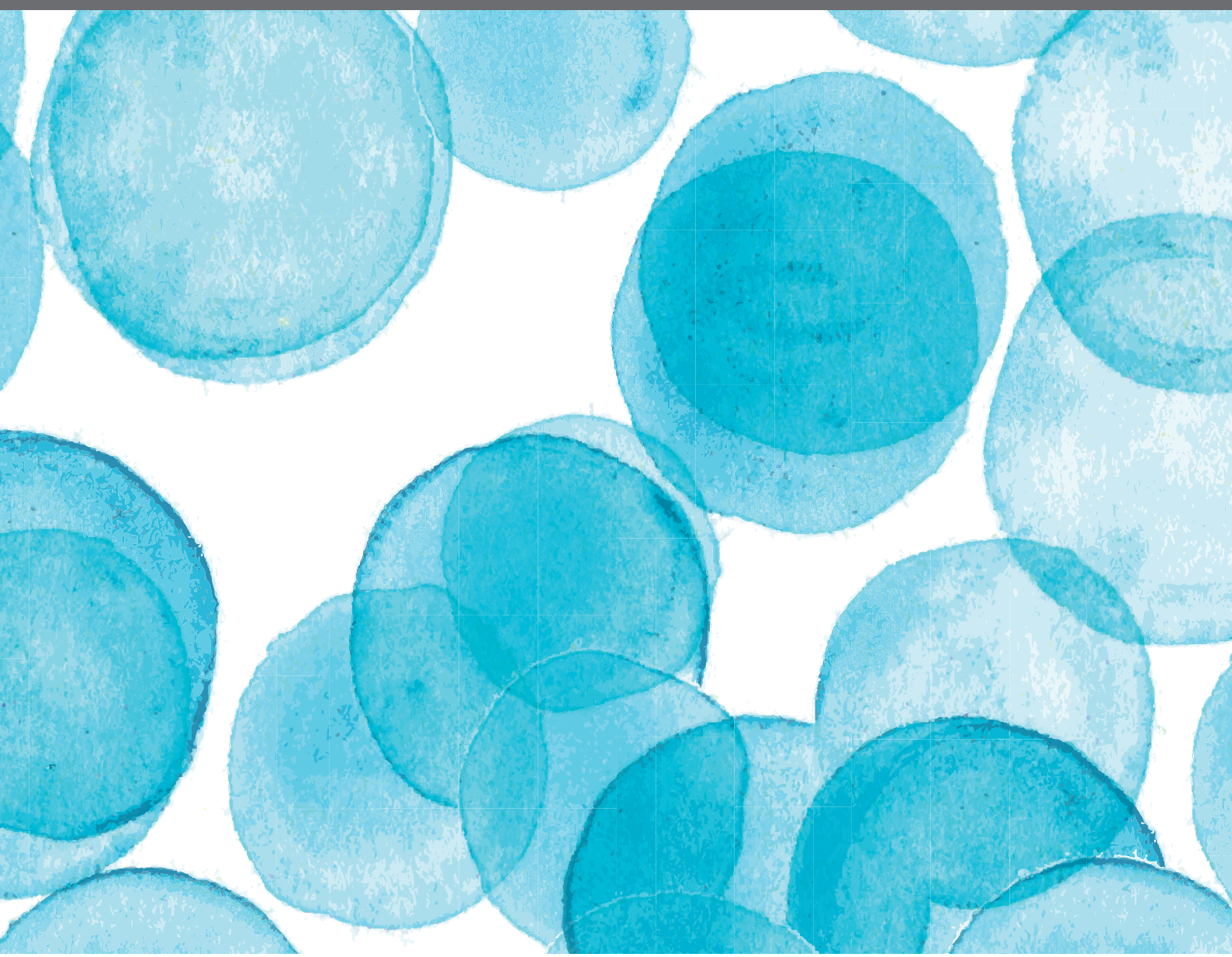

frontiers Research Topics

ISSN 1664-8714
ISBN 978-2-83250-596-0
DOI 10.3389/978-2-83250-596-0

About Frontiers

Frontiers is more than just an open-access publisher of scholarly articles: it is a pioneering approach to the world of academia, radically improving the way scholarly research is managed. The grand vision of Frontiers is a world where all people have an equal opportunity to seek, share and generate knowledge. Frontiers provides immediate and permanent online open access to all its publications, but this alone is not enough to realize our grand goals.

Frontiers Journal Series

The Frontiers Journal Series is a multi-tier and interdisciplinary set of open-access, online journals, promising a paradigm shift from the current review, selection and dissemination processes in academic publishing. All Frontiers journals are driven by researchers for researchers; therefore, they constitute a service to the scholarly community. At the same time, the Frontiers Journal Series operates on a revolutionary invention, the tiered publishing system, initially addressing specific communities of scholars, and gradually climbing up to broader public understanding, thus serving the interests of the lay society, too.

Dedication to Quality

Each Frontiers article is a landmark of the highest quality, thanks to genuinely collaborative interactions between authors and review editors, who include some of the world's best academicians. Research must be certified by peers before entering a stream of knowledge that may eventually reach the public - and shape society; therefore, Frontiers only applies the most rigorous and unbiased reviews.
Frontiers revolutionizes research publishing by freely delivering the most outstanding research, evaluated with no bias from both the academic and social point of view. By applying the most advanced information technologies, Frontiers is catapulting scholarly publishing into a new generation.

What are Frontiers Research Topics?

Frontiers Research Topics are very popular trademarks of the Frontiers Journals Series: they are collections of at least ten articles, all centered on a particular subject. With their unique mix of varied contributions from Original Research to Review Articles, Frontiers Research Topics unify the most influential researchers, the latest key findings and historical advances in a hot research area! Find out more on how to host your own Frontiers Research Topic or contribute to one as an author by contacting the Frontiers Editorial Office: frontiersin.org/about/contact

INSIGHTS IN ANTIMICROBIALS, RESISTANCE & CHEMOTHERAPY: 2021

Topic Editor:
Rustam Aminov, University of Aberdeen, United Kingdom

Citation: Aminov, R., ed. (2022). Insights in Antimicrobials, Resistance & Chemotherapy: 2021. Lausanne: Frontiers Media SA.
doi: 10.3389/978-2-83250-596-0

Table of Contents

05 ***Editorial: Insights in Antimicrobials, Resistance, and Chemotherapy: 2021***
Rustam Aminov

08 ***Eradication of Resistant and Susceptible Aerobic Gram-Negative Bacteria From the Digestive Tract in Critically Ill Patients; an Observational Cohort Study***
Sophie H. Buitinck, Rogier Jansen, Rob J. Bosman, Nardo J. M. van der Meer and Peter H. J. van der Voort

18 ***Identification of Distinct Characteristics of Antibiofilm Peptides and Prospection of Diverse Sources for Efficacious Sequences***
Bipasa Bose, Taylor Downey, Anand K. Ramasubramanian and David C. Anastasiu

38 ***Comparative Metabolic Pathways Analysis and Subtractive Genomics Profiling to Prioritize Potential Drug Targets Against* Streptococcus pneumoniae**
Kanwal Khan, Khurshid Jalal, Ajmal Khan, Ahmed Al-Harrasi and Reaz Uddin

54 ***Phage-Derived Depolymerase as an Antibiotic Adjuvant Against Multidrug-Resistant* Acinetobacter baumannii**
Xi Chen, Miao Liu, Pengfei Zhang, Miao Xu, Weihao Yuan, Liming Bian, Yannan Liu, Jiang Xia and Sharon S. Y. Leung

70 ***Antimicrobial Peptides Controlling Resistant Bacteria in Animal Production***
Gisele Rodrigues, Lucas Souza Santos and Octávio Luiz Franco

84 ***Repeated Exposure of* Escherichia coli *to High Ciprofloxacin Concentrations Selects* gyrB *Mutants That Show Fluoroquinolone-Specific Hyperpersistence***
Aurore Perault, Catherine Turlan, Nathalie Eynard, Quentin Vallé, Alain Bousquet-Mélou and Etienne Giraud

93 ***Scientists' Assessments of Research on Lactic Acid Bacterial Bacteriocins 1990–2010***
Laura D. Martinenghi and Jørgen J. Leisner

105 ***New Mutations in* cls *Lead to Daptomycin Resistance in a Clinical Vancomycin- and Daptomycin-Resistant* Enterococcus faecium *Strain***
Weiwei Li, Jiamin Hu, Ling Li, Mengge Zhang, Qingyu Cui, Yanan Ma, Hainan Su, Xuhua Zhang, Hai Xu and Mingyu Wang

120 ***Ecological Effects of Daily Antiseptic Treatment on Microbial Composition of Saliva-Grown Microcosm Biofilms and Selection of Resistant Phenotypes***
Xiaojun Mao, Andreas Hiergeist, David L. Auer, Konstantin J. Scholz, Denise Muehler, Karl-Anton Hiller, Tim Maisch, Wolfgang Buchalla, Elmar Hellwig, André Gessner, Ali Al-Ahmad and Fabian Cieplik

135 ***A Preliminary* in vitro *and* in vivo *Evaluation of the Effect and Action Mechanism of 17-AAG Combined With Azoles Against Azole-Resistant* Candida *spp.***
Luyao Liu, Xueying Zhang, Shruti Kayastha, Lihua Tan, Heng Zhang, Jingwen Tan, Linyun Li, Jinghua Mao and Yi Sun

146 ***Proteome Profiling of Evolved Methicillin-Resistant* Staphylococcus aureus *Strains With Distinct Daptomycin Tolerance and Resistance Phenotypes***
Jordy Evan Sulaiman, Lexin Long, Pei-Yuan Qian and Henry Lam

162 ***Expert Workshop Summary: Advancing Toward a Standardized Murine Model to Evaluate Treatments for Antimicrobial Resistance Lung Infections***
Rakel Arrazuria, Bernhard Kerscher, Karen E. Huber, Jennifer L. Hoover, Carina Vingsbo Lundberg, Jon Ulf Hansen, Sylvie Sordello, Stephane Renard, Vincent Aranzana-Climent, Diarmaid Hughes, Philip Gribbon, Lena E. Friberg and Isabelle Bekeredjian-Ding

170 ***Variability of Murine Bacterial Pneumonia Models Used to Evaluate Antimicrobial Agents***
Rakel Arrazuria, Bernhard Kerscher, Karen E. Huber, Jennifer L. Hoover, Carina Vingsbo Lundberg, Jon Ulf Hansen, Sylvie Sordello, Stephane Renard, Vincent Aranzana-Climent, Diarmaid Hughes, Philip Gribbon, Lena E. Friberg and Isabelle Bekeredjian-Ding

frontiers | Frontiers in Microbiology

TYPE Editorial
PUBLISHED 12 October 2022
DOI 10.3389/fmicb.2022.1037326

OPEN ACCESS

EDITED AND REVIEWED BY
Paul David Cotter,
Teagasc, Ireland

*CORRESPONDENCE
Rustam Aminov
rustam.aminov@abdn.ac.uk

SPECIALTY SECTION
This article was submitted to Antimicrobials, Resistance and Chemotherapy, a section of the journal Frontiers in Microbiology

RECEIVED 05 September 2022
ACCEPTED 22 September 2022
PUBLISHED 12 October 2022

CITATION
Aminov R (2022) Editorial: Insights in antimicrobials, resistance, and chemotherapy: 2021.
Front. Microbiol. 13:1037326.
doi: 10.3389/fmicb.2022.1037326

Editorial: Insights in antimicrobials, resistance, and chemotherapy: 2021

Rustam Aminov*

The School of Medicine, Medical Sciences and Nutrition, University of Aberdeen, Aberdeen, United Kingdom

KEYWORDS

antimicrobial resistance, drug target, antimicrobial peptides, phage therapy, antiseptics, animal models, digestive tract decontamination, combination therapy

Editorial on the Research Topic
Insights in antimicrobials, resistance, and chemotherapy: 2021

Antimicrobial resistance (AMR) is a problem, which has emerged during the past several decades, and which is now familiar to many (Aminov, 2010). AMR infections require more expensive treatments and result in extended hospital stays and, most importantly, these infections claim human lives. Thus, there are continuous research and development efforts to counteract the current AMR crisis. The aim of this Research Topic was to gather some recent insights in this important area of research.

The vast majority of AMs in the current use target bacterial cell wall biosynthesis, bacterial membranes and replication, transcription, and translation machineries. Metabolomic approach opened new prospects in identification of novel bacterial targets for antimicrobials (AMs; Aminov, 2022). In this Research Topic, Khan et al. analyzed metabolic pathways of *Streptococcus pneumoniae* strains *via* the computational subtractive genomics approach to identify potential drug targets. In total, 47 potential drug targets were identified, with two of them, 4-oxalocrotonate tautomerase and sensor histidine kinase, being of particular interest, because they are unique to *S. pneumoniae,* and thus drugs targeting these proteins could be very specific.

Antimicrobial peptides (AMPs) are produced by many organisms from all three domains of life (Hao et al., 2022). In eukaryotes such as animals, AMPs comprise a part of their immune system in the form of innate immunity, while in bacteria and archaea as well as in lower eukaryotes they presumably protect their own ecological niches from invasion by other organisms. AMPs have attracted a considerable attention due to their AM potential. In particular, as noted by Martinenghi and Leisner, bacteriocins from lactic acid bacteria have been extensively studied during the past 35 years. While there has been, undoubtedly, a great progress in understanding the basic science of bacteriocins, applications of these findings, with the exception of food preservation, have been limited. The drawbacks of bacteriocins are in narrow target spectrum, target resistance, protease sensitivity, poor yields, and also in economic and regulatory hurdles. Potentials of AMPs in clinical or veterinary medicine have not been evaluated in large-scale clinical trials.

With the diminishing arsenal and efficiency of the current antimicrobials, however, AMPs have a potential to assist to at least some of the deficiencies of antimicrobial therapy. For example, AMs are less efficient against the biofilms that are formed by the majority of microbial infections. Bose et al. developed machine learning models for identification of AMPs with antibiofilm actives from a variety of sources. This *in silico* approach may help to identify new antibiofilm AMP leads and predict their antibiofilm efficacy.

It is a well-known fact that the vast majority of globally produced antimicrobials are used in agriculture (Van Boeckel et al., 2019). There is also a link, well-established within the One Health framework, between the antimicrobial use in agriculture and the rise of human AMR pathogens (Woolhouse et al., 2015). Thus, replacement of AMs in agriculture may have a considerable impact on reducing the rate of emergence and dissemination of AMR. Rodrigues et al. extensively reviewed potentials of AMs replacement by AMPs in agriculture. Presently, however, the use of AMPs in agriculture is limited due to low i*n vivo* efficacy, inadequate stability, and production costs. These deficiencies can be addressed *via* engineering of AMPs, association of AMPs with nanoparticles, and production optimization to reduce the cost.

Phage therapy has recently received a renewed attention as one of the possible antimicrobial alternatives (Abedon et al., 2017). Especially promising are the lytic components of bacteriophages that are potentially easier for accommodation under the current pharmacological regulations compared to native phage particles. One of these phage components are depolymerizes that degrade capsular polysaccharides, lipopolysaccharides and exopolysaccharides of the host bacteria thus making them more susceptible to antimicrobials and the immune system. Chen et al. investigated Dpo71 depolymerize from a lytic bacteriophage vB_AbaM-IME-AB2 that infects *Acinetobacter baumannii*. Dpo71 sensitized the multidrug-resistant (MDR) *A. baumannii* strains to the host immunity and increased their susceptibility to antimicrobials such as colistin. The downside of Dpo71, however, was in its narrow range, with the lack of activity against the phage-resistant *A. baumannii* strains. This limitation can be addressed using of cocktails of phage depolymerases or by engineering Dpo71 to broaden its host range and enhance its activity.

Similarly to any other drug, preclinical investigation of antimicrobial candidates in animal models is one of the prerequisites during the antimicrobial drug development. Animal models most frequently used during this stage are rodents, in particular mice. Two articles in this Research Topic discussed the role of murine models of lung infection in evaluation of AM efficiency. Review by Arrazuria et al. revealed pronounced variations in the experimental design of the murine pneumonia models. Importantly, differences in the immune status of animals, their age, infection routes, and sample processing had strong impact on the effect of AMs. Thus, preclinical models of disease need to be standardized to generate consistent and comparable results during the evaluation of AM candidates. Arrazuria et al. also came up with recommendations for a standardized design of preclinical murine pneumonia models that could help to harmonize the results obtained during the evaluation of novel AMs in different laboratories.

Antiseptics such as chlorhexidine digluconate (CHX) and cetylpyridinium chloride (CPC) are widely used in oral care products. Mao et al. revealed rather unexpected effects of these antiseptics, with CHX selecting for caries-associated saccharolytic taxa and CPC—for gingivitis-associated proteolytic taxa in oral biofilms. Antiseptic-resistant isolates were also resistant to various antibiotics. Thus, antiseptics in dental care products may have undesirable effects on oral microbiota, which warrant further investigations.

Selective Decontamination of the Digestive tract (SDD) is aimed at prevention of nosocomial infections by eliminating potentially pathogenic microbiota from the gastrointestinal tract (GIT). Buitinck et al. evaluated the SDD protocol with tobramycin, polymyxin B, and amphotericin B in patients colonized by at least one facultative aerobic Gram-negative bacterium on admission. SDD successfully eradicated the vast majority of susceptible and resistant bacteria from the upper and lower GIT. Eradication of AMR bacteria from the lower GIT, however, required a longer time period compared to patients colonized by susceptible bacteria.

Combination AM therapy is used to treat MDR infections. The fungal infections caused by *Candida* species become increasingly resistant toward the first-line anti-fungal drugs such as azoles that obstruct ergosterol biosynthesis by inhibiting the enzyme 14-alpha-demethylase. Liu et al. explored another target in *Candida*, heat shock proteins 90 (Hsp90). For this, they used a synthetic variant of geldanamycin, 17-Allylamino-17-demethoxygeldamycin (17-AAG), which belong to the benzoquinone ansamycins family of drugs, inhibiting ATPase activity of Hsp90. Although 17-AAG alone exerted a limited antifungal activity, its combination with azoles displayed synergistic effects.

Although the majority of AMR mechanisms are acquired horizontally, there is still a sizeable proportion of AMR due to chromosomal mutations. Li et al. investigated the daptomycin resistance mechanism in a clinical isolate of *Enterococcus faecium*. They established that the resistance is conferred by mutations in the chromosomal *cis* gene, which encodes cardiolipin synthase. These mutations led to the redistribution of lipids and to the decrease of surface negative charges in the cell membrane. In another study with daptomycin, Sulaiman et al. generated tolerance and resistance toward it in methicillin-resistant *Staphylococcus aureus in vitro*. Proteomic analyses of mutants suggested that daptomycin resistance was due to peptidoglycan changes, with a more positive surface charge to repel the antibiotic. But the tolerant phenotype displayed different cell wall changes,

not involving peptidoglycan or surface charge alterations. Quinolone resistance emergence in *Escherichia coli in vitro* was evaluated by Perault et al. Repeated selection by a high ciprofloxacin concentration led to the emergence of *gyrB* mutants with a hyperpersistent phenotype but not a significant MIC increase. Interestingly, mutations were located outside of the canonical GyrB QRDR. Attention should be paid to the tolerant/persister variants since they are frequently the cause of therapeutic failure.

Author contributions

The author confirms being the sole contributor of this work and has approved it for publication.

Conflict of interest

The author declares that the research was conducted in the absence of any commercial or financial relationships that could be construed as a potential conflict of interest.

Publisher's note

References

Abedon, S. T., García, P., Mullany, P., and Aminov, R. (2017). Editorial: Phage therapy: past, present and future. *Front. Microbiol.* 8, 981. doi: 10.3389/fmicb.2017.00981

Aminov, R. (2022). Metabolomics in antimicrobial drug discovery. *Expert Opin. Drug Discov*. doi: 10.1080/17460441.2022.2113774. [Epub ahead of print].

Aminov, R. I. (2010). A brief history of the antibiotic era: lessons learned and challenges for the future. *Front. Microbio*. 1, 134. doi: 10.3389/fmicb.2010.00134

Hao, Y., Wang, J., de la Fuente-Nunez, C., and Franco, O. L. (2022). Editorial: Antimicrobial peptides: molecular design, structure-function relationship, and biosynthesis optimization. *Front. Microbiol.* 13, 888540. doi: 10.3389/fmicb.2022.888540

Van Boeckel, T. P., Pires, J., Silvester, R., Zhao, C., Song, J., Criscuolo, N. G., et al. (2019). Global trends in antimicrobial resistance in animals in low-and middle-income countries. *Science* 365, eaaw1944. doi: 10.1126/science.aaw1944

Woolhouse, M., Ward, M., van Bunnik, B., and Farrar, J. (2015). Antimicrobial resistance in humans, livestock and the wider environment. *Philos. Trans. R. Soc. Lond. B Biol. Sci.* 370, 20140083. doi: 10.1098/rstb.2014.0083

frontiers in Microbiology

ORIGINAL RESEARCH
published: 03 February 2022
doi: 10.3389/fmicb.2021.779805

Eradication of Resistant and Susceptible Aerobic Gram-Negative Bacteria From the Digestive Tract in Critically Ill Patients; an Observational Cohort Study

Sophie H. Buitinck[1,2], Rogier Jansen[3], Rob J. Bosman[1], Nardo J. M. van der Meer[2] and Peter H. J. van der Voort[2,4]**

[1] Department of Intensive Care, OLVG Hospital, Amsterdam, Netherlands, [2] TIAS School for Business and Society, Tilburg, Netherlands, [3] Department of Medical Microbiology, OLVG Hospital, Amsterdam, Netherlands, [4] Department of Critical Care Medicine, University Medical Center Groningen, University of Groningen, Groningen, Netherlands

OPEN ACCESS

Edited by:
Rustam Aminov,
University of Aberdeen,
United Kingdom

Reviewed by:
Miriam Cordovana,
Bruker Daltonik GmbH, Germany
Marnix Kuindersma,
Gelre Hospitals, Netherlands

***Correspondence:**
Sophie H. Buitinck
s.h.buitinck@gmail.com
Peter H. J. van der Voort
p.h.j.van.der.voort@umcg.nl

Specialty section:
This article was submitted to Antimicrobials, Resistance and Chemotherapy, a section of the journal Frontiers in Microbiology

Received: 19 September 2021
Accepted: 22 December 2021
Published: 03 February 2022

Citation:
Buitinck SH, Jansen R, Bosman RJ, van der Meer NJM and van der Voort PHJ (2022) Eradication of Resistant and Susceptible Aerobic Gram-Negative Bacteria From the Digestive Tract in Critically Ill Patients; an Observational Cohort Study. Front. Microbiol. 12:779805. doi: 10.3389/fmicb.2021.779805

Background: Selective Decontamination of the Digestive tract (SDD) aims to prevent nosocomial infections, by eradication of potentially pathogenic micro-organisms from the digestive tract.

Objectives: To estimate the rate of and the time to eradication of resistant vs. susceptible facultative aerobic gram-negative bacteria (AGNB) in patients treated with SDD.

Methods: This observational and retrospective study included patients admitted to the ICU between January 2001 and August 2017. Patients were included when treated with SDD (tobramycin, polymyxin B, and amphotericin B) and colonized in the upper or lower gastro-intestinal (GI) tract with at least one AGNB present on admission. Decontamination was determined after the first negative set of cultures (rectal and throat). An additional analysis was performed of two consecutive negative cultures.

Results: Of the 281 susceptible AGNB in the throat and 1,087 in the rectum on admission, 97.9 and 93.7%, respectively, of these microorganisms were successfully eradicated. In the upper GI-tract no differences in eradication rates were found between susceptible and resistant microorganisms. However, the median duration until eradication was significantly longer for aminoglycosides resistant vs. susceptible microorganisms (5 vs. 4 days, $p < 0.01$). In the lower GI-tract, differences in eradication rates between susceptible and resistant microorganisms were found for cephalosporins (90.0 vs. 95.6%), aminoglycosides (84.4 vs. 95.5%) and ciprofloxacin (90.0 vs. 95.2%). Differences in median duration until eradication between susceptible and resistant microorganisms were found for aminoglycosides and ciprofloxacin (both 5 days vs. 6 days, $p = 0.001$). Decontamination defined as two negative cultures was achieved in a lower rate (77–98% for the upper GI tract and 64–77% for the lower GI tract) and a median of 1 day later.

Conclusion: The vast majority of both susceptible and resistant microorganisms are effectively eradicated from the upper and lower GI tract. In the lower GI tract decontamination rates of susceptible microorganisms are significantly higher and achieved in a shorter time period compared to resistant strains.

Keywords: selective digestive tract decontamination, SDD, resistance, decontamination, critically ill, ICU

INTRODUCTION

Selective Digestive Decontamination (SDD) aims to prevent secondary infection by eradication of potentially pathogenic micro-organisms (PPM's) from the respiratory and digestive tract (van Saene et al., 2003). This intervention has been studied in more than 70 RCTs and has been proven to be effective in infection prevention and mortality reduction (Silvestri et al., 2007; Silvestri and van Saene, 2012; Plantinga et al., 2018). Despite these results, SDD is still debated. The main concern is the emergence or selection of resistant micro-organisms when applying SDD (Cuthbertson et al., 2013).

In a systematic review of 35 studies on SDD and selective oral decontamination (SOD) the emergence of resistant strains was studied (Daneman et al., 2013). No association between the use of SDD and colonization or infection with resistant micro-organisms in ICU-patients was found. Some studies reported even a decline in the prevalence and incidence of antimicrobial resistant micro-organisms in respiratory and digestive tract cultures when applying SDD (Ochoa-Ardila et al., 2011; Smet et al., 2011; Houben et al., 2014; Wittekamp et al., 2015; Sanchez-Ramirez et al., 2018). The longest follow-up of 21 years continuous use of SDD confirmed that the fear for increased development of resistance could not be confirmed (Buitinck et al., 2019).

Moreover, in some studies application of SDD was initiated to eradicate resistant microorganisms from the gut. Oostdijk et al. (2012) studied the eradication rates of cephalosporin-resistant and cephalosporin-susceptible enterobacteriaceae and found that 73% of patients colonized with cephalosporin-resistant enterobacteriaceae were successful eradicated before ICU-discharge. In patients colonized with cephalosporin- susceptible enterobacteriaceae successful decolonization was reached in 80% (p = 0.17) (Oostdijk et al., 2012). For aminoglycoside-resistance, this percentage was 62% in resistant bacteria and 81% in susceptible bacteria, respectively ($P < 0.01$). Already in 1987, Stoutenbeek et al. (1987) reported that in almost all patients colonized with cefotaxime-resistant Gram-negative bacilli successful decolonization was accomplished within 1 week.

Despite these reports, the evidence on the eradication of resistant bacteria with the administration of SDD is scarce and its efficacy is not yet clear. The objective of this observational retrospective cohort is therefore to compare the rate and timing of successful decolonization for susceptible and resistant potentially pathogenic aerobic gram-negative bacteria (AGNB) from both upper and lower digestive tract in ICU-patients treated with SDD.

Abbreviations: ACWO, Advies Commissie Wetenschappelijk Onderzoek; AGNB, Aerobic Gram Negative Bacteria; GI, gastro-intestinal; ICU, Intensive Care Unit; I.v., intravenous; PPM, Potential Pathogenic Microorganism; RCT, Randomized Controlled Trial; SDD, Selective Digestive Tract Decontamination.

MATERIALS AND METHODS

Study Design

This is a retrospective cohort analysis of microbiology data from all consecutive ICU patients admitted between January 2001 and August 2017. This study is conducted in a Dutch 20-bed adult mixed medical, surgical and cardiac surgery tertiary intensive care unit in an inner-city teaching hospital in Amsterdam. In this ICU, SDD is implemented in 1986 and has been used consistently, unchanged and without interruption. The local medical ethical review board (ACWO OLVG) approved the study and waived informed consent due to its retrospective and observational design in accordance to Dutch and European legislation (study no. WO 18.017).

Patients

Patients were eligible for analysis when they had a primary carrier state with one or more potentially pathogenic *Enterobacteriaceae* (*Citrobacter* sp., *Enterobacter* sp., *E* coli, *Klebsiella* sp., *Morganella* sp., *Proteus* sp., *Serratia* sp.) or gram-negative non-fermenters (*Acinetobacter* sp., *Pseudomonas* sp.) in the upper or lower gastro-intestinal tract in the first surveillance cultures in the ICU irrespective of the number of colony-forming units. In addition, at least two follow up surveillance cultures taken during ICU-admission (cultures drawn on two different days) should be available and patients must have been treated with SDD during ICU-admission. Data on baseline characteristics of all included patients were prospectively recorded in the ICU database and extracted for this analysis. This data includes sex, age, APACHE IV predicted mortality, length of stay, patient category, date of admission, ICU-mortality, and antimicrobial treatment, both intravenously and topically applied. The general policy in this ICU is to promote defecation with laxatives from the second day of ICU admission onward to achieve defecation within 4 days.

Cultures

Data on surveillance cultures taken during ICU-admission were extracted from the hospital database. Cultures of the throat were performed to determine carrier state in the upper gastro-intestinal tract. For the lower tract rectal cultures were performed. Routinely, cultures from throat and rectum were taken twice a week and tracheal aspirate 3 times a week for surveillance in patients treated with SDD. All culture samples taken in the context of SDD surveillance were plated on an

unselective blood agar and four specific agars selecting for gram-positive bacteria, gram-negative bacteria, yeast and vancomycin resistant enterococci. AGNB's were tested for antimicrobial susceptibility using agar disk-diffusion. These microorganisms were only included for further analysis if susceptibility testing to aminoglycosides (tobramycin or gentamicin), third generation cephalosporins, polymyxin and ciprofloxacin was performed. Strains were defined as resistant when they were tested intermediate or resistant, for at least one of the before mentioned groups. The cut off values for resistance were set following the guidelines of the "clinical and laboratory standards institute" (CLSI) until July 2011 and "the European committee on antimicrobial susceptibility testing" (EUCAST) from July 2011 until 2017 (Wayne, 2010; European Committee on Antimicrobial Susceptibility Testing (Eu-Cast), 2021). Susceptibility tests of cephalosporins were reported as measured, irrespective of potential presence of beta-lactamases such as AmpC beta-lactamase.

Antimicrobial Treatment 2001–2017

Patients were treated with SDD when the expected ICU stay was more than 24 h, irrespective of the need for mechanical ventilation. This decision whether or not to start SDD was left to the discretion of the attending physician. According to the original SDD formulation, the SDD regimen consists of four times daily Orabase®, a sticky oral paste enriched with 2% polymyxin B, amphotericin B and tobramycin. In addition, 10 ml of a suspension containing 500 mg amphotericin B, 100 mg polymyxin B and 80 mg tobramycin is administered four times daily in the gastric tube or swallowed in patients without gastric tube. An i.v. course of cefotaxime is administered to all patients for 4 days but is prolonged in case of active infection with susceptible microorganisms or replaced by another antimicrobial agent in case of infection with a cefotaxime resistant microorganism. The choice for polymyxin B instead of polymyxin E might imply a more effective therapy when given in the same dose (Evans et al., 1999).

To the discretion of the attending physician, empirical antimicrobial treatment on admission is extended with ciprofloxacin i.v. or tobramycin i.v. In case of peritonitis metronidazole is added as well. Other i.v. antimicrobials can be given when previous culture results necessitate another choice. Penicillins are carefully avoided whenever possible due to their negative effects on the indigenous aerobic and anaerobic intestinal flora which could lead to a loss of the protective effect to invading pathogens (colonization resistance) (Vollaard, 1991). When the surveillance cultures showed Enterobacteriaceae with a combined polymyxin and tobramycin resistance, co-trimoxazole 2% was added in the oral paste and twice daily 960 mg in the enteral suspension until decontamination was obtained.

Data-Analysis and Statistics

The microorganisms cultured on admission were categorized in resistant and susceptible microorganisms per agent. Analysis was performed for all unique strains of AGNB found in the upper or lower GI tract. We analyzed the anti-microbial agents separately: third generation cephalosporins, aminoglycosides, polymyxin B/E and ciprofloxacin (**Figure 1**). Depending on whether susceptibility testing for the different agents was performed,

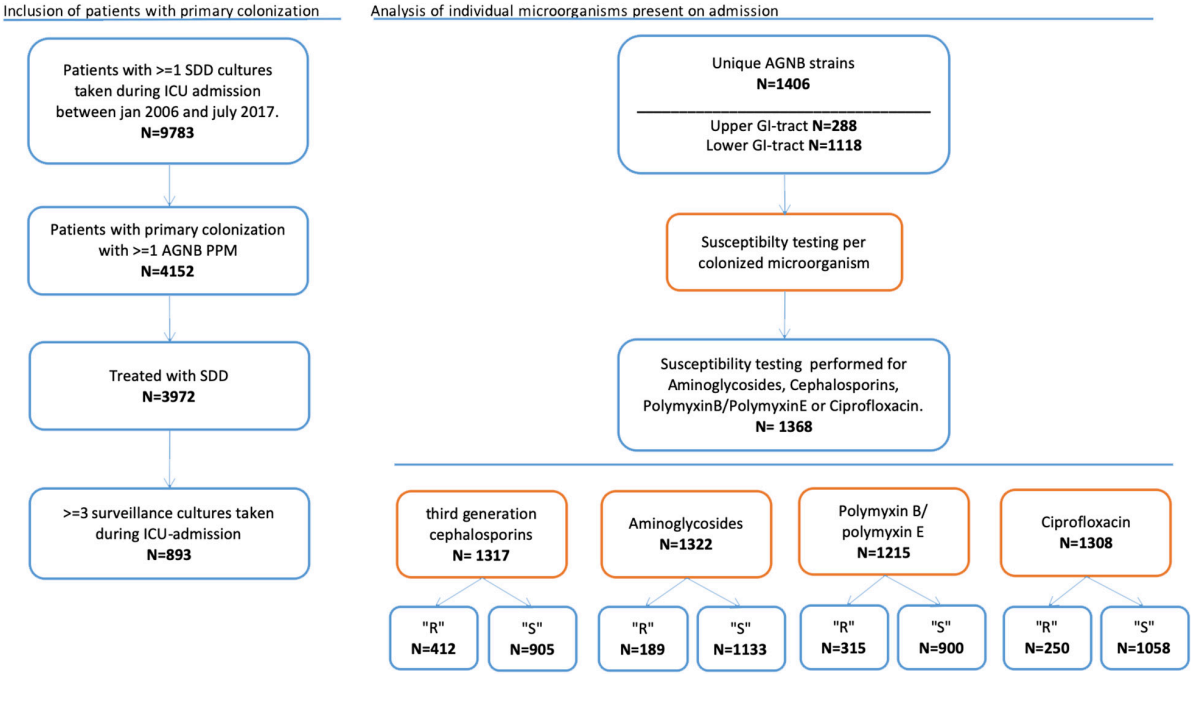

FIGURE 1 | Flowchart of patients and study procedures.

TABLE 1 | Mean and median duration until decontamination in days.

	Cephalosporins		Aminoglycosides		Colistin/Polymyxin B		Ciprofloxacin	
	Resistant	**Susceptible**	**Resistant**	**Susceptible**	**Resistant**	**Susceptible**	**Resistant**	**Susceptible**
Upper GI-tract								
Mean duration until eradication	5.1	4.2	5.9	4.5	4.9	4.5	5.3	4.5
Median duration until eradication	4.0	4.0	5.0	4.0	4.0	4.0	4.0	4.0
Standard error	0.19	0.15	0.45	0.12	0.20	0.16	0.40	0.12
	$P = 0.14$		$p = 0.03$		$p = 0.21$		$p = 0.63$	
Lower GI-tract								
Mean duration until eradication	6.6	5.9	7.7	5.7	5.6	6.1	5.7	7.4
Median duration until eradication	5.0	5.0	6.0	5.0	5.0	5.0	6.0	5.0
Standard error	0.21	0.11	0.42	0.10	0.19	0.12	0.27	0.10
	$p = 0.001$		$p = 0.001$		$P = 0.015$		$P = 0.001$	

microorganisms were included for each particular analysis. This implicates that most cultured microorganisms were included in more than one analysis.

The primary outcome was successful decontamination. Decontamination rates are reported as the percentage of AGNB's present on admission that are successfully decontaminated from either the upper- or lower gastrointestinal tract. We have performed two analyses: (1) decontamination is achieved as soon as one follow-up culture is negative. (2) decontamination is achieved when two consecutive follow-up cultures are negative. Patients with one negative culture followed by ICU discharge were in this analysis considered as not-decontaminated. Differences in decontamination rates between susceptible and resistant micro-organisms are tested using Chi-square test.

The secondary outcomes of this study are the time to achieve successful decontamination and the rate of decontamination in case of co-resistance. Time to successful decontamination was given in days. Time to decontamination between susceptible and resistant strains was tested with the Mann-Whitney *U*-test (**Table 1**). The distributions of time to successful decontamination was estimated using the Kaplan Meier analysis and tested with the log-rank test.

RESULTS

Patients and Cultures

A total of 867 patients with a primary carrier state with one or more aerobic Gram-negative microorganisms and treated with SDD were included. This accounts for 893 admissions (re-admissions included). In **Table 2** baseline characteristics of the included admissions are summarized and shows that it is a mixed medical and surgical group of ICU patients with high APACHE scores. SDD was started on admission day 1 or 2 in 97.8% of patients. Patients included in the study were colonized with 288 unique AGNB's in the upper gastro-intestinal tract (throat culture) of which 281 had antimicrobial sensitivity tested. In the lower gastro-intestinal tract (rectal culture) 1,118 unique AGNB's were found of which 1,087 had susceptibility tested.

TABLE 2 | Baseline characteristics.

Number of patients included		867	
Number of admissions		893	
Age in years, mean (SD)		69	(15)
Males, *N* (%)/Females *N* (%)		573 (64.2%)/320 (35.8%)	
Length of ICU stay in days, median (IQR)		12	(6.5–17.5)
APACHE IV predicted mortality		0.42	(0.18–0.67)
Readmission, *N* (%)		66	(11.8%)
Patient category	Cardiothoracic surgery, N (%)	198	(22.2%)
	Internal medicine, *N* (%)	170	(19.0%)
	Surgery, *N* (%)	233	(26.1%)
	Cardiology, *N* (%)	125	(14.0%)
	Pulmonology, *N* (%)	119	(13.3%)
	Neurology, *N* (%)	28	(3.1%)
	other, *N* (%)	20	(2.2%)
Mechanically ventilated (*N*,%)	706		(81.4%)
ICU mortality, *N* (%)		175	(19.6%)
Number of days treated with SDD, median (IQR)		12	(6.5–17.5)
SDD started on day 1 or day 2, *N* (%)		874	(97.8%)

The microorganisms cultured on admission in the upper gastro-intestinal tract were: *Acinetobacter* sp. ($N = 21$), *Citrobacter* sp. ($N = 10$), *Enterobacter* sp. ($N = 23$), *E. coli* ($N = 39$), *Klebsiella* sp. ($N = 22$), *Morganella* sp. ($N = 9$), *Proteus* sp. ($N = 31$), *Pseudomonas* sp. ($N = 84$) and *Serratia* sp. ($N = 49$). Unique strains of aerobic Gram-negative microorganisms in the lower GI-tract were: *Acinetobacter* sp. ($N = 10$), *Citrobacter* sp. ($N = 36$), *Enterobacter* sp. ($N = 50$), *E. coli* ($N = 446$), *Klebsiella* sp. ($N = 70$),

TABLE 3 | Rates of successful decontamination according to location and antimicrobial agent, for resistant and sensitive strains.

Antimicrobial agent tested		Total number of colonization on admission with susceptibility testing.	Successful de-colonization, N	% Successful de-contamination	
Upper GI-tract					
Cephalosporins	R	121	116	95.9%	$p = 0.07$
	S	150	149	99.3%	
Aminoglycosides	R	35	33	94.3%	$p = 0.17$
	S	242	238	98.3%	
Colistin	R	93	90	96.8%	$p = 0.07$
	S	163	160	98.2%	
Ciprofloxacin	R	40	38	95.0%	$p = 0.21$
	S	233	229	98.3%	
Lower GI-tract					
Cephalosporins	R	291	262	90.0%	$p < 0.01$
	S	755	722	95.6%	
Aminoglycosides	R	154	130	84.4%	$p < 0.01$
	S	891	851	95.5%	
Colistin	R	222	211	95.0%	$p = 0.35$
	S	737	693	94.0%	
Ciprofloxacin	R	210	189	90.0%	$p < 0.01$
	S	825	785	95.2%	

Morganella sp. ($n = 44$), *Proteus* sp. ($N = 161$), *Pseudomonas* sp. ($N = 283$), and *Serratia* sp. ($N = 18$). Susceptibility testing was performed for third generation cephalosporins in 1,317 cases and for aminoglycosides in 1,322; for colistin in 1,215 cases and for ciprofloxacin in 1,308 cases respectively.

Decontamination Defined as One Follow-Up Culture Negative for Aerobic Gram-Negative Bacteria

Successful decontamination of aerobic Gram-negative microorganisms cultured on admission in the upper GI-tract was achieved for 275 out of 281 unique (susceptibility tested) strains (97.9%) before discharge. In the lower GI-tract the number of successfully decontaminated strains was 1,019 out of 1,087 unique strains (93.7%). **Table 3** shows the success rates for decontamination in resistant and susceptible microorganisms for primary carrier state of the upper GI-tract and lower GI-tract separately. Decontamination appears to be achieved in over 90% for all cases except for aminoglycosides resistant strains in the lower GI tract (84%). The upper GI tract did not show significant differences in decontamination rates between susceptible strains and strains resistant for a specific antibiotic. Decontamination of the lower GI tract was significantly less successful in strains resistant to cephalosporins, aminoglycosides and ciprofloxacin compared to susceptible strains.

Table 4 show the decontamination rates for micro-organisms with co-resistance for two or more antimicrobial agents for the upper and lower GI tract, respectively. These rates are 95% or higher in both resistant and sensitive strains in the upper GI tract. In the lower GI tract co-resistant strains are significantly less often decontaminated when co-resistance is present.

TABLE 4 | Decontamination rates for antimicrobial agents with co-resistance in the upper and lower gastrointestinal (GI) tract.

		N	Successful decolonization *N*	%	*p*- value
Upper GI-tract					
Co-resistance for at least two agents	Yes	75	71	94.7%	0.04
	No	206	204	99.0%	
Co-resistance for tobramycin and cefalosporins	Yes	24	22	91.7%	0.08
	No	257	253	98.4%	
Co-resistance for tobramycin and colistin	Yes	43	41	95.3%	0.23
	No	238	234	98.3%	
Co-resistance for tobramycin, colistin and cefalosporins.	Yes	7	7	100.0%	1.00
	No	274	268	97.8%	
Lower GI tract					
Co-resistance for at least two agents	Yes	219	189	86.3%	<0.01
	No	868	830	95.6%	
Co-resistance for tobramycin and cefalosporins	Yes	93	75	80.6%	<0.01
	No	994	944	95.0%	
Co-resistance for tobramycin and colistin	Yes	56	48	85.7%	0.02
	No	1,031	971	94.2%	
Co-resistance for tobramycin, colistin and cefalosporins	Yes	12	8	66.7%	<0.01
	No	1,075	1,011	94.0%	

The decontamination rates for specific microorganisms are summarized in **Supplementary Table 1** and shows successful decontamination in more than 90% for all species except for Morganella (79%).

The analysis of the time to decontamination was performed for colonization of the upper and lower GI-tract separately. **Figure 2** shows the Kaplan-Meyer curves for the different antimicrobial agents tested in the upper GI tract. The same information in shown in **Figure 3** for the lower GI-tract.

The time to successful decontamination appears to be significantly longer for resistant microorganisms compared to sensitive microorganisms (**Table 1**).

Decontamination Defined as Two Consecutive Follow-Up Cultures Negative for Aerobic Gram-Negative Bacteria

We also analyzed decontamination defined as two negative follow-up cultures before ICU discharge. For susceptible strains the rates were between 91.4 and 98.0% in the

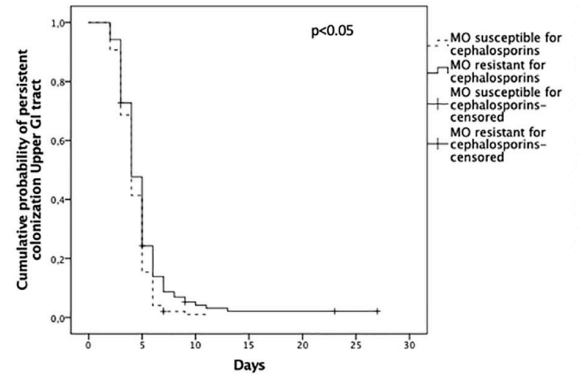

Susceptible for cephalosporin	day 2	day 4	day 6	day 8	day 10	day 12
no. of events	14	88	144	147	148	149
% eradicated of total no. cases	9,3%	58,7%	96,0%	98,0%	98,7%	99,3%
no. censored	0	0	0	1	1	1

Resistant for cephalosporins	day 2	day 4	day 6	day 8	day 10	day 27
no. of events	7	63	103	111	114	116
% eradicated of total no. cases	5,8%	52,1%	85,1%	91,7%	94,2%	95,9%

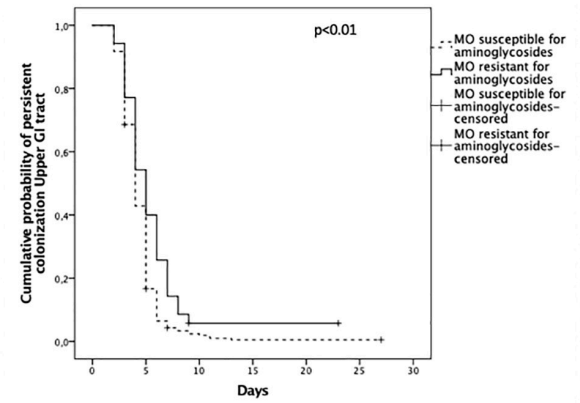

Susceptible for Aminoglycosi	day 2	day 4	day 6	day 8	day 10	day 27
no. of events	20	138	225	232	235	238
% eradicated of total no. cases	8,3%	57,0%	93,0%	95,9%	97,1%	98,3%
no. censored	0	1	2	3	3	4

Resistant for Aminoglycosid	day 2	day 4	day 6	day 8	day 10	day 23
no. of events	2	16	26	32	33	33
% eradicated of total no. cases	5,7%	45,7%	74,3%	91,4%	94,3%	94,3%

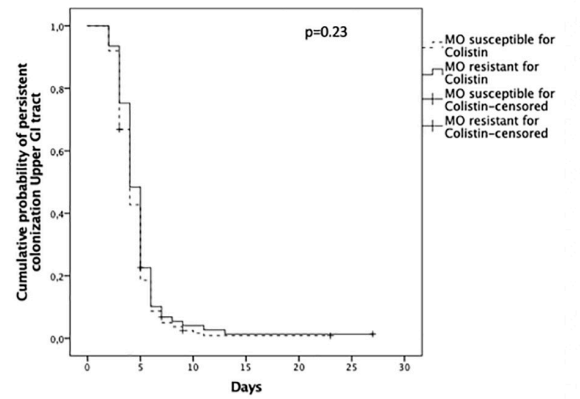

Susceptible for Colistin	day 2	day 4	day 6	day 8	day 10	day 23
no. of events	13	93	148	156	159	160
% eradicated of total no. cases	8,0%	57,1%	90,8%	95,7%	97,5%	98,2%
no. censored	0	1	1	2	3	3

Resistant for Colistin	day 2	day 4	day 6	day 8	day 10	day 27
no. of events	6	48	83	87	88	90
% eradicated of total no. cases	6,5%	51,6%	89,2%	93,5%	94,6%	96,8%
no. censored	0	0	1	2	2	3

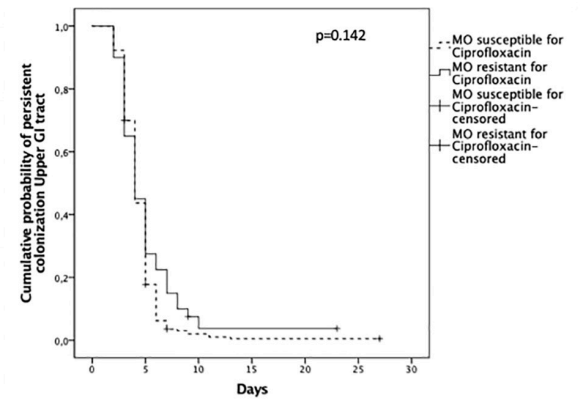

Susceptible for Ciprofloxacin	day 2	day 4	day 6	day 8	day 10	day 27
no. of events	18	131	217	224	226	229
% eradicated of total no. cases	7,7%	56,2%	93,1%	96,1%	97,0%	98,3%
no. censored	0	1	2	3	3	4

Resistant for Ciprofloxacin	day 2	day 4	day 6	day 8	day 10	day 23
no. of events	4	22	31	36	38	38
% eradicated of total no. cases	10,0%	55,0%	77,5%	90,0%	95,0%	95,0%
no. censored	0	0	0	0	1	2

FIGURE 2 | Cumulative decontamination over time for susceptible and resistant microorganisms for the upper gastrointestinal (GI) tract.

upper gastrointestinal tract and between 73.7 and 76.6% in the lower gastrointestinal tract. For resistant strains the decontamination rates were between 77.1 and 90.3% in the upper gastrointestinal tract and between 61.7 and 76.6% for resistant strains in the lower gastrointestinal tract (**Table 5**). The median time to decontamination of the upper GI tract was 4 days for susceptible strains and 5 days for resistant strains except for colistin it was 4 days in both susceptible and resistant groups. The median time to decontamination of the lower GI tract was 5 days for susceptible and 8 days for ciprofloxacin resistant strains, 6 vs. 8 days for aminoglycosides resistant strains, 6 days for both cephalosporins susceptible and resistant strains and 4 days for both colistin susceptible and resistant strains.

The cumulative proportion of decontamination and Kaplan-Meier curves for susceptible and resistant strains are shown in **Supplementary Figures 1**, **2**.

DISCUSSION

We have shown that high rates of decontamination in both susceptible and resistant microorganisms are achieved. SDD resulted in an overall level of decontamination in the upper

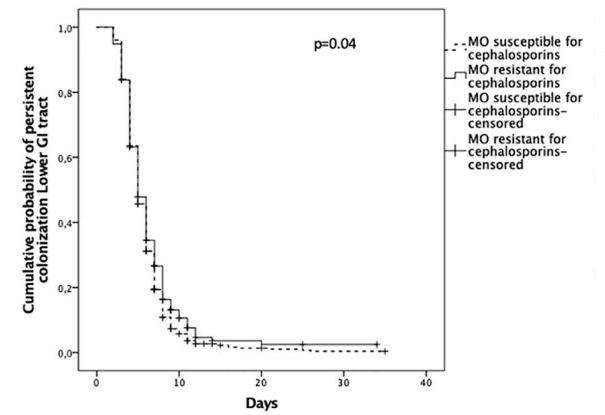

Susceptible for cephalosporins	day 2	day 4	day 6	day 8	day 10	day 35
no. of events	30	275	517	663	696	722
% eradicated of total no. cases	4,0%	36,4%	68,5%	87,8%	92,2%	95,6%
no. censored	0	3	9	21	24	33

Resistant for cephalosporins	day 2	day 4	day 6	day 8	day 10	day 34
no. of events	15	107	189	238	251	262
% eradicated of total no. cases	5,2%	36,8%	64,9%	81,8%	86,3%	90,0%
no. censored	0	2	6	13	22	29

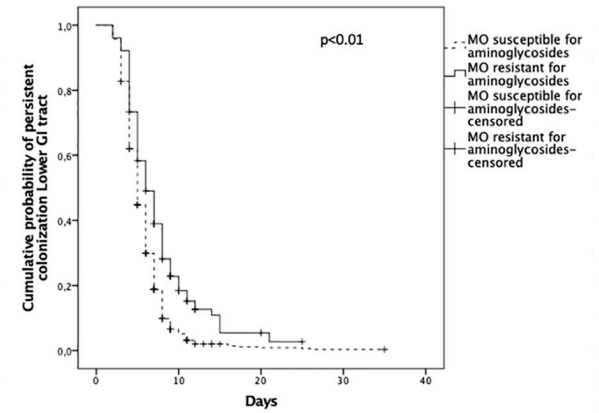

Susceptible for Aminoglycoside	day 2	day 4	day 6	day 8	day 10	day 35
no. of events	38	338	621	789	824	851
% eradicated of total no. cases	4,3%	37,9%	69,7%	88,6%	92,5%	95,5%
no. censored	0	4	14	27	31	40

Resistant for Aminoglycosides	day 2	day 4	day 6	day 8	day 10	day25
no. of events	6	41	78	108	120	130
% eradicated of total no. cases	3,9%	26,6%	50,6%	70,1%	77,9%	84,4%
no. censored	0	1	3	9	17	24

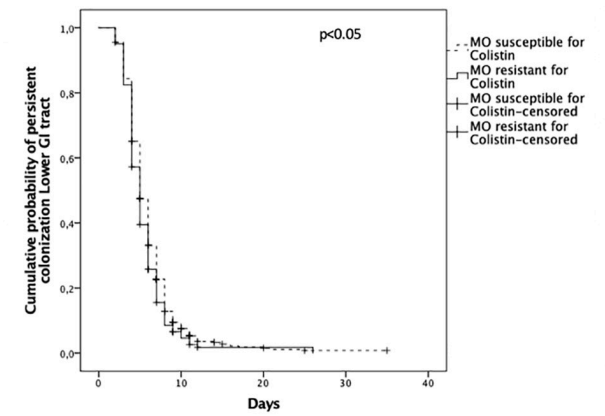

Susceptible for Colistin	day 2	day 4	day 6	day 8	day 10	day 41
no. of events	33	257	490	632	664	693
% eradicated of total no. cases	4,5%	34,9%	66,5%	85,8%	90,1%	94,0%
no. censored	1	3	9	24	33	44

Resistant for Colistin	day 2	day 4	day 6	day 8	day 10	day 26
no. of events	11	95	164	199	206	211
% eradicated of total no. cases	5,0%	42,8%	73,9%	89,6%	92,8%	95,0%
no. censored	0	1	5	6	9	11

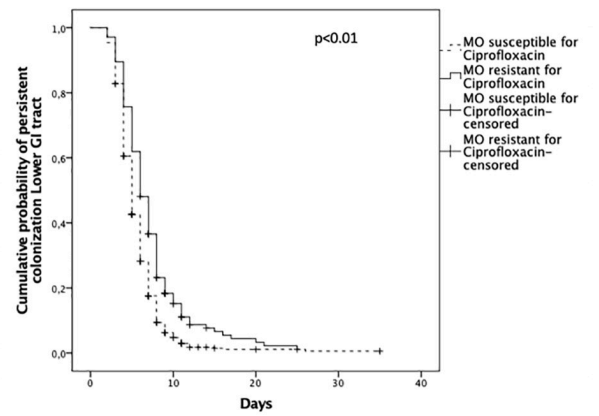

Susceptible for Ciprofloxacin	day 2	day 4	day 6	day 8	day 10	day 35
no. of events	38	325	588	733	765	785
% eradicated of total no. cases	4,6%	39,4%	71,3%	88,8%	92,7%	95,2%
no. censored	0	5	14	26	31	40

Resistant for Ciprofloxacin	day 2	day 4	day 6	day 8	day 10	day 41
no. of events	6	51	109	159	173	189
% eradicated of total no. cases	2,9%	24,3%	51,9%	75,7%	82,4%	90,0%
no. censored	0	0	1	8	15	21

FIGURE 3 | Cumulative decontamination over time for susceptible and resistant microorganisms for the lower gastrointestinal (GI) tract.

GI tract of 97.9, and 93.7% in the lower GI tract before discharge from the ICU. We found significant differences in decontamination rates of the lower GI tract between susceptible and resistant micro-organisms for all antimicrobial agents, except for colistin, probably because of the high concentrations in the gut lumen. These findings demonstrate that many susceptible and resistant microorganisms can be decontaminated from the gut with SDD. The decontamination rate was lower when co-resistance was present. This finding was significant for microorganisms present in the lower GI-tract. Nonetheless, decontamination of the lower GI-tract was successful in 80.6% of microorganisms with co-resistance to tobramycin and cefalosporins, 85.7% of microorganisms with co-resistance to tobramycin and colistin; and 66.7% of microorganisms with combined resistant to tobramycin, colistin and cefalosporins. Decontamination rates in the presence of co-resistance was even higher in microorganisms found in the upper GI-tract. So, despite of co-resistance, decontamination was still possible in the majority of these microorganisms. It should be emphasized that successful decontamination is important

TABLE 5 | Decontamination rates when decontamination is defined as two consecutive negative cultures.

Antimicrobial agent tested		Total number of colonization on admission with susceptibility testing.	Successful de-colonization, N	Successful de-contamination %	*p*-value
Upper GI-tract					
Cephalosporins	R	121	103	85.1%	$p < 0.01$
	S	150	147	98.0%	
Aminoglycosides	R	35	27	77.1%	$p < 0.01$
	S	242	227	93.8%	
Colistin	R	93	84	90.3%	$p = 0.47$
	S	163	149	91.4%	
Ciprofloxacin	R	40	31	77.5%	$p < 0.01$
	S	233	220	94.4%	
Lower GI-tract					
Cephalosporins	R	291	196	67.4%	$p < 0.01$
	S	755	576	76.3%	
Aminoglycosides	R	154	95	61.7%	$p < 0.01$
	S	891	677	76.0%	
Colistin	R	222	170	76.6%	$p = 0.39$
	S	737	543	73.7%	
Ciprofloxacin	R	210	135	64.3%	$p < 0.01$
	S	825	632	76.6%	

to achieve the goals of SDD, the prevention of secondary bacterial infections in particular pneumonia and bacteremia. When decontamination is not achieved, the successful prevention of these infections will diminish.

In this study, when resistance to third generation cephalosporins, aminoglycosides or ciprofloxacin was present the duration until successful decontamination was longer compared to susceptible microorganisms. The Kaplan- Meier curves show that most of the micro-organisms are decontaminated in the first 6 days, both for resistant and susceptible micro-organisms. After day 8–10 after admission, much less cases were successfully decontaminated. We hypothesize that this may be due to the high concentrations of tobramycin and polymyxin, which exceed high MIC values, resulting in high elimination rates of (co) resistant and susceptible microorganisms (Vollaard, 1991). New resistant microorganisms during SDD treatment rarely appear, as was shown by our group previously (Buitinck et al., 2019).

The few studies on decontamination of Gram-negative microorganisms that have been performed show similar decontamination rates. Oostdijk et al. (2012) found decontamination rates of 62–81% with the lowest rates for aminoglycoside resistant Enterobacteriaceae. They defined decontamination as two consecutive negative cultures. Our decontamination rates with two consecutive negative cultures are reported as well and figures and tables as **Supplementary Material**. **Table 5** shows similar or higher rates as Oostdijk et al. (2012). This is, however, an underreporting as patients with only one negative follow-up culture and subsequent ICU discharge are considered not-decontaminated while a prolonged stay in the ICU might show a second negative culture and thus successful decontamination. Therefore, our primary outcome measure was one negative culture. The one-negative culture rates are slightly overestimating as occasionally a patient is tested positive again in the next culture. Stoutenbeek et al. (1987) reported in cephalosporin resistant enterobacteriaceae an elimination rate of 82%. In contrast, Abecasis et al. (2011) in pediatric patients showed a much lower rate of 54% in ESBL-producing AGNB's. In this study AGNB-ESBL susceptible for tobramycin and AGNB-ESBL resistant to tobramycin were also analyzed separately. In the tobramycin susceptible group, no failures of clearance were reported, whereas in the tobramycin resistant group a failure rate of 39% was reported.

The fact that not all patients are successfully decontaminated stresses the importance of surveillance cultures and a pro-active approach when decontamination is not reached a week after admission. The reasons for decontamination failure may be a slow transit time or ileus that prevents the substances to reach the rectal cavity. In our unit we have a general policy to achieve defecation within 4 days by using laxatives. This may be an explanation, next to the definition of one instead of two cultures, for the relatively fast decontamination time in comparison with other studies. Our analysis for two consecutive cultures also shows a faster decontamination than other studies (**Supplementary Figures 1**, **2**). When the throat is not successfully decontaminated, *foreign bodies,* e.g., a nasogastric tube that is in place for more than a week, may maintain pathological colonization (Van Der Voort et al., 2019). In addition, modification of the components of SDD, e.g., the addition of co-trimoxazole or amikacin, could lead to decontamination in specific cases (Nahar et al., 2019; Van Der Voort et al., 2019).

The present study has several strengths and limitations. First, in this cohort study the protocol of SDD is consequently applied in patients with expected ICU stay of more than 24 h irrespective of the need for mechanical ventilation over the complete 10-year study period. SDD was started in 97.8% of patients on admission day 1 or admission day 2. Second, surveillance cultures were consistently taken twice weekly. Third, only surveillance cultures were used for the determination of successful decontamination instead of organ site cultures. SDD surveillance cultures have been shown in previous research to have a greater sensitivity for culturing potentially pathogenic microorganisms than organ sites (Viviani et al., 2010).

This study has several limitations too. The observational design limits the possibility for correction of confounders. A previously determined factor in studies that influences the rate of decontamination is ileus and gastroparesis. These situations limit the propulsion of enteral antimicrobial agents through the gut and therefore limit the success rate of decontamination. We could not reliably determine from our database which patients suffered from ileus or gastroparesis and who did not. On the other hand, our study describes the real-life situation and daily practice.

In practice, successful decontamination is usually determined after two negative cultures. In this study we analyzed one and also two consecutive negative cultures as a definition of decontamination. Two negative cultures give a fair amount of underreporting as quite a number of patients are discharged

after one negative culture and are, in that case, counted as not-decontaminated. We have shown (**Table 5** and **Supplementary Figures 1**, **2**) that the rectal cultures show lower decontamination rates when defined as two negative cultures and also a slower decontamination compared to the results of one negative culture (median 5 days for the upper GI tract vs. 4 days, and 6 days for the lower GI tract vs. 5 days). It is emphasized that a first negative culture implies a great reduction in the number of AGNB in this patient, which will probably reduce both transmission and secondary infection. In addition, this approach was chosen to include more patients as most patients were discharged within a week, the time needed to have three consecutive cultures. Defining decontamination as one negative culture leads to somewhat higher decontamination rates compared to the decontamination rates for two consecutive negative cultures which might be a slight overestimation of the decontamination rate in case a follow-up culture becomes positive again.

A statistical limitation is in the Kaplan-Meier survival analysis as one of the assumptions for this analysis is that the event is precisely measured. In practice, surveillance cultures are taken on admission and twice weekly. The exact date of decontamination could not be determined because of the 3–4-day interval between cultures. Interval censoring may lead to false positive results (Rucker and Messerer, 1988). Also, due to differences in censoring patterns, the result of log-rank testing could be partly the effect of differences in censoring than differences in probability distributions. However, when looking at the Kaplan Meier curves, not only a difference in censoring, but also a difference in time to decontamination can be seen. We used the Kaplan Meier curves more as a tool to show the dynamics in decontamination than as a tool to proof differences between groups.

The interval between the cultures might also have caused an underestimation of the rate of successful decontamination. Patients who were discharged some days after a positive culture may have been decontaminated at the time of discharge without being recognized as such because of the absence of new cultures at discharge. Last, it is unknown whether rebound colonization occurs after ICU discharge.

This study shows that in most, but not all patients, aerobic Gram-negative microorganisms are eliminated from the gut in critically ill patients during SDD treatment. Moreover, when decontamination is not achieved but the growth density in the cultures is decreased than the risk for secondary infection and cross-contamination is probably reduced as infection usually occurs after a state of overgrowth (van Saene et al., 2003). Future research might focus on the reasons why some patients experience prolonged and abnormal carrier state. In addition, the use of alternative antimicrobials can be studied to their efficacy to decontaminate.

CONCLUSION

In conclusion, we have shown that most susceptible and resistant microorganisms can be cleared from the gut. However, microorganisms that are resistant to aminoglycosides, cephalosporins or ciprofloxacin are less frequently eradicated and the duration until decontamination is prolonged.

DATA AVAILABILITY STATEMENT

The raw data supporting the conclusions of this article will be made available by the authors, without undue reservation.

ETHICS STATEMENT

The studies involving human participants were reviewed and approved by ACWO. Written informed consent for participation was not required for this study in accordance with the national legislation and the institutional requirements.

AUTHOR CONTRIBUTIONS

SB analyzed the data and drafted the manuscript. PV, SB, and RJ designed the study. RJ gave access to the microbiology data. All authors were involved in writing the manuscript.

ACKNOWLEDGMENTS

We would like to thank C. J. van der Mark for the extensive data extraction from the microbiology laboratory information system.

SUPPLEMENTARY MATERIAL

The Supplementary Material for this article can be found online at: https://www.frontiersin.org/articles/10.3389/fmicb.2021.779805/full#supplementary-material

Supplementary Figure 1 | The cumulative proportion of decontamination and Kaplan-Meier curves for susceptible and resistant strains in the upper gastrointestinal tract.

Supplementary Figure 2 | The cumulative proportion of decontamination and Kaplan-Meier curves for susceptible and resistant strains in the lower gastrointestinal tract.

Supplementary Table 1 | Decontamination rates per microorganism.

REFERENCES

Abecasis, F., Sarginson, R. E., Kerr, S., Taylor, N., and van Saene, H. K. F. (2011). Is selective digestive decontamination useful in controlling aerobic gram-negative bacilli producing extended spectrum beta-lactamases? *Microb. Drug Resist.* 17, 17–23. doi: 10.1089/mdr.2010.0060

Buitinck, S., Jansen, R., Rijkenberg, S., Wester, J. P. J., Bosman, R. J., van der Meer, N. J. M., et al. (2019). The ecological effects of selective decontamination of

the digestive tract (SDD) on antimicrobial resistance: a 21-year longitudinal single-centre study. *Crit. Care* 23:208. doi: 10.1186/s13054-019-2480-z

Cuthbertson, B. H., Campbell, M. K., MacLennan, G., Duncan, E. M., Marshall, A. P., Wells, E. C., et al. (2013). Clinical stakeholders' opinions on the use of selective decontamination of the digestive tract in critically ill patients in intensive care units: an international Delphi study. *Crit. Care* 17:R266. doi: 10.1186/cc13096

Daneman, N., Sarwar, S., Fowler, R. A., and Cuthbertson, B. H. (2013). SuDDICU canadian study group. effect of selective decontamination on antimicrobial resistance in intensive care units: a systematic review and meta-analysis. *Lancet Infect. Dis.* 13, 328–341. doi: 10.1016/S1473-3099(12)70322-5

European Committee on Antimicrobial Susceptibility Testing (Eu-Cast) (2021). *EUCAST Breakpoint Table Version 1.0*. Sweden: European Committee on Antimicrobial Susceptibility Testing.

Evans, M. E., Feola, D. J., and Rapp, R. P. (1999). Polymyxin B Sulfate and colistin: old antibiotics for emerging multiresistant gram-negative bacteria. *Ann. Pharmacother.* 33, 960–967. doi: 10.1345/aph.18426

Houben, A. J. M., Oostdijk, E. A. N., van der Voort, P. H. J., Monen, J. C. M., Bonten, M. J. M., van der Bij, A. K., et al. (2014). Selective decontamination of the oropharynx and the digestive tract, and antimicrobial resistance: a 4 year ecological study in 38 intensive care units in the Netherlands. *J. Antimicrob. Chemother.* 69, 797–804.

Nahar, J., Buitinck, S., Jansen, R., Haak, E. J. F., and van der Voort, P. H. J. (2019). Use of enteral amikacin to eliminate carriership with multidrug resistant *Enterobacteriaceae*. *J. Infect.* 78, 409–421. doi: 10.1016/j.jinf.2019.02.007

Ochoa-Ardila, M. E., Garcia-Canas, A., Gomez-Mediavilla, K., González-Torralba, A., Alía, I., Garciá-Hierro, P., et al. (2011). Long-term use of selective decontamination of the digestive tract does not increase antibiotic resistance: a 5-year prospective cohort study. *Intensive Care Med.* 37, 1458–1465. doi: 10.1007/s00134-011-2307-0

Oostdijk, E. A. N., de Smet, A. M. G. A., Kesecioglu, J., and Bonten, M. J. M. (2012). Decontamination of cephalosporin-resistant *Enterobacteriaceae* during selective digestive tract decontamination in intensive care units. *J. Antimicrob. Chemother.* 67, 2250–2253. doi: 10.1093/jac/dks187

Plantinga, N. L., de Smet, A. M. G. A., Oostdijk, E. A. N., de Jonge, E., Camus, C., Krueger, W. A., et al. (2018). Selective digestive and oropharyngeal decontamination in medical and surgical ICU patients: individual patient data meta-analysis. *Clin. Microbiol. Infect.* 24, 505–513. doi: 10.1016/j.cmi.2017.08.019

Rucker, G., and Messerer, D. (1988). Remission duration: an example of interval-censored observations. *Stat. Med.* 7, 1139–1145. doi: 10.1002/sim.4780071106

Sanchez-Ramirez, C., Hipola-Escalada, S., Cabrera-Santana, M., Hernández-Viera, M. A., Caipe-Balcázar, L., Saavedra, P., et al. (2018). Long-term use of selective digestive decontamination in an ICU highly endemic for bacterial resistance. *Crit. Care* 22:141. doi: 10.1186/s13054-018-2057-2

Silvestri, L., and van Saene, H. K. F. (2012). Selective decontamination of the digestive tract: an update of the evidence. *HSR Proc. Intensive Care Cardiovasc. Anesth.* 4, 21–29.

Silvestri, L., van Saene, H. K. F., Milanese, M., Gregori, D., and Gullo, A. (2007). Selective decontamination of the digestive tract reduces bacterial bloodstream infection and mortality in critically ill patients. Systematic review of randomized, controlled trials. *J. Hosp. Infect.* 65, 187–203. doi: 10.1016/j.jhin.2006.10.014

Smet, A. M., Kluytmans, J. A., Blok, H. E., Mascini, E. M., Benus, R. F. J., Bernards, A. T., et al. (2011). Selective digestive tract decontamination and selective oropharyngeal decontamination and antibiotic resistance in patients in intensive-care units: an open-label, clustered group-randomised, crossover study. *Lancet Infect. Dis.* 11, 372–380. doi: 10.1016/S1473-3099(11)70035-4

Stoutenbeek, C. P., van Saene, H. K., and Zandstra, D. F. (1987). The effect of oral non-absorbable antibiotics on the emergence of resistant bacteria in patients in an intensive care unit. *J. Antimicrob. Chemother.* 19, 513–520. doi: 10.1093/jac/19.4.513

Van Der Voort, P. H. J., Buitinck, S., Jansen, R. R., Franssen, E. J. F., and Determann, R. M. (2019). Ten tips and tricks for successful digestive tract decontamination. *Netherlands J. Crit. Care* 27, 87–90.

van Saene, H. K. F., Petros, A. J., Ramsay, G., and Baxby, D. (2003). All great truths are iconoclastic: selective decontamination of the digestive tract moves from heresy to level 1 truth. *Intensive Care Med.* 29, 677–690. doi: 10.1007/s00134-003-1722-2

Viviani, M., Van Saene, H. K. F., Pisa, F., Lucangelo, U., Silvestri, L., Momesso, E., et al. (2010). The role of admission surveillance cultures in patients requiring prolonged mechanical ventilation in the intensive care unit. *Anaesth. Intensive Care* 38, 325–335. doi: 10.1177/0310057X1003800215

Vollaard, E. J. (1991). *The Concept of Colonization Resistance, A Study of the Influence of Antimicrobial Agents on Aerobic Flora of the Bowel.* Ph. D Thesis. Benda: Nijmegen.

Wayne, P. (2010). *Performance Standards for Antimicrobial Susceptibility Testing. Twentieth Informational Supplement*. Wayne, PA: CLSI.

Wittekamp, B. H. J., Oostdijk, E. A. N., de Smet, A. M. G. A., and Bonten, M. J. M. (2015). Colistin and tobramycin resistance during long- term use of selective decontamination strategies in the intensive care unit: a post hoc analysis. *Crit. Care* 19:113. doi: 10.1186/s13054-015-0838-4

Conflict of Interest: The authors declare that the research was conducted in the absence of any commercial or financial relationships that could be construed as a potential conflict of interest.

Publisher's Note: All claims expressed in this article are solely those of the authors and do not necessarily represent those of their affiliated organizations, or those of the publisher, the editors and the reviewers. Any product that may be evaluated in this article, or claim that may be made by its manufacturer, is not guaranteed or endorsed by the publisher.

frontiers in Microbiology

ORIGINAL RESEARCH
published: 04 February 2022
doi: 10.3389/fmicb.2021.783284

Identification of Distinct Characteristics of Antibiofilm Peptides and Prospection of Diverse Sources for Efficacious Sequences

Bipasa Bose[1], *Taylor Downey*[2], *Anand K. Ramasubramanian*[3]* *and David C. Anastasiu*[2]*

[1] *Department of Biomedical Engineering, San Jose State University, San Jose, CA, United States,* [2] *Department of Computer Science and Engineering, Santa Clara University, Santa Clara, CA, United States,* [3] *Department of Chemical and Materials Engineering, San Jose State University, San Jose, CA, United States*

OPEN ACCESS

Edited by:
Octavio Luiz Franco, Catholic University of Brasilia (UCB), Brazil

Reviewed by:
Sinosh Skariyachan, St. Pius X College, India
Koshy Philip, University of Malaya, Malaysia
Állan Pires, Catholic University of Brasilia (UCB), Brazil

***Correspondence:**
Anand K. Ramasubramanian
anand.ramasubramanian@sjsu.edu
David C. Anastasiu
danastasiu@scu.edu

Specialty section:
This article was submitted to Antimicrobials, Resistance and Chemotherapy, a section of the journal Frontiers in Microbiology

Received: *25 September 2021*
Accepted: *30 December 2021*
Published: *04 February 2022*

Citation:
Bose B, Downey T, Ramasubramanian AK and Anastasiu DC (2022) Identification of Distinct Characteristics of Antibiofilm Peptides and Prospection of Diverse Sources for Efficacious Sequences. Front. Microbiol. 12:783284. doi: 10.3389/fmicb.2021.783284

A majority of microbial infections are associated with biofilms. Targeting biofilms is considered an effective strategy to limit microbial virulence while minimizing the development of antibiotic resistance. Toward this need, antibiofilm peptides are an attractive arsenal since they are bestowed with properties orthogonal to small molecule drugs. In this work, we developed machine learning models to identify the distinguishing characteristics of known antibiofilm peptides, and to mine peptide databases from diverse habitats to classify new peptides with potential antibiofilm activities. Additionally, we used the reported minimum inhibitory/eradication concentration (MBIC/MBEC) of the antibiofilm peptides to create a regression model on top of the classification model to predict the effectiveness of new antibiofilm peptides. We used a positive dataset containing 242 antibiofilm peptides, and a negative dataset which, unlike previous datasets, contains peptides that are likely to promote biofilm formation. Our model achieved a classification accuracy greater than 98% and harmonic mean of precision-recall (F1) and Matthews correlation coefficient (MCC) scores greater than 0.90; the regression model achieved an MCC score greater than 0.81. We utilized our classification-regression pipeline to evaluate 135,015 peptides from diverse sources for potential antibiofilm activity, and we identified 185 candidates that are likely to be effective against preformed biofilms at micromolar concentrations. Structural analysis of the top 37 hits revealed a larger distribution of helices and coils than sheets, and common functional motifs. Sequence alignment of these hits with known antibiofilm peptides revealed that, while some of the hits showed relatively high sequence similarity with known peptides, some others did not indicate the presence of antibiofilm activity in novel sources or sequences. Further, some of the hits had previously recognized therapeutic properties or host defense traits suggestive of drug repurposing applications. Taken together, this work demonstrates a new *in silico* approach to predicting antibiofilm efficacy, and identifies promising new candidates for biofilm eradication.

Keywords: antimicrobial, antibiofilm, machine learning, MBEC, MBIC, drug discovery

1. INTRODUCTION

Many microbes in their natural habitats are found not as free-floating (planktonic) organisms, but as three dimensional aggregates encased in a polymeric matrix called biofilms (Costerton et al., 1987). Biofilms are responsible for 65–80% of recalcitrant infections in humans. Once established, biofilms have the potential to initiate or prolong infections by providing a safe sanctuary from which organisms can invade local tissue, seed new infection sites and resist eradication efforts. Both bacteria and fungi form biofilms on abiotic (e.g., catheters and implants) or biotic (e.g., skin, wounds) surfaces (Torres et al., 2018; Ramasubramanian and Lopez-Ribot, 2019). Cells within the biofilms display high levels of resistance against clinically-administered antibiotics, which often leads to morbidity and mortality (Srinivasan et al., 2017). Therefore, there is an urgent need to develop agents that are effective against biofilm infections (de la Fuente-Núñez et al., 2013; Pierce et al., 2015).

The traditional antibiotic screening paradigm first established during the "golden era" of antibiotics (1940–1960), which has continued until very recently, was heavily biased toward the discovery of "magic bullets" that have either bacteriostatic or bactericidal properties but elicited waves of antibiotic resistance. This approach has had little success against multidrug resistant (MDR) highly virulent *Enterococcus faecium*, *Staphylococcus aureus*, *Klebsiella pneumoniae*, *Acinetobacter baumannii*, *Pseudomonas aeruginosa*, and *Enterobacter spp* (ESKAPE) pathogens (De Oliveira et al., 2020). Antimicrobial peptides (AMP) have emerged as a promising alternative or complement to chemical compounds in treating microbial infections (Margit et al., 2016). More than 4,700 such peptides have been identified in all forms of life, and are deposited in the Antimicrobial peptide database (APD) (Wang et al., 2015). Compared to chemical antibiotics, AMPs are particularly attractive for several reasons: (i) AMPs appear to have a lower rate of inducing bacterial resistance and they continue to be developed clinically (Spohn et al., 2019); (ii) AMPs appear to be the last resort for recalcitrant infections as exemplified by Polymyxin B, colistin, daptomycin against the MDR ESKAPE pathogens (Zavascki et al., 2007); (iii) AMPs can work synergistically with antibiotics (Sheard et al., 2019).

In the recent past, several Machine Learning (ML)-based approaches have been developed for the characterization and prediction of novel AMPs including AntiBP - for predicting antibacterial peptides (Lata et al., 2007), iAMP-2L-for identifying antimicrobial peptides (Xiao et al., 2013), iAMPred-for predicting antimicrobial peptides by using physico-chemical and structural properties (Meher et al., 2017), AmPEP-for sequence based prediction of antimicrobial peptides (Bhadra et al., 2018). These studies have clearly demonstrated that pattern-based computational approaches to establish structure-function relationships are a powerful alternative or augmentation to experimental biochemical assays, which are inherently lower throughput, and expensive. More importantly, ML approaches have been used to discover new AMP sequences (Lee et al., 2016), predict unknown peptides from known ones (Fjell et al., 2008), identify peptides with multiple functions (Haney et al., 2018), and to discover previously unknown interrelationships between existing peptides (Lee et al., 2016).

While a vast majority of work has focused on AMPs effective against microbial infections in general, relatively fewer experimental or computational efforts have been invested on discovering peptides that are effective against biofilm infections. These peptides, called Antibiofilm peptides (ABP) are a subset of AMPs that inhibit biofilm formation or eradicate previously formed biofilms. Nearly 200–300 peptides have been identified to be effective against biofilms and are listed in the antibiofilm peptide database, BaAMPs (Luca et al., 2015). ABPs can be particularly attractive as a strategy to limit microbial virulence without necessarily killing the organisms, or risking the development of antibiotic resistance. ABPs can be used as an alternative to antibiotics in microbial infections (Pletzer and Hancock, 2016).

Previous ML approaches have focused on establishing patterns from existing antibiofilm peptides that enable the classification of candidate peptides for potential antibiofilm activity (Gupta et al., 2016; Sharma et al., 2016; Fallah Atanaki et al., 2020). Gupta et al. developed sequence-based support vector machine (SVM) and random forest (RF) models to predict antibiofilm activity using the peptides listed in the BaAMP database. Their model achieved reasonable success with a Matthews's correlation coefficient (MCC) score of 0.84 (Gupta et al., 2016). Sharma et al. developed SVM- and Weka-based models using BaAMP data as their positive dataset, and quorum-sensing peptides as their negative set. They achieved an MCC of 0.91 (Sharma et al., 2016). Another web-based model, BIPEP, was developed by Fallah Atanaki et al. (2020) wherein peptides from the APD and BaAMP databases were used as the positive set, along with a negative dataset consisting fewer quorum sensing peptides that in the positive set. Their SVM model achieved an MCC value of 0.89. While these studies developed important quantitative structure and activity relationships in ABPs, they suffered from some drawbacks which may affect the model performance. The model of Atankai et al. did not account for the lower abundance of ABPs in nature. The model of Gupta et al. might have used the pattern recognition sequences ("motifs") as a privileged information prior in the classification model, while the model of Sharma et al. considered a smaller negative set compared to their positive data set. Most importantly, these models can only classify ABPs but do not provide any insights into the efficacy of these peptides against biofilms.

The objectives of this work are 3-fold: first, we seek to improve the classification algorithm for ABPs by using a more realistic, curated negative dataset with mostly biofilm-favoring peptides which is 10-fold larger than the positive dataset; our model identifies the most useful amino-acid composition features and short-repeating patterns ("motifs") indicative of antibiofilm activity; second, we seek to develop a regression model using the minimum biofilm inhibitory concentration (MBIC) and minimum biofilm eradication concentration (MBEC) of ABPs to predict the effectiveness of the novel peptides classified as antibiofilm candidates; third, we seek to understand the putative mechanisms of action of the peptide hits using their

previously known properties, secondary structure, and similarity with known antibiofilm peptides.

2. METHODS

2.1. Dataset Preparation

In this work, we collected data with the aim to improve the performance of antibiofilm prediction models. Since biofilm eradication is a well-defined physiological phenomenon, any peptide will have less than a random 50% chance to be active against preformed biofilms. Therefore, instead of using a balanced dataset consisting of equal amounts of ABP and non-ABP, we used an imbalanced, operationally tractable dataset consisting of ten times more non-ABP peptides in the negative dataset compared to ABP peptides in the positive dataset. We chose to work with real peptides instead of randomly generated peptides so that a more realistic performance may be obtained from our classifier models. Therefore, we collected peptides which directly or indirectly could play a role in biofilm formation as elaborated in section 2.1.1. For establishing the efficacy, we performed an extensive literature search to obtain peptides with minimum biofilm inhibitory concentration (MBIC), and minimum biofilm eradication concentration (MBEC).

2.1.1. Dataset 1

We extracted ABPs from the Antimicrobial Peptide Database (APD), and the Biofilm-active Antimicrobial Peptide database (BaAMP). After removing duplicates, we obtained 242 ABPs, which served as our positive dataset (**Supplementary Tables S14–S18** in Supplementary Note 6). For the negative dataset, we curated peptides from different databases such as UniProt (Consortium, 2020), Quorum Sensing Peptide Prediction Server (QSPProd) (Rajput et al., 2015) and NCBI protein database (Coordinators, 2016). The peptides from the UniProt database were screened for their direct or indirect contribution to biofilm formation, including regulation, association with biofilm matrix polysaccharide or proteins, and association with the cells themselves. For example, we added protein Q59U10, which is a biofilm and cell wall regulator in *Candida albicans*. We also screened the proteomic profiles of different biofilm-forming bacteria like *Staphylococcus aureus* and *Escherichia coli*, and included peptides from the NCBI and UniProt databases that promote biofilm formation. For example, we included fibronectin-binding protein B, which promotes the accumulation and surface attachment of biofilm by *Staphylococcus aureus*. We also included quorum sensing peptides, which promote biofilm formation, from QSPProd in our negative dataset. To have a sequence length distribution in the negative dataset that is similar to the positive dataset, we considered either only the signal peptide length of the original protein, or we divided the whole sequence into several sequences of length 70–75, depending on the protein length. One caveat with this approach is that fragments from a biofilm-promoting protein may not retain the property of the parent protein. The negative dataset has peptides of length 4–75.

Eighty percent of the positive and negative datasets were used for training and 10-fold cross-validation while the remaining 20% was kept aside as a test/validation set. The performances of different machine learning algorithms were evaluated on this out-of-scope test dataset.

2.1.2. Dataset 2

We curated the minimum biofilm inhibitory concentration (MBIC), and the minimum biofilm eradication concentration (MBEC) for our positive dataset against different gram-positive and gram-negative bacteria from the source publications. In cases where these values were not listed in the source publication, the approximate values were obtained from images or graphs in the respective articles. For example, for LL-37, we consider the case where *P. aeruginosa* biofilm were grown previously and then peptides were added in various concentration (Nagant et al., 2012). The bacteria was tagged with green fluorescent protein and the killed biofilm appeared as red in the result. We analyzed the figures, which indicate that the killing starts at 20 μM concentration. Therefore, we considered 20 μM as the MBEC value of LL-37 against *P. aeruginosa*. Likewise we did the search of all the ABPs from our positive dataset. Of the 242 peptides in our positive dataset, we obtained MBIC and MBEC values for 178 and 57 peptides (**Supplementary Tables S19**, **S20** in Supplementary Note 4), respectively.

We did not consider the peptides which showed inhibition/eradication against fungal pathogens like *Candida* and others.

2.1.3. Candidate Dataset

In addition to the labeled dataset we used to train and evaluate the performance of our computational antibiofilm prediction models, we constructed a large *candidate dataset* from various sources, including 74 anticancer, 220 antiviral, and more than 4,770 antimicrobial peptides from the Data Repository of AntiMicrobial peptides (DRAM) (Kang et al., 2019). Additionally, we collected all 202,716 peptides from UniProt of sequence length 11–20. After removing duplicates, our candidate dataset contains 109,807 unique UniProt peptides. We also included peptides from the Swiss-Prot section of UniProt (Duvaud et al., 2021) with sequence length 4–10 and 20–80. In total, we tested our model against 135,015 unique peptides from different data sources.

2.2. Feature Extraction

We used the "propy3" (Cao, 2020) and the "protParam" (Cock et al., 2009) software packages to extract different peptide features, which are numerical representations of the peptide sequence, structure, and physicochemical properties as described below.

2.2.1. Amino Acid Composition

The Amino Acid Composition (AAC) features represent the percentage of each amino acid present in the peptide sequence. The biopython package returns a 20-element vector of the naturally occurring amino acids. Equation 1 provides the formula for computing the AAC of a given amino acid *i*:

$$AAC(i) = \frac{\#\ amino\ acids\ of\ type\ (i)}{\#\ amino\ acids} \times 100 \qquad (1)$$

2.2.2. Dipeptide Composition

Dipeptide Composition (DPC) represents the percentage of the dipeptides present in the peptide sequence. The DPC feature returns 400 named vectors with a non-zero value for any amino acid pair (dipeptide) present in the peptide.

$$DPC(i,j) = \frac{\#\ dipeptide\ (i\ and\ j)}{\#\ possible\ dipeptides} \times 100 \quad (2)$$

2.2.3. Composition, Transition, Distribution

The Composition, Transition, Distribution (CTD) descriptor is a 147-element vector representing different physio-chemical properties of the peptides (Xiao et al., 2015). The properties of peptides that are part of the CTD descriptor include "hydrophobicity," "normalized van der Waals volume," "polarity," "polarizability," "charge," "secondary structure," and "solvent accessibility." The amino acids are divided into three groups depending on their property and functionality. The "composition" features represent the percentage of each group of amino acids in the peptide. The "transition" features represent the relative frequencies of a given amino acid from one group being followed by an amino acid from a different group. Finally, the "distribution" features represent the percentage residue of each attribute present in the peptide in their first, 25%, 50%, 75%, and 100% of residues, respectively.

2.2.4. Motif

"Motifs" are maximal length amino acid sequences present in peptides which may represent a unique biological or chemical function. We used the "MERCI" software (Vens et al., 2011) to identify distinct patterns in ABPs that are not present in non ABPs (non-antibiofilm peptides). The MERCI software provides two scripts to extract motifs. One script can essentially find all the motifs that are present in the positive dataset and absent in the negative dataset, which was used to discover and store, in each experiment, motifs found in our training dataset. We then used the second script to identify which of those training set motifs were present in the test samples. Finally, we used the number of identified motifs found in a given peptide as the motif-based single-variate feature.

2.2.5. Other Features

We extracted other critical, global features, such as sequence length, molecular weight, aromaticity, and isoelectric point, using the "ProteinAnalysis" module of the "protParam" software.

2.3. Machine Learning Models

We developed our prediction model using several machine learning algorithms, including Support Vector Machines (SVM), Random Forest (RF), and Extreme Gradient Boosting (XGBoost) classifiers. Our goal was to select the algorithm that provides the best predictive performance for antibiofilm activity on out-of-sample data. We used the "Scikit-learn" (Pedregosa, 2011) package to train and test models for our work.

2.3.1. Support Vector Machine

Support Vector Machine (SVM) is one of the most commonly used classifiers for peptide prediction (Ng et al., 2015). SVM works particularly well for binary classification problems. The model works by separating samples in different classes using a hyperplane, which can be expressed in a high dimensional space through kernel transformations. Since our dataset is not relatively large, we used a nonparametric method that SVM supports and a radial basis function (RBF) kernel. SVM is a robust model that can be used for both classification and regression. Literature shows that SVM has performed exceptionally well in predicting peptide function (Gupta et al., 2013).

2.3.2. Support Vector Regressor

The Support Vector Regressor (SVR) model uses the same principle as SVM, but for regression problems. Instead of separating samples into different classes using a hyperplane, the hyperplane is used to create a best fit line that has the maximum number of points between the decision boundaries. Like the classifications models, we used a radial basis function (RBF) kernel to create a nonlinear hyperplane. The SVR was used to predict minimum biofilm eradication/inhibitory concentration (MBEC/MBIC).

2.3.3. Random Forest

The Random Forest (RF) model is an ensemble prediction model, which also supports both regression and classification. RF has been used to classify peptides and to solve other biological problems (Manavalan et al., 2018). Although RF may not be the best choice as a classifier for an imbalanced dataset, we used this algorithm to compare the performance with other classification algorithms.

2.3.4. Extreme Gradient Boosting

The Extreme Gradient Boosting (XGBoost) model is comparatively a new prediction method used in machine learning, which can also be used for both classification and regression problems. In our work we used the XGBClassifier. The XGBoost algorithm has regularization parameters that can be tuned to reduce overfitting in an imbalanced dataset. This algorithm is also used in prior work for the prediction of peptides with an accuracy greater than 98% (Wang et al., 2020).

2.4. Cross-Validation and Stratified Sampling

To address potential overfitting problems, we performed 10-fold cross-validation of our training dataset, wherein one part of the dataset, called the validation set, was used for testing, and the other nine were used for training. This process was iterated over ten times, using, in turn, each of the ten parts as the validation set. Since our dataset is imbalanced, having ten negative peptides for every positive one, we used stratified sampling to ensure that each fold receives an equal percentage of positive and negative peptides while doing cross-validation. Additionally, we used stratified sampling to ensure that the out-of-sample test dataset also has precisely 20% of the positive data, i.e., 48 peptides, and 20% of the negative data, i.e., 485 peptides. The details of the distribution of dataset is available in **Supplementary Table S1** in Supplementary Note 1.

2.5. Performance Evaluation

We used several standard metrics to evaluate our models" performance, including sensitivity (Sen), specificity (Spec), accuracy (Acc), Matthews's correlation coefficient (MCC), and harmonic mean of the precision-recall (F1) Score. The metrics are defined as,

$$Specificity = \frac{TN}{FP + TN} \tag{3}$$

$$Sensitivity = \frac{TP}{TP + FN} \tag{4}$$

$$Accuracy = \frac{TP + TN}{TP + FP + TN + FN} \tag{5}$$

$$F1 = \frac{TP}{TP + \frac{FP + FN}{2}} \tag{6}$$

$$MCC = \frac{(TP)(TN) - (FP)(FN)}{\sqrt{(TP + FP)(TP + FN)(TN + FP)(TN + FN)}} \tag{7}$$

where, TP = True Positive, TN = True Negative, FP = False Positive, and FN = False Negative. For each model we tested, we used 10-fold cross-validation to tune meta-parameters and find the best model performance on the training set. We report the effectiveness of that model on the out-of-sample test set in the following section.

2.6. Principal Component Analysis (PCA)

During feature selection, the samples were transformed into a lower dimensional space via Principal Component Analysis (PCA). Several hyperparameters were tuned, namely the regularization parameter (C) and kernel coefficient (γ) for the SVM/SVR models, and the number of principal components for the dimensionality reduction. We employed 5-fold stratified cross validation for classification and 5-fold cross validation for regression to ensure we trained a generic enough model that would not overfit the training set.

2.7. Sequence Alignment and Structure Prediction

Sequence alignment of peptides was performed to identify structural similarities between peptides using Clustal Omega, and visualized using Jalview (Madeira et al., 2019). The BLOSUM62 raw scores were used to confirm pairwise homology. To obtain consensus sequences from multiple sequence alignments, the first phylogenetic relationship was established based on BLOSUM62 scores. Then, from peptides in closely related trees, same or highly similar residues were extracted. To obtain the degree of disorder, the DisEMBL algorithm was used, and sequences with a threshold value greater than 0.55 were classified as "hotloops" or highly disordered regions. The 2D and 3D structures of the peptides were predicted using the PEP2D (Singh et al., 2019) and PEP-FOLD3 (Lamiable et al., 2016) servers, respectively.

3. RESULTS AND DISCUSSION

Our pipeline to predict peptides active against biofilms may be grouped into four key steps: identification of positive and negative datasets; development of a robust machine learning algorithm for classification of ABPs; collection of candidate potential ABPs from diverse habitats; and prediction of the efficacy of the novel peptides using our antibiofilm peptide classification model and a regression model based on known MBEC data. In the following, we will describe each of these tasks, which are also portrayed in **Figure 1**.

3.1. Characteristics of Peptides in the Positive Dataset

3.1.1. Sequence Length

The number of amino acids in our positive dataset varies between 4–70 (**Figure 2A**). Almost all the peptides have a sequence length less than 50. Only 2 peptides have a sequence length between 50–60 and 2 peptides have a sequence length between 60–70. Most of the ABPs were relatively short, i.e., two-thirds of the peptides contain less 20 amino acids with half of the peptides containing between 11–20 amino acids.

3.1.2. Amino Acid Composition

We compared the distribution of 20 amino acids in the peptides in the positive and negative datasets (**Figure 2B**). We observed that, compared to the negative dataset, the ABPs contained a significantly higher percentage of lysine (K), arginine (R), tryptophan (W), and a significantly lower percentage of aspartic acid (D), glutamic acid (E), threonine (T) serine (S), asparagine (N), and methionine (M). This clearly indicates that the ABPs are positively charged, and contain a lower fraction of polar but uncharged side chains. The higher percentage of W indicates a higher hydrophobic nature of ABPs. This is further exemplified when the distribution of amino acids in the positive dataset were grouped by sequence length: K, R, and W make up 50% of the amino acid composition in the short peptides (<20 amino acids), which make up two-thirds of the positive dataset (**Figure 2C**). We also observed that peptides contain non-polar amino acids isoleucine (I), leucine (L), glycine (G), and alanine (A), which provide an amphipathic character to the ABPs.

3.1.3. Dipeptide Composition

Figure 2D and **Supplementary Figure S1** in Supplementary Note 2 show the most commonly encountered dipeptides in our positive and negative datasets, respectively. In our analysis, we focused on the top 3 dipeptide components in different sequence ranges. With the higher prevalence of K, R, and W in the ABPs, all the top candidates for dipeptides contained these amino acids. When arranged by sequence length, it can be seen that the majority of the peptides (>80%, with lengths in the range 4–30) contained "WR/RW," "RI/IR," "KK," and "RR" as the most commonly encountered dipeptides. In contrast, the non-ABPs have non-polar aliphatic amino acid leucine (L) and alanine (A) in the top 5 dipeptide candidates. The dipeptide components most prominent in the positive and negative datasets clearly indicate the presence of a higher

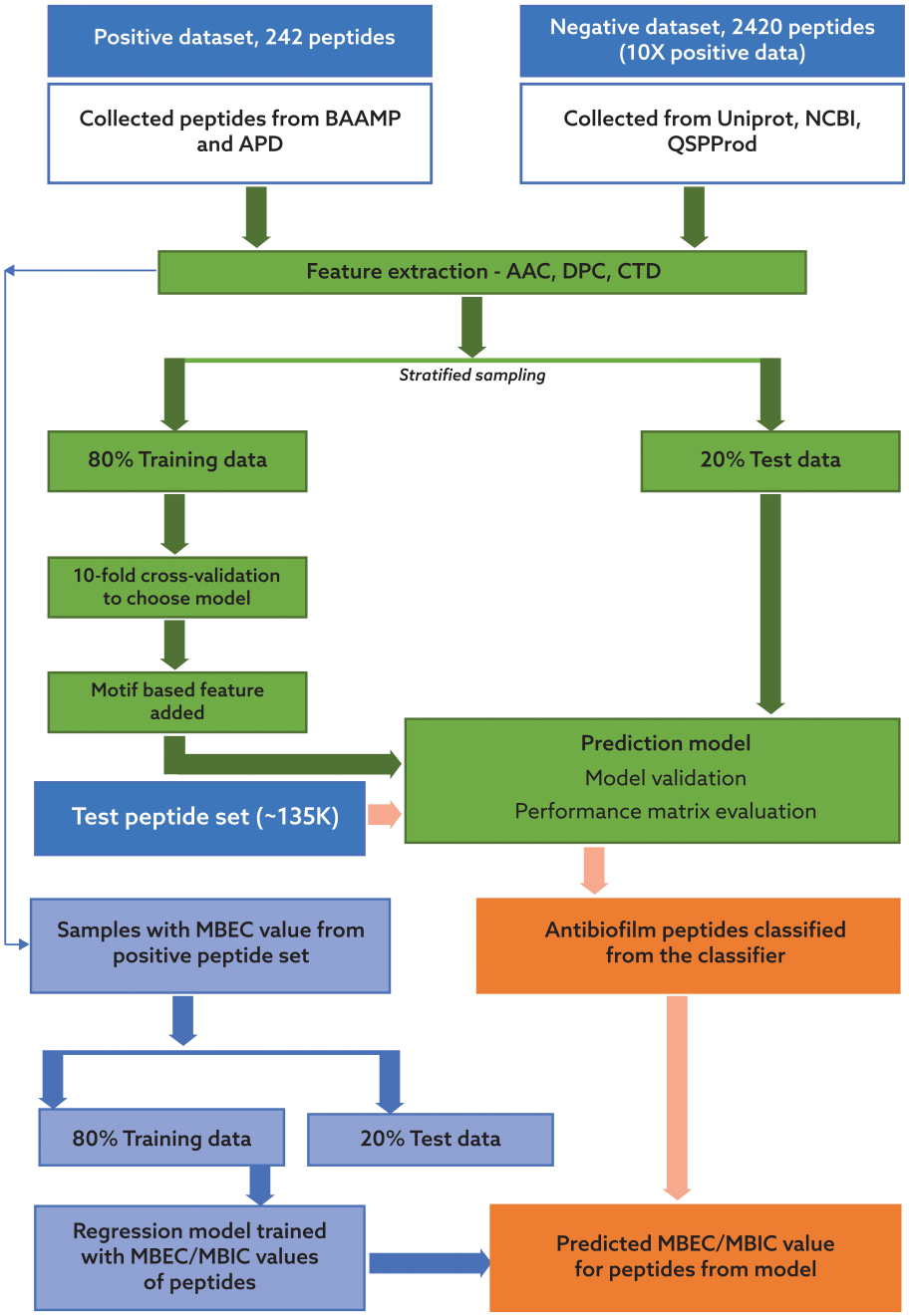

FIGURE 1 | Process flow for the classification of potential antibiofilm peptides and prediction of antibiofilm activity. The process consists of two distinct, sequential steps. In the first step, a binary classification model was trained using a dataset with 242 peptides with reported antibiofilm activity and 2420 peptides with no known or suspected antibiofilm activity. In the second step, two regression models were trained using a subset of the peptides with known minimum biofilm eradication concentration (MBEC) and minimum biofilm inhibitory concentration (MBIC) values. Candidate peptides will be first evaluated for potential antibiofilm activity using the classification model, and then their effectiveness will be predicted using the regression model.

percentage of cationic and hydrophobic amino acids, and charge-hydrophobicity as a recurring theme in the antibiofilm (positive) dataset. It is this recurring presence of the charge-hydrophobicity combination exemplified by the dipeptide composition that underscores the amphipathic characteristic typically attributed to the action of ABPs.

3.1.4. Motifs

Motifs represent short sequences that are commonly found in the datasets. We observed that the motifs "RIRV," "RIVQRIK," and "IGKEFKR" appeared more frequently in the positive dataset (**Figure 2E**), indicating a combination of polar and non-polar amino acids as one of the main reasons of amphipathicity.

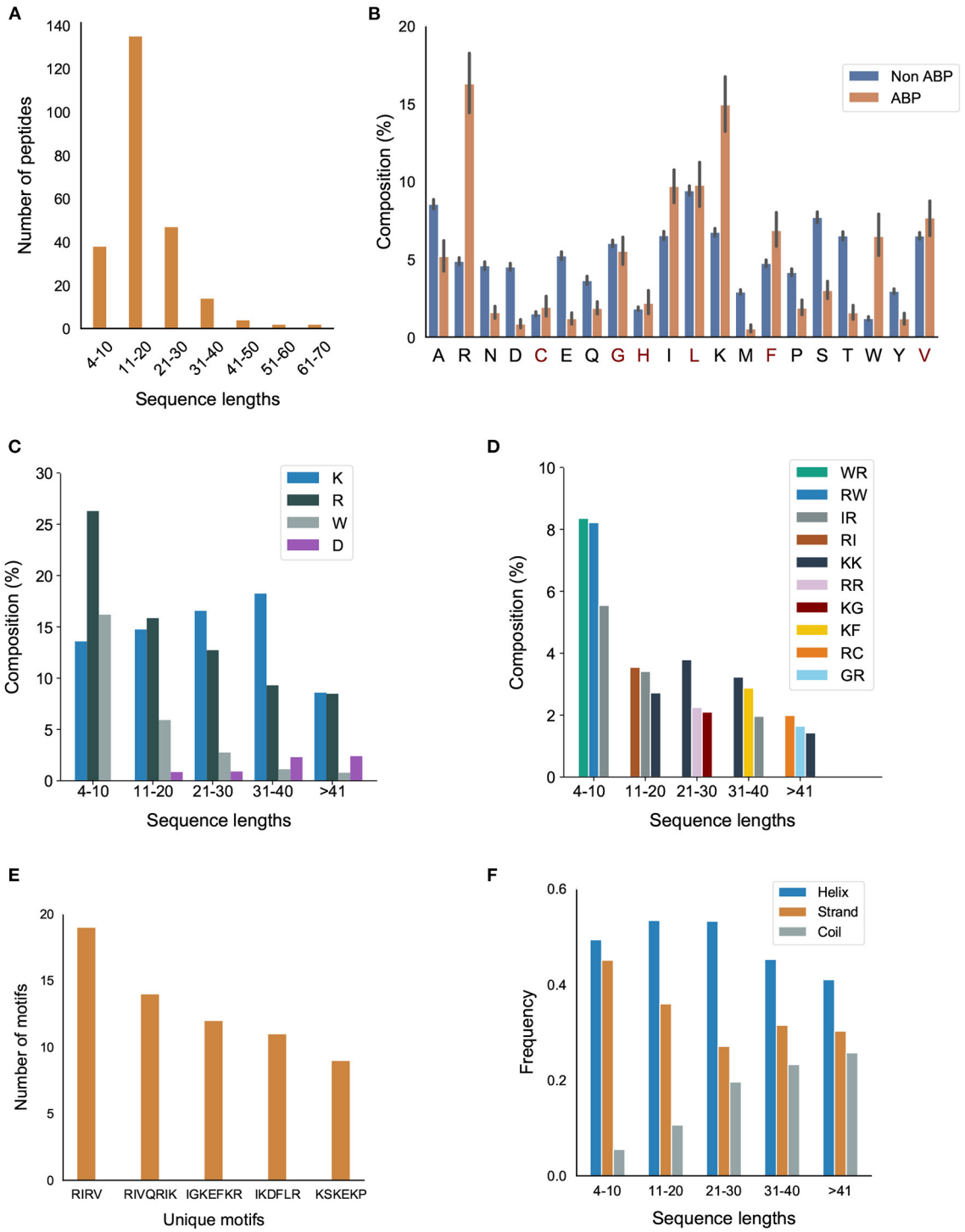

FIGURE 2 | Primary and secondary structural characteristics of antibiofilm peptides. **(A)** Distribution of antibiofilm peptides over different sequence lengths; **(B)** Comparison of amino acid distribution in the positive and negative datasets. Statistical significance ($p \leq 0.001$) was established using Mann-Whitney U-test; Amino acids marked in "red" on the x-axis of the figure are not statistically significant; **(C)** Distribution of K, R, and W, grouped based on the peptide length; **(D)** Dipeptide composition analysis shows IR, RI, WR, RW, and KK are the most common dipeptide sequences present in the antibiofilm peptide database (AA, LL, AL, or LA are most common in the negative dataset); **(E)** Most commonly found motifs in the antibiofilm peptides; **(F)** Antibiofilm peptides contain more alpha helices than beta sheets or coils.

In contrast, the most prevalent motifs in non-ABPs were "SE," "ET," and "VD," mainly consisting of acidic amino acids, i.e., aspartic acids and glutamic acids. This analysis shows that certain motifs, although present in a relatively smaller fraction, can be effective in conferring antibiofilm properties. For instance, human cathelicidin LL-37 prevents biofilm formation of *P.aeruginosa* at a concentration lower than its MIC value by probably blocking the growth of the extracellular matrix (Nagant et al., 2012). While the truncated LL19-37 did not affect biofilm growth, the addition of "IGKEFK" (LL13-37) inhibited biofilm formation at 50 μM. "IGKEFK" is one of the motifs we found in high numbers in our positive dataset during motif analysis. As stated in Nagant et al. (2012) LL-19 has no activity against bacterial membrane permeability, but adding a motif of "IVQRIK" increases permeability in LL-25. "IVQRIK" is another motif that we found in our positive dataset.

3.1.5. Secondary Structure Analysis

We observed that ABPs of any sequence length are more likely to form α-helix structures (**Figure 2F**). In smaller length peptides, we noticed a prevalence of α-helix structures. As the peptide length increases, we noticed a greater percentage of coils in the peptides. The presence of positively charged and hydrophobic amino acids, together with the propensity to form α-helices suggests that the predominant mechanism of antibiofilm activity consists of positively charged, amphipathic helical peptides.

3.1.6. Physicochemical Properties

We also compared different physicochemical properties, namely, polarity, hydrophobicity, and solvent accessibility between the positive and negative datasets (**Figure 3**). First, as expected from the AAC, the ABPs, compared to the negative dataset, contained a significantly larger fraction of charged polar residues but a smaller fraction of uncharged polar residues. Second, the comparison of hydrophobic properties between ABPs and non-ABPs showed that ABPs in our dataset consisted of a much lower number of hydropathically neutral peptides but significantly higher number of hydrophobic or charged residues. The hydrophobic portion of ABPs leads to insertion of the peptides into the less polar bacterial membrane and to destabilizing membrane barriers (Schmidt and Wong, 2013). The higher percentage of alanine, valine, leucine, isoleucine, and phenylalanine could be a potential reason for the ABP's hydrophobic nature. Third, ABPs, compared to the negative dataset, had a significantly lower percentage of compounds that were neutral in their interactions with solvent water but contained more residues that will be buried or exposed when exposed to water. This compositional analysis shows that the ABPs are composed of amino acids with strongly polar and hydrophobic tendencies which together provide an amphipathic nature rather than neutral amino acids.

3.2. Performance of Machine Learning Models

3.2.1. Classifier Performance

Having characterized the antibiofilm peptide dataset, we used primary and secondary structure information of the peptides to develop machine learning models to identify and understand features that may be unique to ABPs. We used a total of 572 features obtained from AAC, DPC, and CTD analysis, and motifs, in various combinations, to describe our peptide samples numerically and train our machine learning models. For the SVM model, we used a linear kernel with and without *recursive feature elimination*, and a RBF kernel. Recursive feature elimination is a heuristic method used to select a subset of the features that may lead to superior performance compared to using all initial features; it works by iteratively eliminating the feature whose elimination produces the most improvement in performance, until no such performance improvement can be achieved. The linear kernel in SVM did not perform well and only achieved an MCC score less than 0.75. Additionally, recursive feature elimination did not lead to improvements in our classification model performance. Using the radial bias kernel provided the highest model performance. For the XGBoost and Random Forest models, the model parameters, number of estimators and maximum depth, were tuned. The performance of the models are presented in **Figure 4** and **Supplementary Tables S2–S4** in Supplementary Note 3. The accuracy for all the models was more than 95% while the model specificity varies between 98 and 100%. Since our model is a binary classifier and our dataset is not balanced, we used F1 score and MCC as the two key metrics to evaluate the performance of these machine learning models (**Figure 4**).

We observed that using either AAC, DPC, or CTD alone resulted in an F1-score between 0.80 and 0.85 in all our models. In contrast, using a combination of two of the three sets of features significantly improved the model performance with F1-scores between 0.82 and 0.88 in all our models. Using a combination of all three sets of features further, though modestly, improved model performance. We also observed that the addition of motifs as a feature improved the performance of our classifier model with SVM (**Figure 4A**). Similar observations have been noticed with MCC scores. While only considering DPC gave an MCC as low as 0.79, adding the remaining features lead to an MCC score of 0.9 (**Figure 4B**).

To adequately compare the performance of our model with that of previously published models on ABPs, we applied our best-performing model to the dataset used by Gupta et al. (2016). It is important to mention here that the performance obtained by one model vs. another on the same task cannot be directly compared unless experiments were conducted using the same dataset and evaluation metrics. Our best performing model is SVM with a radial bias kernel that utilizes AAC, DPC, CTD, and motif as features. Our model outperformed the previously reported results by a significant margin as seen by the increase in MCC from the published value of 0.84 in Gupta et al. (2016) to 0.90 (**Supplementary Table S5** in Supplementary Note 3).

3.2.2. Distinguishing Characteristics of Antibiofilm Peptides Predicted by the SVM Model

Next, we ranked features that are distinct in the positive dataset compared to the negative dataset, so that we may be able to ferret out higher level information that may be unique about the ABPs. To this end, the features were ranked in the order of

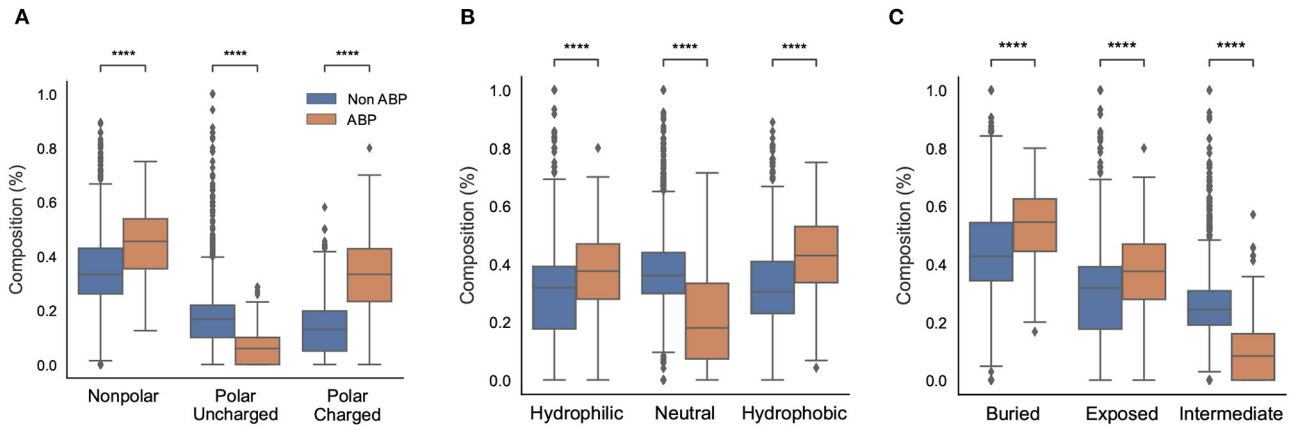

FIGURE 3 | Physicochemical characteristics of antibiofilm peptides. **(A)** Polarity; **(B)** Hydrophobicity; **(C)** Solvent accessibility. Statistical significance (****$p \leq 0.001$) was established using the Mann-Whitney *U*-test using python package.

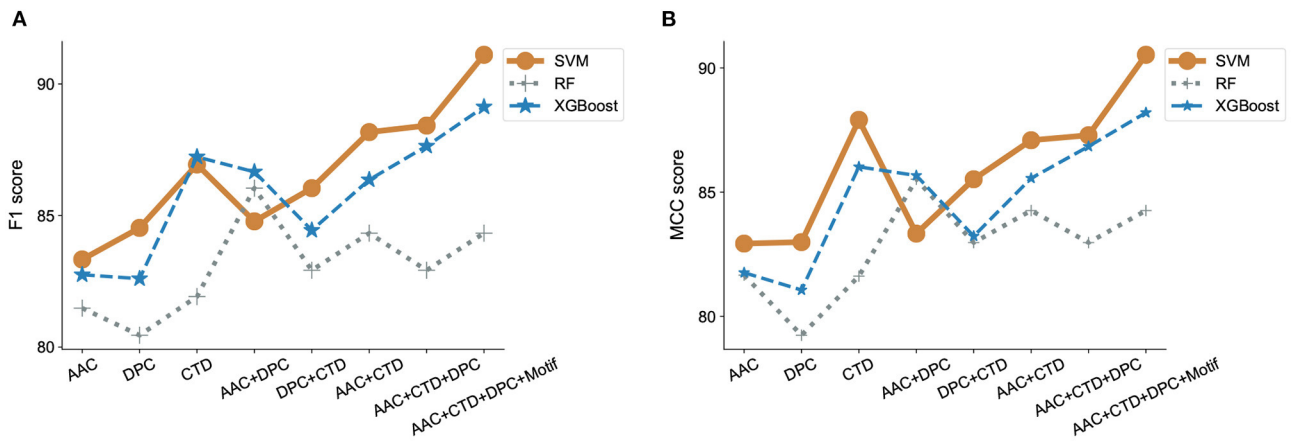

FIGURE 4 | Evaluation of classification models and features. F1 scores **(A)** and MCC **(B)** were estimated for three different machine learning algorithms, SVM, RandomForest and XGBoost, incorporating features that contain combinations of amino acid composition (AAC), dipeptide composition (DPC), composition-transition-distribution parameters (CTD), and motifs. SVM performed best when run against all features, including motif.

increasing importance, as determined by the SVM with radial RBF kernel model.

There is no available API in the *scikit learn* RBF kernel SVM package to get the top feature. Therefore, we used a forward selection method to choose the top features. This is a computationally intensive iterative process where we start with zero features and iteratively add each feature that leads to the most performance improvement, until all 572 features are exhausted. In essence, it is the opposite of the recursive feature elimination method. With each iteration, the algorithm identifies the next best performing feature. The performance score was measured using the MCC score.

We observed that the first feature generated an MCC score of 0.61, and the first four features generated an MCC score of 0.79. The addition of the next four and eight features generated an MCC score of 0.81, and 0.82, respectively; the inclusion of all 572 features generated an MCC score of 0.91 (**Figure 5A**). The first four features that contributed most to the MCC score were all associated with the physicochemical properties of the peptides, namely, number of transitions from apolar to polar amino acids, fraction of polar amino acids, fraction of amino acids that are buried and least accessible to solvent, and distribution of solvent accessibility for amino acids that are buried from first residue to 25% residue. The distributions of these parameters in the positive and negative datasets reveal non-overlapping distributions, which further explains their performance impact in the classification task (**Figure 5B**). This analysis confirmed the importance of the alternation between charge and hydrophobicity. The most discerning feature from the forward selection process, "polarity-transition-group-1-3," is the transition from polar group 1, i.e., from non-polar sequences like Gly, Ala, Val, Leu, Ilu, Pro to group 3, i.e., charged-polar

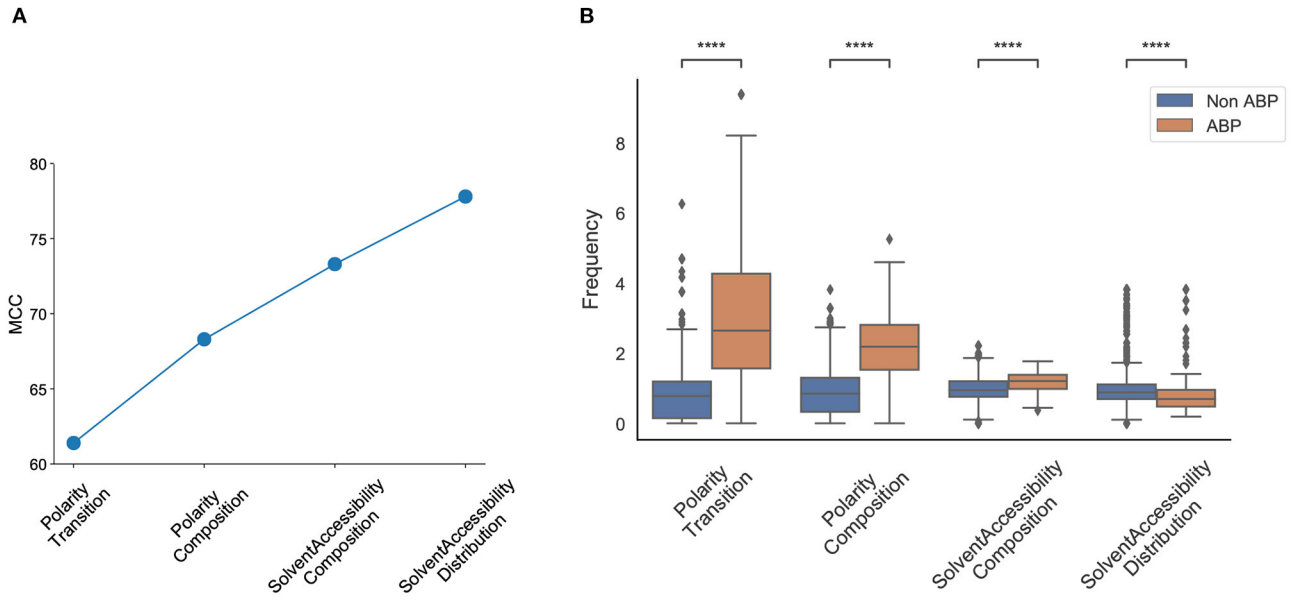

FIGURE 5 | Most discriminant features obtained from the SVM model using Forward Selection. **(A)** Cumulative increase in MCC with top features shows that polarity and solvent accessibility are sufficient to account for nearly all the differences between the positive and negative datasets; **(B)** Distribution of top features between the positive and negative datasets. Polarity Transition means transition from group1 (non-charged) to group3 (highly charged) amino acids; Polarity Composition means composition of highly charged amino acids; Solvent Accessibility Composition means composition of buried amino acids; Solvent Accessibility Distribution means the fraction of first 25% of residues in the sequence are buried amino acids. Statistical significance ($p \leq 0.001$) was established using the Mann-Whitney U-test from python package.

amino acids like His, Lys, and Arg. The other discerning features consist of "polarity-composition-group-3" or composition of highly charged amino acids like His, Lys and Arg, "Solvent-Accessibility-composition-group-1" or composition of buried amino acids, and "Solvent-Accessibility-Distribution-group1" or distribution of amino acids like Ala, Leu, etc.

3.2.3. Prediction of Antibiofilm Efficacy Using Regression Models

The effectiveness of ABPs are evaluated based on their minimum biofilm inhibitory concentration (MBIC) and minimum biofilm eradication concentration (MBEC) levels. The MBIC represents the concentration of the peptide that will prevent biofilm formation, while MBEC represents the concentration of the peptide that can remove preformed biofilms. datasets containing both concentrations were modeled and evaluated for efficacy, with the goal of predicting these values for antibiofilm peptide hits.

3.2.3.1. Models for the Prediction of Minimum Biofilm Inhibitory Concentration

The positive peptide dataset for the classification model contains 242 anti-biofilm peptides, 178 of which we were able to obtain MBIC values for. Although MBIC spanned from 0 to 640 μM, the data was largely skewed with approximately 80% of the values less than 64 μM and 52% of the values less than 20 μM. Given this imbalance, we trained an SVM to classify peptides above or below 64 μM, and a separate Support Vector Regression (SVR) model to predict the MBIC value of a peptide. Both models used an RBF kernel and a dataset consisting of only those peptides with MBIC values less than or equal to 64 μM. Each peptide consisted of 571 features and, due to this large dimensionality, feature selection was implemented using the *forward selection* algorithm to choose the most effective features. While iterating through forward selection, Root Mean Square Error (RMSE) for the training set peptides was minimized in the case of SVR and MCC was maximized in the case of SVM. Forward selection was halted upon 5 consecutive iterations where RMSE had not decreased or MCC increased. During feature selection, the samples were transformed into a lower dimensional space via Principal Component Analysis (PCA). Several hyperparameters were tuned, namely the regularization parameter (C) and kernel coefficient (γ) for the SVM/SVR models, and the number of principal components for the dimensionality reduction. We employed 5-fold stratified cross validation for classification and 5-fold cross validation for regression to ensure we trained a generic enough model that would not overfit the training set. For both models, a grid search between 0.001 to 1000 was used for both C and γ and the number of principal components spanned from 1 to the number of forward selection features. The best SVM model we found contained 9 features and was trained with parameters $C = 10$, $\gamma = 950$, and 6 principal components. The best SVR model contained 9 features as well and used parameters $C = 45$, $\gamma = 40$, and 8 principal components. The final model was able to achieve an MCC of 0.81 and an RMSE of 8.51 on the out-of-sample test sets. **Figure 6A** shows several ranges of

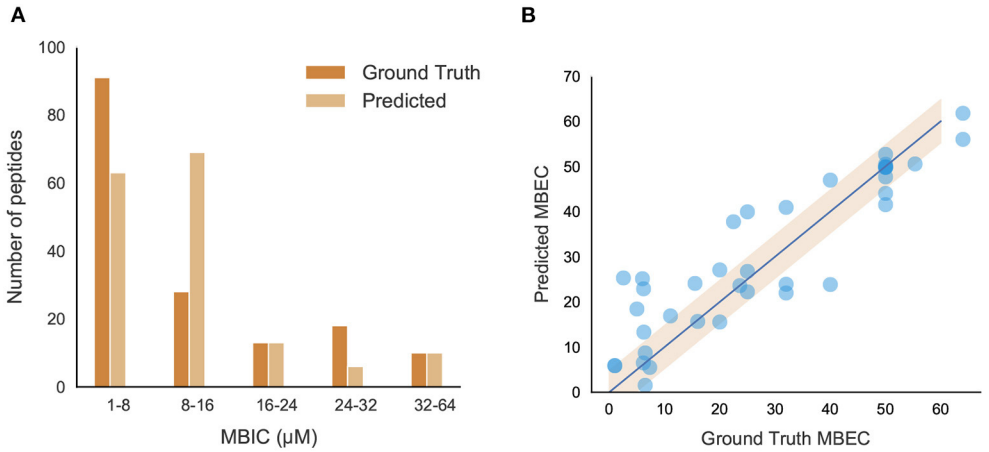

FIGURE 6 | Performance and characteristics of peptides with MBIC/MBEC values. **(A)** Comparison between original and predicted MBIC values using the best regression model; **(B)** Performance of the best MBEC regression model. Best fit line ($R^2 = 0.832$) and 95% confidence interval are shown.

MBIC values and the number of actual predicted MBIC values in each range.

3.2.3.2. Models for the Prediction of Minimum Biofilm Eradication Concentration

We further evaluated the peptides and found only 57 from literature where the MBEC values have been reported. The analysis of peptides showed almost 85% of peptides having a sequence length < 30. These peptides showed a high percentage of positively charged amino acids like arginine and lysine as well as aromatic amino acids like tryptophan. Additionally, secondary structure analysis showed a high percentage of helices present in those peptides (figures in Supplementary Note 4). After eliminating peptides with MBEC values greater than 64 μM, our dataset consisted of 42 peptides for further regression analysis.

A Support Vector Regression (SVR) model built with an RBF kernel was found to be the most effective model to predict MBEC values given the limited training dataset. The same dimensionality reduction methodology was used as in the MBIC models in addition to the same hyperparameter grid search. The best SVR model contained 12 features and used hyperparameters $C = 900$, $\gamma = 20$, and 7 principal components. It was trained using 5-fold cross-validation and the best performing model had an RMSE of 8.41. When ground truth MBEC values were plotted against the regression predictions, we found the R-squared value to be 0.832 (**Figure 6B**).

3.3. Classification of Novel Antibiofilm Peptides

We used our best machine learning models to predict peptides with potential for antibiofilm activity from diverse sources. We queried various peptide databases to identify peptides with antibiofilm activity. We searched 4,700 antimicrobial peptides, 74 anticancer peptides, and 212 antiviral peptides in the DRAMP database. We also considered more than 131,298 unique peptides from UniProt which have a sequence length of 4–80. After removing duplicates, we ran our classification model on 135,015 unique peptides from these varied sources, and selected 5468 unique peptides which were predicted as positive or hits by our model. The overall hit rate for this initial set of predicted peptides is 4.04% while the hit rate only from DRAMP database is 30.49%. This higher value is due to the inclusion of peptides with established antimicrobial activity in the antimicrobial databases, which is likely to be skewed for high antibiofilm activity.

Due to the relatively large number of peptides selected by our classification model, we used the decision function of each of the peptides to narrow down the hits. The decision function estimates the sample position with respect to the discriminating hyperplane of the model. While training our model, we noticed that the peptides with decision function values higher than 0.99 were ABPs, whereas those with a negative decision function were non-ABPs (**Figure 7A**). More importantly, we noticed a clear discontinuity in the decision function as we transition from the positive to the negative dataset, which further showcases the effectiveness of our computational prediction model. Therefore, we used this confidence value as a filtering criteria to narrow down our list of peptides in the candidate set which were initially predicted as antibiofilm by our classification model and set a cut-off threshold of 0.99. As a result, we chose candidate peptides with decision function values higher than 0.99 as more likely to have antibiofilm activity, which further narrowed down the hits to 296 peptides or a hit rate less than 0.2% overall. A vast majority of these peptides have lengths between 6 and 21 amino acids (**Figure 7B**).

3.4. Prediction of Activity in Novel Antibiofilm Peptides

Having classified potential ABPs, we used the regression models to predict the MBIC and MBEC values of the 296 peptides. Since we are interested in peptides that are efficacious against preformed biofilms, we used an operational cut-off of decision function ≥ 0.99, and MBEC ≤ 64 μM. We obtained 185 peptides

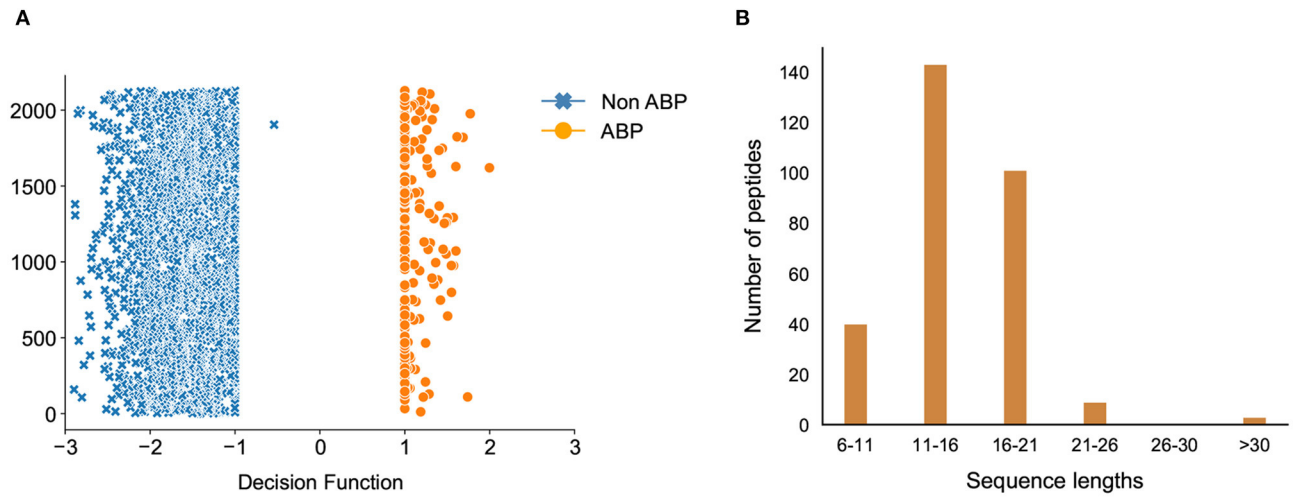

FIGURE 7 | Classification of antibiofilm peptides. **(A)** Decision Function of the training data, decision function values >0.99 are the antibiofilm peptides whereas values <0 are the non-antibiofilm peptides; one antibiofilm peptide was misclassified by the model; **(B)** Distribution of predicted antibiofilm peptides based on their sequence lengths.

(**Supplementary Tables S6–S12** in Supplementary Note 5) of interest (**Figure 8A**). Among these peptides, 40 showed high effectiveness (MBEC between 1.0–8.0 μM) and another 48 peptides had comparatively lower effectiveness (MBEC more than 32 μM) (**Figure 8B**). We noticed that most of the peptides (67 peptides) had moderate predicted effectiveness between 16.0 and 24.0 μM. When we evaluated the source of the peptides, most of them were synthetic (116), and the naturally occurring peptides were from expected sources such as plants, amphibians, insects, and mammals (**Figure 8C**). We grouped the hits into those with known antimicrobial activity as archived in the DRAMP database (**Supplementary Tables S6–S10** in Supplementary Note 5), and those that are not archived in the DRAMP database that were obtained from the UniProt database (**Supplementary Tables S11–S13** in Supplementary Note 5). Of the 185 hits, 131 peptides were from the DRAMP database, and 54 were from the UniProt database. We also grouped the peptide hits based on their function. As expected, most of the peptides have some previously reported antibacterial properties. The hits also contained 19 peptides with anti-tumor/cancer activity, 26 peptides with antifungal properties, and 1 peptide with antiplasmoidal activity, suggesting potentially useful dual function therapeutics (**Figure 8D**).

Some of these peptide hits have already shown promise as antimicrobial agents (but not as antibiofilm agents) (Sahoo et al., 2021). The two anticancer peptides DRAMP03575 and DRAMP03829 are reported to exhibit an MIC of 16 μM and 10 μM, respectively, against *Escherichia coli* (Kang et al., 2019). The sperm protamine peptides from catshark and bat showed activity against 12 pathogens at a concentration of 0.01–20 mg/mL (Kim et al., 2015). Mastoparan-1 has an MIC value between 2 and 32 mg/L against *Staphylococcus aureus*, and is known to have antibacterial and antibiofilm properties (Memariani et al., 2018). Ponericins, peptides from the Ponerine ant, have structural similarity with well-known antimicrobial and antibiofilm peptide cecropins (Orivel et al., 2001). While no known antimicrobial activity has been listed for the histamine releasing peptide from the oriental hornet, studies are ongoing for alpha-conotoxin obtained from cone snails, mainly used in pain management, to establish its antimicrobial activity (Ebou et al., 2021). An analog, ω-conotoxin MVIIA shows the peptide is effective against *Candida kefyr* and *Candida tropicalis* with moderate MIC values between 28 and 40 μM but it was not effective against any bacterial assay up to 500 μM (Hemu and Tam, 2017).

3.5. Prediction of Secondary Structure of Novel Antibiofilm Peptide Hits

We sought to understand the possible mechanisms of action of newly found potential antibiofilm hits in the top quadrant of (**Figure 8A**). Since we were interested in peptides with previously unreported antimicrobial activities, and therefore novel, we focused on the 54 peptides from the UniProt database. Even amongst these 54 peptides, 14 peptides have been reported to have antimicrobial activities as per the UniProt annotation although they were not listed in any of the antimicrobial databases. For instance, the peptides P0CF03, P82420, and C0HK43 have been reported to have antimicrobial properties as well non-hemolytic properties, and anticancer properties (C0HK43) suggesting that these peptides may serve as good antibiofilm candidates. Other peptides such as P30259, P0C424, C0HLM2, Q9U8M9, A0A1C8YA26, P85874, and Q16228 are not reported to have any antimicrobial/antibacterial activity as per their UniProt annotation. Of the 40 peptides that do not have any annotations or references to antimicrobial activity, we found 5 peptides from the mastoparan group, 3 peptides from the poneritoxin group, 2 peptides each from the conotoxin, lasioglossin and protamine groups, and 17 uncharacterized peptides that are mostly derived from plant sources. Of note,

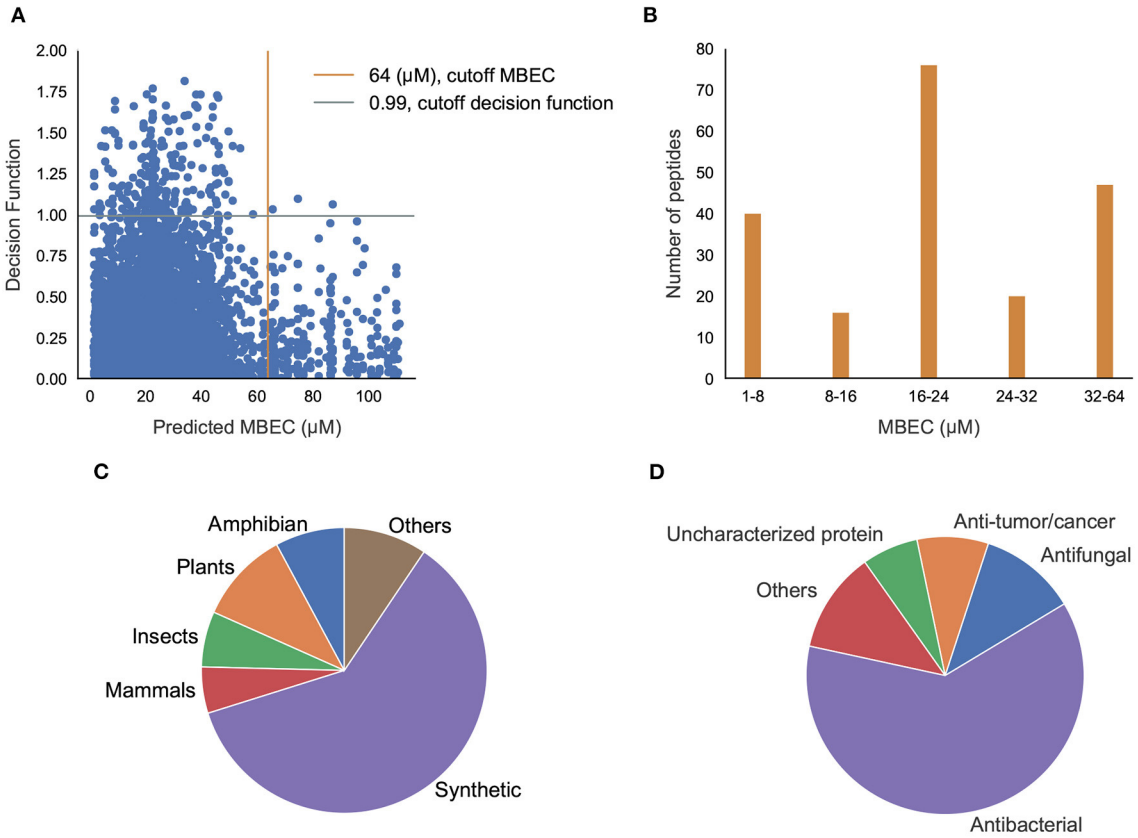

FIGURE 8 | Prediction of antibiofilm activity using an integrated classification-regression scheme. **(A)** Decision Function of the classifier and Predicted MBEC from the regression model of the peptides; **(B)** Distribution of MBEC values in the 1-64 μM range; **(C,D)** Distribution of the peptides with predicted antibiofilm activity based the source **(C)**, or the function **(D)**.

our positive dataset did not contain any peptides from the mastoparan, poneritoxin, conotoxin, lasioglossin or protamine groups indicating that these are indeed novel hits. Since the function of peptides from the mastoparan, ponericin, and conotoxin groups is to protect the host organism, they belong the category of host defense peptides (HDPs). Interestingly, we also obtained non-host defense peptide hits which have varied functions—DNA intercalation (protamine), intemediate filaments in neurons (peripherin), and metabolic enzymes (alcohol dehydrogenase, beta-amylase).

We chose the 37 novel peptides for further analysis, and their decision function and predicted MBEC values are listed in **Table 1**. In this Table, the first 16 peptides have been characterized previously, and the next 21 peptides have not been characterized (i.e., listed as uncharacterized in the Uniprot database). Next, we predicted the secondary structures of these peptides using the PEP2D server (Singh et al., 2019) and PEP-FOLD3 server (Lamiable et al., 2016). **Figures 9**, **10** show the predicted 3D structures, and **Supplementary Figures S3**, **S4** in Supplementary Note 5 show the predicted 2D structures of previously characterized and uncharacterized peptides, respectively. Most peptides show helical or coil structures. Specifically, the mastoparan, poneritoxin, and lasioglossin peptides show helical structure, while the conotoxin peptides have a purely coil structure (**Supplementary Figure S3** in Supplementary Note 5). The peptides not belonging to any specific class or uncharacterized peptides as per Uniprot annotation also showed mostly helical or coil structures with only one or two peptides folding as sheets (**Supplementary Figure S4** in Supplementary Note 5). Using the DisEMBL predictor from JalView, we also observed that three hits (A0A0D3HK27, A0A2P2N8A3, E9I8P2) are likely to be highly mobile and not fold to a stable structure.

3.6. Alignment of Sequences to Identify Consensus Patterns

To characterize the unique sequences or common functional motifs among the 37 peptide hits, we performed multiple sequence alignment and generated the phylogenetic relationship between the hits. Based on these results, the peptide hits were classified into subgroups to obtain consensus sequences. The results are shown in **Figure 11**. We found that previously

TABLE 1 | Antibiofilm peptide hits.

Name	Type	Sequence	Decision function	Predicted MBEC (μM)
P17238	Mastoparan	INLKAIAALVKKVL	1.142	22.669
P85874	Mastoparan-like-peptide PMM2	INWKKIASIGKEVLKAL	1.109	22.679
P69036	Mastoparan	INWLKLGKAVIDAL	1.065	22.679
P69034	Mastoparan	INWLKLGKKVSAIL	1.011	22.679
P82420	U1-poneritoxin-Ng3g	GLVDVLGKVGGLIKKLLPG	1.326	27.710
P82419	M-poneritoxin-Ng3f	GLVDVLGKVGGLIKKLLP	1.299	28.502
P0CF03	U1-poneritoxin-Da2a	FLGGLIGPLMSLIPGLLK	1.001	19.722
C0HLM2	Alpha-conotoxin	SGCCKHPACGKNRC	1.729	39.130
P0C424	Conotoxin	CCAPSACRLGCRPCCR	1.348	2.967
C0HK43	Lasioglossin	VNWKKILGKIIKVAK	1.252	3.071
C0HK42	Lasioglossin	VNWKKVLGKIIKVAK	1.169	3.071
P30259	Protamine	GCKKRKARKRPKCKKARKRP-KCKRRKVAKKKC	1.278	4.289
Q8WMD3	Protamine	MARYRRCRSRSRCRRRRRRCH-RRRRRCCRRRRRRRACCRRYRCRRR	1.043	21.567
Q16228	Peripherin	WRWRRACRRPGRPFWRV	1.533	61.163
Q9U8M9	Alcohol dehydrogenase	AGLGGIGLDTNREIVKSGPK	1.079	20.531
A0A1C8YA26	beta-amylase	FLGCRVQLAIKISGI	1.072	22.358
A0A0A9FN30	Uncharacterized	MFRSLRKELKSKLL	1.052	22.845
A0A0A9M1Q7	Uncharacterized	MGRKFKWKLWT	1.448	14.309
A0A0A9U210	Uncharacterized	MTRIRRRRRHLLLLR	1.066	22.612
A0A0D3HK27	Uncharacterized	MFGGSGPLKLL	1.027	22.008
A0A0E9SZ00	Uncharacterized	MCTRWRVLLTCVRRR	1.299	28.711
A0A0K1NW40	Uncharacterized	KAIALALGKSGCK	1.226	22.678
A0A2P2N8A3	Uncharacterized	MGGKSDFRFCHVKKKVL	1.082	11.138
A0A2P2Q2Y8	Uncharacterized	MLKLWLRIKLLRKAL	1.225	35.601
A0A3D5SU75	Uncharacterized	PCPCGSGKKYKHCHGKLS	1.040	1.854
A0A3Q7GQZ6	Uncharacterized	GLAYRLVNLHFCKTKR	1.073	22.656
A0A5K0UXG7	Uncharacterized	ALLKSKPKLLRSGL	1.662	22.694
A0A5K1B3V0	Uncharacterized	VIRIGCKWKRTA	1.416	6.260
A0A5K1BN05	Uncharacterized	LGCGHGLPGIFACLK	1.030	3.071
A0A5K1D9T8	Uncharacterized	AKALGKRLRIKGRFQS	0.999	61.036
A0A5K1DCQ4	Uncharacterized	LGCGHGLPGIYACLK	1.233	3.071
A0A5K1F988	Uncharacterized	EKFKIHKSGKRWM	1.062	46.811
A0A5K1FWL9	Uncharacterized	FRARLLRTAFR	1.115	22.722
E4Z311	Uncharacterized	IKGILLRKIIKVR	1.138	35.514
E9I8P2	Uncharacterized	MLKKFLGKSGRRILR	1.173	8.156
E9JAR4	Uncharacterized	KLVLRRILALCIIAVCK	1.259	22.923
S7IKV4	Uncharacterized	SGLFCKGCSKL	1.030	60.153

characterized peptides grouped into four subgroups: Subgroup-1, –2, –3 and −4, consisting of mastoparan and lassioglossin, poneritoxin, conotoxin, and protamine peptides, respectively. The previously uncharacterized peptides were grouped in Subgroups-5 through –9. The remaining hits that did show significant alignment with any other hit were placed in Subgroup-10. Some of the uncharacterized peptides aligned well with previously characterized peptides: E9I8P2 aligned with the poneritoxin group, and A0A0E9Z00 and A0A2P2N8A3 aligned with the protamine group. The common functional motifs were diverse but do not contain any anionic residues, and most commonly contain R, K, L, I, and G. We found sequences that were either R- or K-rich (Subgroup-1, −2, −4, −5, and −7), C-rich (Subgroup-3), I- or L-rich (Subgroup-1, −2, −5, −8 and −9). Interestingly, some of the common functional motifs, such as those from Subgroup-3, and −9, are unlike what is typically observed in AMPs.

Using helical wheel diagrams, we visualized helical peptides and their hydrophobic moment in **Supplementary Figure S5** in Supplementary Note 5. The helical wheel diagrams show that the mastoparan and lassioglossin peptides (Subgroup-1) and A0A2P2Q2Y8 (Subgroup-5) form a nearly perfect amphipathic helix with hydrophilic and hydrophobic amino acids on either side of the helix. Other peptides such as A0A0A9210, A0A3Q7GQZ6, and E9JAR4 form helices but do

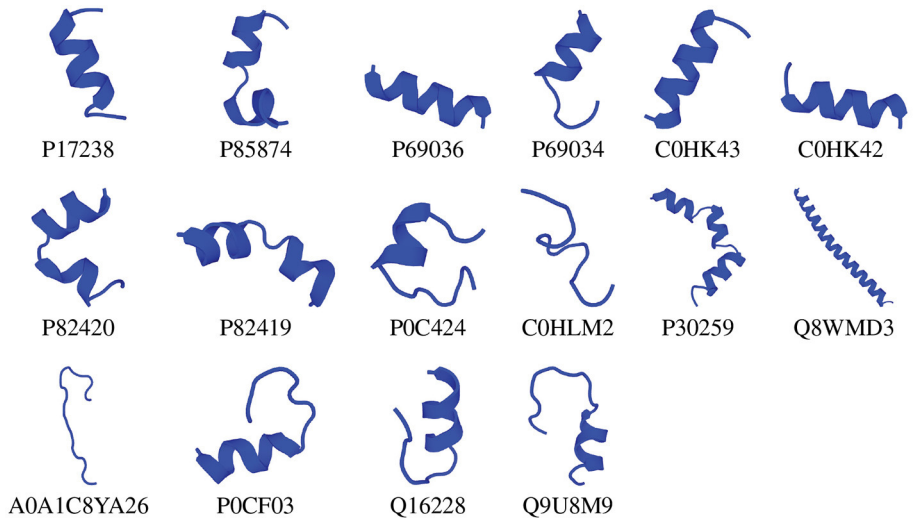

FIGURE 9 | 3D structures of previously characterized potential antibiofilm peptides. The 3D structures were predicted using the PEP-FOLD 3 server. All structures are depicted with N-terminal at the top, and C-terminal at the bottom.

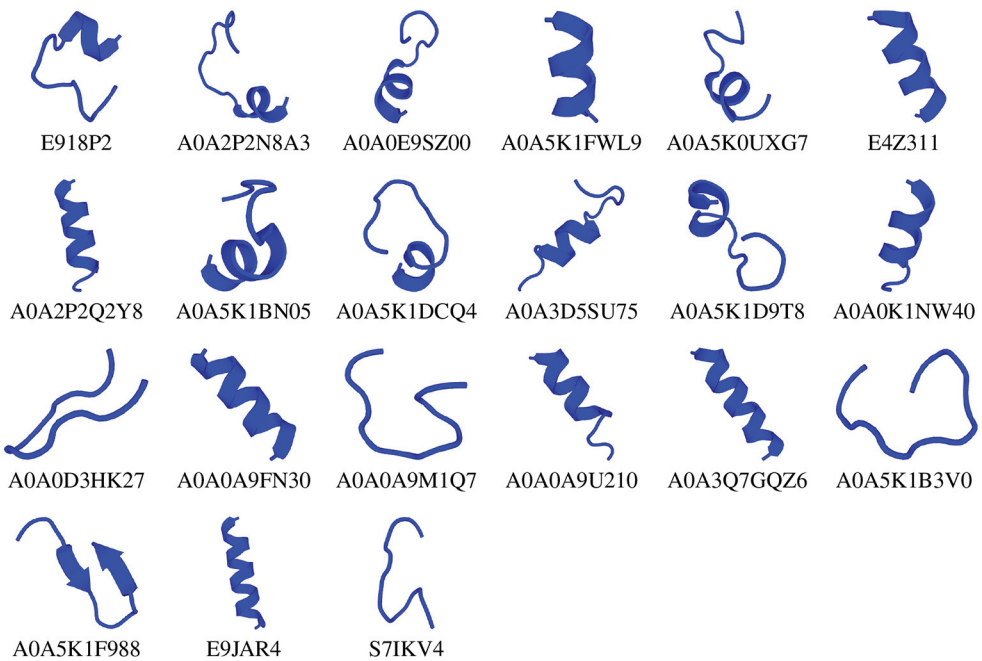

FIGURE 10 | 3D structures of previously uncharacterized potential antibiofilm peptides. The 3D structures were predicted using the PEP-FOLD 3 server. All structures are depicted with N-terminal at the top, and C-terminal at the bottom.

not show amphipathic character as indicated by the lower value of hydrophobic moment.

To obtain insights into the mechanisms of action of these peptide hits, we sought to compare the sequences of these peptides with those in the positive dataset with known low MBEC values (<64 μM). Upon sifting through the positive dataset, we identified 5 peptides (LL-37, coprisin, melittin, RT2 and 1018) that have unique sequences and also have well established antibiofilm activity with known mechanisms of action (**Supplementary Tables S19**, **S20** in Supplementary Note 6). We performed sequence alignment of the 37 peptide hits (16 characterized peptides and 21 uncharacterized peptides) with these 5 antibiofilm peptides using Clustal Omega, and the pairwise alignment score is shown in **Table 2**. As representative examples, the sequence alignments for the peptide pairs with the highest pairwise alignment scores are presented

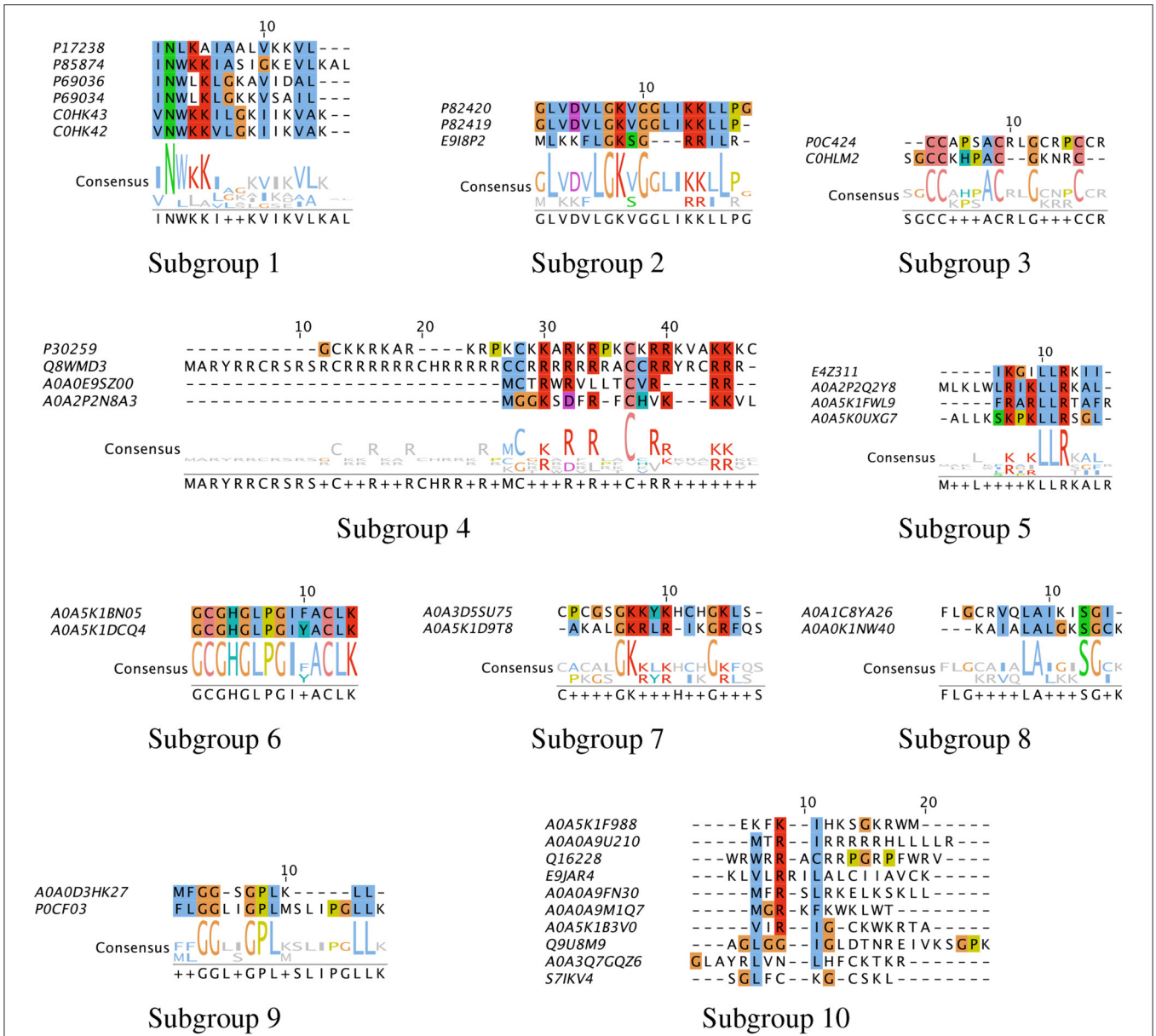

FIGURE 11 | Multiple sequence alignment of peptide hits. The peptide hits listed in **Table 1** were placed in Subgroups based on their BLOSUM62 neighbor in the phylogenetic tree, and Multiple Sequence Alignment with ClustalW was performed. The most conserved sequences for the Subgroups are: (1) INWKKI—V–VL; (2) L—LGK-G—KRLL; (3) CC—AC–G—C; (4) C-R-R-R–C-RR—RR; (5) LR-KLLR–L; (6) GCGHGLPGIFACLK; (7) GKRLR—GKL; (8) I-LAL–SG; (9) GG—GPL—LL. The default color scheme used as per ClustalX. Colorcode—blue: residue A, I, L, M, F, W, V, C; red: residue K, R; green: residue N, Q, S, T; magenta: E, D; yellow: residue P.

in **Supplementary Figure S6** in Supplementary Note 5. The alignment scores are relative. The scores depend on both the length of the sequences and the number of identical or similar amino acids in those sequences. For instance, the self-alignment scores for the 37-amino acid long LL-37 is 1850, while the same score for alignment with the first five amino acids of LL-37 is 260.

Of the previously characterized peptides, the hits which have a helical structure encompassing the mastoparan, poneritoxin, and lasioglossin groups showed significant sequence similarity with the melittin and LL-37 peptides. Conotoxin peptides with coiled structure share sequence similarity with coprisin. Interestingly, peripherin shared relatively high sequence similarity with LL-37, 1018 and RT2, demonstrating the highest pairwise alignment score with RT2 amongst all the peptides tested in this work. On the other hand, we notice that a few of the peptide hits (Q8MWD3 and P30259-protamines, Q9U8M9-alcohol dehydrogenase) showed low sequence similarity to the five known antibiofilm peptide sequences. These three peptides have an acceptable MBEC predicted to be less than 20 μM.

Of the uncharacterized peptides (**Table 3**), a majority of the peptides shared sequences similar to either melittin or LL-37. Among others, A0A0K1NW40 and E9JAR4 showed higher

TABLE 2 | Pairwise alignment scores of known vs. previously characterized potential antibiofilm peptides along with predicted secondary structure.

Peptide Name	Melittin	LL-37	Coprisin	RT2	1018	Secondary structure
Q16228	90	160	40	**230**	150	helix-coil
P69034	**200**	140	90	60	70	helix-coil
P82420	**210**	120	0	40	40	helix-coil-helix
P0CF03	**190**	120	10	20	30	coil-helix
P69036	**180**	50	90	60	50	helix
C0HK43	**170**	**170**	70	50	90	helix
C0HK42	**170**	160	70	50	90	helix
C0HLM2	10	40	**170**	30	20	coil
P0C424	20	0	**160**	110	40	coil
P85874	140	**160**	30	50	90	helix-coil-helix
P82419	**150**	140	0	40	50	helix-coil-helix
P17238	**130**	120	50	0	80	helix
A0A1C8YA26	**130**	40	**130**	100	80	coil
P30259	**110**	50	80	0	20	helix-coil-helix
Q8WMD3	80	40	60	60	**90**	helix
Q9U8M9	**90**	70	50	60	0	coil-helix

*High-low scores are denoted in blue-white-red scale; Most match with known peptide is highlighted in bold; Secondary structure predicted using the PEP-FOLD 3 as shown in **Figure 9**.*

TABLE 3 | Pairwise alignment scores of known vs. previously uncharacterized potential antibiofilm peptides along with predicted secondary structure.

Peptide name	Melittin	LL-37	Coprisin	RT2	1018	Secondary structure
E9I8P2	30	**230**	40	0	60	coil
A0A0A9M1Q7	50	130	30	**220**	60	coil
A0A0K1NW40	30	50	**200**	70	50	helix
A0A5K1F988	30	**190**	40	180	50	sheet
E4Z311	90	110	50	10	**190**	helix
A0A5K1DCQ4	**190**	20	70	60	30	coil
A0A5K1BN05	**190**	40	50	20	30	coil-helix
A0A0A9U210	**180**	90	50	10	150	helix
A0A2P2Q2Y8	120	90	10	80	**180**	helix
A0A0E9SZ00	**170**	60	90	90	90	coil-helix
A0A0D3HK27	**140**	80	30	10	90	coil
A0A5K0UXG7	**140**	70	110	80	10	coil-helix
A0A5K1B3V0	50	**150**	50	50	140	coil
E9JAR4	100	80	**150**	0	80	helix
A0A3Q7GQZ6	50	**140**	70	0	30	helix
A0A3D5SU75	40	70	**130**	20	20	coil-helix
A0A0A9FN30	60	**120**	50	20	60	helix
A0A5K1D9T8	20	**110**	10	20	80	coil
S7IKV4	50	**110**	90	20	40	coil
A0A2P2N8A3	40	60	**110**	20	40	coil
A0A5K1FWL9	30	**50**	**50**	40	0	helix

*High-low scores are denoted in blue-white-red scale; Most match with known peptide is highlighted in bold; Secondary structure predicted using the PEP-FOLD 3 as shown in **Figure 10**.*

sequence similarity to coprisin, A0A0A9M1Q7 and A0A5K1F988 showed higher sequence similarity to RT2, and E4Z311 showed similarity to the 1018 peptide. A few peptides (A0A5K1FWL9, A0A5K1D9T8, S71KV4, A0A2P2N8A3) showed poor alignment with any of the five known antibiofilm peptides. Of these five peptides, A0A2P2N8A3 and A0A5K1FWL9 are predicted to have low MBEC values. A0A2P2N8A3 is rich in lysine and hydrophilic residues while A0A5K1FWL9 is rich in arginine and hydrophobic residues, indicating the diversity in the sequences of the hits.

The results from secondary structure prediction and sequence alignment analysis provide insights into the possible mechanisms of action of the novel antibiofilm peptides. Although poorly understood, the antibiofilm peptides work through a variety of mechanisms including membrane disruption, inhibition of motility, disruption of essential proteins, and interruption of genetic elements (Raheem and Straus, 2019). The interaction with cell membrane is naturally favored by the amphipathic helices which is commonly found in most antimicrobial peptides, and in antibiofilm peptides (Zeng et al., 2021). Therefore, we expect that peptides from Subgroup-1 and Subgroup-5 including mastoparan and poneritoxin peptides may show membrane disrupting activity similar to the AMP. The Subgroup-4 peptides with high overall positive charge may interact favorably with negatively charged membrane. The coiled peptides (conotoxin, peripherin and protamine) may elicit antibiofilm action through mechanisms different from membrane interactions, possibly by interfering with vital cellular processes through specific binding interactions. For instance, the 1018 peptide is believed to interact with the signaling molecule ppGpp, and LL-37 by interfering with several pathways including quorum sensing (Overhage et al., 2008; Wieczorek et al., 2010). Lastly, the biofilm environment is generally acidic with pH 5–6, which may promote a change in secondary structure depending upon the pI of the amino acids (Xiong et al., 2017). Therefore, while this work provides some insights into novel peptide sequences and their mechanisms, detailed genetic and molecular biofilm inhibition assays are necessary to confirm the proposed mechanisms or delineate the mechanisms of action of novel peptides identified in this study.

3.7. Significance and Limitations of the Models

Unlike many other machine learning applications for antimicrobial peptides, we focused on the smaller subset of antibiofilm peptides instead of the much larger set of antimicrobial peptides because most recalcitrant infections are due to biofilms. Therefore, the drug development strategy should focus on efficacy against the biofilm mode of growth rather than the planktonic mode. Our approach differs from the previous models of antibiofilm peptide discovery in many significant ways. First, our negative dataset was curated as peptides which are likely to directly or indirectly promote biofilm formation rather than randomly generated sequences. Second, our model is built on the idea that the antibiofilm peptides are rarer to find in nature than biofilm-inhibiting peptides. To mimic that concept, we used ten times more peptides in the negative dataset than in the positive dataset. We

considered stratified sampling and ten-fold cross-validation to eliminate the overfitting problem due to an imbalanced dataset. Third, we used motifs that are unique to the antibiofilm peptides not as privileged information but as a discovered entity while cross-validating the training dataset. This unbiased approach not only improved the performance of the model but also enabled the identification of truly discerning motifs, which changed the performance compared to the "without motif" model. Fourth, we developed SVR-based regression models for the prediction of the efficacy, i.e., the MBIC and MBEC values of novel peptides that were classified as ABPs by our classification model. Fifth, we used sequence alignment and secondary structure predictions to predict putative mechanisms of action of antibiofilm hits. Lastly, our work identified two broad classes of peptides: those peptides that have previously known bioactivity but not antibiofilm activity, i.e., those that may be considered for drug re-purposing; and those peptides without any previously reported bioactivity, i.e., those that may be considered as novel drug candidates.

One important limitation of using MBIC/MBEC values from the literature is that the peptides were not all tested against a single organism or using a single experimental technique but against a wide range of microorganisms (gram positive and gram negative bacteria, fungi), and using both dilution, plate-based or other techniques. This key limitation notwithstanding, the regression model performed very well, with an RMSE of 10–25% of the mean MBIC/MBEC values, for most peptides in the training set. We expect the effectiveness of our model to increase given more adequate MBIC/MBEC measurements on a wide range of ABPs. As an independent validation of our regression model, the predicted MBIC of these peptides matched well with experimentally determined antimicrobial activity (MIC). For instance, the peptide C0HK43 is active against gram-negative bacteria at concentrations of 1–14 μM as reported in the DRAMP database (MIC 1.4 μM against *E. coli*, MIC 14.1 μM against *P. aeruginosa*) while our model predicted an MBIC/MBEC value between 1 and 8 μM. The identification of a number of host defense peptides, which are considered to be a physiologically relevant response to biofilms, through a mechanism-agnostic sequence search further bolsters confidence in our approach (Hancock et al., 2021). Despite these limitations, our work has clearly demonstrated not only the feasibility of our sequence-based and mechanism-agnostic machine learning pipeline to predict efficacious antibiofilm peptides, but has also unearthed the vast diversity in sequences that have the potential to eradicate biofilms. Our platform may also be easily expanded to incorporate features such as the various post-translational modifications which may enhance the antibiofilm activity of the peptide backbone (Wang, 2012).

4. CONCLUSIONS

In this work, we have developed a machine learning pipeline for the classification of antibiofilm peptides followed by the determination of their efficacy. Using this pipeline, we identified a small set of novel antibiofilm peptides by mining diverse peptide libraries, and evaluated the efficacy of the hits. The peptide hits comprised of both novel peptides and peptides with other reported functions. Classical bioinformatics approaches of sequence alignment showed that some of the peptide hits may act through known mechanisms of antibiofilm activity while some others may follow less understood mechanisms to confer antibiofilm activity.

The two-tiered model enabled the classification and prediction of antibiofilm activity. Our SVM-based model with 572 features performed exceptionally well with an MCC of 0.91, which is significantly higher than current models. The higher performance is due to considering the physicochemical properties and motifs along with the compositions of peptides. Consistent with previously published studies, our model showed that the ABPs are characterized by the abundance of positively charged amino acids K and R, and higher hydrophobicity due to W and I. Our SVR-based model predicted the efficacy of ABPs with high confidence. To our knowledge, no previous studies have attempted to predict peptide efficacy using machine learning approaches. To this end, we built a regression model using the MBIC and MBEC values curated from the literature that have experimentally determined these values. In this work, we were careful to distinguish the biological significance of MBIC and MBEC values, as the former represents efficacy against biofilm formation, and the latter represents efficacy against pre-formed biofilms. An antibiofilm peptide with a lower MBIC but high MBEC may not effectively eradicate pre-formed biofilm. For instance, Dermaseptin-AC is useful in the inhibition of biofilm (MBIC 32 μM) formed by *Staphylococcus aureus* but is not effective in eradicating preformed biofilm (MBEC 256 μM) (Gong et al., 2020). Therefore, in this work, we developed models to predict both MBIC and MBEC for ABPs. *In vitro* biofilm inhibition and *in vivo* virulence assays beyond the scope of this work are warranted to confirm the validity and translational potential of the peptide hits.

DATA AVAILABILITY STATEMENT

The datasets presented in this study can be found in online repositories. The names of the repository/repositories and accession number(s) can be found in the article/**Supplementary Material**. The source code and instructions may be accessed at: https://github.com/davidanastasiu/antibiofilm.

AUTHOR CONTRIBUTIONS

BB, AR, and DA designed the research, analyzed the data, wrote the manuscript, and prepared the figures. BB collected data from databases and literature, performed classification experiments. TD developed and optimized the regression model. All authors approved the final version of the manuscript.

FUNDING

This work was supported by an award from the NIH (R15AI138146).

ACKNOWLEDGMENTS

Computational resources were made possible by the San José State University Computer Engineering department HPC and the Santa Clara University WAVE HPC.

SUPPLEMENTARY MATERIAL

The Supplementary Material for this article can be found online at: https://www.frontiersin.org/articles/10.3389/fmicb.2021.783284/full#supplementary-material

REFERENCES

Bhadra, P., Yan, J., Li, J., Fong, S., and Siu, S. W. I. (2018). Ampep: sequence-based prediction of antimicrobial peptides using distribution patterns of amino acid properties and random forest. *Sci. Rep*. 8, 1697. doi: 10.1038/s41598-018-19752-w

Cao, D. (2020). *propy3. pypi*. Available online at: https://pypi.org/project/propy3/

Cock, P. J. A., Antao, T., Chang, J. T., Chapman, B. A., Cox, C. J., Dalke, A., et al. (2009). Biopython: freely available python tools for computational molecular biology and bioinformatics. *Bioinformatics* 25, 1422–1423. doi: 10.1093/bioinformatics/btp163

Consortium, T. U. (2020). Uniprot: the universal protein knowledgebase in 2021. *Nucleic Acids Res*. 49, D480–D489. doi: 10.1093/nar/gkaa1100

Coordinators, N. R. (2016). Database resources of the national center for biotechnology information. *Nucleic Acids Res*. 44, D7–D19. doi: 10.1093/nar/gkv1290

Costerton, J. W., Cheng, K. J., Geesey, G. G., Ladd, T. I., Nickel, J. C., Dasgupta, M., et al. (1987). Bacterial biofilms in nature and disease. *Annu. Rev. Microbiol*. 41, 435–464. doi: 10.1146/annurev.mi.41.100187.002251

de la Fuente-Nú nez, C., Reffuveille, F., nde, L. F., and Hancock, R. E. (2013). Bacterial biofilm development as a multicellular adaptation: antibiotic resistance and new therapeutic strategies. *Curr. Opin. Microbiol*. 16, 580–589. doi: 10.1016/j.mib.2013.06.013

De Oliveira, D. M. P., Forde, B. M., Kidd, T. J., Harris, P. N. A., Schembri, M. A., Beatson, S. A., et al. (2020). Antimicrobial resistance in eskape pathogens. *Clin. Microbiol. Rev*. 33:e00181-19. doi: 10.1128/CMR.00181-19

Duvaud, S., Gabella, C., Lisacek, F., Stockinger, H., Ioannidis, V., and Durinx, C. (2021). Expasy, the swiss bioinformatics resource portal, as designed by its users. *Nucleic Acids Res*. 49, W216–W227. doi: 10.1093/nar/gkab225

Ebou, A., Koua, D., Addablah, A., Kakou-Ngazoa, S., and Dutertre, S. (2021). Combined proteotranscriptomic-based strategy to discover novel antimicrobial peptides from cone snails. *Biomedicines* 9, 344. doi: 10.3390/biomedicines9040344

Fallah Atanaki, F., Behrouzi, S., Ariaeenejad, S., Boroomand, A., and Kavousi, K. (2020). Bipep: Sequence-based prediction of biofilm inhibitory peptides using a combination of nmr and physicochemical descriptors. *ACS Omega* 5, 7290–7297. doi: 10.1021/acsomega.9b04119

Fjell, C. D., Jenssen, H., Fries, P., Aich, P., Griebel, P., Hilpert, K., et al. (2008). Identification of novel host defense peptides and the absence of alpha-defensins in the bovine genome. *Proteins* 73, 420–430. doi: 10.1002/prot.22059

Gong, Z., Pei, X., Ren, S., Chen, X., Wang, L., Ma, C., et al. (2020). Identification and rational design of a novel antibacterial peptide dermaseptin-ac from the skin secretion of the red-eyed tree frog agalychnis callidryas. *Antibiotics* 9:243. doi: 10.3390/antibiotics9050243

Gupta, S., Kapoor, P., Chaudhary, K., Gautam, A., Kumar, R., and Raghava, G. P. (2013). In silico approach for predicting toxicity of peptides and proteins. *PLoS ONE* 8:e73957. doi: 10.1371/journal.pone.0073957

Gupta, S., Sharma, A. K., Jaiswal, S. K., and Sharma, V. K. (2016). Prediction of biofilm inhibiting peptides: an *in silico* approach. *Front. Microbiol*. 7:949. doi: 10.3389/fmicb.2016.00949

Hancock, R. E. W., Alford, M. A., and Haney, E. F. (2021). Antibiofilm activity of host defence peptides: complexity provides opportunities. *Nat. Rev. Microbiol*. 19, 786–797. doi: 10.1038/s41579-021-00585-w

Haney, E. F., Brito-Sánchez, Y., Trimble, M. J., Mansour, S. C., Cherkasov, A., and Hancock, R. E. W. (2018). Computer-aided discovery of peptides that specifically attack bacterial biofilms. *Sci. Rep*. 8, 1871. doi: 10.1038/s41598-018-19669-4

Hemu, X., and Tam, J. P. (2017). Macrocyclic antimicrobial peptides engineered from ω-conotoxin. *Curr. Pharmaceut. Design* 23, 2131–2138. doi: 10.2174/1381612822666161027120518

Kang, X., Dong, F., Shi, C., Liu, S., Sun, J., Chen, J., et al. (2019). Dramp 2.0, an updated data repository of antimicrobial peptides. *Scientific Data* 6, 148. doi: 10.1038/s41597-019-0154-y

Kim, Y.-H., Kim, S. M., and Lee, S. Y. (2015). Antimicrobial activity of protamine against oral microorganisms. *Biocontrol Sci*. 20, 275–280. doi: 10.4265/bio.20.275

Lamiable, A., Thévenet, P., Rey, J., Vavrusa, M., Derreumaux, P., and Tufféry, P. (2016). Pep-fold3: faster de novo structure prediction for linear peptides in solution and in complex. *Nucleic Acids Res*. 44, W449–W454. doi: 10.1093/nar/gkw329

Lata, S., Sharma, B. K., and Raghava, G. P. S. (2007). Analysis and prediction of antibacterial peptides. *BMC Bioinformatics* 8:263. doi: 10.1186/1471-2105-8-263

Lee, E. Y., Fulan, B. M., Wong, G. C. L., and Ferguson, A. L. (2016). Mapping membrane activity in undiscovered peptide sequence space using machine learning. *Proc. Natl. Acad. Sci. U.S.A*. 113, 13588–13593. doi: 10.1073/pnas.1609893113

Luca, M. D., Maccari, G., Maisetta, G., and Batoni, G. (2015). Baamps: the database of biofilm-active antimicrobial peptides. *Biofouling* 31, 193–199. doi: 10.1080/08927014.2015.1021340

Madeira, F., Park, Y. M., Lee, J., Buso, N., Gur, T., Madhusoodanan, N., et al. (2019). The embl-ebi search and sequence analysis tools apis in 2019. *Nucleic Acids Res*. 47, W636–W641. doi: 10.1093/nar/gkz268

Manavalan, B., Shin, T. H., Kim, M. O., and Lee, G. (2018). Aippred: Sequence-based prediction of anti-inflammatory peptides using random forest. *Front. Pharmacol*. 9:276. doi: 10.3389/fphar.2018.00276

Margit, M., Joakim, H., Lovisa, R., and Camilla, B. (2016). Antimicrobial peptides: an emerging category of therapeutic agents. *Front. Cell. Infect. Microbiol*. 6:194. doi: 10.3389/fcimb.2016.00194

Meher, P. K., Sahu, T. K., Saini, V., and Rao, A. R. (2017). Predicting antimicrobial peptides with improved accuracy by incorporating the compositional, physico-chemical and structural features into chou's general pseaac. *Sci. Rep*. 7, 42362. doi: 10.1038/srep42362

Memariani, H., Memariani, M., and Pourmand, M. R. (2018). Venom-derived peptide mastoparan-1 eradicates planktonic and biofilm-embedded methicillin-resistant staphylococcus aureus isolates. *Microb. Pathog*. 119, 72–80. doi: 10.1016/j.micpath.2018.04.008

Nagant, C., Pitts, B., Nazmi, K., Vandenbranden, M., Bolscher, J. G., Stewart, P. S., et al. (2012). Identification of peptides derived from the human antimicrobial peptide ll-37 active against biofilms formed by pseudomonas aeruginosa using a library of truncated fragments. *Antimicrob. Agents Chemother*. 56, 5698–5708. doi: 10.1128/AAC.00918-12

Ng, X. Y., Rosdi, B. A., and Shahrudin, S. (2015). Prediction of antimicrobial peptides based on sequence alignment and support vector machine-pairwise algorithm utilizing lz-complexity. *Biomed. Res. Int*. 2015:212715. doi: 10.1155/2015/212715

Orivel, J., Redeker, V., Le Caer, J. P., Krier, F., Revol-Junelles, A. M., Longeon, A., et al. (2001). Ponericins, new antibacterial and insecticidal peptides from the venom of the ant *Pachycondyla goeldii*. *J. Biol. Chem*. 276, 17823–17829. doi: 10.1074/jbc.M100216200

Overhage, J., Campisano, A., Bains, M., Torfs, E. C., Rehm, B. H., and Hancock, R. E. (2008). Human host defense peptide LL-37 prevents bacterial biofilm formation. *Infect. Immun* 76, 4176–4182. doi: 10.1128/IAI.00318-08

Pedregosa, F. (2011). Scikit-learn: machine learning in python. *J Mach Learn Res*. 12, 2825–2830.

Pierce, C. G., Srinivasan, A., Ramasubramanian, A. K., and López-Ribot, J. L. (2015). From biology to drug development: new approaches to combat the threat of fungal biofilms. *Microbiol. Spectrum* 3:10.1128/microbiolspec.MB-0007-2014. doi: 10.1128/microbiolspec.MB-0007-2014

Pletzer, D., and Hancock, R. E. W. (2016). Antibiofilm peptides: Potential as broad-spectrum agents. *J. Bacteriol.* 198, 2572–2578. doi: 10.1128/JB.00017-16

Raheem, N., and Straus, S. K. (2019). Mechanisms of action for antimicrobial peptides with antibacterial and antibiofilm functions. *Front. Microbiol.* 10:2866. doi: 10.3389/fmicb.2019.02866

Rajput, A., Gupta, A. K., and Kumar, M. (2015). Prediction and analysis of quorum sensing peptides based on sequence features. *PLoS ONE* 10:e0120066. doi: 10.1371/journal.pone.0120066

Ramasubramanian, A. K., and Lopez-Ribot, J. L. (2019). Nano-biofilm arrays as a novel universal platform for microscale microbial culture and high-throughput downstream applications. *Curr. Med. Chem.* 26, 2529–2535. doi: 10.2174/0929867326666190107155953

Sahoo, A., Swain, S. S., Behera, A., Sahoo, G., Mahapatra, P. K., and Panda, S. K. (2021). Antimicrobial peptides derived from insects offer a novel therapeutic option to combat biofilm: a review. *Front. Microbiol.* 12:1077. doi: 10.3389/fmicb.2021.661195

Schmidt, N. W., and Wong, G. C. (2013). Antimicrobial peptides and induced membrane curvature: geometry, coordination chemistry, and molecular engineering. *Curr. Opin. Solid State Mater. Sci.* 17, 151–163. doi: 10.1016/j.cossms.2013.09.004

Sharma, A., Gupta, P., Kumar, R., and Bhardwaj, A. (2016). dpabbs: A novel in silico approach for predicting and designing anti-biofilm peptides. *Sci. Rep.* 6:21839. doi: 10.1038/srep21839

Sheard, D. E., O'Brien-Simpson, N. M., Wade, J. D., and Separovic, F. (2019). Combating bacterial resistance by combination of antibiotics with antimicrobial peptides. *Pure Appl. Chem.* 91, 199–209. doi: 10.1515/pac-2018-0707

Singh, H., Singh, S., and Singh Raghava, G. P. (2019). Peptide secondary structure prediction using evolutionary information. *bioRxiv*. doi: 10.1101/558791

Spohn, R., Daruka, L., Lázár, V., Martins, A., Vidovics, F., Grézal, G., et al. (2019). Integrated evolutionary analysis reveals antimicrobial peptides with limited resistance. *Nat. Commun.* 10, 4538. doi: 10.1038/s41467-019-12364-6

Srinivasan, A., Torres, N. S., Leung, K. P., Lopez-Ribot, J. L., and Ramasubramanian, A. K. (2017). nbiochip, a lab-on-a-chip platform of mono- and polymicrobial biofilms for high-throughput downstream applications. *mSphere* 2, e00247-17. doi: 10.1128/mSphere.00247-17

Torres, N. S., Montelongo-Jauregui, D., Abercrombie, J. J., Srinivasan, A., Lopez-Ribot, J. L., Ramasubramanian, A. K., et al. (2018). Antimicrobial and antibiofilm activity of synergistic combinations of a commercially available small compound library with colistin against pseudomonas aeruginosa. *Front. Microbiol.* 9:2541. doi: 10.3389/fmicb.2018.02541

Vens, C., Rosso, M.-N., and Danchin, E. G. J. (2011). Identifying discriminative classification-based motifs in biological sequences. *Bioinformatics* 27, 1231–1238. doi: 10.1093/bioinformatics/btr110

Wang, G. (2012). Post-translational modifications of natural antimicrobial peptides and strategies for peptide engineering. *Curr. Biotechnol.* 1, 72–79. doi: 10.2174/2211550111201010072

Wang, G., Li, X., and Wang, Z. (2015). APD3: the antimicrobial peptide database as a tool for research and education. *Nucleic Acids Res.* 44, D1087–D1093. doi: 10.1093/nar/gkv1278

Wang, L., Niu, D., Wang, X., Shen, Q., and Xue, Y. (2020). A novel machine learning strategy for prediction of antihypertensive peptides derived from food with high efficiency. *bioRxiv*. doi: 10.1101/2020.08.12.248955

Wieczorek, M., Jenssen, H., Kindrachuk, J., Scott, W. R., Elliott, M., Hilpert, K., et al. (2010). Structural studies of a peptide with immune modulating and direct antimicrobial activity. *Chem. Biol.* 17, 970–980. doi: 10.1016/j.chembiol.2010.07.007

Xiao, N., Cao, D.-S., Zhu, M.-F., and Xu, Q.-S. (2015). protr/protrweb: R package and web server for generating various numerical representation schemes of protein sequences. *Bioinformatics* 31, 1857–1859. doi: 10.1093/bioinformatics/btv042

Xiao, X., Wang, P., Lin, W.-Z., Jia, J.-H., and Chou, K.-C. (2013). iamp-2l: a two-level multi-label classifier for identifying antimicrobial peptides and their functional types. *Anal. Biochem.* 436, 168–177. doi: 10.1016/j.ab.2013.01.019

Xiong, M., Bao, Y., Xu, X., Wang, H., Han, Z., Wang, Z., et al. (2017). with pH-responsive helix-coil conformation transitionable antimicrobial polypeptides. *Proc. Natl. Acad. Sci. U.S.A.* 114, 12675–12680. doi: 10.1073/pnas.1710408114

Zavascki, A. P., Goldani, L. Z., Li, J., and Nation, R. L. (2007). Polymyxin b for the treatment of multidrug-resistant pathogens: a critical review. *J. Antimicrob. Chemother.* 60, 1206–1215. doi: 10.1093/jac/dkm357

Zeng, P., Yi, L., Xu, J., Gao, W., Xu, C., Chen, S., et al. (2021). Investigation of antibiofilm activity, antibacterial activity, and mechanistic studies of an amphiphilic peptide against acinetobacter baumannii. *Biochim. Biophys. Acta* 1863, 183600. doi: 10.1016/j.bbamem.2021.183600

Conflict of Interest: The authors declare that the research was conducted in the absence of any commercial or financial relationships that could be construed as a potential conflict of interest.

Publisher's Note: All claims expressed in this article are solely those of the authors and do not necessarily represent those of their affiliated organizations, or those of the publisher, the editors and the reviewers. Any product that may be evaluated in this article, or claim that may be made by its manufacturer, is not guaranteed or endorsed by the publisher.

frontiers in Microbiology

ORIGINAL RESEARCH
published: 10 February 2022
doi: 10.3389/fmicb.2021.796363

Comparative Metabolic Pathways Analysis and Subtractive Genomics Profiling to Prioritize Potential Drug Targets Against *Streptococcus pneumoniae*

Kanwal Khan[1], Khurshid Jalal[2], Ajmal Khan[3], Ahmed Al-Harrasi[3]* and Reaz Uddin[1]**

[1] Dr. Panjwani Center for Molecular Medicine and Drug Research, International Center for Chemical and Biological Sciences, University of Karachi, Karachi, Pakistan, [2] HEJ Research Institute of Chemistry, International Center for Chemical and Biological Sciences, University of Karachi, Karachi, Pakistan, [3] Natural and Medical Sciences Research Center, University of Nizwa, Nizwa, Oman

OPEN ACCESS

Edited by:
Mattias Collin,
Lund University, Sweden

Reviewed by:
Jitendraa Vashistt,
Jaypee University of Information Technology, India
Anders P. Hakansson,
Lund University, Sweden

***Correspondence:**
Ajmal Khan
ajmalkhan@unizwa.edu.om
Ahmed Al-Harrasi
aharrasi@unizwa.edu.om
Reaz Uddin
mriazuddin@iccs.edu

Specialty section:
This article was submitted to Antimicrobials, Resistance and Chemotherapy, a section of the journal Frontiers in Microbiology

Received: *16 October 2021*
Accepted: *28 December 2021*
Published: *10 February 2022*

Citation:
Khan K, Jalal K, Khan A, Al-Harrasi A and Uddin R (2022) Comparative Metabolic Pathways Analysis and Subtractive Genomics Profiling to Prioritize Potential Drug Targets Against Streptococcus pneumoniae. Front. Microbiol. 12:796363. doi: 10.3389/fmicb.2021.796363

Streptococcus pneumoniae is a notorious pathogen that affects ∼450 million people worldwide and causes up to four million deaths per annum. Despite availability of antibiotics (i.e., penicillin, doxycycline, or clarithromycin) and conjugate vaccines (e.g., PCVs), it is still challenging to treat because of its drug resistance ability. The rise of antibiotic resistance in *S. pneumoniae* is a major source of concern across the world. Computational subtractive genomics is one of the most applied techniques in which the whole proteome of the bacterial pathogen is gradually reduced to a limited number of potential therapeutic targets. Whole-genome sequencing has greatly reduced the time required and provides more opportunities for drug target identification. The goal of this work is to evaluate and analyze metabolic pathways in serotype 14 of *S. pneumonia* to identify potential drug targets. In the present study, 47 potent drug targets were identified against *S. pneumonia* by employing the computational subtractive genomics approach. Among these, two proteins are prioritized (i.e., 4-oxalocrotonate tautomerase and Sensor histidine kinase uniquely present in *S. pneumonia*) as novel drug targets and selected for further structure-based studies. The identified proteins may provide a platform for the discovery of a lead drug candidate that may be capable of inhibiting these proteins and, therefore, could be helpful in minimizing the associated risk related to the drug-resistant *S. pneumoniae*. Finally, these enzymatic proteins could be of prime interest against *S. pneumoniae* to design rational targeted therapy.

Keywords: *Streptococcus pneumoniae*, subtractive genomics, serotype 14, metabolic pathways, 4-oxalocrotonate tautomerase and sensor histidine kinase

INTRODUCTION

Streptococcus pneumoniae is a gram-positive, spherical, alpha-beta hemolytic, and facultatively anaerobic bacterium. It is classified primarily as one of the major pathogenic species resulting in high mortality and morbidity rate. It is responsible for causing meningitis, otitis media, septicemia, bacteremia, and community-acquired pneumonia, otherwise called Invasive Pneumococcal

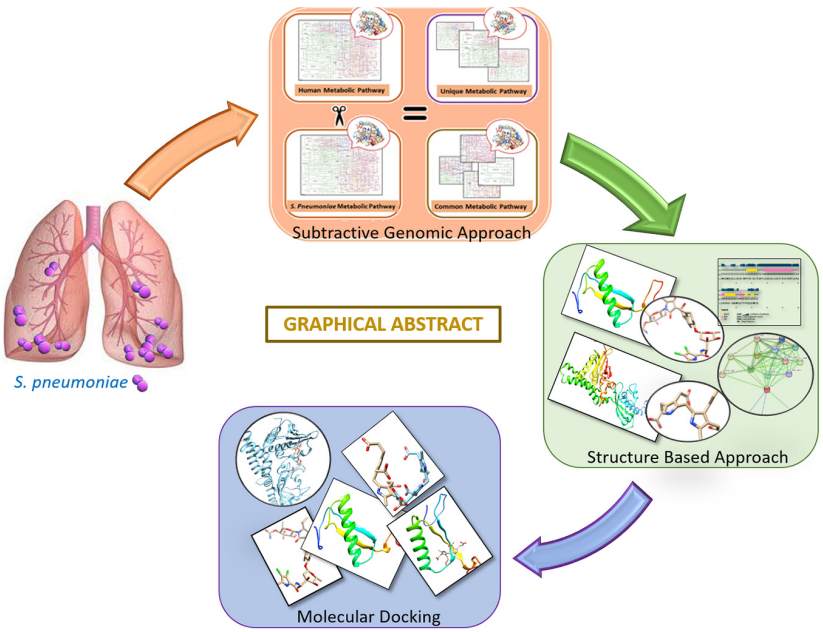

GRAPHICAL ABSTRACT |

Disease (IPD) (Lo et al., 2019). Nearly ∼600,000 children, ∼200,000 elders, and immuno-compromised individuals die due to pneumococcal diseases caused by *streptococci* annually (Watt et al., 2009). Surprisingly, in 2019, >600,000 deaths were reported due to pneumonia as well as >385,000 deaths during the COVID-19 pandemic (Elflein, 2021). Antibiotics are used as the most common anti-infection therapy (e.g., beta-lactam antibiotics) for the treatment of pneumonia. Unfortunately, the increasing resistance against common antibiotics as well as the emergence of Multiple Drug Resistant strains (MDRs) worldwide makes the management and treatment of pneumococcal infections highly difficult (Hakenbeck et al., 2012). Surveillance of serotypes and prevalence of drug-resistant strains in the general population is critical to create appropriate prevention and treatment protocol for *S. pneumoniae* (Ediriweera et al., 2016).

Evidently, the serotype 14 is most frequently responsible for Invasive Pneumococcal Disease (IPD) (Geno et al., 2015) among the 101 defined *S. pneumoniae* serotypes. The conjugated pneumococcal vaccines are developed against *S. pneumoniae* infections based on the polysaccharide capsular serotypes (Chiba et al., 2014). Specifically, Polysaccharide Pneumococcal Vaccine (PPV) 23-valent was developed for serotype 14 to cure IPD. Unfortunately, PPSV23 led to poor immunogenicity for pneumococci (Cilloniz et al., 2016). Currently, there is Pneumococcal Polysaccharide Vaccine (PPSV23), 10-valent Pneumococcal Conjugate Vaccine (PCV10), 7-valent Pneumococcal Conjugate Vaccine (PCV7), and 13-valent Pneumococcal Conjugate Vaccine (PCV13) in use. Even after the distribution of multi-valent Pneumococcal Conjugate Vaccine (PCV7), the percentage of serotype 14 infection has increased over time due to the increase in drug resistance (Bouskraoui et al., 2011).

Experimentally, molecular serotyping such as MultiLocus Sequence Typing (MLST) and Pulse-Field Gel Electrophoresis (PFGE) are the gold standard methods used to study the outbreaks and identification of pneumococcal isolates (Enright and Spratt, 1998), but with high associated cost. Thus, accurate determination of the serotypes remained a challenge (Hu et al., 2014). It is therefore imperative that s novel therapeutic drug target is identified against *S. pneumoniae*. The discovery of a new drug target may lead to better therapeutics (Lodha et al., 2013). Fortunately, the arrival of the post-genomic era and whole-genome sequencing of the pathogens opened up new avenues, such as comparative subtractive genomics, to design new drugs and vaccine candidates. Computational approaches make it possible to identify potential drug targets against such pathogens (Fair and Tor, 2014).

Certain gaps from previous studies against *S. pneumoniae,* such as metabolic pathways coverage, consideration of hub nodes, and conserved drug targets of bacterial pneumonia (Henriques et al., 2000), are covered in this study. The current study includes comparative and subtractive genomics analysis, subcellular localization, Protein-Protein Interaction (PPI) network analysis, essentiality and druggability of the target proteins, and metabolic pathway analysis. Furthermore, the study proposed that antibacterial lead compounds could be developed against the shortlisted potential drug targets.

MATERIALS AND METHODS

The drug target prioritization and identification against *S. pneumoniae* was performed by employing a subtractive genomics approach along with the analysis of the metabolic

pathways. Various databases and tools, as illustrated in the flow chart (**Figure 1**), were used for the determination of therapeutic targets against *S. pneumoniae.*

Data Collection of Proteome and Metabolic Pathways

The Kyoto Encyclopedia of Genes and Genomes (KEGG) database (Kanehisa and Goto, 2000) was used for the metabolic pathways retrieval of the pathogen (*S. pneumoniae,* i.e., spw01100*)* and host (*Homo sapiens,* i.e., hsa01100*)*. The human and *S. pneumoniae* proteomes were retrieved from the Universal Protein Resource (UniProt) database (Apweiler et al., 2021) with accession numbers UP000005640 and UP000001682 (strain CGSP14), respectively. The Database of Essential Genes (DEG database) (Luo et al., 2021) was used to investigate the essentiality of the drug targets and the DrugBank database (Wishart et al., 2018) was used to assess the druggability of the shortlisted targets.

Subtractive Genomics Approach

In the current study, a "Subtractive Genomic Approach," which is one of the most commonly applied methodologies, was applied. Subtractive Genomics is a powerful approach that applies the sequence subtraction between the host, the pathogen proteomes, and metabolic pathways. It provides necessary information on a set of proteins essential for the microorganism that do not exist in the respective host. Subtractive Genomics plays a role of great

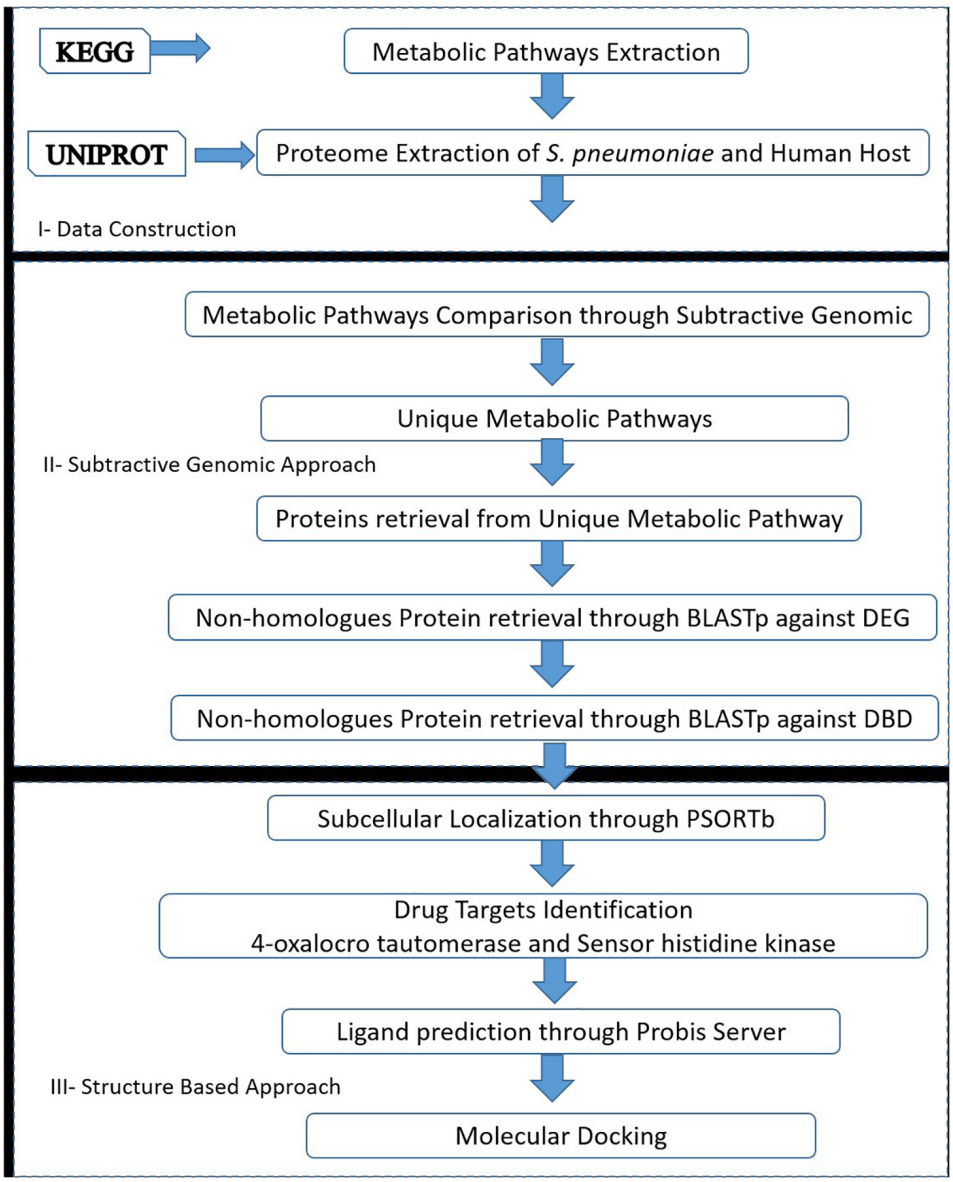

FIGURE 1 | Flow chart: A general sketch of the current study integrated with the use of various computational approaches and tools to identify potential drug targets candidates.

importance in potential drug target identification that is unique and essential to the pathogen survival without altering the host's (human) systematic metabolic pathways (Fenoll et al., 2009).

Host and Pathogen Metabolic Pathway Analysis

As mentioned above, the KEGG database (Kanehisa and Goto, 2000) was used for the genome-wide pathways analysis of *S. pneumoniae* and human. A standalone comparison was performed between the host and pathogen to identify unique and commonly found metabolic pathways. Unique pathways are classified as those pathways that are present only in the pathogen, while common pathways are those pathways that are present in both organisms (i.e., pathogen and host) (Linares et al., 2010). In the present study, the common metabolic pathways proteins were discarded while the protein sequences of unique metabolic pathways were retrieved from the UniProt for further downstream study.

Non-homologous Protein Identification

Accordingly, the protein sequences retrieved from the unique metabolic pathways were subjected to BLASTp (with *E*-value 10-3) against *Homo sapiens*. The BLASTp resulted in "Hits" (Homologous sequences between host and pathogen) and "No-Hits" (Non-homologous sequences). For further analysis, the non-homologous sequences that showed no similarity with the human host were selected.

Essential Non-homologous Genes Identification

Proteins that play a major role in cellular metabolism are said to be essential for any organism's survival (Deng et al., 2011). Thus, to shortlist proteins essential to pathogen's survival, BLASTp of non-homolog *S. pneumoniae* proteins was performed against DEG with cut-off parameters of *E* value 10^{-5}. Consequently, the obtained Hits protein sequences (homologous proteins) were used for further analysis while "No-Hits" (non-homologous proteins) protein sequences were discarded.

Druggability of Essential Protein

Furthermore, the essential non-homologous proteins were assessed through BLASTp with an *E* value 10^{-3} against the DrugBank database to determine the drug–target-like ability of shortlisted proteins to finally identify novel drug targets against *S. pneumoniae*. Similarly, the identified Hits protein sequences were retrieved and analyzed for the prioritization of a potent drug target while obtained "No-Hits" proteins sequences were discarded.

Sub-Cellular Location Prediction

The subcellular location of final shortlisted drug-like protein targets was determined by using PSORTb v.3.0. tool (Yu et al., 2010). The PSORTb predicts results based on the sub-cellular localization, i.e., cytoplasmic membrane, cell wall, cytoplasmic, extracellular, and unknown.

Protein Structure Prediction, Validation, and Conservancy Analysis

The structures from the proteins shortlisted from the above approach were searched for in PDB. The suitable template for the protein structure modeling was found through BLASTp against the PDB. It resulted in the shortlisting of various proteins with different query coverage and percent identity that can be further filtered to select a suitable template for protein structure modeling. Eventually, the 3D structures of shortlisted drug targets were then modeled by using the Homology modeler tool. Based on DOPE score, the best optimized structure from five modeled structures was selected. In order to perform the docking experiment against shortlisted proteins, PSIPRED (Buchan and Jones, 2019), ProSA-web (Wiederstein and Sippl, 2007), and PROCHECK (Laskowski et al., 2006) were applied for the model structure evaluation based on secondary structure analysis, error in 3D model identification, and tertiary structure stereochemistry analysis, respectively.

The shortlisted proteins were further analyzed to investigate the conservancy of these proteins in the *S. pneumoniae* strains. Therefore, BLASTp of shortlisted proteins was performed and resultant matched sequences were retrieved. These sequences were further aligned through Clustal Omega tool to study conservation among these proteins from other serotypes of *S. pneumoniae*.

Active Site Prediction

As the structure was modeled, there is a need to find the active site where a ligand could bind to alter its function. The DogSite Scorer[1] was used to find the possible binding sites of the modeled protein. The DogSite Scorer identifies active site pockets based on the physico-chemical properties of the protein residues. These active sites can be selected to dock ligand against respective proteins.

Network Topology Studies

Furthermore, to identify whether these proteins can be a hub protein and validate their functional interactions, the PPIs network of pathogen proteins as potential drug targets were generated through the STRING database (Szklarczyk et al., 2021). The STRING is a database of experimentally known and predicted PPIs, including direct (physical) and indirect (functional) network. Node degrees and clustering coefficient are used to classify these PPIs as hub proteins.

Ligand Prediction

As the protein structure was not available, the ligand information was also missing. The ProBis server (Konc et al., 2015) was used to find the probable ligands and also used for the assessment of the fundamental interaction between the ligand and drug targets. The ProBis predicts the best possible ligand for proteins through molecular simulation based on a theoretical approach. On the basis of the proposed ligand, one may design new drugs in further drug discovery stages.

[1] https://proteins.plus/

Molecular Docking Studies

In molecular docking, the most effective ligand shows the minimal score of docking for its target proteins. The proteins with the modeled structure were used as target proteins while identified ligands were docked. The ligand was docked following the standard docking parameters of 250 times Lamarckian GA settings resulting in 27,000 generations (Tanchuk et al., 2016). The MOE software was used to investigate the docked ligand-protein interactions, and to visualize the hydrogen bond and hydrophobic interactions of the ligand with docked protein within the range of 5 Å.

RESULTS

Identification of Metabolic Pathways in *Streptococcus pneumoniae*

Currently, the KEGG database has 115 metabolic pathways for *S. pneumoniae* serotype 14 and 375 for human, as shown in **Table 1**. Unique and common metabolic pathways among pathogen and host (human) were identified through standalone BLASTp. Consequently, 25 unique pathways are identified for the pathogen that are crucial for the persistence of *S. pneumoniae* (**Table 2**) with 90 pathways commonly present in both organisms (**Table 3**).

Metabolic Pathway Analysis

Furthermore, BLASTp of proteins that are uniquely present in the shortlisted unique metabolic pathways was performed against the human proteome to encounter further cross-reactivity of drug-like compounds with the host protein. Metabolic pathway analysis through KEGG showed 318 proteins present in the unique metabolic pathways in which the shortlisted proteins are playing significant roles, as shown in **Table 2**.

Non-homologous Proteins Identification

As described above, a total of 318 proteins were retrieved from the unique metabolic pathways. These 318 proteins were subjected to BLASTp to determine the non-homologous protein sequences against the host proteome. The BLASTp revealed 150 proteins classified as non-homologous proteins that are present only in the pathogen. These proteins are further analyzed in subsequent steps.

TABLE 1 | Steps involved in the current study: Subtractive filtering of proteins and metabolic pathways against *S. pneumoniae*.

S. no	Steps involved in the current study	*Streptococcus pneumoniae*
1	Complete pathways of the pathogen from KEGG (spw)	115
2	Complete pathways of the human from KEGG (hsa)	375
3	Common metabolic pathways	90
4	Unique metabolic pathways	25
5	Number of proteins presents in unique metabolic pathways	318
6	Removal of redundant KEGG IDs	207
7	BLASTp of unique metabolic proteins against human host proteome (*E* value 10^{-3})	150
8	BLASTp of unique metabolic proteins against DEG (*E* value 10^{-5})	105
9	BLASTp of unique metabolic proteins against DBD (*E* value 10^{-3})	47

TABLE 2 | Unique metabolic pathways: List of all unique metabolic pathways and uniquely present proteins in these metabolic pathways present in *S. pneumoniae*.

S. no	Metabolic pathways	Pathway Ids	Proteins in the pathway
1	Aminobenzoate degradation	spw00627	2
2	Antimicrobial resistance genes	spw01504	17
3	Bacterial secretion system	spw03070	13
4	Benzoate degradation	spw00362	2
5	C5-Branched dibasic acid metabolism	spw00660	5
6	Carbapenem biosynthesis	spw00332	2
7	Cationic antimicrobial peptide (CAMP) resistance	spw01503	6
8	Chloroalkane and chloroalkene degradation	spw00625	2
9	Cyanoamino acid metabolism	spw00460	4
10	D-Alanine metabolism	spw00473	4
11	Lysine biosynthesis	spw00300	12
12	Methane metabolism	spw00680	9
13	Monobactam biosynthesis	spw00261	4
14	Naphthalene degradation	spw00626	2
15	Peptidoglycan biosynthesis	spw00550	25
16	Peptidoglycan biosynthesis and degradation protein	spw01011	24
17	Phosphotransferase system	spw02060	45
18	Photosynthesis proteins	spw00194	8
19	Quorum sensing	spw02024	52
20	Streptomycin biosynthesis	spw00521	3
21	Two-component system	spw02022	37
22	Two-component system	spw02020	16
23	Vancomycin resistance	spw01502	6
24	Xylene degradation	spw00622	2
25	beta-Lactam resistance	spw01501	16

Identification of Essential Proteins

The essentiality of all non-homologous proteins was determined by using BLASTp from the DEG database with the *E* value of 10^{-5}. About 105 non-homolog proteins were classified as essential proteins required for the survival of *S. pneumoniae* and could be proposed as the potential drug targets (**Supplementary Table 1**). These non-homologous essential proteins can be safely recommended as possible therapeutic targets for pathogens. Theoretically, bacteria may survive but expected to be less virulent if such proteins are targeted, or numerous important processes could be inhibited, resulting in pathogenicity being eradicated. The DEG database is being updated periodically, however, it is limited to the studies of *S. pneumoniae* survival in rich growth medium only. Despite the DEG's limitation it is a well cited database and provided reliable results for known organisms. The essentiality of *S. pneumoniae* proteins can be

TABLE 3 | Common metabolic pathways: List of all common metabolic pathways, commonly shared by both organisms (*S. pneumoniae* and Human).

S. no	Metabolic pathways	Pathway ids	Protein in pathways
1	ABC transporters	pw02010	97
2	Alanine, aspartate, and glutamate metabolism	spw00250	17
3	Amino acid related enzymes	spw01007	27
4	Amino sugar and nucleotide sugar metabolism	spw00520	35
5	Aminoacyl-tRNA biosynthesis	spw00970	84
6	Arachidonic acid metabolism	spw00590	1
7	Arginine and proline metabolism	spw00330	7
8	Arginine biosynthesis	spw00220	7
9	Ascorbate and aldarate metabolism	spw00053	11
10	Bacterial toxins	spw02042	4
11	Base excision repair	spw03410	9
12	Biotin metabolism	spw00780	5
13	Butanoate metabolism	spw00650	7
14	CD molecules	spw04090	1
15	Chaperones and folding catalysts	spw03110	18
16	Chloroalkane and chloroalkene degradation	spw00625	2
17	Chromosome and associated proteins	spw03036	29
18	Citrate cycle (TCA cycle)	spw00020	4
19	Cysteine and methionine metabolism	spw00270	21
20	Cytoskeleton proteins	spw04812	3
21	D-Glutamine and D-glutamate metabolism	spw00471	3
22	DNA repair and recombination proteins	spw03400	67
23	DNA replication	spw03030	15
24	DNA replication proteins	spw03032	25
25	Enzymes	spw01000	1
26	Exosome	spw04147	26
27	Fatty acid biosynthesis	spw00061	15
28	Folate biosynthesis	spw00790	9
29	Fructose and mannose metabolism	spw00051	20
30	Galactose metabolism	spw00052	27
31	Glutathione metabolism	spw00480	8
32	Glycerolipid metabolism	spw00052	10
33	Glycerophospholipid metabolism	spw00564	8
34	Glycine, serine, and threonine metabolism	spw00260	16
35	Glycolysis/Gluconeogenesis	spw00010	26
36	Glycosyltransferases	spw01003	6
37	Glyoxylate and dicarboxylate metabolism	spw00630	7
38	Homologous recombination	spw03440	21
39	Inositol phosphate metabolism	spw00562	4
40	Ion channels	spw04040	1
41	Lipid biosynthesis proteins	spw01004	12
42	Lysine degradation	spw00310	2
43	Membrane trafficking	spw04131	5
44	Messenger RNA biogenesis	spw03019	14
45	Mismatch repair	spw03430	18
46	Mitochondrial biogenesis	spw03029	27
47	Nicotinate and nicotinamide metabolism	spw00760	8
48	Nitrogen metabolism	spw00910	4
49	Non-coding RNAs	spw03100	74
50	Nucleotide excision repair	spw03420	8
51	One carbon pool by folate	spw00670	10
52	Other glycan degradation	spw00511	10
53	Oxidative phosphorylation	spw00190	18
54	Pantothenate and CoA biosynthesis	spw00770	11
55	Pentose and glucuronate interconversions	spw00040	9
56	Pentose phosphate pathway	spw00030	19
57	Peptidases and inhibitors	spw01002	38
58	Phenylalanine, tyrosine, and tryptophan biosynthesis	spw00400	18
59	Porphyrin and chlorophyll metabolism	spw00860	1
60	Prenyltransferases	spw01006	3
61	Prokaryotic defense system	spw02048	25
62	Propanoate metabolism	spw00640	12
63	Protein export	spw03060	14
64	Protein kinases	spw01001	10
65	Protein phosphatases and associated proteins	spw01009	3
66	Purine metabolism	spw00230	36
67	Pyrimidine metabolism	spw00240	30
68	Pyruvate metabolism	spw00620	22
69	RNA degradation	spw03018	10
70	RNA polymerase	spw03020	6
71	Riboflavin metabolism	spw00740	6
72	Ribosome	spw03011	63
73	Ribosome biogenesis	spw03009	52
74	Secretion system	spw02044	13
75	Selenocompound metabolism	spw00450	7
76	Sphingolipid metabolism	spw00600	6
77	Starch and sucrose metabolism	spw00500	40
78	Sulfur metabolism	spw00920	5
79	Sulfur relay system	spw04122	5
80	Taurine and hypotaurine metabolism	spw00430	4
81	Terpenoid backbone biosynthesis	spw00900	8
82	Thiamine metabolism	spw00730	13
83	Transcription factors	spw03000	41
84	Transcription machinery	spw03021	11
85	Transfer RNA biogenesis	spw03016	52
86	Translation factors	spw03012	14
87	Transporters	spw02000	264
88	Valine, leucine, and isoleucine biosynthesis	spw00290	11
89	Valine, leucine, and isoleucine degradation	spw00280	3
90	Vitamin B6 metabolism	spw00750	4

further evaluated through experimental studies for the survival of pathogen in environmental or other biological conditions such as saliva (van Opijnen et al., 2009; Liu et al., 2017, 2021).

Druggability of Therapeutic Targets

Eventually, the non-homologous essential 105 proteins were BLASTp-ed against the DrugBank database and any sequence similarities with the drug target proteins in the DrugBank were found. Only proteins with significant sequence similarity to FDA-approved therapeutic targets were chosen, while the remaining

were eliminated from the database. As a result, only 47 proteins were identified as being essential, non-homologous, and drug target-like against *S. pneumoniae*. These 47 proteins showed significant similarities with the FDA approved drug targets found in DrugBank and, therefore, subsequently followed up in the next step. On the other hand, the excluded 58 proteins at this stage have not shown any significant similarity to the drug targets found in DrugBank. Although those 58 proteins were excluded they still may be studied as potential drug targets by the scientific community owing to their essentiality and non-homologous nature. The list of these 47 drug target-like proteins are provided in **Supplementary Table 2**.

Subcellular Localization Prediction

Protein localization is important to understand throughout the drug development process because it influences the design of novel drugs and vaccines. Cell membrane proteins, for example, are frequently employed as vaccine targets, while cytoplasmic proteins are frequently used as therapeutic targets. Among these 47 essential proteins, 30 were found to be cytoplasmic proteins, 11 were cytoplasmic membrane proteins, three were cell wall proteins, and one was identified as an extracellular protein, as shown in **Table 4**. **Figure 2** showed the location distribution of all essential proteins in *S. pneumoniae*. The step-wise filtering of the proteins during the current study is shown in **Table 1**.

Novel Drug Targets Prediction and Significance of Selected Proteins

The literature is full of examples of cytoplasmic proteins as proven therapeutic targets because of easy reach by the drugs (Anis Ahamed et al., 2021). Additionally, ∼70% FDA approved drugs are reported as enzymatic proteins because of their significant role in multiple pathways. Finally, among 47 potential drug targets, two proteins were shortlisted as essential, non-homologous, druggable targets against *S. pneumoniae* i.e., 4-oxalocrotonate tautomerase (B2IPH4) and sensor histidine kinase CiaH (B2INS3). Based on their cytoplasmic subcellular localization, length > 100 amino acids, their enzymatic nature, and involvement in essential metabolic pathways, these identified proteins were subjected to further structure-based studies. **Figure 3** showed the comprehensive outcome of the current study.

4-Oxalocrotonate Tautomerase

4-oxalocrotonate tautomerase enzyme (EC 5.3.2.-4-OT) belongs to a family of isomerases that readily convert hydroxymuconate to the αβ-unsaturated ketone (van Diemen et al., 2017). It is involved in benzonate degradation and xylene degradation pathways uniquely found in *S. pneumoniae*.

$$\text{Aromatic compound} \xrightarrow{4-\text{OT}} \alpha, \beta - \text{unsaturated ketone}$$

Through this enzyme, bacteria utilize aromatic compounds and amino acids to essential hydrocarbons which are the sole source of carbon and energy that is further used in the citric acid cycle.

TABLE 4 | Subcellular localization: Distribution of essential non-homologous proteins in a different area of cell.

S. no	PSORTb results	No. of proteins
1	Cell wall	3
2	Cytoplasmic	30
3	Cytoplasmic Membrane	11
4	Extracellular	1
5	Unknown	2

Sensor Histidine Kinase CiaH

Sensor histidine kinase CiaH (EC:2.7.13.3) is an ATP binding signal transduction protein involved in the Two-component system of *S. pneumoniae* (Singh et al., 2011). These sensor histidine kinases sense the changes in the environment (in stress or presence of drug) surrounding the pathogen and provide such signals that alter the inside mechanism of bacterial cells, preparing it to utilize these changes. It has been reported that the changes in these sensor kinases showed resistance to many antibacterial drugs such as cefotaxime (Möglich, 2019). The protein helps in the catalysis of reactions such as,

$$\text{ATP} + \text{protein L-histidine} \xrightarrow{\text{CiaH}} \text{ADP} + \text{protein}$$
$$\text{N} - \text{phospho} - \text{L} - \text{histidine}$$

Environmental variables influence the synthesis of virulence proteins, and two-component regulatory mechanisms are involved in detecting these influences. Tatsuno et al. (2014) reported the effected regulation of Streptococcus and significant growth reduction in knockout CiaH strains. Additionally, CiaH is highly conserved in *S. pneumoniae*, and deletion of the gene encoding its cognate response regulator (ciaR*pn*) made pneumococcal strains more susceptible to oxidative stress (Kaiser et al., 2020). Furthermore, it has been widely studied for its mutations resulting in the beta-lactamase resistance (Schweizer et al., 2017; Peters et al., 2021). It is used as a drug target to inhibit *ESKAPE* pathogens (Velikova et al., 2016), *Staphylococcus aureus* (Xie et al., 2020), and *Corynebacterium diphtheriae* (Khalid et al., 2018). However, CiaH protein has never been studied as drug target against *S. pneumoniae* and thus in the current study it is proposed as a potential drug target.

Conservancy Analysis of Shortlisted Proteins

Furthermore, the conservancy analysis was performed for 4-oxalocrotonate tautomerase and sensor histidine kinase CiaH proteins. The BLASTp of 4-oxalocrotonate tautomerase resulted in the local alignment of XylH with P67530 *S. pneumoniae* (serotype 4), P67531 (strain ATCC BAA-255/R6), A5MAV1 (strain SP14-BS69), and J0V2K5 (from strain 2070335). The alignments of these identified proteins were further analyzed through multiple sequence alignment using Clustal Omega. The percent matric analysis showed that these proteins are 100–98% conserved among them (**Supplementary Figure 1**). Additionally, the BLASTp of sensor histidine kinase CiaH showed similarities

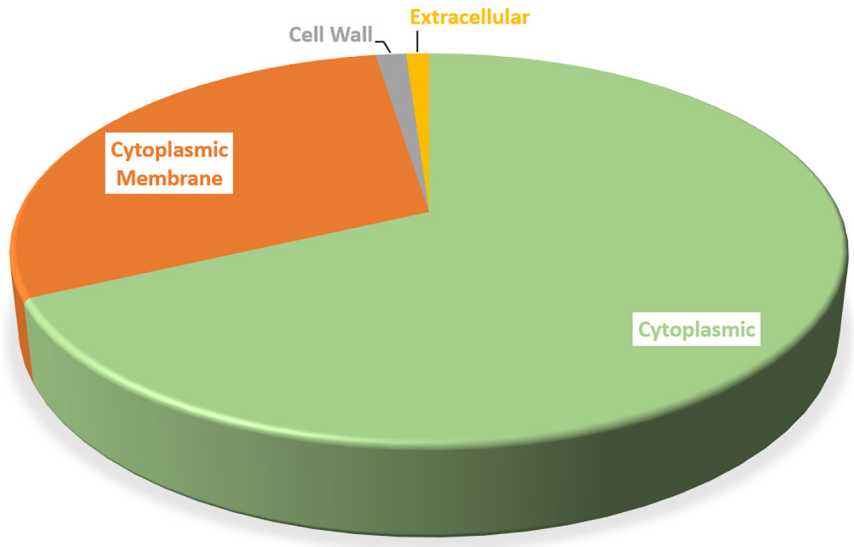

FIGURE 2 | Subcellular localization: PSORTb results showing the subcellular distribution of essential proteins occur in *S. pneumoniae*.

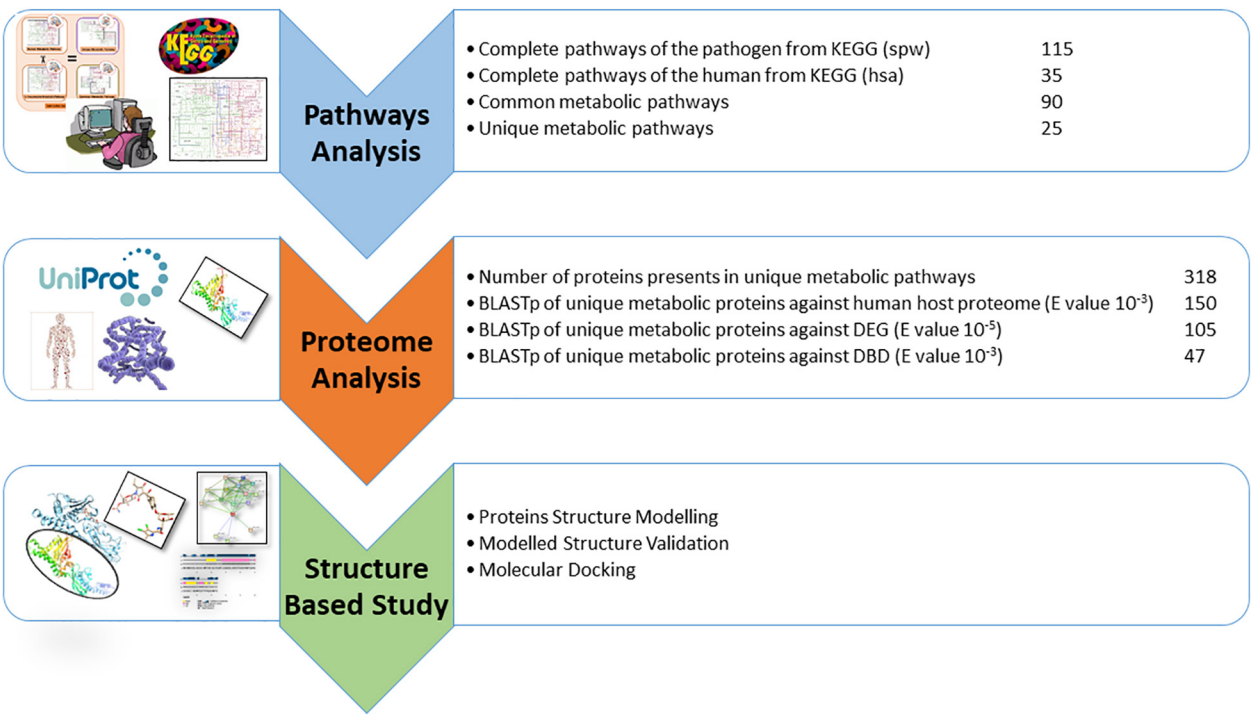

FIGURE 3 | Current study summary for target protein identification: Stepwise analysis of subtractive genomic approach for drug targets identification in *S. pneumoniae*.

with P0A4I6 (strain ATCC BAA-255/R6), P0A4I5 (serotype 4 strain ATCC BAA-334/TIGR4), A0A0H2ZQ10 (serotype 2 strain D39/NCTC 7466), J1DIP7 (strain 2070335), A5M9S1 (SP14-BS69), and A5M9S2 (strain SP14-BS69), respectively. These proteins showed conservancy of 100–93% when analyzed through MSA (**Supplementary Figure 2**).

Comparative Structure Prediction and Evaluation

The 3D structures of shortlisted proteins were not yet available in the PDB. Therefore, its homology modeling was performed by taking the FASTA sequence of the protein from the UniProt database with the accession numbers B2IPH4 and B2INS3 as mentioned in the database. Structural and functional studies of 4-oxalocrotonate tautomerase and sensor histidine kinase CiaH, were further evaluated by performing BLASTp against the PDB database to find a possible template. For 4-oxalocrotonate tautomerase, the template PDB ID: 6FPS was identified with 41% sequence similarity (**Figure 4A**). Likewise, for sensor histidine kinase CiaH, template PDB ID: 4I5S with a 40% sequence similarity was selected (**Figure 4B**). Using these identified template proteins, the 3D structure of 4-oxalocrotonate tautomerase and sensor histidine kinase CiaH was modeled. Structures with high DOPE score (i.e., modeled structure 4) were further evaluated for ligand screening.

Validation of the Modeled Structure

Different tools were used to verify the modeled protein structure. In the following, the structure verification procedure is discussed.

Confirmation of Proteins Through PSIPRED

The PSIPRED resulted in the prediction of a higher number of alpha helices than beta sheets formation as shown in **Supplementary Figure 3** for both XylH and CiaH. The PSIPRED results verified the protein on the basis of their sequence for the alpha helices and beta sheets formation as modeled through modeler tool.

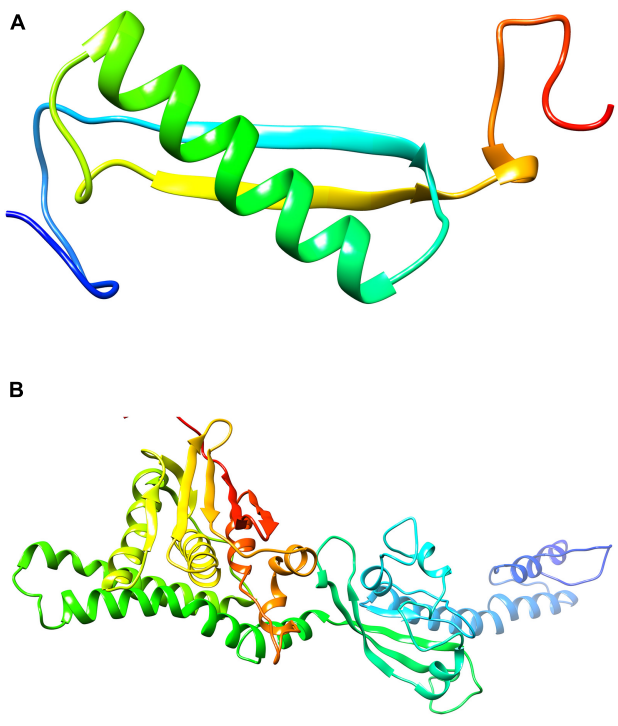

FIGURE 4 | Modeled structure of proteins (drug targets): Structure modeled through Homology modeler for 4-oxalocrotonate tautomerase **(A)** and sensor histidine kinases **(B)** using the respective template.

PROCHECK Validation of Proteins

The PROCHECK was used to generate a Ramachandran plot for the modeled protein structures. For XylH, the Ramachandran plot showed about 93.8% residues in the favorable region and four residues in additionally allowed regions (6.2%). While in the case of CiaH, validation showed about 84.4% residues in the favorable region, with seven residues in the disallowed region and 51 and 7 residues in the additionally allowed and generously allowed regions responsible for about 12.2 and 1.7%, respectively, as shown in **Supplementary Figure 4**.

Structure Validation Through ProSA

Additionally, the cross validation of modeled structure through ProSA tool predicted a *Z*-score value of −2.66 for XylH and −4.62 for CiaH, indicating the model falls within the range of NMR/X-ray crystallography derived structures (**Supplementary Figure 5**).

Network Topology for Protein-Protein Interactions

Many functional and physical interactions between various types of proteins develop, and these interactions are critical for many biological processes involving cellular machinery. Filtering and analyzing functional genomic data for annotating functional, structural, and evolutionary information of proteins may be performed using this information. Investigating the predicted PPIs might open up new avenues for experimental research and computer-assisted drug discovery in the future (Schwartz et al., 2009). The PPI and functional annotation of selected proteins (XylH and CiaH) were determined using the STRING server. The STRING results showed different nodes and edges of each protein and showed that the prioritized target proteins may act as hub protein inter-acting with more than ten proteins. Therefore, targeting such proteins may affect the activity of all interactor proteins.

The interaction of XylH protein with other proteins in *S. pneumoniae* was identified using the STRING database, which was submitted with the protein sequence of XylH. It resulted in 16 PPI networks for 4-oxalocrotonate tautomerase (**Figure 5A**) represented as (XylH in red node) with neighbor proteins as SPD_0131 (Conserved hypothetical protein), SPD_0182 (Conserved hypothetical protein), SPD_0072 (Catechol 2,3-dioxygenase), SPD_1834 (Acetaldehyde dehydrogenase), TrmE (Trna modification gtpase trme), glyA (Glycine hydroxymethyltransferase), PolA (In addition to polymerase activity), prfA (Peptide chain release factor 1), tdk (Thymidine kinase), SPD_0905 (Acetyltransferase), SPD_0908 (L-threonylcarbamoyladenylate synthase), SPD_0911 (Uncharacterized protein), PvaA (Pneumococcal vaccine antigen A), and HemK (Release factor glutamine methyltransferase). The XylH protein has a total number of edges of 62, expected number of edges of 23, number of nodes of 16, and an average nodes degree of 7.75, according to the results. The enrichment

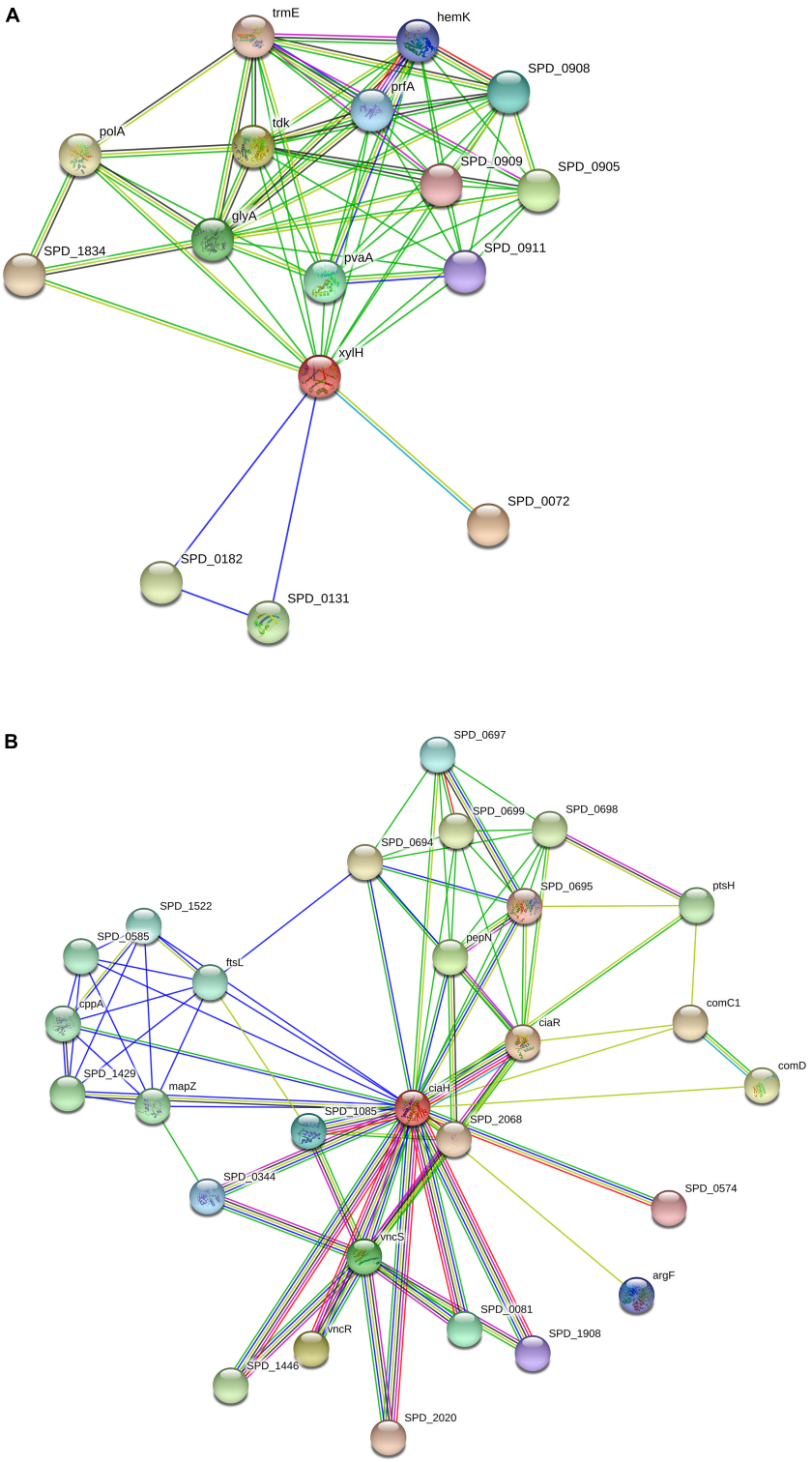

FIGURE 5 | Protein-protein interactions: Schematic PPI network generated through the STRING database for XylH **(A)** and CiaH **(B)**.

p-value for Protein-Protein Interactions is 7.79e-12, with an average local clustering coefficient of 0.908. These proteins are involved in a variety of critical functions. As a result, targeting the XylH protein may result in the loss of function of the other associated proteins. As a result, we can suggest this protein as a therapeutic target.

Similarly, the CiaH protein sequence was uploaded to the STRING database. The STRING resulted in 28 PPI networks for sensor histidine kinase CiaH, verifying that the selected proteins are hub proteins (**Figure 5B**). The CiaH was represented by a red node having interactions with CiaR (DNA-binding response regulator ciaR), SPD_2068 (DNA-binding response regulator), SPD_0574 (DNA-binding response regulator), ArgF (Ornithine carbamoyltransferase), SPD_1908 (Response regulator), SPD_0081 (Response regulator), VncS (Histidine kinase), VncR (DNA-binding response regulator VncR), SPD_1446 (DNA-binding response regulator), SPD_2020 (DNA-binding response regulator protein), SPD_0344 (DNA-binding response regulator), SPD _1085 (response regulator saer), SPD_0574 (DNA-binding response regulator), ComD (sensor histidine kinase comd), ComC1 (Competence stimulating peptide precursor 1), PtsH (phosphocsrrier protein), SPD_0698 (Uncharacterized protein), SPD_0695 (Oxidoreductase), SPD_0699 (Uncharacterized protein), SPD_0694 (Uncharacterized protein), SPD_0697 (Acetyltransferase), PepN (Aminopeptidase), mapZ (Conserved hypothetical protein), SPD_1429 (Uncharacterized protein), CppA (C_3-degrading proteinase), SPD_0585 (Uncharacterized protein), SPD_1522 (Replication initiation and membrane attachment protein), and FtsL (Cell division protein ftsl). It has a total of 28 number of nodes, 90 edges, 6.43 average node degree, average clustering coefficient as 0.824, expected number of edges as 38, and PPI enrichment *p*-value of 6.97e-13.

Active Site Prediction

Accordingly, as the protein structures were modeled, there is a need to find an interactive interface for the binding of the ligand. For that purpose, the DogSite Scorer tool was used to identify such binding sites. It predicted only one binding pocket for XylH protein with a drug score of 0.82 as shown in **Supplementary Figure 6A**. **Table 5** showed the residues present in the selected binding pocket. As for CiaH, it predicted 16 binding pockets. Among these pockets, the binding site with a high drug score 0.81 was selected, as shown in **Supplementary Figure 6B**. **Table 5** showed the residues present in the selected binding pocket.

TABLE 5 | Active site: Residues present in the Active site of XylH and CiaH protein.

XylH protein active site residues				CiaH protein active site residues		
S. no	**Chain**	**Position**	**Residue**	**Chain**	**Position**	**Residue**
1	A	1	Met	A	211	Leu
2	A	2	Val	A	212	Glu
3	A	3	Lys	A	218	Gln
4	A	4	Trp	A	219	Ser
5	A	5	Lys	A	223	Asn
6	A	6	Lys	A	226	His
7	A	7	Ser	A	227	Glu
8	A	8	Lys	A	228	Leu
9	A	9	Leu	A	229	Arg
10	A	10	Val	A	230	Thr
11	A	11	Glu	A	231	Pro
12	A	12	Glu	A	233	Ala
13	A	13	Ala	A	234	Val
14	A	14	Ile	A	235	Leu
15	A	15	Met	A	236	Gln
16	A	16	Pro	A	237	Asn
17	A	17	Phe	A	238	Arg
18	A	28	Leu	A	256	Ser
19	A	31	Lys	A	259	Ser
20	A	32	Lys	A	260	Ser
21	A	35	Ala	A	262	Glu
22	A	36	Lys	A	263	Glu
23	A	39	Thr	A	266	Asn
24	A	48	Ala	A	267	Met
25	A	49	Pro	A	269	Phe
26	A	50	Gln	A	270	Leu
27	A	51	Ser	A	273	Ser
28	A	52	Ala	A	274	Leu
29	A	53	Val	A	280	Arg
30	A	54	His	A	281	Asp
31	A	56	Val	A	282	Asp
32				A	284	Ile
33				A	289	Ala
34				A	290	Glu
35				A	294	Ser
36				A	295	Phe
37				A	298	Thr
38				A	301	Thr
39				A	332	Lys
40				A	351	Glu
41				A	385	Arg
42				A	402	Leu
43				A	407	Ala
44				A	410	Ile
45				A	413	Ala

Protein-Ligand Interactions Study Through Docking

The protein-ligand interactions were analyzed through AutoDock Vina.

Ligand Identification

The identification of protein binding site and their corresponding ligands have an important role in drug target identification and drug research. The protein binding sites are structurally and functionally important regions on the protein surface on which different type of drugs interact to perform a desired action (Konc and Janežič, 2017). The ProBis server was used for the ligand identification. For 4-oxalocrotonate tautomerase, DPM commonly named as DIPYRROMETHANE COFACTOR with IUPAC name: 3-[5-[[3-(2-carboxyethyl)-4-(carboxymethyl)-5-methyl-1H-pyrrol-2-yl]methyl]-4-(carboxymethyl)-1H-pyrrol-3-yl] propanoic acid was used. The ligand was identified from a template protein PDB ID: 3EQ1 (from Human) and for sensor histidine kinase CiaH, XAM commonly named as Amycolamicin antibiotic, IUPAC name (1R,4aS,5S,6S,8aR)-5-{[(5S)-1-(3-O-acetyl-4-O-carbamoyl-6-deoxy-2-O-methyl-alpha-L-talopyranosyl)-4-hydroxy-2-oxo-5-(propan-2-yl)-2,5-dihydro-1H-pyrrol-3-yl]carbonyl}-6-methyl-4-methylidene-1,2,3,4,4a,5,6,8a-octahydronaphthalen-1-yl-2,6-dideoxy-3-C-[(1S)-1-{[(3,4-dichloro-5-methyl-1H-pyrrol-2-yl)carbonyl]amino} ethyl]-beta-D-ribo-hexopyranosideligand was identified from

a template PDB ID: 4URL (from *Escherichia coli* BL21) (**Supplementary Figure 7**).

Molecular Docking With AutoDock

Molecular docking analysis was performed with the identified ligand from ProBis server and modeled structure of CiaH and XylH protein through the AutoDock 4.2 tool. The XAM compound resulted in the binding score of –5.09 kcal/mol while DPM showed more potency toward XylH i.e., –7.59 kcal/mol. Furthermore, the post-docking analysis was performed to study the interaction of protein compounds complex. The analysis showed that XAM mediates five hydrogen bonds with Glu377, Lys424, and Arg393 whereas DPM mediates one hydrogen bond through its side chain oxygen with Val55 residue, as shown in **Figure 6**. The detailed interaction analysis of XAM and DPM is highlighted in **Table 6**.

DISCUSSION

Streptococcus pneumoniae is the most common cause of pneumonia in children and the number of antimicrobial-resistant cases of *S. pneumoniae* has increased globally. The situation tends to the worst due to limited medication for acute and chronic illnesses (Yang et al., 2019). Recently, computational methods gained more attention for the development of numerous alternative approaches for treating the resistant pathogens (Boeckmann et al., 2003). The subtractive genomics has been widely applied on various pathogens for the prediction and identification of therapeutic targets. Despite the methodological advancements, the high throughput experimental results are yet not available for the majority of pathogens. As a result, the efforts to find essential drug targets now mostly rely on bioinformatics based predictions (Uddin and Rafi, 2017). *In silico* based subtractive genomic analysis has been widely applied for strain-specific drug target identifications, particularly for the resistant pathogens (Uddin et al., 2019).

In the current study, a subtractive genomics based metabolic pathways analysis was applied for the prediction of drug targets against the clinically relevant *S. pneumoniae* serotype 14. In the present study, metabolic pathway analysis of *S. pneumoniae* against human host was performed that resulted in the prediction of 25 metabolic pathways uniquely present in *S. pneumoniae*. The proteins involved in these pathways were retrieved and

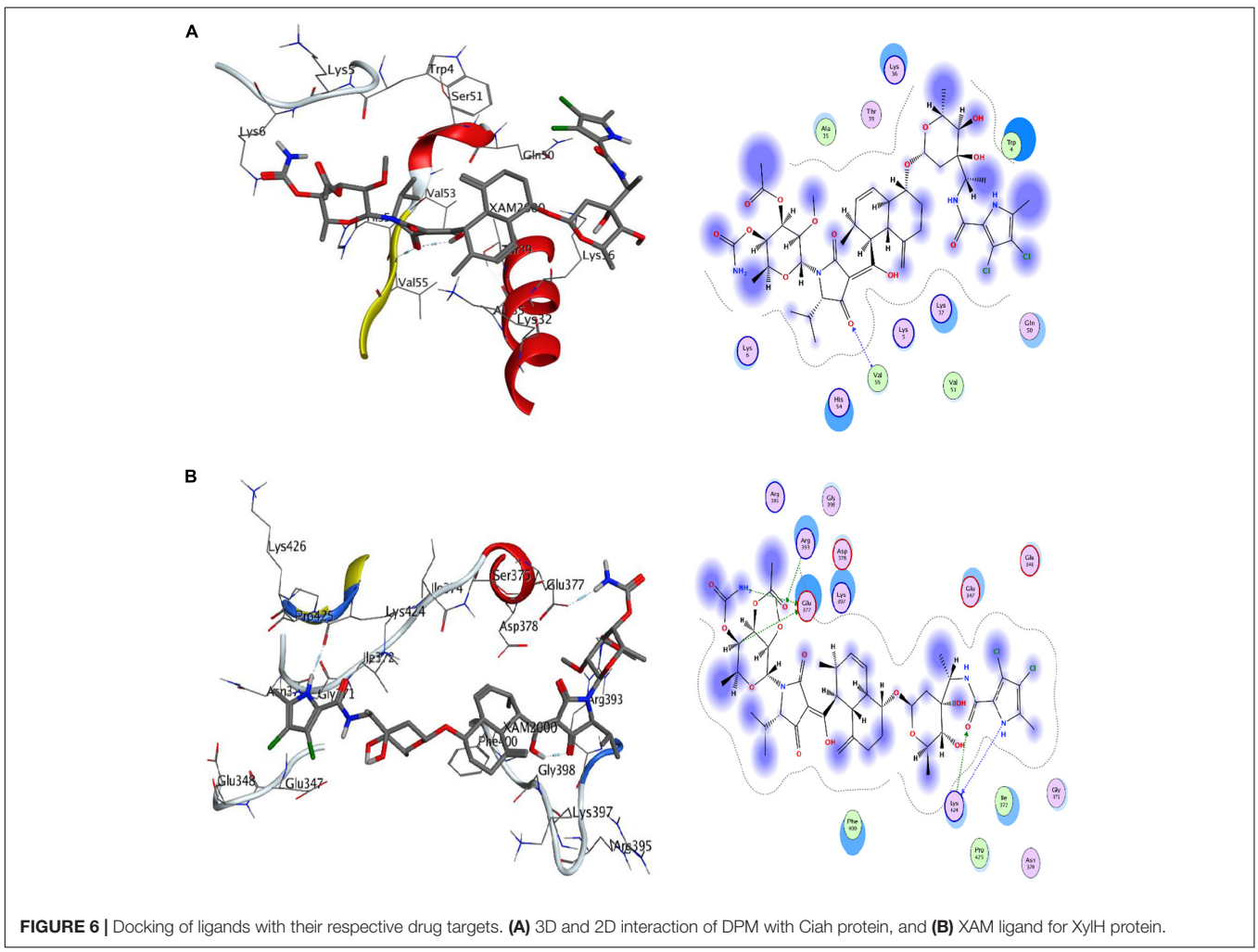

FIGURE 6 | Docking of ligands with their respective drug targets. **(A)** 3D and 2D interaction of DPM with Ciah protein, and **(B)** XAM ligand for XylH protein.

TABLE 6 | Post-docking interactional analysis of XAM and DPM with XylH and CiaH protein.

Compounds	Ligand	Receptor	Interaction	Distance	E (kcal/mol)	Binding affinity (kcal/mol)
XAM	C4 1	OE2 GLU377	H-donor	3.21	−0.7	−7.59
	NAV 20	O LYS424	H-donor	2.98	−4.5	
	NCA 115	OE2 GLU377	H-donor	3.09	−5.0	
	OAQ 24	CB LYS424	H-acceptor	3.54	−0.7	
	OBY 120	NH2 ARG393	H-acceptor	3.45	−0.6	
DPM	OBI 88	N VAL55	H-acceptor	3.11	−2.6	−5.09

further studied for homologous proteins identification and also to identify proteins that are only found in pathogens. The computational subtractive genomics is a powerful tool to prioritize those proteins that are essential and play a role in the pathogenicity. However, the unique pathways found exclusively in bacteria may still share the common proteins that are found in the bacterial pathogens as well as in human host. Similarly, there are common pathways between the pathogen and human host that may also have unique proteins and those unique proteins may also act as drug targets. That common proteins may still be looked for and studied to find the drug targets since the mere similarity among proteins is not the only criterion to exclude them from the search of drug targets. There are many examples of successful drugs which target common proteins of the pathogens that are shared by the human host. One such drug target is a bacterial enzyme known as *Pantothenate synthetase* that has a homolog present in human host, however, with low similarity (∼40%) and it is safely considered as a drug target for numerous other bacterial pathogens including *M. tuberculosis* (Suresh et al., 2020; Rahman et al., 2021). It is the matter of focus of the current study that we considered the unique and non-homologous proteins only from the bacterial pathogen to proceed in our work pipeline. This could be considered as a limitation of the current applied protocol. However, one may explore the unique pathways for common proteins and also the common pathways for the unique proteins depending upon the similarity thresholds.

Furthermore, the filtration for essential proteins/genes were performed by the DEG database. The essential genes from the DEG database are identified by *in vitro* rich medium for the growth of the bacteria, therefore, it may result in identifying those proteins which may not be essential during the *in vivo* (i.e., in the host) infection phase. This is the major limitation of working with the DEG. Even with this limitation the DEG has been well studied in literature examples and produced the reliable results that led to the identification of novel *in vivo* drug targets (Umland et al., 2012).

In the next step, the drug target-like proteins were searched with the help of DrugBank database. Consequently, a total of 47 essential druggable and unique proteins were prioritized as potential drug targets against *S. pneumoniae* serotype 14. Finally, only two enzymes out of the 47 shortlisted proteins were selected for further ligand discovery as potential drug candidates against *S. pneumonia*. The selected two proteins are 4-oxalocrotonate tautomerase and sensor histidine kinases. These two proteins were selected because of their role in benzoate degradation and two-component system as both are critical for the growth and survival of the bacteria (Gupta et al., 2020). Though the focus of the current study is on the above mentioned two proteins, the other proteins can also be equally considered for further study to characterize them as potential drug targets against which lead compounds can be developed as potent drugs.

The 4-oxalocrotonate tautomerase enzyme is involved in benzonate and xylene degradation pathways which is unique to *S. pneumonia*. The benzonate and xylene degradation pathways degrade the aromatic compounds and amino acids into essential hydrocarbons to fulfill its carbon and energy requirements (Medellin et al., 2020; Baas et al., 2021). On the other hand, the sensor histidine kinase is involved in the Two-Component System (TCS) of *S. pneumonia* and regulates certain physiological conditions. The TCS is a basic signaling mechanism that allows bacteria to detect environmental signals and develop an appropriate stress response by expressing genes that allow for environmental adaptability. The function of these proteins elaborate their importance and hence can be considered as potential drug targets (Rosales-Hurtado et al., 2020). The shortlisted proteins were modeled through modeler and validated through PROCHECK, PSIPRED, and ProSA. Furthermore, the inhibitors, i.e., XAM (against CiaH) and DPM (for XylH), were predicted against through probis server and were screened using AutoDock tool. Subsequently, the interaction analysis was performed through MOE tool. These compounds showed favorable potency against each respective protein with the estimated binding affinities of –5.09 kcal/mol for XAM against CiaH and –7.59 kcal/mol of DPM against XylH. The results we achieved in the current study are presented here and are open for the experimental validation of compounds against respective drug targets in future by the scientific community.

The above study predicted the essential proteins that may most likely act as potential drug targets due to their involvement in essential pathways of *S. pneumoniae* (Lo et al., 2019). Additionally, the metabolic pathways associated with the cytoplasmic proteins may be used to formulate the drug targets, whereas the membrane-associated proteins may be used to formulate peptide vaccines (Masomian et al., 2020). All of the remaining non-homologous essential proteins, on the other hand, might be good therapeutic targets. The vaccines and therapies that target the activities of these proteins may eventually lead to the destruction and eradication of pathogen from the respective hosts. The current study covered all important

and potent pharmacological targets in *S. pneumoniae* that will certainly aid future researchers in developing effective treatment or vaccine candidates. Therefore, various other computational approaches along with this approach in collaboration with experimental researchers could be used in the future to produce potential therapeutic strategy not only against *S. pneumoniae* but for other pathogens too.

CONCLUSION

The analysis of the genome and proteome of many pathogens has aided the prediction of drug targets. In the current study, a subtractive genomic-based metabolic pathway analysis approach was applied to predict non-homologous essential druggable proteins against *S. pneumoniae* participating in the unique metabolic pathway. However, all the non-homologous essential proteins may also act as promising drug targets. Targeting these protein's functions through novel drug candidates may lead to the destruction and the eradication of pathogen from the respective host. The analysis and results of the study covered all essential, potent drug targets in *S. pneumoniae* and thus it may facilitate future researchers to develop effective drug compounds and vaccines against strain-specific *S. pneumoniae* serotype 14.

DATA AVAILABILITY STATEMENT

The original contributions presented in the study are included in the article/**Supplementary Material**, further inquiries can be directed to the corresponding authors.

AUTHOR CONTRIBUTIONS

RU, AK, and AA-H conceived and designed the study. KK and KJ performed data collection and analysis and contributed to drafting the manuscript. RU provided technical and material support and supervised the study. All authors approved the final version of the manuscript.

FUNDING

This project was supported by grant from The Oman Research Council (TRC) through the funded project (BFP/RGP/CBS/19/220) and Pakistan Science Foundation under research support grant # PSF/Res/S-ICCBS/Med (431).

ACKNOWLEDGMENTS

We would like to acknowledge the Pakistan Science Foundation for providing financial support under research support grant # PSF/Res/S-ICCBS/Med (431). We would also like to thank the University of Nizwa for the generous support of this project and Oman Research Council (TRC) through the funded project (BFP/RGP/HSS/19/198). We thank technical staff for assistance.

SUPPLEMENTARY MATERIAL

The Supplementary Material for this article can be found online at: https://www.frontiersin.org/articles/10.3389/fmicb.2021.796363/full#supplementary-material

REFERENCES

Anis Ahamed, N., Panneerselvam, A., Arif, I. A., Syed Abuthakir, M. H., Jeyam, M., Ambikapathy, V., et al. (2021). Identification of potential drug targets in human pathogen *Bacillus cereus* and insight for finding inhibitor through subtractive proteome and molecular docking studies. *J. Infect. Public Health* 14, 160–168. doi: 10.1016/j.jiph.2020.12.005

Apweiler, R., Bairoch, A., Wu, C. H., Barker, W. C., Boeckmann, B., Ferro, S., et al. (2021). UniProt: the universal protein knowledgebase in 2021. *Nucleic Acids Res.* 49, D480–D489. doi: 10.1093/nar/gkaa1100

Baas, B.-J., Medellin, B. P., Levieux, J. A., Erwin, K., Lancaster, E. B., Johnson, W. H. Jr., et al. (2021). Kinetic and structural analysis of two linkers in the tautomerase superfamily: analysis and implications. *Biochemistry* 60, 1776–1786. doi: 10.1021/acs.biochem.1c00220

Boeckmann, B., Bairoch, A., Apweiler, R., Blatter, M.-C., Estreicher, A., Gasteiger, E., et al. (2003). The SWISS-PROT protein knowledgebase and its supplement TrEMBL in 2003. *Nucleic Acids Res.* 31, 365–370. doi: 10.1093/nar/gkg095

Bouskraoui, M., Soraa, N., Zahlane, K., Arsalane, L., Doit, C., Mariani, P., et al. (2011). Étude du portage rhinopharyngé de *Streptococcus pneumoniae* et de sa sensibilité aux antibiotiques chez les enfants en bonne santé âgés de moins de 2 ans dans la région de Marrakech (Maroc). *Arch. Pediatr.* 18, 1265–1270. doi: 10.1016/j.arcped.2011.08.028

Buchan, D. W., and Jones, D. T. (2019). The PSIPRED protein analysis workbench: 20 years on. *Nucleic Acids Res.* 47, W402–W407. doi: 10.1093/nar/gkz297

Chiba, N., Morozumi, M., Shouji, M., Wajima, T., Iwata, S., Ubukata, K., et al. (2014). Changes in capsule and drug resistance of pneumococci after introduction of PCV7, Japan, 2010–2013. *Emerg. Infect. Dis.* 20, 1132–1139. doi: 10.3201/eid2007.131485

Cilloniz, C., Martin-Loeches, I., Garcia-Vidal, C., San Jose, A., and Torres, A. (2016). Microbial etiology of pneumonia: epidemiology, diagnosis and resistance patterns. *Int. J. Mol. Sci.* 17:2120. doi: 10.3390/ijms17122120

Deng, J., Deng, L., Su, S., Zhang, M., Lin, X., Wei, L., et al. (2011). Investigating the predictability of essential genes across distantly related organisms using an integrative approach. *Nucleic Acids Res.* 39, 795–807. doi: 10.1093/nar/gkq784

Ediriweera, D. S., Kasturiratne, A., Pathmeswaran, A., Gunawardena, N. K., Wijayawickrama, B. A., Jayamanne, S. F., et al. (2016). Mapping the risk of snakebite in Sri Lanka-a national survey with geospatial analysis. *PLoS Negl. Trop. Dis.* 10:e0004813. doi: 10.1371/journal.pntd.0004813

Elflein, J. (2021). *COVID-19, Pneumonia, and Influenza Deaths Reported in the U.S. November* 5, 2021. Available online at: https://www.mckinsey.com/industries/healthcare-systems-and-services/our-insights/when-will-the-covid-19-pandemic-end (accessed December 19, 2021).

Enright, M. C., and Spratt, B. G. (1998). A multilocus sequence typing scheme for *Streptococcus pneumoniae*: identification of clones associated with serious invasive disease. *Microbiology* 144, 3049–3060. doi: 10.1099/00221287-144-11-3049

Fair, R., and Tor, Y. (2014). Antibiotics and bacterial resistance in the 21st century. *Perspect. Med. Chem.* 6, 25–64. doi: 10.4137/PMC.S14459

Fenoll, A., Granizo, J., Aguilar, L., Giménez, M., Aragoneses-Fenoll, L., Hanquet, G., et al. (2009). Temporal trends of invasive *Streptococcus pneumoniae* serotypes and antimicrobial resistance patterns in Spain from 1979 to 2007. *J. Clin. Microbiol.* 47, 1012–1020. doi: 10.1128/JCM.01454-08

Geno, K. A., Gilbert, G. L., Song, J. Y., Skovsted, I. C., Klugman, K. P., Jones, C., et al. (2015). Pneumococcal capsules and their types: past, present, and future. *Clin. Microbiol. Rev.* 28, 871–899. doi: 10.1128/cmr.00024-15

Gupta, S. R., Gupta, E., Ohri, A., Shrivastava, S. K., Kachhwaha, S., Sharma, V., et al. (2020). Comparative proteome analysis of *Mycobacterium tuberculosis* Strains-H37Ra, H37Rv, CCDC5180, and CAS/NITR204: a step forward to identify novel drug targets. *Lett. Drug Des. Discov.* 17, 1422–1431.

Hakenbeck, R., Brückner, R., Denapaite, D., and Maurer, P. (2012). Molecular mechanisms of β-lactam resistance in *Streptococcus pneumoniae*. *Future Microbiol.* 7, 395–410. doi: 10.2217/fmb.12.2

Henriques, B., Kalin, M., Örtqvist, Å., Liljequist, B. O., Almela, M., Marrie, T. J., et al. (2000). Molecular epidemiology of *Streptococcus pneumoniae* causing invasive disease in 5 countries. *J. Infect. Dis.* 182, 833–839. doi: 10.1086/315761

Hu, S., Shi, Q., Song, S., Du, L., He, J., Chen, C.-I., et al. (2014). Estimating the cost-effectiveness of the 7-valent pneumococcal conjugate vaccine in Shanghai, China. *Value Health Reg. Issues* 3, 197–204. doi: 10.1016/j.vhri.2014.04.007

Kaiser, S., Hoppstädter, L. M., Bilici, K., Heieck, K., and Brückner, R. (2020). Control of acetyl phosphate-dependent phosphorylation of the response regulator CiaR by acetate kinase in *Streptococcus pneumoniae*. *Microbiology* 166, 411–421. doi: 10.1099/mic.0.000894

Kanehisa, M., and Goto, S. (2000). KEGG: kyoto encyclopedia of genes and genomes. *Nucleic Acids Res.* 28, 27–30.

Khalid, Z., Ahmad, S., Raza, S., and Azam, S. S. (2018). Subtractive proteomics revealed plausible drug candidates in the proteome of multi-drug resistant *Corynebacterium diphtheriae*. *Meta Gene* 17, 34–42.

Konc, J., and Janežič, D. (2017). ProBiS tools (algorithm, database, and web servers) for predicting and modeling of biologically interesting proteins. *Prog. Biophys. Mol. Biol.* 128, 24–32. doi: 10.1016/j.pbiomolbio.2017.02.005

Konc, J., Miller, B. T., Štular, T., Lešnik, S., Woodcock, H. L., Brooks, B. R., et al. (2015). ProBiS-CHARMMing: web Interface for Prediction and Optimization of Ligands in Protein Binding Sites. *J. Chem. Inf. Model.* 55, 2308–2314. doi: 10.1021/acs.jcim.5b00534

Laskowski, R., Macarthur, M., and Thornton, J. (2006). PROCHECK: validation of protein structure coordinates. *J. Biol. Macromol.* doi: 10.1107/9780955360206000882 [Epub ahead of print].

Linares, J., Ardanuy, C., Pallares, R., and Fenoll, A. (2010). Changes in antimicrobial resistance, serotypes and genotypes in *Streptococcus pneumoniae* over a 30-year period. *Clin. Microbiol. Infect.* 16, 402–410. doi: 10.1111/j.1469-0691.2010.03182.x

Liu, X., Gallay, C., Kjos, M., Domenech, A., Slager, J., Van Kessel, S. P., et al. (2017). High-throughput CRISPRi phenotyping identifies new essential genes in *Streptococcus pneumoniae*. *Mol. Syst. Biol.* 13:931. doi: 10.15252/msb.20167449

Liu, X., Kimmey, J. M., Matarazzo, L., De Bakker, V., Van Maele, L., Sirard, J. C., et al. (2021). Exploration of Bacterial Bottlenecks and *Streptococcus pneumoniae* Pathogenesis by CRISPRi-Seq. *Cell Host Microbe* 29, 107–120.e6. doi: 10.1016/j.chom.2020.10.001

Lo, S. W., Gladstone, R. A., Van Tonder, A. J., Lees, J. A., Du Plessis, M., Benisty, R., et al. (2019). Pneumococcal lineages associated with serotype replacement and antibiotic resistance in childhood invasive pneumococcal disease in the post-PCV13 era: an international whole-genome sequencing study. *Lancet* 19, 759–769. doi: 10.1016/S1473-3099(19)30297-X

Lodha, R., Kabra, S. K., and Pandey, R. M. (2013). Antibiotics for community-acquired pneumonia in children. *Cochrane Database Syst. Rev.* 2013:CD004874.

Luo, H., Lin, Y., Liu, T., Lai, F.-L., Zhang, C.-T., Gao, F., et al. (2021). DEG 15, an update of the Database of Essential Genes that includes built-in analysis tools. *Nucleic Acids Res.* 49, D677–D686. doi: 10.1093/nar/gkaa917

Masomian, M., Ahmad, Z., Ti Gew, L., and Poh, C. L. (2020). Development of next generation *Streptococcus pneumoniae* vaccines conferring broad protection. *Vaccines* 8:132. doi: 10.3390/vaccines8010132

Medellin, B. P., Lancaster, E. B., Brown, S. D., Rakhade, S., Babbitt, P. C., Whitman, C. P., et al. (2020). Structural Basis for the Asymmetry of a 4-Oxalocrotonate Tautomerase Trimer. *Biochemistry* 59, 1592–1603. doi: 10.1021/acs.biochem.0c00211

Möglich, A. (2019). Signal transduction in photoreceptor histidine kinases. *Protein Sci.* 28, 1923–1946. doi: 10.1002/pro.3705

Peters, K., Schweizer, I., Hakenbeck, R., and Denapaite, D. (2021). New Insights into Beta-Lactam Resistance of *Streptococcus pneumoniae*: serine Protease HtrA Degrades Altered Penicillin-Binding Protein 2x. *Microorganisms* 9:1685. doi: 10.3390/microorganisms9081685

Rahman, N., Shah, M., Muhammad, I., Khan, H., and Imran, M. (2021). Genome-wide core proteome analysis of *Brucella melitensis* strains for potential drug target prediction. *Mini Rev. Med. Chem.* 21, 2778–2787. doi: 10.2174/1389557520666200707133347

Rosales-Hurtado, M., Meffre, P., Szurmant, H., and Benfodda, Z. (2020). Synthesis of histidine kinase inhibitors and their biological properties. *Med. Res. Rev.* 40, 1440–1495. doi: 10.1002/med.21651

Schwartz, A. S., Yu, J., Gardenour, K. R., Finley, R. L. Jr., and Ideker, T. (2009). Cost-effective strategies for completing the interactome. *Nat. Methods* 6, 55–61. doi: 10.1038/nmeth.1283

Schweizer, I., Blättner, S., Maurer, P., Peters, K., Vollmer, D., Vollmer, W., et al. (2017). New aspects of the interplay between penicillin binding proteins, murM, and the two-component system CiaRH of penicillin-resistant *Streptococcus pneumoniae* serotype 19A isolates from Hungary. *Antimicrob. Agents Chemother.* 61:e00414-17. doi: 10.1128/AAC.00414-17

Singh, A. P., Mishra, M., Chandra, A., and Dhawan, S. (2011). Graphene oxide/ferrofluid/cement composites for electromagnetic interference shielding application. *Nanotechnology* 22:465701. doi: 10.1088/0957-4484/22/46/465701

Suresh, A., Srinivasarao, S., Khetmalis, Y. M., Nizalapur, S., Sankaranarayanan, M., and Sekhar, K. V. G. C. (2020). Inhibitors of pantothenate synthetase of *Mycobacterium tuberculosis*–a medicinal chemist perspective. *RSC Adv.* 10, 37098–37115. doi: 10.1039/d0ra07398a

Szklarczyk, D., Gable, A. L., Nastou, K. C., Lyon, D., Kirsch, R., Pyysalo, S., et al. (2021). The STRING database in 2021: customizable protein–protein networks, and functional characterization of user-uploaded gene/measurement sets. *Nucleic Acids Res.* 49, D605–D612.

Tanchuk, V. Y., Tanin, V. O., Vovk, A. I., and Poda, G. (2016). A new, improved hybrid scoring function for molecular docking and scoring based on AutoDock and AutoDock Vina. *Chem. Biol. Drug Des.* 87, 618–625. doi: 10.1111/cbdd.12697

Tatsuno, I., Isaka, M., Okada, R., Zhang, Y., and Hasegawa, T. (2014). Relevance of the two-component sensor protein CiaH to acid and oxidative stress responses in *Streptococcus pyogenes*. *BMC Res. Notes* 7:189. doi: 10.1186/1756-0500-7-189

Uddin, R., and Rafi, S. (2017). Structural and functional characterization of a unique hypothetical protein (WP_003901628. 1) of *Mycobacterium tuberculosis*: a computational approach. *Med. Chem. Res.* 26, 1029–1041. doi: 10.1007/s00044-017-1822-0

Uddin, R., Siddiqui, Q. N., Sufian, M., Azam, S. S., and Wadood, A. (2019). Proteome-wide subtractive approach to prioritize a hypothetical protein of XDR-*Mycobacterium tuberculosis* as potential drug target. *Genes Genomics* 41, 1281–1292. doi: 10.1007/s13258-019-00857-z

Umland, T. C., Schultz, L. W., Macdonald, U., Beanan, J. M., Olson, R., and Russo, T. A. (2012). *In vivo*-validated essential genes identified in *Acinetobacter baumannii* by using human ascites overlap poorly with essential genes detected on laboratory media. *mBio* 3:e00113-12. doi: 10.1128/mBio.00113-12

van Diemen, P. M., Leneghan, D. B., Brian, I. J., Miura, K., Long, C. A., Milicic, A., et al. (2017). The *S. aureus* 4-oxalocrotonate tautomerase SAR1376 enhances immune responses when fused to several antigens. *Sci. Rep.* 7:1745. doi: 10.1038/s41598-017-01421-z

van Opijnen, T., Bodi, K. L., and Camilli, A. (2009). Tn-seq: high-throughput parallel sequencing for fitness and genetic interaction studies in microorganisms. *Nat. Methods* 6, 767–772. doi: 10.1038/nmeth.1377

Velikova, N., Fulle, S., Manso, A. S., Mechkarska, M., Finn, P., Conlon, J. M., et al. (2016). Putative histidine kinase inhibitors with antibacterial effect against multi-drug resistant clinical isolates identified by *in vitro* and *in silico* screens. *Sci. Rep.* 6:26085. doi: 10.1038/srep26085

Watt, J. P., Wolfson, L. J., O'brien, K. L., Henkle, E., Deloria-Knoll, M., Mccall, N., et al. (2009). Burden of disease caused by *Haemophilus influenzae* type b in children younger than 5 years: global estimates. *Lancet* 374, 903–911. doi: 10.1016/S0140-6736(09)61203-4

Wiederstein, M., and Sippl, M. J. (2007). ProSA-web: intercation web service for the recognition of errors in three-dimensional structure of proteins. *Nucleic Acids Res.* 35, W407–W410. doi: 10.1093/nar/gkm290

Wishart, D. S., Feunang, Y. D., Guo, A. C., Lo, E. J., Marcu, A., Grant, J. R., et al. (2018). DrugBank 5.0: a major update to the DrugBank database for 2018. *Nucleic Acids Res.* 46, D1074–D1082. doi: 10.1093/nar/gkx1037

Xie, Q., Wiedmann, M. M., Zhao, A., Pagan, I. R., Novick, R. P., Suga, H., et al. (2020). Discovery of quorum quenchers targeting the membrane-embedded sensor domain of the *Staphylococcus aureus* receptor histidine kinase, AgrC. *Chem. Commun.* 56, 11223–11226. doi: 10.1039/d0cc04873a

Yang, T.-I., Chang, T.-H., Lu, C.-Y., Chen, J.-M., Lee, P.-I., Huang, L.-M., et al. (2019). Mycoplasma pneumoniae in pediatric patients: Do macrolide-resistance and/or delayed treatment matter? *J. Microbiol. Immunol. Infect.* 52, 329–335. doi: 10.1016/j.jmii.2018.09.009

Yu, N. Y., Wagner, J. R., Laird, M. R., Melli, G., Rey, S., Lo, R., et al. (2010). PSORTb 3.0: improved protein subcellular localization prediction with refined localization subcategories and predictive capabilities for all prokaryotes. *Bioinformatics* 26, 1608–1615. doi: 10.1093/bioinformatics/btq249

Conflict of Interest: The authors declare that the research was conducted in the absence of any commercial or financial relationships that could be construed as a potential conflict of interest.

frontiers in Microbiology

ORIGINAL RESEARCH
published: 25 March 2022
doi: 10.3389/fmicb.2022.845500

Phage-Derived Depolymerase as an Antibiotic Adjuvant Against Multidrug-Resistant *Acinetobacter baumannii*

Xi Chen[1], Miao Liu[1], Pengfei Zhang[2], Miao Xu[2], Weihao Yuan[3], Liming Bian[3], Yannan Liu[4], Jiang Xia[1]* and Sharon S. Y. Leung[2]**

[1] Department of Chemistry, The Chinese University of Hong Kong, Sha Tin, Hong Kong SAR, China, [2] School of Pharmacy, The Chinese University of Hong Kong, Sha Tin, Hong Kong SAR, China, [3] Department of Biomedical Engineering, The Chinese University of Hong Kong, Sha Tin, Hong Kong SAR, China, [4] Emergency Medicine Clinical Research Center, Beijing Chao-Yang Hospital, Capital Medical University, Beijing, China

Bacteriophage-encoded depolymerases are responsible for degrading capsular polysaccharides (CPS), lipopolysaccharides (LPS), and exopolysaccharides (EPS) of the host bacteria during phage invasion. They have been considered as promising antivirulence agents in controlling bacterial infections, including those caused by multidrug-resistant (MDR) bacteria. This feature inspires hope of utilizing these enzymes to disarm the polysaccharide capsules of the bacterial cells, which then strengthens the action of antibiotics. Here we have identified, cloned, and expressed a depolymerase Dpo71 from a bacteriophage specific for the gram-negative bacterium *Acinetobacter baumannii* in a heterologous host *Escherichia coli*. Dpo71 sensitizes the MDR *A. baumannii* to the host immune attack, and also acts as an adjuvant to assist or boost the action of antibiotics, for example colistin. Specifically, Dpo71 at 10 μg/ml enables a complete bacterial eradication by human serum at 50% volume ratio. A mechanistic study shows that the enhanced bactericidal effect of colistin is attributed to the improved outer membrane destabilization capacity and binding rate to bacteria after stripping off the bacterial capsule by Dpo71. Dpo71 inhibits biofilm formation and disrupts the pre-formed biofilm. Combination of Dpo71 could significantly enhance the antibiofilm activity of colistin and improve the survival rate of *A. baumannii* infected *Galleria mellonella*. Dpo71 retains the strain-specificity of the parent phage from which Dpo71 is derived: the phage-sensitive *A. baumannii* strains respond to Dpo71 treatment, whereas the phage-insensitive strains do not. In summary, our work demonstrates the feasibility of using recombinant depolymerases as an antibiotic adjuvant to supplement the development of new antibacterials and to battle against MDR pathogens.

Keywords: depolymerase, exopolysaccharide degrading enzymes, antibiotic adjuvant, serum killing, biofilm prevention and degradation

OPEN ACCESS

Edited by:
Benjamin Andrew Evans, University of East Anglia, United Kingdom

Reviewed by:
J. Mark Sutton, Public Health England, United Kingdom
Qingquan Chen, Stanford University, United States

***Correspondence:**
Yannan Liu
yannan_liu@foxmail.com
Jiang Xia
jiangxia@cuhk.edu.hk
Sharon S. Y. Leung
sharon.leung@cuhk.edu.hk

Specialty section:
This article was submitted to Antimicrobials, Resistance and Chemotherapy, a section of the journal Frontiers in Microbiology

Received: *29 December 2021*
Accepted: *08 February 2022*
Published: *25 March 2022*

Citation:
Chen X, Liu M, Zhang P, Xu M, Yuan W, Bian L, Liu Y, Xia J and Leung SSY (2022) Phage-Derived Depolymerase as an Antibiotic Adjuvant Against Multidrug-Resistant Acinetobacter baumannii. Front. Microbiol. 13:845500. doi: 10.3389/fmicb.2022.845500

INTRODUCTION

Carbapenem-resistant *Acinetobacter baumannii* was identified as the number one priority pathogen by World Health Organization [WHO] (2017) and Centers for Disease Control and Prevention [CDC] (2019). *A. baumannii* infection is associated with frequent and hard-to-treat infections, such as pneumonia, bacteremia, urinary tract infections, meningitis, and wound

infections (Peleg et al., 2008). In the past decades, outbreaks of *A. baumannii* resistant to the last-resort antibiotics, such as colistin, are increasingly reported (Pendleton et al., 2013; Fair and Tor, 2014). Alarmingly, the development of novel antibiotics have experienced significant setbacks in recent years (World Health Organization [WHO], 2019), and thereby the field is urgently calling for novel antibacterial agents to address the clinical challenges of *A. baumannii* associated infections.

Bacteriophages (phages), natural co-evolving bacteria killers, are being revitalized to combat multidrug-resistant (MDR) bacteria (Hampton et al., 2020). Although regarded as a promising alternative to conventional antibiotics, phage therapy faces challenges as very few completed clinical trials confirmed the efficacy (Pirnay and Kutter, 2020). The narrow host range and the development of phage-resistance could be the major factors for such failures. The viral nature of phage may also be unacceptable to most clinicians and the general public (Verbeken et al., 2014a,b, 2016). Alternatively, researchers explore the potential of phage-encoded enzymes, including the peptidoglycan hydrolases, polysaccharide depolymerases, and holins, as novel antibacterial agents, drawing inspiration from the life cycle of phage. In contrast to phage, phage-encoded enzymes, as therapeutic proteins without replicating capability are more manageable and acceptable (Pires et al., 2016; Latka et al., 2017; Knecht et al., 2020; Lai et al., 2020).

Phage-encoded depolymerases are polysaccharide hydrolases or lyases responsible for stripping bacterial polysaccharides, including exopolysaccharides (EPS), capsular polysaccharides (CPS), and lipopolysaccharide (LPS), to facilitate the parent phage to inject its DNA materials into the bacterial host (Pires et al., 2016; Knecht et al., 2020). Distinct from other phage-encoded enzymes, depolymerases do not lyse bacterial cells directly. Instead, they disintegrate the CPS of bacteria to make them susceptible to host immune attack and antibacterial treatments (Majkowska-Skrobek et al., 2018). Recombinant depolymerases have been shown to protect mice from fatal systemic bacterial infections (Lin et al., 2014; Chen et al., 2020) and to disrupt biofilms for enhanced antimicrobial activity (Hughes et al., 1998; Gutiérrez et al., 2015; Hernandez-Morales et al., 2018; Mi et al., 2019; Topka-Bielecka et al., 2021).

Combined administration of depolymerases and antibiotics will produce superior antibacterial efficacy – expected but not yet well-supported by experiments. Bansal et al. (2014) were the first to report the adjuvant effect of a depolymerase derived from *Aeromonas punctata* (a facultative anaerobic gram-negative bacterium) with gentamicin in treating mice infected with non-lethal dose of *K. pneumoniae*. Intranasal administration and intravenous administration of the combination for lung infection and systemic infection, respectively, both reduced bacterial counts significantly more than the single-agent treatments. They attributed the improved bacterial killing efficiency to the enhanced bacterial susceptibility toward gentamicin after the bacteria were decapsulated by the depolymerase. Depolymerases also effectively dispersed the EPS matrix in *K. pneumoniae* biofilms to facilitate the penetration of gentamicin (Bansal et al., 2015). A similar synergy was also observed in the treatment of *K. pneumoniae* biofilms using the Dep42 depolymerase and polymyxin B (Wu et al., 2019). On the contrary, Latka and Drulis-Kawa (2020) showed that the KP34p57 depolymerase had no impact on the activity of ciprofloxacin but could significantly enhance the antibiofilm efficiency of non-depolymerase-producing phages. Depolymerase could also enhance the antibiofilm efficacy of a phage-encoded antibacterial enzyme endolysin (Olsen et al., 2018).

Currently, a few *A. baumannii* depolymerases have been identified (Hernandez-Morales et al., 2018; Liu et al., 2019a; Oliveira et al., 2019a,b; Wang et al., 2020; Shahed-Al-Mahmud et al., 2021). Whether they would work with antibiotics in controlling biofilm-associated infections, like those observed for *K. pneumoniae*, remains questionable. In the present study, the combinational effects of a depolymerase Dpo71 encoded by a lytic *A. baumannii* phage, vB_AbaM-IME-AB2 (IME-AB2 in short) (Peng et al., 2014; Liu et al., 2016), with serum or colistin in targeting MDR *A. baumannii* are evaluated.

MATERIALS AND METHODS

Bacterial Strains, Culture Condition and Materials

All bacterial strains used in this study are listed in **Supplementary Table 1**. The multidrug-resistant *A. baumannii* strain MDR-AB2, isolated from the sputum samples of a patient with pneumonia at PLA Hospital 307 was supplied by the Beijing Institute of Microbiology and Epidemiology (Peng et al., 2014). The antibiotic susceptibility profile of this strain was determined, which confirmed its resistance to most of the commonly used antibiotics (Peng et al., 2014). All the bacterial strains were grown in Nutrient Broth (NB) medium at 37°C. Colistin was bought from J&K Scientific (Beijing, China) (Cat No. 437689, >19,000 IU/mg).

Plasmid Construction

The plasmid was constructed using standard cloning methods. Genes encoded Dpo71 (Protein id: YP_009592222.1) was synthesized by BGI (Shenzhen, China) and cloned into the pET28a plasmid using *Bam*HI and *Xho*I site and the protein sequence was listed in supporting information (**Supplementary Table 2**).

Recombinant Proteins Expression and Purification

The constructed plasmid was transformed into *Escherichia coli* BL21 (DE3) cells and colonies were grown overnight at 37°C in LB media supplemented with 50 μg/ml kanamycin. The start culture was grown overnight, and then was used to inoculate LB media supplemented with antibiotics at 1:100 ratio. The cell culture was grown at 37°C to reach OD_{600} ∼0.6 before 0.25 mM IPTG was added to induce protein expression. After grown at 16°C overnight, cells were harvested for protein purification. The enzyme was purified by nickel affinity chromatography using HisTrap™ HP column (GE Healthcare, Chicago, United States). Briefly, harvested cells were re-suspended in lysis buffer

containing 10 mM imidazole, 50 mM phosphate/300 mM sodium chloride (pH 8.0). The cell suspension was lysed by sonication and centrifuged. The supernatant was collected, filtered, and loaded into the column. The bound protein was eluted by imidazole gradient from 10 to 500 mM. Pure protein fractions eluted with imidazole gradient were collected and exchanged with PBS (pH 7.4). After purification, all proteins were flash frozen under liquid nitrogen and stored at −80°C. Protein concentration was determined using NanoDrop (Thermo Fisher Scientific, Massachusetts, United States).

Size Exclusion Chromatography Analysis

Purified depolymerase Dpo71 as well as two gel filtration markers with molecular weight of 150 and 200 kDa (MWGF200, Sigma-Aldrich, Missouri, United States) were used for analysis, performed on an AKTA FPLC instrument installed with a Superose 6 Increase prepacked column (GE Healthcare, Illinois, United States). Proteins were filtered with 0.2 μm membrane and injected into the FPLC system equilibrated with PBS.

Circular Dichroism Spectroscopy

Far-UV CD spectroscopy is commonly used to analyze the secondary structures of proteins with a Jasco J810 CD spectrometer (Oliveira et al., 2020). The spectrum measurement was performed with the Dpo71 of 0.30 mg/ml in PBS buffer (pH 7.4) using a wavelength range from 190 to 260 nm. Thermal denaturation with 1°C/min increments was also employed to measure the secondary structure unfolding at 215 nm, from 20 to 90°C. The melting curves were fitted into a Boltzmann sigmoidal function.

Spot Test Assay

The depolymerase activity of Dpo71 was qualitatively assayed by a modified single-spot assay. In brief, 100 μl of MDR-AB2 overnight bacterial culture was added to 5 ml of molten soft nutrient agar (0.7%) and incubated at 37°C for 3 h to form a bacterial lawn in plates. The purified enzyme was serially diluted, then 5 μl of each dilution (from 0.001 to 10 μg) was dropped onto the MDR-AB2 bacterial lawn for incubation at 37°C overnight. The plates were monitored for the formation of semi-clear spots as a confirmation of the depolymerase activity.

Extraction of Bacterial Surface Polysaccharides

The bacterial polysaccharide extracts (containing both CPS and LPS) were purified, via a modified hot water-phenol method as described previously (Liu et al., 2020). Briefly, *A. baumannii* were cultured overnight in LB with 0.25% glucose. A volume of 1 ml culture was centrifuged (10,000 rpm, 5 min) and resuspended in 200 μl of double distilled water (ddH_2O). An equal volume of water-saturated phenol (pH 6.6; Thermo Fisher Scientific) was added to the bacterial suspension. The mixture was vortexed and incubated at 65°C for 20 min, centrifuged at 10,000 rpm for 10 min. Then the supernatant was extracted with chloroform to remove bacterial debris. The obtained bacterial CPS/LPS were lyophilized and stored at –20°C before use.

Quantification of Depolymerase Activity

The enzymatic activity of Dpo71 degrading the bacterial polysaccharides was determined as described in Liu et al. (2020) with minor modifications. The extracted CPS/LPS powder of *A. baumannii* was resuspended in ddH2O (1 mg/ml) and mixed with Dpo71 (30 μg/ml) or deactivated Dpo71 (by heating at 90°C for 15 min) to a final reaction volume of 200 μl. The extracted CPS/LPS or enzyme alone served as the controls. After 2 h incubation at 37°C, cetylpyridinium chloride (CPC, Sigma-Aldrich, Missouri, United States) was added to the mixture at the final concentration of 5 mg/ml, which was further incubated at room temperature for 5 min. Absorbance was measured at 600 nm using a microplate reader (Multiskan Sky, Thermo Fisher Scientific, Massachusetts, United States). The experiment was performed in triplicate and repeated at least in two independent experiments.

Influence of pH and Storage Time on the Depolymerase Activity

The extracted CPS/LPS powder was dissolved in 100 mM citric acid-Na_2HPO_4 buffer (pH 3.0–8.0) or 100 mM Glycine-NaOH buffer (pH 9.0–10.0) to a final concentration of 1 mg/ml. The CPS/LPS solutions of *A. baumannii* were mixed with Dpo71 (30 μg/ml) to a final reaction volume of 200 μl, respectively. After 2 h incubation at 37°C, the turbidity of residual CPS/LPS in various pH buffers was determined as described above. The effect of pH on the enzymatic activity was determined by this method. The storage stability of Dpo71 at 4°C was determined by measuring the CPS/LPS degradation activity after 1, 3, and 6 months storage. All assays were performed in triplicate and repeated at least in two independent experiments.

Serum Killing Assay

The serum killing assay was performed as previously described (Oliveira et al., 2020). Log phase bacteria were prepared by inoculating overnight culture at 1:100 ratio in NB medium and shaking 180 rpm for 3–4 h at 37°C. Then the cells of each culture (AB#1, AB#2, AB#3, and AB#4) were harvested via centrifugation, washed, and resuspended in PBS, then adjusted to OD_{600} = 0.6. Human serum (Sigma-Aldrich, Missouri, United States) was mixed with (i) only bacteria or (ii) bacteria and Dpo71 mixture. The Dpo71 was fixed at final concentration of 10 μg/ml and the volume ratio of human serum was set at 50%. Experiments with heat-inactivated serum (at 56°C for 30 min) were served as controls. The mixtures were then incubated at 37°C for 4 h for viable bacterial counting. Time-killing assays were also performed for the two sensitive strains (AB#1, AB#2) with the volume ratio of human serum varied from 1 to 50% and at 100 μg/ml Dpo71. Samples were withdrawn at 1, 3, 5, and 24 h for bacterial counting. All assays were performed in triplicate and repeated at least in two independent experiments.

Scanning Electron Microscopy

Scanning Electron Microscopy (SEM) was conducted as described previously (Oliveira et al., 2019a). Log phase *A. baumannii* bacteria were washed twice with PBS and resuspended in PBS buffer at OD_{600} = 0.6. Then approximately

10^8 cells were incubated at 37°C with PBS or Dpo71 for 3 h. Cells were then fixed with 2.5% (v/v) glutaraldehyde at 4°C overnight. Thereafter, the fixed cells were washed twice with PBS and dehydrated with a graded ethanol series (15, 30, 50, 70, 85, and 100% for twice). The bacterial suspensions were then spotted on glass and dried with vacuum. Finally, the samples were coated with gold and observed with Quanta 400F SEM (FEI, Oregon, United States).

Outer Membrane Permeability to 1-N-Phenylnaphthylamine Assay

For the investigation of outer membrane permeability, 1-N-phenylnaphthylamine (NPN) uptake assay was performed (Helander and Mattila-Sandholm, 2000; Chen et al., 2021). *A. baumannii* cells were grown to mid-log phase (OD_{600} = 0.6–0.8), centrifuged, and resuspended in PBS. Then PBS (control), Dpo71 (10 μg/ml), colistin (1 μg/ml) or their combination (Dpo71 + colistin) were incubated with 10^7 CFU/ml cells in the presence of 10 μM NPN for 5 min. The fluorescence intensities were recorded using a microplate reader (CLARIOstar, BMG Labtech, Ortenberg, Germany) with 350 ± 7.5 nm for excitation and 420 ± 10 nm for emission. All experiments were performed in three biological replicates and repeated at least in two independent times.

Assessment of Colistin Binding

The assay described by Campos et al. (2004) was done with minor modifications. Briefly, cells grown as described above were resuspended in PBS buffer about 10^{10} CFU/ml. Then, the bacteria were first treated with Dpo71 or PBS at 37°C for 2 h. Then 50 μg/ml colistin was added, after 5 min of incubation, the cells with the bound colistin were sedimented (12,000 g, 10 min), the supernatant was centrifuged two more times under the same conditions. Finally, the unbound colistin was quantified with HPLC. The integrated areas were recorded and the concentrations of the unbound colistin were calculated from the standard curve of colistin (16–500 μg/ml). All experiments were performed in three biological replicates and repeated at least in two independent times.

Biofilm Inhibition Assay

A. baumannii were grown in NB medium overnight at 37°C with continuous shaking 180 rpm. The overnight bacterial culture was diluted with fresh NB medium to a final density of 10^6 CFU/ml. Then the diluted bacteria cultures were treated with PBS (control), Dpo71 (1, 10, or 40 μg/ml), colistin (1 μg/ml) or their combination (Dpo71 + colistin) with a final volume of 150 μl/well at 37°C for 24 h with gentle shaking (100 rpm). At the end of the incubation time, all media were removed and the wells were stained with 200 μl 0.1% (w/v) crystal violet for 1 h. After staining, the crystal violet solution was removed and the wells were washed with 200 μl PBS for three times. Then, 200 μl of 70% ethanol was added to dissolve the crystal violet and 100 μl solution was transferred to a new plate for quantification of the residual biofilm biomass using a microplate reader (CLARIOstar, BMG Labtech, Ortenberg, Germany) at 570 nm. All experiments were performed in three biological replicates and repeated at least in two independent times.

Biofilm Removal Assay

A. baumannii were grown in NB medium overnight at 37°C with continuous shaking 100 rpm. The overnight bacterial culture was diluted with fresh NB medium to a final density of OD_{600} = 0.2. To initiate the biofilm growth, diluted culture was aliquoted into a 96-well plate at 100 μl/well (Costar, Corning Incorporated, New York, United States) and incubated at 37°C for 24 h at 100 rpm. Biofilm was washed twice with PBS and treated with PBS (control), Dpo71 (10 μg/ml), colistin (4 μg/ml) or their combination (Dpo71 + colistin) with a final volume of 150 μl/well at 37°C for 24 h with gentle shaking (100 rpm). At the end of the incubation time, the residual biomass was quantified using crystal violet as described in the inhibition assay above. The antibiofilm activity was also evaluated by the counting the viable bacteria in the biofilm (Wilson et al., 2017). Briefly, the biofilm was grown and treated as above, then the wells were washed three times with PBS. Then the biofilm-containing wells were mixed fully with a pipetting device, making the biofilm cells become planktonic cells. Each sample was serially diluted and plated for bacterial counting. All experiments were performed in triplicate and repeated at least in two independent times.

Confocal Laser Scanning Microscopy on Biofilm Removal

Confocal dish (NEST, Wuxi NEST Biotechnology, Jiangsu, China) was used instead of the 96-well plate for the antibiofilm study described above. Before microimaging, the biofilms were stained by LIVE/DEAD™ BacLight™ Bacterial Viability Kit (Thermo Fisher Scientific, Massachusetts, United States) for 60 min following the manufacturer's instructions. Then the biofilms were washed three times with PBS before the confocal laser scanning microscopy (Nikon, C2+ confocal, Tokyo, Japan) study. The excitation maximum and emission maximum of SYTO 9 is at 483 and 503 nm, respectively. The excitation maximum and emission maximum of propidium iodide is at 493 and 636 nm, respectively.

Hemolysis Assay

The effect of Dpo71 on the hemolysis of human red blood cells was performed using previously described methods with minor modifications (Liu et al., 2019a). The human blood sample from a healthy donor was centrifuged at 1,000 rpm for 10 min to remove the serum. The red blood cell pellets were washed with PBS (pH = 7.4) at least three times and then diluted to a concentration of 5% (volume ratio) with PBS. The Dpo71 (10, 100, and 500 μg/ml, final concentration) was added to the red blood cells and incubated at 37°C for 1 h, followed by centrifugation at 1,000 rpm for 10 min. Then 100 μl supernatant was transferred to a 96-well microplate and topped up with another 100 μl of PBS to get a final volume of 200 μl. The erythrocytes in PBS and 0.1% Triton X-100 were served as negative and positive controls, respectively. The hemoglobin in supernatant was determined by measuring absorbance at 540 nm using a microplate reader (Multiskan Sky, Thermo Fisher Scientific, Massachusetts, United States). All experiments were performed in three biological replicates and repeated at least in two independent times.

Cytotoxicity of Dpo71 Against BEAS-2B Cell

BEAS-2B (Human Normal Lung Epithelial Cells) cells were cultured in DMEM (GIBCO, New York, United States) containing 10% FBS (GIBCO, New York, United States) under standard conditions in a humidified incubator with 5% CO_2 at 37°C. The cytotoxic effect of the Dpo71 on BEAS-2B cells was measured by Cell Counting Kit-8. The BEAS-2B cells were seeded at density of 10^4 cells/well in a 96-well plate containing 200 μl of culture medium and incubated at 37°C for 24 h. Next, the cells were incubated with Dpo71 for 12 h followed by incubating with 10 μl of WST-8 solution (Beyotime, Shanghai, China) for another 2 h at 37°C. Absorbance was measured at a wavelength of 450 nm using a microplate reader (Multiskan Sky, Thermo Fisher Scientific, Massachusetts, United States). The PBS group was served as a negative control. All experiments were performed in three biological replicates and repeated at least in two independent times.

Galleria mellonella Infection Model

The *G. mellonella* model was conducted following the procedures described by Peleg et al. (2009) with some minor modifications, and referring in other *G. mellonella* studies (Yang et al., 2015; Blasco et al., 2020). The *G. mellonella* larvae were acquired from WAGA company in Hong Kong and the injection was performed with a 10 μl SGE syringe (Sigma-Aldrich, Missouri, United States). To infect the *G. mellonella*, the larvae were first injected with 10^6 CFU *A. baumannii* (MDR-AB2 strain) into the last left proleg. Then the PBS buffer (control group) or 5 μg Dpo71; 1 μg colistin; or 1 μg colistin + 5 μg Dpo71 (treatment group), were injected into the last right proleg within 30 min. The *G. mellonella* were then incubated at 37°C and observed at 24 h intervals over 4 days. The *G. mellonella* which did not respond to physical stimuli were considered dead. Each group included nine *G. mellonella* with individual experiments repeated two times ($n = 18$).

Statistics

All experimental data are presented as means ± standard deviation (SD), and significance was determined using independent Student's *t* tests and the one-way analysis of variance (ANOVA), assuming equal variance at a significance level of 0.05. Comparison of the survival rates of *G. mellonella* between groups was determined by Kaplan–Meier survival analysis with a log-rank test. All statistical analysis was performed using GraphPad Prism software.

RESULTS

Identification and Characterization Depolymerase Dpo71

The IME-AB2 phage exhibits plaque surrounded by a halo-zone, suggesting the presence of a depolymerase protein. Bioinformatic analysis reveals that gp71 is a tail fiber protein (Peng et al., 2014) with 43% sequence similarity as the depolymerase encoded by another *Acinetobacter* phage vB_AbaP_AS12 (Protein Data Bank number 6EU4) (**Figure 1A**). Expression of the ORF71 sequence in *E. coli*. yields a protein with more than 95% purity and a molecular mass of about 80 kDa (**Figure 1B**), matching the calculated value of 80.2 kDa. Size exclusion chromatography shows that the purified Dpo71 elutes as a single peak at a molecular weight larger than 200 kDa (**Figure 1C**). This corresponds to a trimer, consistent with the expected oligomeric form of phage tail fiber protein which is believed to endure extreme conditions for phage infection and survival (Oliveira et al., 2019a, 2020). Circular dichroism (CD) reveals that the Dpo71 protein adopts a well-folded conformation rich in β-sheet structures with a negative dichroic minimum at 215-nm and a positive maximum around 195-nm characteristic peaks (**Figure 1D**). The melting curves following the CD signal at 215 nm show a melting temperature (Tm) of 58.5°C (**Figure 1E**). Spot tests were performed next to confirm the ability of Dpo71 in degrading bacterial capsules of the host bacteria MDR-AB2 of the parent phage. Semi-clear spot formation was observed on the bacterial lawn with the spot sizes increasing with the dose of depolymerase from 0.001 to 10 μg range (**Figure 1F**). The bacterial CPS/LPS degradation activity of Dpo71 was also confirmed by the reduced CPS/LPS concentration and Alcian blue staining (**Supplementary Figure 1**) using protocols documented in previous studies (Liu et al., 2020).

Robustness of Dpo71 Upon Administration and Storage

To evaluate the therapeutic applicability of Dpo71, the enzymatic activity of Dpo71 at various pH values was evaluated by monitoring the turbidity of the residual polysaccharide extracts (CPS/LPS). **Figure 2A** shows that the enzyme remained active in the range of pH 4–8, covering most of the physiological conditions. Then we measured the toxicity of Dpo71 to mammalian cells, human red blood cells and lung bronchial epithelial cell line (BEAS-2B cells). No hemolytic activity was detected even at a high dose of 500 μg/ml (**Figure 2B**). **Figure 2C** also shows Dpo71 has no cytotoxicity against BEAS-2B cells. The result suggests that Dpo71 may be a safe treatment, likely for systemic or pulmonary infections. As stability upon storage is critical for the development of commercially viable protein therapeutics, the storage stability of Dpo71 at 4°C has been evaluated. Results show that Dpo71 is stable for at least 6 months without noticeable activity loss (**Figure 2D**).

Sensitizing Bacteria to Serum Killing and Antibiotic

As depolymerase can disintegrate bacterial capsules and thus sensitize bacteria to be killed by host immune system (Yoshida et al., 2000; Spinosa et al., 2007; Oliveira et al., 2020), we first measured whether serum could kill the Dpo71-treated bacterial cells. Two *A. baumannii* strains (AB#1 and AB#2), belonging to ST208 sequence type (Liu et al., 2019a), sensitive to the parent IME-AB2 phage and two insensitive strains (AB#3 and AB#4) were chosen for the serum killing assays. The four tested strains were resistant to serum killing and continue to

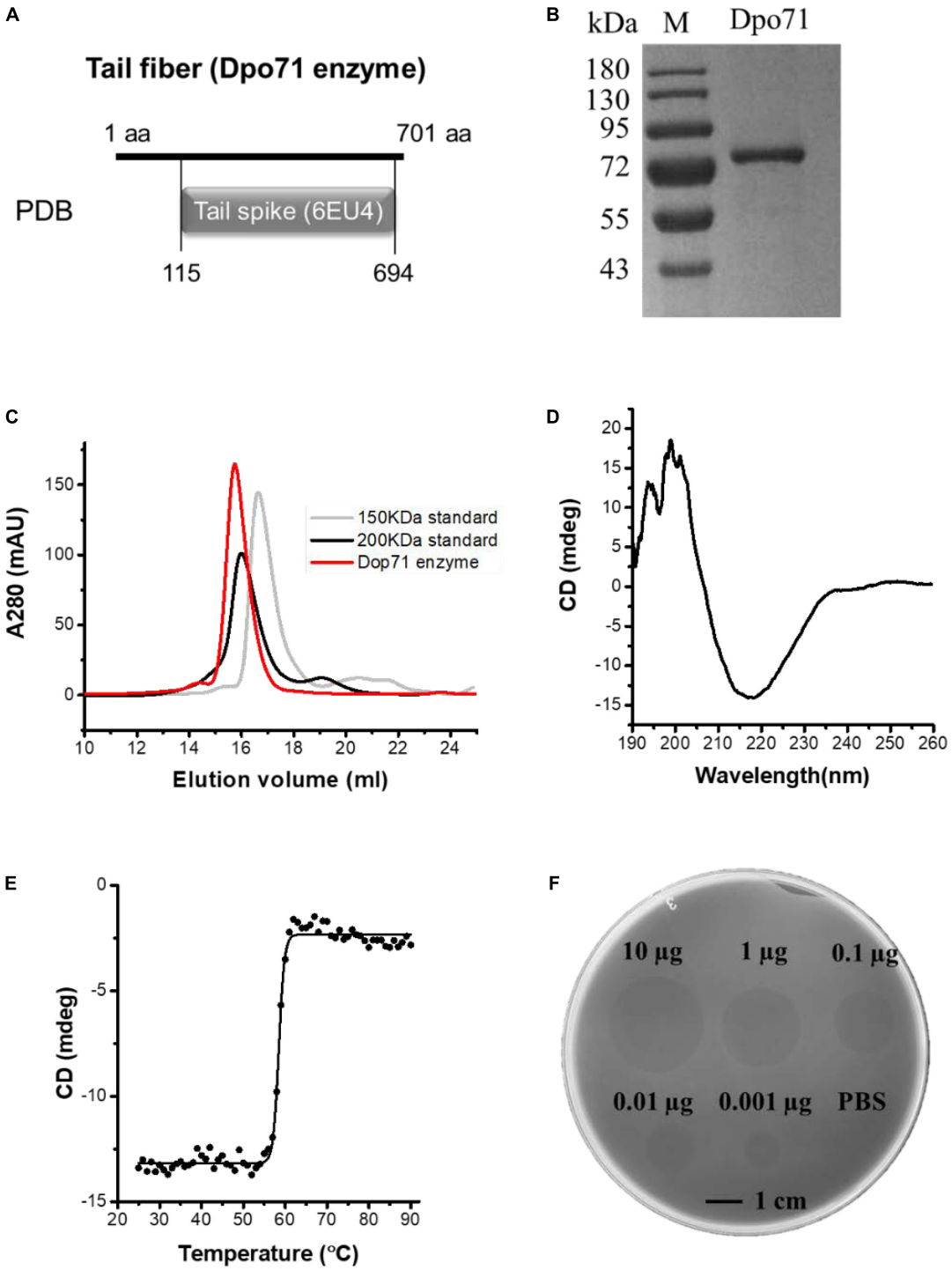

FIGURE 1 | Identification and characterization of Dpo71 depolymerase. **(A)** Bioinformatic analysis indicates the gp71 gene of the IME-AB2 phage. **(B)** SDS gel electrophoresis analysis of purified Dpo71 and a standard molecular mass marker (Lane M). **(C)** Size exclusion chromatography of purified depolymerase protein. **(D)** Circular dichroism analysis of Dpo71 measured in the far-UV (190–260 nm). **(E)** The melting curve of Dpo71 acquired at 215 nm from 20 to 90°C. **(F)** Spot test assay of Dpo71 against *A. baumannii* lawn (0.001–10 μg).

grow in human serum without the presence of depolymerase. Bacteria treated with 10 μg/ml Dpo71 and inactivated serum also showed no antibacterial effect (**Figure 3A**). On the contrary, a remarkable bacterial reduction (8 log) was noted for the two sensitive strains (AB#1 and AB#2), but not for the insensitive ones (AB#3 and AB#4) when the bacteria were treated with

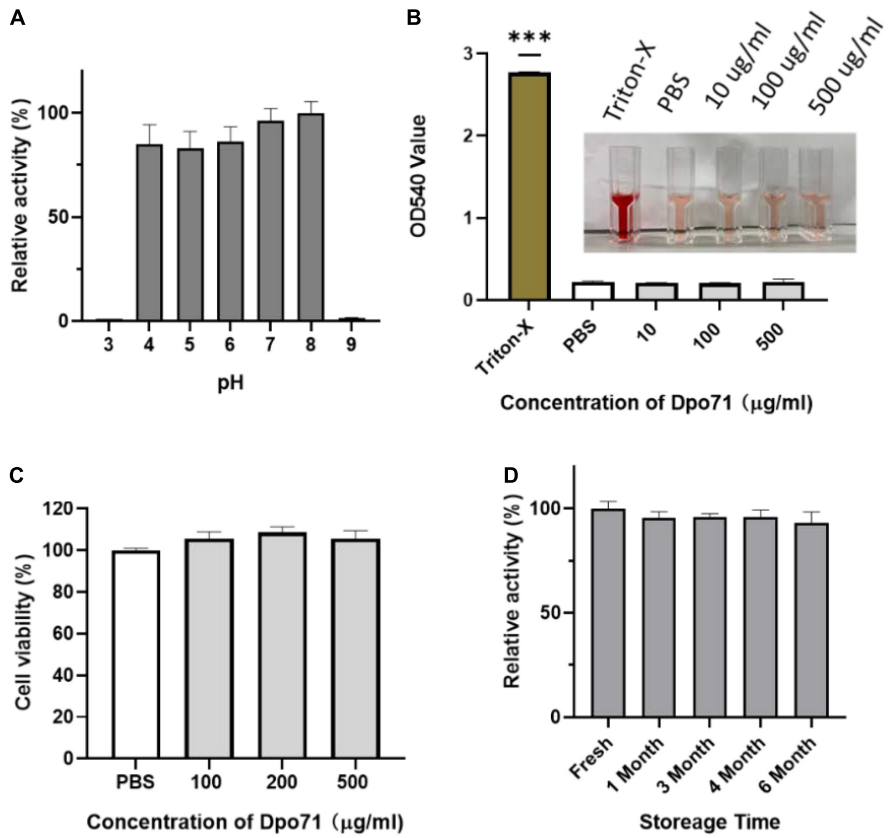

FIGURE 2 | Stability and toxicity of Dpo71. **(A)** The effect of pH on Dpo71 depolymerase activity. CPC turbidity assay was used to measure the polysaccharide extracts (CPS/LPS) degradation activity, the highest activity at pH 8 was set as 100%. **(B)** Hemolysis of red blood cells by Dpo71. PBS and 0.1% Triton X-100 in PBS as the negative and positive controls, respectively. *** indicated $P < 0.001$, Student's *t*-test. **(C)** Cytotoxicity of Dpo71 against human cells (BEAS-2B). **(D)** Stability of Dpo71 after storage at 4°C. The polysaccharide extract (CPS/LPS) degradation activity of the freshly prepared enzyme was set as 100%. Data are expressed as means ± SD ($n = 5$).

active human serum (with a volume ratio of 50%) and Dpo71 (**Figure 3A**). Furthermore, the time-killing assay on the two sensitive strains was performed with a serum ratio of 1–50%. Complete bacterial eradication was observed after a 5-h treatment at 50% human serum for both AB#1 and AB#2 (**Figure 3B** and **Supplementary Figure 2**). It is noteworthy that a 5% serum was sufficient to achieve around 4-log bacterial reduction after 5 h and with minor regrowth after 24 h. This efficacy is significantly higher as compared with previous reports, in which at least 25% human serum is needed to achieve the same killing efficiency (Majkowska-Skrobek et al., 2018; Liu et al., 2019a, 2020; Mi et al., 2019; Oliveira et al., 2020).

We next examined the antibiotic adjuvant effect of Dpo71 against MDR-AB2. Colistin was chosen because it was the only tested antibiotic that the MDR-AB2 strain was susceptible to with a minimum inhibition concentration (MIC) of 2 μg/ml (Peng et al., 2014; **Supplementary Table 3**). The colistin concentration was set at 1 μg/ml, half of the MIC value. **Figure 3C** shows that 1 μg/ml colistin alone or colistin with 5% serum had no antibacterial effect against the inoculation of 10^8 CFU/ml. Dpo71 combined with 5% serum could achieve around 4-log bacterial reduction and the antibacterial effect was further enhanced to nearly complete eradiation (residual viable bacteria reduced from 4.4 ± 0.2 log to 0.7 ± 1.1 log) when Dpo71 was used in combination with 1 μg/ml colistin in the presence of 5% serum (**Figure 3C**). This boosting effect was consistent with a modified checkerboard assay examining the synergy between Dpo71 and colistin that the MIC of colistin dropped from 2 to 0.5 μg/ml with the addition of 5% serum (Data not shown). Notably, these results indicated that Dpo71 could act as an adjuvant to boost the antibacterial activity of colistin in low serum condition.

Mechanisms for the Adjuvant Effect of Depolymerase on Colistin

Although the combined administration of depolymerase and antibiotics was superior to the individual treatments, the underlying mechanisms responsible for the adjuvant effect of Dpo71 have not been fully investigated (Bansal et al., 2014, 2015; Olsen et al., 2018; Wu et al., 2019; Latka and Drulis-Kawa, 2020). We first confirmed that Dpo71 could strip the bacterial capsule using scanning electron microscopy (SEM). **Figure 4A** shows clearly the morphological changes of the bacterial surface after Dpo71 treatment. The bacterial surface of untreated bacteria

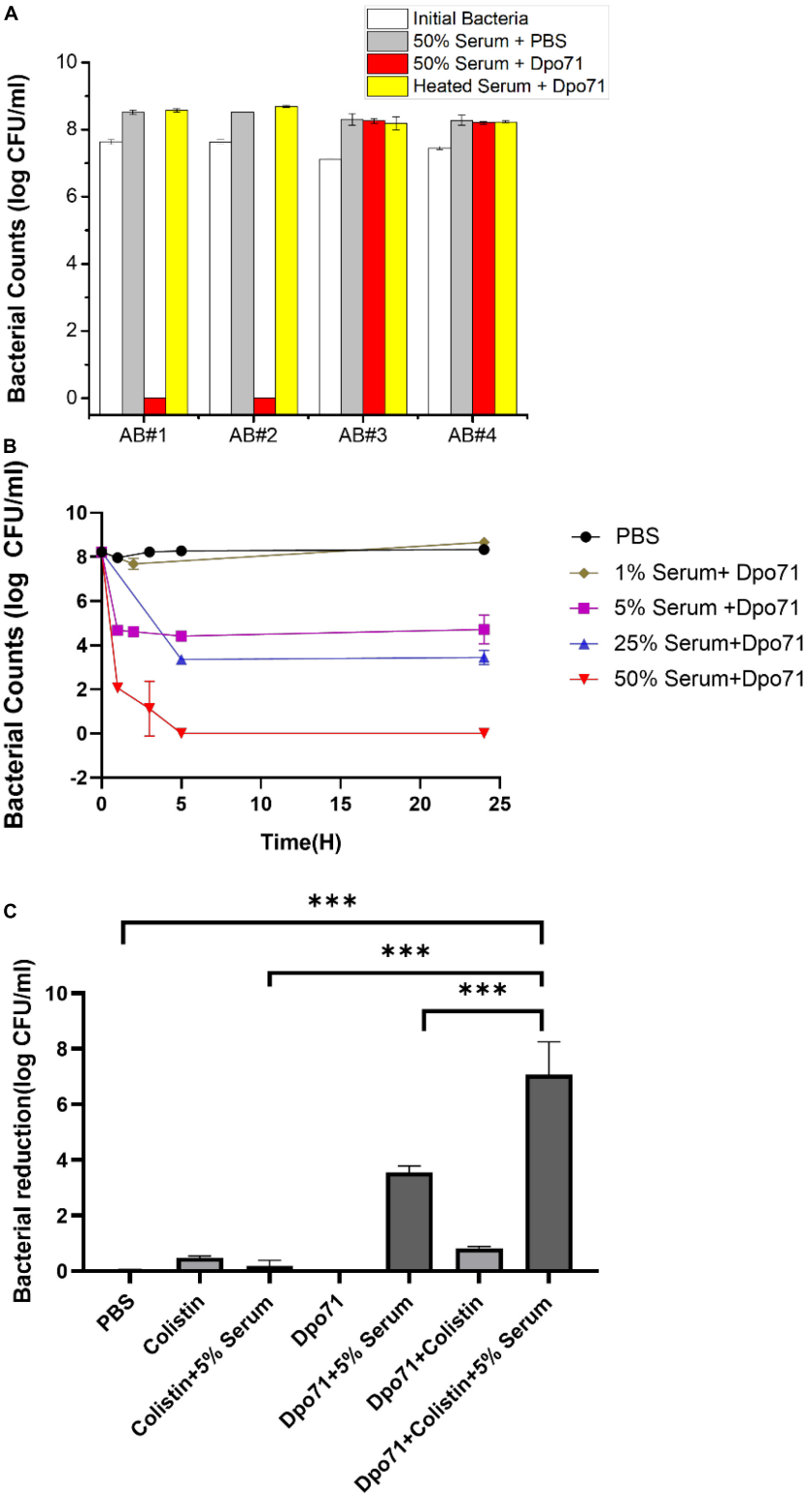

FIGURE 3 | Dpo71 enhanced the serum sensitivity and colistin activity against *A. baumannii.* **(A)** Bacterial susceptibility to the treatment with Dpo71 concentration of 10 μg/ml and 50% serum volume ratio. *A. baumannii* clinical strains sensitive (AB#1 and AB#2) and insensitive (AB#3 and AB#4) to the phage IME-AB2 were tested. **(B)** Time-killing curve of Dpo71 (10 μg/ml) against MDR-AB2 (AB#2 strain) in the presence of 1–50% human serum. **(C)** Dpo71 and colistin activity against *A. baumannii* in the presence/absence of 5% human serum. Data are expressed as means ± SD (n = 3). *** indicates $P < 0.001$, Student's t-test.

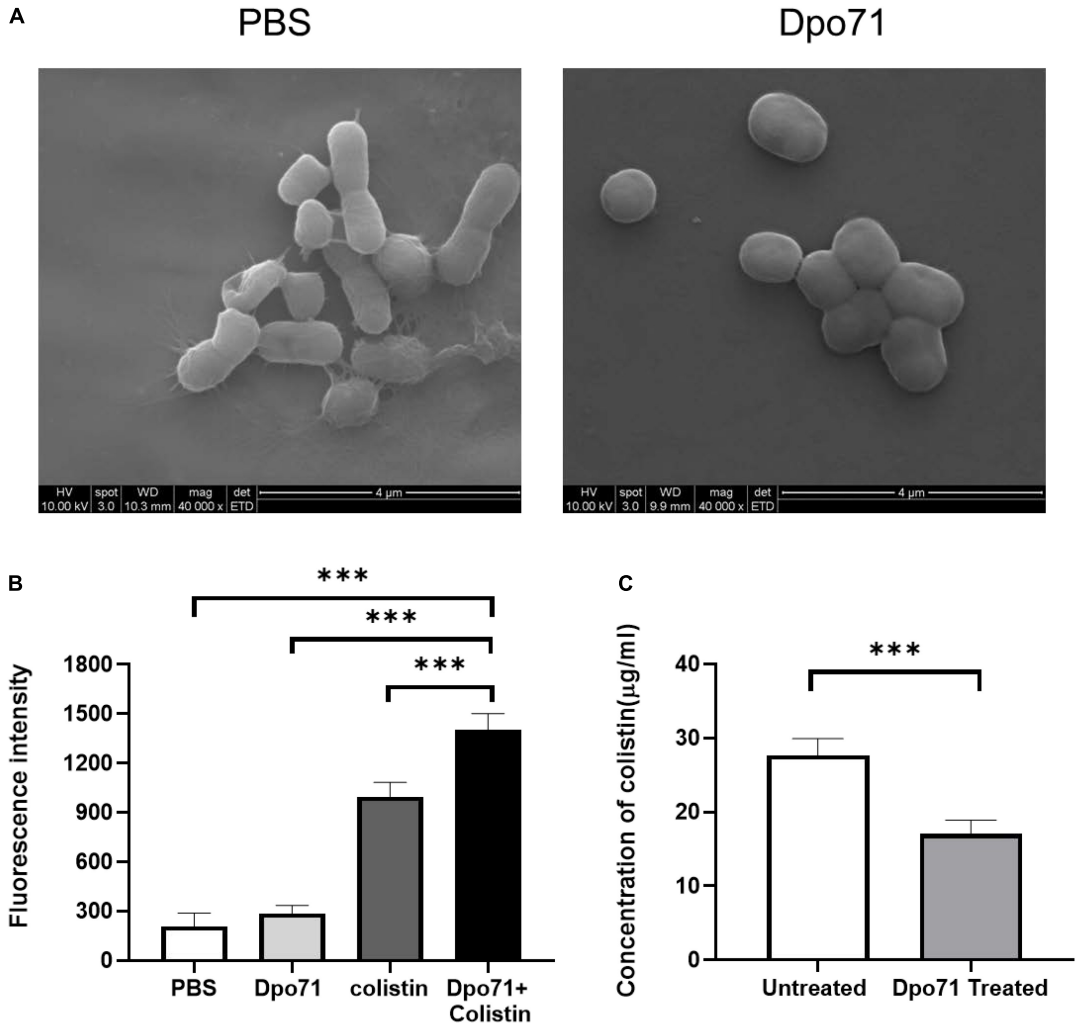

FIGURE 4 | Mechanistic studies using the Dpo71 as an adjuvant agent. **(A)** Representative Scanning Electron Microscope (SEM) images of *A. baumannii* incubated with PBS and Dpo71 (10 μg/ml). Scale bar 4 μm. **(B)** NPN uptake assay of *A. baumannii* induced by PBS buffer; Dpo71; colistin (1 μg/ml); and their combination agents (Dpo71 + colistin). Net fluorescence signals with the background signal of the cells subtracted are used. Data are expressed as means ± SD (n = 3) with ***$p < 0.001$ determined by Student's t-test. **(C)** Assessment concentration of the unbounded colistin. *A. baumannii* were treated with Dpo71 or PBS for 2 h, then after 5 min incubation of the colistin, the cells with the bound colistin were sedimented. The supernatant was centrifuged and the unbound colistin was measured with the HPLC. Data are expressed as means ± SD (n = 3) with ***$p < 0.001$ determined by Student's t-test.

possessed a complex polysaccharide capsule with pilus-shaped protrusions, while the surface of the Dpo71-treated group showed the absence of these pilus-shaped protrusions, suggesting the loss of the capsule. Then we evaluated the impact of the capsule on the outer membrane (OM) destabilization capacity of colistin using the 1-N-phenylnaphthylamine (NPN) uptake assay. The fluorescence intensity of NPN for the Dpo71-alone group was comparable with the control group and that of the Dpo71-colistin treated bacteria (decapsulated) was significantly higher than the colistin-alone groups (**Figure 4B**). These results indicate that Dpo71 depolymerase only acted on bacterial capsules and the removal of the capsule could significantly enhance the OM destabilization capability of colistin. The binding efficiency of colistin with native and decapsulated bacteria was estimated. The Dpo71 treated bacteria had a lower level of free colistin in the supernatant compared with the untreated group, indicating that more colistin binds onto the capsule-stripped bacteria (**Figure 4C**). These results all suggested that depolymerase can function as an antibiotic adjuvant by disintegrating the bacteria capsule to promote interaction between antibiotics and the bacteria, and hence their entry to the bacterial host.

Anti-biofilm Activity

We next measured the inhibition effect of Dpo71 on biofilm formation (Wilson et al., 2017). **Figure 5A** shows Dpo71 inhibits biofilm formation in a dose-dependent manner. At 1 μg/ml Dpo71, the residual biomass was 80% as compared with the PBS-treated control. The residual biomass was further reduced to 60.0 ± 7.2% at 10 μg/ml Dpo71 and 58.2 ± 7.0% at 40 μg/ml. Therefore, 10 μg/ml Dpo71 was chosen for the evaluation of

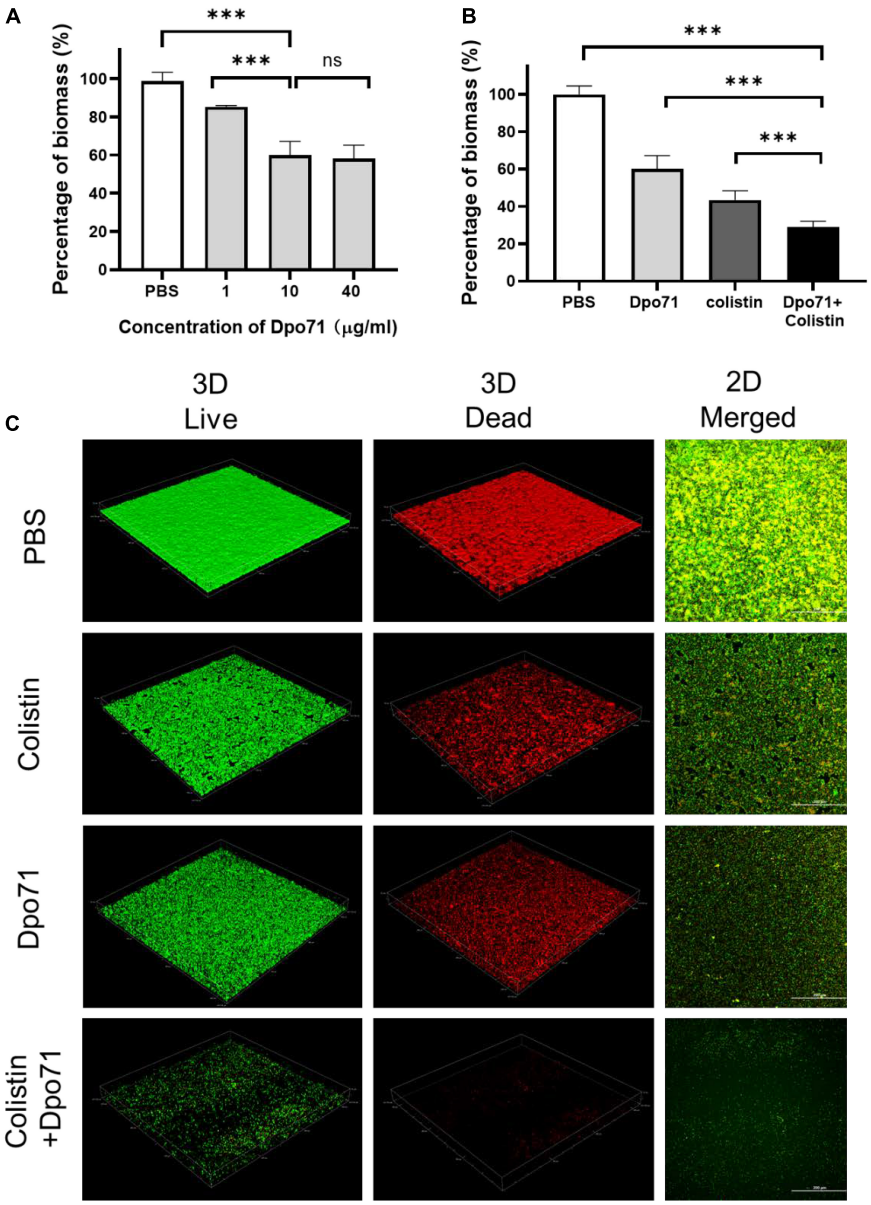

FIGURE 5 | Dpo71 and colistin inhibited biofilm formation. **(A)** Dpo71-alone inhibited the biofilm in a dose-dependent manner. **(B)** Dpo71 and colistin combination inhibited the biofilm formation. *A. baumannii* were incubated with PBS buffer; Dpo71; colistin (1 μg/ml); and their combination agents (Dpo71 + colistin) in 96-well plates for 24 h, followed with crystal violet staining. The OD value of the PBS control was 1.55 ± 0.11. Data are expressed as means ± SD ($n = 3$) with $^{***}p < 0.001$ determined by Student's *t*-test. **(C)** The Representative confocal fluorescence microscopic images of LIVE/DEAD stained *A. baumannii* biofilm (Scale bar, 200 μm). ns: No significant difference.

adjuvant effects with 1 μg/ml colistin (1/2 MIC) in inhibiting biofilm formation. Colistin alone brought down the biomass to 43.5 ± 4.9%, and further reduced it to 28.9 ± 3.1% when used in combination with Dpo71 (**Figure 5B**). The biofilm was visualized by the LIVE/DEAD staining, in which live cells were stained with green fluorescence and dead cells with damaged membrane were stained red (**Figure 5C**). Consistent with the results from the CV staining assay, confocal imaging showed Dpo71 alone and colistin alone could prevent the biofilm formation to a certain extent compared with the PBS-treated sample, but the combination of Dpo71 and colistin yielded the most effective biofilm inhibition. Our results confirmed the capability of both Dpo71-alone and co-treatment with colistin in preventing *A. baumannii* biofilm formation.

We next assessed whether Dpo71 or its combination with colistin can remove pre-formed biofilm (Wilson et al., 2017). According to the CV staining assay, the biomass could be disrupted by a single treatment of Dpo71 (10 μg/ml) or colistin (4 μg/ml, 2× MIC) to around 60% residual biomass of the PBS control (**Figure 6A**). The combined treatment could further

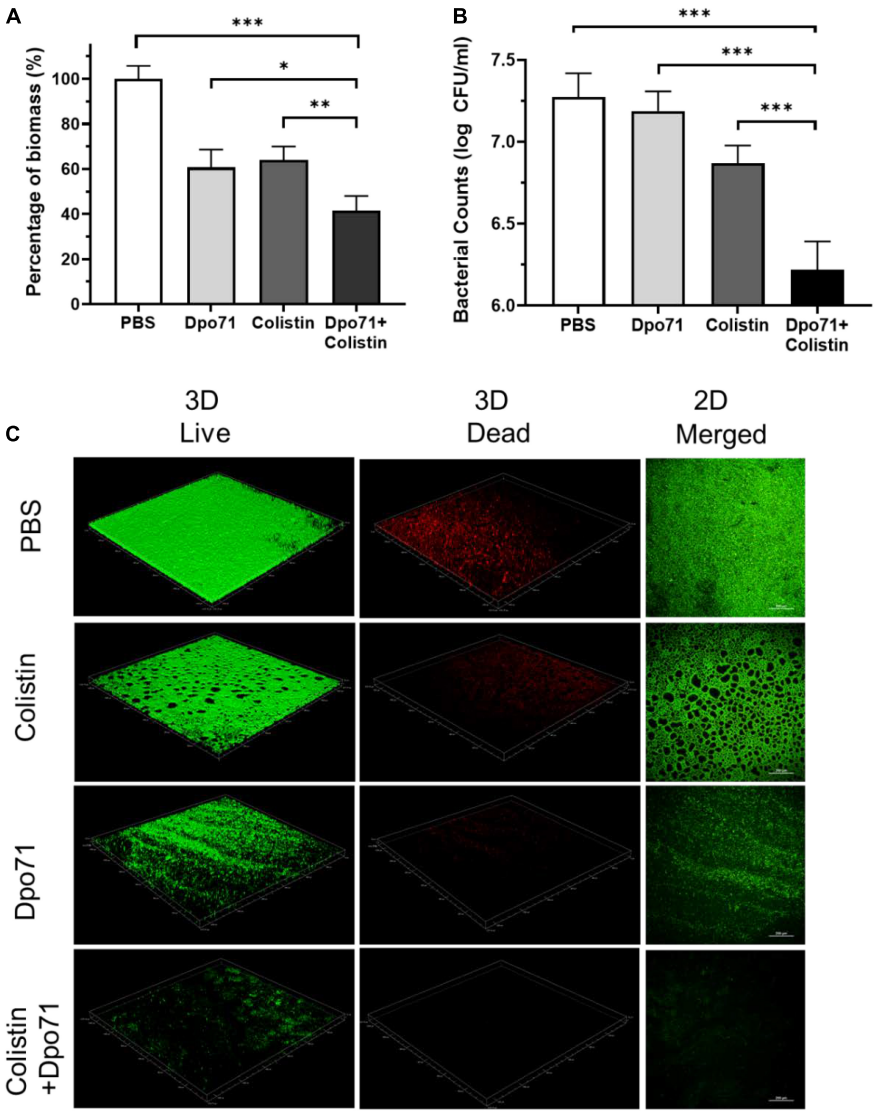

FIGURE 6 | Dpo71 and colistin disrupted the pre-formed biofilm. The residual biofilm was assessed by **(A)** crystal violet staining (the OD value of the PBS control was 2.12 ± 0.14) and **(B)** *A. baumannii* bacterial counts. Briefly *A. baumannii* strain was grown on 96-well plates for 24 h for biofilm formation first, and then the biofilm was treated with PBS buffer, Dpo71 (10 μg/ml), colistin (4 μg/ml) or Dpo71 + colistin for 24 h, followed with crystal violet staining and bacterial counting. Data are expressed as means ± SD ($n = 3$). *$p < 0.05$, **$p < 0.01$, ***$p < 0.001$, Student's *t*-test. **(C)** Representative confocal fluorescence microscopic images of live/dead stained *A. baumannii* biofilm (Scale bar, 200 μm). Confocal dish was used instead of the 96-well plate here.

reduce the residual biomass to 41.5 ± 6.6%. We reached the same conclusion when we compared the number of viable bacterial cells in the dispersed biofilms (**Figure 6B**). In the absence of Dpo71, colistin was inefficient in killing bacteria embedded in the biofilm (<0.5 log reduction), whereas with the help of Dpo71, more than 90% of the bacterial cells in biofilm were killed (from 7.3 ± 0.1 to 6.2 ± 0.2 in log scale). In the LIVE/DEAD viability assay, the pre-formed biofilm network was dismantled by Dpo71 (**Figure 6C**). These results show that Dpo71 can efficiently disrupt per-formed biofilm. For biofilms treated with the combination of Dpo71 and colistin, both 2D and 3D confocal images showed only weak fluorescence signals, confirming that the biofilm was effectively removed (**Figure 6C**). These data indicate that Dpo71 could boost the antibiofilm activity of colistin.

Antibacterial Activity in a *Galleria mellonella* Infection Model

We next evaluated the *in vivo* efficacy of Dpo71 and colistin in combating bacterial infections in a *Galleria mellonella* infection model (**Figure 7A**). In the control group, approximately 70% of the *G. mellonella* died within 18 h and the death rate increased to 90% at 48 h (**Figure 7B**). The survival rate of the colistin-treated group increased to 50% after 24 h post-infection, and around 30% endured to the end of the monitoring

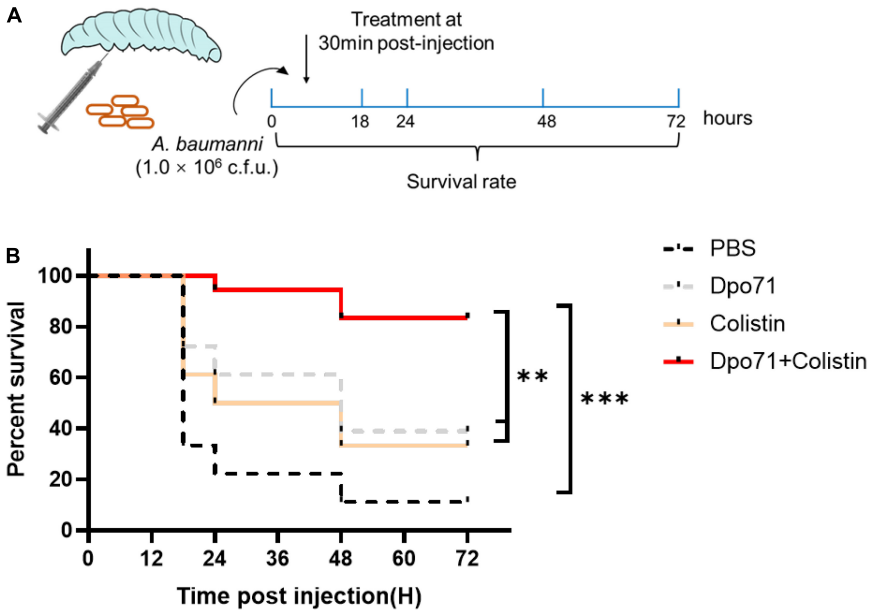

FIGURE 7 | Antivirulent activity in the *Galleria mellonella* infection model. **(A)** Scheme of the experimental protocol for the *G. mellonella*. **(B)** Survival curves for *G. mellonella* infected with 10^6 CFU *A. baumannii* then followed by the injection of PBS buffer (control group); 5 μg Dpo71; 1 μg colistin; or 1 μg colistin + 5 μg Dpo71 (treatment group) (n = 18, $^{**}p < 0.01$, $^{***}p < 0.001$, Kaplan–Meier survival analysis with log-rank test).

period (72 h post-infection). Although depolymerase itself is not bactericidal, the Dpo71-alone treatment was found to be effective in rescuing the infected worms with 40% of the *G. mellonella* surviving for 72 h. The combination treatment increased the survival rate of the infected worms to 80% till the end of the monitoring period, significantly higher than the monotherapy groups ($^{**}p < 0.01$, log-rank test).

DISCUSSION

A. baumannii, one of the most alarming nosocomial gram-negative pathogens, has drawn significant attention in clinical settings due to its exceptional ability to acquire resistance to the commonly used antibiotics (Wieland et al., 2018). Although the knowledge on the mechanisms involved in the pathogenicity of *A. baumannii* is still limited, the production of bacterial capsular polysaccharides has been regarded as an important virulence factor, conferring its intrinsic resistance to peptide antibiotics and protecting it from host immune attack (Wilson et al., 2002; Geisinger and Isberg, 2015; Pettis and Mukerji, 2020). *A. baumannii* has previously shown a much higher biofilm formation rate (80∼91%) compared with other species (5–24%) (Martí et al., 2011). Its excellent capability of forming biofilms also contributes to the bacterial pathogenicity and resistance toward antibiotics. As CPS and EPS (a major component of the biofilms) are the substrates of phage-encoded depolymerases, the application of recombinant depolymerases has received compelling interest as novel antivirulence agents to control multidrug-resistant infections (Pires et al., 2016; Knecht et al., 2020). A few depolymerases encoded by *A. baumannii* phage have been identified in recent years with demonstrated *in vivo* efficacy (Lin et al., 2017; Liu et al., 2019b; Oliveira et al., 2019b; Wang et al., 2020; Shahed-Al-Mahmud et al., 2021). However, the adjuvant effect of depolymerases on SOC antibiotics in controlling infections caused by *A. baumannii* has never been attempted.

In this study, depolymerase Dpo71, derived from an *A. baumannii* phage, IME-AB2 was found to remain active at a pH range of 4-8 and have a Tm of 58.5°C, suggesting it can be used under most physiological conditions. These properties of Dpo71 were consistent with that of other depolymerases (Oliveira et al., 2019a, 2020). Importantly, this study demonstrated the excellent storage stability of a depolymerase with no noticeable activity loss for at least 6 months storing at 4°C. This would offer great advantages in developing depolymerases as commercially viable antibacterial agents. Depolymerases are known to be highly specific to the capsular type of the bacteria (Whitfield, 2006; Schmid et al., 2015; Singh et al., 2018, 2019). Dpo71 was sensitive to AB#1 and AB#2 but insensitive to AB#3 and AB#4. The reason for this discrepancy is rooted in the mechanism of action of Dpo71, which still remains elusive. The remarkable diversity of bacterial capsules and the narrow host-spectrum of phage and phage-derived enzymes might raise a concern about the general applicability of phage therapy and therapies based on phage-derived enzymes, although in some scenarios this narrow spectrum can be harnessed to eradicate pathogens while leaving beneficial bacterial strains in the flora unharmed. Furthermore, the recombinant Dpo71 effectively decapsulates the host bacteria of its parent phage (AB#1 and AB#2) and re-sensitizes them to serum killing in a serum ratio-dependent manner (**Figure 3B**). The depolymerase treatment was largely

limited for systemic infections because bacterial killing required the aid from the host immune attack such as complement-mediate killing. In the present study, the Dpo71 treated bacteria were significantly reduced in the presence of 5% serum (4 logs of killing from a density of 10^8 CFU/ml), representing the possibility of applying this depolymerase beyond systemic infection to environments with a low serum level, like lung infections. When the serum ratio increased to 50%, complete bacterial eradication was achieved with Dpo71. This was significantly higher than that reported in previous studies (Lin et al., 2017; Majkowska-Skrobek et al., 2018; Liu et al., 2019a, 2020; Mi et al., 2019; Oliveira et al., 2020), in which a 50% serum (complement) ratio could only kill 2-5 log of the depolymerase treated bacteria and no further killing was noted when the serum (complement) ratio increased to 75%. Liu et al. (2019a) postulated that the incomplete bacteria-killing was due to the emergence of resistant phenotypes. Therefore, resistance development toward the depolymerase treatment was assessed and compared with the parent phage treatment. While the bacteria developed phage resistance after 24-h co-incubation, they remained sensitive to the Dpo71 depolymerase (**Supplementary Table 4**). The sensitivity of the bacteria incubating with Dpo71 and 5% serum was also examined. Dpo71 could still yield a clear halo spot on the treated bacteria lawn (**Supplementary Figure 3**), suggesting they were still sensitive to the depolymerase. It is mainly because depolymerases do not directly kill the bacteria during the antibacterial treatment, reducing the impetus for bacteria to evolve mechanisms against the depolymerases.

While the Dpo71 treatment could effectively remove the bacterial capsules and promoted their interactions with colistin (**Figure 4**), no enhanced antibacterial effect was noted for the mixture of Dpo71 and colistin in the absence of serum. However, the addition of a small amount of serum (5% volume ratio) significantly boosted the bacterial killing efficiency (**Figure 3C**). These results suggested that serum was also essential for the combination treatments. Colistin first binds to the LPS at the cell surface followed by displacing the divalent cations (Ca^{2+} and Mg^{2+}) to disturb the integrity of the outer membrane, resulting in bacterial cell death. Previous reports showed that the MIC values in serum was lower than those in other culture media (Loose et al., 2020). Therefore, the enhanced antibacterial effect in the presence of serum is likely attributed to the combination effect of colistin and depolymerase on the bacterial cell surface facilitating the host immune attack.

Biofilm formation is one of the major contributors for the chronicity of *A. baumannii* infections and their increased antibiotic resistance (Martí et al., 2011). As the EPS can account for 80–90% of the biofilm matrix, the ability of phage in eradicating biofilms was reported to be accounted for the action of their tailspike depolymerases degrading the EPS, facilitating their diffusion through the dispersed biofilms to get access to the underneath bacteria (Dunsing et al., 2019). The effectiveness of recombinant depolymerases in preventing biofilm formation and disrupting the established biofilms has also been studied. The susceptibility of biofilms to phage depolymerase treatments varied, depending on the bacterial strains and the activity of depolymerases. In most reported antibiofilm studies, depolymerases were able to cause a 10–40% biofilm reduction compared with the untreated controls in a dose-dependent manner (Gutiérrez et al., 2015; Hernandez-Morales et al., 2018; Wu et al., 2019; Shahed-Al-Mahmud et al., 2021; Topka-Bielecka et al., 2021). However, there were also reports showing depolymerases were ineffective in dispersing the biofilms, though they were capable of decapsulating bacterial CPS (Latka and Drulis-Kawa, 2020). Overall, the depolymerase treatment were unable to completely inhibit or remove biofilms and the number of viable bacterial counts in the biofilms were similar to the untreated controls (Gutiérrez et al., 2015; Hernandez-Morales et al., 2018; Wu et al., 2019; Topka-Bielecka et al., 2021), with a few exceptions (Bansal et al., 2015; Shahed-Al-Mahmud et al., 2021). These suggested that using depolymerases as a stand-alone treatment might not be sufficient in controlling infections associated with biofilms. Impairing drug diffusion (subdiffusion) within the biofilm matrix is a major contributor to the sub-optimal treatment to biofilm-related infections (Sweeney et al., 2020). Improving the penetration of antibiotics into the biofilm matrix may hold the key to better clinical outcomes. In the present study, Dpo71 demonstrated moderate biofilm inhibition and removal capacities, both around 40% reduction compared with the PBS control, at an optimal concentration of 10 μg/ml (**Figures 5**, **6**). Consistent with most previous studies, Dpo71 could effectively disperse the biofilms but failed to reduce the viable bacterial counts in the biofilms and this was also visually reflected in the LIVE/DEAD confocal images. Combination treatment with colistin, which is the only antibiotic that the MDR-AB2 strain is susceptible to, was studied. The residual biomass and the number of viable bacterial counts within the biofilms were both significantly reduced compared with the depolymerase-alone and colistin-alone treatments, confirming the positive effect of depolymerase-antibiotic combination treatment noted in other bacterial species (Bansal et al., 2014, 2015; Wu et al., 2019). Previously, Dunsing et al. (2019) have proved that treating established *Pantoea stewartii* biofilms with phage tailspike proteins could rapidly restore unhindered diffusion of nanoparticles. Therefore, the improved antibiofilm ability with the combined Dpo71 and colistin treatment noted here was likely attributed to the improved colistin penetration within the biofilm matrix after the EPS depolymerization by the Dpo71. Overall, our data support the depolymerase and antibiotic combination as a promising alternative treatment strategy in managing biofilm-associated infections caused by *A. baumannii*.

The *G. mellonella* infection model was first developed to study the bacterial pathogenicity by Peleg et al. (2009) and has emerged as a valuable inset model to evaluate the effectiveness of novel antibacterial reagents (Yang et al., 2015; Blasco et al., 2020). Several reasons make it a popular model: the larvae (1) can survive at 37°C to mimic the physiological condition of humans; (2) have fast reproduction time to allow high-throughput of experiments compared with mammalian systems; (3) have a semi-complex cellular and humoral innate immunity, which shares remarkable similarities with mammals, but no adaptive immune response to interfere with the therapeutic outcome (Kay et al., 2019). Importantly, the *G. mellonella* model does not

require ethical approval to provide informed data in reducing the number of mammals used for further identification/confirmation of the potential lead compounds. Liu et al. (2019b) first evaluated the *in vivo* efficacy of Dpo48 identified from an *A. baumannii* phage (IME200) using a *G. mellonella* infection model. They showed that the Dpo48 treated *G. mellonella* had a higher survival rate (10-30%) than the untreated group at all the time points throughout the study period (72 h). Although the Dpo48 treatment outcome was not particularly profound in the *G. mellonella* infection model, they showed that the Dpo48 could significantly reduce the bacterial load 6 h post-treatment and rescue 100% of the infected mice (both normal and immunocompromised) from fatal sepsis. They attributed the difference in the insect and mammal infection models to the simpler innate immune response of insects. Nonetheless, their results confirmed that the *G. mellonella* infection model is sufficient to predict the antivirulence capacity of depolymerase and their ability to control *A. baumannii* infections in mammals. As shown in **Figure 7B**, the survival rate of infected *G. mellonella* treated by Dpo71 or colistin monotherapy was around 40%, but the survival rate of those treated by the combination of Dpo71 and colistin could be significantly enhanced to 80%. The results confirmed that Dpo71 was effective in reducing the virulence level of MDR-AB2 *in vivo* and prolonged the survival time of the infected worms as demonstrated in Liu et al. (2019b). Moreover, the adjuvant effect of depolymerase to colistin was demonstrated *in vivo*, consistent with the *in vitro* biofilm experiments. These results warrant further studies on assessing the potential of the combination in treating biofilm-associated infections in mammals.

While promising effects on the use of depolymerase as antivirulence agents have been demonstrated *in vivo*, knowledge on the exact mechanisms of *A. baumannii* CPS cleavage by phage depolymerases are still largely missing (Popova et al., 2020). In addition, depolymerases also present high specificity toward a narrow range of target polysaccharides (specific capsular type of the bacteria) (Blundell-Hunter et al., 2021). In some cases, depolymerases might only be active against a subset of bacteria of their parent phage which are already specific to a small set of bacteria strains (Liu et al., 2020; Topka-Bielecka et al., 2021). Such narrow host spectrum would greatly limit the wider therapeutic application of depolymerases. To address this limitation, the use of cocktails of depolymerases, an approach widely adopted for phage therapy in human use, may be a feasible solution. Further work on elucidating mechanisms of action of depolymerases would allow protein engineering to extend their host range and activity (Latka et al., 2021), facilitating their application as a stand-alone treatment or as an adjuvant with SOC antibiotics.

CONCLUSION

In summary, phage tail fiber proteins with depolymerase activity are promising antivirulence agents to re-sensitize *A. baumannii*, even the drug-resistant strains, to host immune attack. The identified Dpo71 depolymerase was found to effectively degrade bacterial capsules with excellent stability at various pH and upon storage. In addition, Dop71 alone can be utilized to prevent and remove *A. baumannii* biofilms. The combination of Dpo71 and colistin was further demonstrated to significantly enhance the antibiofilm activity compared with the monotherapies. Furthermore, this depolymerase was able to enhance the colistin antibacterial activity *in vivo*, markedly improving the survival rate of infected *G. mellonella*. As carbapenem-resistant *A. baumannii* has been ranked as the number one priority pathogen by the WHO and there are no antibiotics which have reached the advanced stage in the development pipeline to target this superbug, depolymerases as a stand-alone treatment or adjuvant to antibiotics may represent promising treatment strategies in controlling multidrug-resistant *A. baumannii* infections.

DATA AVAILABILITY STATEMENT

The datasets presented in this study can be found in online repositories. The names of the repository/repositories and accession number(s) can be found below: https://www.ncbi.nlm.nih.gov/genbank/, JX976549.

AUTHOR CONTRIBUTIONS

XC was responsible for data collection and interpretation for the overall study and manuscript writing. ML was responsible for data collection and interpretation for the depolymerase characterization. PZ was responsible for data collection and interpretation for the *Galleria mellonella* infection model. MX and WY were responsible for the SEM and confocal imaging experiments. LB, YL, and JX were responsible for the conceptual design of the study, data interpretation, and manuscript review. SL was responsible for the coordination of the study, conceptual design, data interpretation, and manuscript review. All authors contributed to the article and approved the submitted version.

FUNDING

This work was partially funded by the University Grants Committee of Hong Kong (ref. N_CUHK422/18 and ref. 14112921).

ACKNOWLEDGMENTS

We are thankful to Changqing Bai from the Fifth Medical Center of Chinese PLA General Hospital, Beijing, China and Lin Zhang from Prince of Wales Hospital, Hong Kong for their kind donation of bacterial strains tested in the present study.

SUPPLEMENTARY MATERIAL

The Supplementary Material for this article can be found online at: https://www.frontiersin.org/articles/10.3389/fmicb.2022.845500/full#supplementary-material

REFERENCES

Bansal, S., Harjai, K., and Chhibber, S. (2014). Depolymerase improves gentamicin efficacy during *Klebsiella pneumoniae* induced murine infection. *BMC Infect. Dis.* 14:456. doi: 10.1186/1471-2334-14-456

Bansal, S., Harjai, K., and Chhibber, S. (2015). Aeromonas punctata derived depolymerase improves susceptibility of *Klebsiella pneumoniae* biofilm to gentamicin. *BMC Microbiol.* 15:119. doi: 10.1186/s12866-015-0455-z

Blasco, L., Ambroa, A., Trastoy, R., Bleriot, I., Moscoso, M., Fernández-Garcia, L., et al. (2020). In vitro and in vivo efficacy of combinations of colistin and different endolysins against clinical strains of multi-drug resistant pathogens. *Sci. Rep.* 10:7163. doi: 10.1038/s41598-020-64145-7

Blundell-Hunter, G., Enright, M. C., Negus, D., Dorman, M. J., Beecham, G. E., Pickard, D. J., et al. (2021). Characterisation of bacteriophage-encoded depolymerases selective for key *Klebsiella Pneumoniae* capsular exopolysaccharides. *Front. Cell. Infect. Microbiol.* 11:686090. doi: 10.3389/fcimb.2021.686090

Campos, M. A., Vargas, M. A., Regueiro, V., Llompart, C. M., Albertí, S., and Bengoechea, J. A. (2004). Capsule polysaccharide mediates bacterial resistance to antimicrobial peptides. *Infect. Immun.* 72, 7107–7114. doi: 10.1128/IAI.72.12.7107-7114.2004

Centers for Disease Control and Prevention [CDC] (2019). *Antibiotic resistance threats in the United States*. Atlanta, GA: U.S. Department of Health and Human Services, CDC

Chen, X., Liu, M., Zhang, P., Leung, S. S. Y., and Xia, J. (2021). Membrane-Permeable Antibacterial Enzyme against Multidrug-Resistant *Acinetobacter baumannii*. *ACS Infect. Dis.* 7, 2192–2204. doi: 10.1021/acsinfecdis.1c00222

Chen, Y., Li, X., Wang, S., Guan, L., Li, X., Hu, D., et al. (2020). A novel tail-associated O91-specific polysaccharide depolymerase from a *Podophage* reveals lytic efficacy of Shiga toxin-producing *Escherichia coli*. *Appl. Environ. Microbiol.* 86, e00145–20. doi: 10.1128/AEM.00145-20

Dunsing, V., Irmscher, T., Barbirz, S., and Chiantia, S. (2019). Purely polysaccharide-based biofilm matrix provides size-selective diffusion barriers for nanoparticles and bacteriophages. *Biomacromolecules* 20, 3842–3854. doi: 10.1021/acs.biomac.9b00938

Fair, R. J., and Tor, Y. (2014). Antibiotics and bacterial resistance in the 21st century. *Perspect. Medicin. Chem.* 6, 25–64. doi: 10.4137/PMC.S14459

Geisinger, E., and Isberg, R. R. (2015). Antibiotic modulation of capsular exopolysaccharide and virulence in *Acinetobacter baumannii*. *PLoS Pathog.* 11:e1004691. doi: 10.1371/journal.ppat.1004691

Gutiérrez, D., Briers, Y., Rodríguez-Rubio, L., Martínez, B., Rodríguez, A., Lavigne, R., et al. (2015). Role of the pre-neck appendage protein (Dpo7) from phage vB_SepiS-phiIPLA7 as an anti-biofilm agent in *Staphylococcal* species. *Front. Microbiol.* 6:1315. doi: 10.3389/fmicb.2015.01315

Hampton, H. G., Watson, B. N. J., and Fineran, P. C. (2020). The arms race between bacteria and their phage foes. *Nature* 577, 327–336. doi: 10.1038/s41586-019-1894-8

Helander, I. M., and Mattila-Sandholm, T. (2000). Fluorometric assessment of gram-negative bacterial permeabilization. *J. Appl. Microbiol.* 88, 213–219. doi: 10.1046/j.1365-2672.2000.00971.x

Hernandez-Morales, A. C., Lessor, L. L., Wood, T. L., Migl, D., Mijalis, E. M., Cahill, J., et al. (2018). Genomic and biochemical characterization of Acinetobacter *Podophage Petty* reveals a novel lysis mechanism and tail-associated depolymerase activity. *J. Virol.* 92, e01064–17. doi: 10.1128/JVI.01064-17

Hughes, K. A., Sutherland, I. W., and Jones, M. V. (1998). Biofilm susceptibility to bacteriophage attack: the role of phage-borne polysaccharide depolymerase. *Microbiology* 144, 3039–3047. doi: 10.1099/00221287-144-11-3039

Kay, S., Edwards, J., Brown, J., and Dixon, R. (2019). *Galleria mellonella* infection model identifies both high and low lethality of clostridium perfringens toxigenic strains and their response to antimicrobials. *Front. Microbiol.* 10:1281. doi: 10.3389/fmicb.2019.01281

Knecht, L. E., Veljkovic, M., and Fieseler, L. (2020). Diversity and function of phage encoded depolymerases. *Front. Microbiol.* 10:2949. doi: 10.3389/fmicb.2019.02949

Lai, W. C. B., Chen, X., Ho, M. K. Y., Xia, J., and Leung, S. S. Y. (2020). Bacteriophage-derived endolysins to target gram-negative bacteria. *Int. J. Pharm.* 589:119833. doi: 10.1016/j.ijpharm.2020.119833

Latka, A., and Drulis-Kawa, Z. (2020). Advantages and limitations of microtiter biofilm assays in the model of antibiofilm activity of *Klebsiella* phage KP34 and its depolymerase. *Sci. Rep.* 10:20338. doi: 10.1038/s41598-020-77198-5

Latka, A., Lemire, S., Grimon, D., Dams, D., Maciejewska, B., Lu, T., et al. (2021). Engineering the modular receptor-binding proteins of *Klebsiella* phages switches their capsule serotype specificity. *mBio* 12, e00455–21. doi: 10.1128/mBio.00455-21

Latka, A., Maciejewska, B., Majkowska-Skrobek, G., Briers, Y., and Drulis-Kawa, Z. (2017). Bacteriophage-encoded virion-associated enzymes to overcome the carbohydrate barriers during the infection process. *Appl. Microbiol. Biotechnol.* 101, 3103–3119. doi: 10.1007/s00253-017-8224-6

Lin, H., Paff, M. L., Molineux, I. J., and Bull, J. J. (2017). Therapeutic application of phage capsule depolymerases against K1, K5, and K30 capsulated *E. coli* in mice. *Front. Microbiol.* 8:2257. doi: 10.3389/fmicb.2017.02257

Lin, T. L., Hsieh, P. F., Huang, Y. T., Lee, W. C., Tsai, Y. T., Su, P. A., et al. (2014). Isolation of a bacteriophage and its depolymerase specific for K1 capsule of *Klebsiella pneumoniae*: implication in typing and treatment. *J. Infect. Dis.* 210, 1734–1744. doi: 10.1093/infdis/jiu332

Liu, Y., Leung, S. S. Y., Huang, Y., Guo, Y., Jiang, N., Li, P., et al. (2020). Identification of two depolymerases from phage IME205 and their antivirulent functions on K47 capsule of *Klebsiella pneumoniae*. *Front. Microbiol.* 11:218. doi: 10.3389/fmicb.2020.00218

Liu, Y., Mi, Z., Mi, L., Huang, Y., Li, P., Liu, H., et al. (2019a). Identification and characterization of capsule depolymerase Dpo48 from *Acinetobacter baumannii* phage IME200. *PeerJ* 7:e6173. doi: 10.7717/peerj.6173

Liu, Y., Leung, S. S. Y., Guo, Y., Zhao, L., Jiang, N., Mi, L., et al. (2019b). The capsule depolymerase Dpo48 rescues *Galleria mellonella* and mice from *Acinetobacter baumannii* systemic infections. *Front. Microbiol.* 10:942. doi: 10.3389/fmicb.2019.00942

Liu, Y., Mi, Z., Niu, W., An, X., Yuan, X., Liu, H., et al. (2016). Potential of a lytic bacteriophage to disrupt *Acinetobacter baumannii* biofilms in vitro. *Future Microbiol.* 11, 1383–1393. doi: 10.2217/fmb-2016-0104

Loose, M., Naber, K. G., Coates, A., Wagenlehner, F. M. E., and Hu, Y. (2020). Effect of different media on the bactericidal activity of colistin and on the synergistic combination with azidothymidine against mcr-1-positive colistin-resistant *Escherichia coli*. *Front. Microbiol.* 11:54. doi: 10.3389/fmicb.2020.00054

Majkowska-Skrobek, G., Latka, A., Berisio, R., Squeglia, F., Maciejewska, B., Briers, Y., et al. (2018). Phage-borne depolymerases decrease *Klebsiella pneumoniae* resistance to innate defense mechanisms. *Front. Microbiol.* 9:2517. doi: 10.3389/fmicb.2018.02517

Martí, S., Rodríguez-Baño, J., Catel-Ferreira, M., Jouenne, T., Vila, J., Seifert, H., et al. (2011). Biofilm formation at the solid-liquid and air-liquid interfaces by *Acinetobacter* species. *BMC Res. Notes* 4:5. doi: 10.1186/1756-0500-4-5

Mi, L., Liu, Y., Wang, C., He, T., Gao, S., Xing, S., et al. (2019). Identification of a lytic *Pseudomonas aeruginosa* phage depolymerase and its anti-biofilm effect and bactericidal contribution to serum. *Virus Gene* 55, 394–405. doi: 10.1007/s11262-019-01660-4

Oliveira, H., Costa, A. R., Ferreira, A., Konstantinides, N., Santos, S. B., Boon, M., et al. (2019a). Functional Analysis and antivirulence properties of a new depolymerase from a myovirus that infects *Acinetobacter baumannii* capsule K45. *J. Virol.* 93, e01163–18. doi: 10.1128/JVI.01163-18

Oliveira, H., Mendes, A., Fraga, A. G., Ferreira, A., Pimenta, A. I., Mil-Homens, D., et al. (2019b). K2 capsule depolymerase is highly stable, is refractory to resistance, and protects larvae and mice from *Acinetobacter baumannii* sepsis. *Appl. Environ. Microbiol.* 85, e00934–19. doi: 10.1128/AEM.00934-19

Oliveira, H., Pinto, G., Mendes, B., Dias, O., Hendrix, H., Akturk, E., et al. (2020). A tailspike with exopolysaccharide depolymerase activity from a new *Providencia Stuartii* phage makes multidrug-resistant bacteria susceptible to serum-mediated killing. *Appl. Environ. Microbiol.* 86, e00073–20. doi: 10.1128/AEM.00073-20

Olsen, N. M. C., Thiran, E., Hasler, T., Vanzieleghem, T., Belibasakis, G. N., Mahillon, J., et al. (2018). Synergistic removal of static and dynamic *Staphylococcus aureus* biofilms by combined treatment with a bacteriophage endolysin and a polysaccharide depolymerase. *Viruses* 10:438. doi: 10.3390/v10080438

Peleg, A. Y., Jara, S., Monga, D., Eliopoulos, G. M., Moellering, R. C. Jr., and Mylonakis, E. (2009). *Galleria mellonella* as a model system to study

Acinetobacter baumannii pathogenesis and therapeutics. *Antimicrob. Agents Chemother.* 53, 2605–2609.

Peleg, A. Y., Seifert, H., and Paterson, D. L. (2008). *Acinetobacter baumannii*: emergence of a successful pathogen. *Clin. Microbiol. Rev.* 21, 538–582. doi: 10.1128/CMR.00058-07

Pendleton, J. N., Gorman, S. P., and Gilmore, B. F. (2013). Clinical relevance of the ESKAPE pathogens. *Expert Rev. Anti Infect. Ther.* 11, 297–308. doi: 10.1586/eri.13.12

Peng, F., Mi, Z., Huang, Y., Yuan, X., Niu, W., Wang, Y., et al. (2014). Characterization, sequencing and comparative genomic analysis of vB_AbaM-IME-AB2, a novel lytic bacteriophage that infects multidrug-resistant *Acinetobacter baumannii* clinical isolates. *BMC Microbiol.* 14:181. doi: 10.1186/1471-2180-14-181

Pettis, G. S., and Mukerji, A. S. (2020). Structure, function, and regulation of the essential virulence factor capsular polysaccharide of Vibrio Vulnificus. *Int. J. Mol. Sci.* 21:3259. doi: 10.3390/ijms21093259

Pires, D. P., Oliveira, H., Melo, L. D., Sillankorva, S., and Azeredo, J. (2016). Bacteriophage-encoded depolymerases: their diversity and biotechnological applications. *Appl. Microbiol. Biotechnol.* 100, 2141–2151. doi: 10.1007/s00253-015-7247-0

Pirnay, J.-P., and Kutter, E. (2020). Bacteriophage: it's a medicine, Jim, but not as we know it. *Lancet Infect. Dis.* 21, 309–311. doi: 10.1016/S1473-3099(20)30464-3

Popova, A. V., Shneider, M. M., Arbatsky, N. P., Kasimova, A. A., Senchenkova, S. N., Shashkov, A. S., et al. (2020). Specific interaction of novel *Friunavirus* phages encoding tailspike depolymerases with corresponding *Acinetobacter baumannii* capsular types. *J. Virol.* 95, e01714–20. doi: 10.1128/JVI.01714-20

Schmid, J., Sieber, V., and Rehm, B. (2015). Bacterial exopolysaccharides: biosynthesis pathways and engineering strategies. *Front. Microbiol.* 6:496. doi: 10.3389/fmicb.2015.00496

Shahed-Al-Mahmud, M., Roy, R., Sugiokto, F. G., Islam, M. N., Lin, M. D., Lin, L. C., et al. (2021). Phage φAB6-Borne depolymerase combats *Acinetobacter baumannii* biofilm formation and infection. *Antibiotics* 10:279. doi: 10.3390/antibiotics10030279

Singh, J. K., Adams, F. G., and Brown, M. H. (2018). Diversity-generating machines: genetics of bacterial sugar-coating. *Trends Microbiol.* 26, 1008–1021. doi: 10.1016/j.tim.2018.06.006

Singh, J. K., Adams, F. G., and Brown, M. H. (2019). Diversity and function of capsular polysaccharide in *Acinetobacter baumannii*. *Front. Microbiol.* 9:3301. doi: 10.3389/fmicb.2018.03301

Spinosa, M. R., Progida, C., Talà, A., Cogli, L., Alifano, P., and Bucci, C. (2007). The *Neisseria meningitidis* capsule is important for intracellular survival in human cells. *Infect. Immun.* 75, 3594–3603. doi: 10.1128/IAI.01945-06

Sweeney, E., Sabnis, A., Edwards, A. M., and Harrison, F. (2020). Effect of host-mimicking medium and biofilm growth on the ability of colistin to kill *Pseudomonas aeruginosa*. *Microbiology* 166, 1171–1180. doi: 10.1099/mic.0.000995

Topka-Bielecka, G., Dydecka, A., Necel, A., Bloch, S., Nejman-Faleńczyk, B., Węgrzyn, G., et al. (2021). Bacteriophage-derived depolymerases against bacterial biofilm. *Antibiotics* 10:175. doi: 10.3390/antibiotics10020175

Verbeken, G., Huys, I., De Vos, D., De Coninck, A., Roseeuw, D., Kets, E., et al. (2016). Access to bacteriophage therapy: discouraging experiences from the human cell and tissue legal framework. *FEMS Microbiol. Lett.* 363:fnv241. doi: 10.1093/femsle/fnv241

Verbeken, G., Huys, I., Pirnay, J. P., Jennes, S., Chanishvili, N., Scheres, J., et al. (2014a). Taking bacteriophage therapy seriously: a moral argument. *Biomed Res. Int.* 2014:621316. doi: 10.1155/2014/621316

Verbeken, G., Pirnay, J. P., Lavigne, R., Jennes, S., De Vos, D., Casteels, M., et al. (2014b). Call for a dedicated European legal framework for bacteriophage therapy. *Arch. Immunol. Ther. Exp.* 62, 117–129. doi: 10.1007/s00005-014-0269-y

Wang, C., Li, P., Zhu, Y., Huang, Y., Gao, M., Yuan, X., et al. (2020). Identification of a novel *Acinetobacter baumannii* phage-derived depolymerase and its therapeutic application in mice. *Front. Microbiol.* 11:1407. doi: 10.3389/fmicb.2020.01407

Whitfield, C. (2006). Biosynthesis and assembly of capsular polysaccharides in *Escherichia coli*. *Annu. Rev. Biochem.* 75, 39–68.

Wieland, K., Chhatwal, P., and Vonberg, R. P. (2018). Nosocomial outbreaks caused by *Acinetobacter baumannii* and *Pseudomonas aeruginosa*: results of a systematic review. *Am. J. Infect. Control* 46, 643–648. doi: 10.1016/j.ajic.2017.12.014

Wilson, C., Lukowicz, R., Merchant, S., Valquier-Flynn, H., Caballero, J., Sandoval, J., et al. (2017). Quantitative and qualitative assessment methods for biofilm growth: a mini-review. *Res. Rev. J. Eng. Technol.* 6, 1–25.

Wilson, J. W., Schurr, M. J., LeBlanc, C. L., Ramamurthy, R., Buchanan, K. L., and Nickerson, C. A. (2002). Mechanisms of bacterial pathogenicity. *Postgrad. Med. J.* 78, 216–224. doi: 10.1136/pmj.78.918.216

World Health Organization [WHO] (2017). *Global priority list of antibiotic-resistant bacteria to guide research, discovery, and development of new antibiotics*. Geneva: World-Health-Organization

World Health Organization [WHO] (2019). *Antibacterial agents in clinical development: an analysis of the antibacterial clinical development pipeline*. Available Online at: https://apps.who.int/iris/bitstream/handle/10665/330420/9789240000193-eng.pdf. (accessed 15 January 2020).

Wu, Y., Wang, R., Xu, M., Liu, Y., Zhu, X., Qiu, J., et al. (2019). A Novel Polysaccharide Depolymerase encoded by the phage SH-KP152226 confers specific activity against multidrug-resistant *Klebsiella pneumoniae* via biofilm degradation. *Front. Microbiol.* 10:2768. doi: 10.3389/fmicb.2019.02768

Yang, H., Chen, G., Hu, L., Liu, Y., Cheng, J., Li, H., et al. (2015). In vivo activity of daptomycin/colistin combination therapy in a *Galleria mellonella* model of *Acinetobacter baumannii* infection. *Int. J. Antimicrob. Agents* 45, 188–191. doi: 10.1016/j.ijantimicag.2014.10.012

Yoshida, K., Matsumoto, T., Tateda, K., Uchida, K., Tsujimoto, S., and Yamaguchi, K. (2000). Role of bacterial capsule in local and systemic inflammatory responses of mice during pulmonary infection with *Klebsiella pneumoniae*. *J. Med. Microbiol.* 49, 1003–1010. doi: 10.1099/0022-1317-49-11-1003

Conflict of Interest: The authors declare that the research was conducted in the absence of any commercial or financial relationships that could be construed as a potential conflict of interest.

Publisher's Note: All claims expressed in this article are solely those of the authors and do not necessarily represent those of their affiliated organizations, or those of the publisher, the editors and the reviewers. Any product that may be evaluated in this article, or claim that may be made by its manufacturer, is not guaranteed or endorsed by the publisher.

frontiers | Frontiers in Microbiology

REVIEW
published: 19 May 2022
doi: 10.3389/fmicb.2022.874153

Antimicrobial Peptides Controlling Resistant Bacteria in Animal Production

Gisele Rodrigues[1,2], *Lucas Souza Santos*[1] *and Octávio Luiz Franco*[1,2]*

[1] Centro de Análises Proteômicas e Bioquímicas, Programa de Pós-Graduação em Ciências Genômicas e Biotecnologia, Universidade Católica de Brasília, Brasília, Brazil, [2] S-Inova Biotech, Programa de Pós-Graduação em Biotecnologia, Universidade Católica Dom Bosco, Campo Grande, Brazil

In the last few decades, antimicrobial resistance (AMR) has been a worldwide concern. The excessive use of antibiotics affects animal and human health. In the last few years, livestock production has used antibiotics as food supplementation. This massive use can be considered a principal factor in the accelerated development of genetic modifications in bacteria. These modifications are responsible for AMR and can be widespread to pathogenic and commensal bacteria. In addition, these antibiotic residues can be dispersed by water and sewer water systems, the contamination of soil and, water and plants, in addition, can be stocked in tissues such as muscle, milk, eggs, fat, and others. These residues can be spread to humans by the consumption of water or contaminated food. In addition, studies have demonstrated that antimicrobial resistance may be developed by vertical and horizontal gene transfer, producing a risk to public health. Hence, the World Health Organization in 2000 forbid the use of antibiotics for feed supplementation in livestock. In this context, to obtain safe food production, one of the potential substitutes for traditional antibiotics is the use of antimicrobial peptides (AMPs). In general, AMPs present anti-infective activity, and in some cases immune response. A limited number of AMP-based drugs are now available for use in animals and humans. This use is still not widespread due to a few problems like *in-vivo* effectiveness, stability, and high cost of production. This review will elucidate the different AMPs applications in animal diets, in an effort to generate safe food and control AMR.

Keywords: antimicrobial resistance, growth promoters, antimicrobial peptides, livestock, feed supplementation

OPEN ACCESS

Edited by:
Josep M. Sierra,
University of Barcelona, Spain

Reviewed by:
Piyush Baindara,
University of Missouri, United States
Bruno Rivas-Santiago,
Unidad de Investigación Biomédica de Zacatecas (IMSS), Mexico
Jian Li,
Hubei University of Medicine, China

***Correspondence:**
Octávio Luiz Franco
ocfranco@gmail.com

Specialty section:
This article was submitted to Antimicrobials, Resistance and Chemotherapy, a section of the journal Frontiers in Microbiology

Received: *11 February 2022*
Accepted: *06 April 2022*
Published: *19 May 2022*

Citation:
Rodrigues G, Souza Santos L and Franco OL (2022) Antimicrobial Peptides Controlling Resistant Bacteria in Animal Production. Front. Microbiol. 13:874153. doi: 10.3389/fmicb.2022.874153

INTRODUCTION

In the last decades, antimicrobial resistance (AMR) has been a worldwide concern. The indiscriminate use of such drugs for a long time led to the formation of significant reservoirs of microorganisms with AMR genes in human and animal production (World Health Organization., 2014; Sharma et al., 2018).

The use of antimicrobials in animal feedstuff as therapeutic, metaphylactic, prophylactic, and growth promoter agents started in the year 1950, to boost food production (Krishnasamy et al., 2015; Woolhouse et al., 2015; Lagha et al., 2017; Magouras et al., 2017). The indiscriminate use of such drugs for a long time led to the formation of significant reservoirs of microorganisms

with AMR genes in livestock production (World Health Organization., 2014; Sharma et al., 2018). Moreover, drug-resistant bacteria can disseminate in two ways: through direct contact with animals and humans or indirectly through the food chain, and contaminated environment (Soucy et al., 2015; Lagha et al., 2017; Magouras et al., 2017; Vidovic and Vidovic, 2020). In 2014, the World Health Organization (WHO), emphasized the abusive use of antibiotics in the treatment of infectious diseases can result in bacteria with genes resistant to these drugs (Brown et al., 2017) (**Table 1**). Hence, in 2000, the WHO Advisory Group on Integrated Surveillance of Antimicrobial Resistance (AGISAR) (2011) classified AMR as a global public health concern, recommending the eradication of the use of antibiotics for feed supplementation in livestock.

In this sense, the use of alternative treatments such as phages therapy (Ferriol-González and Domingo-Calap, 2021; Loponte et al., 2021) and antimicrobial peptides treatment (Vieco-Saiz et al., 2019; Silveira et al., 2021) are considered to combat the advance of resistant microorganisms. In this review, we described information about antimicrobial peptides treatment.

Thus, the use of antimicrobial peptides (AMPs) suggests a possible alternative to traditional antibiotics, given their several modes of action, facility for degradation in nature, avoiding the accumulation, low resistance frequency, host immunity enhancement, and ability to neutralize the activity of many microbes (Jenssen et al., 2006; Zhao et al., 2016; Li et al., 2018). AMPs can be found in all organisms and demonstrated activity against several microorganisms even cancer cells (Saido-Sakanaka et al., 2004; Brogden, 2005; Hwang et al., 2011; Rodrigues G. et al., 2019; Rodrigues G. R. et al., 2019; Spohn et al., 2019; Vilas et al., 2019; Cardoso et al., 2020). Likewise, AMPs have sequences with variable structures, and mechanisms of action (Gomes et al., 2018; Spohn et al., 2019; Cardoso et al., 2020). Due to their cationic characteristics, AMPs may be capable of set electrostatic interactions with the external bacterial membrane, which is generally present negatively charged phospholipids (Hancock and Chapple, 1999; Shai, 2002). AMPs have the capacity to connect the outer membrane and act in the disturbed. In addition, they can also be translocated across the membrane and also react to internal targets (Hancock and Sahl, 2006). Furthermore, these peptides present the ability to stimulate the host's immune system indirectly (Hancock, 2001; Ward et al., 2013; Wang et al., 2016; Ageitos et al., 2017).

Therefore, this review will examine the different applications of AMPs supplemented in ruminants and non-ruminant feed, in an attempt to increase food production safety and control AMR.

ANTIMICROBIAL RESISTANCE AND ENVIRONMENTAL PROBLEMS

The discovery of penicillin represented an unprecedented milestone for modern medicine, transforming human history (Swann, 1983). Penicillin over the years has been collaborated to a massive reduction in mortality and caused an increase in life expectancy, besides offering essential support for invasive surgeries, and chemotherapy treatments (Blair and Piddock, 2009). Likewise, antibiotics also brought benefits to animal health when used as feed supplementation improving the growth and rentability of animal production (Cheng et al., 2014; Lhermie et al., 2017).

However, the antimicrobials used for animal food supplementation are the same as those administered as medicine for humans (World Health Organization., 2014; Sharma et al., 2018; Wu et al., 2018; Medina et al., 2020). The abusive use of antibiotics is the major factor in developing genetic modifications in bacteria. That is the main cause of antimicrobial resistance (AMR), which can be widespread in pathogenic and commensal bacteria (Thomas and Nielsen, 2005; Founou et al., 2016; Aslam et al., 2018; Li et al., 2018; Innes et al., 2020). AMR can be diffused into the food chain, by animal contact, or by environmental routes (Li et al., 2018; Scott et al., 2019) (**Figure 1**). Additionally, most of these drugs are not totally degraded in the body of animals and humans, and those residues are eliminated by excreted urine and feces, which then accumulate in soils, wastewater, manure causing profound, and complex impacts (Lim et al., 2013; Wu et al., 2014; Thanner et al., 2016; Li et al., 2018). Contact with or ingestion of antibiotic residues can give rise to several health problems, such as allergic hypersensitivity reactions, hepatotoxicity, nephropathy, mutagenicity, carcinogenicity, and antibiotic resistance (Mensah et al., 2014).

Presently, 700,000 annual worldwide death are associated with AMR, and the number of deaths in 2050 is estimated to reach 10 million (Aria and Murray, 2009; Munita and Arias, 2016; World-Health-Organisation [WHO], 2018; Ghosh et al., 2019). Considering all this information, the WHO recommended the suspension or elimination of the use of antimicrobial agents in animal feed supplementation. Following the recommendations of the WHO Advisory Group on Integrated Surveillance of Antimicrobial Resistance (AGISAR) (2011), countries of the European Union forbade feed supplementation with antibiotics in livestock production in 2006 (Magouras et al., 2017). In an attempt to standardize the measures to be taken and the information generated, surveillance and monitoring programs were created, advised by the WHO the OIE (OIE World Organisation for Animal Health., 2012), and the Food and Agriculture Organization (FAO) (FAO et al., 2018).

ANTIMICROBIAL PEPTIDES AS AN ALTERNATIVE FOR LIVESTOCK TREATMENT

Livestock production is a sector that has expanded immensely, in an attempt to keep up with meat consumption. According to the FAO, cattle (including meat and dairy), pigs, and poultry together represent approximately 80% of the meat production (FAO, 2016, 2018). Current meat production is 200 million tons, and in 2050, this production will need to expand to 470 million tons, under current rates and predictions (Clifford et al., 2018). This rise causes concern regarding the quality of the meat produced (Vieco-Saiz et al., 2019), as accelerated production on large farms can cause health problems like weight loss, mastitis, and

TABLE 1 | Antimicrobial agents used in animals and humans.

Antimicrobial class	Antibiotics	Animal use	Activity human	References
Aminoglycosides	Gentamicin B	Therapeutic use for poultry and swine	Yes	Heuer et al. (2009)
	Lasalocid	AGP*	No	Heuer et al. (2009)
	Neomycin	Therapeutic use and AGP in cattle, swine, poultry and aquiculture	Yes	Jones and Ricke (2003)
	Streptomycin B	Feed supplementation for aquiculture	Yes	National Research Council. (1999)
Amphenicols	Florfenicol	Therapeutic use in cattle and swine	No	Dibner and Richards (2005)
	Carbomycin B	Feed supplementation for aquiculture	Yes	Bywater (2005)
Aminocoumarins	Novobiocin	Therapeutic use in bovine mastitis	Yes	Katsunuma et al. (2007)
Aminopenicillins	Amoxicillin, B ampicillin B	Therapeutic use in cattle, mastitis, swine, poultry and aquiculture	Yes	Aarestrup et al, 2007
Arsenicals	Roxarsone	AGP for poultry, swine and therapeutic use in swine	No	Witte (2000)
Beta-lactams	Procaine penicillin	AGP in poultry and swine	Yes	Witte (2000)
Cyclopolypeptides	Colistin	Feed supplementation for cattle, swine and broiler	Yes	Witte (2000)
Diaminopyrimidines	Ormetoprim	AGP and therapeutic use for poultry	No	Andleeb et al. (2020)
Elfamycins	Efrotomycin	AGP for swine	No	Bywater (2005)
Fluoroquinolones	Enrofloxacin B	Therapeutic use for cattle, swine	No	Bywater (2005)
	Flumequin B	Therapeutic use in aquaculture	No	Dibner and Richards (2005)
Glycopeptides	Ardacin	AGP for broilers	No	Arestrup et al. (2001)
	Avoparcin B	AGP	No	Arestrup et al. (2001)
Ionophores	Narasin	Feed supplementation and therapeutic use for poultry and AGP for cattle	No	Katsunuma et al. (2007)
	Maduramycin	Feed supplementation for poultry	No	Jones and Ricke (2003)
	Monensin	AGP in cattle and poultry	No	Jones and Ricke (2003)
	Salinomycin	AGP and therapeutic use for swine	No	Witte (2000)
Lincosamides	Lincomycin	Therapeutic use for poultry and swine	Rare	Heuer et al. (2009)
Macrolides	Macrolides	Therapeutic use for poultry	No	Bywater (2005)
	Tylosin B	AGP for swine and therapeutic use for mastitis	No	McEwen and Fedorka-Cray (2002)
	Oleandomycin B	AGP for swine and poultry	Yes	Andleeb et al. (2020)
	Erythromycin*b*	AGP in cattle, poultry, swine and therapeutic use in aquaculture	Yes	Dibner and Richards (2005)
	Spiramycin B	AGP for swine and therapeutic use in bovine mastitis	Yes	Witte (2000)
Nitrofurans	Furazolidone	Therapeutic use in aquaculture	Yes	Dibner and Richards (2005)
Orthosomysins	Avilamycin	AGP for broilers	No	Arestrup et al. (2001)
Phosphoglycolipids	Bambermycin	AGP	No	Butaye et al. (2003)
Pleuromutilins	Tiamulin	Therapeutic use and AGP for swine	No	McEwen and Fedorka-Cray (2002)
Polypeptides	Bacitracin/zinc bacitracin	AGP and therapeutic use in several livestock infections	Yes	Butaye et al. (2003)
Quinolones	Oxolinic acid B	Feed supplementation for aquiculture	No	Andleeb et al. (2020)
Quinoxalines	Carbadox	Therapeutic use in swine	No	Butaye et al. (2003)
	Olaquindox	AGP an therapeutic use in swine	No	Katsunuma et al. (2007)
Streptogramins	Pristinamycin	AGP	Yes	Andleeb et al. (2020)
	Virginiamycin	AGP for broilers	Yes	McEwen and Fedorka-Cray (2002)
Streptothricins	Nourseothricin	AGP for swine	No	Katsunuma et al. (2007)
Sulfonamides	Sulfonamides	Therapeutic use in aquiculture, and AGP in poultry and swine	Yes	National Research Council. (1999)
Tetracylines	Tetracyclines (oxy- and chlor-) B	AGP in cattle, poultry, swine and therapeutic use for livestock infection	Yes	National Research Council. (1999)

**Antimicrobial growth promoters.*

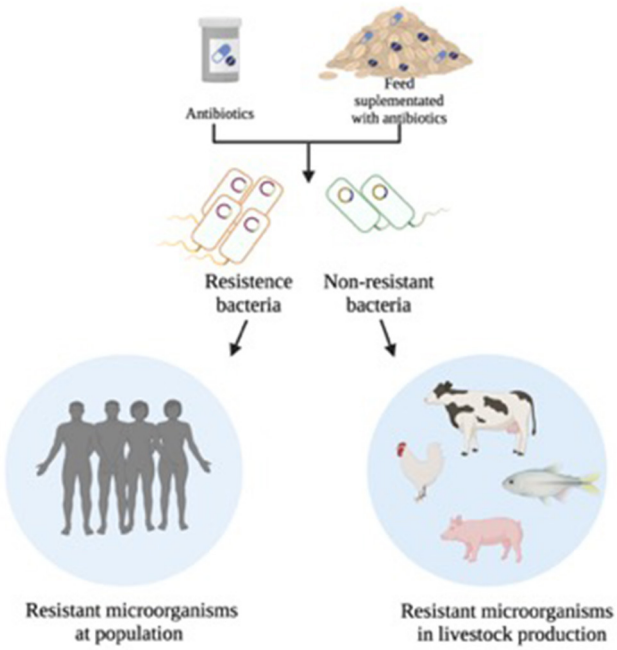

FIGURE 1 | Representation of antibiotic-resistant bacteria in different ecosystems: antimicrobial usage may select the genes encoding resistance. Drug-resistant bacteria can spread when domestic animals receive antibiotics and develop antibiotic-resistant bacteria in their gastrointestinal tracts (GIT). This contamination can occur through humans, among vulnerable patients in hospitals or with contact with contaminated surfaces. These bacteria can be propagated in humans either through the food supply chain (meat and dairy products) or by direct animal contact. In addition, they can spread via water containing animal feces used for animal crops, or drug-resistant bacteria can remain on crops and be eaten. In this way, bacteria can remain in human and animal guts and spread in the community.

other infectious diseases (Krehbiel, 2013; Li et al., 2018; Sharma et al., 2018). Furthermore, farmers have been using antibiotics in their livestock production in an effort to prevent animal health problems, but the broad use of antimicrobials is one of the causes of the development of resistant microorganisms (World Health Organization., 2014; Sharma et al., 2018).

As described above AMPs, in general, demonstrated efficient activity against antimicrobial infection, due to the rapid action against pathogens, non-specific action, these result in a low resistance rate (Wimley and Hristova, 2011; Maria-Neto et al., 2015; Ageitos et al., 2017; Li et al., 2018). According to this, the overexposure of AMPs to the pathogens can generate the development of AMP-resistant strains.

Antimicrobial Peptides Issues

AMPs demonstrated an efficient result acting as antimicrobial and immunomodulation activity. Despite this, AMPs may present some issues like bacterial resistance (Fry, 2018). This mechanism is unclear, but studies described that bacterial AMPs resistance cause alterations in membranes, cell walls, and cellular metabolism. In the case of membrane modification, bacteria can switch the AMP target, decreasing AMPs interactions with membrane components (Huhand and Kwon, 2011; Zucca et al., 2011). Also, these modifications can affect the permeability and fluidity of the membrane (Li et al., 2007; Otto, 2009).

Other resistance mechanisms result in a modification of bacterial ionic cell wall potential in specific interaction spots that can reduce the binding of antibiotic peptides (Henderson et al., 2014). In addition, AMPs activities against the bacteria could generate high metabolic stress levels like the production of proteases, modification of surface structures, and biofilm (Yeaman and Yount, 2003). Furthermore, AMPs also present problems related to high production costs compared with antibiotics, susceptible to enzymatic and pH degradation. AMPs that act in the gastrointestinal tract (GIT) occur in intestinal absorption, bioavailability, distribution, renal clearance, and peptide elimination (Fry, 2018; Meade et al., 2020).

In general, these issues can be avoided using computational strategies to overcome challenges associated with the high cost of production, the potency of AMPs, and reduce the rate of resistance, degradation, toxicity, and instability (Cardoso et al., 2020; Dijksteel et al., 2021). Another option is the use of multi-omics (including genomics, transcriptomics, and proteomics) which allows identifying a novel sequence of AMPs (Chen et al., 2019; Burgos-Toro et al., 2021).

Problems related above are responsible for the low number of peptides approved in a clinical trial because the efficiency of the results *in vitro* does not always the same as *in vivo*. Nevertheless, AMPs remain a great option to control microbial infections. **Table 2** summarized some AMPs recently approved or in advanced clinical trials (Dijksteel et al., 2021).

AMP to Control Microbiota in Livestock Production

The microbiota profile relates to the growth performance of animals since the presence of specific groups of microorganisms promotes the absorption of nutrients inside the gastrointestinal tract (Yadav and Jha, 2019). The modulation of microbiota may also lead to the reduction of pathogenic species, decreasing the frequency and lethality of some diseases (Cheema et al., 2011; Wang et al., 2015b; Yadav and Jha, 2019).

Despite that, several diseases affected the livestock production causing intestinal mucosa inflammation, and diarrhea associated with morphological changes in the intestinal epithelium. These pathologies are caused by toxins produced by bacteria (Xiao et al., 2015). For decades, all diseases were treated using antibiotics which boosted the increase of antibiotic-resistant microorganisms. This increase in resistant bacteria in the animal microbiota has been demonstrated in resistome studies (Wang et al., 2021). Resitsome studies described the existence of a broad spectrum of antimicrobial resistance genes (ARGs) in the digestive tract of food-producing animals. The presence of ARGs is not necessarily associated with the direct use of antibiotics but can occur with the administration through feed or water or by injectable antimicrobials (Ma et al., 2021).

In this context, the uses of AMPs utilization have demonstrated their ability to recover and maintain the GIT of animals by epithelial barrier integrity stabilization and

TABLE 2 | AMPs recently tested and approved by FDA.

Peptide	Description	Target	Phase	Clinical Trial ID	Mechanism	References
Topical						
PXL01	Analog of Lactoferrin	Postsurgical adhesions	II	NCT01022242	Immunomodulation	Edsfeldt et al., 2017
Wap-8294A2 (Lotilibcin)	Produced by Lysobacter species	Gram-positive bacteria	II/III		Membrane disruption	Itoh et al., 2018
Novexatin (NP213)	Cyclic Cationic peptide	Fungal nail infection	II	NCT02933879	Membrane disruption	Mercer et al., 2020
Melamine	Chimeric peptide	Contact lenses microbials	II/III		Membrane disruption	Yasir et al., 2019
Mel4	Derivative of melamine	Contact lenses microbials	II/III	ACTRN1261500072556	Membrane disruption	Yasir et al., 2020
D2A21	Synthetic peptide	Burn wound infections	III		Membrane disruption	Muchintala et al., 2020
Delmitide (RDP58)	Derivative of HLA	Inflammatory bowel disease	II		Immunomodulation	Travis et al., 2005
XOMA-629 (XMP-629)	Derivative of BPI	Impetigo/acne rosacea	III		Immunomodulation	Easton et al., 2009
PL-5	Synthetic peptide	Skin infections			Membrane disruption	Miyake et al., 2004
LTX-109	Synthetic tripeptide	MRSA/impetigo	I/II	NCT01803035; NCT01158235	Membrane disruption	Isaksson et al., 2011; Sivertsen et al., 2014
Intravenous						
hLF1-11	Fragment of human lactoferrin	Bacterial/fungal infections	I/II	NCT00430469	Membrane disruption/immunomodulation	Brouwer et al., 2018
EA-230	Oligopeptide	Sepsis	II	NCT03145220	Immunomodulation	van Groenendael, 2018
DPK-060	Derivative of Kininogen	Acute external otitis	II	NCT01447017	Membrane disruption/immunomodulation	Håkansson et al., 2019
Friulimicin	Cyclic lipopeptide	MRSA/pneumonia	I	NCT00492271	Membrane disruption	Schneider et al., 2009
Murepavadin (POL7080)	Analog of Protegrin	*P. aeruginosa, K. pneumoniae*	II	EUCTR2017-	Binding to LptD	Srinivas et al., 2010
IDR-1	Bactenecin	Infection prevention	I		Immunomodulation	Yu et al., 2009
Ghrelin	Endogenous peptide	Chronic respiratory infection	II	NCT00763477	Immunomodulation	Gualillo et al., 2003
PMX-30063 (Brilacidin)	Defensin mimetic	Acute bacterial skin infection	II	NCT01211470; NCT02052388	Membrane disruption/immunomodulation	Mensa et al., 2014
Oral						
Ramoplanin (NTI-851)	Glycolipodepsipeptide	*C. difficile*	III		Inhibition of cell wall synthesis	Fulco and Wenzel, 2006
SGX942 (Dusquetide)	Analog of IDR-1	Oral mucositis	III	NCT03237325	Immunomodulation	Kudrimoti et al., 2016
GSK1322322 (Lanopepden)	Synthetic hydrazide	Bacterial skin infection	II	NCT01209078	Peptide deformylase inhibitor	Peyrusson et al., 2015
NVB-302	Lantibiotic	*C. difficile*	I	ISRCTN40071144	Inhibition of cell wall synthesis	Crowther et al., 2013
Nisin bacteria	Polycyclic lantibiotic	Gram-positive		NCT02928042; NCT02467972	Depolarization of cell membrane	Prince et al., 2016

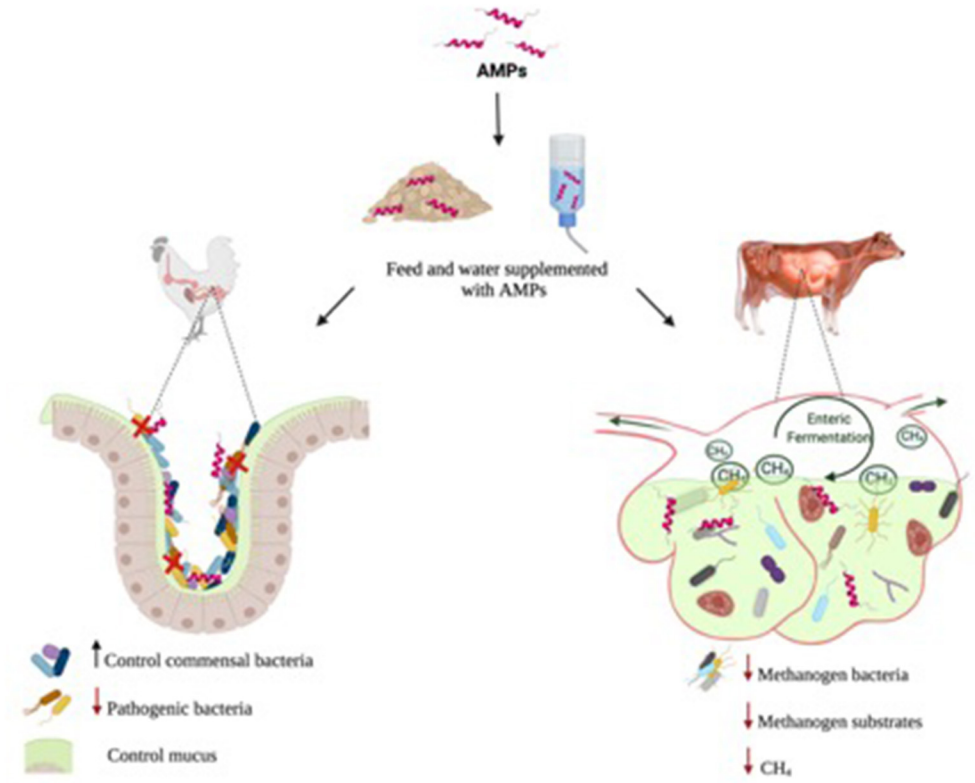

FIGURE 2 | Antimicrobial peptides (AMPs) affects intestinal mucosa and rumen: AMP as growth promoters in poultry and swine intestinal can act altering the composition of the microbiota to reduce competition for nutrients, reduce pathogen, and control mucus. In rumen the AMPs as growth promoters acting reducing the methanogen bacteria and substrates. In addition, decrease the rate of methane (CH_4) production and release.

by boosting intestinal epithelium colonization susceptibility (Murphy et al., 1993; Gallo et al., 1994; Podolsky, 2000; Tollin et al., 2003; Xiao et al., 2015) (**Figure 2**). Furthermore, some AMPs can act by inhibiting LPS-induced pro-inflammatory cytokine production, behaving as chemokines, or modulating the dendritic cell and T cell response (Mookherjee et al., 2006; Xiao et al., 2015).

Likewise, antibiotics have been used in ruminants with the goal to control the ruminal microbiota reducing losses during the enteric fermentation process. Moreover, ruminants are relevant sources of greenhouse gas (GHG) emissions (Eisler et al., 2014; Reisinger and Clark, 2018). The CH_4 liberated for enteric fermentation suggests that 90% GHG is present in the atmosphere (Lan and Yang, 2019; Leahy et al., 2019). Other problems related to CH_4 are the conversion to ammonia by rumen fermentation and its further excretion as urea in the urine can accumulate in the soil, and also cause groundwater pollution (Firkins et al., 2007) (**Figure 2**).

In this context, AMPs are used as a sustainable alternative to the rising production and mitigated contaminants. Peptides like LL32, Lpep 19-2.5, and NK2 derivatives of porcine NK-lysin have demonstrated activity against methanogenic archaeal strains and also observed in the control of rumen fermentation (Bang et al., 2012). This modulation can occur as an influence on electron flow, acting as the hydrogen acceptor to effectively compete with rumen methane production, or killing some nitrate-reducing Gram-positive bacteria (Bang et al., 2012; Shen et al., 2016, 2017; Varnava et al., 2017). Besides, some peptides use rumen microbiota to reduce amino acid deamination and methanogenesis, without having a negative impact on dry matter digestibility or volatile fatty acid production (Varnava et al., 2017). Additionally, the sheep feed supplemented with peptides showed a decrease in methane emission of 10% (Callaway et al., 1997; Shen et al., 2016). Thus, the use of AMPs in livestock can be an alternative method to solve problems with digestibility and microbiota, improving the sustainability of livestock production (Santoso et al., 2004; Sar et al., 2005; Wang et al., 2015a,b; Vieco-Saiz et al., 2019).

AMPs Used as Growth Promoters

AMPs in feed supplementation have been extensively evaluated in several studies, and some characteristics are listed in **Table 3**. The peptide microcin J25 (MccJ25), a bacterial RNA polymerase inhibitor, increases the broilers' growth and attenuates the injuries to the intestine morphology caused by microbial infection. The application of MccJ25 in a range from 0.5 to

TABLE 3 | AMPs using livestock production.

AMP	Source	Activity	Target bacteria	Animal	References
Microcin J25	*E. coli*	Immune Regulation, and Intestinal Microbiota	*Escherichia coli, Salmonella* CVCC519	Broiler	Wang et al. (2020) and Iseppi et al. (2021)
Pediocin A	*Pediococcus pentosaceus*	Dietary supplementation	*Clostridium perfringens*	Broilers	Grilli et al. (2009) and Hernández-González et al. (2021)
Gallinacin-6	*Gallus gallus domesticus*	Antimicrobial	*Campylobacter jejuni, Salmonella enterica, Clostridium perfringens, E. coli*	Broilers	van Dijk et al. (2007)
Plectasin	*Pseudoplectania nigrella*	Dietary supplementation		Broilers	Ma et al. (2019)
RSRP	*Oryctolagus cuniculus*—sacculus rotundus	Dietary supplementation Intestinal mucosal immune responses	Reducing the viable counts of *E. coli*	Broilers	Liu et al. (2008)
Lactoferrin (bLf)	*Bos taurus*	Dietary supplementation Intestinal mucosal	Reducing the total viable counts of *E. coli* and Salmonella	Broilers	Tang et al. (2008), Messaoudi et al. (2012), Aguirre et al. (2015)
SMXD51	*Lactobacillus salivarius*	Intestinal Microbiota	*Campylobacter jejuni*	Poultry	Cao et al. (2007), Ceotto-Vigoder et al. (2016)
BT	*Brevibacillus texasporus*	Dietary supplementation Intestinal mucosal	*Salmonella enterica serovar Enteritidis.*	Neonatal poultry	Kogut et al. (2013)
Nissin*	*Lactococcus sp. Streptococcus sp*.	Food preservation; Antimicrobial	*E. coli, Staphylococcus aureus, Streptococcus agalactiae, S. dysagalactiae, S. uberis S. aureus* biofilm	Cattle	Santoso et al. (2004), Sar et al. (2005), Cao et al. (2007), Ceotto-Vigoder et al. (2016), Shen et al. (2016, 2017), Shin et al. (2016), Hernández-González et al. (2021)
Lysostaphin	*Staphylococcus sp.*	Antimicrobial	*S. aureus* biofilm	Cattle	Ceotto-Vigoder et al. (2016)
AP-CECT712	*Enterococcus faecalis*	Antimicrobia	*S. aureus*, *S. dysgalactiae*, S. *uberis*, S. *agalactia*	Cattle	Sparo et al. (2009)
Colicin	*E. coli*	Antimicrobial	*E. coli*	Swine	Stahl et al. (2004), Cutler et al. (2007)
Porcine (pBD-1)	Porcine blood	Antimicrobial, immune responses	*Bordetella pertussis*	Newborn Piglets	Elahi et al. (2006)
Cathelicidin-BF (C-BF)	*Bungarus fascia*	Intestinal immune responses		Weanling piglets	Wang et al. (2008), Yi et al. (2015)

**Commercial use—FDA liberation.*

1.0 mg.kg^{-1} was able to reduce body weight loss by up to 70%, in comparison to 54.6% with antibiotic treatment (Wang et al., 2020). The recombinant cecropin A-D-Asn is formed by a chimeric peptide, from cecropin A, and cecropin D C-termini. Moreover, asparagine residue was added and amidated in C-terminus. The inclusion of 6 mg/kg^{-1} of the peptide to the basal feed of broilers boosts by 20% the weight when compared with feed without peptide addition (Wen and He, 2012).

Pediocin A was administrated in poultry food and demonstrated efficient results as a growth promoter (Daeschel and Klaenhammer, 1985). A similar result with a gain of body weight was described using the combination of bacteriocins (divercin AS7 and nisin) as a food additive for broilers (Józefiak et al., 2013; Hernández-González et al., 2021). *In vivo* studies have shown AMPs also improve growth performance and digestive capacity in poultry and pigs (Wang et al., 2016). The use of AMP-A3 and AMP-P5 (both derived from the amino acid substitution of the *Helicobacter pylori* HP and the cecropin-magainin2 fusion, respectively), can raise the F:G ratio of weanling pigs and broilers, with additional benefits concerning nutrient uptake and intestinal morphology. The AMP-A3 (90 mg.kg^{-1}) and AMP-P5 (60 mg.kg^{-1}), display effective results showing elevated weight gain and reduced intestinal damage (Yoon et al., 2012, 2013, 2014; Choi et al., 2013a,b).

Ren et al. (2019) demonstrated the use of the recombinant swine defensin PBD-mI with a molecular mass of 5.4 kDa, and LUC-n with a molecular mass of 21.18 kDa, in 18 4-month-old Chuanzhong black goats. The animals were split into three groups (basal diet; basal diet + 2g AMP/goat/day; basal diet + 3g AMP/goat/day), and rumen fluid was collected and analyzed. Dietary supplementation with both AMPs demonstrated that the goats enhanced rumen microbiota diversity, updated ruminal fermentation, improved efficiency of food usage, and boosted growth performance. Although studies demonstrated positive results of AMPs in feed supplementation for poultry and pigs, the same is not observed for ruminants.

Use of AMPs to Control Infectious Disease

AMPs present an important role in controlling infection disease and the immunity system of non-ruminants maintaining (Hernández-González et al., 2021). Daneshmand et al. (2019), demonstrated that the use of a lactoferrin-derived peptide, cLF36 utilization can diminish infection by modulating the expression of cytokines IL-2 and IL-6 and mucine in broilers challenged with enterotoxigenic *Escherichia coli*. Adding 20 $mg.kg^{-1}$ of cLF36 in feed reduced the population of *E. coli* and *Clostridium* spp. by 25% and 20%, respectively. Besides, the number of beneficial *Lactobacillus spp.* and *Bifidobacterium spp*. increased by up to 36%. Moreover, sublacin, a peptide obtained from *Bacillus*, may decrease harmful bacteria without causing any change in the *Lactobacillus* community. The peptide was supplemented with water (5.76 mg. L^{-1}) (Wang et al., 2015a,b).

Another host defense peptide, ß-defensin-1 (pDB-1), has potential veterinary application. This peptide has shown its expression in the respiratory tract of old pigs, and demonstrated to be resistant against the infection of the respiratory pathogen *Bordetella pertussis*. Otherwise, newborn piglets do not seem to have pDB-1, and are susceptible to the disease. Thus, the application of 500 μg of tpDB-1 to the respiratory tract of these piglets was able to totally inhibit clinical symptoms (Elahi et al., 2006).

Furthermore, the peptide C-BF, which originates from *Bungarus fasciatus* venom, also demonstrated beneficial results in controlling bacterial disease in animal production (Elahi et al., 2006). C-BF used 0.5 $mg.kg^{-1}$ in piglets via intraperitoneal application, and the peptide minimized the inflammatory molecule's TNF-α and IL-6. The level of cell apoptosis and intestinal barrier damage caused by bacterial lipopolysaccharide also decreased (Zhang et al., 2017). S100A8 and S100A9 showed beneficial results against ruminant infections. These peptides reduced uterine inflammation (which appears after calving in association with bacterial contamination) and modulated the early endometrial response against infection in Holstein–Friesian cows (Swangchan-Uthai et al., 2013).

Another application for AMPs is in aquaculture, a sector which dedicated to producing aquatic plants and animals, with a recent growth rate higher than any other land-based livestock (Gyan et al., 2020; León et al., 2020). *In vitro* study demonstrated high efficacy of synthetic peptides (frog caerin1.1, European sea bass dicentracin (Dic) and NK-lysin peptides (NKLPs) and tongue sole NKLP27) against viral fish pathogens, such as nodavirus (NNV), viral septicemia hemorrhagic virus (VHSV), infectious pancreatic necrosis virus (IPNV) and spring viremia carp virus (SVCV) (León et al., 2020).

In addition, **Table 2** summarized many AMPs used in veterinary treatment with an efficient result.

APPLICATION OF AMPs IN DIFFERENT SECTORS

AMPs presented beneficial results in the control of microbial infections and in food supplementation. However, peptides have different functions in the food industry (Bemena et al., 2014; Rai et al., 2016), and artificial breeding in livestock (Schulze et al., 2014, 2020; Speck et al., 2014; Shaoyong et al., 2019).

The food industry normally uses nitrites and sulfur dioxide (chemical preservatives), which can cause negative effects on human health and the nutritional level of food (Bemena et al., 2014). Recently, AMPs have been used instead, to maintain the properties of the food without modifying quality, besides not being harmful (Wang et al., 2016). The lactic acid bacteria are a good example because they are recognized as safe by the Food and Drug Administration, and are extensively used in human and animal food as a preservative, and to control pathogenic and spoilage bacteria (Rai et al., 2016; Venegas-Ortega et al., 2019; Iseppi et al., 2021).

AMPs are also being studied and applied to semen preservation in the artificial breeding process. A recent study used two synthetics cyclic hexapeptides, c-WFW and c-WWW, and magainin II (MK5E). These peptides were tested for boar semen preservation, indicating that cyclic hexapeptides can be promising candidates, due to proteolytic stability, capacity to control bacterial proliferation, and synergistic interaction with conventional antibiotics. The peptide ε-PL also showed effective results at a low concentration (0.16 g. L^{-1}), suggesting that it could be a possible substitute for gentamicin to enhance sperm quality parameters, sperm capacitation, and *in vitro* fertilization by reducing bacterial concentrations (Shaoyong et al., 2019).

CONCLUDING REMARKS AND PROSPECTS

The excessive use of antibiotics as a growth promoter in livestock causes microbial resistance, which is associated with increased consumption of animal protein, while production has difficulties in keeping up with this demand (Eisler et al., 2014).

Hence, various countries prohibited antibiotics in animal supplementation, thus stimulating the expansion of research to sustainable approaches (Wang et al., 2016; Li et al., 2018; Leahy et al., 2019). Besides that, livestock products have faced challenges such as reduced productivity, loss of biodiversity, rising GHG emissions, sick animals, and diseases that can cause human illness (Grace et al., 2012; Michalk et al., 2019). Thus, sustainable animal production is the next step to increasing healthy livestock production and at the same time reducing environmental impacts (Kemp and Michalk, 2011; Godfray and Garnett, 2015; Vidovic and Vidovic, 2020).

Herein, we demonstrated positive results in the use of AMPs, which have shown to be promising in controlling microbial infection (Stahl et al., 2004; Ceotto-Vigoder et al., 2016), and methane gas emissions (Santoso et al., 2004; Sar et al., 2005), while also providing in-feed supplementation (Wang et al., 2008, 2016; Ren et al., 2019).

In this context, synthetic biology (SB) is an approach responsible for improving or completely creating systems and organisms, providing novel diagnostic tools, and enabling the economic production of new therapeutics drugs (Weber and Fussenegger, 2012; Takano and Breitling, 2014). SB has the skills to produce antibiotic drug advances, using different approaches like synthetic gene circuits (Weber et al., 2008) and protein engineering (King et al., 2016). It can foster the development of new drugs using faster and more efficient protocols, allowing the development of more accessible medicines that demonstrate greater precision (Noel, 2010; Jakobus et al., 2012). The rational design seeks to improve AMP sequence optimization and enhance biological activities, aiming to develop new drugs with high specificity against microorganisms and a reduction in adverse effects (Porto et al., 2012; Cardoso et al., 2020). In this context, computational tools like quantitative structure-activity relationship (QSAR), *de novo*, linguistic, pattern insertion, and evolutionary/genetic algorithms are very useful in designing AMP variants (Chen and Bahar, 2004; Loose et al., 2006; Hiss et al., 2010; Mitchell, 2014; Torres and De La Fuente-Nunez, 2019). In addition, these computational tools can be used separately or in association to construct novel peptide-based drug candidates (Cardoso et al., 2020).

In addition, AMPs can be used associated with nanoparticles (NPs) (Sharma et al., 2018). They could have several shapes and formulations (e.g., nitric oxide-releasing nanoparticles, chitosan-containing, and metal-containing nanoparticles) (Huhand and Kwon, 2011; Pelgrift and Friedman, 2013), and delivery systems, such as microencapsulation (Ganesh and Hettiarachchy, 2016; Kaikabo et al., 2016; Suresh et al., 2018), improving the bacterial control system. NPs can boost the effectiveness in the treatment of infectious diseases, besides protecting the peptide from degradation in the physiological environment (Rodrigues G. et al., 2019; Rodrigues G. R. et al., 2019). These tools are able to produce new drugs with fewer side effects, low costs, and with ability to abolish or control infectious diseases.

Different studies have been executed in the search for AMPs with anti-infective activities, but it is essential that these studies proceed to *in vivo* models and also to clinical trials.

All alternate strategies suggested can be successfully implemented with the prudent use of antibiotics, and strengthen the supervision associated with policies and regulation of use. These steps will allow farmers and veterinarians to prescribe treatment options for livestock production without causing chain effects. Thus, the use of AMPs in livestock allows the safe production of quality food, contributing to the maximization of agricultural output in a sustainable and economically satisfactory way.

AUTHOR CONTRIBUTIONS

All authors listed have made a substantial, direct, and intellectual contribution to the work and approved it for publication.

FUNDING

This work was supported by grants from Fundação de Apoio à Pesquisa do Distrito Federal (FAPDF), Coordenação de Aperfeiçoamento de Pessoal de Nível Superior (CAPES) (MC 88887.351521/2019-00), Conselho Nacional de Desenvolvimento e Tecnológico (CNPq), and Fundação de Apoio ao Desenvolvimento do Ensino, Ciência e Tecnologia do Estado de Mato Grosso do Sul (FUNDECT), Brazil.

REFERENCES

Ageitos, J. M., Sánchez-Pérez, A., Calo-Mata, P., and Villa, T. G. (2017). Antimicrobial peptides (AMPs): ancient compounds that represent novel weapons in the fight against bacteria. *Biochem. Pharmacol.* 133, 117–138. doi: 10.1016/j.bcp.2016.09.018

Aguirre, A. T. A., Acda, S. P., Angeles, A. A., Oliveros, M. C. R., Merca, F. E., and Cruz, F. A. (2015). Effect of bovine lactoferrin on growth performance and intestinal histologic features of broiler. *Philipp. J. Vet. Anim. Sci.* 41, 12–20.

Andleeb, S., Jamal, M., Bukhari, S. M., Sardar, S., and Majid, M. (2020). "Trends in antimicrobial use in food animals, aquaculture, and hospital waste," in *Antibiotics and Antimicrobial Resistance Genes*, ed M. Z. Hashmi (Cham: Springer), 95–138. doi: 10.1007/978-3-030-40422-2_5

Arestrup, F. M., Seyfarth, A. M., Emborg, H. N., Pedersen, K., Hendriksen, R. S., and Bager, F. (2001). Effect of abolishment of the use of antimicrobial resistance in fecal Enterococci from food animals in Denmark. *Antimicrob. Agents Chemother.* 45, 2054–2059. doi: 10.1128/AAC.45.7.2054-2059.2001

Aarestrup, F. M., Knöchel, S., and Hasman, H. (2007). Antimicrobial susceptibility of Listeria monocytogenes from food products. *Foodborne Pathog. Dis.* 4, 216–221. doi: 10.1089/fpd.2006.0078

Aria, C. A., and Murray, B. E. (2009). Antibiotic-resistant bugs in the 21st century—a clinical super-challenge. *N. Engl. J. Med.* 360: 439–443. doi: 10.1056/NEJMp0804651

Aslam, B., Wang, W., Arshad, M. I., Khurshid, M., Muzammil, S., Rasool, M. H., et al. (2018). Antibiotic resistance: a rundown of a global crisis. *Infect. Drug Resist.* 11, 1645. doi: 10.2147/IDR.S173867

Bang, C., Schilhabel, A., Weidenbach, K., Kopp, A., Goldmann, T., Gutsmann, T., et al. (2012). Effects of antimicrobial peptides on methanogenic archaea. *Antimicrob. Agents Chemother.* 56, 4123–4130. doi: 10.1128/AAC.00661-12

Bemena, L. D., Mohamed, L. A., Fernandes, A. M., and Lee, B. H. (2014). Applications of bacteriocins in food, livestock health and medicine. *Int. J. Curr. Microbiol. Appl. Sci.* 3, 924–949.

Blair, J. M., and Piddock, L. J. (2009). Structure, function and inhibition of RND efflux pumps in Gram-negative bacteria: an update. *Curr. Opin. Microbiol.* 12, 512–519. doi: 10.1016/j.mib.2009.07.003

Brogden, K. A. (2005). Antimicrobial peptides: pore formers or metabolic inhibitors in bacteria? *Nat. Rev. Microbiol.* 3, 238–250. 1098. doi: 10.1038/nrmicro1098

Brouwer, C. P. J. M., Roscini, L., Cardinali, G., Corte, L., Pierantoni, D. C., Robert, V., et al. (2018). Structure-activity relationship study of synthetic variants derived from the highly potent human antimicrobial peptide hLF (1-11). *Cohesive J. Microbiol. Infect. Dis.* 1, 1–19. doi: 10.31031/CJMI.2018.01.000512

Brown, K., Uwiera, R. R., Kalmokoff, M. L., Brooks, S. P., and Inglis, G. D. (2017). Antimicrobial growth promoter use in livestock: a requirement

to understand their modes of action to develop effective alternatives. *Int. J. Antimicrob, Agents* 49, 12–24. doi: 10.1016/j.ijantimicag.2016.08.006

Burgos-Toro, A., Dippe, M., Vásquez, A. F., Pierschel, E., Wessjohann, L. A., and Fernández-Niño, M. (2021). "Multi-omics data mining: A novel tool for biobrick design," in *Synthetic Genomics-From Natural to Synthetic Genomes* (IntechOpen).

Butaye, P., Devriese, L. A., and Haesebrouck, F. (2003). Antimicrobial growth promoters used in animal feed: effects of less well-known antibiotics on gram-positive bacteria. *Clin. Microbiol. Rev.* 16, 175–188. doi: 10.1128/CMR.16.2.175-188.2003

Bywater, R. J. (2005). Identification and surveillance of antimicrobial resistance dissemination in animal production. *Poult. Sci. J.* 84, 644–648. doi: 10.1093/ps/84.4.644

Callaway, T. R., Carneiro De Melo, A. M. S., and Russell, J. B. (1997). The effect of nisin and monensin on ruminal fermentations *in vitro*. *Curr. Microbiol.* 35, 90–96. doi: 10.1007/s002849900218

Cao, L. T., Wu, J. Q., Xie, F., Hu, S. H., and Mo, Y. (2007). Efficacy of nisin in treatment of clinical mastitis in lactating dairy cows. *Int. J. Dairy Sci.* 90, 3980–3985. doi: 10.3168/jds.2007-0153

Cardoso, M. H., Orozco, R. Q., Rezende, S. B., Rodrigues, G., Oshiro, K. G., Cândido, E. S., et al. (2020). Computer-aided design of antimicrobial peptides: are we generating effective drug candidates? *Front. Microbiol.* 10, 3097. doi: 10.3389/fmicb.2019.03097

Ceotto-Vigoder, H., Marques, S. L. S., Santos, I. N. S., Alves, M. D. B., Barrias, E. S., Potter, A., et al. (2016). Nisin and lysostaphin activity against preformed biofilm of *Staphylococcus aureus* involved in bovine mastitis. *J. Appl. Microbiol.* 121, 101–114. doi: 10.1111/jam.13136

Cheema, U. B., Younas, M., Sultan, J. I., Iqbal, A., Tariq, M., and Waheed, A. (2011). Antimicrobial peptides: an alternative of antibiotics in ruminants. *Adv. Agric. Biotechnol.* 2, 15–21.

Chen, S. C., and Bahar, I. (2004). Mining frequent patterns in protein structures: a study of protease families. *J. Bioinform.* 20, i77–i85. doi: 10.1093/bioinformatics/bth912

Chen, X., Yi, Y., You, X., Liu, J., and Shi, Q. (2019). High-throughput identification of putative antimicrobial peptides from multi-omics data of the lined seahorse (*Hippocampus erectus*). *Marine Drugs* 18, 30. doi: 10.3390/md18010030

Cheng, G., Hao, H., Xie, S., Wang, X., Dai, M., Huang, L., et al. (2014). Antibiotic alternatives: the substitution of antibiotics in animal husbandry? *Front. Microbiol.* 5, 217. doi: 10.3389/fmicb.2014.00217

Choi, S. C., Ingale, S. L., Kim, J. S., Park, Y. K., Kwon, I. K., and Chae, B. J. (2013a). Effects of dietary supplementation with an antimicrobial peptide-P5 on growth performance, nutrient retention, excreta and intestinal microflora and intestinal morphology of broilers. *Anim. Feed. Sci. Technol.* 185, 78–84. doi: 10.1016/j.anifeedsci.2013.07.005

Choi, S. C., Ingale, S. L., Kim, J. S., Park, Y. K., Kwon, I. K., and Chae, B. J. (2013b). An antimicrobial peptide-A3: effects on growth performance, nutrient retention, intestinal and fecal microflora and intestinal morphology of broilers. *Br. Poult. Sci.* 54, 738–746. doi: 10.1080/00071668.2013.838746

Clifford, K., Desai, D., Prazeres da Costa, C., Meyer, H., Klohe, W.inkler A. S., Rahman, T., et al. (2018). Antimicrobial resistance in livestock and poor-quality veterinary medicines. *Bull. World Health Orga.* 96, 662–664. doi: 10.2471/BLT.18.209585

Crowther, G. S., Baines, S. D., Todhunter, S. L., Freeman, J., Chilton, C. H., and Wilcox, M. H. (2013). Evaluation of NVB302 versus vancomycin activity inan *in vitro* human gut model of *Clostridium difficile* infection. *J. Antimicrob. Chemother.* 68, 168–176. doi: 10.1093/jac/dks359

Cutler, S. A., Lonergan, S. M., Cornick, N., Johnson, A. K., and Stahl, C. H. (2007). Dietary inclusion of colicin e1 is effective in preventing postweaning diarrhea caused by F18-positive *Escherichia coli* in pigs. *Antimicrob. Agents Chemother.* 51, 3830–3835. doi: 10.1128/AAC.00360-07

Daeschel, M. A., and Klaenhammer, T. R. (1985). Association of a 13.6-megadalton plasmid in *Pediococcus pentosaceus* with bacteriocin activity. *Appl. Environ. Microbiol.* 50, 1538–1541. doi: 10.1128/aem.50.6.1538-1541.1985

Daneshmand, A., Kermanshahi, H., Sekhavati, M. H., Javadmanesh, A., and Ahmadian, M. (2019). Antimicrobial peptide, cLF36, affects performance and intestinal morphology, microflora, junctional proteins, and immune cells in broilers challenged with *E. coli*. *Sci. Rep.* 9, 14176. doi: 10.1038/s41598-019-50511-7

Dibner, J. J., and Richards, J. D. (2005). Antibiotic growth promoters in agriculture: history and mode of action. *Poult. Sci.* 84, 634–643. doi: 10.1093/ps/84.4.634

Dijksteel, G. S., Ulrich, M. M., Middelkoop, E., and Boekema, B. K. (2021). lessons learned from clinical trials using antimicrobial peptides (AMPs). *Front. Microbiol.* 12, 287. doi: 10.3389/fmicb.2021.616979

Easton, D. M., Nijnik, A., Mayer, M. L., and Hancock, R. E. W. (2009). Potential of immunomodulatory host defense peptides as novel anti-infectives. *Trends Biotechnol.* 27, 582–590. doi: 10.1016/j.tibtech.2009.07.004

Edsfeldt, S., Holm, B., Mahlapuu, M., Reno, C., Hart, D. A., and Wiig, M. (2017). PXL01 in sodium hyaluronate results in increased PRG4 expression: a potential mechanism for anti-adhesion. *Ups. J. Med. Sci.* 122, 28–34. doi: 10.1080/03009734.2016.1230157

Eisler, M. C., Lee, M. R., Tarlton, J. F., Martin, G. B., Beddington, J., Dungait, J. A., et al. (2014). Agriculture: steps to sustainable livestock. *Nat. News* 507, 32–34. doi: 10.1038/507032a

Elahi, S., Buchanan, R. M., Attah-Poku, S., Townsend, H. G., Babiuk, L. A., and Gerdts, V. (2006). The host defense peptide beta-defensin 1 confers protection against Bordetella pertussis in newborn piglets. *Infect. Immun.* 74, 2338–2352. doi: 10.1128/IAI.74.4.2338-2352.2006

FAO (2016). *The FAO Action Plan on Antimicrobial Resistance. Rome: Food and Agriculture Organization of the United Nations*. 3–25. Available online at: http://www.fao.org/3/a-i5996e.pdf (accessed May 25, 2021).

FAO (2018). *World Livestock: Transforming the Livestock Sector Through the Sustainable Development Goals*. Rome: FAO. 222.

FAO, IFAD, UNICEF, WFP, and WHO (2018). *The State of Food Security and Nutrition in the World 2018. Building Climate Resilience for Food Security and Nutrition*. Rome: FAO.

Ferriol-González, C., and Domingo-Calap, P. (2021). Phage therapy in livestock and companion animals. *Antibiotics* 10, 559. doi: 10.3390/antibiotics10050559

Firkins, J. L., Yu, Z., and Morrison, M. (2007). Ruminal nitrogen metabolism: perspectives for integration of microbiology and nutrition for dairy. *J. Dairy Sci.* 90, E1–E16. doi: 10.3168/jds.2006-518

Founou, L. L., Founou, R. C., and Essack, S. Y. (2016). Antibiotic resistance in the food chain: a developing country-perspective. *Front. Microbiol.* 7, 1881. doi: 10.3389/fmicb.2016.01881

Fry, D. E. (2018). Antimicrobial peptides. *Surg. Infect.* 19, 804–811. doi: 10.1089/sur.2018.194

Fulco, P., and Wenzel, R. P. (2006). Ramoplanin: a topical lipoglycodepsipeptide antibacterial agent. *Expert Rev. Anti Infect. Ther.* 4, 939–945. doi: 10.1586/14787210.4.6.939

Gallo, R. L., Ono, M., Povsic, T., Page, C., Eriksson, E., Klagsbrun, M., et al. (1994). Syndecans, cell surface heparan sulfate proteo- glycans, are induced by a proline-rich antimicrobial peptide from wounds. *Proc. Natl. Acad. Sci. U. S. A.* 91, 11035-11039. doi: 10.1073/pnas.91.23.11035

Ganesh, V., and Hettiarachchy, N. S. (2016). A review: supplementation of foods with essential fatty acids—can it turn a breeze without further ado? *Crit. Rev. Food Sci. Nutr.* 56, 1417–1427. doi: 10.1080/10408398.2013.765383

Ghosh, C., Sarkar, P., Issa, R., and Haldar, J. (2019). Alternatives to conventional antibiotics in the Era of antimicrobial resistance. *Trends Microbiol.* 27, 323–338. doi: 10.1016/j.tim.2018.12.010

Godfray, H. C. J., and Garnett, T. (2015). Food security and sustainable intensification. *Philos. Trans. R. Soc. B.* 369, 20120273. doi: 10.1098/rstb.2012.0273

Gomes, B., Augusto, M. T., Felício, M. R., Hollmann, A., Franco, O. L., Gonçalves, S., et al. (2018). Designing improved active peptides for therapeutic approaches against infectious diseases. *Biotechnol. Adv.* 36, 415–429. doi: 10.1016/j.biotechadv.2018.01.004

Grace, D., Mutua, F., Ochungo, P., Kruska, R. L., Jones, K., Brierley, L., et al. (2012). *Mapping of Poverty and Likely Zoonoses Hotspots*. Available online at: https://hdl.handle.net/10568/2116 (accessed May 10, 2021).

Grilli, E., Messina, M. R., Catelli, E., Morlacchini, M., and Piva, A. (2009). Pediocin A improves growth performance of broilers challenged with *Clostridium perfringens*. *Poult. Sci. J.* 88, 2152–2158. doi: 10.3382/ps.2009-00160

Gualillo, O., Lago, Gómez-Reino, J., Casanueva, F. F., and Dieguez, C. (2003). Ghrelin, a widespread hormone: insights into molecular and cellular regulation

of its expression and mechanism of action. *FEBS Lett.* 552, 105–109. doi: 10.1016/S0014-5793(03)00965-7

Gyan, W. R., Yang, Q., Tan, B., Jan, S. S., Jiang, L., Chi, S., et al. (2020). Effects of antimicrobial peptides on growth, feed utilization, serum biochemical indices and disease resistance of juvenile shrimp, *Litopenaeus vannamei*. *Aquac Res* 51, 1222–1231. doi: 10.1111/are.14473

Hancock, R., and Chapple, D. (1999). MINIREVIEW peptide antibiotics. *Antimicrob. Agents Chemother.* 43, 1317–1323. doi: 10.1128/AAC.43.6.1317

Hancock, R. E. (2001). Cationic peptides: effectors in innate immunity and novel antimicrobials. *Lancet Infect. Dis.* 1, 156–164. doi: 10.1016/S1473-3099(01)00092-5

Hancock, R. E., and Sahl, H. G. (2006). Antimicrobial and host-defense peptides as new anti-infective therapeutic strategies. *Nat. Biotechnol.* 24, 1551–1557. doi: 10.1038/nbt1267

Håkansson, J., Ringstad, L., Umerska, A., Johansson, J., Andersson, T., Boge, L., et al. (2019). Characterization of the in vitro, ex vivo, and in vivo efficacy of the antimicrobial peptide dpk-060 used for topical treatment. *Front. Cell. Infect. Microbiol.* 9,174. doi: 10.3389/fcimb.2019.00174

Henderson, J. C., Fage, C. D., Cannon, J. R., Brodbelt, J. S., Keatinge-Clay, A. T., and Trent, M. S. (2014). Antimicrobial peptide resistance of *Vibrio cholerae* results from an LPS modification pathway related to nonribosomal peptide synthetases. *ACS Chem. Biol.* 9, 2382–2392. doi: 10.1021/cb500438x

Hernández-González, J. C., Martínez-Tapia, A., Lazcano-Hernández, G., García-Pérez, B. E., and Castrejón-Jiménez, N. S. (2021). Bacteriocins from lactic acid bacteria. A powerful alternative as antimicrobials, probiotics, and immunomodulators in veterinary medicine. *Animals* 11, 979. doi: 10.3390/ani11040979

Heuer, O. E., Kruse, H., Grave, K., Collignon, P., Karunasagar, I., and Angulo, F. J. (2009). Human health consequences of use of antimicrobial agents in aquaculture. *Clin. Infect. Dis.* 49, 1248–1253. doi: 10.1086/605667

Hiss, J. A., Hartenfeller, M., and Schneider, G. (2010). Concepts and applications of "natural computing" techniques in de novo drug and peptide design. *Curr. Pharm. Des.* 16, 1656–1665. doi: 10.2174/138161210791164009

Huhand, Y. A. J., and Kwon, J. (2011). Nanoantibiotics': a new paradigm for treating infectious dis-eases using nanomaterials in the antibiotics-resistant era. *J. Control Release* 156, 128–145. doi: 10.1016/j.jconrel.2011.07.002

Hwang, B., Hwang, J. S., Lee, J., and Lee, D. G. (2011). The antimicrobial peptide, psacotheasin induces reactive oxygen species and triggers apoptosis in *Candida albicans*. *Biochem. Biophys. Res. Commun.* 405, 267–271. doi: 10.1016/j.bbrc.2011.01.026

Innes, G. K., Randad, P. R., Korinek, A., Davis, M. F., Price, L. B., So, A. D., et al. (2020). External societal costs of antimicrobial resistance in humans attributable to antimicrobial use in livestock. *Annu. Rev. Public Health* 41, 111–157. doi: 10.1146/annurev-publhealth-040218-043954

Isaksson, J., Brandsdal, B. O., Engqvist, M., Flaten, G. E., Svendsen, J. S. M., and Stensen, W. (2011). A synthetic antimicrobial peptidomimetic (LTX 109): stereochemical impact on membrane disruption. *J. Med. Chem.* 54, 5786–5795. doi: 10.1021/jm200450h

Iseppi, R., Andrea, L., and Sabia, C. (2021). Bacteriocin-producing probiotic bacteria: a natural solution for increasing efficiency and safety of livestock food production. *Front. Microbiol.* 12, 675483. doi: 10.3389/fmicb.2021.675483

Itoh, H., Tokumoto, K., Kaji, T., Paudel, A., Panthee, S., Hamamoto, H., et al. (2018). Total synthesis and biological mode of action of WAP-8294A2: A menaquinone-targeting antibiotic. *J. Org. Chem.* 83, 6924–6935. doi: 10.1021/acs.joc.7b02318

Jakobus, K., Wend, S., and Weber, W. (2012). Synthetic mammalian gene networks as a blueprint for the design of interactive biohybrid materials. *Chem. Soc. Rev.* 41, 1000–1018. doi: 10.1039/C1CS15176B

Jenssen, H., Hamill, P., and Hancock, R. E. (2006). Peptide antimicrobial agents. *Clin. Microbiol. Rev.* 19, 491–511. doi: 10.1128/CMR.00056-05

Jones, F. T., and Ricke, S. C. (2003). Observations on the history of the development of antimicrobials and their use in poultry feeds. *Poult. Sci. J.* 82, 613–617. doi: 10.1093/ps/82.4.613

Józefiak, D., Kierończyk, B., Juśkiewicz, J., Zduńczyk, Z., Rawski, M., Długosz, J., et al. (2013). Dietary nisin modulates the gastrointestinal microbial ecology and enhances growth performance of the broiler chickens. *PLoS ONE* 8, e85347. doi: 10.1371/journal.pone.0085347

Kaikabo, A. A., Sabo Mohammed, A., and Abas, F. (2016). Chitosan nanoparticles as carriers for the delivery of ΦKAZ14 bacteriophage for oral biological control of colibacillosis in chickens. *Molecules* 21, 256. doi: 10.3390/molecules21030256

Katsunuma, Y., Hanazumi, M., Fujisaki, H., Minato, H., Hashimoto, Y., and Yonemochi, C. (2007). Associations between the use of antimicrobial agents for growth promotion and the occurrence of antimicrobial-resistant *Escherichia coli* and enterococci in the feces of livestock and livestock farmers in Japan. *J. Gen. Appl. Microbiol.* 53, 273–279. doi: 10.2323/jgam.53.273

Kemp, D. R., and Michalk, D. L. (eds.). (2011). *Development of Sustainable Livestock Systems on Grasslands in North-Western China ACIAR Proceedings No. 134*. Canberra, ACT: Australian Centre for International Agricultural Research.

King, J. R.,Edgar, S., Qiao, K., and Stephanopoulos, G. (2016). Accessing nature's diversity through metabolic engineering and synthetic biology. *F1000 Res.* 5, 1–11. doi: 10.12688/f1000research.7311.1

Kogut, M. H., Genovese, K. J., He, H., Swaggerty, C. L., and Jiang, Y. (2013). Modulation of chicken intestinal immune gene expression by small cationic peptides as feed additives during the first week posthatch. *Clin. Vaccine Immunol.* 20, 1440–1448. doi: 10.1128/CVI.00322-13

Krehbiel, C. (2013). The role of new technologies in global food security: improvinganimal production efficiency and minimizing impacts. *Anim. Front.* 3, 4–7. doi: 10.2527/af.2013-0017

Krishnasamy, V., Otte, J., and Silbergeld, E. (2015). Antimicrobial use in Chinese swine and broiler poultry production. *Antimicrob. Resist. Infect. Control* 4, 17. doi: 10.1186/s13756-015-0050-y

Kudrimoti, M., Curtis, A., Azawi, S., Worden, F., Katz, S., Adkins, D., et al. (2016). Dusquetide: a novel innate defense regulator demonstrating a significant and consistent reduction in the duration of oral mucositis in preclinical data and a randomized, placebo-controlled Phase 2a clinical study. *J. Biotechnol.* 239, 115–125. doi: 10.1016/j.jbiotec.2016.10.010

Lagha, A. B., Haas, B., Gottschalk, M., and Grenier, D. (2017). Antimicrobial potential of bacteriocins in poultry and swine production. *Vet. Res.* 48, 22. doi: 10.1186/s13567-017-0425-6

Lan, W., and Yang, C. (2019). Ruminal methane production: associated microorganisms and the potential of applying hydrogen-utilizing bacteria for mitigation. *Sci. Total Environ.* 654, 1270–1283. doi: 10.1016/j.scitotenv.2018.11.180

Leahy, S. C., Doyle, N., Mbandlwa, P., Attwood, G. T., Li, Y., Ross, P., et al. (2019). Use of lactic acid bacteria to reduce methane production in ruminants, a critical review. *Front. Microbiol.* 10, 2207. doi: 10.3389/fmicb.2019.02207

León, R., Ruiz, M., Valero, Y., Cárdenas, C., Guzman, F., Vila, M., et al. (2020). Exploring small cationic peptides of different origin as potential antimicrobial agents in aquaculture. *Fish Shellfish Immunol.* 98, 720–727. doi: 10.1016/j.fsi.2019.11.019

Lhermie, G., Gröhn, Y. T., and Raboisson, D. (2017). Addressing antimicrobial resistance: an overview of priority actions to prevent suboptimal antimicrobial use in food-animal production. *Front. Microbiol.* 7, 2114. doi: 10.3389/fmicb.2016.02114

Li, M., Cha, D. J., Lai, Y., Villaruz, A. E., Sturdevant, D. E., and Otto, M. (2007). The antimicrobial peptide-sensing system aps of *Staphylococcus aureus*. *Mol. Microbiol.* 66, 1136–1147. doi: 10.1111/j.1365-2958.2007.05986.x

Li, Z., Hu, Y., Yang, Y., Lu, Z., and Wang, Y. (2018). Antimicrobial resistance in livestock: antimicrobial peptides provide a new solution for a growing challenge. *Anim. Front.* 8, 21–29. doi: 10.1093/af/vfy005

Lim, S. J., Seo, C. K., Kim, T. H., and Myung, S. W. (2013). Occurrence and ecological hazard assessment of selected veterinary medicines in livestock wastewater treatment plants. *J. Environ. Sci. Health B.* 48, 658–670. doi: 10.1080/03601234.2013.778604

Liu, T., She, R., Wang, K., Bao, H., Zhang, Y., Luo, D., et al. (2008). Effects of rabbit *Sacculus rotundus* antimicrobial peptides on the intestinal mucosal immunity in chickens. *Poult. Sci.* 87, 250–254. doi: 10.3382/ps.2007-00353

Loose, C., Jensen, K., Rigoutsos, I., and Stephanopoulos, G. (2006). A linguistic model for the rational design of antimicrobial peptides. *Nature* 443, 867–869. doi: 10.1038/nature05233

Loponte, R., Pagnini, U., Iovane, G., and Pisanelli, G. (2021). Phage therapy in veterinary medicine. *Antibiotics* 10, 421. doi: 10.3390/antibiotics10040421

Ma, J. L., Zhao, L. H., Sun, D. D., Zhang, J., Guo, Y. P., Zhang, Z. Q., et al. (2019). Effects of dietary supplementation of recombinant plectasin on growth

performance, intestinal health and innate immunity response in broilers. *Probiotics Antimicrob. Proteins* 12, 214–223. doi: 10.1007/s12602-019-9515-2

Ma, T., McAllister,T. A., and Guan, L. L. (2021). A review of the resistome within the digestive tract of livestock. *Anim. Sci. Biotechnol.* 12, 1–20. doi: 10.1186/s40104-021-00643-6

Magouras, I., Carmo, L. P., Stärk, K. D., and Schüpbach-Regula, G. (2017). Antimicrobial usage and-resistance in livestock: where should we focus? *Front. Vet. Sci.* 4, 148. doi: 10.3389/fvets.2017.00148

Maria-Neto, S., de Almeida, K. C., Macedo, M. L. R., and Franco, O. L. (2015). Understanding bacterial resistance to antimicrobial peptides: from the surface to deep inside. *Biochimica et Biophys. Acta Biomemb.* 1848, 3078–3088. doi: 10.1016/j.bbamem.2015.02.017

McEwen, S. A., and Fedorka-Cray, P. J. (2002). Antimicrobial use and resistance in animals. *Clin. Infect. Dis.* 34(Suppl. 3), S93–S106. doi: 10.1086/340246

Meade, E., Slattery, M. A., and Garvey, M. (2020). Bacteriocins, potent antimicrobial peptides and the fight against multi drug resistant species: resistance is futile? *Antibiotics* 9, 32. doi: 10.3390/antibiotics9010032

Medina, M. J., Legido-Quigley, H., and Hsu, L. Y. (2020). *Antimicrobial Resistance in One Health. Global Health Security.* Cham: Springer. 209–229. doi: 10.1007/978-3-030-23491-1_10

Mensa, B., Howell, G., Scott, R., and DeGrado, W. (2014). Comparative mechanistic studies of brilacidin, daptomycin, and the antimicrobial peptide LL16. *Antimicrob. Agents Chemother.* 58, 5136–5145. doi: 10.1128/AAC.02955-14

Mensah, S. E., Koudande, O. D., Sanders, P., Laurentie, M., Mensah, G. A., and Abiola, F. A. (2014). Antimicrobial residues in foods of animal origin in Africa: public health risks. *Rev. Sci. Tech.* 33, 987–996. doi: 10.20506/rst.33.3.2335

Mercer, D. K., Robertson, J. C., Miller, L., Stewart, C. S., and O'Neil, D. A. (2020). NP213 (NovexatinR): a unique therapy candidate for onychomycosis with a differentiated safety and efficacy profile. *Med. Mycol.* 58, 1064–1072. doi: 10.1093/mmy/myaa015

Messaoudi, S., Madi, A., Prévost, H., Feuilloley, M., Manai, M., Dousset, X., et al. (2012). *In vitro* evaluation of the probiotic potential of *Lactobacillus salivarius* SMXD51. *Anaerobe* 18, 584–589. doi: 10.1016/j.anaerobe.2012.10.004

Michalk, D. L., Kemp, D. R., Badgery, W. B., Wu, J., Zhang, Y., and Thomassin, P. J. (2019). Sustainability and future food security—A global perspective for livestock production. *Land Degrad. Dev.* 30, 561–573. doi: 10.1002/ldr.3217

Mitchell, J. B. (2014). Machine learning methods in chemoinformatics. *Wiley Interdiscipl. Rev. Comput. Mol. Sci.* 4, 468–481. doi: 10.1002/wcms.1183

Miyake, O., Ochia, A., Hashimoto, W., and Murata, K. (2004). Origin and diversity of alginate lyases of families PL-5 and−7 in *Sphingomonas sp*.strain A1. *J. Bacteriol.* 186, 2891–2896. doi: 10.1128/JB.186.9.2891-2896.2004

Mookherjee, N., Brown, K. L., Bowdish, D. M., Doria, S., Falsafi, R., Hokamp, K., et al. (2006). Modulation of the TLR-mediated inflammatory response by the endogenous human host defense peptide LL-37. *J. Immunol.* 176, 2455–2464. doi: 10.4049/jimmunol.176.4.2455

Muchintala, D., Suresh, V., Raju, D., and Sashidhar, R. B. (2020). Synthesis and characterization of cecropin peptide-based silver nanocomposites: its antibacterial activity and mode of action. *Mater. Sci. Eng. C.* 110, 110712. doi: 10.1016/j.msec.2020.110712

Munita, J. M., and Arias, C. A. (2016). Mechanisms of antibiotic resistance. *Microbiol Spectr.* 4, 10.1128/microbiolspec. VMBF-0016- 2015. doi: 10.1128/microbiolspec

Murphy, C. J., Foster, B. A., Mannis, M. J., Selsted, M. E., and Reid, T. W. (1993). Defensins are mitogenic for epithelial cells and fibroblasts. *J. Cell Physiol.* 155, 408–413. doi: 10.1002/jcp.1041550223

National Research Council. (1999). *The Use of Drugs in Food Animals: Benefits and Risks.* Washington, DC: National Academies Press.

Noel, J. P. (2010). Synthetic metabolism goes green. *Nature* 468, 380–381. doi: 10.1038/468380a

OIE World Organisation for Animal Health. (2012). *Terrestrial Animal Health Code. 21st Edn.* Paris: OIE. Available online at: http://www.oie.int/international-standard-setting/terrestrial-code/ (accessed March 30, 2021).

Otto, M. (2009). Bacterial sensing of antimicrobial peptides. *Bacterial Sens. Signal.* 16, 136–149. doi: 10.1159/000219377

Pelgrift, R. Y., and Friedman, A. J. (2013). Nanotechnology as a therapeutic tool to combat microbial resistance. *Adv. Drug Deliv. Rev.* 65, 1803–1815. doi: 10.1016/j.addr.2013.07.011

Peyrusson, F., Butler, D., Tulkens, P. M., and Van Bambeke, F. (2015). Cellular pharmacokinetics and intracellular activity of the novel peptide deformylase inhibitor GSK1322322 against Staphylococcus aureus laboratory and clinical strains with various resistance phenotypes: studies with human THP-1monocytes and J774 murine macrophages. *Antimicrob. Agents Chemother.* 59, 5747–5760. doi: 10.1128/AAC.00827-15

Podolsky, D. K. (2000). Healing after inflammatory injury–coordination of a regulatory peptide network. *Aliment. Pharmacol. Ther.* 14, 87–93. doi: 10.1046/j.1365-2036.2000.014s1087.x

Porto, W. F., Silva, O. N., and Franco, O. L. (2012). "Prediction and rational design of antimicrobial peptides," in *Protein Structure, 1st Edn.*, ed E. Faraggi (InTech), 20.

Prince, A., Sandhu, P., Ror, P., Dash, E., Sharma, S., Arakha, M., et al. (2016). Lipid-II independent antimicrobial mechanism of nisin depends on its crowding and degree of oligomerization. *Sci. Rep.* 6, 1–15. doi: 10.1038/srep37908

Rai, M., Pandit, R., Gaikwad, S., and Kövics, G. (2016). Antimicrobial peptides as natural bio-preservative to enhance the shelf-life of food. *J. Food Sci. Technol.* 53, 3381–3394. doi: 10.1007/s13197-016-2318-5

Reisinger, A., and Clark, H. (2018). How much do direct livestock emissions actually contribute to global warming? *Glob. Change Biol.* 24, 1749–1761. doi: 10.1111/gcb.13975

Ren, Z., Yao, R., Liu, Q., Deng, Y., Shen, L., Deng, H., et al. (2019). Effects of antibacterial peptides on rumen fermentation function and rumen microorganisms in goats. *PLoS ONE* 14, e221815. doi: 10.1371/journal.pone.0221815

Rodrigues, G., Silva, G. G. O., Buccini, D. F., Duque, H. M., Dias, S. C., and Franco, O. L. (2019). Bacterial proteinaceous compounds with multiple activities toward cancers and microbial infection. *Front. Microbiol.* 10, 1690. doi: 10.3389/fmicb.2019.01690

Rodrigues, G. R., López-Abarrategui, C., de la Serna Gómez, I., Dias, S. C., Otero-González, A. J., and Franco, O. L. (2019). Antimicrobial magnetic nanoparticles based-therapies for controlling infectious diseases. *Int. J. Pharm.* 555, 356–367. doi: 10.1016/j.ijpharm.2018.11.043

Saido-Sakanaka, H., Ishibashi, J., Momotani, E., Amano, F., and Yamakawa, M. (2004). *In vitro* and *in vivo* activity of antimicrobial peptides synthesized based on the insect defensin. *Peptides* 25, 19–27. doi: 10.1016/j.peptides.2003.12.009

Santoso, B., Mwenya, B., Sar, C., Gamo, Y., Kobayashi, T., Morikawa, R., et al. (2004). Effects of supplementing galacto-oligosaccharides, Yucca schidigera or nisin on rumen methanogenesis, nitrogen and energy metabolism in sheep. *Livest. Prod. Sci.* 91, 209–217. doi: 10.1016/j.livprodsci.2004.08.004

Sar, C., Mwenya, B., Pen, B., Morikawa, R., Takaura, K., Kobayashi, T., et al. (2005). Effect of nisin on ruminal methane production and nitrate/nitrite reduction *in vitro*. *Aust. J. Agric. Res.* 56, 803–810. doi: 10.1071/AR04294

Schneider, T., Gries, K., Josten, M., Wiedemann, I., Pelzer, S., Labischinski, H., et al. (2009). The lipopeptide antibiotic friulimicin B inhibits cell wall biosynthesis through complex formation with bactoprenol phosphate. *Antimicrob. Agents Chemother.* 53, 1610–1618. doi: 10.1128/AAC.01040-08

Schulze, M., Junkes, C., Mueller, P., Speck, S., Ruediger, K., Dathe, M., et al. (2014). Effects of cationic antimicrobial peptides on liquid-preserved boar spermatozoa. *PLoS ONE* 9, e100490. doi: 10.1371/journal.pone.0100490

Schulze, M., Nitsche-Melkus, E., Hensel, B., Jung, M., and Jakop, U. (2020). Antibiotics and their alternatives in artificial breeding in livestock. *Anim. Reprod. Sci.* 220, 106284. doi: 10.1016/j.anireprosci.2020.106284

Scott, H. M., Acuff, G., Bergeron, G., Bourassa, M. W., Gill, J., Graham, D. W., et al. (2019). Critically important antibiotics: criteria and approaches for measuring and reducing their use in food animal agriculture. *Ann. N. Y. Acad. Sci.* 1441, 8. doi: 10.1111/nyas.14058

Shai, Y. (2002). Mode of action of membrane active antimicrobial peptides. *Pep. Sci.* 66, 236–248. doi: 10.1002/bip.10260

Shaoyong, W., Li, Q., Ren, Z. Q., Wei, C. S., Chu, G. Y., Dong, W. Z., et al. (2019). Evaluation of ε-polylysine as antimicrobial alternative for liquid-stored boar semen. *Theriogenology* 130, 146. doi: 10.1016/j.theriogenology.2019.03.005

Sharma, C., Rokana, N., Chandra, M., Singh, B. P., Gulhane, R. D., Gill, J. P. S., et al. (2018). Antimicrobial resistance: its surveillance, impact, and

alternative management strategies in dairy animals. *Front. Vet. Sci.* 4, 237. doi: 10.3389/fvets.2017.00237

Shen, J., Liu, Z., Yu, Z., and Zhu, W. (2017). Monensin and nisin affect rumen fermentation and microbiota differently *in vitro*. *Front. Microbiol.* 8, 1111. doi: 10.3389/fmicb.2017.01111

Shen, J. S., Liu, Z., Chen, Y. Y., Lv, P. A., and Zhu, W. Y. (2016). Effects of nisin on *in vitro* fermentation, methanogenesis and functional microbial populations of the rumen. *Acta Microbiol. Sin.* 56, 1348–1357. doi: 10.13343/j.cnki.wsxb. 20150559

Shin, J. M., Gwak, J. W., Kamarajan, P., Fenno, J. C., Rickard, A. H., and Kapila, Y. L. (2016). Biomedical applications of nisin. *J. Appl. Microbiol.* 120, 1449–1465. doi: 10.1111/jam.13033

Silveira, R. F., Roque-Borda, C. A., and Vicente, E. F. (2021). Antimicrobial peptides as a feed additive alternative to animal production, food safety and public health implications: an overview. *Anim. Nutr.* 7, 896–904. doi: 10.1016/j.aninu.2021.01.004

Sivertsen, A., Isaksson, J., Leiros, H.-K. S., Svenson, J., Svendsen, J.-S., and Brandsdal, B. O. (2014). Synthetic cationic antimicrobial peptides bind with their hydrophobic parts to drug site II of human serum albumin. *BMC Struct. Biol.* 14:4. doi: 10.1186/1472-6807-14-4

Soucy, S. M., Huang, J., and Gogarten, J. P. (2015). Horizontal gene transfer: building the web of life. *Nat. Rev. Genet.* 16, 472–482. doi: 10.1038/nrg3962

Sparo, M. D., Jones, D. G., and Sánchez Bruni, S. F. (2009). *In vitro* efficacy of the novel peptide CECT7121 against bacteria isolated from mastitic dairy cattle. *Lett. Appl. Microbiol.* 48, 187–192. doi: 10.1111/j.1472-765X.2008.02507.x

Speck, S., Courtiol, A., Junkes, C., Dathe, M., Müller, K., and Schulze, M. (2014). Cationic synthetic peptides: assessment of their antimicrobial potency in liquid preserved boar semen. *PLoS ONE* 9, e105949. doi: 10.1371/journal.pone.0105949

Spohn, R., Daruka, L., Lázár, V., Martins, A., Vidovics, F., Grézal, G., et al. (2019). Integrated evolutionary analysis reveals antimicrobial peptides with limited resistance. *Nat. Commun.* 10, 1–13. doi: 10.1038/s41467-019-12364-6

Srinivas, N., Jetter, P., Ueberbacher, B. J., Werneburg, M., Zerbe, K., Steinmann, J., et al. (2010). Peptidomimetic antibiotics target outer-membrane biogenesis in *Pseudomonas aeruginosa*. *Science* 327, 1010–1013. doi: 10.1126/science.1182749

Stahl, C. H., Callaway, T. R., Lincoln, L. M., Lonergan, S. M., and Genovese, K. J. (2004). Inhibitory activities of colicins against *Escherichia coli* strains responsible for postweaning diarrhea and edema disease in swine. *Antimicrob. Agents Chemother.* 48, 3119–3121. doi: 10.1128/AAC.48.8.3119-3121.2004

Suresh, G., Das, R. K., Kaur Brar, S., Rouissi, T., Avalos Ramirez, A., Chorfi, Y., et al. (2018). Alternatives to antibiotics in poultry feed: molecular perspectives. *Crit. Rev. Microbiol.* 44, 318–335. doi: 10.1080/1040841X.2017.1373062

Swangchan-Uthai, T., Chen, Q., Kirton, S. E., Fenwick, M. A., Cheng, Z., Patton, J., et al. (2013). Influence of energy balance on the antimicrobial peptides S100A8 and S100A9 in the endometrium of the post-partum dairy cow. *Reproduction* 145, 527. doi: 10.1530/REP-12-0513

Swann, J. P. (1983). The search for synthetic penicillin during World War II. *Br. J. Hist. Sci.* 16, 154–190. doi: 10.1017/S0007087400026789

Takano, E., and Breitling, R. (2014). *Antimicrobial Resistance – A New Drug Perspective Using Synthetic Biology*. Houston, TX: Emerging and Persistent Infectious Diseases (EPID): Focus on Antimicrobial Resistance.

Tang, Z., Yin, Y., Zhang, Y., Huang, R., Sun, Z., Li, T., et al. (2008). Effects of dietary supplementation with an expressed fusion peptide bovine lactoferricin–lactoferrampin on performance, immune function and intestinal mucosal morphology in piglets weaned at age 21 d. *Br. J. Nutr.* 101, 998–1005. doi: 10.1017/S0007114508055633

Thanner, S., Drissner, D., and Walsh, F. (2016). Antimicrobial resistance in agriculture. *MBio* 7, e02227–e02215. doi: 10.1128/mBio.02227-15

Thomas, C. M., and Nielsen, K. M. (2005). Mechanisms of, and barriers to, horizontal gene transfer between bacteria. *Nat. Rev. Microbiol.* 3, 711–721. doi: 10.1038/nrmicro1234

Tollin, M., Bergman, P., Svenberg, T., Jornvall, H., Gudmundsson, G. H., and Agerberth, B. (2003). Antimicrobial peptides in the first line defence of human colon mucosa. *Peptides* 24, 523–530. doi: 10.1016/S0196-9781(03)00114-1

Torres, M. D. T., and De La Fuente-Nunez, C. (2019). Toward computer-made artificial antibiotics. *Curr. Opin. Microbiol.* 51, 30–38. doi: 10.1016/j.mib.2019.03.004

Travis, S., Yap, L. M., Hawkey, C., Warren, B., Lazarov, M., Fong, T., et al. (2005). RDP58 is a novel and potentially effective oral therapy for ulcerative colitis. *Inflamm. Bowel Dis.* 11, 713–719. doi: 10.1097/01.MIB.0000172807.26748.16

van Dijk, A., Veldhuizen, E. J., Kalkhove, S. I., Tjeerdsma-van Bokhoven, J. L., Romijn, R. A., and Haagsman, H. P. (2007). The β-defensin gallinacin-6 is expressed in the chicken digestive tract and has antimicrobial activity against food-borne pathogens. *Antimicrob. Agents Chemother.* 51, 912–922. doi: 10.1128/AAC.00568-06

van Groenendael, R., Kox, M., van Eijk, L. T., and Pickkers, P. (2018). Immunomodulatory and kidney-protective effects of the human chorionic gonadotropin derivate EA-230. *Nephron*. 140, 148–151. doi: 10.1159/000490772

Varnava, K. G., Ronimus, R. S., and Sarojini, V. (2017). A review on comparative mechanistic studies of antimicrobial peptides against archaea. *Biotechnol. Bioeng.* 114, 2457–2473. doi: 10.1002/bit.26387

Venegas-Ortega, M. G., Flores-Gallegos, A. C., Martínez-Hernández, J. L., Aguilar, C. N., and Nevárez-Moorillón, G. V. (2019). Production of bioactive peptides from lactic acid bacteria: a sustainable approach for healthier foods. *Compr. Rev. Food Sci. Food Saf.* 18, 1039–1051. doi: 10.1111/1541-4337.12455

Vidovic, N., and Vidovic, S. (2020). Antimicrobial resistance and food animals: influence of livestock environment on the emergence and dissemination of antimicrobial resistance. *Antibiotics* 9, 52. doi: 10.3390/antibiotics9020052

Vieco-Saiz, N., Belguesmia, Y., Raspoet, R., Auclair, E., Gancel, F., Kempf, I., et al. (2019). Benefits and inputs from lactic acid bacteria and their bacteriocins as alternatives to antibiotic growth promoters during food-animal production. *Front. Microbiol.* 10, 57. doi: 10.3389/fmicb.2019.00057

Vilas, L. B., Campos, M. L., Berlanda, R. L. A., and Franco, O. L. (2019). Antiviral peptides as promising therapeutic drugs. *Cell Mol. Life Sci*. 76, 3525–3542. doi: 10.1007/s00018-019-03138-w

Wang, G., Song, Q., Huang, S., Wang, Y., Cai, S., Yu, H., et al. (2020). Effect of antimicrobial peptide microcin J25 on growth performance, immune regulation, and intestinal microbiota in broiler chickens challenged with *Escherichia coli* and *Salmonella*. *Animals* 10, 345. doi: 10.3390/ani10020345

Wang, S., Thacker, P., A., Watford, M., and Qiao, S. (2015a). Functions of antimicrobial peptides in gut homeostasis. *Curr. Prot. Pept. Sci.* 16, 582–591. doi: 10.2174/1389203716666150630135847

Wang, S., Zeng, X., Yang, Q., and Qiao, S. (2016). Antimicrobial peptides as potential alternatives to antibiotics in food animal industry. *Int. J. Mol. Sci.* 17, 603. doi: 10.7150/ijms.13264

Wang, S., Zeng, X. F., Wang, Q. W., Zhu, J. L., Peng, Q., Hou, C. L., et al. (2015b). The antimicrobial peptide sublancin ameliorates necrotic enteritis induced by *Clostridium perfringens* in broilers. *J. Anim. Sci.* 93, 4750–4760. doi: 10.2527/jas.2015-9284

Wang, Y., Hong, J., Liu, X., Yang, H., Liu, R., Wu, J., et al. (2008). Snake cathelicidin from *Bungarus fasciatus* is a potent peptide antibiotic. *PLoS ONE* 3, e3217. doi: 10.1371/journal.pone.0003217

Wang, Y., Lyu, N., Liu, F., Liu, W. J., Bi, Y., Zhang, Z., et al. (2021). More diversified antibiotic resistance genes in chickens and workers of the live poultry markets. *Environ. Int.* 153, 106534. doi: 10.1016/j.envint.2021.106534

Ward, B. P., Ottaway, N. L., Perez-Tilve, D., Ma, D., Gelfanov, V. M., Tschöp, M. H., et al. (2013). Peptide lipidation stabilizes structure to enhance biological function. *Mol. Metab.* 2, 468–479. doi: 10.1016/j.molmet.2013.08.008

Weber, W., and Fussenegger, M. (2012). Emerging biomedical applications of synthetic biology. *Nat. Rev. Genet.* 13, 21–35. doi: 10.1038/nrg3094

Weber, W., Schoenmakers, R., Keller, B., Gitzinger, M., Grau, T., Daoud-El Baba, M., et al. (2008). A synthetic mammalian gene circuit reveals antituberculosis compounds. *Proc. Natl. Acad. Sci. U. S. A.* 105, 9994–9998. doi: 10.1073/pnas.0800663105

Wen, L. F., and He, J. G. (2012). Dose-response effects of an antimicrobial peptide, a cecropin hybrid, on growth performance, nutrient utilisation, bacterial counts in the digesta and intestinal morphology in broilers. *Br. J. Nutr.* 108, 1756–1763. doi: 10.1017/S0007114511007240

WHO Advisory Group on Integrated Surveillance of Antimicrobial Resistance (AGISAR) (2011). *Critically Important Antimicrobials for Human Medicine – 3rd Revision 2011*. 1–38. Available online at: http://apps.who.int/iris/bitstream/10665/77376/1/9789241504485_eng.pdf (accessed 15 April 2021).

Wimley, W. C., and Hristova, K. (2011). Antimicrobial peptides: successes,challenges and unanswered questions. *J. Membr. Biol.* 239, 27–34. doi: 10.1007/s00232-011-9343-0

Witte, W. (2000). Selective pressure by antibiotic use in livestock. *Int. J. Antimicrob. Agents* 16, 19–24. doi: 10.1016/S0924-8579(00)00301-0

Woolhouse, M., Ward, M., van Bunnik, B., and Farrar, J. (2015). Antimicrobial resistance in humans, livestock and the wider environment. *Philos. Trans. R. Soc. B. Biol. Sci.* 370, 20140083. doi: 10.1098/rstb.2014.0083

World Health Organization. (2014). *WHO's First Global Report on Antibiotic Resistance Reveals Serious, Worldwide Threat to Public Health*. Available online at: http://www.who.int/mediacentre/news/releases/2014/amr-report/en/ (accessed April 10, 2021).

World-Health-Organisation [WHO] (2018). *Cancer: World Cancer Report*. Geneva: World-Health-Organisation.

Wu, W., Yu, Q., You, L., Chen, K., Tang, H., and Liu, J. (2018). Global cropping intensity gaps: increasing food production without cropland expansion. *Land Use Policy* 76, 515–525. doi: 10.1016/j.landusepol.2018.02.032

Wu, X. L., Xiang, L., Yan, Q. Y., Jiang, Y. N., Li, Y. W., Huang, X. P., et al. (2014). Distribution and risk assessment of quinolone antibiotics in the soils from organic vegetable farms of a subtropical city, Southern China. *Sci. Total Environ.* 487, 399–406. doi: 10.1016/j.scitotenv.2014.04.015

Xiao, H., Shao, F., Wu, M., Ren, W., Xiong, X., Tan, B., et al. (2015). The application of antimicrobial peptides as growth and health promoters for swine. *Anim. Sci. Biotechnol.* 6, 1–6. doi: 10.1186/s40104-015-0018-z

Yadav, S., and Jha, R. (2019). Strategies to modulate the intestinal microbiota and their effects on nutrient utilization, performance, and health of poultry. *J. Anim. Sci. Biotechnol.* 10, 2 doi: 10.1186/s40104-018-0310-9

Yasir, M., Dutta, D., and Willcox, M. D. P. (2019). Comparative mode of action of the antimicrobial peptide melimine and its derivative Mel4 against Pseudomonas aeruginosa. *Sci. Rep.* 9, 7063. doi: 10.1038/s41598-019-42440-2

Yasir, M., Dutta, D., Hossain, K. R., Chen, R., Ho, K. K. K., Kuppusamy, R., et al. (2020). Mechanism of action of surface immobilized antimicrobial peptides against *Pseudomonas aeruginosa*. *Front. Microbiol.* 10:3053. doi: 10.3389/fmicb.2019.03053

Yeaman, M. R., and Yount, N. Y. (2003). Mechanisms of antimicrobial peptide action and resistance. *Pharmacol. Rev.* 55, 27–55. doi: 10.1124/pr.55.1.2

Yi, H., Yu, C., Zhang, H., Song, D., Jiang, D., Du, H., et al. (2015). Cathelicidin-BF suppresses intestinal inflammation by inhibiting the nuclear factor-κB signaling pathway and enhancing the phagocytosis of immune cells via STAT-1 in weanling piglets. *Inter. Immunopharmacol.* 28, 61–69. doi: 10.1016/j.intimp.2015.05.034

Yoon, J. H., Ingale, S. L., Kim, J. S., Kim, K. H., Lee, S. H., Park, Y. K., et al. (2012). Effects of dietary supplementation of antimicrobial peptide-A3 on growth performance, nutrient digestibility, intestinal and fecal microflora and intestinal morphology in weanling pigs. *Anim. Feed Sci. Technol.* 177, 98–107. doi: 10.1016/j.anifeedsci.2012.06.009

Yoon, J. H., Ingale, S. L., Kim, J. S., Kim, K. H., Lee, S. H., Park, Y. K., et al. (2014). Effects of dietary supplementation of synthetic antimicrobial peptide-A3 and P5 on growth performance, apparent total tract digestibility of nutrients, fecal and intestinal microflora and intestinal morphology in weanling pigs. *Livest. Sci.* 159, 53–60. doi: 10.1016/j.livsci.2013.10.025

Yoon, J. H., Ingale, S. L., Kim, J. S., Kim, K. H., Lohakare, J., Park, Y. K., et al. (2013). Effects of dietary supplementation with antimicrobial peptide-P5 on growth performance, apparent total tract digestibility, faecal and intestinal microflora and intestinal morphology of weanling pigs. *J. Sci. Food Agric.* 93, 587–592. doi: 10.1002/jsfa.5840

Yu, H. B., Kielczewska, A., Rozek, A., Takenaka, S., Li, Y., Thorson, L., et al. (2009). Sequestosome-1/p62 is the key intracellular target of innate defense regulator peptide. *J. Biol. Chem.* 284, 36007–36011. doi: 10.1074/jbc.C109.073627

Zhang, H., Zhang, B., Zhang, X., Wang, X., Wu, K., and Guan, Q. (2017). Effects of cathelicidin-derived peptide from reptiles on lipopolysaccharide-induced intestinal inflammation in weaned piglets. *Vet. Immunol. Immunopathol.* 192, 41–53.doi: 10.1016/j.vetimm.2017.09.005

Zhao, Y., Zhang, M., Qiu, S., Wang, J., Peng, J., Zhao, P., et al. (2016). Antimicrobial activity and stability of the D-amino acid substituted derivatives of antimicrobial peptide polybia-MPI. *AMB Express* 6, 122. doi: 10.1186/s13568-016-0295-8

Zucca, M., Scutera, S., and Savoia, D. (2011). New antimicrobial frontiers. *Mini Rev. Med. Chem.* 11, 888–900. doi: 10.2174/138955711796575498

Conflict of Interest: The authors declare that the research was conducted in the absence of any commercial or financial relationships that could be construed as a potential conflict of interest.

Publisher's Note: All claims expressed in this article are solely those of the authors and do not necessarily represent those of their affiliated organizations, or those of the publisher, the editors and the reviewers. Any product that may be evaluated in this article, or claim that may be made by its manufacturer, is not guaranteed or endorsed by the publisher.

frontiers | Frontiers in Microbiology

ORIGINAL RESEARCH
published: 30 May 2022
doi: 10.3389/fmicb.2022.908296

Repeated Exposure of *Escherichia coli* to High Ciprofloxacin Concentrations Selects *gyrB* Mutants That Show Fluoroquinolone-Specific Hyperpersistence

*Aurore Perault[1], Catherine Turlan[2], Nathalie Eynard[2], Quentin Vallé[1], Alain Bousquet-Mélou[1] and Etienne Giraud[1]**

[1]INTHERES, Université de Toulouse, INRAE, ENVT, Toulouse, France, [2]Service d'Ingénierie Génétique du LMGM (SIG-LMGM-CBI), CNRS, Toulouse, France

OPEN ACCESS

Edited by:
Miklos Fuzi, Independent Researcher, Budapest, Hungary

Reviewed by:
José Manuel Rodriguez-Martínez, Sevilla University, Spain
Torahiko Okubo, Hokkaido University, Japan
Xiaoqiang Liu

***Correspondence:**
Etienne Giraud
etienne.giraud@inrae.fr

Specialty section:
This article was submitted to Antimicrobials, Resistance and Chemotherapy, a section of the journal Frontiers in Microbiology

Received: *30 March 2022*
Accepted: *29 April 2022*
Published: *30 May 2022*

Citation:
Perault A, Turlan C, Eynard N, Vallé Q, Bousquet-Melou A and Giraud E (2022) Repeated Exposure of Escherichia coli to High Ciprofloxacin Concentrations Selects gyrB Mutants That Show Fluoroquinolone-Specific Hyperpersistence. Front. Microbiol. 13:908296. doi: 10.3389/fmicb.2022.908296

Recent studies have shown that not only resistance, but also tolerance/persistence levels can evolve rapidly in bacteria exposed to repeated antibiotic treatments. We used *in vitro* evolution to assess whether tolerant/hyperpersistent *Escherichia coli* ATCC25922 mutants could be selected under repeated exposure to a high ciprofloxacin concentration. Among two out of three independent evolution lines, we observed the emergence of *gyrB* mutants showing an hyperpersistence phenotype specific to fluoroquinolones, but no significant MIC increase. The identified mutation gives rise to a L422P substitution in GyrB, that is, outside of the canonical GyrB QRDR. Our results indicate that mutations in overlooked regions of quinolone target genes may impair the efficacy of treatments *via* an increase of persistence rather than resistance level, and support the idea that, in addition to resistance, phenotypes of tolerance/persistence of infectious bacterial strains should receive considerations in the choice of antibiotic therapies.

Keywords: experimental evolution, DNA gyrase, tolerance, persisters, quinolones

INTRODUCTION

Since the discovery of the antibacterial activity of penicillin (Fleming, 1929), antibiotics have been used to treat bacterial infections. However, their overuse and misuse over the decades have contributed to the development in many bacterial pathogens of strategies allowing them to overcome antibiotic treatments. In addition to antibiotic resistance, which has been extensively studied, tolerance and persistence mechanisms are now increasingly looked at as important factors of antibiotic treatments failures (Windels et al., 2019, 2020).

Resistance is the inherited ability of bacteria to grow in the presence of therapeutic concentrations of antibiotics, regardless of the duration of treatment (Brauner et al., 2016). Resistance levels can be quantified by several *in vitro* methods, one of them being the determination of the Minimum Inhibitory Concentration (MIC; Balaban et al., 2019), that is, the minimal antibiotic concentration that prevents growth of a bacterial population for a specific antibiotic. MICs are routinely determined in clinical settings and are crucial for antibiotic,

dosing, and regimen selection. However, resistance is not the only strategy used by bacteria to survive antibiotic treatments.

Tolerance is defined as the ability of a bacterial population to transiently survive high antibiotic concentrations without an increase in the MIC (Balaban et al., 2019). Experimental *in vitro* studies of bacterial evolution have shown the existence of tolerance mutations resulting in a slower killing of the whole bacterial population (Balaban et al., 2019). Tolerance has long been considered as a simple phenotypic adaptation allowing bacteria to prevent total eradication under stress conditions. However it has been highlighted that increased tolerance levels can be conferred by chromosomal mutations in genes involved in global metabolism or stress regulation (Van den Bergh et al., 2017; Chebotar' et al., 2021). For example, mutations have been identified in genes involved in activation of the stringent response and thus in the inhibition of bacterial growth, such as genes encoding the *hipAB* toxin–antitoxin module (Korch et al., 2003) or the methionine-tRNA ligase in *Escherichia coli* (Girgis et al., 2012; Levin-Reisman et al., 2017). Importantly, these mutations subsequently promote the secondary selection of resistance mutations (Van den Bergh et al., 2016; Levin-Reisman et al., 2017).

Another phenomenon called persistence has been defined in a recent consensus statement, as the ability of a subset of bacteria, called persisters, to survive a transient exposure to a bactericidal antibiotic concentration (Balaban et al., 2019). Persisters are stochastically produced drug-tolerant cells. They are phenotypic variants that do not grow and are killed much more slowly than the major antibiotic-susceptible bacterial population, which typically results in biphasic killing curves when performing time-kill assays (Brauner et al., 2016; Balaban et al., 2019). The dormancy state of persisters cells is considered to be responsible for their high tolerance to antibiotics. Upon removal of antibiotics, persisters can resume growth. This makes them a recognized cause of recalcitrance of bacterial infections to antibiotic treatments. Bacterial strains that produce increased persisters subpopulations are termed high persistence or hyperpersistent strains. Experimental *in vitro* studies of bacterial evolution have shown the existence of high persistence mutations that increase the persisters fraction (Khare and Tavazoie, 2020; Sulaiman and Lam, 2020). Recent laboratory evolution experiments have shown that repeated exposure of an *E. coli* strain to high antibiotic concentrations including fluoroquinolones can select hyperpersistent mutants with mutations in translation-related genes (Khare and Tavazoie, 2020; Sulaiman and Lam, 2020).

Tolerance and persistence phenomena can be evidenced by time-kill measurements and quantified by MDK ("Minimum Duration for Killing"), which is the minimum time required to kill a certain percentage of the bacterial population. For example, MDK_{99} and $MDK_{99.99}$ are the minimum duration to kill 99 and 99.99% of the bacterial population, respectively (Brauner et al., 2016).

In this context, we wondered whether tolerance or hyperpersistence mutations could be selected by repeated exposure of a wild-type susceptible *E. coli* strain to clinically relevant concentrations of ciprofloxacin, an antibiotic which targets type II topoisomerases, and primarily DNA gyrase (Vance-Bryan et al., 1990). An Adaptative Laboratory Evolution (ALE) experiment was therefore conducted and evolved clones showing an increased survival during antibiotic treatment or resistance were phenotypically and genotypically analyzed. A summary diagram is presented at **Supplementary Figure S1**. Our results showed that *gyrB* mutations conferring a fluoroquinolone-specific hyperpersistent phenotype, rather than a classical resistance phenotype, could be selected under repeated exposition to clinically relevant ciprofloxacin concentrations.

MATERIALS AND METHODS

Bacterial Strains and Culture Conditions

We used *E. coli* ATCC25922-GFP-Amp^R, named H1 thereafter as the parental strain in our evolution experiments. All strains were grown in Mueller–Hinton Broth (MHB) at 37°C, except during site-directed mutagenesis experiments, where Luria-Bertani Broth (LB) was used. Three different strains of *E. coli* (*E. coli* ATCC25922, *E. coli* BL21, and *E. coli* MG1655) were used in site-directed mutagenesis. For bacterial counts in persistence assays, we used tryptic soy agar supplemented with magnesium heptahydrate sulfate and activated charcoal.

Adaptative Laboratory Evolution Experiment

Three independent evolution lines (named I, II, and III thereafter) were conducted in parallel, starting from overnight cultures of the parental *E. coli* ATCC25922-GFP-Amp^R strain in MHB supplemented with 50 μg/ml ampicillin. A total of 10 selection cycles were performed for each line (**Figures 1A,B**) as follows. At each cycle, 1 ml of overnight cultures grown from the previous cycle were transferred to 29 ml of MHB (1:30 dilution) in Erlenmeyer flasks. Bacteria were enumerated and, ciprofloxacin was then added at a final concentration of 1 μg/ml. Cultures were then incubated for 5 h at 37°C with agitation at 180 rpm. This ciprofloxacin concentration far above the MIC of the parental strain (0.008 μg/ml) was used to prevent the probability of selecting resistant bacteria and rather promote the selection of tolerant or hyperpersistent mutants. Cells from the treated cultures were collected by centrifugation, washed to remove ciprofloxacin, and resuspended in 10 ml of MHB. Ten-fold serial dilutions were prepared to enumerate surviving bacteria. Cultures were then incubated overnight at 37°C with ampicillin at 50 μg/ml, and newly grown bacteria were used for the next selection cycle. Samples of bacterial populations from all overnight cultures were conserved at −80°C.

Selection of a Resistant *gyrB* Mutant

A spontaneous resistant mutant "R" was selected by plating cultures of the *E. coli* ATCC25922-GFP-Amp^R strain on MH agar medium supplemented with ciprofloxacin at 4-fold the parental MIC.

Susceptibility Testing

Minimum Inhibitory Concentration determinations were performed on evolving bacterial populations and on isolated clones according to the microdilution method (Andrews, 2001).

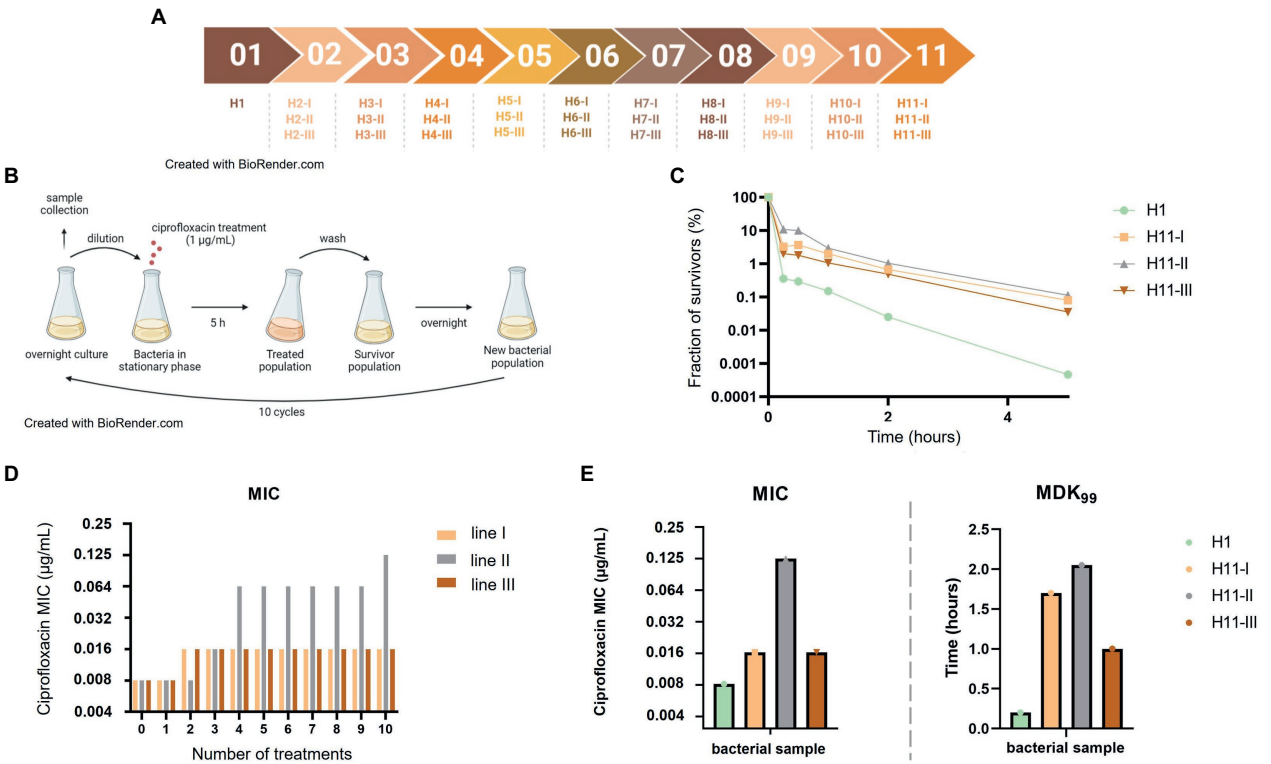

FIGURE 1 | Repeated exposures to ciprofloxacin lead to the emergence of hyperpersistence and resistance phenotypes. **(A)** Chronological set up of the different antibiotic treatments and bacterial population samples evolved from the H1 parental strain. **(B)** Set up of the evolutionary experience with repeated ciprofloxacin treatments. Bacteria were exposed to 10 ciprofloxacin treatments as follows: bacteria were grown overnight, stationary phase cultures were sampled and diluted by a factor of 1:30 before addition of ciprofloxacin at 1 µg/ml for 5 h. After antibiotic removal by centrifugation and washing, all bacteria were grown again overnight in fresh medium for the next cycle. **(C)** Time-kill assays performed on bacterial populations obtained after 10 ciprofloxacin treatments. **(D)** Evolution of ciprofloxacin MIC of bacterial populations along treatments. **(E)** Evolved bacteria from the three evolution lines showed increased MDK_{99}.

The MIC was determined as the lowest antibiotic concentration where no bacterial growth occurred. Results were validated by comparison with reference values provided by EUCAST for the *E. coli* ATCC25922 strain (The European Committee on Antimicrobial Susceptibility Testing, 2022).

Persistence Assays

Overnight cultures were first diluted 1:6 or 1:600 in fresh MHB for 10^7–10^8 CFU/ml inocula and 10^5–10^6 CFU/ml inocula, respectively. Initial CFU counts were determined by serial dilution and plating as described above. To overcome resistance phenotypes, time-kill assays were performed at antibiotic concentrations much higher than the MICs (128- or 256-fold higher) for each strain. Antibiotic used were ciprofloxacin, enrofloxacin, norfloxacin, nalidixic acid, flumequine, tetracycline, and gentamicin (Sigma and Fluka). The survival fraction was calculated as the ratio of bacterial numeration at a given time of the treatment versus the bacterial numeration before treatment.

Whole-Genome Sequencing and Identification of Mutations

Genomic DNA was extracted using the DNEasy Blood and Tissue kit (QIAGEN). A whole-genome sequencing (WGS) was performed using IonTorrent technology at the GeT-PlaGe Genotoul Platform, Toulouse, France. Sequence assembly was performed, and mutations were identified by comparison with the *E. coli* ATCC25922 reference genome (GenBank accession number: CP009072).

Strain Reconstruction by Site-Directed Mutagenesis

Mutagenesis was based on the one-step inactivation of chromosomal gene strategy (Datsenko and Wanner, 2000). The different recombination substrates were obtained by PCR amplification and assembly. Primers used for this directed mutagenesis are described in **Supplementary Table S1**. The plasmid pKD3 was used as template to amplify the FRT-flanked chloramphenicol resistance (cat) gene, antibiotic that will be used later for the selection of recombinant clones. PCR reaction was performed using the PrimeSTAR® Max DNA Polymerase (Takara). DNA fragments isolated from agarose gels were purified using the GFX PCR DNA and gel band purification kit (Sigma Aldrich). For this mutagenesis, we used plasmids pKD46 and pE-FLP containing an ampicillin resistance gene and a heat-sensitive replication origin, and from which λRed proteins or FLP are constitutively produced.

Fifty microliters of electrocompetent cells were mixed with 500 ng of recombinant substrates or 50 ng of plasmid and incubated for 20 min in ice. Electroporation was performed at 2.5 kV, 25 µF, 200 Ω during 4.5 ms into a chilled 2 mm cuvette 1 ml of SOC has been added, and cells recovery was done at 30°C or 37°C for 2 h. Cells were plated on LB Ampicillin or LB Chloramphenicol and incubated at 30°C or 37°C.

To verify the introduction of the *gyrB* gene mutations, PCR sequencing was performed from an overnight culture diluted at 1:13 and preincubated at 95°C 5 min, using the PrimerSTAR® Max DNA Polymerase (Takara) with the RecF5 and RecF6 primers (**Supplementary Table S1**). This amplification produced a 1,070 bp fragment which was then sequenced.

To eliminate the chloramphenicol resistance gene, Cm^R mutants were transformed with pE-FLP plasmid, as previously described (Datsenko and Wanner, 2000) and ampicillin-resistant transformants were selected at 30°C. Transformant clones were streaked and incubated at 42°C on non-selective media and then tested for chloramphenicol sensitivity. Excision of the *cat* gene was verified by PCR using the Taq DNA polymerase (MP Biomedical) with the RecF5 and RecF14 primers (**Supplementary Table S1**) and sequencing from RecF13.

Statistical Analysis

All statistical analyses were performed using data from independent biological replicates. Differences between groups of quantitative variables were assessed using the Kruskal–Wallis test. Differences were considered significant when *p*-values were ≤ 0.05.

RESULTS

After 10 Days of Ciprofloxacin Treatment, Altered Bactericidal Activity Is Observed With Increased Persisters Fraction and MDK Levels

An experimental evolution experiment was set up in order to select tolerant or hyperpersistent bacteria from a susceptible parental strain (**Figure 1A**). The fully quinolone-susceptible *E. coli* ATCC25922-GFP strain, which was used as the parental strain H1, was repeatedly exposed to 1 µg/ml ciprofloxacin, a concentration 128-fold higher than its MIC (0.008 µg/ml). Ten selection cycles were performed along 15 days, each cycle consisting in the ciprofloxacin treatment of a stationary phase culture obtained from growth of bacteria that had survived the previous treatment. Three independent evolution lines were conducted in parallel (**Figures 1A,B**). To evaluate how resistance and tolerance evolved in the three lines, samples of bacterial populations were collected at each cycle and their ciprofloxacin MICs and survival fractions under ciprofloxacin treatment were determined.

For unevolved population directly grown from the parental strain (H1), the ciprofloxacin MIC was 0.008 µg/ml and the survival fraction after a 5-h exposure to 1 µg/ml ciprofloxacin was in the 5.10^{-5}–10^{-6} range (**Figure 1C**). In lines I and III, the ciprofloxacin MIC of bacterial populations increased 2-fold after two treatments but did not change thereafter (**Figure 1D**). In contrast, the ciprofloxacin MIC of the bacterial population of line II increased 16-fold along the 10 treatments, to reach the value of 0.125 µg/ml.

Time-kill assays were performed on bacterial populations evolved along 10 treatments (H11-I, H11-II, and H11-III; **Figure 1C**), and MDK_{99} values were deduced from killing curves. Bacterial populations from all three evolutionary lines showed similarly altered killing, with a 100-fold increased persisters fraction after a 5-h ciprofloxacin treatment, compared to the parental strain they derive from.

MDK_{99} values of evolved bacterial populations increased 5- to 10-fold for all three lines (**Figure 1E**). For H11-I and H11-III (i.e., evolved populations from lines I and III, respectively), the increase in survival fraction and MDK_{99} was associated with a ciprofloxacin MIC similar (only 2-fold higher) to that of the parental strain, indicating that the altered killing was due to a tolerance or hyperpersistence mechanism. In contrast, increased survival and MDK_{99} observed for population H11-II was associated to a significantly increased ciprofloxacin MIC (16-fold higher than the MIC of the H1 parental strain), indicating that the killing in bacteria evolved in this line was altered probably due to a higher level of resistance.

In summary, it appeared that increased survival observed for the bacterial populations of the three evolutions lines after 10 treatments were due to a tolerant or hyperpersistent phenotype in line I and III, but rather to a resistance mechanism in line II. This was confirmed by analysis of individual clones isolated from populations of the three evolution lines. **Table 1** shows resistance and persistence characteristics of representative clones.

The GyrB L422P Substitution Is Associated to an Hyperpersistence Phenotype

To identify the mutations responsible for the previously identified hyperpersistence and resistance phenotypes, whole-genome sequencing was performed on clones isolated from the different lines. In addition, for comparison purpose, a spontaneous resistant mutant (named R) obtained by plating a culture of the parental strain on a ciprofloxacin-supplemented solid medium, was also sequenced. Interestingly, all spontaneous and evolved mutants had a mutation on one of the two subunits of the DNA gyrase, which is the enzyme primarily targeted by quinolones (**Table 1**).

The R mutant (ciprofloxacin MIC: 0.062 µg/ml) showed a mutation on the *gyrB* gene giving rise to the S464Y amino acid change. Mutations at this position are known to confer a quinolone resistance phenotype. This substitution has already been described in other Gram-negative species, such as *Salmonella* spp. (Correia et al., 2017), *Pseudomonas aeruginosa* (Mouneimné et al., 1999), and *Proteus mirabilis* (Weigel et al., 2002).

Clone H11-II4 isolated from evolution line II, showing a resistance phenotype, carried a mutation on the *gyrA* gene giving rise to the D87G amino acid substitution. This substitution is frequent in fluoroquinolone-resistant gram-negative bacteria and particularly in enterobacterales (Conrad et al., 1996; Correia et al., 2017).

TABLE 1 | Mutations identified in resistant and hyperpersistent mutants and their phenotypic characteristics in the presence of ciprofloxacin.

Strain	Identified mutations	Gene	Ciprofloxacin MICs (μg/ml)	Ciprofloxacin MDK_{99} (h)	Ciprofloxacin $MDK_{99.99}$ (h)	Survival fraction at 24 h
H1	/	/	0.008	0.4	4.2	2.5×10^{-7}
Resistant R	S464Y (TCT → TAT)	*gyrB*	0.062	2.1	7.6	3.6×10^{-7}
H11-I1	L422P (CTG → TTG)	*gyrB*	0.016	16	>24	3.8×10^{-3}
H11-III2	L422P (CTG → TTG)	*gyrB*	0.016	1.6	9.5	2.6×10^{-5}
	T insertion at nucleotide position 2093745	MFS family				
H11-II4	D87G (GAC → GGC)	*gyrA*	0.125	1.6	6.6	1.1×10^{-5}

Survival fraction was determined after exposing bacteria for 24 h to a ciprofloxacin concentration of 256 times their MIC. The survival fraction was calculated by dividing the number of surviving bacteria by the number of live bacteria that were present before the antibiotic treatment. The nucleotide position refers to the Escherichia coli ATCC25922 genome (GenBank accession number CP009072).

More interestingly, three sequenced clones from line I (H11-I1, H11-I3, and H11-I5) and clone H11-III2 from line III carried the same mutation of the *gyrB* gene giving rise to the amino acid change L422P. In clone H11-III2, an additional mutation consisting in a single nucleotide insertion was also identified in a major facilitator superfamily (MFS) gene (**Table 1**). This frameshift mutation probably causes a loss of function of the corresponding MFS protein.

The L422P substitution was associated in our isolates with a small (2-fold) increase of ciprofloxacin MIC, but with a high persistence level. From there, we focused our investigations on isolate H11-I1, as representative of the hyperpersistence-associated genotype. This isolate displays a MDK_{99} increased 40-fold and a survival fraction after a 24-h treatment increased more than 10^4-fold, compared to its parental strain.

The Hyperpersistent Phenotype Associated With the Mutation L422P Is Specific to Fluoroquinolones

Identification of mutations in the DNA gyrase genes suggested that the phenotypes selected in our experiments were specific to quinolones. Therefore, we investigated whether experimental selections for tolerance/persistence and resistance to ciprofloxacin also resulted in persistence and resistance to other quinolone antibiotics.

The MIC of three fluoroquinolones (ciprofloxacin, enrofloxacin, norfloxacin) and of two quinolones (flumequine, nalidixic acid) were measured for the susceptible (H1), hyperpersistent (H11-I1) and resistant (R) strains (**Figure 2A**). The susceptibility level of the hyperpersistent strain for these five antibiotics was similar (unchanged or only doubled MICs) to that of the parental H1 strain. In contrast, the MICs of the resistant strain showed an 8-fold increase for ciprofloxacin, norfloxacin, enrofloxacin, and nalidixic acid and 4-fold for flumequine.

Tolerance and persistence levels were also measured for the five antibiotics (**Figures 2B–F**). All killing curves showed the same biphasic profile characteristic of a persistence phenotype, that is, presence in bacterial populations of persisters tolerant to the tested antibiotics. The bactericidal activity of ciprofloxacin, norfloxacin, and enrofloxacin against the hyperpersistent H11-I1 strain was significantly decreased compared to that observed against the H1 parental and the resistant strains (**Figures 2B–D**). This resulted in increased MDK_{99}, $MDK_{99.99}$, and 24-h survival rates (**Supplementary Table S2**). Interestingly, results were different for flumequine and nalidixic acid, which are not fluoroquinolones. For these two older generation quinolones, bactericidal profiles observed for resistant and tolerant mutant were not significantly different from those obtained for the susceptible parental strain (**Figures 2E,F**).

Effect of the inoculum size was also analyzed, since many studies have shown that it can influence killing profiles during treatments with fluoroquinolones (Li et al., 2017). An inoculum of 10^5 bacteria was therefore exposed to the same concentrations of ciprofloxacin as in previously described killing assays. As with the large size inoculum, a bimodal killing pattern was observed with a significantly higher persisters rate for the H11-I1 strain compared to its parental strain (H1; **Supplementary Figure S2**). This shows that the hyperpersistent phenotype of this mutant is not dependent on inoculum size.

These results show that the hyperpersistent mutant H11-I1, despite displaying no significant increase in resistance, is killed much less efficiently by fluoroquinolones than its susceptible parental strain and than a resistant mutant. This hyperpersistence phenotype appears to be specific to fluoroquinolones since it is not observed for flumequine and nalidixic acid.

In a second step, we addressed whether experimental selections of tolerance and resistance to ciprofloxacin also resulted in cross-persistence and cross-resistance to antibiotic of other families.

For the three strains studied, parental (H1), hyperpersistent (H11-I1), and resistant (R), MICs of tetracycline and of gentamicin (aminoglycoside family) were measured. Susceptibility levels of the hyperpersistent and resistant mutant strains to these two antibiotics appeared identical to that of the parental H1 strain (**Supplementary Figure S3A**).

Tolerance/persistence levels of the susceptible, hyperpersistent, and resistant strains were then measured for the two antibiotics. No significant difference in the bactericidal activity of gentamicin and tetracycline against the resistant and hyperpersistent strains was observed compared to the susceptible strain (**Supplementary Figures S3B,C**). No difference in MDK_{99} and $MDK_{99.99}$ was observed between the three strains when treated with gentamicin. Nevertheless, the MDK_{99} of the H11-I1 mutant was increased about 2-fold during tetracycline treatment compared to those of the parental and resistant strains (**Supplementary Figure S3D**). In summary, the hyperpersistence phenotype of the H11-I1

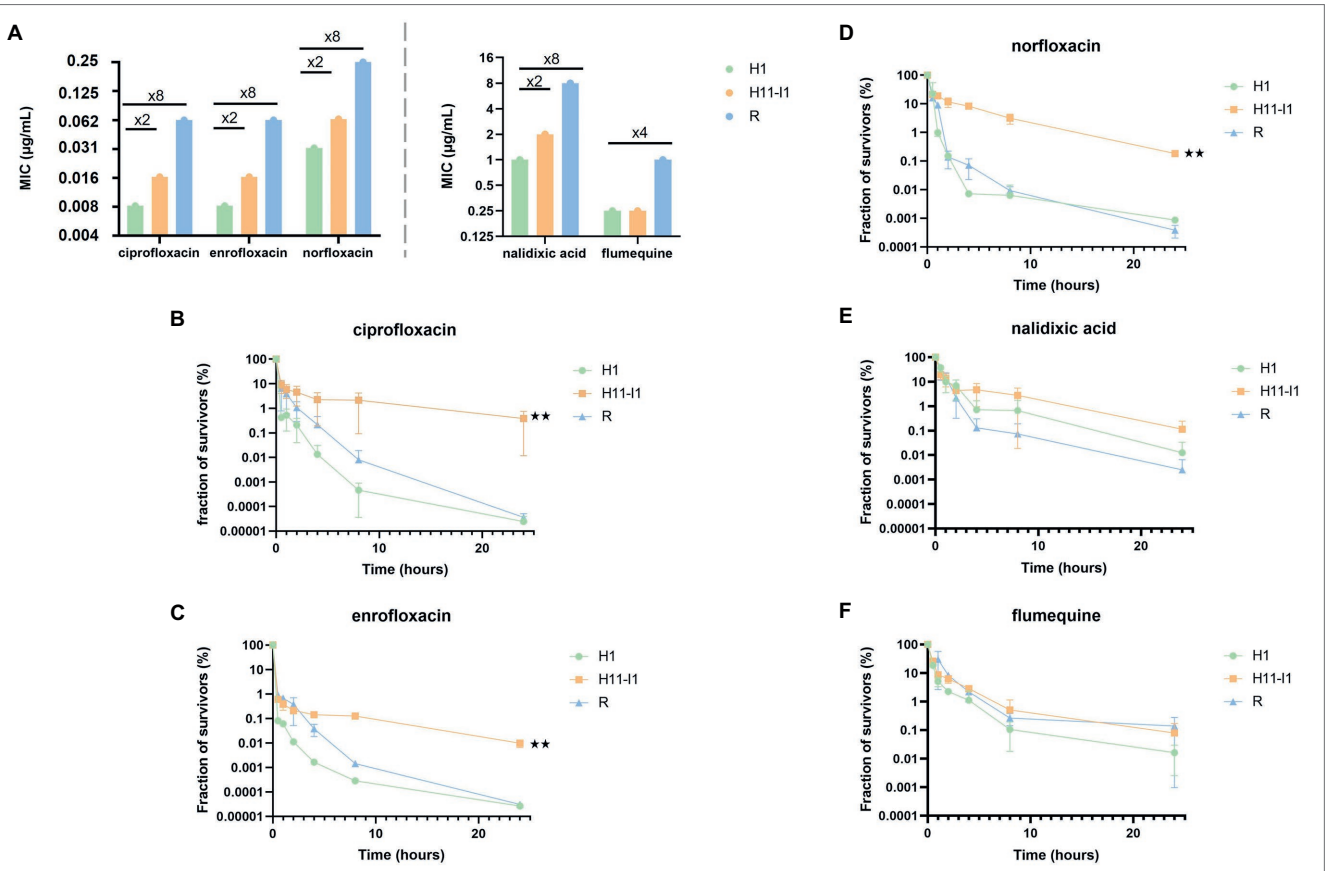

FIGURE 2 | The L422P substitution in GyrB is associated with an hyperpersistence phenotype specific to fluoroquinolones. **(A)** MICs of the parental strain (H1), of the H11-I1 mutant clone from line I and of a spontaneous resistant mutant (R) were determined for three fluoroquinolones (ciprofloxacin, norfloxacin, and enrofloxacin) and two older generation quinolones (nalidixic acid and flumequine). **(B–D)** Bactericidal assays in the presence of fluoroquinolones at 256-fold the MIC of each strain (ciprofloxacin, enrofloxacin, and norfloxacin) showed an altered bactericidal effect for the H11-I1 mutant, with a fraction of persisters increased by a factor 100 to 1,000. **(E,F)** Bactericidal essays in the presence of old generation quinolones (nalidixic acid and flumequine) showed no significant alteration of bactericidal effect for the H11-I1 mutant. Significant *p*-values compared with the H1 strain are noted (**$p \leq 0.01$).

mutant seems to be associated with fluoroquinolones only and no cross-persistence is observed.

Induction of the Hyperpersistence Phenotype in the Presence of the GyrB Mutation L422P Is Strain-Dependent

In order to confirm that the GyrB L422P substitution was causal to the hyperpersistence phenotype of H11-I1 mutant and test the influence of the genetic background, the mutation was introduced by directed mutagenesis in 3 *E. coli* strains (*E. coli* ATCC25922, MG1655, and BL21). As a control, the resistance mutation identified in the R mutant was also reconstructed in the three genetic backgrounds. All strains were then submitted to MIC determinations and time-kill assays.

In the reconstructed strains, introduction of the GyrB L422P and S464Y substitutions resulted in ciprofloxacin MICs increases similar to those observed in the mutants selected during the experimental evolution, that is, a 2-fold increase for the L422P substitution and a 8- to 16-fold increase for the S464Y substitution (**Figure 3A**).

As expected, the survival fraction at 24 h of the *E. coli* ATCC25922 (L422P) reconstructed mutant was increased 100-fold, confirming the causality of L422P substitution to the phenotype of hyperpersistent to ciprofloxacin (**Figure 3B**). Killing assays also conducted on *E. coli* ATCC25922 (L422P) with other fluoroquinolones, older quinolones, an aminoglycoside, and tetracycline gave results similar to those observed with the strains selected during ALE experiments. These results confirmed that L422P substitution conferred an hyperpersistent phenotype specific to fluoroquinolones (**Supplementary Figure S4**).

In contrast, no alteration of bacterial killing was observed when bacteria were treated with fluoroquinolones after introduction of the L422P substitution in *E. coli* MG1655 and BL21 strains (**Figures 3C,D**). This indicates that expression of hyperpersistence phenotype associated to GyrB L422P substitution does not occur in all genetic backgrounds but is actually strain-dependent.

DISCUSSION

Antibiotic tolerance and hyperpersistence have been associated to chronic and recurrent infections (Lewis, 2010, 2019;

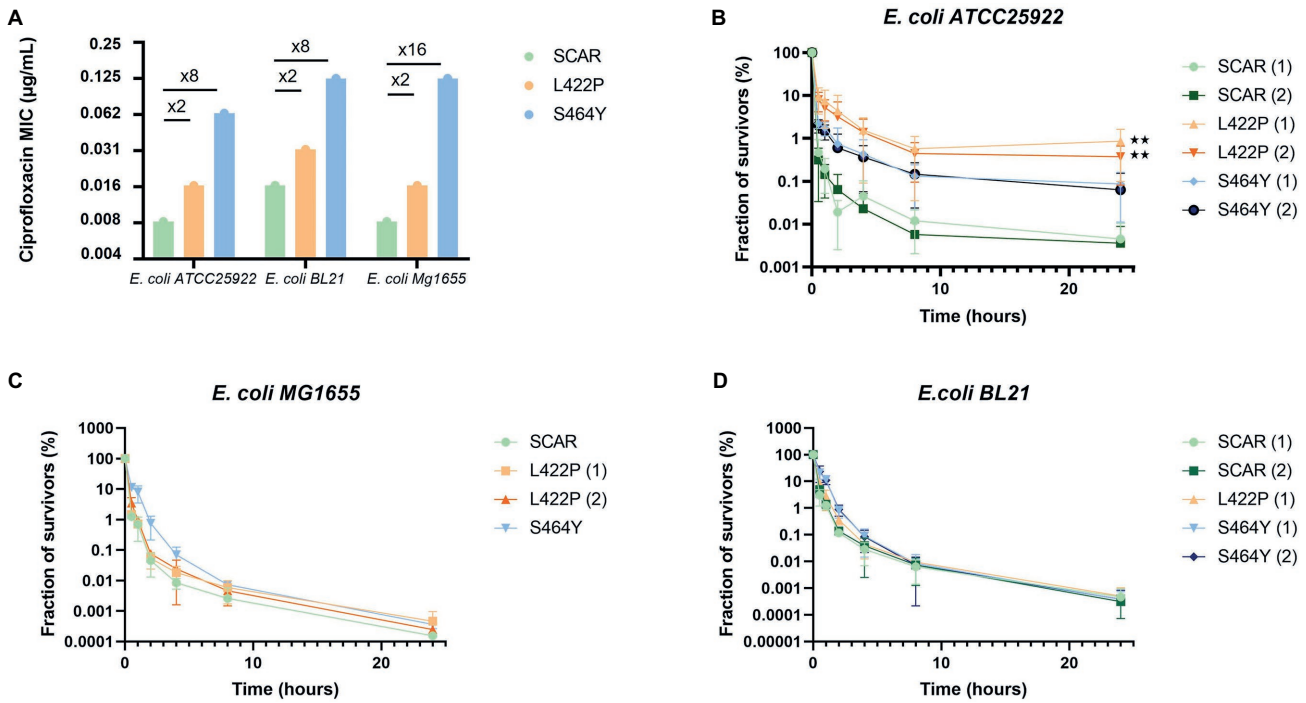

FIGURE 3 | The hyperpersistent phenotype associated with the GyrB L422P substitution is strain-dependent. **(A)** Levels of resistance to ciprofloxacin of reconstructed mutants of *Escherichia coli* ATCC25922, BL21, and MG1655 carrying the GyrB L422P or S464Y substitutions. SCAR strains are susceptible controls with no introduced mutation in *gyrB*, but containing the scar left by removal of the chloramphenicol resistance gene used for selection of recombinant clones. For each mutation, when possible, two independent recombinant clones were analyzed and then named (1) and (2). MICs of the three strains of *E. coli* with the L422P substitution were similar to those of the susceptible strains (SCAR) with only a 2-fold factor difference. **(B)** Bactericidal assays performed on the reconstructed *E. coli* ATCC25922 strains showed an alteration in bactericidal activity in the presence of ciprofloxacin for *E. coli* ATCC25922 (L422P) clones. **(C,D)** Bactericidal assays conducted on strains *E. coli* MG1655 and BL21 (L422P), (S464Y), and (SCAR) showed no alteration in bactericidal activity in the presence of ciprofloxacin. Significant *p*-values compared to SCAR1 and SCAR2 control clones are noted (**$p \leq 0.01$).

Van den Bergh et al., 2017). In particular, tolerance and hyperpersistence mechanisms are suspected to be involved in the recurrency of Urinary Track Infections (UTI; Murray et al., 2021). As these infections are often caused by *E. coli* and may be treated with ciprofloxacin, we designed this study to address whether repeated *in vitro* exposure of an *E. coli* strain to high concentrations of ciprofloxacin could select tolerant or hyperpersistent clones. Study of such phenotypes is important since previous studies have shown that selection of antibiotic resistance, which is the main cause of recalcitrance to antibiotic therapy, is more likely to occur in tolerant or hyperpersistent strains (Levin-Reisman et al., 2017).

Starting from a susceptible *E. coli* strain, we observed the selection of bacterial clones displaying a significantly higher persistence rate in time-kill assays carried out with ciprofloxacin, but a resistance similar to their parental strain. Interestingly, we discovered that this hyperpersistence phenotype was associated with a mutation in the *gyrB* gene coding for the B subunit of DNA gyrase, which is the main target enzyme of quinolones. This result was unexpected since mutations in quinolone target genes usually confer increased resistance to antibiotics of this family (Hooper and Jacoby, 2015). In contrast, tolerance/persistence mechanisms are generally associated with mutations located outside the antibiotic target genes, in global metabolism or stress regulation genes (Van den Bergh et al., 2017; Chebotar' et al., 2021). Quinolone resistance mutations appear at specific codons of regions called QRDR (Quinolone Resistance Determining Region). They are more frequent in the *gyrA* QRDR (spanning codons 64–106) than in the *gyrB* QRDR (codons 426–464; Bhatnagar and Wong, 2019). The mutation identified in our hyperpersistent mutant, which gives rise to the L422P amino acid substitution, is therefore outside but close to the *E. coli gyrB* QRDR. Interestingly, the 422 amino acid position is located into the TOPRIM domain which is the catalytic domain involved in DNA strand breakage and rejoining (Bhatnagar and Wong, 2019). The presence of this mutation in a quinolone target gene suggested that the hyperpersistence phenotype could be specific to these antibiotics. Indeed, our mutant did not show increased persistence when exposed to antibiotics of the tetracycline and aminoglycoside family. Furthermore, increased persistence of our *gyrB* mutant was also observed with fluoroquinolones others than ciprofloxacin, but not with older quinolones, such as nalidixic acid and flumequine. This indicates that the hyperpersistence phenotype we selected by repeated exposure to ciprofloxacin is likely specific of compounds that are structurally close to this fluoroquinolone. Sulaiman and Lam (2020) obtained similar results in *E. coli* by demonstrating that tolerance could be specific to the type of antibiotic used during evolution experiment. In

summary, our study shows that a *gyrB* mutation, even located outside of the QRDR and conferring a barely significant resistance level, can significantly increase persistence against ciprofloxacin. To our knowledge, it is the first study to report a mutation in a quinolone target gene which confers an hyperpersistence phenotype rather than an increased resistance level. In a recent study, it was also shown that low level quinolone resistance mechanisms mediated by type II topoisomerase modifications increased tolerance and persistence against ciprofloxacin (Ortiz-Padilla et al., 2020). The mechanism involved in this apparently fluoroquinolone-specific hyperpersistence occurring in our mutant remains unknown.

Reconstruction of this *gyrB* mutation in *E. coli* ATCC25922 proved that it was responsible for the hyperpersistent phenotype in this genetic background. However, when reconstructed in two other *E. coli* genetic backgrounds (K12 and B type), this mutation did not confer any hyperpersistence phenotype. This indicates that phenotypic expression of the *gyrB* mutation depends on genetic background and is possibly restricted to a narrow panel of strains. To our knowledge, the GyrB L422P amino acid substitution has not been reported in any *E. coli* clinical or laboratory isolate, or at an equivalent position in another bacterial species. We cannot exclude that its selection was influenced by our *in vitro* experimental design and that its selection would be unlikely *in vivo*. However, it should be noticed that strains bearing such a hyperpersistence-conferring mutation would probably not be remarked in a clinical setting, where antibiotic resistance is the only bacterial phenotype that is measured and considered to make antibiotic therapy decisions. Our study shows that a mutation located outside of the QRDRs of target genes can lead to strong alterations of the bactericidal effect of fluoroquinolones without increasing significantly the resistance level. In a more general manner, it is possible that some mutations detected in antibiotic target genes and which are overlooked because they are not associated with a resistance phenotype, actually confer a tolerance or hyperpersistence phenotype that can compromise treatments.

Knowing the role played by tolerant and persistent bacteria during therapeutic failure, it now seems essential to take these phenotypes into consideration when choosing an antibiotic treatment. Currently, analyses carried out in clinical settings (antibiograms, MIC determinations) allow measurement of susceptibility level but not detection of tolerance and hyperpersistence phenotypes. This can lead to classify bacterial isolates as susceptible whereas they could be difficult to treat and lead to antibiotic treatment failure and infection relapse due to an undetected tolerance or persistence phenotype. Although techniques have been developed, such as Tolerance Disk test (TDtest), which is based on the disk-diffusion assay (Gefen et al., 2017), they remain unreliable and tedious to implement on a large scale. There is a clinical need to develop technical means to detect hyperpersistence and tolerance phenotypes in an automated and rapid way.

DATA AVAILABILITY STATEMENT

The nucleotide sequence data are deposited in the EMBL-EBI European Nucleotide Archive repository under accession number PRJEB52382.

AUTHOR CONTRIBUTIONS

EG contributed to conception and design of the study and supervised this project. AP, QV, CT, and NE performed the experiments. CT and NE designed mutagenesis experiments. AP, QV, and EG analyzed the data. AP wrote the first draft of the manuscript. CT, NE, QV, AB-M, and EG revised the manuscript. All authors contributed to the article and approved the submitted version.

ACKNOWLEDGMENTS

We thank Thi Hai Ha Phung for her help with the microbiological experiments, Nathalie Arpaillange for technical support, and Veronique Dupuy for technical advices.

SUPPLEMENTARY MATERIAL

The Supplementary Material for this article can be found online at: https://www.frontiersin.org/articles/10.3389/fmicb.2022.908296/full#supplementary-material

REFERENCES

Andrews, J. M. (2001). Determination of minimum inhibitory concentrations. *J. Antimicrob. Chemother.* 48, 5–16. doi: 10.1093/jac/48.suppl_1.5

Balaban, N. Q., Helaine, S., Lewis, K., Ackermann, M., Aldridge, B., Andersson, D. I., et al. (2019). Definitions and guidelines for research on antibiotic persistence. *Nat. Rev. Microbiol.* 17, 441–448. doi: 10.1038/s41579-019-0196-3

Bhatnagar, K., and Wong, A. (2019). The mutational landscape of quinolone resistance in *Escherichia coli*. *PLoS One* 14:e0224650. doi: 10.1371/journal.pone.0224650

Brauner, A., Fridman, O., Gefen, O., and Balaban, N. Q. (2016). Distinguishing between resistance, tolerance and persistence to antibiotic treatment. *Nat. Rev. Microbiol.* 14, 320–330. doi: 10.1038/nrmicro.2016.34

Chebotar', I. V., Emelyanova, M. A., Bocharova, J. A., Mayansky, N. A., Kopantseva, E. E., and Mikhailovich, V. M. (2021). The classification of bacterial survival strategies in the presence of antimicrobials. *Microb. Pathog.* 155:104901. doi: 10.1016/j.micpath.2021.104901

Conrad, S., Saunders, J. R., Oethinger, M., Kaifel, K., Klotz, G., Marre, R., et al. (1996). *gyrA* mutations in high-level fluoroquinolone-resistant clinical isolates of *Escherichia coli*. *J. Antimicrob. Chemother.* 38, 443–456. doi: 10.1093/jac/38.3.443

Correia, S., Poeta, P., Hébraud, M., Capelo, J. L., and Igrejas, G. (2017). Mechanisms of quinolone action and resistance: where do we stand? *J. Med. Microbiol.* 66, 551–559. doi: 10.1099/jmm.0.000475

Datsenko, K. A., and Wanner, B. L. (2000). One-step inactivation of chromosomal genes in *Escherichia coli* K-12 using PCR products. *Proc. Natl. Acad. Sci. U. S. A.* 97, 6640–6645. doi: 10.1073/pnas.120163297

Fleming, A. (1929). On the antibacterial action of cultures of a penicillium, with special reference to their use in the isolation of *B. influenzae*. *Br. J. Exp. Pathol.* 10, 226–236.

Gefen, O., Chekol, B., Strahilevitz, J., and Balaban, N. Q. (2017). TDtest: easy detection of bacterial tolerance and persistence in clinical isolates by a modified disk-diffusion assay. *Sci. Rep.* 7:41284. doi: 10.1038/srep41284

Girgis, H. S., Harris, K., and Tavazoie, S. (2012). Large mutational target size for rapid emergence of bacterial persistence. *Proc. Natl. Acad. Sci. U. S. A.* 109, 12740–12745. doi: 10.1073/pnas.1205124109

Hooper, D. C., and Jacoby, G. A. (2015). Mechanisms of drug resistance: quinolone resistance. *Ann. N. Acad. Sci.* 1354, 12–31. doi: 10.1111/nyas.12830

Khare, A., and Tavazoie, S. (2020). Extreme antibiotic persistence via heterogeneity-generating mutations targeting translation. *mSystems* 5:e00847–19. doi: 10.1128/mSystems.00847-19

Korch, S. B., Henderson, T. A., and Hill, T. M. (2003). Characterization of the hipA7 allele of Escherichia coli and evidence that high persistence is governed by (p)ppGpp synthesis: persistence and (p)ppGpp synthesis in *E. coli*. *Mol. Microbiol.* 50, 1199–1213. doi: 10.1046/j.1365-2958.2003.03779.x

Levin-Reisman, I., Ronin, I., Gefen, O., Braniss, I., Shoresh, N., and Balaban, N. Q. (2017). Antibiotic tolerance facilitates the evolution of resistance. *Science* 355, 826–830. doi: 10.1126/science.aaj2191

Lewis, K. (2010). Persister Cells. *Annu. Rev. Microbiol.* 64, 357–372. doi: 10.1146/annurev.micro.112408.134306

Lewis, K. (2019). *Persister Cells and Infectious Disease*. Cham: Springer International Publishing.

Li, J., Xie, S., Ahmed, S., Wang, F., Gu, Y., Zhang, C., et al. (2017). Antimicrobial activity and resistance: influencing factors. *Front. Pharmacol.* 8:364. doi: 10.3389/fphar.2017.00364

Mouneimné, H., Robert, J., Jarlier, V., and Cambau, E. (1999). Type II topoisomerase mutations in ciprofloxacin-resistant strains of *Pseudomonas aeruginosa*. *Antimicrob. Agents Chemother.* 43, 62–66. doi: 10.1128/AAC.43.1.62

Murray, B. O., Flores, C., Williams, C., Flusberg, D. A., Marr, E. E., Kwiatkowska, K. M., et al. (2021). Recurrent urinary tract infection: a mystery in search of better model systems. *Front. Cell. Infect. Microbiol.* 11:691210. doi: 10.3389/fcimb.2021.691210

Ortiz-Padilla, M., Diaz-Diaz, S., Machuca, J., Tejada-Gonzalez, A., Recacha, E., Docobo-Pérez, F., et al. (2020). Role of low-level quinolone resistance in generating tolerance in *Escherichia coli* under therapeutic concentrations of ciprofloxacin. *J. Antimicrob. Chemother.* 75, 2124–2132. doi: 10.1093/jac/dkaa151

Sulaiman, J. E., and Lam, H. (2020). Proteomic investigation of tolerant *Escherichia coli* populations from cyclic antibiotic treatment. *J. Proteome Res.* 19, 900–913. doi: 10.1021/acs.jproteome.9b00687

The European Committee on Antimicrobial Susceptibility Testing (2022). Routine and extended internal quality control for MIC determination and disk diffusion as recommended by EUCAST, Version 12.0.

Van den Bergh, B., Fauvart, M., and Michiels, J. (2017). Formation, physiology, ecology, evolution and clinical importance of bacterial persisters. *FEMS Microbiol. Rev.* 41, 219–251. doi: 10.1093/femsre/fux001

Van den Bergh, B., Michiels, J. E., Wenseleers, T., Windels, E. M., Boer, P. V., Kestemont, D., et al. (2016). Frequency of antibiotic application drives rapid evolutionary adaptation of *Escherichia coli* persistence. *Nat. Microbiol.* 1:16020. doi: 10.1038/nmicrobiol.2016.20

Vance-Bryan, K., Guay, D. R. P., and Rotschafer, J. C. (1990). Clinical pharmacokinetics of ciprofloxacin. *Clin. Pharmacokinet.* 19, 434–461. doi: 10.2165/00003088-199019060-00003

Weigel, L. M., Anderson, G. J., and Tenover, F. C. (2002). DNA Gyrase and topoisomerase IV mutations associated with fluoroquinolone resistance in *Proteus mirabilis*. *Antimicrob. Agents Chemother.* 46, 2582–2587. doi: 10.1128/AAC.46.8.2582-2587.2002

Windels, E. M., Michiels, J. E., Van den Bergh, B., Fauvart, M., and Michiels, J. (2019). Antibiotics: combatting tolerance to stop resistance. *MBio* 10:e02095-19. doi: 10.1128/mBio.02095-19

Windels, E. M., Van den Bergh, B., and Michiels, J. (2020). Bacteria under antibiotic attack: different strategies for evolutionary adaptation. *PLoS Pathog.* 16:e1008431. doi: 10.1371/journal.ppat.1008431

Conflict of Interest: The authors declare that the research was conducted in the absence of any commercial or financial relationships that could be construed as a potential conflict of interest.

Publisher's Note: All claims expressed in this article are solely those of the authors and do not necessarily represent those of their affiliated organizations, or those of the publisher, the editors and the reviewers. Any product that may be evaluated in this article, or claim that may be made by its manufacturer, is not guaranteed or endorsed by the publisher.

frontiers | Frontiers in Microbiology

ORIGINAL RESEARCH
published: 03 June 2022
doi: 10.3389/fmicb.2022.908336

Scientists' Assessments of Research on Lactic Acid Bacterial Bacteriocins 1990–2010

*Laura D. Martinenghi and Jørgen J. Leisner**

Department of Veterinary and Animal Sciences, Faculty of Health and Medical Sciences, University of Copenhagen, Frederiksberg, Denmark

The antimicrobial activity of bacteriocins from lactic acid bacteria has constituted a very active research field within the last 35 years. Here, we report the results of a questionnaire survey with assessments of progress within this field during the two decades of the 1990s and the 2000s by 48 scientists active at that time. The scientists had research positions at the time ranging from the levels of Master's and Ph.D. students to principal investigators in 19 Asian, European, Oceanian and North American countries. This time period was evaluated by the respondents to have resulted in valuable progress regarding the basic science of bacteriocins, whereas this was not achieved to the same degree with regard to their applications. For the most important area of application, food biopreservation, there were some success stories, but overall the objectives had not been entirely met due to a number of issues, such as limited target spectrum, target resistance, poor yield as well as economic and regulatory challenges. Other applications of bacteriocins such as enhancers of the effects of probiotics or serving as antimicrobials in human clinical or veterinary microbiology, were not evaluated as having been implemented successfully to any large extent at the time. However, developments in genomic and chemical methodologies illustrate, together with an interest in combining bacteriocins with other antimicrobials, the current progress of the field regarding potential applications in human clinical microbiology and food biopreservation. In conclusion, this study illuminates parameters of importance not only for R&D of bacteriocins, but also for the broader field of antimicrobial research.

Keywords: antibiotic, antimicrobial, biopreservation, lantibiotic, nisin, pediocin, bacteriocin, lactic acid bacteria

OPEN ACCESS

Edited by:
Des Field,
University College Cork, Ireland

Reviewed by:
Svetoslav Todorov,
University of São Paulo, Brazil
Takeshi Zendo,
Kyushu University, Japan

***Correspondence:**
Jørgen J. Leisner
jjl@sund.ku.dk

Specialty section:
This article was submitted to Antimicrobials, Resistance and Chemotherapy, a section of the journal Frontiers in Microbiology

Received: *30 March 2022*
Accepted: *28 April 2022*
Published: *03 June 2022*

Citation:
Martinenghi LD and Leisner JJ (2022) Scientists' Assessments of Research on Lactic Acid Bacterial Bacteriocins 1990–2010. Front. Microbiol. 13:908336. doi: 10.3389/fmicb.2022.908336

INTRODUCTION

The antimicrobial activity of lactic acid bacterial (LAB) bacteriocins—especially class I (containing lanthionine and β-methyllanthionine) and class II (small, heat-stable) peptides (1990s classifications applied)—has constituted a very active research field within the last 35 years. Their application as food biopreservatives has been an important objective; as a partially purified compound (nisin), a component in fermentates (pediocin PA-1) or by *in situ* production by an added culture (Holzapfel et al., 1995; Stiles, 1996; Ennahar et al., 2000; Cleveland et al., 2001; Twomey et al., 2002; Cotter et al., 2005; Drider et al., 2006; O'Connor et al., 2020). Bacteriocins have

also been examined for applications in veterinary microbiology and human clinical microbiology (Twomey et al., 2002; Servin, 2004; Drider et al., 2006; Hassan et al., 2012; Cotter et al., 2013; Yang et al., 2014; Alvarez-Sieiro et al., 2016; Chikindas et al., 2018; O'Connor et al., 2020; Soltani et al., 2021).

Investigations of bacteriocin structures and biosynthesis, mode of action, secretion, and genetic regulation, e.g., by quorum sensing, have constituted important parts of this field (Nes et al., 1996; Kleerebezem et al., 1997; Kuipers et al., 1998; Sahl and Bierbaum, 1998; Ennahar et al., 2000; Cintas et al., 2001; Kleerebezem and Quadri, 2001; Eijsink et al., 2002; Garneau et al., 2002; Héchard and Sahl, 2002; Fimland et al., 2005; Nissen-Meyer et al., 2009). On the other hand, the ecological functions of LAB bacteriocins have only attracted relatively limited attention, although their role appears to differ from colicins that constitute an established model for our understanding of the ecology of bacterial antimicrobial peptides (Dykes and Hastings, 1997; Eijsink et al., 2002; Leisner and Haaber, 2012; Snyder and Worobo, 2013).

Historically, research on LAB bacteriocins began with empirical screenings of antimicrobial activity by producer cultures, typically originating from foods, starting in earnest in the late 1980s and the early 1990s. This research typically focused on GRAS species among the bacteriocinogenic LAB but also on other potential bacteriocin producers within the Firmicutes and other phyla (Héchard and Sahl, 2002; Arnison et al., 2013; Acedo et al., 2018). During the 1990s and 2000s, it became apparent that resistance by target organisms was a common phenomenon (Montville et al., 1995; Gravesen et al., 2002; Cotter et al., 2005, 2013; Drider et al., 2006; Naghmouchi et al., 2007). This situation, combined with the fact that the antimicrobial spectra of many bacteriocins are relatively narrow, promoted research into synergy effects by combining them, also with other antimicrobial compounds or even phages (Lüders et al., 2003; Mathur et al., 2017; Rendueles et al., 2022). Research has also been devoted to synthetic or bioengineered bacteriocins (Ennahar et al., 2000; Ongey and Neubauer, 2016; Soltani et al., 2021).

Here, we present the accounts of scientists involved in research on bacteriocins from 1990 to 2010 in the form of their responses to a questionnaire probing their choices of producer and target organisms, types of bacteriocins, studies of the mode of action and underlying genetics, intended applications, and their opinion then and now on whether research objectives were met, both in relation to their own studies and to the field as such. This study serves as an informal supplement to a large number of reviews and opinions that have been published on LAB bacteriocins over the last 30 years.

MATERIALS AND METHODS

Bibliometric Analyses

A topic search was done using Web of Science (WoS) with the key terms "Lactic acid bacteria AND bacteriocin(s)" for 1990–2010. The search returned 1,504 hits with information on numbers of articles, reviews, letters, and proceedings papers and information on WoS categories, authors, and institutions. The search also resulted in a full record for all 1,504 publications as well as citations for the individual publications. Citation windows (10 years) were manually extracted and number of patents were extracted from Scopus (Elsevier).

Questionnaire

Respondents were contacted by e-mails containing individual links to the online questionnaire hosted by Userneeds (Copenhagen, Denmark), which supplies web-based questionnaire surveys. Individual answers were kept anonymously according to existing GDPR rules.

Potential participants were selected by a combination of personal knowledge of the field at the time by one of us (JJL) and by identifying individual research groups from the bibliometric search using the terms "lactic acid bacteria" AND "bacteriocin(s)" for publications from 1990 to 2010. Respondents were then found among the 20 institutions with the most publications, including researchers with high or low amounts of publications on the topic. In addition, a number of respondents was selected from additional institutions. In general, the selection contained a range of researchers with variations in research outputs for bacteriocins. Among the 30 researchers with the highest output from 1990 to 2010, 22 were contacted and 12 completed the questionnaire. Overall, 94 researchers were contacted, with 54 responding and 48 completing the questionnaire.

The questionnaire (**Supplementary Datasheet 1**) was organized into four sections: profiles (eight questions), details on respondents', research on bacteriocins (22 questions), respondents' memories of their opinions during the 1990s and 2000s on the research (11 questions), and current opinions of respondents on whether research objectives were reached at the time (seven questions), in total 48 questions (question 9 was divided into two; see **Supplementary Datasheet 1** for questionnaire text). In the first two sections, most questions were open, but in a few cases, we used a five-point scale for answers. In the last two sections, we employed a seven-point scale for answers including the following terms: completely agree, strongly agree, agree, neither agree/disagree, somewhat disagree, strongly disagree, and completely disagree. Re-analysis of results pooling the responses into three categories—agree, neither agree nor disagree, and disagree—gave similar results. It was possible to add comments to nearly all questions. A total of 29 out of 48 respondents used this possibility, with 10 respondents (all associated with different institutions) adding at least four comments each. Comments are listed in **Supplementary Datasheet 2**.

RESULTS

Profile of Respondents and Details on Their Research on Bacteriocins

The respondents represented a broad spectrum of researchers in the field from 1990 to 2010, as reflected by their information on age, years of research in the field, and job positions, ranging from Master students to PI's [Question (Q) 1–8]; **Supplementary Table 1**. The number of active researchers among the respondents

was higher in the 1990s (40) than in the 2000s (34). The numbers of PhD. students and post-docs were highest in the 1990s (17 and 10 compared to 3 and 6, respectively in the 2000s), whereas the numbers of PI's, Professors, and Associate Professors were higher in the 2000s (results not shown). The data gave the impression of a cohort and input from respondents at Ph.D. and post-doc levels in the latter decade were therefore underrepresented.

Among the respondents, 19 (26.8%) were among 71 researchers with at least 10 publications in the 1990s and 2000s found using the search term "Lactic acid bacteria AND bacteriocin(s)." Two respondents were among the top five regarding publication output. An additional 15 respondents had between five and nine publications, whereas the remaining 14 had below five publications. Individual searches revealed higher numbers of publications on bacteriocins for some respondents as the search term applied would not cover all research aspects.

Respondents were associated with laboratories in 19 countries, including Brazil, Canada, Japan, Malaysia, New Zealand, South Africa, the United States, and 12 European countries (Q8; **Supplementary Table 2**). Countries with the most respondents included Canada, France, Ireland, Netherlands, Norway, and the United States.

The researchers had worked with a wide range of LAB bacteriocin producers, including especially the genera *Carnobacterium*, *Enterococcus*, and *Lactobacillus* (including some of the new genera created after a recent taxonomic revision; Zheng et al., 2020), *Lactococcus* and *Pediococcus* (Q16; **Supplementary Table 3**). In addition, a number of bacteriocin producers other than LAB had also been examined by some researchers, especially species belonging to *Bacillus* or *Staphylococcus* (Q17; **Supplementary Table 4**). The number of respondents who had worked on probiotics amounted to 18 out of 48 (37.5%; Q21).

A number of different non-pathogenic LAB target strains were included in research on antimicrobial spectra (Q9a; **Supplementary Table 5**). Among the Gram-positive foodborne pathogens, especially *Listeria monocytogenes* followed by *Staphylococcus aureus*, *Enterococcus* spp., *Bacillus* spp., and *Clostridium* spp. were used as targets (Q9b; **Supplementary Table 6**). Gram-negative foodborne pathogens were also included by many respondents as target strains, but it is safe to assume, that they under most conditions, were not sensitive toward the majority of bacteriocins (Q10; **Supplementary Table 6**). A selection of Gram-positive foodborne spoilage organisms were examined by some respondents (Q11; **Supplementary Table 6**). The majority of applied research on bacteriocins was devoted to biopreservation of foods, especially (in the following order) meat, milk/dairy, and seafood (Q18; **Supplementary Table 7**).

Regarding Gram-positive and Gram-negative human clinical species as target strains, some were also listed under foodborne pathogens by a number of respondents [e.g., *Escherichia coli*, *Salmonella, S. aureus*, and *Streptococcus pyogenes* (but see Falkenhorst et al., 2008); Q12, 13]. A minority of respondents mentioned some additional pathogens: *Cutibacterium acnes*, *Clostridium* (now Clostridiodes) *difficile*, *Streptococcus agalactiae*, *Streptococcus mutans*, *Streptococcus pneumoniae*, *Streptococcus pyogenes* (all Gram-positive; 10 respondents), *Acinetobacter baumannii*, *Helicobacter pylori*, *Klebsiella pneumoniae*, *Legionella pneumophila*, *Pseudomonas aeruginosa* (five respondents), and antibiotic-resistant variants of pathogenic bacteria (MRSA: Methicillin Resistant *Staphylococcus aureus*; ESKAPE: *Enterococcus faecium*, *Staphylococcus aureus*, *Klebsiella pneumoniae*, *Acinetobacter baumannii*, *Pseudomonas aeruginosa*, and *Enterobacter* spp.; VRE: Vancomycin Resistant Enterococci; four respondents; Q12, 13). A minority of respondents also worked with target strains from species important in veterinary microbiology, including *Enterococcus faecium*, *Enterococcus faecalis*, *Lactococcus garvieae* (fish pathogen), *Listeria ivanovii*, *Listeria monocytogenes*, *Staphylococcus aureus* (mastitis research), *Streptococcus* spp. (mastitis research) including *Streptococcus uberis*, *Streptococcus dysgalactiae* (all Gram-positive; 14 respondents), and *Aeromonas* spp. including *Aeromonas salmonicida* (fish pathogen), *Tenacibaculum* spp. (fish pathogen), *Vibrio* spp., and *Yersinia* spp. (all Gram-negative; 11 respondents) in addition to *Mycobacterium avium* subsp. *paratuberculosis* (one respondent; Q14, 15).

The respondents obtained bacteriocin producers and target strains from many sources, but external (public) and internal collections constituted a higher proportion of sources for target strains (Q22–24; **Figure 1**). It might be speculated that the variety among target strains from culture collections was relatively low but further research is needed to clarify this issue.

Empirical screenings, mode of action, and genetic characterization of expression all constituted relatively high degrees of research activities among the respondents (Q25, 26, and 28; **Figure 2**). Further, for both studies of mode of action and genetic characterization, obtaining basic knowledge was the most important objective, followed by examining applicability, whereas the issue of obtaining patents was not perceived as important (Q27 and 29; **Figure 3**).

The research focused on class I and class II bacteriocins, mostly as purified or partially purified compounds, whereas class III bacteriocins (all classes as defined in the 1990s) attracted less attention (Q19 and 20; **Figure 4**). Overall, the respondents had worked with a broad range of both LAB and non-LAB bacteriocins (comments 1–17 and 18–35, respectively).

Details on Opinion on the Field of Research and Research Objectives

The respondents were asked about their opinion on the number of research groups with LAB bacteriocins as one of the primary topics in the 1990s and the 2000s. These were difficult questions to answer and only a few respondents suggested numbers that varied widely; average values were around 60 and 55 research groups for the 1990s and 2000s, respectively (Q30, 31; comments 65–73). The bibliometric data showed that relatively few institutions and researchers had significant higher publication outputs for "Lactic acid bacteria AND bacteriocin(s)" with Norwegian University of Life Sciences (four of the top 20 researchers with highest publication outputs within the topic), Stellenbosch University (two researchers), National Research Institute for Agriculture, Food and Environment (INRAE), Vrije Universiteit Brussel (two researchers), and University of Alberta (two researchers) in the top five.

Questions Q32–40 were concerning respondents' memories of opinions about the different aspects of the bacteriocin research

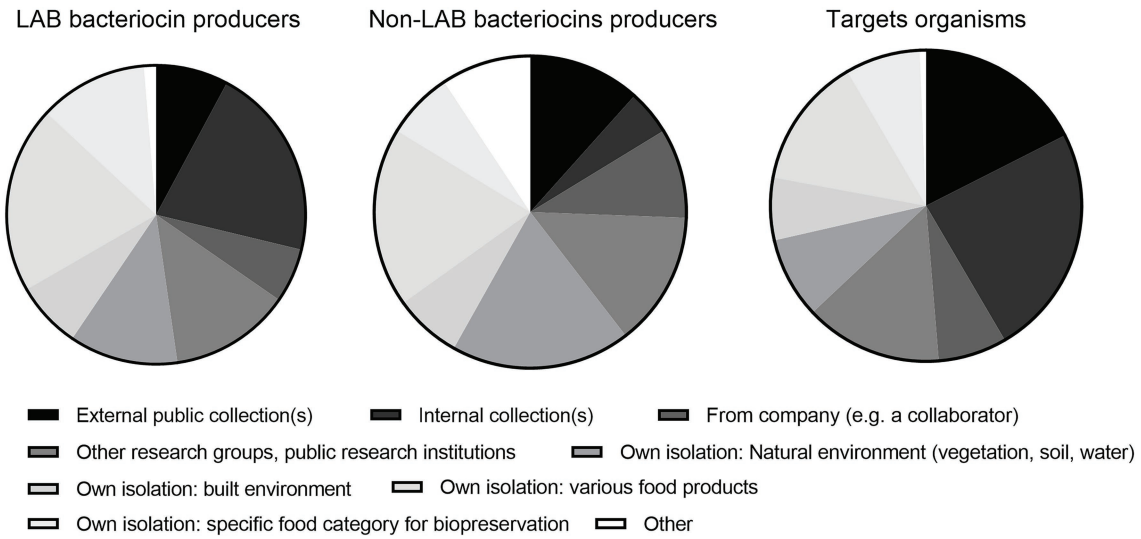

FIGURE 1 | Sources of strains of lactic acid bacterial (LAB) bacteriocin producers (47 respondents), non-LAB producers (26 respondents), and target strains (48 respondents; Q22–24).

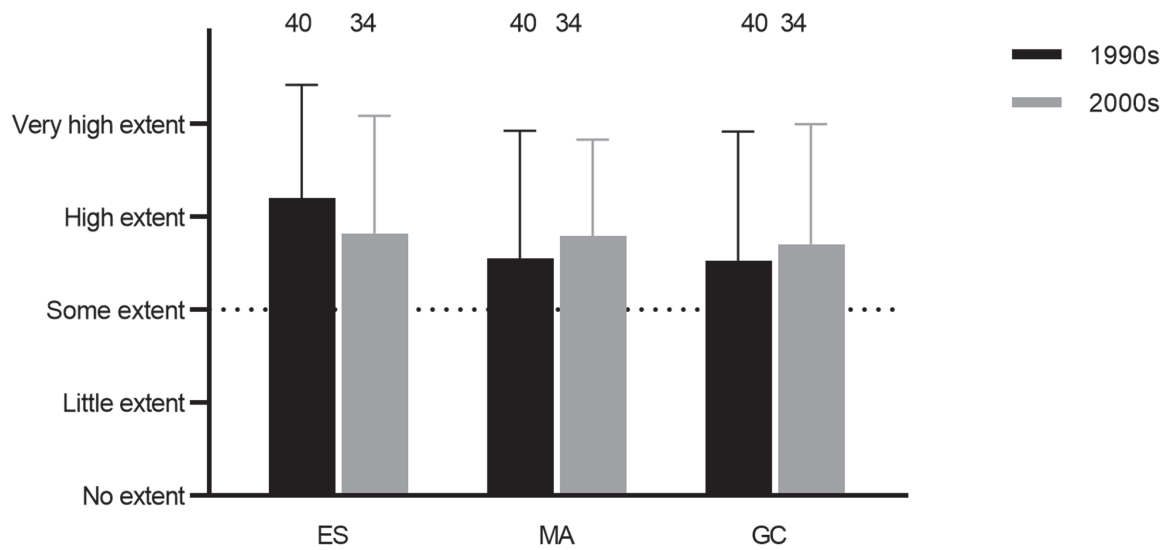

FIGURE 2 | Average degrees of research activities in the 1990s and 2000s involving empirical screenings (ES), studies of mode of action (MA), and genetic characterization (GC; Q25, 26, and 28).

field back in the 1990s and/or the 2000s. On average, the researchers agreed or strongly agreed that the chances of finding new bacteriocins were high, especially in the 1990s (Q32; **Figure 5**; but see the variations in answers provided by comments 46–48, 50–51, 152, 154, and 159). The chances of finding new bacteriocins with potential practical applications for biopreservation of foods were perceived positively (Q33; **Figure 5**), although some comments did not support this (86–87). Further, the researchers did not agree to the same extent that the chances were high of finding bacteriocins for practical applications for the treatment of infections by human clinical pathogens or veterinary pathogens in the 1990s (Q34 and 35; **Figure 5**; comments 111–115 and 122–124). A similar pattern was observed for the evaluation of whether the chances were high for finding new practical applicable antimicrobial peptides from other organisms than lactic acid bacteria, including eukaryotic organisms (animals, plants, and/or fungi) for treatment of infections by human clinical pathogens (Q36; **Figure 5**). It should be noted that the degree of variation in responses was higher for Q34–36 than for Q32 and Q33. One factor that weighs in regarding the evaluation of chances for application of bacteriocins was the issue of target resistance, which the researchers to some extent agreed was a cause for concern (Q37; **Figure 5**; comments 62–64).

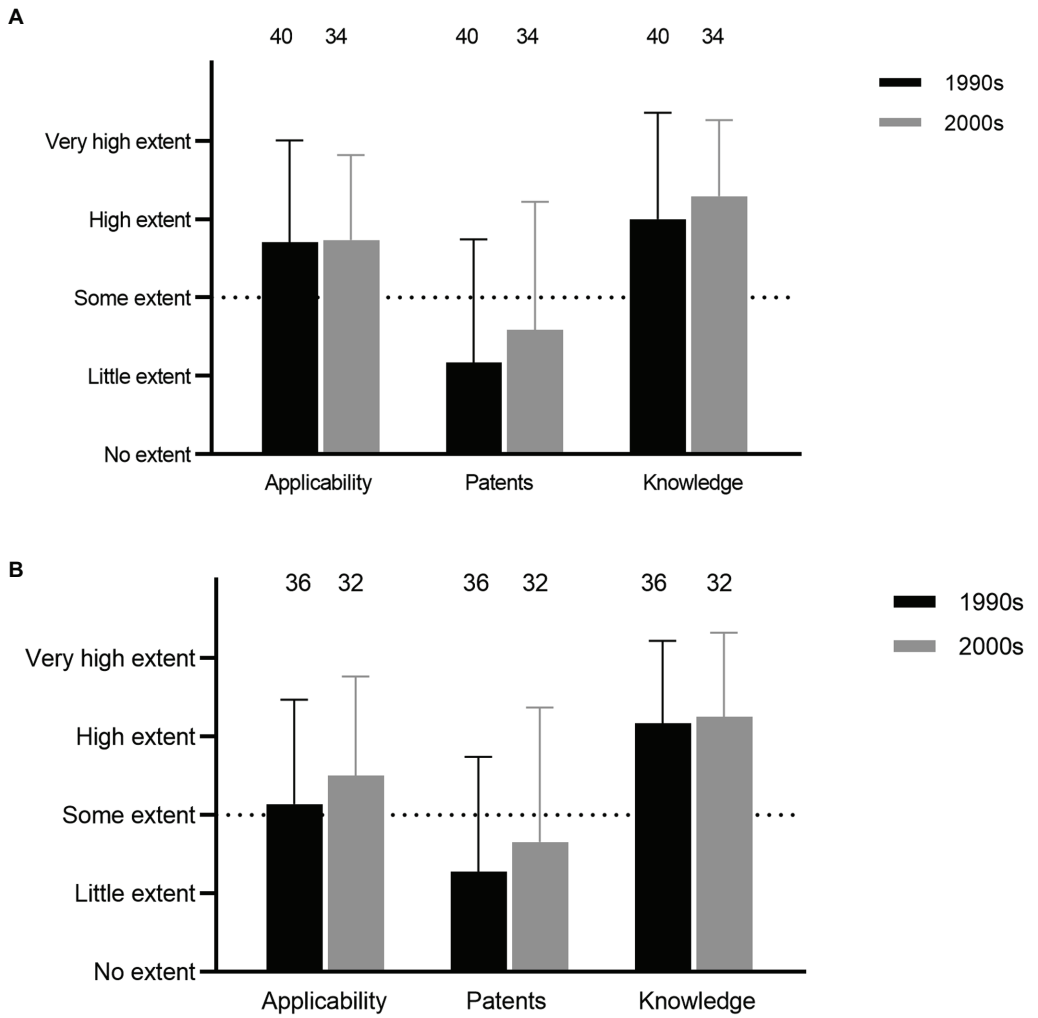

FIGURE 3 | Objectives for research on mode of action **(A)** and genetic characterization (**B**; Q27 and 29).

Regarding inspiration, the researchers neither agreed nor disagreed that previous research on antibiotics and colicins provided such a source (Q38, 39, **Figure 5**, comment 74–76). The same outcome was noted regarding inspiration from contemporary screening studies in the related field of new animal, plant, and/or fungal antimicrobial peptides (Q40, **Figure 5**).

Questions Q41–46 were concerning current opinions by respondents on whether bacteriocin research reached the objectives in the 1990s and/or the 2000s. The researchers, on average, agreed that bacteriocin research met the personal objectives set by the individual researcher from 1990 to 2010, including that the field presented an important training ground for researchers early on in their careers (Q41; **Figure 6**; comments 77–81). This positive outcome was even more pronounced regarding opinions on whether the overall field of research on lactic acid bacterial bacteriocins met the objectives in terms of contributing to basic knowledge on bacteria antagonism (Q42; **Figure 6**; comment 82 but see comments 83–84).

However, there was, on average, some skepticism about whether the bacteriocin research had met the objectives from 1990 to 2010 in the applied aspects (Q43–46; **Figure 6**). The best outcome was perceived for food biopreservation (**Figure 6**, comments 88–97). Views on probiotic applications were relatively similar to what were perceived for biopreservation, whereas applications for veterinary microbiology and human clinical microbiology were viewed somewhat less favorable (**Figure 6**; see comments 98–110 for probiotics; 116–119 for human clinical microbiology and 125 for veterinary microbiology).

An additional question (Q47) inquired whether the bacteriocin research field has benefitted from developments in sequence-based methodology and associated bioinformatics. These developments were generally perceived very positively (comments 126–162), although it was noted that additional research was required to illuminate functional and applied aspects (comments 129, 137, 141–142, 149, 151, 152, 154, 156, and 159).

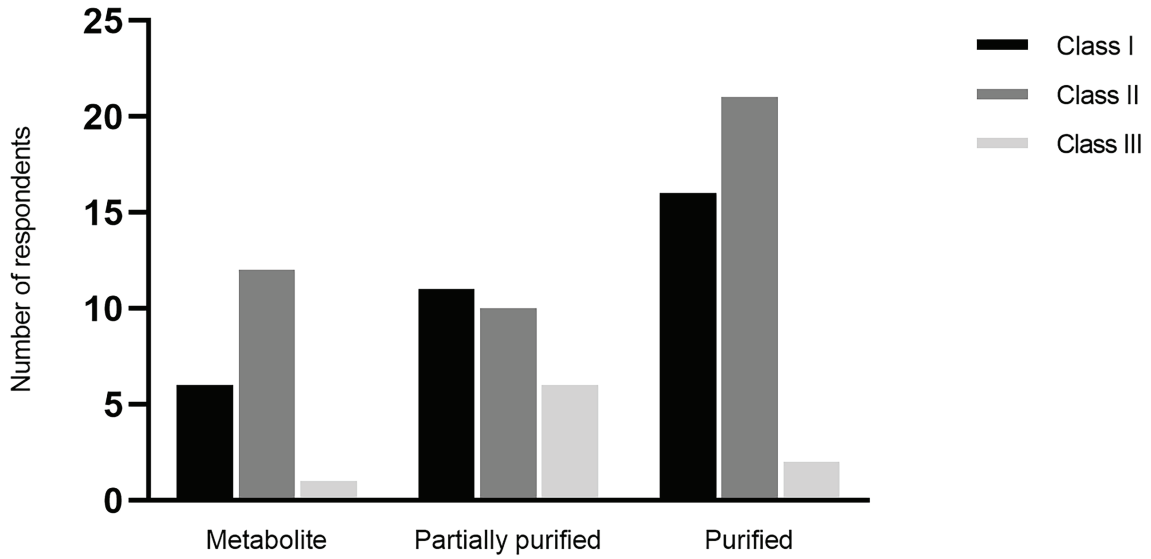

FIGURE 4 | Class and level of purification of bacteriocins included in respondents' research (Q19).

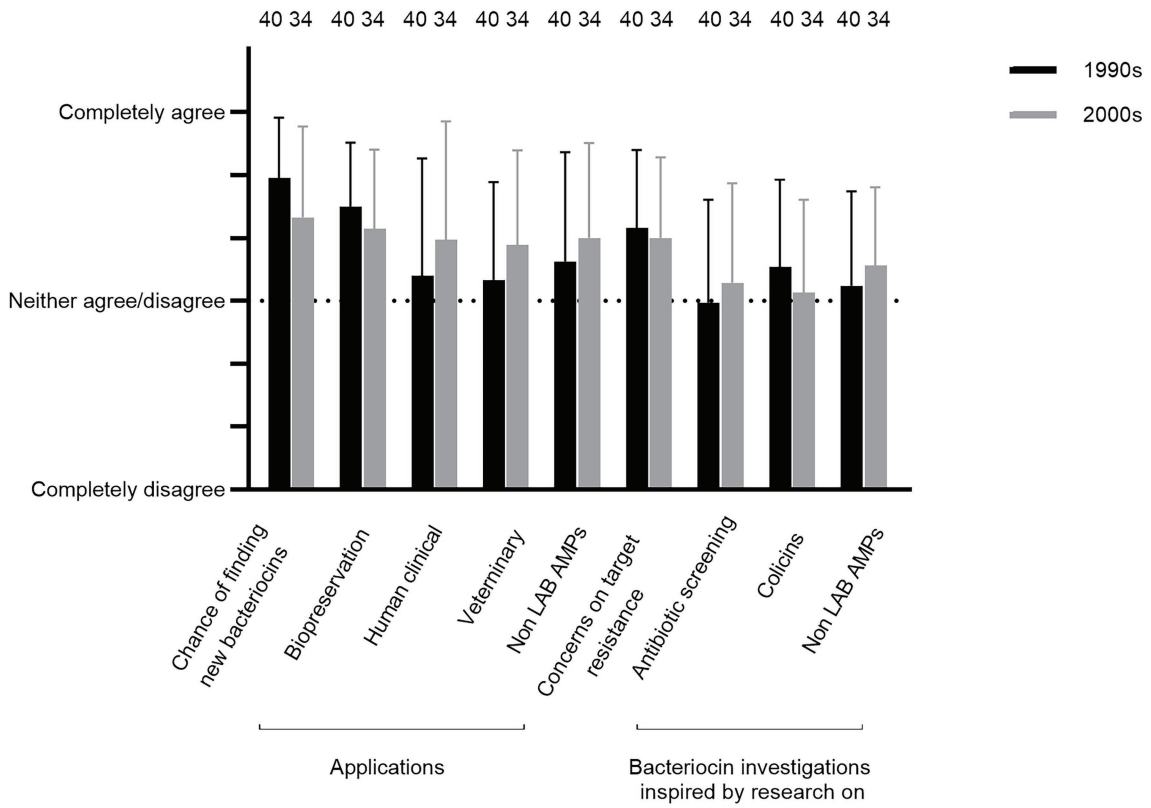

FIGURE 5 | Respondents' memories of their opinions in the 1990s and/or the 2000s about whether the chances were high regarding finding new bacteriocins including compounds useful for various applications and whether they were inspired by related research fields (Q32–40).

At the end of the questionnaire, the respondents were encouraged to add any additional comment/memory/insight in relation to their bacteriocin research. Those comments were allocated to the specific questions they addressed.

DISCUSSION

Examples of lactic acid bacterial bacteriocins have been known since the 1960s (nisin since the late 1920s/early 1930s), but

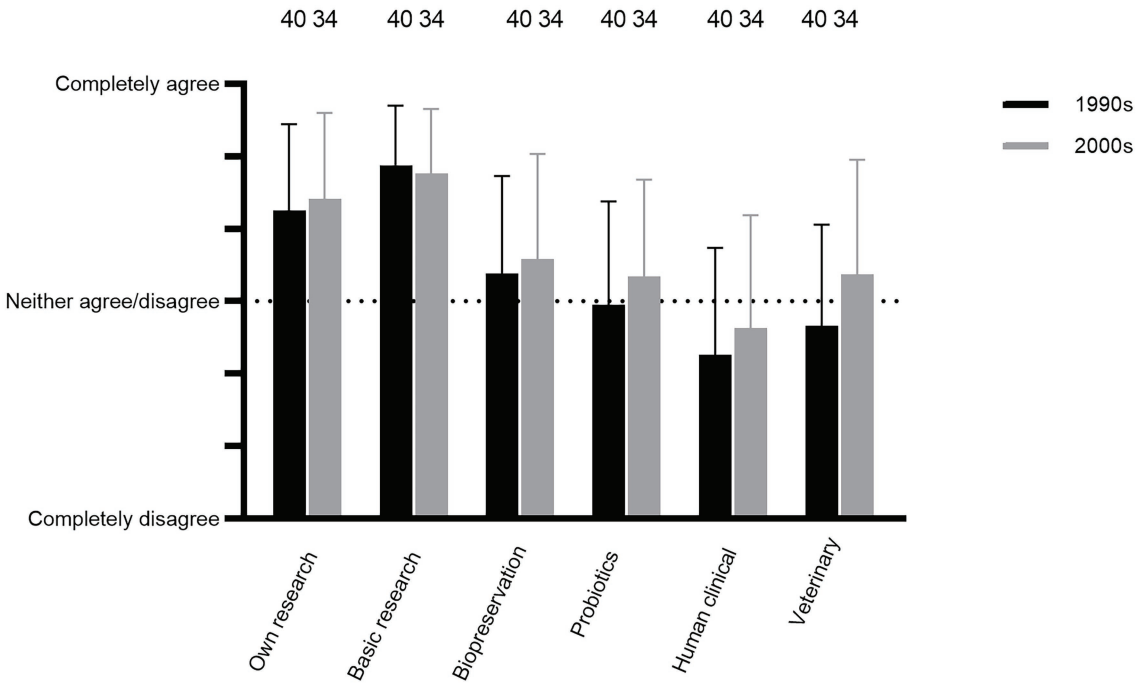

FIGURE 6 | Respondents' current opinions about whether LAB bacteriocin research in the 1990s and 2000s fulfilled the objectives (Q41–46).

they first became an active area of research from the late 1980s and onwards (**Figure 7**; De Klerk and Coetzee, 1961; Brock et al., 1963; Delves-Broughton et al., 1996), the period of time covered by this questionnaire study. Some respondents indicated an increase in research groups in the 1990s but stagnation or even a decrease in the 2000s (Comments 65–73). The total research output increased during both decades, but the number of citations leveled during the latter part of the 2000s (**Figure 7**). Interestingly, the number of patents shows another trend with relatively few granted in the 1990s followed by a sharp increase in the first half of the 2000s, although this issue was not an important motivator for research (**Figures 3**, **7**). The increase in patents over time agrees with the findings by López-Cuellar et al. (2016), although their overall number of patents were substantially lower.

Two classes of bacteriocins, class I—lantibiotics, containing lanthionine and β-methyllanthionine residues and sometimes other unusual residues due to post-translational modifications and class II—small, heat-stable peptides, were the focuses for research. In contrast, larger antimicrobial class III proteins received less attention. It should be noted that the classification of bacteriocins has been a focus for revision with subsequent more elaborate classification systems and transfer between classes as a result. Thus, cyclic peptides were characterized as class II bacteriocins before 2010 but are now considered as posttranslational modified bacteriocins (Franz et al., 2007; Zouhir et al., 2010; Martin-Visscher et al., 2011; Rea et al., 2011; Cotter et al., 2013; Snyder and Worobo, 2013; Gabrielsen et al., 2014; Alvarez-Sieiro et al., 2016; Acedo et al., 2018; Chikindas et al., 2018).

The respondents were generally not inspired by earlier screening efforts for colicins or natural product antibiotics during the 1940s and 1950s (**Figure 5**, comments 74–76). However, that earlier epoch gave some potential important lessons regarding obstacles in antibiotic screening programs worth re-considering in the context of bacteriocins, including the risk of rediscovery, resistance among target organisms and potential toxicity (Peláez, 2006; Silver, 2011; Lewis, 2013; Genilloud, 2014; Wright, 2014; Katz and Baltz, 2016; Aminov, 2017; Abouelhassan et al., 2019; Leisner, 2020). Further, there is some similarity with some antibiotics in routes of activities (comment 54).

The underlying motivation for detailed investigation of antibacterial systems may frequently be found in a desire to explore fundamental aspects as much or even more than examining their potential application. The mode of action of colicins constitutes an early example of this issue as they provided an insight into the functionality of membranes and membrane proteins as described by Luria (1984), one of the pioneers in that field. Overall, the responses in this study agree with the importance of basic science as a major motivator for bacteriocin research (**Figures 5, 6**).

Fundamental aspects of the research involved initial screenings for bacteriocinogenic cultures and subsequent investigations of promising bacteriocinogenic systems, including their antimicrobial spectra, structure and biosynthesis, mode of action, regulation of expression and secretion (Nes et al., 1996; Ennahar et al., 2000; Cintas et al., 2001; Eijsink et al., 2002; Garneau et al., 2002; Héchard and Sahl, 2002; Fimland et al., 2005; Nissen-Meyer et al., 2009; Snyder and Worobo, 2013; Ongey and Neubauer, 2016). In addition, genetic characterization of expressions of bacteriocins also gave insights in relation to the field of bacterial quorum sensing (Kleerebezem et al., 1997;

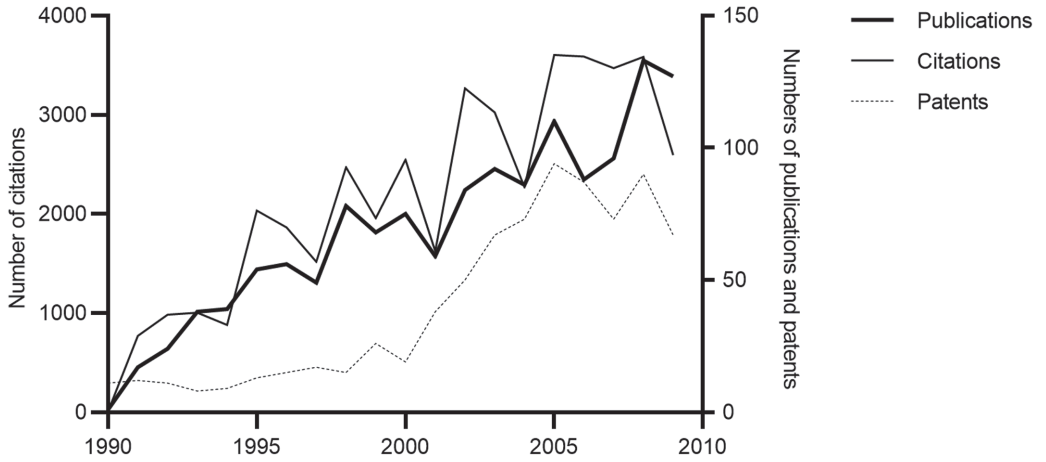

FIGURE 7 | Bibliometric data on number of publications, citations, and patents 1990–2009.

Kuipers et al., 1998; Kleerebezem and Quadri, 2001). Overall, these fundamental studies were evaluated as having obtained a relatively high degree of success in the 1990s and 2000s (**Figures 5, 6**). However, some respondents expressed doubts regarding how much natural variation exists among bacteriocins and whether that had a negative impact on the discovery of novel compounds already in the 2000s (comments 48, 50, 51, 152, 154, and 159).

One fundamental area that, to some extent, was overlooked concerns the ecology of class I and II bacteriocins, as they do not readily fit into the ecological functionality described for colicins (Dykes and Hastings, 1997; Eijsink et al., 2002; Kirkup and Riley, 2004; Leisner and Haaber, 2012; Snyder and Worobo, 2013; comment 83). Their utilization as signals have been proposed, a function that mirrors previous suggestions for antibiotics (Linares et al., 2006; Snyder and Worobo, 2013; Chikindas et al., 2018). Among other possibilities can be mentioned that bacteriocins may mediate a supply of nutrients from lysed target cells (Leisner and Haaber, 2012) or facilitate the transfer of DNA *via* transformation (Snyder and Worobo, 2013). Further research would be relevant for the broader area of microbial interactions and may support application of bacteriocins in food systems (Gálvez et al., 2007; Ramia et al., 2020).

Class I and II bacteriocins were perceived early on to have potential for application as "natural" food preservatives, either by addition of bacteriocinogenic cultures or bacteriocins, e.g., in the form of encapsulation (Holzapfel et al., 1995; Stiles, 1996; Cleveland et al., 2001; Cotter et al., 2005; Drider et al., 2006; Boualem et al., 2013; Chikindas et al., 2018; O'Connor et al., 2020). In addition, bacteriocinogenic cultures were potentially useful in food technological applications such as for acceleration of cheese ripening (Oumer et al., 2001). Cooked or fermented meat products, dairy products, and (lightly preserved) fish products constituted the main food categories among the respondents for potential application of biopreservation (**Supplementary Table 7**). Foods served as the obvious choice for isolating potential bacteriocinogenic cultures for this purpose (Hastings and Stiles, 1991; Lewus et al., 1991; Garver and Muriana, 1993; Ruiz-Barba et al., 1994; Jones et al., 2008). Biopreservation was evaluated by respondents as having obtained a moderate degree of success in the 1990s and 2000s, although narrow target spectra, resistance, sensitivity to proteases, low level of production and legislation all presented challenges, as detailed below (**Figures 6, 7**; comments 86–94, 96–97, and 153).

In addition, bacteriocins were of interest as enhancers of probiotic actions, including fish probiotics in aquaculture (Ringø and Gatesoupe, 1998; Desriac et al., 2010; O'Connor et al., 2020). Further, they were considered as potential antimicrobial compounds in relation to veterinary and human clinical bacteriology—especially targeting antibiotic-resistant pathogens—but also in virology in addition to serving as potential anti-cancer agents (Wachsman et al., 2003; Servin, 2004; Drider et al., 2006; Montalbán-López et al., 2011; Hassan et al., 2012; Yang et al., 2014; Alvarez-Sieiro et al., 2016; Chikindas et al., 2018; Soltani et al., 2021). The bacteriocinogenic cultures were sometimes isolated from the same source for which they were intended for (veterinary) application (comment 38). The degree of success of these applications in the 1990s and 2000s was a subject of critical evaluation by some of the respondents in this study due to, e.g., the issue of toxicity in relation to systemic applications (**Figures 5, 6**; comments 16, 98–119, and 122–125). Biomedical applications against biofilms present another possible application (Bower et al., 2001; Mathur et al., 2017). This topic was not mentioned in the questionnaire and it was not commented upon by respondents. Further, bacteriocins found relatively few applications in a veterinary context except for topical applications such as mastitis (Ross et al., 1999; comments 122–125). Finally, a few comments mention the application of bacteriocins as feed additives, which are of interest in the light of controversies concerning the use of antibiotics for this purpose (Kirchhelle, 2018; Silveira et al., 2021; comments 120–121).

The relatively narrow antimicrobial spectra for many bacteriocins might be desirable in a human therapeutic context

to minimize damage to the commensal human microbiota (Cotter et al., 2013). However, this would not be the case for many biopreservative applications. Combinations of bacteriocins with food-grade antimicrobials/stressors is a potential solution in that context (Gálvez et al., 2007; Mathur et al., 2017). Bacteriocins typically only inhibit related taxons (Eijsink et al., 1998, comment 84) and then frequently only some strains within a given species (Rasch and Knøchel, 1998; Carl et al., 2004), an issue that requires careful selection of a wider panoply of target strains in screening scenarios. The respondents informed on a higher usage of external and internal culture collections as a source for target strains compared with producer strains. With a bit of caution, this might be interpreted as perhaps involving a relatively narrow common range of target strains, making it more difficult to accurately estimate the frequency of resistance within a given target species (**Figure 1**).

In addition, as revealed by a few comments by the questionnaire respondents, resistance development among target organisms represented a challenge that was addressed by some research groups in the 1990s and onwards (Gravesen et al., 2002; Cotter et al., 2005; Naghmouchi et al., 2007, comments 62–64). Resistance had, however, a potential positive element in an explorative context, somewhat similar to dereplication screening efforts in searches for antibiotics (Leisner, 2020). Thus, target resistance to known bacteriocins was employed as a selection method to find new bacteriocins (comment 61).

Overall, a limited number of bacteriocins were introduced for applications from 1990 to 2010. Partially purified nisin and pediocin PA-1 (in the form of an added fermentate) were two commonly applied bacteriocins for food biopreservation at the time. They were, however, both discovered, and in the case of nisin, applied before the 1990s (Frazer et al., 1962; Bhunia et al., 1988; Delves-Broughton et al., 1996; Stiles, 1996; Rodríguez et al., 2002; Cotter et al., 2005; O'Connor et al., 2020). Thus, some of the few low-hanging fruits were found early on, and it was difficult to find new compounds with enhanced desired properties relative to the initial compounds (comments 48, 51, 152, 154, and 159). In this context, the phenomenon of rediscoveries of well-known bacteriocins represented an additional challenge (comment 46). This situation was not too different from the outcome of screening of natural product antibiotics in the 1940s and 1950s (Greenwood, 2008; Silver, 2011; Lewis, 2013; Wright, 2014; Leisner, 2020).

One additional important obstacle to the application of bacteriocins, both in relation to food biopreservation as well as in relation to medical and veterinary applications, is presented in the form of legislative demands such as bacteriocins should be safe to consume, and bacteriocinogenic cultures should also not contain genes encoding virulence factors or antibiotic resistance (Montville et al., 1995; Stiles, 1996; O'Connor et al., 2020). This made the use of enterococci for biopreservation a topic for discussion already in the 1990s (Jett et al., 1994; Franz et al., 1999; for a more positive account, see also Moreno et al., 2006). Finally, although the antimicrobial activity of bacteriocinogenic cultures might be improved by, e.g., combining the genetic systems for different bacteriocins in one organism or construction of strains that can produce the compounds in a heterologous manner (Hanlin et al., 1993; Ennahar et al., 2000; O'Sullivan et al., 2003), genetically modified LAB is still a controversial issue that meets regulatory demands (Plavec and Berlec, 2020).

Another obstacle at the time was represented by the difficulties in obtaining funding for searching for new bacteriocins (comments 85, 93–94, and 138). This might partially have been due to the lack of enthusiasm by some of the players in the food industry (comment 96, 97).

Overall, the objectives for research into bacteriocin applications in the 1990s and 2000s were only met to a partial degree, even within the area of food biopreservation, which constituted the single most important objective. The research did, however, provide important fundamental insights useful for the next ongoing phase that in addition to food biopreservation or probiotics focuses on potential medical applications of a wider range of antimicrobial peptides. These include, among others, post-translationally modified LAB and non-LAB peptides (RiPPs, among them class I bacteriocins), e.g., in combination with other antimicrobials (Arnison et al., 2013, Cotter et al., 2013; Yang et al., 2014; Alvarez-Sieiro et al., 2016; Mathur et al., 2017; Perez et al., 2018; O'Connor et al., 2020; Chen et al., 2021; Soltani et al., 2021). The introduction of genomics, including bioinformatics software already during the 2000s, such as BAGEL and antiSMASH (comments 146 and 149) has been important (de Jong et al., 2006, 2010; Medema et al., 2011; Nes, 2011; van Heel et al., 2013; several of the comments 126–162). This approach serves as a mean for dereplication in screenings (comment 149). There were, however, some notes of caution among respondents, as functional and applied aspects are not always easy to decipher from obtained sequences (Eijsink et al., 2002; comments 129, 137, 141–142, 151, 152, 154, 156, and 159) and could be supplemented with other approaches such as mass-spectrometry to characterize modification patterns of RiPPs (comment 149).

An important aspect not covered in the questionnaire concerns the chemical approach by targeted engineering of new peptides. This is an area that has attracted research from the 1990s and up to now but has been met with some challenges (Fimland et al., 1996, Ongey and Neubauer, 2016; comments 138, 149, 150, and 152). However, this scenario, if implemented, to some degree resembles the shift in antibiotics R&D during the 1960s from large screenings of natural compounds to the construction of semisynthetic variants (Leisner, 2020).

In conclusion, this questionnaire survey illuminates the formative years of research on class I, II, and III bacteriocins from lactic acid bacteria and other sources. The research was evaluated by respondents to have resulted in valuable progress regarding the basic science of bacteriocins, and there were some success stories within the area of food biopreservation (see e.g., Chikindas et al., 2018). However, issues such as limited target spectrum, target resistance, sensitivity to proteases, poor yield, and economic and regulatory challenges limited the overall success of this approach. Applications also met difficulties in relation to human clinical and veterinary microbiology. The findings in this study highlight how progress in the studies of bacteriocins depended on a number of parameters, some of which are also of interest in the broader field of antimicrobial research.

DATA AVAILABILITY STATEMENT

The raw data supporting the conclusions of this article will be made available by the authors, without undue reservation. Any requests should be directed to the corresponding author.

ETHICS STATEMENT

Ethical review and approval were not required for the study on human participants in accordance with the local legislation and institutional requirements. Written informed consent for participation was not required for this study in accordance with the national legislation and the institutional requirements.

AUTHOR CONTRIBUTIONS

JL designed the study. LM and JL performed the research and wrote the manuscript. All authors contributed to the article and approved the submitted version.

FUNDING

This study was funded by a research grant from the Norwegian Research Council (grant 314490-FORSKER20).

ACKNOWLEDGMENTS

The authors would like to thank all the respondents for their generous time completing the questionnaire, including their additional valuable comments. We thank Liselotte Nielsen, Benjamin Derksen, and Philine Zeinert (all from The Royal Library/Copenhagen University Library, Denmark) for valuable support in retrieving the bibliometric data and Rebecca Futtrup from Userneeds for support in designing the questionnaire.

SUPPLEMENTARY MATERIAL

The Supplementary Material for this article can be found online at: https://www.frontiersin.org/articles/10.3389/fmicb.2022.908336/full#supplementary-material

REFERENCES

Abouelhassan, Y., Garrison, A. T., Yang, H., Chávez-Riveros, A., Burch, G. M., and Huigens, R. W. (2019). Recent progress in natural-product-inspired programs aimed to address antibiotic resistance and tolerance. *J. Med. Chem.* 62, 7618–7642. doi: 10.1021/acs.jmedchem.9b00370

Acedo, J. Z., Chiorean, S., Vederas, J. C., and van Belkum, M. (2018). The expanding structural variety among bacteriocins from gram-positive bacteria. *FEMS Microbiol. Rev.* 42, 805–828. doi: 10.1093/femsre/fuy033

Alvarez-Sieiro, P., Montalbán-López, M., Mu, D., and Kuipers, O. P. (2016). Bacteriocins of lactic acid bacteria: extending the family. *Appl. Microbiol. Biotechnol.* 100, 2939–2951. doi: 10.1007/s00253-016-7343-9

Aminov, R. (2017). History of antimicrobial drug discovery: major classes and health impact. *Biochem. Pharmacol.* 133, 4–19. doi: 10.1016/j.bcp.2016.10.001

Arnison, P. G., Bibb, M. J., Bierbaum, G., Bowers, A. A., Bugni, T. S., Bulaj, G., et al. (2013). Ribosomally synthesized and post-translationally modified peptide natural products: overview and recommendations for a universal nomenclature. *Nat. Prod. Rep.* 30, 108–160. doi: 10.1039/C2NP20085F

Bhunia, A. K., Johnson, M. C., and Ray, B. (1988). Purification, characterization and antimicrobial spectrum of a bacteriocin produced by *Pediococcus acidilactici*. *J. Appl. Bacteriol.* 65, 261–268. doi: 10.1111/j.1365-2672.1988.tb01893.x

Boualem, K., Subirade, M., Desjardins, Y., and Saucier, L. (2013). Development of an encapsulation system for the protection and controlled release of antimicrobial nisin at meat cooking temperature. *J. Food Res.* 2, 36–45. doi: 10.5539/jfr.v2n3p36

Bower, C. K., Bothwell, M. K., and McGuire, J. (2001). Lantibiotics as surface active agents for biomedical applications. *Colloids Surf. B: Biointerfaces* 22, 259–265. doi: 10.1016/S0927-7765(01)00199-0

Brock, T. D., Peacher, B., and Pierson, D. (1963). Survey of the bacteriocines of enterococci. *J. Bacteriol.* 86, 702–707. doi: 10.1128/jb.86.4.702-707.1963

Carl, G. D., Leisner, J. J., Swings, J., and Vancanneyt, M. (2004). Intra-specific variation of *Lactobacillus plantarum* and *Lactobacillus pentosus* in sensitivity towards various bacteriocins. *Antonie Van Leeuwenhoek* 85, 209–216. doi: 10.1023/B:ANTO.0000020155.79931.d7

Chen, Y., Wang, J., Li, G., Yang, Y., and Ding, W. (2021). Current advancements in sactipeptide natural products. *Front. Chem.* 9:595991. doi: 10.3389/fchem.2021.595991

Chikindas, M. L., Weeks, R., Drider, D., Chistyakov, V. A., and Dicks, L. M. T. (2018). Functions and emerging applications of bacteriocins. *Curr. Opin. Biotechnol.* 49, 23–28. doi: 10.1016/j.copbio.2017.07.011

Cintas, L. M., Casaus, M. P., Herranz, C., Nes, I. F., and Hernández, P. E. (2001). Review: bacteriocins of lactic acid bacteria. *Food Sci. Technol. Int.* 7, 281–305. doi: 10.1106/R8DE-P6HU-CLXP-5RYT

Cleveland, J., Montville, T. J., Nes, I. F., and Chikindas, M. L. (2001). Bacteriocins: safe, natural antimicrobials for food preservation. *Int. J. Food Microbiol.* 71, 1–20. doi: 10.1016/S0168-1605(01)00560-8

Cotter, P. D., Hill, C., and Ross, R. P. (2005). Bacteriocins: developing innate immunity for food. *Nat. Rev. Microbiol.* 3, 777–788. doi: 10.1038/nrmicro1273

Cotter, P. D., Ross, R. P., and Hill, C. (2013). Bacteriocins—a viable alternative to antibiotics? *Nat. Rev. Microbiol.* 11, 95–105. doi: 10.1038/nrmicro2937

de Jong, A., van Heel, A. J., Kok, J., and Kuipers, O. P. (2010). BAGEL2: mining for bacteriocins in genomic data. *Nucleic Acids Res.* 38, W647–W651. doi: 10.1093/nar/gkq365

de Jong, A., van Hijum, S. A. F. T., Bijlsma, J. J. E., Kok, J., and Kuipers, O. P. (2006). BAGEL: a web-based bacteriocin genome mining tool. *Nucleic Acids Res.* 34, W273–W279. doi: 10.1093/nar/gkl237

De Klerk, H. C., and Coetzee, J. N. (1961). Antibiosis among lactobacilli. *Nature* 192, 340–341. doi: 10.1038/192340a0

Delves-Broughton, J., Blackburn, P., Evans, R. J., and Hugenholtz, J. (1996). Applications of the bacteriocin, nisin. *Antonie Van Leeuwenhoek* 69, 193–202. doi: 10.1007/BF00399424

Desriac, F., Defer, D., Bourgougnon, N., Brillet, B., Le Chevalier, P., and Fleury, Y. (2010). Bacteriocins as weapons in the marine animal-associated bacteria warfare: inventory and potential applications as an aquaculture probiotic. *Mar. Drugs* 8, 1153–1177. doi: 10.3390/md8041153

Drider, D., Fimland, G., Héchard, Y., McMullen, L. M., and Prévost, H. (2006). The continuing story of class II bacteriocins. *Microbiol. Mol. Biol. Rev.* 70, 564–582. doi: 10.1128/MMBR.00016-05

Dykes, G. A., and Hastings, J. W. (1997). Selection and fitness in bacteriocin–producing bacteria. *Proc. R. Soc. Lond. B* 264, 683–687. doi: 10.1098/rspb.1997.0097

Eijsink, V. C., Skeie, M., Middelhoven, P. H., Brurberg, M. B., and Nes, I. F. (1998). Comparative studies of class IIa bacteriocins of lactic acid bacteria. *Appl. Environ. Microbiol.* 64, 3275–3281. doi: 10.1128/AEM.64.9.3275-3281.1998

Eijsink, V. G. H., Axelsson, L., Diep, D. B., Håvardstein, L. V., Holo, H., and Nes, I. F. (2002). Production of class II bacteriocins by lactic acid bacteria: an example of biological warfare and communication. *Antonie Van Leeuwenhoek* 81, 639–654. doi: 10.1023/A:1020582211262

Ennahar, S., Sashihara, T., Sonomoto, K., and Ishizaki, A. (2000). Class IIa bacteriocins: biosynthesis, structure and activity. *FEMS Microbiol. Rev.* 24, 85–106. doi: 10.1111/j.1574-6976.2000.tb00534.x

Falkenhorst, G., Bagdonaite, J., Lisby, M., Madsen, S., Lambertsen, L., Olsen, K., et al. (2008). Outbreak of group A streptococcal throat infection: don't forget to ask about food. *Epidemiol. Infect.* 136, 1165–1171. doi: 10.1017/S0950268807009764

Fimland, G., Blingsmo, O. R., Sletten, K., Jung, G., Nes, I. F., and Nissen-Meyer, J. (1996). New biological active hybrid bacteriocins constructed by combining regions from various pediocin-like bacteriocins: the C-terminal region is important for determining specificity. *Appl. Environ. Microbiol.* 62, 3313–3318. doi: 10.1128/aem.62.9.3313-3318.1996

Fimland, G., Johnsen, L., Dalhus, B., and Nissen-Meyer, J. (2005). Pediocin-like antimicrobial peptides (class IIa bacteriocins) and their immunity proteins: biosynthesis, structure, and mode of action. *J. Pept. Sci.* 11, 688–696. doi: 10.1002/psc.699

Franz, C. M. A. P., Holzapfel, W. H., and Stiles, M. E. (1999). Enterococci at the crossroads of food safety? *Int. J. Food Microbiol.* 47, 1–24. doi: 10.1016/S0168-1605(99)00007-0

Franz, M. A. P., van Belkum, M. J., Holzapfel, W. H., Abriouel, H., and Gálvez, A. (2007). Diversity of enterococcal bacteriocins and their grouping in a new classification scheme. *FEMS Microbiol. Rev.* 31, 293–310. doi: 10.1111/j.1574-6976.2007.00064.x

Frazer, A. C., Sharratt, M., and Hickman, J. R. (1962). The biological effects of food additives. I.-Nisin. *J. Sci. Food Agric.* 13, 32–42. doi: 10.1002/jsfa.2740130106

Gabrielsen, C., Brede, D. A., Nes, I. F., and Diep, D. B. (2014). Circular bacteriocins: biosynthesis and mode of action. *Appl. Environ. Microbiol.* 80, 6854–6862. doi: 10.1128/AEM.02284-14

Gálvez, A., Abriouel, H., López, R. L., and Omar, N. B. (2007). Bacteriocin-based strategies for food biopreservation. *Int. J. Food Microbiol.* 120, 51–70. doi: 10.1016/j.ijfoodmicro.2007.06.001

Garneau, S., Martin, N. I., and Vederas, J. C. (2002). Two-peptide bacteriocins produced by lactic acid bacteria. *Biochimie* 84, 577–592. doi: 10.1016/S0300-9084(02)01414-1

Garver, K. I., and Muriana, P. M. (1993). Detection, identification and characterization of bacteriocin-producing lactic acid bacteria from retail food products. *Int. J. Food Microbiol.* 19, 241–258. doi: 10.1016/0168-1605(93)90017-B

Genilloud, O. (2014). The re-emerging role of microbial natural products in antibiotic discovery. *Antonie Van Leeuwenhoek* 106, 173–178. doi: 10.1007/s10482-014-0204-6

Gravesen, A., Axelsen, A.-M. J., Mendes da Silva, J., Hansen, T. B., and Knøchel, S. (2002). Frequency of bacteriocin resistance development and associated fitness costs in *Listeria monocytogenes*. *Appl. Environ. Microbiol.* 68, 756–764. doi: 10.1128/AEM.68.2.756-764.2002

Greenwood, D. (2008). *Antimicrobial Drugs. Chronicle of a Twentieth Century Medical Triumph*. Oxford: Oxford University Press.

Hanlin, M. B., Kalchayanand, N., Ray, P., and Ray, B. (1993). Bacteriocins of lactic acid bacteria in combination have greater antibacterial activity. *J. Food Prot.* 56, 252–255. doi: 10.4315/0362-028X-56.3.252

Hassan, M., Kjos, M., Nes, I. F., Diep, D. B., and Lotfipour, F. (2012). Natural antimicrobial peptides from bacteria: characteristics and potential applications to fight against antibiotic resistance. *J. Appl. Microbiol.* 113, 723–736. doi: 10.1111/j.1365-2672.2012.05338.x

Hastings, J. W., and Stiles, M. E. (1991). Antibiosis of *Leuconostoc gelidum* isolated from meat. *J. Appl. Bacteriol.* 70, 127–134. doi: 10.1111/j.1365-2672.1991.tb04438.x

Héchard, Y., and Sahl, H.-G. (2002). Mode of action of modified and unmodified bacteriocins from gram-positive bacteria. *Biochimie* 84, 545–557. doi: 10.1016/S0300-9084(02)01417-7

Holzapfel, W. H., Geisen, R., and Schillinger, U. (1995). Biological preservation of foods with reference to protective cultures, bacteriocins and food-grade enzymes. *Int. J. Food Microbiol.* 24, 343–362. doi: 10.1016/0168-1605(94)00036-6

Jett, B. D., Huycke, M. M., and Gilmore, M. S. (1994). Virulence of enterococci. *Clin. Microbiol. Rev.* 7, 462–478. doi: 10.1128/CMR.7.4.462

Jones, R. J., Hussein, H. M., Zagorec, M., Brightwell, G., and Tagg, J. R. (2008). Isolation of lactic acid bacteria with inhibitory activity against pathogens and spoilage organisms associated with fresh meat. *Food Microbiol.* 25, 228–234. doi: 10.1016/j.fm.2007.11.001

Katz, L., and Baltz, R. H. (2016). Natural product discovery: past, present and future. *J. Ind. Microbiol. Biotechnol.* 43, 155–176. doi: 10.1007/s10295-015-1723-5

Kirchhelle, C. (2018). Pharming animals: a global history of antibiotics in food production (1935–2017). *Palgrave Commun.* 4:96. doi: 10.1057/s41599-018-0152-2

Kirkup, B. C., and Riley, M. A. (2004). Antibiotic-mediated antagonism leads to a bacterial game of rock–paper–scissors in vivo. *Nature* 428, 412–414. doi: 10.1038/nature02429

Kleerebezem, M., and Quadri, L. E. N. (2001). Peptide pheromone-dependent regulation of antimicrobial peptide production in gram-positive bacteria: a case of multicellular behavior. *Peptides* 22, 1579–1596. doi: 10.1016/S0196-9781(01)00493-4

Kleerebezem, M., Quadri, L. E. N., Kuipers, O. P., and De Vos, W. M. (1997). Quorum sensing by peptide pheromones and two-component signal-transduction systems in gram-positive bacteria. *Mol. Microbiol.* 24, 895–904. doi: 10.1046/j.1365-2958.1997.4251782.x

Kuipers, O. P., Ruyter, P. G. G. A., Kleerebezem, M., and de Vos, W. M. (1998). Quorum sensing-controlled gene expression in lactic acid bacteria. *J. Biotechnol.* 64, 15–21. doi: 10.1016/S0168-1656(98)00100-X

Leisner, J. J. (2020). The diverse search for synthetic, semisynthetic and natural product antibiotics from the 1940s and up to 1960 exemplified by a small pharmaceutical player. *Front. Microbiol.* 11:976. doi: 10.3389/fmicb.2020.00976

Leisner, J. J., and Haaber, J. (2012). Intraguild predation provides a selection mechanism for bacterial antagonistic compounds. *Proc. R. Soc. B* 279, 4513–4521. doi: 10.1098/rspb.2012.1179

Lewis, K. (2013). Platforms for antibiotic discovery. *Nat. Rev. Drug Discov.* 12, 371–387. doi: 10.1038/nrd3975

Lewus, C. B., Kaiser, A., and Montville, T. J. (1991). Inhibition of food-borne bacterial pathogens by bacteriocins from lactic acid bacteria isolated from meat. *Appl. Environ. Microbiol.* 57, 1683–1688. doi: 10.1128/aem.57.6.1683-1688.1991

Linares, J. F., Gustafsson, I., Baquero, F., and Martinez, J. L. (2006). Antibiotics as intermicrobial signaling agents instead of weapons. *Proc. Natl. Acad. Sci. U. S. A.* 103, 19484–19489. doi: 10.1073/pnas.0608949103

López-Cuellar, M. R., Rodríguez-Hernández, A. I., and Chavarría-Hernández, N. (2016). LAB bacteriocin applications in the last decade. *Biotechnol. Biotechnol. Equip.* 30, 1039–1050. doi: 10.1080/13102818.2016.1232605

Lüders, T., Birkemo, G. A., Fimland, G., Nissen-Meyer, J., and Nes, I. F. (2003). Strong synergy between a eukaryotic antimicrobial peptide and bacteriocins from lactic acid bacteria. *Appl. Environ. Microbiol.* 69, 1797–1799. doi: 10.1128/AEM.69.3.1797-1799.2003

Luria, S.E. (1984). *A Slot Machine, A Broken Test Tube. An Autobiography*. New York: Harper & Row, Publishers.

Martin-Visscher, L. A., van Belkum, M. J., and Vederas, J. C. (2011). "Class IIc or circular bacteriocins," in *Prokaryotic Microbial Peptides*. eds. D. Drider and S. Rebuffat (New York, Dordrecht, Heidelberg, London: Springer), 213–236.

Mathur, H., Field, D., Rea, M. C., Cotter, P. D., Hill, C., and Ross, P. R. (2017). Bacteriocin-antimicrobial synergy: a medical and food perspective. *Front. Microbiol.* 8:1205. doi: 10.3389/fmicb.2017.01205

Medema, M. H., Blin, K., Cimermancic, P., de Jager, V., Zakrzewski, P., Fischbach, M. A., et al. (2011). AntiSMASH: rapid identification, annotation and analysis of secondary metabolite biosynthesis gene clusters in bacterial and fungal genome sequences. *Nucleic Acids Res.* 39, W339–W346. doi: 10.1093/nar/gkr466

Montalbán-López, M., Sánchez-Hidalgo, M., Valdivia, E., Martínez-Bueno, M., and Maqueda, M. (2011). Are bacteriocins underexploited? NOVEL applications for OLD antimicrobials. *Curr. Pharm. Biotechnol.* 12, 1205–1220. doi: 10.2174/138920111796117364

Montville, T. J., Winkowski, K., and Ludescher, R. D. (1995). Models and mechanisms for bacteriocin action and application. *Int. Dairy J.* 5, 797–814. doi: 10.1016/0958-6946(95)00034-8

Moreno, M. R. F., Sarantinopoulos, P., Tsakalidou, E., and De Vuyst, L. (2006). The role and application of enterococci in food and health. *Int. J. Food Microbiol.* 106, 1–24. doi: 10.1016/j.ijfoodmicro.2005.06.026

Naghmouchi, K., Kheadr, E., Lacroix, C., and Fliss, I. (2007). Class I/Class IIa bacteriocin cross-resistance phenomenon in *Listeria monocytogenes*. *Food Microbiol.* 24, 718–727. doi: 10.1016/j.fm.2007.03.012

Nes, I. F. (2011). "History, current knowledge, and future directions on bacteriocin research in lactic acid bacteria," in *Prokaryotic Microbial Peptides*. eds. D. Drider and S. Rebuffat (New York, Dordrecht, Heidelberg, London: Springer), 3–12.

Nes, I. F., Diep, D. B., Håvardstein, L. H., Brurberg, M. B., Eijsink, V., and Holo, H. (1996). Biosynthesis of bacteriocins in lactic acid bacteria. *Antonie Van Leeuwenhoek* 70, 113–128. doi: 10.1007/BF00395929

Nissen-Meyer, J., Rogne, P., Oppegård, C., Haugen, H., and Kristiansen, P. E. (2009). Structure-function relationships of the non-lanthionine-containing peptide (class II) bacteriocins produced by gram-positive bacteria. *Curr. Pharm. Biotechnol.* 10, 19–37. doi: 10.2174/138920109787048661

O'Connor, P. M., Kuniyoshi, T. M., Oliveira, R. P. S., Hill, C., Ross, R. P., and Cotter, P. D. (2020). Antimicrobials for food and feed: a bacteriocin perspective. *Curr. Opin. Biotechnol.* 61, 160–167. doi: 10.1016/j.copbio.2019.12.023

O'Sullivan, L., Ryan, M. P., Ross, R. P., and Hill, C. (2003). Generation of food-grade lactococcal starters which produce the lantibiotics 3147 and lacticin 481. *Appl. Environ. Microbiol.* 69, 3681–3685. doi: 10.1128/AEM.69.6.3681-3685.2003

Ongey, E. L., and Neubauer, P. (2016). Lanthipeptides: chemical synthesis versus in vivo biosynthesis as tools for pharmaceutical production. *Microb. Cell Factories* 15:97. doi: 10.1186/s12934-016-0502-y

Oumer, A., Garde, S., Gaya, P., Medina, M., and Nuñez, M. (2001). The effects of cultivating lactic starter cultures with bacteriocin-producing lactic acid bacteria. *J. Food Prot.* 64, 81–86. doi: 10.4315/0362-028X-64.1.81

Peláez, F. (2006). The historical delivery of antibiotics from microbial natural products—can history repeat? *Biochem. Pharmacol.* 71, 981–990. doi: 10.1016/j.bcp.2005.10.010

Perez, R. H., Zendo, T., and Sonomoto, K. (2018). Circular and leaderless bacteriocins: biosynthesis, mode of actions, applications and prospects. *Front. Microbiol.* 9:2085. doi: 10.3389/fmicb.2018.02085

Plavec, T. V., and Berlec, A. (2020). Safety aspects of genetically modified lactic acid bacteria. *Microorganisms* 8:297. doi: 10.3390/microorganisms8020297

Ramia, N. E., Mangavel, C., Gaiani, C., Muller-Gueudin, A., Taha, S., Revol-Junelles, A.-M., et al. (2020). Nested structure of intraspecific competition network in *Carnobacterium maltaromaticum*. *Sci. Rep.* 10:7335. doi: 10.1038/s41598-020-63844-5

Rasch, M., and Knøchel, S. (1998). Variations in tolerance of *Listeria monocytogenes* to nisin, pediocin PA-1 and bavaricin A. *Lett. Appl. Microbiol.* 27, 275–278. doi: 10.1046/j.1472-765X.1998.00433.x

Rea, M. C., Ross, R. P., Cotter, P. D., and Hill, C. C. (2011). "Classification of bacteriocins from gram-positive bacteria," in *Prokaryotic Microbial Peptides*. eds. D. Drider and S. Rebuffat (New York, Dordrecht, Heidelberg, London: Springer), 29–54.

Rendueles, C., Duarte, A. C., Escobedo, S., Fernández, L., Rodríguez, A., García, P., et al. (2022). Combined use of bacteriocins and bacteriophages as food biopreservatives. A review. *Int. J. Food Microbiol.* 368:109611. doi: 10.1016/j.ijfoodmicro.2022.109611

Ringø, E., and Gatesoupe, F.-J. (1998). Lactic acid bacteria in fish: a review. *Aquaculture* 160, 177–203. doi: 10.1016/S0044-8486(97)00299-8

Rodríguez, J. M., Martínez, M. I., and Kok, J. (2002). Pediocin PA-1, a wide-spectrum bacteriocin from lactic acid bacteria. *Crit. Rev. Food Sci. Nutr.* 42, 91–121. doi: 10.1080/10408690290825475

Ross, R. P., Galvin, M., McAuliffe, O., Morgan, S. M., Ryan, M. P., Twomey, D. P., et al. (1999). Developing applications for lactococcal bacteriocins. *Anton Leeuw. Int. J. G.* 76, 337–346. doi: 10.1023/A:1002069416067

Ruiz-Barba, J. L., Cathcart, D. P., Warner, P. J., and Jiménez-Díaz, R. (1994). Use of *Lactobacillus plantarum* LPCO10, a bacteriocin producer, as a starter culture in Spanish-style green olive fermentations. *Appl. Environ. Microbiol.* 60, 2059–2064. doi: 10.1128/aem.60.6.2059-2064.1994

Sahl, H. G., and Bierbaum, G. (1998). Lantibiotics: biosynthesis and biological activities of uniquely modified peptides from gram-positive bacteria. *Annu. Rev. Microbiol.* 52, 41–79. doi: 10.1146/annurev.micro.52.1.41

Servin, A. L. (2004). Antagonistic activities of lactobacilli and bifidobacteria against microbial pathogens. *FEMS Microbiol. Rev.* 28, 405–440. doi: 10.1016/j.femsre.2004.01.003

Silveira, R. F., Roque-Borda, C. A., and Vicente, E. F. (2021). Antimicrobial peptides as a feed additive alternative to animal production, food safety and public health implications: an overview. *Anim. Nutr.* 7, 896–904. doi: 10.1016/j.aninu.2021.01.004

Silver, L. L. (2011). Challenges of antibacterial discovery. *Clin. Microbiol. Rev.* 24, 71–109. doi: 10.1128/CMR.00030-10

Snyder, A. B., and Worobo, R. W. (2013). Chemical and genetic characterization of bacteriocins: antimicrobial peptides for food safety. *J. Sci. Food Agric.* 94, 28–44. doi: 10.1002/jsfa.6293

Soltani, S., Hammami, R., Cotter, P. D., Rebuffat, S., Said, L. B., Gaudreau, H., et al. (2021). Bacteriocins as a new generation of antimicrobials: toxicity aspects and regulations. *FEMS Microbiol. Rev.* 45:fuaa039. doi: 10.1093/femsre/fuaa039

Stiles, M. E. (1996). Biopreservation by lactic acid bacteria. *Anton Leeuw. Int. J. G.* 70, 331–345. doi: 10.1007/BF00395940

Twomey, D., Ross, R. P., Ryan, M., Meaney, B., and Hill, C. (2002). Lantibiotics produced by lactic acid bacteria: structure, function and applications. *Anton Leeuw. Int. J. G.* 82, 165–185. doi: 10.1023/A:1020660321724

van Heel, A. J., de Jong, A., Montalbán-López, M., Kok, J., and Kuipers, O. P. (2013). BAGEL3: automated identification of genes encoding bacteriocins and (non-)bactericidal posttranslationally modified peptides. *Nucleic Acids Res.* 41, W448–W453. doi: 10.1093/nar/gkt391

Wachsman, M. B., Castilla, V., de Ruiz Holgado, A. P., de Torres, R. A., Sesma, F., and Coto, C. E. (2003). Enterocin CRL35 inhibits late stages of HSV-1 and HSV-2 replication in vitro. *Antivir. Res.* 58, 17–24. doi: 10.1016/S0166-3542(02)00099-2

Wright, G. D. (2014). Something old, something new: revisiting natural products in antibiotic drug discovery. *Can. J. Microbiol.* 60, 147–154. doi: 10.1139/cjm-2014-0063

Yang, S.-C., Lin, C.-H., Sung, C. T., and Fang, J.-Y. (2014). Antibacterial activities of bacteriocins: application in foods and pharmaceuticals. *Front. Microbiol.* 5:241. doi: 10.3389/fmicb.2014.00241

Zheng, J., Wittouck, S., Salvetti, S., Franz, C. M. A. P., Harris, H. M. B., Mattarelli, P., et al. (2020). A taxonomic note on the genus *Lactobacillus*. Description of 23 novel genera, emended description of the genus *Lactobacillus* Beijerinck 1901, and union of Lactobacillaceae and Leuconostocaceae. *Int. J. Syst. Evol. Microbiol.* 70, 2782–2858. doi: 10.1099/ijsem.0.004107

Zouhir, A., Hammami, R., Fliss, I., and Hamida, J. B. (2010). A new structure-based classification of gram-positive bacteriocins. *Protein J.* 29, 432–439. doi: 10.1007/s10930-010-9270-4

Conflict of Interest: JL has a minor share in a company that sell probiotic cultures.

The remaining author declares that the research was conducted in the absence of any commercial or financial relationships that could be construed as a potential conflict of interest.

Publisher's Note: All claims expressed in this article are solely those of the authors and do not necessarily represent those of their affiliated organizations, or those of the publisher, the editors and the reviewers. Any product that may be evaluated in this article, or claim that may be made by its manufacturer, is not guaranteed or endorsed by the publisher.

frontiers | Frontiers in Microbiology

ORIGINAL RESEARCH
published: 21 June 2022
doi: 10.3389/fmicb.2022.896916

New Mutations in *cls* Lead to Daptomycin Resistance in a Clinical Vancomycin- and Daptomycin-Resistant *Enterococcus faecium* Strain

Weiwei Li[1,2], Jiamin Hu[1], Ling Li[1], Mengge Zhang[1], Qingyu Cui[1], Yanan Ma[1], Hainan Su[1], Xuhua Zhang[3], Hai Xu[1]*and Mingyu Wang[1]**

[1]State Key Laboratory of Microbial Technology, Microbial Technology Institute, Shandong University, Qingdao, China, [2]Division of Science and Technology, Ludong University, Yantai, China, [3]Laboratory Medicine Center, The Second Hospital of Shandong University, Jinan, China

OPEN ACCESS

Edited by:
Hidetada Hirakawa,
Gunma University, Japan

Reviewed by:
Milya Davlieva,
Quantapore, United States
Xiaogang Xu,
Fudan University, China

***Correspondence:**
Xuhua Zhang
chh8105@126.com
Hai Xu
haixu@sdu.edu.cn
Mingyu Wang
wangmingyu@sdu.edu.cn

Specialty section:
This article was submitted to Antimicrobials, Resistance and Chemotherapy, a section of the journal Frontiers in Microbiology

Received: 15 March 2022
Accepted: 19 May 2022
Published: 21 June 2022

Citation:
Li W, Hu J, Li L, Zhang M, Cui Q, Ma Y, Su H, Zhang X, Xu H and Wang M (2022) New Mutations in cls Lead to Daptomycin Resistance in a Clinical Vancomycin- and Daptomycin-Resistant Enterococcus faecium Strain. Front. Microbiol. 13:896916. doi: 10.3389/fmicb.2022.896916

Daptomycin (DAP), a last-resort antibiotic for treating Gram-positive bacterial infection, has been widely used in the treatment of vancomycin-resistant enterococci (VRE). Resistance to both daptomycin and vancomycin leads to difficulties in controlling infections of enterococci. A clinical multidrug-resistant *Enterococcus faecium* EF332 strain that shows resistance to both daptomycin and vancomycin was identified, for which resistance mechanisms were investigated in this work. Whole-genome sequencing and comparative genomic analysis were performed by third-generation PacBio sequencing, showing that *E. faecium* EF332 contains four plasmids, including a new multidrug-resistant pEF332-2 plasmid. Two vancomycin resistance-conferring gene clusters *vanA* and *vanM* were found on this plasmid, making it the second reported vancomycin-resistant plasmid containing both clusters. New mutations in chromosomal genes *cls* and *gdpD* that, respectively, encode cardiolipin synthase and glycerophosphoryl diester phosphodiesterase were identified. Their potential roles in leading to daptomycin resistance were further investigated. Through molecular cloning and phenotypic screening, two-dimensional thin-layer chromatography, fluorescence surface charge test, and analysis of cardiolipin distribution patterns, we found that mutations in *cls* decrease surface negative charges of the cell membrane (CM) and led to redistribution of lipids of CM. Both events contribute to the DAP resistance of *E. faecium* EF332. Mutation in *gdpD* leads to changes in CM phospholipid compositions, but cannot confer DAP resistance. Neither mutation could result in changes in cellular septa. Therefore, we conclude that the daptomycin resistance of *E. faecium* EF332 is conferred by new *cls* mutations. This work reports the genetic basis for vancomycin and daptomycin resistance of a multidrug-resistant *E. faecium* strain, with the finding of new mutations of *cls* that leads to daptomycin resistance.

Keywords: vancomycin-resistant enterococci, *Enterococcus faecium*, daptomycin resistance, vancomycin resistance, membrane surface charge, *gdpD*, *cls*

INTRODUCTION

Enterococcus faecium, a Gram-positive coccus, is an important nosocomial pathogen that can cause fatal bacteremia and myocarditis (Arias and Murray, 2012). The emergence of multidrug-resistant (MDR) *E. faecium*, particularly vancomycin-resistant enterococci (VRE), led to high morbidity and mortality in hospitalized patients (Tran et al., 2013a, 2015; Herc et al., 2017; Lebreton et al., 2018). To make matters worse, the horizontal transfer of antibiotic resistance genes (ARGs) directly led to the rapid increase in VRE. In recent decades, VRE was gradually recognized as a major cause of MDR hospital infection in many countries (Uttley et al., 1988; Cattoir and Giard, 2014). A rapid increase of VRE undoubtedly brings more difficulties for the treatment of *E. faecium* infections (Depardieu et al., 2007; Lebreton et al., 2018). Initially, linezolid and quinupristin–dalfopristin were used to treat VRE infections, but their use was hampered by their strong adverse drug effects (Carver et al., 2003; Hogan et al., 2010; Matsumoto et al., 2010). By contrast, daptomycin (DAP) was generally considered to be a safer antimicrobial agent and gradually became the front-line drug for the patients who have VRE infections (Chow et al., 2016; Gonzalez-Ruiz et al., 2016; Herc et al., 2017; Suleyman et al., 2017).

Daptomycin is a cyclic lipopeptide antibiotic produced by *Streptomyces roseosporus* (Heidary et al., 2018), which has a special mechanism that binds to Ca^{2+} and inserts into the cell membrane (CM) causing leakage of intracellular ions and ATP, thus killing bacteria (LaPlante and Rybak, 2004; Heidary et al., 2018). Unfortunately, the widespread use of daptomycin resulted in the emergence of daptomycin non-susceptible VRE (DNVRE), which undoubtedly further reduced the option of treatment for VRE infections (Munoz-Price et al., 2005; Lellek et al., 2015; Chow et al., 2016; Hussain et al., 2016; Herc et al., 2017). Multiple studies suggested that the mechanism of daptomycin resistance is mainly related to mutations in chromosomal genes, including *mprF*, *gdpD*, *yycG*, *rpoB*, *rpoC*, *pgsA*, *cls*, *liaFSR*, etc. (Fischer et al., 2011; Tran et al., 2013a,b; Heidary et al., 2018). With the increase of reports on DNVRE, a series of investigations were carried out to try to find the resistance mechanisms of daptomycin and effective applications of DAP (Munoz-Price et al., 2005; Lellek et al., 2015; Chow et al., 2016; Hussain et al., 2016; Suleyman et al., 2017). However, the mechanism of DAP resistance has not been fully elucidated: One view is that DAP is diverted from effective targets at the septum by redistribution of anionic phospholipids; another view is that resistant bacteria achieve electrostatic repulsion to DAP by reducing the negative surface charge of CM (Heidary et al., 2018). In summary, the reports on DAP resistance mainly focus on the interaction between CM and DAP–Ca^{2+} complex.

In view of this, in the present study, a clinical multidrug-resistant *E. faecium* from a hospital showing daptomycin resistance and high-level vancomycin resistance was identified. Whole-genome sequencing and subsequent mechanistic investigations were performed, hoping to find the answers to the following questions: (1) the genetic basis of the multidrug resistance; (2) the risk of multiple resistance transmission; and (3) the mechanism of daptomycin resistance.

MATERIALS AND METHODS

Strains

Enterococcus faecium EF332 strain used in this study was isolated in the Laboratory Medicine Center of the Second Hospital of Shandong University. The laboratory maintains an opportunistic pathogen library isolated from patient samples and routinely screens them for possible new findings. The strain was identified by the analysis of 16S rDNA sequence.

Antibiotic Susceptibility Tests

Antibiotic susceptibility tests were conducted according to CLSI/EUCAST guidelines (EUCAST, 2017; CLSI, 2018). The tested antibiotics include: penicillin (PEN), ampicillin (AMP), ciprofloxacin (CIP), gatifloxacin (GAT), chloramphenicol (CHL), tetracycline (TET), tigecycline (TGC), fosfomycin (FOF), erythromycin (ERY), linezolid (LZD), rifampicin (RIF), vancomycin (VAN), and daptomycin (DAP). K-B Disk diffusion assays were performed as previously documented (Vading et al., 2011). Agar dilution method (for FOF) and broth microdilution method (for the rest antibiotics) were adopted to determine MICs of antibiotics. *Staphylococcus aureus* ATCC 25923 and *Enterococcus faecalis* ATCC 29212 were used as control strains for disk diffusion and dilution method, respectively, according to CLSI and EUCAST standards (EUCAST, 2017; CLSI, 2018).

Extraction and Sequencing of Genomic DNA

The genomic DNA of *E. faecium* EF332 and constructed strains (29212-pDL278, EFDO-*cls*, EF332-*cls*) was extracted following previous reported protocol (Qian and Zhao, 2014), and the purity and integrity of the DNA were confirmed by agarose gel electrophoresis. DNA samples of *E. faecium* EF332 were constructed into a 10-kb SMRTbell DNA library, and PacBio single-molecule sequencing was used to obtain at least 50× of sequencing data. In addition, a 350-bp small fragment library was constructed, and Illumina NovaSeq PE150 platform was used for paired-end sequencing to obtain at least 100× clean data for auxiliary assembly. DNA samples of constructed strains were used as templates for quantitative polymerase chain reaction (qPCR) to detect the relative copy number of plasmids.

Conjugation and Transformation of Plasmid

To verify the transferability of plasmid pEF332-2, we conducted conjugation and transformation experiments. A chloramphenicol-resistant and vancomycin-sensitive *E. faecalis* 3–147 strain was used as the recipient for conjugations, and vancomycin-sensitive *E. faecalis* ATCC 29212 was used as recipient for transformation. Transconjugants were identified on the plates containing 32 μg/ml of vancomycin and 50 μg/ml of chloramphenicol, and transformants were identified on the plates containing 32 μg/ml of vancomycin.

Acquisition, Cloning, and Transformation of Presumed DAP Resistance Genes

Genomic DNA of *E. faecium* EF332 strain was used as template to amplify the presumed DAP resistance genes *cls* and *gdpD* by PCR using Phanta super-fidelity DNA polymerase (Vazyme Biotech Co. Ltd. Nanjing, China). All the PCR products were analyzed by 1% agarose gel electrophoresis and purified by DNA clean-up kit (TIANGEN, Beijing, China).

All primer sequences are shown in **Supplementary Table 1**, in which the cleavage sites of BamHI and SalI were added to the 5′ ends for the next step of cloning. The shuttle plasmid pDL278 with spectinomycin resistance was used for molecular cloning (Genbank accession number AF216802.1). The *cls*, *gdpD* fragments and pDL278 vector, were digested by BamHI and SalI endonuclease, respectively, and then, the gene fragments were ligated to pDL278 vector by T4 DNA ligase to generate recombinant shuttle plasmids (pDL278-*cls*, pDL278-*gdpD*). These recombinant plasmids were transferred into *Escherichia coli* DH5α chemically competent cells, respectively, according to the manufacturer's protocols, and Luria-Bertani (LB) agar plates with 500 mg/L spectinomycin were used to select for positive transformants. The plasmids of the positive clones were extracted and transformed into the electroporation competent cells of *E. faecalis* ATCC 29212, and tryptic soy broth (TSB) agar plates with 1,000 mg/L spectinomycin were used to select for positive transformants. The successfully transferred gene fragments were validated by Sanger sequencing using primer M13 (as shown in **Supplementary Table 1**). Finally, we obtained the EF332-*cls* and EF332-*gdpD* strains for downstream analysis. A summary of constructed strains is shown in **Table 1** for easier comparison.

Site-Directed Mutagenesis

In order to further confirm the role of mutations in *cls* and *gdpD* genes, site-directed mutagenesis was performed using overlap extension PCR (SOE-PCR; Ho et al., 1989). The *cls* gene was divided into four fragments at three mutated sites, and *gdpD* gene was divided into two fragments at one mutated site. The primers used are shown in **Supplementary Table 1**.

The SOE-PCR process consisted of two consecutive reactions. First-round PCR: Genomic DNA of *E. faecium* EF332 was used as a template to obtain the corresponding gene fragments. PCR products obtained were purified using the DNA purification kit (TIANGEN, Beijing, China). Second-round PCR: The purified PCR products obtained from the previous step were used as templates, and corresponding primers were added to the reaction system for amplification.

These point mutations led to the amino acid substitutions T269I, V203I, T298S in Cls, and S201P in GdpD. Plasmids carrying these mutated gene fragments were transformed to obtain EFDO-*cls* and EFDO-*gdpD* strains by the method described above.

TABLE 1 | Constructed strains in this study.

Strain	Description
EF332-*cls*	*Enterococcus faecalis* ATCC 29212 harboring plasmid pDL278 that carries *cls* gene originated from *E. faecium* EF332
EFDO-*cls*	*Enterococcus faecalis* ATCC 29212 harboring plasmid pDL278 that carries site-directed mutated *cls* gene originated from *E. faecium* DO
EF332-*gdpD*	*Enterococcus faecalis* ATCC 29212 harboring plasmid pDL278 that carries *gdpD* gene originated from *E. faecium* EF332
EFDO-*gdpD*	*Enterococcus faecalis* ATCC 29212 harboring plasmid pDL278 that carries site-directed mutated *gdpD* gene originated from *E. faecium* DO
29,212-pDL278	*Enterococcus faecalis* ATCC 29212 harboring shuttle plasmid pDL278

Analysis of Membrane Surface Charge

Poly-$_L$-lysine conjugated to fluorescein isothiocyanate (PLL:FITC) was used to assay cell surface charges according to previous studies (Prater et al., 2021). In brief, the strains grew until OD_{600} reached 0.5 in TSB. Cells were then washed three times with sterilized HEPES buffer (20 mM, pH 7.0) and diluted to OD_{600} of 0.1. Cells were incubated with 50 μg/ml PLL:FITC (final concentration) at room temperature with shaking for 10 min and were then washed once using HEPES buffer to remove unbound PLL:FITC. Treated cells were spread on poly-$_L$-lysine-treated glass slides, followed by the addition of 20 μl fluorescent anti-quenching agent. Fluorescence images were observed under NIKON Ti-E inverted fluorescence microscope (Nikon Instruments Co., LTD, Japan) and quantified by ImageJ, with duplicates per strain.

Observation of Cardiolipin Distribution on CM

The fluorescent probe 10-*N*-nonyl acridine orange (NAO) specifically binds to cardiolipin, and the change of cardiolipin distribution caused by *cls* mutation can be determined by observing the NAO fluorescence distribution on the membrane (Mileykovskaya et al., 2001). NAO fluorescence assay was performed according to previous studies (Tran et al., 2013b). In brief, the bacteria were activated in TSB overnight and transferred to new TSB to grow to exponential phase (OD_{600} of ~0.5), after which NAO was added to the medium at a final concentration of 2.5 μM. The sample was oscillated at 100 rpm and 37°C for 4 h under dark conditions. The cells were washed three times (5,000 rpm, 3 min) with sterilized 0.9% saline and immediately mixed with 2× volume of fluorescent anti-quenching agent and fixed on the poly-$_L$-lysine-treated glass slides. Fluorescence observation was performed using a laser scanning confocal microscope with 100× objective and airyscan detector (LSM880, ZEISIS, Germany).

CM Lipid Analysis

Membrane lipids were extracted using previous methods (Komagata and Suzuki, 1988). The lipid components of tested strains were separated by two-dimensional thin-layer chromatography (2D-TLC, Silica 60 F254 TLC plates; Merck) and stained with phosphomolybdic acid (blue for all lipids) and ninhydrin (red for lipids with amino groups), respectively, with three replicates for each strain. The first dimension was developed with chloroform/methanol/water (65:25:4, by volume),

and the second dimension was developed with chloroform/acetic acid/methanol/water (80:15:12:4, by volume). The dried TLC plates were heated for 15 min in a 110°C oven to find phospholipid composition.

Transmission Electron Microscopy

Bacteria were inoculated in 30-ml TSB and grew to exponential phase by shaking at 160 rpm and 37°C. The cultures were centrifuged at 5,000 rpm for 3 min to pellet cells. Cells were fixed at 4°C for 1 h with 500 µl 2.5% glutaraldehyde, washed with PBS (pH 7.2, 0.01 M) for five times (20 min each), fixed with 1% osmium acid at 4°C for 1 h, and washed with PBS (pH 7.2, 0.01 M) for three times, 15 min each. The samples were sequentially dehydrated with 30, 50, 70, 90, and 100% ethanol (twice) and replaced twice by acetone, 15 min each time. Different proportions of embedding agent (EPON812: acetone =1:3,1:1,3:1) were used to penetrate for 1 h successively, and then, pure embedding agent (100% EPON812) was used for penetration overnight. The samples were embedded in EPON812 and then subjected to temperature-programmed curing for 48 h before ultra-thin section. The sections were stained with 2% uranium acetate solution for 20 min (in dark), washed with ddH_2O three times for 5 min each, stained with 1% lead citrate solution for 10 min, and then washed with ddH_2O three times for 5 min each. The prepared samples were observed by Focused Ion Beam-Scanning Transmission Electron Microscope (Crossbeam 550, ZEISIS, Germany).

Quantitative Polymerase Chain Reactions

qPCRs were used to assay the copy numbers of pDL278 vector and variants in *E. faecium* strains (29212-pDL278, EFDO-*cls*, EF332-*cls*) to verify the stability of this vector. Plasmid levels were calculated using the $2^{-\Delta\Delta Ct}$ method. 16S rDNA was used as the housekeeping gene. The primers used are listed in **Supplementary Table 1**. The qPCR system (20 µl) contains the following: 10 µl of 2× SYBR green premix pro taq HS premix (Accurate Biotechnology Co., Ltd., China), 7.8 µl dd H_2O, 0.4 µl of forward and reverse primers each (10 µM), 0.4 µl of ROX reference dye (20 µM, Accurate Biotechnology Co., Ltd., China), and 1 µl template DNA (100 ng/µl). The qPCRs were performed with the following programs: denaturation at 95°C for 30 s, followed by 40 cycles of denaturation at 95°C for 5 s, annealing at 60°C for 30 s. Three biological replicates were performed for each sample, and each qPCR was conducted in triplicate using the ABI StepOnePlus system (Applied Biosystems Inc., Waltham, MA, United States).

Survival Assay

Survival analysis was performed according to the previously published method to compare the survival of different strains under daptomycin stress (Grein et al., 2020). After the bacteria grew to exponential phase (OD_{600} = 0.5) in 5 ml Müller Hinton broth containing 0.05 g/L Ca^{2+} (CAMHB), 100 µl of the cultures were diluted 10^5-fold. One hundred microliters of the diluted bacterial solution was inoculated on TSB agar plates (three replications) for CFU calculation. The remaining cultures were incubated with 32 µg/ml (4 ×MIC) daptomycin (final concentration) at 37°C with shaking at 180 rpm for 1 h. During incubation, 100 µl cultures were taken every 15 min, diluted, and counted as described above. In order to avoid the influence of the change of bacterial solution volume during incubation, an equal volume of CAMHB was added after 100 µl bacterial solution was taken each time. Colony counts at different time points were recorded after overnight incubation at 37°C, and survival rate was calculated as the percentage of colony counts to those without treatment of daptomycin.

Bioinformatics

Whole-genome sequencing reads were assembled into a preliminary genome using SMRT Link v5.1.0 software (Ardui et al., 2018), and arrow software was used to optimize the assembly results. The optimized assembly results were analyzed and compared with original data to discriminate chromosomes and plasmid sequences. Final circular genomes were obtained, followed by gene prediction using GeneMarkS v4.17 software (Besemer et al., 2001). Genomic Islands (GIs) were predicted using IslandPath-DIOMB v0.12 software (Hsiao et al., 2003). Prophage prediction was completed by online prediction server PHASTER (Zhou et al., 2011; Arndt et al., 2016). Functional annotation of coding genes was performed using GO (Ashburner et al., 2000), COG (Galperin et al., 2014), NR (Li et al., 2002), Pfam (Punta et al., 2011), TCDB (Saier et al., 2013), and SWISS-PROT (Bairoch and Apweiler, 2000) databases. ARG annotation used Resistance Gene Identifier (RGI) v5.1.0 software provided by CARD database (Jia et al., 2016). Multilocus sequence typing (MLST) and plasmid classification of *E. faecium* EF332 were performed using MLST[1] and PlasmidFinder databases,[2] respectively, provided by Center for Genomic Epidemiology. AlphaFold 2 software was used to construct Cls structure model (Jumper et al., 2021). Pfam database was used to predict Cls protein domain structure (Mistry et al., 2021), and DOG 2.0 software was used to draw the protein domain structure map (Ren et al., 2009). The relative intensity of fluorescence was quantified by ImageJ 1.52a, resulting in the mean of two biological duplicates, and the significance level was analyzed by Student's *t*-test. The ggplot2 package in R Studio 1.3.929 software (based on R 3.6.3) was used to draw the box charts of fluorescence intensity, and the gggenes and ggplot2 packages were used to generate the gene structure diagrams.

RESULTS

Isolation and Identification of a Vancomycin- and Daptomycin-Resistant *Enterococcus faecium* EF332 Strain

Enterococcus faecium EF332 strain used in this study was isolated in the Laboratory Medicine Center of the Second Hospital of

[1]https://cge.food.dtu.dk/services/MLST/
[2]https://cge.food.dtu.dk/services/PlasmidFinder/

TABLE 2 | Antibiotic susceptibility of *Enterococcus faecium* EF332.

Antibiotics class	Antibiotic	Inhibition zone (mm)	MIC (μg/ml)
Ansamycins	RIF	11 (R)	4 (R)
Macrolides	ERY	0 (R)	>256 (R)
Fluoroquinolones	CIP	0 (R)	32 (R)
	GAT	0 (R)	32 (R)
Phenicols	CHL	21 (S)	4 (S)
Tetracyclines	TET	10 (R)	32 (R)
	TGC	22 (S)	0.0375 (S)
Glycopeptides	VAN	0 (R)	128 (R)
β-lactams	PEN	0 (R)	>256 (R)
	AMP	0 (R)	>256 (R)
Lipopeptides	DAP	n.a.	8 (R)
Fosfomycins	FOF	34 (S)	64 (S)
Oxazolidinones	LZD	23 (S)	1 (S)

n.a.: K-B disk diffusion method is unavailable in both CLSI and EUCAST standards. RIF, rifampicin; ERY, erythromycin; CIP, ciprofloxacin; GAT, gatifloxacin; CHL, chloramphenicol; TET, tetracycline; TGC, tigecycline; VAN, vancomycin; PEN, penicillin; AMP, ampicillin; DAP, daptomycin; FOF, fosfomycin; LZD, linezolid; R, resistant; S, sensitive.

Shandong University during routine screening of pathogens. Antimicrobial susceptibility tests were performed for this strain using 13 antibiotics in 10 classes by both Kirby–Bauer disk diffusion method and determination of minimum inhibitory concentration (MIC) levels. It was shown that *E. faecium* EF332 was resistant to most antibiotics (**Table 2**), suggesting that it is multidrug-resistant. A striking observation is that *E. faecium* EF332 is resistant to both last-line antibiotics against enterococcal infections: vancomycin and daptomycin (Bender et al., 2018). This unusual phenomenon drove us to further investigate the mechanisms underlying multidrug resistance of this strain, particularly for the two last-resort antibiotics vancomycin and daptomycin.

Multidrug-Resistant Determinants of *Enterococcus faecium* EF332 Revealed by Whole-Genome Sequencing

To fully understand the genetic basis of multidrug resistance in *E. faecium* EF332, whole-genome sequences were obtained with third-generation PacBio sequencing accompanied by second-generation Illumina sequencing (The sequencing data were deposited in GenBank with accession numbers CP058891-CP058895). Full sequences for a circular chromosome and four plasmids were obtained. The size of the chromosome is 2,755,510 bp, similarly to previously sequenced *E. faecium* strains. The four plasmids, pEF332-1, pEF332-2, pEF332-3, and pEF332-4, are, respectively, 12,341, 87,675p, 28,308, and 203,652 bp long (**Supplementary Figure 1; Supplementary Table 2**). Multilocus sequence typing (MLST) result showed that *E. faecium* EF332 belongs to ST192, one type of the CC17 clone complex (clade A1), which is believed to have evolved in infections of hospital environment (Freitas et al., 2010).

With accurate gene prediction algorithms, a total of 3,121 genes were predicted to be encoded by *E. faecium* EF332, of which 2,735 are chromosome-borne and 386 are plasmid-borne (**Supplementary Table 2**). Annotation with Comprehensive Antibiotic Resistance Database (CARD) showed that 9, 0, 12, 0, and 2 ARGs were encoded on the chromosome, pEF332-1, pEF332-2, pEF332-3, and pEF332-4, respectively (**Table 3; Supplementary Table 2**). Determinants for all antibiotics were found, most of which are chromosome-borne. Only pEF332-2 and pEF332-4 are antibiotic-resistant plasmids. While pEF332-4 only carries ARGs for aminoglycosides and was previously found in *E. faecium* VRE1 (Sun et al., 2020), pEF332-2 is a new plasmid that carries both *vanA* and *vanM* gene clusters. To the best of our knowledge, plasmids carrying both *vanA* and *vanM* genes are very rare, and only one such plasmid (pELF1) has been found so far in Japan, which is associated with high vancomycin resistance and high risk of transmission (Hashimoto et al., 2019). pEF332-2 is therefore the second plasmid that bears both *vanA* and *vanM* clusters identified so far. This is also in consistency with the high level of vancomycin resistance (128 μg/ml) observed with *E. faecium* EF332. In addition, *vanA* gene clusters are encoded on a genomic island GIs011 that is also part of a multidrug-resistant prophage (**Figure 1; Supplementary Table 3**). This is a strong implication that these ARGs are acquired by horizontal gene transfer. Therefore, this new pEF332-2 plasmid is a strong vancomycin-resistant plasmid that also has a strong implication for ARG mobility. Further phylogenetic analysis of *E. faecium* EF332 plasmids and 55 other plasmids, along with subtyping of pEF332-2 with PlasmidFinder, suggests pEF332-2 belongs to type rep2 (**Figure 2**). Previous report suggested type rep2 plasmids originate from a variety of sources, including hospitals, poultry, and foods (Schwarz et al., 2001; Sletvold et al., 2007; Sun et al., 2020), suggesting that these plasmids may spread between multiple environments. Nevertheless, attempts to transfer

TABLE 3 | Predicted antimicrobial resistance determinants in *Enterococcus faecium* EF332 with CARD.

Antibiotics class	Chromosome	pEF332-2	pEF332-4
Fluoroquinolones	*gyrA* mutation *gyrB* mutation		
Elfamycins/kirromycins	*EF-Tu* mutation		
Lipopeptides	*cls* mutation* *gdpD* mutation*		
Peptide/ansamycins antibiotics	*rpoB*		
Diaminopyrimidines	*dfrE*		
Tetracyclines	*tetM*		
Aminoglycosides	*AAC(6′)-Ii*	*APH(3′)-IIIa*	*AAC(6′)-Ie-APH(2″)-Ia1* *AAC(6′)-Ie-APH(2″)-Ia2*
Macrolides/ lincosamides/ streptogramins		*ermB*	
Glycopeptides		*vanM* *vanHM* *vanYM* *vanSM* *vanRM* *vanA* *vanSA* *vanHA* *vanXA* *vanRA*	
Total	9	12	2

**Genes associated with DAP resistance.*

pEF332-2 from the host *E. faecium* EF332 strain to another bacterium *via* conjugation or transformation were unsuccessful, showing the limited efficiency of horizontal gene transfer.

While comparing the genomic sequences of *E. faecium* EF332 and daptomycin-sensitive *E. faecium* DO strain, mutations were found on *cls* and *gdpD* that, respectively, encode cardiolipin synthase and glycerophosphoryl diester phosphodiesterase (**Table 4**). It was previously reported that mutations in these genes can lead to daptomycin resistance (Humphries et al., 2012; Davlieva et al., 2013; Kelesidis et al., 2013; Lellek et al., 2015; Prater et al., 2019). However, known mutations that confer DAP resistance on these genes were not present in *E. faecium* EF332, leading to the hypothesis that new mutations of the two genes could lead to daptomycin resistance.

New *cls* Mutations Lead to Daptomycin Resistance in *Enterococcus faecium* EF332

In order to find out which mutations on *cls* and/or *gdpD* lead to daptomycin resistance in *E. faecium* EF332 strains, a series of clones were constructed using daptomycin-sensitive *E. faecalis* ATCC 29212 as the parent strain: the EF332-*cls* strain that harbors *cls* from *E. faecium* EF332; the EFDO-*cls* strain that harbors *cls* from *E. faecium* EF332 with identified mutations (V_{203}, T_{269}, T_{298}) reverted to I_{203}, I_{269}, and S_{298}; the EF332-*gdpD* strain that harbors *gdpD* from *E. faecium* EF332; and the EFDO-*gdpD* strain that harbors *gdpD* from *E. faecium* EF332 with identified mutation S_{201} reverted to P_{201}; the 29212-pDL278 strain that harbors pDL278 empty vector as control for constructed strains (**Table 1**). It is shown that the DAP MIC of *E. faecalis* ATCC 29212 increased from 1 to 8 with the introduction of pDL278 vector (**Supplementary Table 4**). A twofold increase in MIC values for daptomycin was found for EF332-*cls* strain (16 μg/ml) over the EFDO-*cls* strain (8 μg/ml), whereas no change of MIC values for daptomycin was found for EF332-*gdpD* strain (8 μg/ml) over the EFDO-*gdpD* strain (8 μg/ml; **Supplementary Table 4**). These results suggest that mutations in *cls* can lead to daptomycin resistance, while mutations in *gdpD* cannot.

Further susceptibility tests including K-B disk diffusion assays and survival assays support this finding. The inhibition zones of daptomycin with the EF332-*cls* strain are significantly smaller than the EFDO-*cls* strain ($p = 2.09 \times 10^{-5}$, **Figure 3**), while no significant difference was found between EFDO-*cls* strain and 29212-pDL278. Similarly, in survival assays, a significantly higher daptomycin resistance strength was found for EF332-*cls* in comparison with EFDO-*cls*, while EFDO-*cls* and 29212-pDL278 respond to daptomycin stress similarly (**Figure 4**). Additional analysis of plasmid copy numbers confirmed that introducing variants of *cls* did not lead to plasmid copy number fluctuation (**Figure 5**). It is further

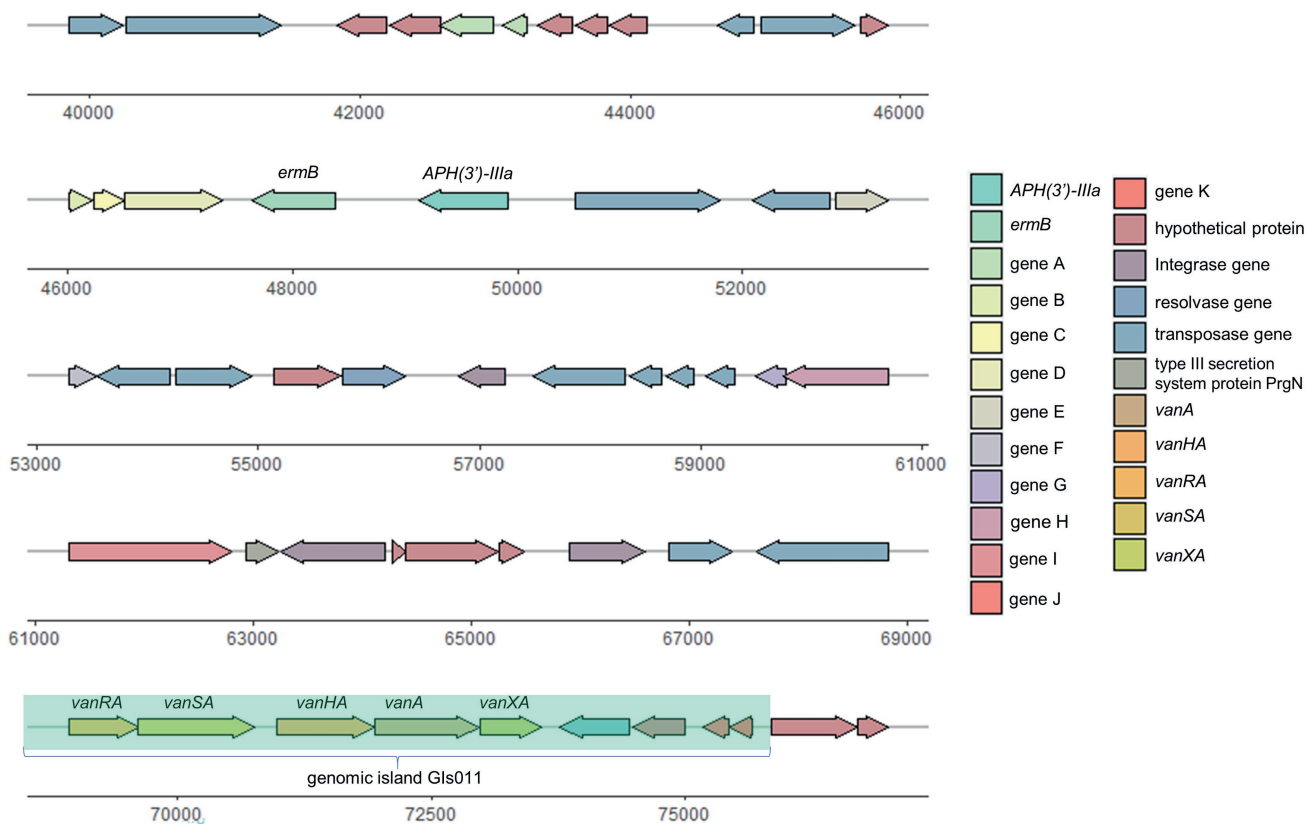

FIGURE 1 | Genetic organization of prophage in pEF332-2.

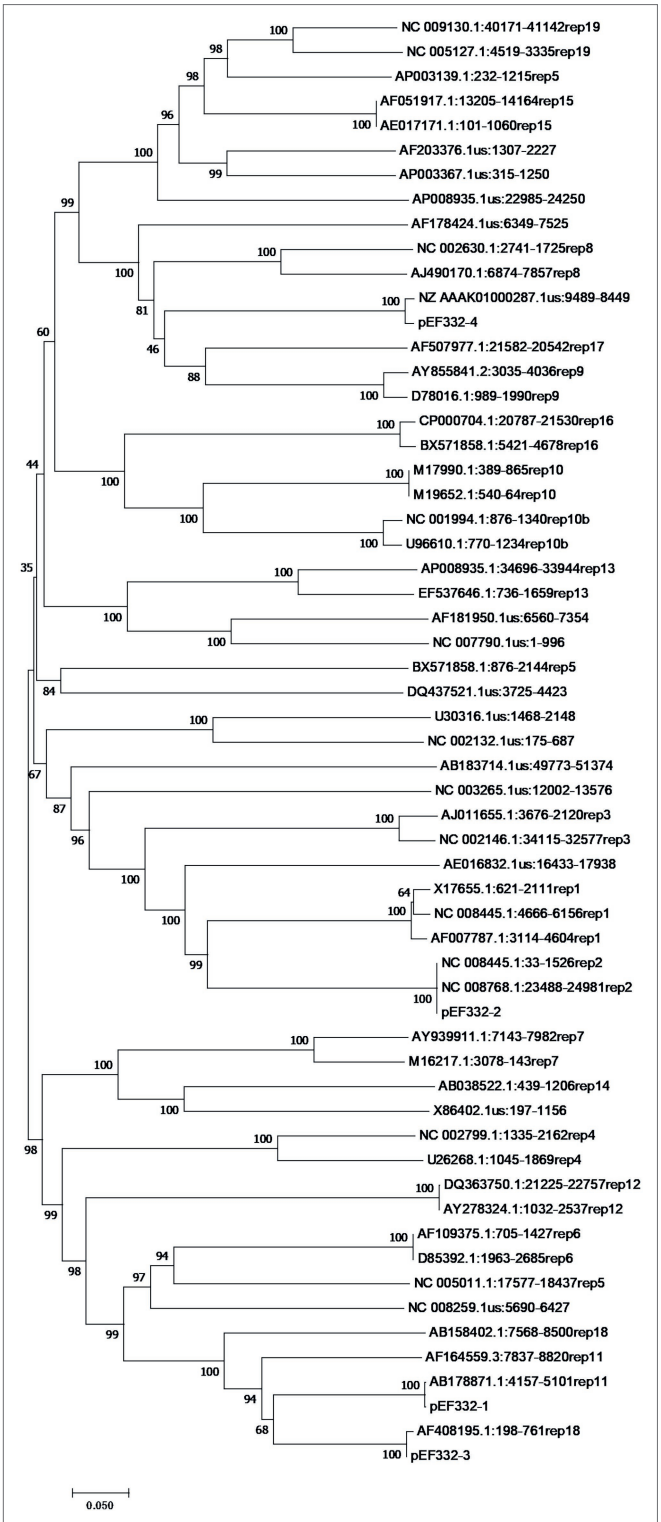

FIGURE 2 | Phylogenetic analysis of *rep* genes of *Enterococcus faecium* EF332 plasmids. The bootstrap values are displayed on the branches with 1,000 times of replications. Bar, evolutionary distance.

interesting to find that in both liquid-media-based analyses, aka the MIC determination and survival analysis, pDL278 introduction increased daptomycin resistance (**Figure 4**), while in the plate-based K-B disk diffusion assay, pDL278 introduction led to little difference in daptomycin resistance (**Figure 3**). This prompted us to hypothesize that maybe pDL278 can result in growth status-specific response to daptomycin, but without further evidence we cannot suggest the specific mechanism behind this phenomenon. Despite this difference, in all scenarios and in all assays, introducing *cls* from *E. faecium* EF332 leads to significantly stronger daptomycin resistance than introducing *cls* from *E. faecium* DO, confirming the above suggestion that mutations in *cls* found in *E. faecium* EF332 lead to daptomycin resistance.

TABLE 4 | Mutations in *cls* and *gdpD* that are associated with DAP resistance.

Genes	Mutations	References
cls	N13I, H215R, R218Q, +MPL110-112	Arias et al., 2011
cls	N13T, K59T	Kelesidis et al., 2013
cls	H215R, R218Q	Davlieva et al., 2013
cls	H215R	Humphries et al., 2012
cls	A20D, D27N, R218Q, R267H	Lellek et al., 2015
cls	I203V, I269T, S298T	This study
gdpD[a]	H29R	Prater et al., 2019
gdpD	P201S	This study

[a]*This mutation was found in DAP-resistant Enterococcus faecium but has not been shown to confer DAP resistance.*

Impact of *cls* and *gdpD* Mutations on Membrane Properties

Both *cls* and *gdpD* genes are related to phospholipid metabolism in CM: The *cls* gene encodes cardiolipin synthase, and *gdpD* gene encodes glycerophosphoryl diester phosphodiesterase (Arias et al., 2011). We therefore hypothesized that mutations in these two genes alter membrane properties, which in turn leads to alteration in membrane–daptomycin interactions. To confirm this, two-dimensional thin-layer chromatography (2D-TLC) was performed to analyze the changes of membrane lipids components caused by mutations. As shown in **Figure 6**, mutation in *gdpD* altered the aminolipid composition of CM, while mutations in *cls* did not significantly alter the lipid composition of CM. This finding suggests a putative role of *gdpD* in the biosynthesis of relatively poorly characterized aminolipid. Furthermore, membrane surface charges were quantified using positively charged fluorescence dye poly-$_L$-lysine conjugated to fluorescein isothiocyanate (PLL: FITC). A significant reduction of binding to PLL: FITC was found between EF332-*cls* and *E. faecalis* ATCC 29212 ($p = 6.27 \times 10^{-65}$), as well as between EF332-*cls* and EFDO-*cls* ($p = 2.20 \times 10^{-101}$; **Figure 7**). This significant change suggests that a reduction of membrane negative charges followed *cls* mutations, which can lead to weakened binding of positively charged DAP-Ca^{2+} to the membrane, the target for the bactericidal effect of daptomycin. This finding suggests that *cls* mutations lead to daptomycin resistance by reduction of membrane negative charges. Only minor changes of membrane negative potentials were found for *gdpD* mutation strain (**Figure 7**), in consistent with the finding that *gdpD* mutation did not lead to increase of daptomycin resistance.

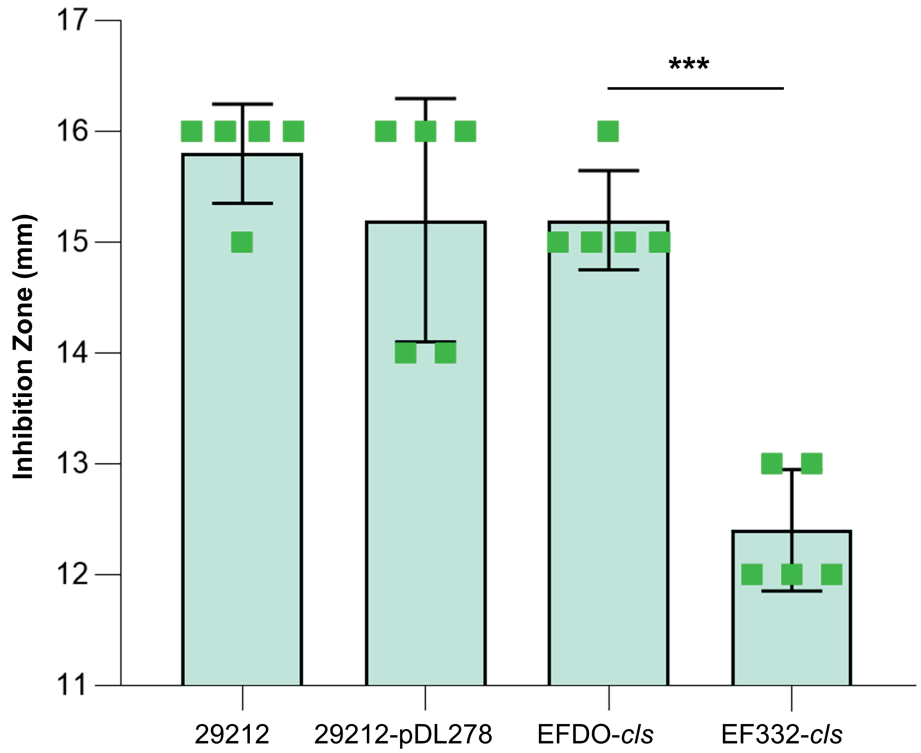

FIGURE 3 | Susceptibility tests of strains based on K-B disk diffusion method. 29212, *Enterococcus faecalis* ATCC 29212; ***$p<0.001$; bar, standard deviation.

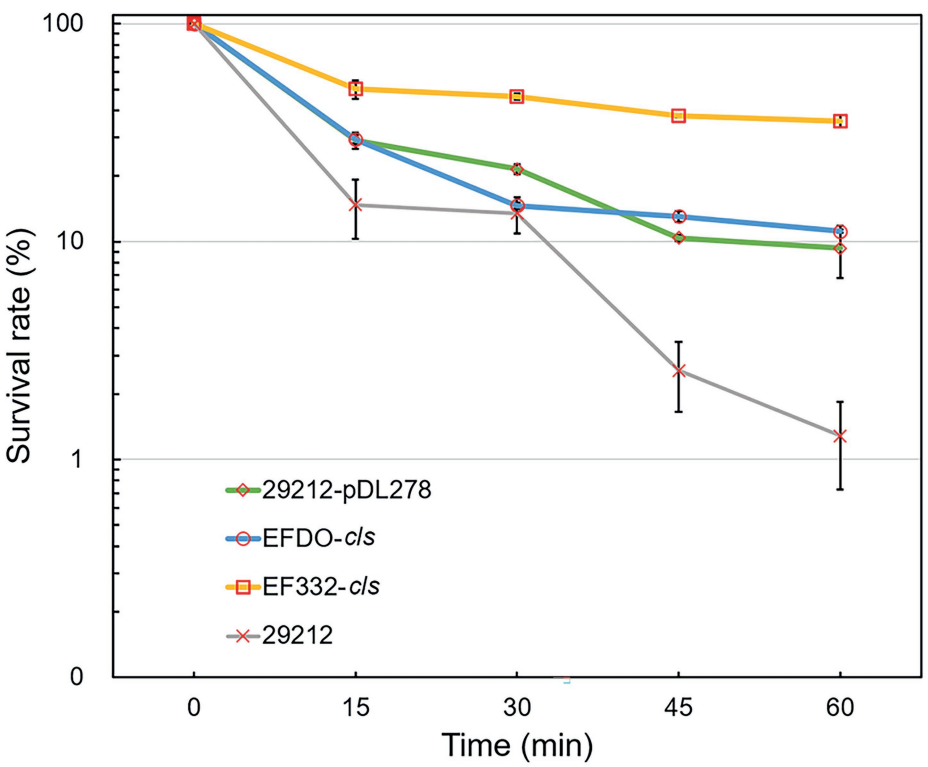

FIGURE 4 | Daptomycin survival assays of *Enterococcus faecalis* strains. 29212, *E. faecalis* ATCC 29212; bar, standard deviation.

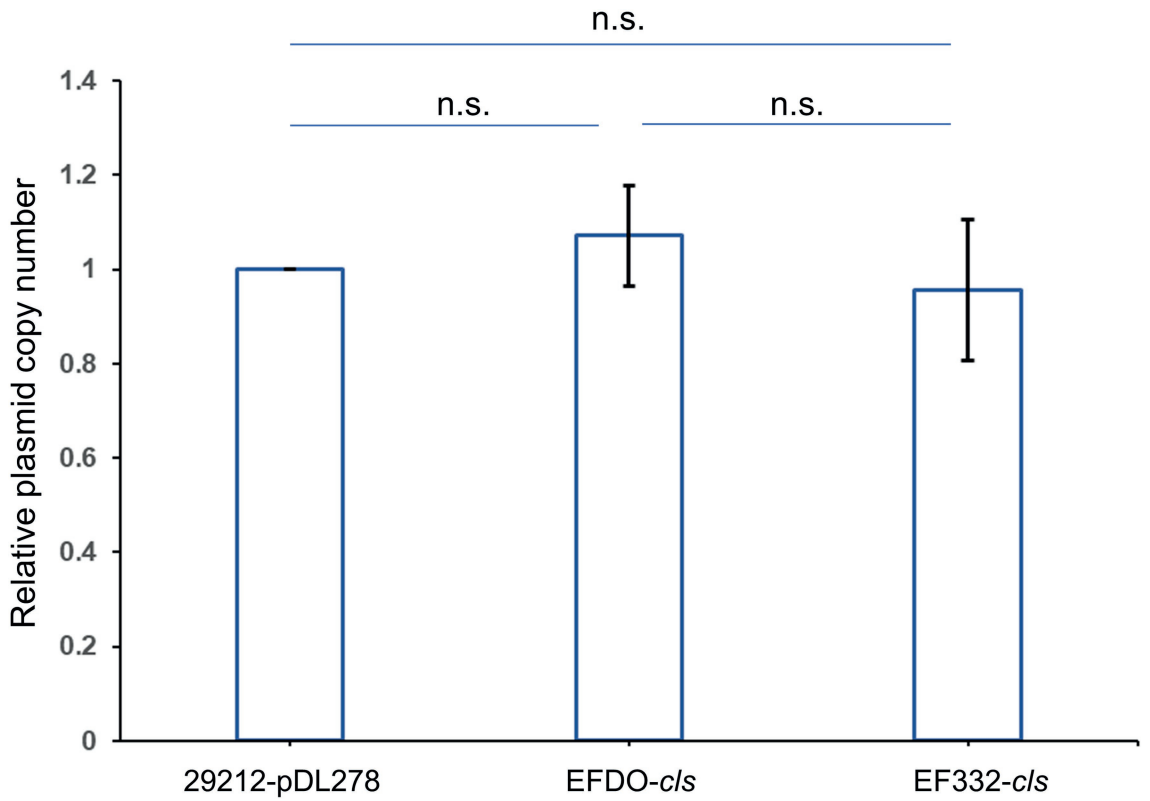

FIGURE 5 | Relative plasmid copy numbers. Relative plasmid copy numbers are defined as relative normalized plasmid copy numbers to 29212-pDL278 strain. Bar, standard deviation; n.s., not significant.

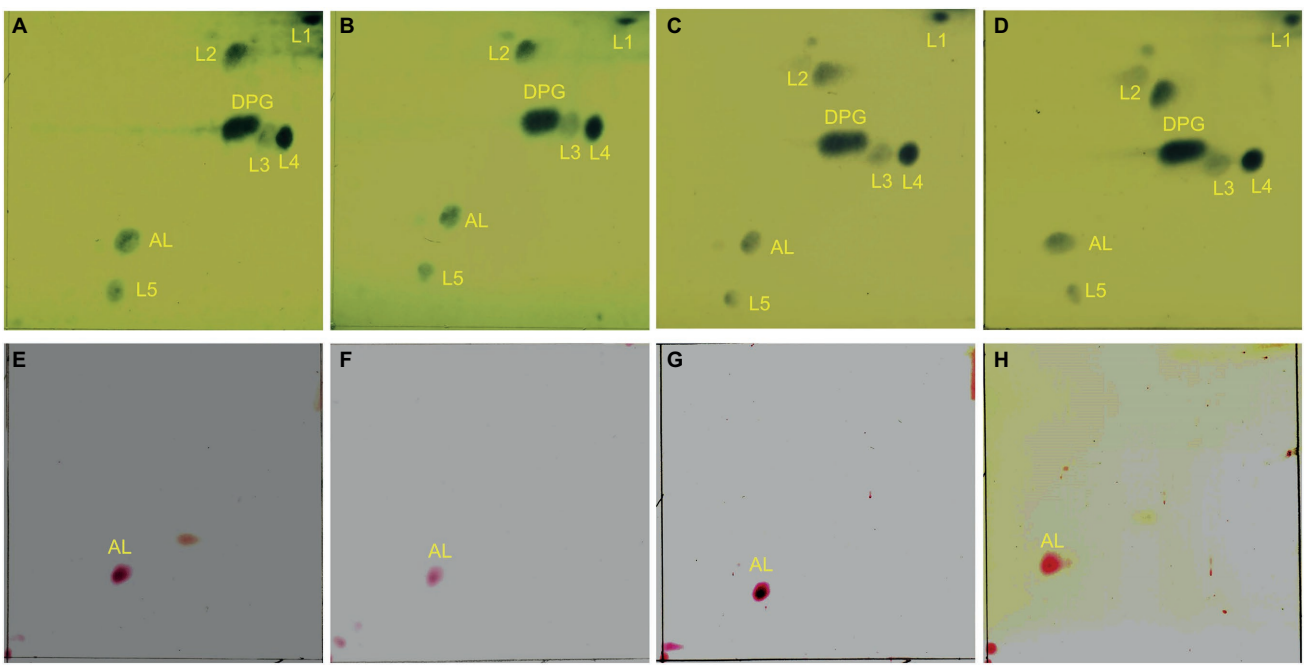

FIGURE 6 | Two-dimensional thin-layer chromatography of phospholipids in *Enterococcus faecium* EF332 strains. Panels **(A–D)** are results of phosphomolybdic acid staining, and all lipids are dyed blue; Panels **(E–H)** are results of ninhydrin staining, and aminolipids are dyed red. Panels **(A,E)** EFDO-*cls*; Panels **(B,F)** EF332-*cls*; Panels **(C,G)** EFDO-*gdpD*; Panels **(D,H)** EF332-*gdpD*. DPG: diphosphatidyl glycerol (cardiolipin); AL, aminolipids; L1–L5, lipids.

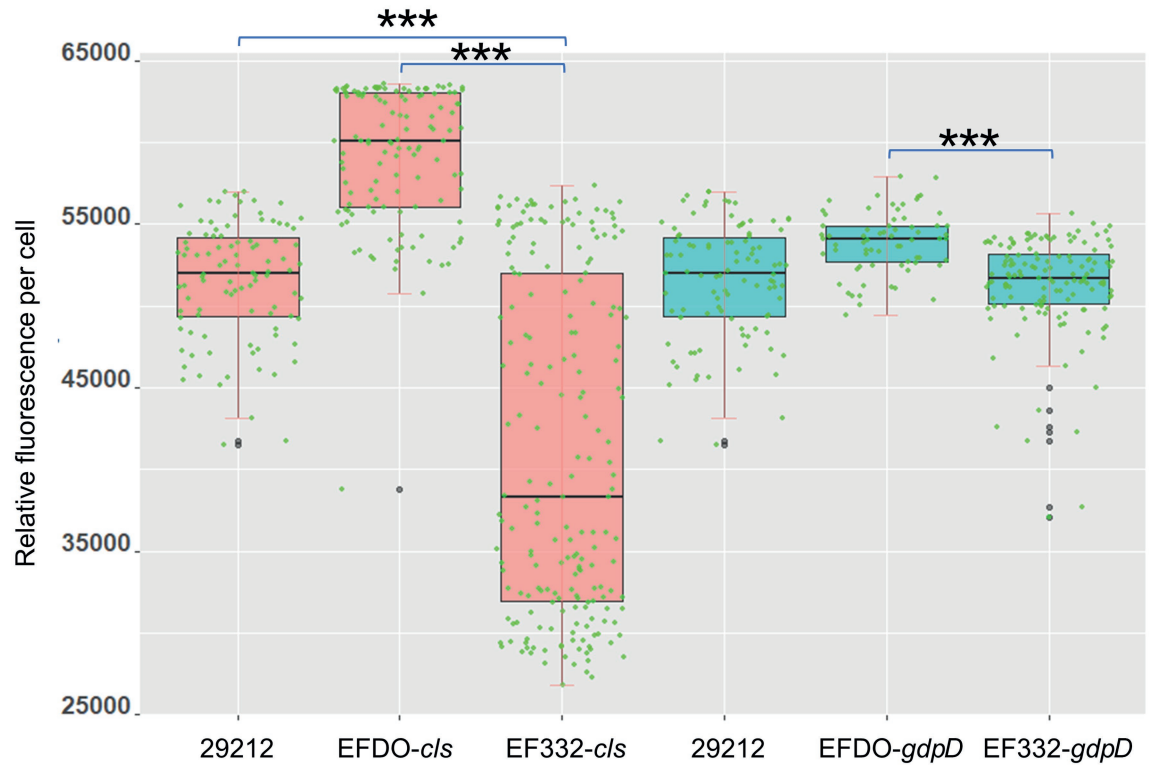

FIGURE 7 | Cell surface charge measured with PLL: FITC fluorescence. 29212, *Enterococcus faecalis* ATCC 29212, ***$p < 0.001$.

We further sought to investigate whether *cls* mutations also alter the distribution of cardiolipin produced by *cls*-encoded cardiolipin synthase. A specific cardiolipin binding fluorescent probe, 10-*N*-nonyl acridine orange (NAO), was used to observe the distribution of cardiolipins in CM. A redistribution of cardiolipin in CM was found (**Figure 8**). In *E. faecalis* ATCC 29212 (**Figures 8A,D**) and EFDO-*cls* (**Figures 8B,E**), the cardiolipin-rich regions were mainly located at the cell septum or at both poles, while in the *cls*-mutant strain EF332-*cls*, the cardiolipin-rich regions were scattered all over the cell, leading to a more even distribution and reduced abundance at septa (**Figures 8C,F**). This is in agreement with previous suggestion that daptomycin resistance may be resulted from redistribution of phospholipids and diverting DAP from effective targets at the septum (Heidary et al., 2018).

Structure Predictions Suggest That Cls Mutations May Affect Phospholipase Activity

Pfam was used to predict Cls domain structures, leading to the finding that the identified I269T mutation in this work is located in one of phospholipase D-like domains (**Figure 9**). As a three-dimensional structure of Cls is not available, we predicted its three-dimensional structure by AlphaFold 2 (**Figure 10**). Interestingly, T269 of the Cls mutant is located at the bottom of a pocket that could potentially bind substrate for catalysis (**Figure 10B**). This is in agreement with domain structure binding, which leads to the suggestion that mutations of Cls may affect the phospholipase activity of this cardiolipin synthase.

Mutations in *cls* Did Not Lead to Changes in Cell Ultrastructure

Using transmission electron microscopy, we were able to compare whether *cls* mutations caused changes in cell envelope and septa between *cls* mutant and parent strains. As shown in **Figure 11**, for parent strain *E. faecalis* ATCC 29212 and mutant strain EF332-*cls*, the cell surfaces and septum of both strains were smooth, and both single-septum (red arrows) and multiple-septum morphology (blue arrows) were observed and their morphology were similar. This result suggests that *cls* mutations does not change the structure of cell envelope.

DISCUSSION

As VRE has spread extensively and treatment options have become increasingly limited, DAP is considered to be one of last resort antibiotics for VRE. Assessing DAP resistance, particularly in a vancomycin-resistant strain, is therefore of particular interest. In this work, a DAP-resistant VRE (*E. faecium* EF332) was identified and investigated to understand its mechanism for DAP resistance. Based on whole-genome sequencing and genome comparison, new mutations of two genes associated with phospholipid metabolism, *cls* and *gdpD*, were identified and suspected to be involved in DAP resistance.

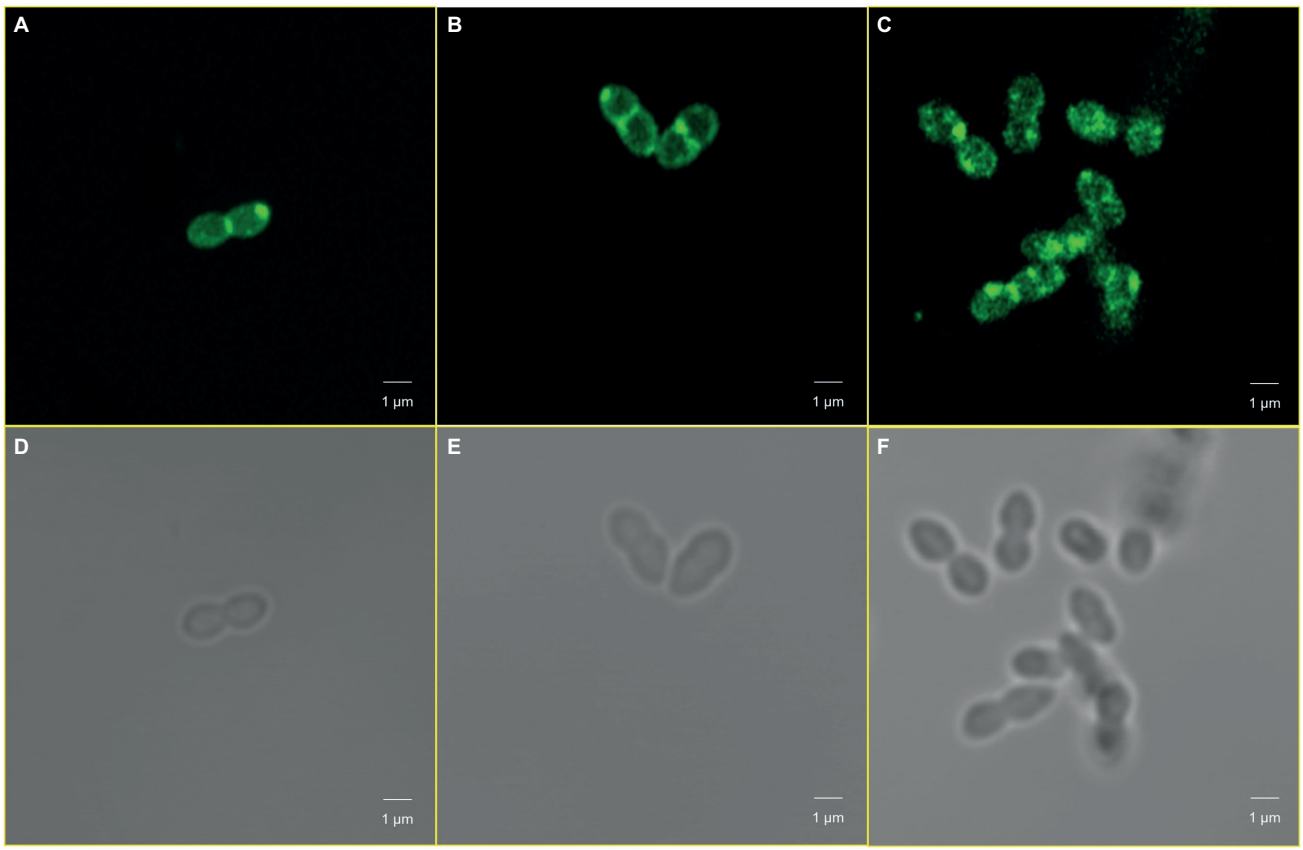

FIGURE 8 | Cardiolipin redistribution caused by *cls* mutations. Panels **(A,D)** *Enterococcus faecalis* ATCC 29212; Panels **(B,E)** EFDO-*cls*; Panels **(C,F)** EF332-*cls*.

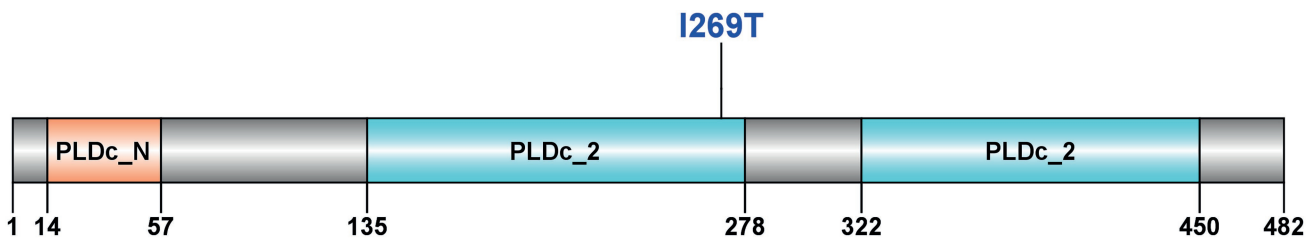

FIGURE 9 | Domain structure prediction of Cls with Pfam.

Mutations in the two genes were shown to be necessary for DAP resistance in previous studies (Arias et al., 2011). Therefore, investigations of the identified new mutations were carried out to verify their relationship with DAP resistance.

Results of this work suggest that mutations in *cls* alone can confer DAP resistance. The *cls* gene encodes a cardiolipin synthase, which catalyzes the production of cardiolipin from two molecules of phosphatidylglycerol. Previous studies have suggested that an increase in the concentration of cardiolipin in CM can divert more DAP from its target septum to other sites, thereby improving DAP resistance (Zhang et al., 2014; Tran et al., 2015). Some bacteria can change the membrane anionic microdomain to resist DAP by reducing the negatively charged membrane phospholipid composition (Mishra et al., 2017). While analysis of phospholipid composition by 2D-TLC showed that the *cls* mutations did not change the phospholipid composition of CM (including cardiolipin levels; **Figure 6**), the *cls* mutations led to decrease in negative charges on the cell surface (**Figure 7**) and may lead to a reduced adhesion to DAP. It has been reported that membrane lipids are asymmetrically distributed in the inner and outer leaflet of CM (Tannert et al., 2003). We therefore postulated that *cls* mutations do not change the level of cardiolipin synthesized but change the distribution of cardiolipin in CM, leading to reduction of cardiolipin in the outer leaflet of CM, thereby reducing membrane surface negative charges and the adhesion of DAP (Mukhopadhyay et al., 2007). It was previously suggested that DAP resistance can also be caused by redistribution of

anionic phospholipids and diverting from effective targets at the septum (Tran et al., 2013b; Heidary et al., 2018). In this work, mutations of *cls* led to a more evenly distributed cardiolipins and reduction in septa (**Figure 8C**), in agreement with this theory. Therefore, we suspect the resistance to DAP found in this work is also attributable to the redistribution of cardiolipin away from the cell septa. Both events, reduction of cellular negative charge and redistribution of phospholipids, may work together or even synergistically to complete the development of DAP resistance in *E. faecium*. We also found that *cls* mutations did not lead to changes in cell ultrastructure, which is inconsistent with the previously reported results observed in S613 (DAP susceptible) and R712 (DAP-resistant, deletion of Lys at position 61) strains (Arias et al., 2011). This may be due to different effects of different mutated sites on the cell envelope and septum.

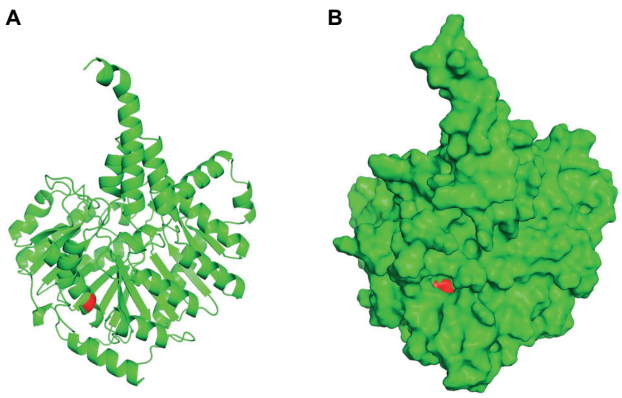

FIGURE 10 | Three-dimensional structure prediction of Cls I269T mutant. Panel **(A)**, cartoon presentation; Panel **(B)**, surface presentation. Red color indicates T269 residue.

Out of the three mutations in *cls*, both I203V and S298T are mutations to similar amino acids, while I269T is a mutation from hydrophobic residue to polar residue. We therefore speculate that I269T is the effective mutation conferring DAP resistance. This is further supported by predictions of domain structure (**Figure 9**) and three-dimensional structure (**Figure 10**), which suggests that I269T mutation may alter the catalytic activity of cardiolipin synthase. Another DAP-resistant strain of *E. faecium* found by our research team also showed the same I269T mutation (data not shown), which also supports our prediction.

Although the MIC of DAP on *E. faecium* EF332 is not high (8 μg/ml), it has a high potential transmission risk. MLST analysis revealed that the sequence type of *E. faecium* EF332 is ST192, belonging to epidemic hospital strains (clade A1), which included polyclonal complex 17 (CC17; Lebreton et al., 2013, 2018). *Enterococcus faecium* of CC17 is high-risk clonal lineages, which is often associated with nosocomial VRE outbreak and leads to severe morbidity and mortality (Lee et al., 2019). Worryingly, plasmid pEF332-2 in this study carried two high-risk gene clusters *vanA* and *vanM*. *VanA* gene clusters were also found on genomic islands GIs011 and prophage (**Figure 1**). This means that vancomycin resistance of this strain could easily disseminate, leading to higher levels of prevalence. One more thing to note is *vanM* gene has only been previously reported in Shanghai, Chengdu, Hangzhou, and Beijing in China (Chen et al., 2014, 2015; Sun et al., 2019a,b). *Enterococcus faecium* EF332 carrying *vanM* genes in this study was found in Jinan of China, suggesting that *vanM* gene may have already spread nationwide.

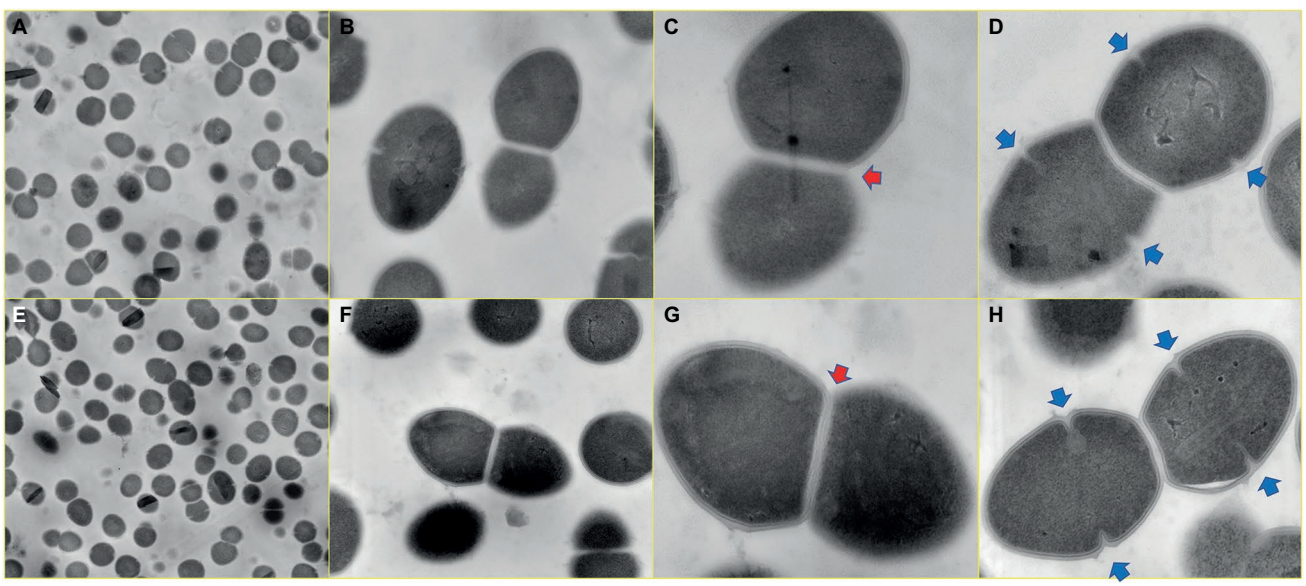

FIGURE 11 | Ultrastructure of *cls* parent and mutant strains. Panels **(A–D)** *Enterococcus faecalis* ATCC 29212; Panels **(E–H)** EF332-*cls*. Image magnifications for Panels **(A,E)**, Panels **(B,F)**, Panels **(C,G)**, and Panels **(D,H)** are 5,000, 20,000, 50,000, and 50,000, respectively. The red arrow marks a single-septum structure, and the blue arrow marks multiple-septum structures.

CONCLUSION

In this study, a clinical DAP-resistant VRE was identified. Whole-genome sequencing revealed the genetic background for multidrug resistance. A new plasmid pEF332-2 was found to carry two vancomycin resistance clusters, a rare phenomenon reported only twice so far. The genetic basis for daptomycin was investigated, suggesting new mutations in *cls* gene confer DAP resistance. The mechanisms of DAP resistance were further investigated, showing that *cls* mutations lead to significant decrease of membrane surface negative charges and the redistribution of cardiolipin in CM, both of which contribute to DAP resistance. This work reports the genetic basis of multidrug resistance of a daptomycin- and vancomycin-resistant *E. faecium*, and new mutations of *cls* that leads to resistance of daptomycin, a key last-resort antibiotic.

DATA AVAILABILITY STATEMENT

To fully understand the genetic basis of multidrug resistance in E. faecium EF332, whole-genome sequences were obtained with third-generation PacBio sequencing accompanied by second-generation Illumina sequencing (The sequencing data were deposited in GenBank with accession numbers CP058891-CP058895).

AUTHOR CONTRIBUTIONS

HX and MW designed this study and revised the manuscript. XZ was responsible for sample collection and strain identification and participated in experimental design. HS helped to analyze membrane lipid compositions. JH, LL, MZ, QC, and YM participated in the experiments and assisted in collecting experimental data. WL performed experiments, collected and analyzed the data, and wrote the draft of the manuscript. All authors contributed to the article and approved the submitted version.

FUNDING

This work was supported by the National Key Research and Development Program of China (grant number 2021YFE0199800), Key R&D Program of Shandong Province (grant number 2020CXGC011305); the National Natural Science Foundation of China (Grant numbers 31770042 and 31770043); and Shandong Provincial Natural Science Foundation (grant number ZR2020MH308).

ACKNOWLEDGMENTS

We thank Sen Wang, Haiyan Yu, and Yuyu Guo of the Core Facilities for Life and Environmental Sciences, State Key Laboratory of Microbial Technology of Shandong University for focused ion beam-scanning transmission electron microscope, inverted fluorescence microscope, and laser scanning confocal microscope analysis. We also thank Jingyi Zhu from State Key Laboratory of Microbial Technology of Shandong University for protein structure prediction.

SUPPLEMENTARY MATERIAL

The Supplementary Material for this article can be found online at: https://www.frontiersin.org/articles/10.3389/fmicb.2022.896916/full#supplementary-material

REFERENCES

Ardui, S., Ameur, A., Vermeesch, J. R., and Hestand, M. S. (2018). Single molecule real-time (SMRT) sequencing comes of age: applications and utilities for medical diagnostics. *Nucleic Acids Res.* 46, 2159–2168. doi: 10.1093/nar/gky066

Arias, C. A., and Murray, B. E. (2012). The rise of the *Enterococcus*: beyond vancomycin resistance. *Nat. Rev. Microbiol.* 10, 266–278. doi: 10.1038/nrmicro2761

Arias, C. A., Panesso, D., McGrath, D. M., Qin, X., Mojica, M. F., Miller, C., et al. (2011). Genetic basis for *in vivo* daptomycin resistance in enterococci. *N. Engl. J. Med.* 365, 892–900. doi: 10.1056/NEJMoa1011138.Genetic

Arndt, D., Grant, J. R., Marcu, A., Sajed, T., Pon, A., Liang, Y., et al. (2016). PHASTER: a better, faster version of the PHAST phage search tool. *Nucleic Acids Res.* 44, W16–W21. doi: 10.1093/nar/gkw387

Ashburner, M., Ball, C. A., Blake, J. A., Botstein, D., Butler, H., Cherry, J. M., et al. (2000). Gene ontology: tool for the unification of biology. *Nat. Genet.* 25, 25–29. doi: 10.1038/75556

Bairoch, A., and Apweiler, R. (2000). The SWISS-PROT protein sequence database and its supplement TrEMBL in 2000. *Nucleic Acids Res.* 28, 45–48. doi: 10.1128/AAC.02435-16

Bender, J. K., Cattoir, V., Hegstad, K., Sadowy, E., Coque, T. M., Westh, H., et al. (2018). Update on prevalence and mechanisms of resistance to linezolid, tigecycline and daptomycin in enterococci in Europe: towards a common nomenclature. *Drug Resist. Updat.* 40, 25–39. doi: 10.1016/j.drup.2018.10.002

Besemer, J., Lomsadze, A., and Borodovsky, M. (2001). GeneMarkS: a self-training method for prediction of gene starts in microbial genomes. Implications for finding sequence motifs in regulatory regions. *Nucleic Acids Res.* 29, 2607–2618. doi: 10.1093/nar/29.12.2607

Carver, P. L., Whang, E., VandenBussche, H. L., Kauffman, C. A., and Malani, P. N. (2003). Risk factors for arthralgias or myalgias associated with quinupristin-dalfopristin therapy. *Pharmacotherapy* 23, 159–164. doi: 10.1592/phco.23.2.159.32078

Cattoir, V., and Giard, J. C. (2014). Antibiotic resistance in *Enterococcus faecium* clinical isolates. *Expert Rev. Anti-Infect. Ther.* 12, 239–248. doi: 10.1586/14787210.2014.870886

Chen, C., Sun, J., Guo, Y., Lin, D., Guo, Q., Hu, F., et al. (2015). High prevalence of *vanM* in vancomycin-resistant *Enterococcus faecium* isolates from Shanghai, China. *Antimicrob. Agents Chemother.* 59, 7795–7798. doi: 10.1128/AAC.01732-15

Chen, C., Xu, X., Qu, T., Yu, Y., Ying, C., Liu, Q., et al. (2014). Prevalence of the fosfomycin-resistance determinant, *fosB3*, in *Enterococcus faecium* clinical isolates from China. *J. Med. Microbiol.* 63, 1484–1489. doi: 10.1099/jmm.0.077701-0

Chow, A., Win, N. N., Ng, P. Y., Lee, W., and Win, M. K. (2016). Vancomycin-resistant enterococci with reduced daptomycin susceptibility in Singapore: prevalence and associated factors. *Epidemiol. Infect.* 144, 2540–2545. doi: 10.1017/S0950268816000923

CLSI (2018). Performance standards for antimicrobial susceptibility testing. *Clin. Lab. Stand. Inst.* 1–296.

Davlieva, M., Zhang, W., Arias, C. A., and Shamoo, Y. (2013). Biochemical characterization of cardiolipin synthase mutations associated with daptomycin resistance in enterococci. *Antimicrob. Agents Chemother.* 57, 289–296. doi: 10.1128/AAC.01743-12

Depardieu, F., Podglajen, I., Leclercq, R., Collatz, E., and Courvalin, P. (2007). Modes and modulations of antibiotic resistance gene expression. *Clin. Microbiol. Rev.* 20, 79–114. doi: 10.1128/CMR.00015-06

EUCAST (2017). The European committee on antimicrobial susceptibility testing. *Eur. Comm. Antimicrob. Susceptibility Test* 1–146.

Fischer, A., Yang, S. J., Bayer, A. S., Vaezzadeh, A. R., Herzig, S., Stenz, L., et al. (2011). Daptomycin resistance mechanisms in clinically derived *Staphylococcus aureus* strains assessed by a combined transcriptomics and proteomics approach. *J. Antimicrob. Chemother.* 66, 1696–1711. doi: 10.1093/jac/dkr195

Freitas, A. R., Tedim, A. P., Novais, C., Ruiz-Garbajosa, P., Werner, G., Laverde-Gomez, J. A., et al. (2010). Global spread of the hylEfm colonization-virulence gene in megaplasmids of the *Enterococcus faecium* CC17 polyclonal subcluster. *Antimicrob. Agents Chemother.* 54, 2660–2665. doi: 10.1128/AAC.00134-10

Galperin, M. Y., Makarova, K. S., Wolf, Y. I., and Koonin, E. V. (2014). Expanded microbial genome coverage and improved protein family annotation in the COG database. *Nucleic Acids Res.* 43, D261–D269. doi: 10.1093/nar/gku1223

Gonzalez-Ruiz, A., Seaton, R. A., and Hamed, K. (2016). Daptomycin: an evidence-based review of its role in the treatment of gram-positive infections. *Infect. Drug Resist.* 9, 47–58. doi: 10.2147/IDR.S99046

Grein, F., Müller, A., Scherer, K. M., Liu, X., Ludwig, K. C., Klöckner, A., et al. (2020). Ca^{2+}-Daptomycin targets cell wall biosynthesis by forming a tripartite complex with undecaprenyl-coupled intermediates and membrane lipids. *Nat. Commun.* 11:1455. doi: 10.1038/s41467-020-15257-1

Hashimoto, Y., Taniguchi, M., Uesaka, K., Nomura, T., Hirakawa, H., Tanimoto, K., et al. (2019). Novel multidrug-resistant enterococcal mobile linear plasmid pELF1 encoding *vanA* and *vanM* gene clusters from a Japanese vancomycin-resistant enterococci isolate. *Front. Microbiol.* 10:2568. doi: 10.3389/fmicb.2019.02568

Heidary, M., Khosravi, A. D., Khoshnood, S., Nasiri, M. J., Soleimani, S., and Goudarzi, M. (2018). Daptomycin. *J. Antimicrob. Chemother.* 73, 1–11. doi: 10.1093/jac/dkx349

Herc, E. S., Kauffman, C. A., Marini, B. L., Perissinotti, A. J., and Miceli, M. H. (2017). Daptomycin nonsusceptible vancomycin resistant *Enterococcus* bloodstream infections in patients with hematological malignancies: risk factors and outcomes. *Leuk. Lymphoma* 58, 2852–2858. doi: 10.1080/10428194.2017.1312665

Ho, S. N., Hunt, H. D., Horton, R. M., Pullen, J. K., and Pease, L. R. (1989). Site-directed mutagenesis by overlap extension using the polymerase chain reaction. *Gene* 77, 51–59. doi: 10.1016/0378-1119(89)90358-2

Hogan, H. L., Hachem, R. Y., Neuhauser, M., Raad, I. I., and Coyle, E. (2010). Clinical experience of linezolid in bone marrow transplantation patients. *J. Pharm. Pract.* 23, 352–357. doi: 10.1177/0897190009358773

Hsiao, W., Wan, I., Jones, S. J., and Brinkman, F. S. L. (2003). IslandPath: aiding detection of genomic islands in prokaryotes. *Bioinformatics* 19, 418–420. doi: 10.1093/bioinformatics/btg004

Humphries, R. M., Kelesidis, T., Tewhey, R., Rose, W. E., Schork, N., Nizet, V., et al. (2012). Genotypic and phenotypic evaluation of the evolution of high-level daptomycin nonsusceptibility in vancomycin-resistant *Enterococcus faecium*. *Antimicrob. Agents Chemother.* 56, 6051–6053. doi: 10.1128/AAC.01318-12

Hussain, K., Ullah, S., Tahir, H., Alkilani, W. Z., Naeem, M., Vinod, N. R., et al. (2016). Daptomycin- vancomycin-resistant *Enterococcus faecium* native valve endocarditis: successfully treated with off-label quinupristin-dalfopristin. *J. Investig. Med. High Impact Case Rep.* 4, 3–5. doi: 10.1177/2324709616665408

Jia, B., Raphenya, A. R., Alcock, B., Waglechner, N., Guo, P., Tsang, K. K., et al. (2016). CARD 2017: expansion and model-centric curation of the comprehensive antibiotic resistance database. *Nucleic Acids Res.* 45, D566–D573. doi: 10.1093/nar/gkw1004

Jumper, J., Evans, R., Pritzel, A., Green, T., Figurnov, M., Ronneberger, O., et al. (2021). Highly accurate protein structure prediction with AlphaFold. *Nature* 596, 583–589. doi: 10.1038/s41586-021-03819-2

Kelesidis, T., Tewhey, R., and Humphries, R. M. (2013). Evolution of high-level daptomycin resistance in *Enterococcus faecium* during daptomycin therapy is associated with limited mutations in the bacterial genome. *J. Antimicrob. Chemother.* 68, 1926–1928. doi: 10.1093/jac/dkt117

Komagata, K., and Suzuki, K. I. (1988). 4 lipid and cell-wall analysis in bacterial systematics. *Methods Microbiol.* 19, 161–207. doi: 10.1016/S0580-9517(08)70410-0

LaPlante, K. L., and Rybak, M. J. (2004). Daptomycin – a novel antibiotic against gram-positive pathogens. *Expert. Opin. Pharmacother.* 5, 2321–2331. doi: 10.1517/14656566.5.11.2321

Lebreton, F., Valentino, M. D., Schaufler, K., Earl, A. M., Cattoir, V., and Gilmore, M. S. (2018). Transferable vancomycin resistance in clade B commensal-type *Enterococcus faecium*. *J. Antimicrob. Chemother.* 73, 1479–1486. doi: 10.1093/jac/dky039

Lebreton, F., van Schaik, W., Manson McGuire, A., Godfrey, P., Griggs, A., Mazumdar, V., et al. (2013). Emergence of epidemic multidrug-resistant *Enterococcus faecium* from animal and commensal strains. *MBio* 4:00534-13. doi: 10.1128/mBio.00534-13

Lee, T., Pang, S., Abraham, S., and Coombs, G. W. (2019). Antimicrobial-resistant CC17 *Enterococcus faecium*: the past, the present and the future. *J. Glob. Antimicrob. Resist.* 16, 36–47. doi: 10.1016/j.jgar.2018.08.016

Lellek, H., Franke, G. C., Ruckert, C., Wolters, M., Wolschke, C., Christner, M., et al. (2015). Emergence of daptomycin non-susceptibility in colonizing vancomycin-resistant *Enterococcus faecium* isolates during daptomycin therapy. *Int. J. Med. Microbiol.* 305, 902–909. doi: 10.1016/j.ijmm.2015.09.005

Li, W., Jaroszewski, L., and Godzik, A. (2002). Tolerating some redundancy significantly speeds up clustering of large protein databases. *Bioinformatics* 18, 77–82. doi: 10.1093/bioinformatics/18.1.77

Matsumoto, K., Takeshita, A., Ikawa, K., Shigemi, A., Yaji, K., Shimodozono, Y., et al. (2010). Higher linezolid exposure and higher frequency of thrombocytopenia in patients with renal dysfunction. *Int. J. Antimicrob. Agents* 36, 179–181. doi: 10.1016/j.ijantimicag.2010.02.019

Mileykovskaya, E., Dowhan, W., Birke, R. L., Zheng, D., Lutterodt, L., and Haines, T. H. (2001). Cardiolipin binds nonyl acridine orange by aggregating the dye at exposed hydrophobic domains on bilayer surfaces. *FEBS Lett.* 507, 187–190. doi: 10.1016/S0014-5793(01)02948-9

Mishra, N. N., Tran, T. T., Seepersaud, R., Garcia-De-La-Maria, C., Faull, K., Yoon, A., et al. (2017). Perturbations of phosphatidate cytidylyltransferase (CdsA) mediate daptomycin resistance in *Streptococcus mitis/oralis* by a novel mechanism. *Antimicrob. Agents Chemother.* 61, 1–13. doi: 10.1128/AAC.02435-16

Mistry, J., Chuguransky, S., Williams, L., Qureshi, M., Salazar, G. A., Sonnhammer, E. L. L., et al. (2021). Pfam: The protein families database in 2021. *Nucleic Acids Res.* 49, D412–D419. doi: 10.1093/nar/gkaa913

Mukhopadhyay, K., Whitmire, W., Xiong, Y. O., Molden, J., Jones, T., Peschel, A., et al. (2007). *In vitro* susceptibility of *Staphylococcus aureus* to thrombin-induced platelet microbicidal protein-1 (tPMP-1) is influenced by cell membrene phospholipid composition and asymmetry. *Microbiology* 153, 1187–1197. doi: 10.1099/mic.0.2006/003111-0

Munoz-Price, L. S., Lolans, K., and Quinn, J. P. (2005). Emergence of resistance to daptomycin during treatment of vancomycin-resistant *Enterococcus faecalis* infection. *Clin. Infect. Dis.* 41, 565–566. doi: 10.1086/432121

Prater, A. G., Mehta, H. H., Beabout, K., Supandy, A., Miller, W. R., Tran, T. T., et al. (2021). Daptomycin resistance in *Enterococcus faecium* can be delayed by disruption of the LiaFSR stress response pathway. *Antimicrob. Agents Chemother.* 65, 1–6. doi: 10.1128/AAC.01317-20

Prater, A. G., Mehta, H. H., Kosgei, A. J., Miller, W. R., Tran, T. T., Arias, C. A., et al. (2019). Environment shapes the accessible daptomycin resistance mechanisms in *Enterococcus faecium*. *Antimicrob. Agents Chemother.* 63, 3–5. doi: 10.1128/AAC.00790-19

Punta, M., Coggill, P. C., Eberhardt, R. Y., Mistry, J., Tate, J., Boursnell, C., et al. (2011). The Pfam protein families database. *Nucleic Acids Res.* 32, 138D–1141D. doi: 10.1093/nar/gkh121

Qian, Y., and Zhao, X. (2014). A comparison of methods for the extraction of bacterial genomic DNA in rat feces. *Sci. Technol. Food Ind.* 35, 166–169. doi: 10.13386/j.issn1002-0306.2014.04.005

Ren, J., Wen, L., Gao, X., Jin, C., Xue, Y., and Yao, X. (2009). DOG 1.0: illustrator of protein domain structures. *Cell Res.* 19, 271–273. doi: 10.1038/cr.2009.6

Saier, M. H. Jr., Reddy, V. S., Tamang, D. G., and Västermark, Å. (2013). The transporter classification database. *Nucleic Acids Res.* 42, D251–D258. doi: 10.1093/nar/gkt1097

Schwarz, F. V., Perreten, V., and Teuber, M. (2001). Sequence of the 50-kb conjugative multiresistance plasmid pRE25 from *Enterococcus faecalis* RE25. *Plasmid* 46, 170–187. doi: 10.1006/plas.2001.1544

Sletvold, H., Johnsen, P. J., Simonsen, G. S., Aasnæs, B., Sundsfjord, A., and Nielsen, K. M. (2007). Comparative DNA analysis of two *vanA* plasmids

from *Enterococcus faecium* strains isolated from poultry and a poultry farmer in Norway. *Antimicrob. Agents Chemother.* 51, 736–739. doi: 10.1128/AAC.00557-06

Suleyman, G., Mahan, M., and Zervos, M. J. (2017). Comparison of daptomycin and linezolid in the treatment of vancomycin-resistant *Enterococcus faecium* in the absence of endocarditis. *Infect. Dis. Clin. Pract.* 25, 151–154. doi: 10.1097/IPC.0000000000000482

Sun, H. L., Liu, C., Zhang, J. J., Zhou, Y. M., and Xu, Y. C. (2019a). Molecular characterization of vancomycin-resistant enterococci isolated from a hospital in Beijing, China. *J. Microbiol. Immunol. Infect.* 52, 433–442. doi: 10.1016/j.jmii.2018.12.008

Sun, L., Qu, T., Wang, D., Chen, Y., Fu, Y., Yang, Q., et al. (2019b). Characterization of *vanM* carrying clinical *Enterococcus* isolates and diversity of the suppressed *vanM* gene cluster. *Infect. Genet. Evol.* 68, 145–152. doi: 10.1016/j.meegid.2018.12.015

Sun, L., Xu, J., Wang, W., and He, F. (2020). Emergence of *vanA*-type vancomycin-resistant *Enterococcus faecium* ST 78 strain with a rep2-type plasmid carrying a Tn1546-like element isolated from a urinary tract infection in China. *Infect. Drug Resist.* 13, 949–955. doi: 10.2147/IDR.S247569

Tannert, A., Pohl, A., Pomorski, T., and Herrmann, A. (2003). Protein-mediated transbilayer movement of lipids in eukaryotes and prokaryotes: the relevance of ABC transporters. *Int. J. Antimicrob. Agents* 22, 177–187. doi: 10.1016/S0924-8579(03)00217-6

Tran, T. T., Munita, J. M., and Arias, C. A. (2015). Mechanisms of drug resistance: daptomycin resistance. *Ann. N. Y. Acad. Sci.* 1354, 32–53. doi: 10.1111/nyas.12948

Tran, T. T., Panesso, D., Gao, H., Roh, J. H., Munita, J. M., Reyes, J., et al. (2013a). Whole-genome analysis of a daptomycin-susceptible *Enterococcus faecium* strain and its daptomycin-resistant variant arising during therapy. *Antimicrob. Agents Chemother.* 57, 261–268. doi: 10.1128/AAC.01454-12

Tran, T. T., Panesso, D., Mishra, N. N., Mileykovskaya, E., Guan, Z., Munita, J. M., et al. (2013b). Daptomycin-resistant *Enterococcus faecalis* diverts the antibiotic molecule from the division septum and remodels cell membrane phospholipids. *MBio* 4:e00281-13. doi: 10.1128/mBio.00281-13

Uttley, A. C., Collins, C. H., Naidoo, J., and George, R. C. (1988). Vancomycin-resistant enterococci. *Lancet* 331, 57–58. doi: 10.1016/S0140-6736(88)91037-9

Vading, M., Samuelsen, H. B., Sundsfjord, A. S., and Giske, C. G. (2011). Comparison of disk diffusion, Etest and VITEK2 for detection of carbapenemase-producing *Klebsiella pneumoniae* with the EUCAST and CLSI breakpoint systems. *Clin. Microbiol. Infect.* 17, 668–674. doi: 10.1111/j.1469-0691.2010.03299.x

Zhang, T. H., Muraih, J. K., Tishbi, N., Herskowitz, J., Victor, R. L., Silverman, J., et al. (2014). Cardiolipin prevents membrane translocation and permeabilization by daptomycin. *J. Biol. Chem.* 289, 11584–11591. doi: 10.1074/jbc.M114.554444

Zhou, Y., Liang, Y., Lynch, K. H., Dennis, J. J., and Wishart, D. S. (2011). PHAST: A fast phage search tool. *Nucleic Acids Res.* 39, W347–W352. doi: 10.1093/nar/gkr485

Conflict of Interest: The authors declare that the research was conducted in the absence of any commercial or financial relationships that could be construed as a potential conflict of interest.

Publisher's Note: All claims expressed in this article are solely those of the authors and do not necessarily represent those of their affiliated organizations, or those of the publisher, the editors and the reviewers. Any product that may be evaluated in this article, or claim that may be made by its manufacturer, is not guaranteed or endorsed by the publisher.

frontiers | Frontiers in Microbiology

ORIGINAL RESEARCH
published: 30 June 2022
doi: 10.3389/fmicb.2022.934525

Ecological Effects of Daily Antiseptic Treatment on Microbial Composition of Saliva-Grown Microcosm Biofilms and Selection of Resistant Phenotypes

*Xiaojun Mao[1†], Andreas Hiergeist[2†], David L. Auer[1], Konstantin J. Scholz[1], Denise Muehler[1], Karl-Anton Hiller[1], Tim Maisch[3], Wolfgang Buchalla[1], Elmar Hellwig[4], André Gessner[2], Ali Al-Ahmad[4] and Fabian Cieplik[1]**

[1] Department of Conservative Dentistry and Periodontology, University Hospital Regensburg, Regensburg, Germany, [2] Institute of Clinical Microbiology and Hygiene, University Hospital Regensburg, Regensburg, Germany, [3] Department of Dermatology, University Hospital Regensburg, Regensburg, Germany, [4] Department of Operative Dentistry and Periodontology, Center for Dental Medicine, University of Freiburg, Freiburg im Breisgau, Germany

OPEN ACCESS

Edited by:
Rustam Aminov,
University of Aberdeen,
United Kingdom

Reviewed by:
Sigrun Eick,
University of Bern, Switzerland
Lei Cheng,
Sichuan University, China

***Correspondence:**
Fabian Cieplik
fabian.cieplik@ukr.de

† These authors have contributed equally to this work and share first authorship

Specialty section:
This article was submitted to Antimicrobials, Resistance and Chemotherapy, a section of the journal Frontiers in Microbiology

Received: 02 May 2022
Accepted: 25 May 2022
Published: 30 June 2022

Citation:
Mao X, Hiergeist A, Auer DL, Scholz KJ, Muehler D, Hiller K-A, Maisch T, Buchalla W, Hellwig E, Gessner A, Al-Ahmad A and Cieplik F (2022) Ecological Effects of Daily Antiseptic Treatment on Microbial Composition of Saliva-Grown Microcosm Biofilms and Selection of Resistant Phenotypes. Front. Microbiol. 13:934525. doi: 10.3389/fmicb.2022.934525

Antiseptics are widely used in dental practice and included in numerous over-the-counter oral care products. However, the effects of routine antiseptic use on microbial composition of oral biofilms and on the emergence of resistant phenotypes remain unclear. Microcosm biofilms were inoculated from saliva samples of four donors and cultured in the *Amsterdam Active Attachment* biofilm model for 3 days. Then, they were treated two times daily with chlorhexidine digluconate (CHX) or cetylpyridinium chloride (CPC) for a period of 7 days. Ecological changes upon these multiple antiseptic treatments were evaluated by semiconductor-based sequencing of bacterial 16S rRNA genes and identification of amplicon sequence variants (ASVs). Furthermore, culture-based approaches were used for colony-forming units (CFU) assay, identification of antiseptic-resistant phenotypes using an agar dilution method, and evaluation of their antibiotic susceptibilities. Both CHX and CPC showed only slight effects on CFU and could not inhibit biofilm growth despite the two times daily treatment for 7 days. Both antiseptics showed significant ecological effects on the microbial compositions of the surviving microbiota, whereby CHX led to enrichment of rather caries-associated saccharolytic taxa and CPC led to enrichment of rather gingivitis-associated proteolytic taxa. Antiseptic-resistant phenotypes were isolated on antiseptic-containing agar plates, which also exhibited phenotypic resistance to various antibiotics. Our results highlight the need for further research into potential detrimental effects of antiseptics on the microbial composition of oral biofilms and on the spread of antimicrobial resistance in the context of their frequent use in oral healthcare.

Keywords: chlorhexidine, cetylpyridinium chloride, antiseptic, biofilm, resistance, biocide, antibiotic, dysbiosis

INTRODUCTION

At present, a wide variety of antiseptics are available as over-the-counter consumer products for daily use in oral care (van der Weijden et al., 2015; Figuero et al., 2019). The use of antiseptic mouthwashes as adjunct to mechanical removal of biofilm and use of fluorides has been recommended for certain high-risk patient populations, such as patients with intellectual disabilities (Waldron et al., 2019), patients following surgical procedures, such as periodontal or implant surgery (Solderer et al., 2019), with fixed orthodontic appliances (Pithon et al., 2015), or elderly persons who are restricted in performing tooth-brushing or other oral hygiene procedures themselves (Grönbeck Lindén et al., 2017). More recently, since the COVID-19 pandemic, antiseptic mouthwashes are also applied as preprocedural mouthrinses for potentially reducing the viral load and infectivity of SARS-CoV-2 in the oral cavity and dental aerosols (Gottsauner et al., 2020; Carrouel et al., 2021; Meister et al., 2022).

Chlorhexidine digluconate (CHX), a symmetric bis-biguanide molecule carrying two positive charges, and cetylpyridinium chloride (CPC), a monocationic quaternary ammonium compound (QAC), can be regarded as the most common antiseptics for dental professional use and as ingredients in oral care products (Jones, 1997; Haps et al., 2008; Sanz et al., 2013; van der Weijden et al., 2015; Cieplik et al., 2019a; Mao et al., 2020). While both CHX and CPC are highly effective against planktonic bacteria (Cieplik et al., 2019a; So Yeon and Si Young, 2019; Mao et al., 2020), it is well known that eradicating bacterial cells in biofilms is much more difficult than killing planktonic bacteria and usually requires the antiseptic concentrations of about 100–1,000 times higher than those required to eliminate planktonic bacteria (Ceri et al., 1999; Shani et al., 2000). Accordingly, in a classic study, Zaura-Arite et al. (2001) showed that treatment with 0.2% CHX for a clinically relevant treatment period of 1 min had some effects on the outer layers of biofilms formed *in situ* for 48 h, but did not affect their inner layers. Likewise, a previous study by our group showed that a single treatment with CHX (0.1 or 0.2%) or CPC (0.05 or 0.1%) on 72 h saliva-grown microcosm biofilms resulted in colony-forming unit (CFU) reductions of only less than 1 $\log_{10}$ step (Schwarz et al., 2021). The biofilm matrix may be the main cause for this low antibacterial efficacy acting as a diffusion barrier for positively charged antiseptics such as CHX or CPC (Jakubovics et al., 2021). Therefore, it seems reasonable that bacteria in deeper layers of biofilms will be exposed to subinhibitory antiseptic concentrations upon application of antiseptic-containing mouthwash (Cieplik et al., 2019a; Mao et al., 2020; Schwarz et al., 2021; Muehler et al., 2022). Previous studies have shown that repeated exposure to subinhibitory concentrations of CHX or CPC *in vitro* may lead to phenotypic adaptation of bacteria to these antiseptics (Kitagawa et al., 2016; Cieplik et al., 2019a; Verspecht et al., 2019; Mao et al., 2020; Schwarz et al., 2021; Auer et al., 2022). Furthermore, selection pressure due to antiseptic treatment may lead to selection of antibiotic-resistant strains (Wand et al., 2017; Verspecht et al., 2019). Accordingly, we recently analyzed the transcriptomic stress response following sublethal treatment of *Streptococcus mutans* with CHX by RNA-sequencing and found considerable numbers of genes and pathways significantly upregulated or downregulated (Muehler et al., 2022). Particularly, upregulation of pathways related to stress response, increased biofilm formation, and regulation of membrane-transporters such as ATP-binding cassettes (ABC) may be linked to development of (cross-)resistances (Muehler et al., 2022).

Despite those concerns about limited antibacterial efficacy and potential risks of resistance, it is also not entirely understood which ecological changes in microbial composition of oral biofilms are induced by the routine use of antiseptic mouthwashes (Al-Kamel et al., 2019; Bescos et al., 2020a; Chatzigiannidou et al., 2020; Brookes et al., 2021; Zayed et al., 2022). Two recent studies have shown that antiseptic treatment of *in vitro* biofilms affected their microbial composition and may potentially result in ecological shifts toward increased abundance of pathobionts (Chatzigiannidou et al., 2020; Zayed et al., 2022).

Therefore, the aim for this study was first, to investigate ecological changes in mature saliva-grown microcosm biofilms upon two times daily application of CHX and CPC for a period of 7 days, and second, to evaluate, whether suchlike multiple application of CHX or CPC selects for resistant phenotypes.

MATERIALS AND METHODS

Test Substances

Chlorhexidine digluconate (CHX; Sigma C9394) and cetylpyridinium chloride (CPC; Merck 6,002,006; both: Merck, Darmstadt, Germany) were used as antiseptics in the present study. CHX and CPC were both dissolved in dH_2O and diluted to the respective treatment concentrations (0.1% and 0.2% for CHX, 0.05% and 0.1% for CPC).

Saliva Collection

Four healthy volunteers (age range: 30–32 years) with no untreated dental caries, periodontitis, or other oral diseases, and no intake of antibiotics within the past 3 months volunteered for collection of saliva. Written informed consents were obtained after a detailed description of the study outline. The study protocol had been approved by the internal review board of the University of Regensburg (ref. 17-782_1-101).

The sampling was performed as described earlier (Schwarz et al., 2021). Unstimulated saliva was collected using the spitting method (Navazesh and Christensen, 1982) with the volunteers not having consumed anything except water on the respective day. The volunteers were asked to let saliva gather on the bottom of their mouth and spit into a tube every 30 s for a total period of 10 min. For separating aggregated bacteria, the collected saliva was vortexed (REAX top, Heidolph Instruments, Schwabach, Germany) for 10 s, placed in an ultrasonic water-bath chamber (Sonorex Super RK 102 H, Bandelin, Berlin, Germany; 35 kHz) for 2 min, and vortexed again for 10 s. Afterwards, saliva was divided into two aliquots, i.e., 2 ml was used for immediate biofilm inoculation and 50 μl was used as a baseline sample for

16S rRNA sequencing. For baseline samples, microbial nucleic acids were immediately stabilized by mixing 50 µl of the saliva 1:2 with magic PBI microbiome preservation buffer (microBIOMix GmbH, Regensburg, Germany). Stabilized samples were stored at –80°C until further processing.

Inoculation and Culture of Saliva-Derived Microcosm Biofilms

Biofilms were cultured using the so-called *Amsterdam Active Attachment* (AAA) biofilm model, which is based on active attachment of the bacteria to a substrate. The AAA model consists of a custom-made stainless-steel lid with 24 clamps, which contain the respective substrates, and fits on top of a 24-well polystyrene microtiter plate, thus allowing 24 individual biofilms to form (Exterkate et al., 2010; Cieplik et al., 2019b; Schwarz et al., 2021). For the present study, hydroxyapatite (HAP) disks (9.5 mm diameter, 2 mm thickness; Clarkson Chromatography Products, South Williamsport, PA, United States) were used as a substrate in the AAA model. As a basal nutrient broth, the complete saliva broth as described by Pratten et al. (1998) was modified by adding sucrose (final concentration: 0.1%) for mimicking caries-associated conditions (caries broth; CB), as described earlier (Schwarz et al., 2021). For inoculation of the biofilms, 800 µl of the collected saliva was mixed with 40 ml CB and vigorously vortexed. Subsequently, 1.5 ml was added per each well of a 24-well plate (Corning® Costar®, Corning, NY, United States). The steel lids containing HAP disks were placed upon, and the AAA models were incubated anaerobically (80% N_2, 10% CO_2, 10% H_2) at 37°C in a microincubator (MI23NK, SCHOLZEN Microbiology Systems, St. Margrethen, Switzerland) for 8 h thus allowing initial attachment to the HAP disks. After this initial attachment period, the lids containing the HAP disks were carefully moved up and down to remove loosely bound bacteria and transferred to 24-well plates containing fresh CB. Medium was refreshed again in the same way after 24 and 48 h of culture.

Two Times Daily Treatment of Saliva-Grown Microcosm Biofilms

After 72 h of culture, the biofilms were treated by placing the steel lid containing the HAP disks in a new 24-well plate containing either 0.1% CHX, 0.05% CPC, or 0.9% NaCl as a negative control for a treatment period of 5 min. Subsequently, the steel lid was placed in a new 24-well plate containing 0.9% NaCl to carefully wash the biofilms. This washing procedure was performed two times. Then, the steel lid was finally placed back onto a new 24-well plate containing fresh CB and incubated again anaerobically at 37°C. The biofilms were treated daily at 8 am and 4 pm for a period of 7 days resulting in 14 treatments. For each of the four donors, eight biofilms formed on separate HAP disks were used for treatment with 0.1% CHX, 0.05% CPC, or 0.9% NaCl each.

Harvesting of the Biofilms

After 7 days of treatment with CHX, CPC, or NaCl two times daily, all biofilms were harvested by carefully removing the HAP disks from the lids using sterile forceps and transferring them to 5 ml Eppendorf tubes containing 1 ml of phosphate-buffered saline (PBS; Biochrom, Berlin, Germany). Biofilm dispersal was ensured by vortexing for 10 s, placing in an ultrasonic water-bath chamber (35 kHz) for 10 min, and vortexing again for 10 s, and confirmed visually. From those harvested samples, 50 µl was immediately stabilized by mixing with 250 µl magic PBI microbiome preservation buffer and stored at –80°C until further processing. The remaining 750 µl was immediately used for culture-based analysis.

Extraction of Nucleic Acids and Semiconductor-Based Sequencing of Bacterial 16S rRNA Genes

Extraction of nucleic acids and semiconductor-based sequencing of bacterial 16S rRNA genes was performed, as described previously (Schwarz et al., 2021). First, pre-lysis of microbial cells was performed by mechanical cell disruption using repeated bead beating. Therefore, the total volumes of 150 µl (inoculum samples) or 300 µl (biofilm samples) stabilized sample material, respectively, were added into lysing matrix Y tubes (MP Biomedicals, Eschwege, Germany) and further processed in the TissueLyser II instrument (Qiagen, Hilden, Germany) at 60 Hz for 3 × 1 min. Nucleic acids were purified from total crude cell extracts using the MagNA Pure 96 instrument (Roche Diagnostics, Mannheim, Germany). Quantification of total nucleic acids was carried out by means of the NanoDrop™ 1000 spectrophotometer (Thermo Fisher Scientific, Darmstadt, Germany).

Copy numbers of bacterial 16S rRNA genes were quantified in nucleic acid extracts by qRT-PCR, as described earlier (Hiergeist et al., 2016). Subsequently, V1–V3 hypervariable regions of bacterial 16S rRNA genes were amplified from a total of 1e + 7 bacterial 16S rDNA copies for each sample using primer S-D-Bact-0008-c-S-20 containing a 10-bp barcode sequence and IonTorrent-specific sequencing adaptor A, and S-D-Bact-0517-a-A-18 containing a 3'-P1 adapter sequence using the Platinum II Taq Hot-Start DNA Polymerase (Thermo Fisher Scientific). After 30 PCR cycles, amplicons were purified two times with a 0.8 bead to DNA ratio using MagSi-NGS^{PREP} Plus beads (Steinbrenner Laborsysteme, Wiesenbach, Germany). Copy numbers of amplicons containing sequencing-adaptors were determined using the KAPA Library Quantification IonTorrent Kit (Roche Diagnostics) and pooled to equimolar amplicon concentrations of each sample. A total of 120 attomol of the final library pool was subjected to isothermal amplification with the IonChef instrument before running 1350 flow cycles during high-throughput sequencing on an Ion Torrent™ S5 Plus machine (Thermo Fisher Scientific).

Sequence Processing and Identification of Amplicon Sequence Variants

First, amplification primer and adapter sequences and low-quality bases were removed using cutadapt 3.5 and Trimmomatic 0.39. Cutadapt was also used for demultiplexing of filtered reads

allowing no errors. All subsequent analyses were conducted with R 4.1.2. Here, the resulting reads (19,573 ± 7,048) were subjected to denoising sequencing data and generation of Amplicon Sequence Variants (ASVs) using dada2 (version 1.16). An unrooted phylogenetic tree was calculated with FastTree 2.1 after sequence alignment with DECIPHER 2.20 for later calculation of UniFrac distances with the phyloseq package. The IDTAXA algorithm and the All-Species Living Tree Project (LTP) reference database 12.2021 release was used for taxonomic classification of ASVs. Significantly altered taxa between groups were assessed with the linear discriminant analysis (LDA) effect size (LEfSe) method which is included within the microbiomeMarker R package (Cao, 2021). All plots were generated using the ggpubr 0.4 package.

Colony-Forming Units Assay, Identification of Antiseptic-Resistant Phenotypes, and Evaluation of Antibiotic Susceptibility

Immediately after harvesting the biofilms, 10-fold serial dilutions (10^{-1} to 10^{-7}) were prepared in PBS and aliquots (180 μl) were plated on Schaedler blood agar plates for determination of total CFU following the two times daily treatment with CHX, CPC, or NaCl over 7 days, and incubated anaerobically at 37°C for 72 h. Afterward, CFU were evaluated.

Furthermore, aliquots (180 μl) from the lowest dilution steps (10^{-1} to 10^{-4}) were plated on Schaedler blood agar plates containing 0.1 or 0.2% CHX for CHX-treated and NaCl-treated biofilms or containing 0.05 or 0.1% CPC for CPC-treated and NaCl-treated biofilms in order to investigate for antiseptic-resistant phenotypes. After anaerobic incubation at 37°C for 72 h, the plates were evaluated for growth of antiseptic-resistant phenotypes. Those colonies were first discriminated according to their respective colony morphology and separated by sub-culturing on fresh agar plates. These colonies were identified at the species level by means of matrix-assisted laser desorption/ionization time-of-flight mass spectrometry (MALDI-TOF MS) employing a Microflex mass spectrometer and BioTyper analysis software (both from Bruker, Billerica, MA, United States), as described earlier (Cieplik et al., 2020).

The antiseptic-resistant isolates (despite Enterobacteriaceae) were analyzed for their antibiotic susceptibilities by means of the ETEST® method (bioMérieux, Marcy l'Etoile, France). In brief, suspensions (McFarland 1.0) of *Capnocytophaga*, *Fusobacterium*, and *Veillonella* spp. were inoculated on Brucella blood agar (bioMérieux), *Campylobacter* spp. on Mueller-Hinton (MH) agar with horse blood (Oxoid, Wesel, Germany), and *Neisseria* spp. on MH blood agar (Oxoid), and the ETEST® strips were placed on the agar plates. Results were evaluated following incubation for 48 h at 37°C under microaerophilic (*Campylobacter* spp.) or anaerobic (*Capnocytophaga*, *Fusobacterium*, *Veillonella,* and *Neisseria* spp.) conditions. Using ETEST®, the following antibiotics were investigated: penicillin G, ampicillin, amoxicillin/clavulanic acid, piperacillin/tazobactam, imipenem, ceftriaxone/cefotaxime, ceftazidime, ciprofloxacin, erythromycin, clindamycin, tetracycline, and metronidazole.

Antibiotic susceptibilities of Enterobacteriaceae were tested using the BD Phoenix NMIC panel (Becton Dickinson, Sparks, MD, United States) according to the instructions of the manufacturer for the following antibiotics: ampicillin/amoxicillin, amoxicillin/clavulanic acid, piperacillin, piperacillin/tazobactam, imipenem, meropenem, ertapenem, aztreonam, cefuroxime, cefoxitin, ceftriaxone/cefotaxime, ceftazidime, cefepime, ciprofloxacin, levofloxacin, gentamicin, amikacin, tobramycin, fosfomycin, and trimethoprim/sulfamethoxazole. Interpretation of the results of both methods was done according to the EUCAST (European Committee on Antimicrobial Susceptibility Testing) 12.0 guidelines, and susceptibility was determined as susceptible (S), intermediate (I), or resistant (R), whereby non-species related breakpoints were used if no species-specific breakpoints were available.

RESULTS

Microbial Composition of Saliva-Grown Microcosm Biofilms and Ecological Effects of Daily Treatment With Chlorhexidine Digluconate or Cetylpyridinium Chloride

A total of 4,036 (mean 294 ± 115 per sample) amplicon sequence variants (ASVs) were detected by high-throughput sequencing of V1–V3 variable regions of bacterial 16S rRNA genes. Alpha-diversity represented by the number of detected ASVs (**Figure 1A**) and the Effective Shannon Index (**Figure 1B**) was significantly lower in CHX-treated biofilms (mean 203 ± 72 ASVs; mean 19 ± 11 Shannon) as compared to NaCl-treated (mean 344 ± 84 ASVs; mean 63 ± 16 Shannon) or CPC-treated biofilms (mean 335 ± 125 ASVs; mean 59 ± 25 Shannon) with no significant differences between the latter.

Figure 2 depicts a heatmap of ASV abundance on genus level for NaCl-treated, CHX-treated, and CPC-treated biofilms from all four donors. The biofilms show a diverse microbial composition with *Streptococcus*, *Veillonella*, *Fusobacterium*, *Haemophilus*, and *Granulicatella* spp. being the most abundant. The heatmap clearly depicts the differences in microbial composition between the biofilms from different donors as well depending on the respective treatment. Accordingly, beta-diversity based on weighted UniFrac distances showed clear clustering depending on the donor (**Figure 3A**; Adonis $R^2 = 0.25$, p.adj = 0.001) and also regarding their respective treatment (**Figure 3B**; Adonis $R^2 = 0.41$, p.adj = 0.001).

Several ASVs were found to be discriminatory between the biofilms treated by CHX, CPC, or NaCl, as revealed by LefSE (**Figure 4**). Accordingly, the CHX-treated biofilms were characterized by the enrichment of several ASVs within the orders Lactobacillales (mainly *Streptococcus* and *Granulicatella* spp.), Neisseriales (mainly *Neisseria* spp.), and Actinomycetales (mainly *Schaalia* spp.). In contrast, CPC-treated biofilms were enriched by several ASVs within the orders Fusobacteriales (mainly *Fusobacterium* and *Leptotrichia* spp.), Selenomonadales

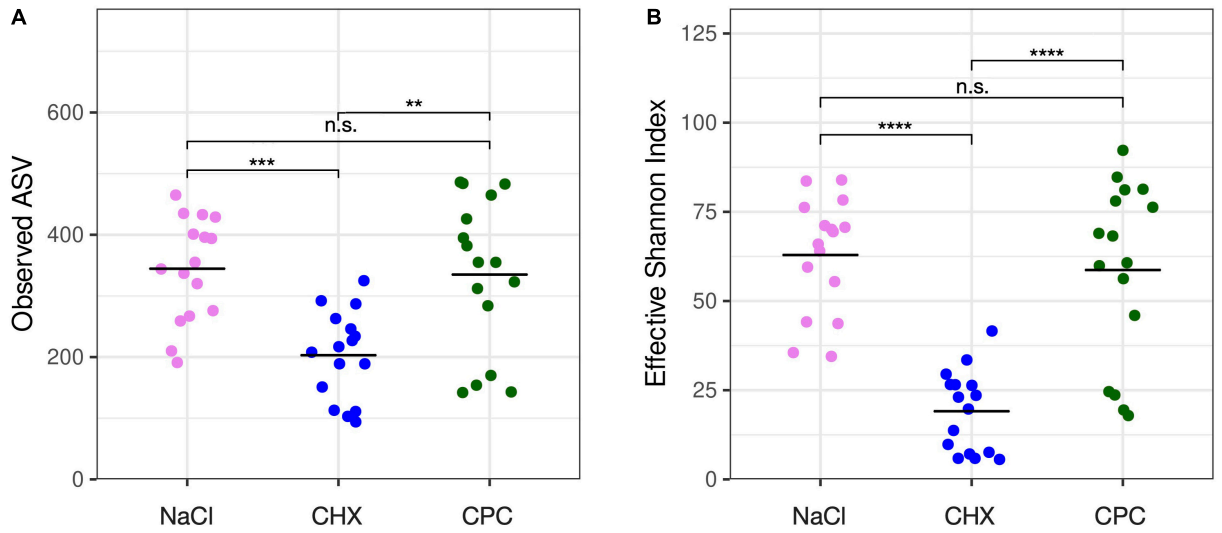

FIGURE 1 | Alpha-diversity of the biofilms as shown by observed ASVs **(A)** and effective Shannon index **(B)**. CHX-treated biofilms showed significantly lower alpha-diversity as compared to NaCl-treated or CPC-treated biofilms with no significant differences between the latter. Significance levels are indicated by asterisks: $^{**}p \leq 0.01$, $^{***}p \leq 0.001$, $^{****}p \leq 0.0001$.

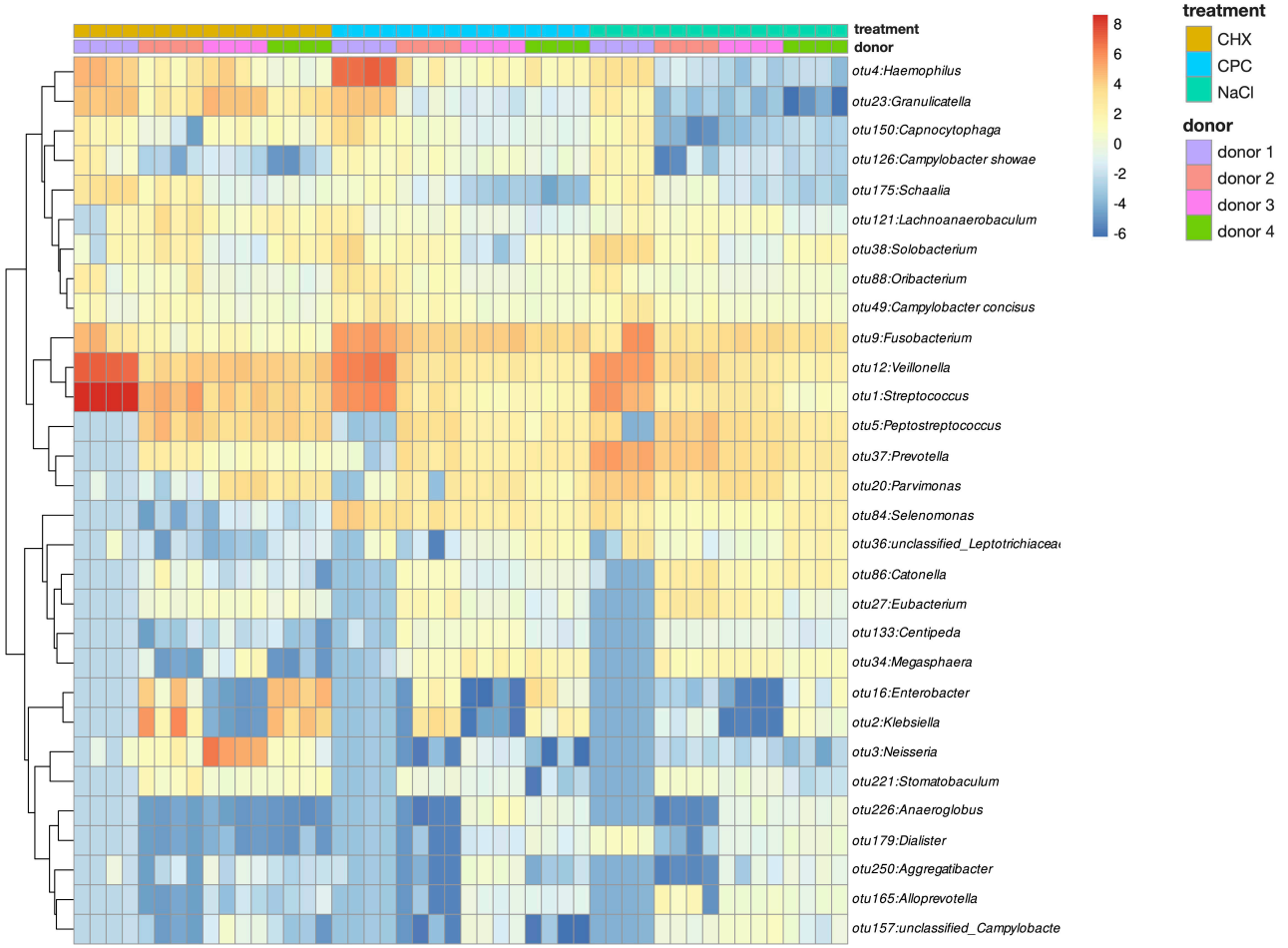

FIGURE 2 | Heatmap of ASV abundance on genus level for NaCl-, CHX-, and CPC-treated biofilms from all four donors.

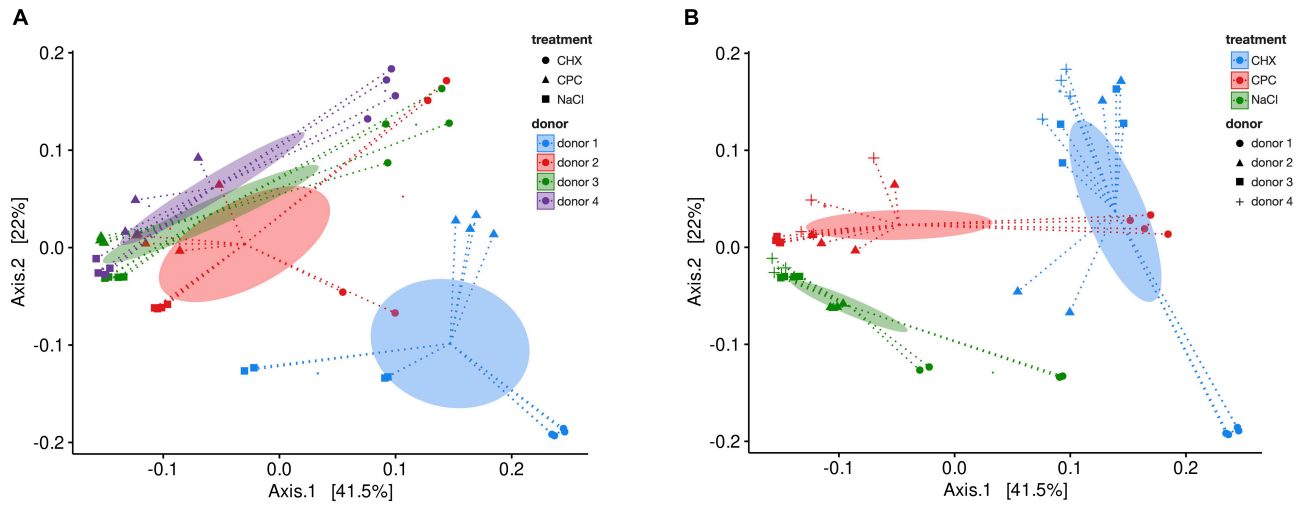

FIGURE 3 | Beta-diversity analysis by principal coordinate analysis (PCoA) of weighted UniFrac distances for NaCl-, CHX-, and CPC-treated biofilms from all four donors. Ellipses indicate the 95% confidence interval of group centroids summarized for donors **(A)** or treatments **(B)**. Depicted are coordinates 1 and 2, which explained 63.5% of the total variance. (Adonis NaCl vs. CHX: $R^2 = 0.42$, p.adj = 0.003, NaCl vs. CPC: $R^2 = 0.23$, p.adj = 0.003, CHX vs. CPC: $R^2 = 0.36$, p.adj = 0.003).

(mainly *Selenomonas* spp.), Pasteurellales (mainly *Haemophilus* spp.), and Campylobacterales, as well as *Oribacterium* and *Prevotella loescheii*. Furthermore, both CHX- and CPC-treated biofilms were characterized by a loss of several *Prevotella*, *Catonella*, and *Parvimonas* spp. as compared to the NaCl-treated biofilms.

Colony-Forming Units Assay and Identification of Antiseptic-Resistant Phenotypes

Figure 5 shows the CFU assay results. Biofilms treated with NaCl exhibited median CFU numbers of 9.3×10^7 CFU, while CHX- or CPC-treated biofilms showed 3.3×10^6 or 2.5×10^7 CFU, respectively, resulting in CFU-reductions of 1.5 $\log_{10}$ steps for CHX and 0.6 $\log_{10}$ steps for CPC as compared to the biofilms treated with NaCl.

Table 1 summarizes the antiseptic-resistant phenotypes as identified by MALDI-TOF MS along with their respective antibiotic susceptibilities as tested using ETEST® or by means of the BD Phoenix NMIC panel. In each donor, at least one taxon could be isolated that was able to grow on the antiseptic-containing agar plates. In donor 1, *Capnocytophaga sputigena* was found on the CHX-containing agar plate from the NaCl-treated biofilm and was susceptible to all tested antibiotics, while *Campylobacter showae*, which was isolated on the CPC-containing agar plate from both NaCl- and CPC-treated biofilms presented resistance to ciprofloxacin and piperacillin/tazobactam. Moreover, *Campylobacter showae*, which was isolated on the CPC-containing agar plate from CPC-treated biofilms, showed additional resistance to Penicillin G. In donor 2, only taxa identified as *Klebsiella oxytoca or Raoultella* sp. were isolated on both CHX- and CPC-containing agar from the corresponding antiseptic-treated biofilms. Both *Klebsiella oxytoca* and *Raoultella* sp. isolates showed resistance to ampicillin/amoxicillin, piperacillin, and fosfomycin. The highest number of antiseptic-resistant phenotypes was isolated from donor 3. *Capnocytophaga sputigena* (susceptible to all tested antibiotics) and *Capnocytophaga gingivalis* (susceptible to all tested antibiotics) were isolated on the CHX-containing agar plate from the NaCl-treated biofilms, while *Fusobacterium* sp. (resistant to penicillin G, ampicillin and ciprofloxacin), *Veillonella rogosae* (resistant to clindamycin and intermediate resistant to ceftazidime), and *Campylobacter curvus* (intermediate resistant to ciprofloxacin) were isolated on the CPC-containing agar plate from the NaCl-treated biofilm. Additionally, *Neisseria perflava* (resistant to penicillin G, ampicillin and ceftriaxone/cefotaxime) was isolated from the CHX-treated biofilm and *Veillonella rogosae* (resistant to clindamycin) was isolated from the CPC-treated biofilm. In donor 4, two strains identified as *Klebsiella oxytoca* or *Raoultella* sp. were collected from NaCl- or CPC-treated biofilms and isolated from CHX- or CPC-containing agar. Both showed resistance to ampicillin/amoxicillin, piperacillin, and fosfomycin. One taxon identified to be from the *Enterobacter cloacae*-complex was isolated on the CHX-containing agar originating from the CHX-treated biofilms growing and exhibited resistance to ampicillin/amoxicillin, amoxicillin/clavulanic acid, piperacillin, piperacillin/tazobactam, and cefazolin.

DISCUSSION

Antiseptics are in widespread use in dental practice and also included in numerous over-the-counter oral care products (Haps et al., 2008; Sanz et al., 2013; van der Weijden et al., 2015), but the effects of routine antiseptic use on microbial composition of oral

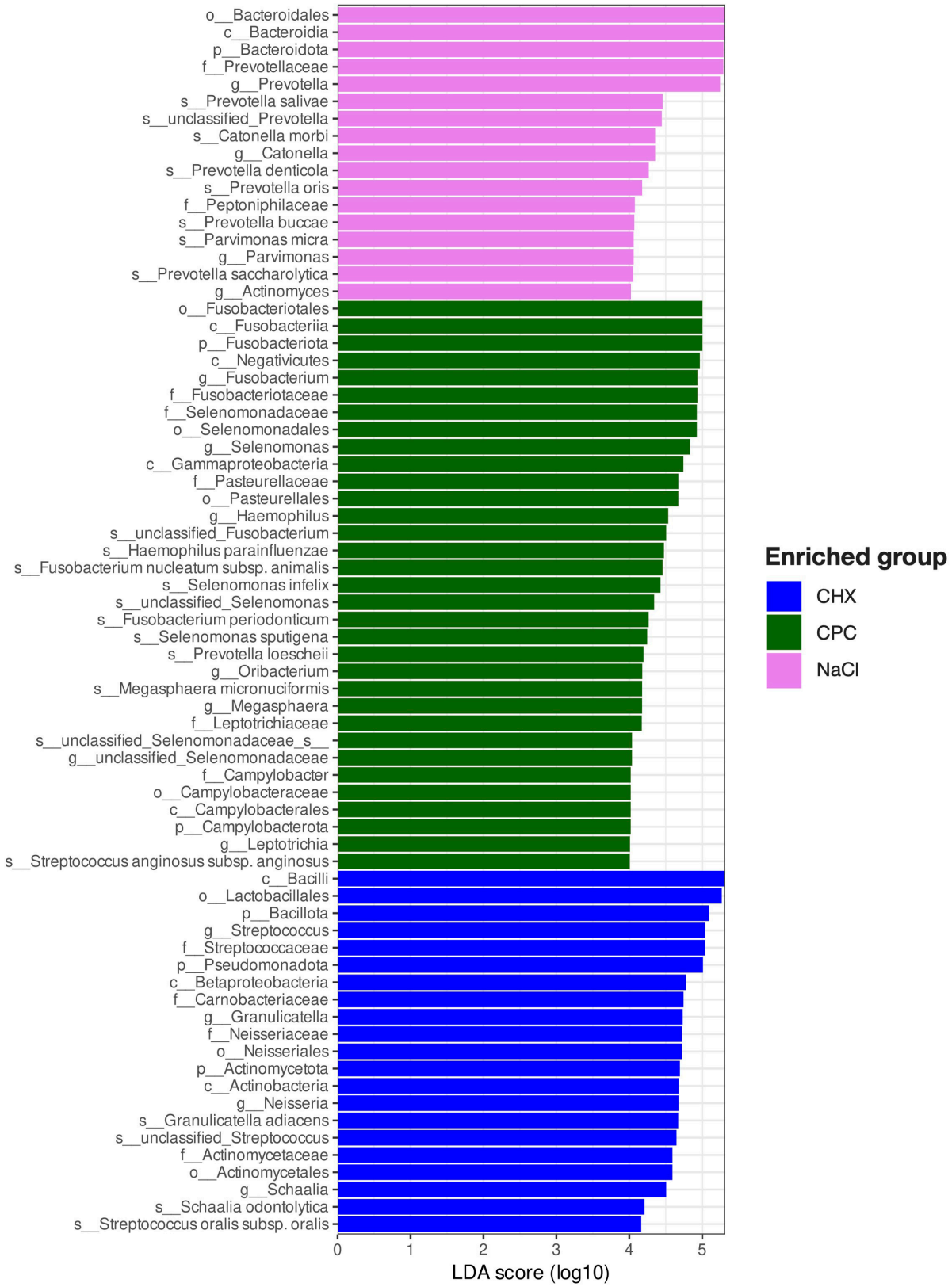

FIGURE 4 | Discriminatory ASVs for biofilms treated with NaCl, CPC, or CHX, respectively, as identified by linear discriminant analysis (LDA) effect size (LEfSe). ASVs exhibiting LDA-score ≥ 4 and adjusted p-values < 0.01 are shown.

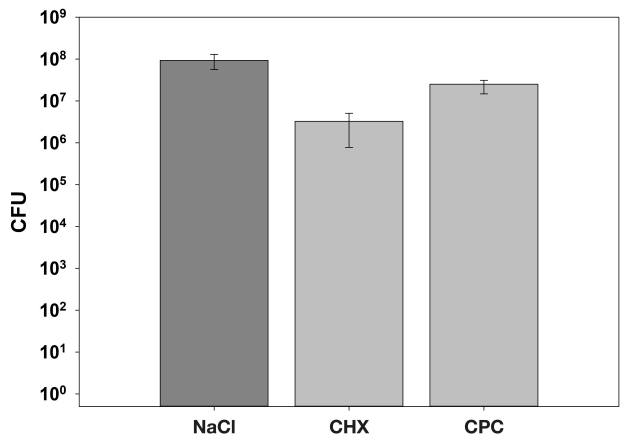

FIGURE 5 | The CFU results following two times daily treatment with either 0.9% NaCl, 0.1% CHX, or 0.05% CPC for a period of 7 days. All results are depicted as medians, 1st and 3rd quartiles from eight individual biological replicates on a $\log_{10}$-scaled ordinate.

biofilms (Chatzigiannidou et al., 2020; Zayed et al., 2022) and on the emergence of resistant phenotypes are still unclear (Cieplik et al., 2019a; Mao et al., 2020). Therefore, this study aimed to investigate the ecological effects of daily treatment with CHX or CPC on mature saliva-grown biofilms and whether a suchlike treatment selects for resistant phenotypes.

For this purpose, microcosm biofilms were cultured from human saliva employing the so-called *Amsterdam Active Attachment* (AAA) biofilm model, as described previously (Schwarz et al., 2021). Sampling was performed from healthy donors, and a basal nutrient broth mimicking human saliva was modified by adding sucrose (Pratten et al., 1998; Cieplik et al., 2013; Schwarz et al., 2021) to provide environmental conditions leading to biofilms that resemble microbial communities in rather early stage of dysbiosis dominated by early colonizers of dental plaque (Schwarz et al., 2021). While the biofilms in this previous study showed rather low alpha-diversity and mostly growth of *Streptococcus* and *Veillonella* spp., a considerably higher alpha-diversity was found for the biofilms in the present study. This may be attributed to several factors: Once, HAP disks were used as a substrate for biofilm culture instead of glass disks as used previously (Schwarz et al., 2021). These HAP disks may better mimic dental hard tissues and might improve bacterial attachment toward the substrate (Hannig and Hannig, 2009), which is particularly crucial for the AAA model used in the present study, as it relies on the active attachment of bacteria (Exterkate et al., 2010; Cieplik et al., 2019b). Furthermore, another important aspect may be the different period for culture of the biofilms. While the biofilms were cultured only for 3 days in the previous study (Schwarz et al., 2021), here, the biofilms were cultured for 10 days in total (3 days of biofilm formation followed by 7 days of treatment with NaCl, CHX, or CPC), which may have given the more fastidious bacteria more time to establish themselves in the biofilms (Edlund et al., 2013; Kistler et al., 2015; Cieplik et al., 2019b). The microbial compositions of the biofilms were found dependent on the respective donor source, which is in line with the results from a previous study, where we found a much stronger clustering of microbial compositions of biofilms per each donor than per niche of each donor even after up to 28 days of *in vitro* culture, indicating a strong donor-driven "fingerprint" (Cieplik et al., 2019b). Similar results were reported by Chatzigiannidou et al. (2020) who also observed a strong donor-dependency regarding microbial composition of their tongue-swab-derived microcosm biofilms. Notably, here, the biofilms from one donor (donor 1) clustered particularly different from the other three donors. This may be explained by the different ethnicity of this donor (Asian, while the other three donors were Caucasian), as also shown in previous studies (Mason et al., 2013; Premaraj et al., 2020). For instance, microbial communities in saliva and subgingival biofilms were found to have distinct ethnicity profiles, and based on these results, it was even possible to identify the ethnicity of individuals from subgingival microbial signatures using a machine learning classifier (Mason et al., 2013). Furthermore, a recent metagenome-wide association study found that human genetics account for at least 10% of oral microbiome compositions between different individuals, which may also explain the stable microbial composition within one single individual over time (Liu et al., 2021).

After undisturbed culture of the biofilms for 3 days, a mouthwash was simulated two times daily using either of the tested compounds for 5 min each. The AAA biofilm model facilitates controlling treatment periods as opposed to other biofilms models, which are based on bacterial sedimentation rather than active bacterial attachment (Exterkate et al., 2010). Due to the well-known high substantivity of CHX and CPC (Elworthy et al., 1996), biofilms were washed after the 5 min treatment period to dilute potentially remaining CHX or CPC and limit potential prolonged effects of both antiseptics. The two times daily treatment with CHX or CPC reduced CFU in the biofilms only by 1.5 $\log_{10}$ or 0.6 $\log_{10}$ steps as compared to the NaCl group. These results clearly show that both antiseptics exhibited only temporary effects and could not inhibit bacterial regrowth, in line with several other studies indicating that antiseptic mouthwashes are not able to effectively limit microbial numbers, particularly when applied to mature biofilms (Cieplik et al., 2019a; Chatzigiannidou et al., 2020; Brookes et al., 2021; Schwarz et al., 2021). Therefore, it is crucial to investigate the ecological effects on the microbial composition of the surviving microbiota, which is still discussed controversially for CHX and has not been investigated so far for CPC (Al-Kamel et al., 2019; Bescos et al., 2020a; Chatzigiannidou et al., 2020; Brookes et al., 2021).

We found that treatment with CHX significantly reduced alpha-diversity in the biofilms as compared to treatment with CPC or NaCl (with no significant difference between the latter), in accordance with several other studies evaluating the effects of CHX on microbial communities *in vitro* and *in vivo* (Fernandez et al., 2017; Tribble et al., 2019; Brookes et al., 2020, 2021; Chatzigiannidou et al., 2020). Furthermore, beta-diversity showed a strong and significant ecological shift following treatment with CHX, resulting in enrichment of

TABLE 1 | Antiseptic-resistant phenotypes isolated from the biofilms and evaluation of antibiotic susceptibilities.

A. Antiseptic-resistant phenotypes and evaluation of their antibiotic susceptibilities by means of ETEST®

				Beta-lactams							Fluoroquinolones	Macrolides and Lincosamides		Tetracycline	Nitroimidazole
Donor	**Treatment group**	**Growth on plate**	**Identification by MALDI-TOF MS**	**Penicillin G**	**Ampicillin**	**Amoxicillin/clavulanic acid**	**Piperacillin/tazobactam**	**Imipenem**	**Ceftriaxone Cefotaxime**	**Ceftazidime**	**Ciprofloxacin**	**Erythromycin**	**Clindamycin**	**Tetracycline**	**Metronidazole**
1	NaCl	0.01% CHX	*Capnocytophaga sputigena*	0.002 S	0.016 S	0.016 S	0.016 S	0.002 S	0.006 S	0.032 S	0.003 S	0.125 –	0.006 –	0.023 –	0.047 –
1	NaCl	0.01% CPC	*Campylobacter showae*	2 S	0.032 S	0.032 S	24 **R**	0.094 S	0.064 S	0.125 S	≥ 32 **R**	4 S	0.25 –	0.19 –	≥ 256 –
1	CPC	0.01% CPC	*Campylobacter showae*	4 **R**	0.094 S	0.032 S	48 **R**	0.125 S	0.094 S	0.25 S	≥32 **R**	4 S	0.75 –	0.75 –	≥256 –
3	NaCl	0.01% CHX	*Capnocytophaga sputigena*	0.002 S	0.016 S	0.016 S	0.016 S	0.002 S	0.002 S	0.016 S	0.006 S	0.125 –	0.016 –	0.023 –	0.016 –
3	NaCl	0.01% CHX	*Capnocytophaga gingivalis*	0.016 S	0.023 S	0.023 S	0.016 S	0.032 S	0.5 S	0.38 S	0.006 S	≥256 –	0.006 –	0.047 –	3 S
3	NaCl	0.01% CPC	*Fusobacterium* sp.	≥32 **R**	≥256 **R**	0.016 S	0.19 S	0.047 S	1 S	3 S	0.75 **R**	4 –	0.75 –	0.19 –	0.016 S
3	NaCl	0.01% CPC	*Veillonella rogosae*	0.125 S	0.094 S	0.094 S	0.75 S	0.125 S	0.25 S	8 I	0.032 S	16 –	≥256 **R**	0.064 –	0.38 S
3	NaCl	0.01% CPC	*Campylobacter curvus*	1 S	0.032 S	0.032 S	24 S	0.19 S	0.032 S	0.38 S	0.047 I	2 S	1.5 –	0.19 S	6 –
3	CHX	0.05% CHX	*Neisseria perflava*	6 **R**	1.5 **R**	1.5 S	1 S	0.75 S	0.19 **R**	*N*	0.012 S	32 -	32 –	1.5 –	256 –
3	CPC	0.05% CPC	*Veillonella rogosae*	0.25 S	0.19 S	0.19 S	0.19 S	0.064 S	0.25 S	8 I	0.047 S	24 -	≥ 256 **R**	0.125 –	0.38 S

(Continued)

TABLE 1 | (Continued)

B. Antiseptic-resistant phenotypes and evaluation of their antibiotic susceptibilities by means of the BD Phoenix NMIC panel.

				Beta-lactams													Fluoroquinolones		Aminoglycosides			Others	
Donor	**Treatment group**	**Growth on plate**	**Identification by MALDITOF-MS**	**Ampicillin/amoxicillin**	**Amoxicillin/clavulanic acid**	**Piperacillin**	**Piperacillin/tazobactam**	**Imipenem**	**Meropenem**	**Ertapenem**	**Aztreonam**	**Cefuroxime**	**Cefoxitin**	**Ceftriaxone/Cefotaxime**	**Ceftazidime**	**Cefepime**	**Ciprofloxacin**	**Levofloxacin**	**Gentamicin**	**Amikacin**	**Tobramycin**	**Fosfomycin**	**Trimethoprim/sulfamethoxazole**
2	CHX	0.01% CHX	*Klebsiella oxytoca/ Raoultella* sp.	>8 **R**	≤2/2 S	8 **R**	≤4/4 S	0.5 S	≤0.125 S	≤0.25 S	≤1 S	≤2 I	≤4 S	≤0.5 S	≤0.5 S	≤1 S	≤0.25 S	≤0.5 S	≤1 S	≤4 S	≤1 S	>128 **R**	≤1/19 S
2	CPC	0.05% CPC	*Klebsiella oxytoca/ Raoultella* sp.	> 8 **R**	≤ 2/2 S	8 **R**	≤ 4/4 S	0.5 S	≤ 0.125 S	≤0.25 S	≤ 1 S	≤2 I	≤ 4 S	≤0.5 S	≤ 0.5 S	≤1 S	≤ 0.25 S	≤0.5 S	≤ 1 S	≤4 S	≤ 1 S	> 128 **R**	≤ 1/19 S
4	NaCl	0.01% CHX	*Klebsiella oxytoca/ Raoultella* sp.	>8 **R**	≤2/2 S	≤4 **R**	≤4/4 S	0.5 S	≤0.125 S	≤0.25 S	≤1 S	≤2 I	≤4 S	≤0.5 S	≤0.5 S	≤1 S	≤0.25 S	≤0.5 S	≤1 S	≤4 S	≤1 S	≤16 S	≤1/19 S
4	CHX	0.05% CHX	*Enterobacter cloacae* complex	>8 **R**	≤32/2 S	16 **R**	≤16/4 S	≤0.25 S	≤0.125 S	≤0.25 S	≤1 S	*N*	>16 **R**	≤0.5 S	1 S	≤1 S	≤0.25 S	≤0.5 S	≤1 S	≤4 S	≤1 S	≤16 S	≤1/19 S
4	CPC	0.05% CPC	*Klebsiella oxytoca/ Raoultella* sp.	>8 **R**	≤2/2 S	≤4 **R**	≤4/4 S	≤0.25 S	≤0.125 S	≤0.25 S	≤1 S	≤2 I	≤4 S	≤0.5 S	≤0.5 S	≤1 S	≤0.25 S	≤0.5 S	≤1 S	≤4 S	≤1 S	≤16 S	≤1/19 S

*(A) The first line shows the respective ETEST® result [μg/mL], while the second line gives the interpretation according to EUCAST 12.0 (S, susceptible; I, intermediate; **R**, resistant; –, no breakpoint given). N, not tested.*

*(B) The first line shows the respective MIC [μg/mL], while the second line gives the interpretation according to EUCAST 12.0 (S, susceptible; I, intermediate; **R**, resistant). N, not tested.*

rather caries-associated taxa such as *Streptococcus*, *Neisseria*, *Schaalia* [genus recently created by subdivision from *Actinomyces* (Nouioui et al., 2018)], and *Granulicatella* spp. For instance, the significantly enriched species *Streptococcus oralis* subsp. *oralis* and *Schaalia odontolytica* (formerly classified as *Actinomyces odontolyticus*) have been associated with dental caries (ElSalhy et al., 2016; Da Costa Rosa et al., 2021). Bescos et al. (2020a) investigated the effects of 7-day use of a CHX mouthwash on the salivary microbiota in 36 healthy individuals. They observed an increase in the abundance of taxa from the genera *Streptococcus*, *Neisseria*, and *Granulicatella*, but a decrease of *Actinomyces* (Bescos et al., 2020a), and a significantly lower salivary pH and buffer capacity after using the CHX mouthwash for 7 days, concluding that CHX may have a significant impact on the oral microbiota, potentially favoring dental caries (Bescos et al., 2020a). Likewise, Chatzigiannidou et al. (2020) found an ecological shift toward a streptococci-dominated microbial community and increased lactate production after treating *in vitro* 14-species biofilms with CHX over 3 days for 5 min each, while they observed a contrary trend with increase in *Granulicatella* and *Fusobacterium* spp. after treating microcosm biofilms inoculated from tongue scrapings.

Interestingly, treatment with CPC had a different effect on the biofilms. Alpha-diversity was not significantly affected as compared to the NaCl-treated biofilms, but beta-diversity also revealed a significant ecological shift, resulting in enrichment of proteolytic and Gram-negative taxa such as *Fusobacterium*, *Leptotrichia*, and *Selemonas* spp. as well as *Oribacterium*, which are mainly associated with gingivitis (Diaz et al., 2016; Bryan et al., 2017; Nowicki et al., 2018).

Both antiseptic treatments led to a loss of *Prevotella* spp., which are known nitrite producers and associated with high nitrate-reduction capacity (Hyde et al., 2014; Rosier et al., 2022). Accordingly, clinical studies have shown that the use of CHX mouthwashes led to lower nitrite concentrations in saliva and plasma followed by slight increases in systolic blood pressure (Tribble et al., 2019; Bescos et al., 2020a). Although the oral microbiota is known to be highly resilient, particularly as compared to the intestinal microbiota (Wade, 2021), clinicians should be aware of potential detrimental effects of long-term use of antiseptic mouthwashes with regard to oral microbial ecology (Bescos et al., 2020b), which may potentially further perturb the commensal microbiota rather than shifting to a health-associated state (Chatzigiannidou et al., 2020). However, it needs to be considered that here the effects of "pure" antiseptics were investigated, whereas the effects of antiseptic mouthwashes seem to be strongly dependent on their respective compositions and formulations, as recently shown (Zayed et al., 2022). Also, a commercially available mouthwash comprising both CHX and CPC showed capability to even improve the microbial ecology of a 14-species biofilm *in vitro* reducing the level of pathobionts to less than 10% (Zayed et al., 2022), whereas in our study, CHX led to enrichment of rather caries-associated saccharolytic taxa and CPC led to enrichment of rather gingivitis-associated proteolytic taxa.

Despite analyzing effects on biofilm ecology, we also sought to investigate whether antiseptic treatment selects for resistant phenotypes. For this purpose, an agar dilution technique was employed, and the biofilms were plated on Schaedler agar plates containing 0.01 or 0.05% CHX or CPC, respectively. Although this method is in line with the guidelines of the Clinical Laboratory Standards Institute (CLSI) (CLSI, 2018a,b) and has also been used in earlier studies investigating antiseptics (Eick et al., 2011; Akca et al., 2016), it should be considered that the biologically available concentrations on the surface of the plates may not necessarily reflect the rather high concentrations mixed into the agar plates, due to potential interactions of the cationic antiseptics and constituents of the solid growth media (Akca et al., 2016). Thus, only qualitative, but no quantitative results (i.e., CFU numbers) are reported in this study. We found antiseptic-resistant phenotypes in biofilms from each donor, which also showed resistance to various antibiotics. As some of them were isolated from the NaCl-treated biofilms, these isolates originate from the inoculum source and could establish in the biofilms even without selection pressure due to the two times daily antiseptic treatment, supporting recent studies, which highlight the oral microbiota as a reservoir of antimicrobial resistance (AMR) genes (Jiang et al., 2018; Arredondo et al., 2020).

The isolated antiseptic-resistant phenotypes were found to be highly donor-dependent: In the biofilms from two donors (1 and 3), typical oral taxa could be isolated from the antiseptic-containing agar plates. *Capnocytophaga* spp. could be isolated from CHX-containing agar, in line with older studies reporting that *Capnocytophaga* spp. exhibited minimum inhibitory concentrations (MICs) for CHX of up to 250 μg/ml (0.025%) and were the least susceptible among all oral bacteria included in these experiments (Stanley et al., 1989; Wade and Addy, 1989). Furthermore, the earliest study probably reporting isolation of this genus was from a group of dental students following use of a 0.2% CHX mouthwash for 22 days (Davies et al., 1972; Leadbetter et al., 1979). Two *V. rogosae* strains, which were both isolated from CPC-containing agar, showed high-level resistance to clindamycin, which was also found in 55% of *Veillonella* isolates in a previous study (Teng et al., 2002). *N. perflava* isolated from CHX-treated biofilms on CHX-containing agar was found resistant to penicillin G, ampicillin, and ceftriaxone/cefotaxime, which is in line with a recent systematic review stating that antimicrobial susceptibilities in commensal as well as pathogenic *Neisseria* spp. have been increasing considerably following decades of antibiotic exposure (Vanbaelen et al., 2022). Remarkably, the MIC of 6 μg/ml found here for penicillin G is higher than all reported for commensal *Neisseria* spp. in this systematic review (Vanbaelen et al., 2022). *Campylobacter* spp. could be isolated from CPC-containing agar. The two *C. showae* isolates showed high-level resistance to ciprofloxacin and piperacillin/tazobactam, while they were sensitive to amoxicillin/clavulanic acid. Resistance to piperacillin has previously been described in poultry isolates of *Campylobacter* spp., although MICs of piperacillin/tazobactam were 16- to 32-fold lower than for piperacillin alone, they still were found quite high (around 32 μg/ml) (Griggs et al., 2009), in line with the MICs found here. In *Campylobacter* spp., resistance to fluoroquinolones like ciprofloxacin is mainly due to single point mutation(s) in the *gyrA* gene (Wieczorek and Osek, 2013; Sproston et al., 2018). An isolate of the genus *Fusobacterium*,

which was obtained from CPC-containing agar, exhibited high-level resistance to penicillin G and ampicillin, which was also found previously and attributed to be due to expression of a class D beta-lactamase (Al-Haroni et al., 2008).

Apart from these typical oral taxa, Enterobacteriaceae could be isolated from the biofilms from donors 2 and 4. Although members of Enterobacteriaceae are usually considered as transient components of the oral microbiota, they have consistently been detected at low numbers in subgingival biofilm samples (Espíndola et al., 2022; Jepsen et al., 2022) and also on toothbrushes (Zinn et al., 2020). For instance, Jepsen et al. (2022) recently analyzed biofilm samples collected between 2008 and 2015 from deep periodontal pockets in 16,612 German adults diagnosed with periodontitis and found mean annual prevalence rates of 3.6% for *K. oxytoca* and 2.5% for *E. cloacae*. The fosfomycin resistance detected in two *K. oxytoca*/*Raoultella* sp. isolates may be attributable to the chromosomal *fosA* gene, which is present in the majority of genomes in *Klebsiella* spp. (Ito et al., 2017). Likewise, the resistance of all Enterobacteriaceae isolated in the present study to aminopenicillins such as ampicillin, amoxicillin, and piperacillin and, in part, to second-generation cephalosporins like cefuroxime or cefoxitin may be mainly attributed to their production of AmpC-type beta-lactamases (Meini et al., 2019). Thus, adjunctive prescription of amoxicillin, e.g., in the course of periodontal treatment, may pose the risk of overgrowth of such taxa in oral biofilms (Jepsen et al., 2022). Accordingly, Baker at al. (2019) reported recently that *K. oxytoca*, *K. pneumoniae,* and *Providencia alcalifaciens* were the only taxa found to be transcriptionally active and recoverable after long-term starvation of a saliva-derived microbial community over 100 days *in vitro*, which may explain that hospital surfaces contaminated with saliva can serve as source of outbreaks of drug-resistant Enterobacteriaceae. Although such long-term starvation does not reflect the environmental conditions in the oral cavity (Baker et al., 2019), it may be similar to long-term selective pressure due to extensive use of antiseptic mouthwashes (Cieplik et al., 2019a; Mao et al., 2020). Besides selection of intrinsically less susceptible phenotypes, adaptation to antiseptics such as CHX may also occur, which was recently linked to development of antibiotic cross-resistance to colistin in *K. pneumoniae* (Wand et al., 2017).

CONCLUSION

This study shows that both CHX and CPC exhibited significant ecological effects on the microbial compositions of microcosm biofilms upon two times daily treatment for a period of 7 days. CHX led to enrichment of rather caries-associated saccharolytic taxa as compared to NaCl-treated biofilms, while CPC led to enrichment of rather gingivitis-associated proteolytic taxa. Antiseptic-resistant phenotypes could be isolated from all biofilms regardless which treatment group they belonged to. These isolates exhibited resistance to various antibiotics. Therefore, further studies are needed to elucidate implications of the widespread use of antiseptics in oral healthcare with regard to their ecological effects on oral biofilms as well as on the spread of antimicrobial resistance. Clinicians should be aware of the potential risks associated with the widespread and indiscriminate use of antiseptics and apply or prescribe them only for appropriate indications and preferably only for short periods of time.

DATA AVAILABILITY STATEMENT

The datasets presented in this study can be found in online repositories. The names of the repository/repositories and accession number(s) can be found below: NCBI – PRJEB52604.

ETHICS STATEMENT

The studies involving human participants were reviewed and approved by the Internal Review Board of the University of Regensburg (ref.: 17-782_1-101). The participants provided their written informed consent to participate in this study.

AUTHOR CONTRIBUTIONS

FC, AA-A, AH, and AG conceived and designed the experiments. XM, AH, DA, KS, and DM performed the experiments. XM, AH, FC, AG, KS, K-AH, TM, WB, and EH analyzed and interpreted the data. FC and AA-A acquired the funding and supervised the study. FC, XM, and AH wrote the manuscript with input from all authors. All authors reviewed and approved the manuscript.

FUNDING

This study was funded by the Deutsche Forschungsgemeinschaft (DFG, German Research Foundation; grants CI 263/3-1 and AL 1179/4-1) and by the Bavarian Ministry of Science and the Arts in the framework of the Bavarian Research Network 'New Strategies Against Multi-Resistant Pathogens by Means of Digital Net-working – bayresq.net, project "IRIS"'. XM and DA thank for funding by doctoral scholarships from the Affiliated Stomatology Hospital of Tongji University (Shanghai, China) or the Medical Faculty of the University of Regensburg (Regensburg, Germany), respectively.

ACKNOWLEDGMENTS

Heike Preuschl and Stefan Lukas are gratefully acknowledged for their excellent technical support.

REFERENCES

Akca, A. E., Akca, G., Topçu, F. T., Macit, E., Pikdöken, L., and Özgen, I. Ş. (2016). The Comparative Evaluation of the Antimicrobial Effect of Propolis with Chlorhexidine against Oral Pathogens: an In Vitro Study. *Biomed Res. Int.* 2016:3627463. doi: 10.1155/2016/3627463

Al-Haroni, M., Skaug, N., Bakken, V., and Cash, P. (2008). Proteomic analysis of ampicillin-resistant oral *Fusobacterium nucleatum*. *Oral Microbiol. Immunol.* 23, 36–42. doi: 10.1111/j.1399-302X.2007.00387.x

Al-Kamel, A., Baraniya, D., Al-Hajj, W. A., Halboub, E., Abdulrab, S., Chen, T., et al. (2019). Subgingival microbiome of experimental gingivitis: shifts associated with the use of chlorhexidine and N-acetyl cysteine mouthwashes. *J. Oral Microbiol.* 11:1608141. doi: 10.1080/20002297.2019.1608141

Arredondo, A., Blanc, V., Mor, C., Nart, J., and León, R. (2020). Tetracycline and multidrug resistance in the oral microbiota: differences between healthy subjects and patients with periodontitis in Spain. *J. Oral Microbiol.* 13:1847431. doi: 10.1080/20002297.2020.1847431

Auer, D. L., Mao, X., Anderson, A. C., Muehler, D., Wittmer, A., von Ohle, C., et al. (2022). Phenotypic Adaptation to Antiseptics and Effects on Biofilm Formation Capacity and Antibiotic Resistance in Clinical Isolates of Early Colonizers in Dental Plaque. *Antibiotics* 11:688. doi: 10.3390/antibiotics11050688

Baker, J. L., Hendrickson, E. L., Tang, X., Lux, R., He, X., Edlund, A., et al. (2019). Klebsiella and Providencia emerge as lone survivors following long-term starvation of oral microbiota. *Proc. Natl. Acad. Sci. U. S. A.* 116, 8499–8504. doi: 10.1073/pnas.1820594116

Bescos, R., Ashworth, A., Cutler, C., Brookes, Z. L., Belfield, L., Rodiles, A., et al. (2020a). Effects of Chlorhexidine mouthwash on the oral microbiome. *Sci. Rep.* 10:5254. doi: 10.1038/s41598-020-61912-4

Bescos, R., Casas-Agustench, P., Belfield, L., Brookes, Z., and Gabaldón, T. (2020b). Coronavirus Disease 2019 (COVID-19): emerging and Future Challenges for Dental and Oral Medicine. *J. Dent. Res.* 99:1113. doi: 10.1177/0022034520932149

Brookes, Z. L. S., Belfield, L. A., Ashworth, A., Casas-Agustench, P., Raja, M., Pollard, A. J., et al. (2021). Effects of chlorhexidine mouthwash on the oral microbiome. *J. Dent.* 113:103768. doi: 10.1016/j.jdent.2021.103768

Brookes, Z. L. S., Bescos, R., Belfield, L. A., Ali, K., and Roberts, A. (2020). Current uses of chlorhexidine for management of oral disease: a narrative review. *J. Dent.* 103:103497. doi: 10.1016/j.jdent.2020.103497

Bryan, N. S., Tribble, G., and Angelov, N. (2017). Oral Microbiome and Nitric Oxide: the Missing Link in the Management of Blood Pressure. *Curr. Hypertens. Rep.* 19:33. doi: 10.1007/s11906-017-0725-2

Cao, Y. (2021). *microbiome R package*. doi: 10.5281/zenodo.3749415

Carrouel, F., Gonçalves, L. S., Conte, M. P., Campus, G., Fisher, J., Fraticelli, L., et al. (2021). Antiviral Activity of Reagents in Mouth Rinses against SARS-CoV-2. *J. Dent. Res.* 100, 124–132. doi: 10.1177/0022034520967933

Ceri, H., Olson, M. E., Stremick, C., Read, R. R., Morck, D., and Buret, A. (1999). The Calgary Biofilm Device: new technology for rapid determination of antibiotic susceptibilities of bacterial biofilms. *J. Clin. Microbiol.* 37, 1771–1776. doi: 10.1128/JCM.37.6.1771-1776.1999

Chatzigiannidou, I., Teughels, W., van de Wiele, T., and Boon, N. (2020). Oral biofilms exposure to chlorhexidine results in altered microbial composition and metabolic profile. *NPJ Biofilms Microbiomes* 6:13. doi: 10.1038/s41522-020-0124-3

Cieplik, F., Jakubovics, N. S., Buchalla, W., Maisch, T., Hellwig, E., and Al-Ahmad, A. (2019a). Resistance Toward Chlorhexidine in Oral Bacteria - Is There Cause for Concern? *Front. Microbiol.* 10:587. doi: 10.3389/fmicb.2019.00587

Cieplik, F., Zaura, E., Brandt, B. W., Buijs, M. J., Buchalla, W., Crielaard, W., et al. (2019b). Microcosm biofilms cultured from different oral niches in periodontitis patients. *J. Oral Microbiol.* 11:1551596. doi: 10.1080/20022727.2018.1551596

Cieplik, F., Späth, A., Regensburger, J., Gollmer, A., Tabenski, L., Hiller, K.-A., et al. (2013). Photodynamic biofilm inactivation by SAPYR–an exclusive singlet oxygen photosensitizer. *Free Radic Biol. Med.* 65, 477–487. doi: 10.1016/j.freeradbiomed.2013.07.031

Cieplik, F., Wiedenhofer, A. M., Pietsch, V., Hiller, K.-A., Hiergeist, A., Wagner, A., et al. (2020). Oral Health, Oral Microbiota, and Incidence of Stroke-Associated Pneumonia-A Prospective Observational Study. *Front. Neurol.* 11:528056. doi: 10.3389/fneur.2020.528056

CLSI (2018a). *M07: Methods For Dilution Antimicrobial Susceptibility Tests For Bacteria That Grow Aerobically,: 11th Edition*. Pennsylvania, USA: Clinical and Laboratory Standards Institute.

CLSI (2018b). *M11: Methods For Antimicrobial Susceptibility Testing Of Anaerobic Bacteria: 9th Edition*. Pennsylvania, USA: Clinical and Laboratory Standards Institute.

Da Costa Rosa, T., de Almeida Neves, A., Azcarate-Peril, M. A., Divaris, K., Wu, D., Cho, H., et al. (2021). The bacterial microbiome and metabolome in caries progression and arrest. *J. Oral Microbiol.* 13:1886748. doi: 10.1080/20002297.2021.1886748

Davies, R. M., Jensen, S. B., Rindom Schiott, C., Löe, H., and Theilade, J. (1972). Anaerobic gliding bacteria isolated from the oral cavity. *Acta. Pathol. Microbiol. Scand. B Microbiol. Immunol.* 80, 397–402. doi: 10.1111/j.1699-0463.1972.tb00052.x

Diaz, P. I., Hoare, A., and Hong, B.-Y. (2016). Subgingival Microbiome Shifts and Community Dynamics in Periodontal Diseases. *J. Calif. Dent. Assoc.* 44, 421–435.

Edlund, A., Yang, Y., Hall, A. P., Guo, L., Lux, R., He, X., et al. (2013). An in vitro biofilm model system maintaining a highly reproducible species and metabolic diversity approaching that of the human oral microbiome. *Microbiome* 1:25. doi: 10.1186/2049-2618-1-25

Eick, S., Goltz, S., Nietzsche, S., Jentsch, H., and Pfister, W. (2011). Efficacy of chlorhexidine digluconate-containing formulations and other mouthrinses against periodontopathogenic microorganisms. *Quintessence Int.* 42, 687–700.

ElSalhy, M., Söderling, E., Honkala, E., Fontana, M., Flannagan, S., Kokaras, A., et al. (2016). Salivary microbiota and caries occurrence in Mutans Streptococci-positive school children. *Eur. J. Paediatr. Dent.* 17, 188–192.

Elworthy, A., Greenman, J., Doherty, F. M., Newcombe, R. G., and Addy, M. (1996). The substantivity of a number of oral hygiene products determined by the duration of effects on salivary bacteria. *J. Periodontol.* 67, 572–576. doi: 10.1902/jop.1996.67.6.572

Espíndola, L. C. P., Picão, R. C., Mançano, S. M. C. N., Martins do Souto, R., and Colombo, A. P. V. (2022). Prevalence and antimicrobial susceptibility of Gram-negative bacilli in subgingival biofilm associated with periodontal diseases. *J. Periodontol.* 93, 69–79. doi: 10.1002/JPER.20-0829

Exterkate, R. A. M., Crielaard, W., and Ten Cate, J. M. (2010). Different response to amine fluoride by Streptococcus mutans and polymicrobial biofilms in a novel high-throughput active attachment model. *Caries Res.* 44, 372–379. doi: 10.1159/000316541

Fernandez, Y., Mostajo, M., Exterkate, R. A. M., Buijs, M. J., Crielaard, W., and Zaura, E. (2017). Effect of mouthwashes on the composition and metabolic activity of oral biofilms grown in vitro. *Clin. Oral Investig.* 21, 1221–1230. doi: 10.1007/s00784-016-1876-2

Figuero, E., Herrera, D., Tobías, A., Serrano, J., Roldán, S., Escribano, M., et al. (2019). Efficacy of adjunctive anti-plaque chemical agents in managing gingivitis: a systematic review and network meta-analyses. *J. Clin. Periodontol.* 46, 723–739. doi: 10.1111/jcpe.13127

Gottsauner, M. J., Michaelides, I., Schmidt, B., Scholz, K. J., Buchalla, W., Widbiller, M., et al. (2020). A prospective clinical pilot study on the effects of a hydrogen peroxide mouthrinse on the intraoral viral load of SARS-CoV-2. *Clin. Oral Investig.* 24, 3707–3713. doi: 10.1007/s00784-020-03549-1

Griggs, D. J., Peake, L., Johnson, M. M., Ghori, S., Mott, A., and Piddock, L. J. V. (2009). Beta-lactamase-mediated beta-lactam resistance in Campylobacter species: prevalence of Cj0299 (bla OXA-61) and evidence for a novel beta-Lactamase in C. jejuni. *Antimicrob. Agents Chemother.* 53, 3357–3364. doi: 10.1128/AAC.01655-08

Grönbeck Lindén, I., Hägglin, C., Gahnberg, L., and Andersson, P. (2017). Factors Affecting Older Persons' Ability to Manage Oral Hygiene: a Qualitative Study. *JDR Clin. Trans. Res.* 2, 223–232. doi: 10.1177/2380084417709267

Hannig, C., and Hannig, M. (2009). The oral cavity–a key system to understand substratum-dependent bioadhesion on solid surfaces in man. *Clin. Oral Investig.* 13, 123–139. doi: 10.1007/s00784-008-0243-3

Haps, S., Slot, D. E., Berchier, C. E., and van der Weijden, G. A. (2008). The effect of cetylpyridinium chloride-containing mouth rinses as adjuncts to toothbrushing

on plaque and parameters of gingival inflammation: a systematic review. *Int. J. Dent. Hyg.* 6, 290–303. doi: 10.1111/j.1601-5037.2008.00344.x

Hiergeist, A., Reischl, U., and Gessner, A. (2016). Multicenter quality assessment of 16S ribosomal DNA-sequencing for microbiome analyses reveals high inter-center variability. *Int. J. Med. Microbiol.* 306, 334–342. doi: 10.1016/j.ijmm.2016.03.005

Hyde, E. R., Andrade, F., Vaksman, Z., Parthasarathy, K., Jiang, H., Parthasarathy, D. K., et al. (2014). Metagenomic analysis of nitrate-reducing bacteria in the oral cavity: implications for nitric oxide homeostasis. *PLoS One* 9:e88645. doi: 10.1371/journal.pone.0088645

Ito, R., Mustapha, M. M., Tomich, A. D., Callaghan, J. D., McElheny, C. L., Mettus, R. T., et al. (2017). Widespread Fosfomycin Resistance in Gram-Negative Bacteria Attributable to the Chromosomal fosA Gene. *mBio* 8, e749–e717. doi: 10.1128/mBio.00749-17

Jakubovics, N. S., Goodman, S. D., Mashburn-Warren, L., Stafford, G. P., and Cieplik, F. (2021). The dental plaque biofilm matrix. *Periodontol. 2000* 86, 32–56. doi: 10.1111/prd.12361

Jepsen, K., Falk, W., Brune, F., Cosgarea, R., Fimmers, R., Bekeredjian-Ding, I., et al. (2022). Prevalence and Antibiotic Susceptibility Trends of Selected *Enterobacteriaceae*, Enterococci, and Candida albicans in the Subgingival Microbiota of German Periodontitis Patients: a Retrospective Surveillance Study. *Antibiotics* 11:385. doi: 10.3390/antibiotics11030385

Jiang, S., Zeng, J., Zhou, X., and Li, Y. (2018). Drug Resistance and Gene Transfer Mechanisms in Respiratory/Oral Bacteria. *J. Dent. Res.* 97, 1092–1099. doi: 10.1177/0022034518782659

Jones, C. G. (1997). Chlorhexidine: is it still the gold standard? *Periodontol. 2000* 15, 55–62. doi: 10.1111/j.1600-0757.1997.tb00105.x

Kistler, J. O., Pesaro, M., and Wade, W. G. (2015). Development and pyrosequencing analysis of an in-vitro oral biofilm model. *BMC Microbiol.* 15:24. doi: 10.1186/s12866-015-0364-1

Kitagawa, H., Izutani, N., Kitagawa, R., Maezono, H., Yamaguchi, M., and Imazato, S. (2016). Evolution of resistance to cationic biocides in Streptococcus mutans and Enterococcus faecalis. *J. Dent.* 47, 18–22. doi: 10.1016/j.jdent.2016.80902.008

Leadbetter, E. R., Holt, S. C., and Socransky, S. S. (1979). Capnocytophaga: new genus of gram-negative gliding bacteria. I. General characteristics, taxonomic considerations and significance. *Arch. Microbiol.* 122, 9–16. doi: 10.1007/BF00408040

Liu, X., Tong, X., Zhu, J., Tian, L., Jie, Z., Zou, Y., et al. (2021). Metagenome-genome-wide association studies reveal human genetic impact on the oral microbiome. *Cell Discov.* 7:117. doi: 10.1038/s41421-021-00356-0

Mao, X., Auer, D. L., Buchalla, W., Hiller, K.-A., Maisch, T., Hellwig, E., et al. (2020). Cetylpyridinium Chloride: mechanism of Action, Antimicrobial Efficacy in Biofilms, and Potential Risks of Resistance. *Antimicrob. Agents Chemother.* 64, e576–e520. doi: 10.1128/AAC.00576-20

Mason, M. R., Nagaraja, H. N., Camerlengo, T., Joshi, V., and Kumar, P. S. (2013). Deep sequencing identifies ethnicity-specific bacterial signatures in the oral microbiome. *PLoS One* 8:e77287. doi: 10.1371/journal.pone.0077287

Meini, S., Tascini, C., Cei, M., Sozio, E., and Rossolini, G. M. (2019). AmpC β-lactamase-producing Enterobacterales: what a clinician should know. *Infection* 47, 363–375. doi: 10.1007/s15010-019-01291-9

Meister, T. L., Gottsauner, J.-M., Schmidt, B., Heinen, N., Todt, D., Audebert, F., et al. (2022). Mouthrinses against SARS-CoV-2 - High antiviral effectivity by membrane disruption in vitro translates to mild effects in a randomized placebo-controlled clinical trial. *Virus Res.* 316:198791. doi: 10.1016/j.virusres.2022.198791

Muehler, D., Mao, X., Czemmel, S., Geißert, J., Engesser, C., Hiller, K.-A., et al. (2022). Transcriptomic Stress Response in Streptococcus mutans following Treatment with a Sublethal Concentration of Chlorhexidine Digluconate. *Microorganisms* 10:561. doi: 10.3390/microorganisms10030561

Navazesh, M., and Christensen, C. M. (1982). A comparison of whole mouth resting and stimulated salivary measurement procedures. *J. Dent. Res.* 61, 1158–1162. doi: 10.1177/00220345820610100901

Nouioui, I., Carro, L., García-López, M., Meier-Kolthoff, J. P., Woyke, T., Kyrpides, N. C., et al. (2018). Genome-Based Taxonomic Classification of the Phylum Actinobacteria. *Front. Microbiol.* 9:2007. doi: 10.3389/fmicb.2018.02007

Nowicki, E. M., Shroff, R., Singleton, J. A., Renaud, D. E., Wallace, D., Drury, J., et al. (2018). Microbiota and Metatranscriptome Changes Accompanying the Onset of Gingivitis. *mBio* 9, e575–e518. doi: 10.1128/mBio.00575-18

Pithon, M. M., Sant'Anna, L. I. D. A., Baião, F. C. S., dos Santos, R. L., Da Coqueiro, R. S., and Maia, L. C. (2015). Assessment of the effectiveness of mouthwashes in reducing cariogenic biofilm in orthodontic patients: a systematic review. *J. Dent.* 43, 297–308. doi: 10.1016/j.jdent.2014.12.010

Pratten, J., Wills, K., Barnett, P., and Wilson, M. (1998). In vitro studies of the effect of antiseptic-containing mouthwashes on the formation and viability of Streptococcus sanguis biofilms. *J. Appl. Microbiol.* 84, 1149–1155. doi: 10.1046/j.1365-2672.1998.00462.x

Premaraj, T. S., Vella, R., Chung, J., Lin, Q., Panier, H., Underwood, K., et al. (2020). Ethnic variation of oral microbiota in children. *Sci. Rep.* 10:14788. doi: 10.1038/s41598-020-71422-y

Rosier, B. T., Takahashi, N., Zaura, E., Krom, B. P., MartÍnez-Espinosa, R. M., van Breda, S. G. J., et al. (2022). The Importance of Nitrate Reduction for Oral Health. *J. Dent. Res.* 23:220345221080982. doi: 10.1177/00220345221080982

Sanz, M., Serrano, J., Iniesta, M., Santa Cruz, I., and Herrera, D. (2013). Antiplaque and antigingivitis toothpastes. *Monogr. Oral Sci.* 23, 27–44. doi: 10.1159/000350465

Schwarz, S. R., Hirsch, S., Hiergeist, A., Kirschneck, C., Muehler, D., Hiller, K.-A., et al. (2021). Limited antimicrobial efficacy of oral care antiseptics in microcosm biofilms and phenotypic adaptation of bacteria upon repeated exposure. *Clin. Oral Investig.* 25, 2939–2950. doi: 10.1007/s00784-020-03613-w

Shani, S., Friedman, M., and Steinberg, D. (2000). The anticariogenic effect of amine fluorides on Streptococcus sobrinus and glucosyltransferase in biofilms. *Caries Res.* 34, 260–267. doi: 10.1159/000016600

So Yeon, L., and Si Young, L. (2019). Susceptibility of Oral Streptococci to Chlorhexidine and Cetylpyridinium Chloride. *Biocontrol. Sci.* 24, 13–21. doi: 10.4265/bio.24.13

Solderer, A., Kaufmann, M., Hofer, D., Wiedemeier, D., Attin, T., and Schmidlin, P. R. (2019). Efficacy of chlorhexidine rinses after periodontal or implant surgery: a systematic review. *Clin. Oral Investig.* 23, 21–32. doi: 10.1007/s00784-018-2761-y

Sproston, E. L., Wimalarathna, H. M. L., and Sheppard, S. K. (2018). Trends in fluoroquinolone resistance in Campylobacter. *Microb. Genom.* 4:e000198. doi: 10.1099/mgen.0.000198

Stanley, A., Wilson, M., and Newman, H. N. (1989). The in vitro effects of chlorhexidine on subgingival plaque bacteria. *J. Clin. Periodontol.* 16, 259–264. doi: 10.1111/j.1600-051x.1989.tb01651.x

Teng, L.-J., Hsueh, P.-R., Tsai, J.-C., Liaw, S.-J., Ho, S.-W., and Luh, K.-T. (2002). High incidence of cefoxitin and clindamycin resistance among anaerobes in Taiwan. *Antimicrob. Agents Chemother.* 46, 2908–2913. doi: 10.1128/AAC.46.9.2908-2913.2002

Tribble, G. D., Angelov, N., Weltman, R., Wang, B.-Y., Eswaran, S. V., Gay, I. C., et al. (2019). Frequency of Tongue Cleaning Impacts the Human Tongue Microbiome Composition and Enterosalivary Circulation of Nitrate. *Front. Cell Infect. Microbiol.* 9:39. doi: 10.3389/fcimb.2019.00039

van der Weijden, F. A., van der Sluijs, E., Ciancio, S. G., and Slot, D. E. (2015). Can Chemical Mouthwash Agents Achieve Plaque/Gingivitis Control? *Dent. Clin. North. Am.* 59, 799–829. doi: 10.1016/j.cden.2015.06.002

Vanbaelen, T., van Dijck, C., Laumen, J., Gonzalez, N., De Baetselier, I., Manoharan-Basil, S. S., et al. (2022). Global epidemiology of antimicrobial resistance in commensal Neisseria species: a systematic review. *Int. J. Med. Microbiol.* 312:151551. doi: 10.1016/j.ijmm.2022.151551

Verspecht, T., Rodriguez Herrero, E., Khodaparast, L., Khodaparast, L., Boon, N., Bernaerts, K., et al. (2019). Development of antiseptic adaptation and cross-adapatation in selected oral pathogens in vitro. *Sci. Rep.* 9:8326. doi: 10.1038/s41598-019-44822-y

Wade, W. G. (2021). Resilience of the oral microbiome. *Periodontol. 2000* 86, 113–122. doi: 10.1111/prd.12365

Wade, W. G., and Addy, M. (1989). In vitro activity of a chlorhexidine-containing mouthwash against subgingival bacteria. *J. Periodontol.* 60, 521–525. doi: 10.1902/jop.1989.60.9.521

Waldron, C., Nunn, J., Mac Giolla Phadraig, C., Comiskey, C., Guerin, S., van Harten, M. T., et al. (2019). Oral hygiene interventions for people with intellectual disabilities. *Cochrane Database Syst. Rev.* 5, CD012628. doi: 10.1002/14651858.CD012628.pub2

Wand, M. E., Bock, L. J., Bonney, L. C., and Sutton, J. M. (2017). Mechanisms of Increased Resistance to Chlorhexidine and Cross-Resistance to Colistin following Exposure of *Klebsiella pneumoniae* Clinical Isolates to Chlorhexidine. *Antimicrob. Agents Chemother.* 61, e1162–e1116. doi: 10.1128/AAC.01162-16

Wieczorek, K., and Osek, J. (2013). Antimicrobial resistance mechanisms among Campylobacter. *Biomed. Res. Int.* 2013:340605. doi: 10.1155/2013/340605

Zaura-Arite, E., van Marle, J., and ten Cate, J. M. (2001). Conofocal microscopy study of undisturbed and chlorhexidine-treated dental biofilm. *J. Dent. Res.* 80, 1436–1440. doi: 10.1177/00220345010800051001

Zayed, N., Boon, N., Bernaerts, K., Chatzigiannidou, I., van Holm, W., Verspecht, T., et al. (2022). Differences in chlorhexidine mouthrinses formulations influence the quantitative and qualitative changes in in-vitro oral biofilms. *J. Periodontal. Res.* 57, 52–62. doi: 10.1111/jre.12937

Zinn, M.-K., Schages, L., and Bockmühl, D. (2020). The Toothbrush Microbiome: impact of User Age, Period of Use and Bristle Material on the Microbial Communities of Toothbrushes. *Microorganisms* 8:1379. doi: 10.3390/microorganisms8091379

Conflict of Interest: The authors declare that the research was conducted in the absence of any commercial or financial relationships that could be construed as a potential conflict of interest.

frontiers | Frontiers in Microbiology

ORIGINAL RESEARCH
published: 07 July 2022
doi: 10.3389/fmicb.2022.825745

A Preliminary *in vitro* and *in vivo* Evaluation of the Effect and Action Mechanism of 17-AAG Combined With Azoles Against Azole-Resistant *Candida* spp.

Luyao Liu[1†], Xueying Zhang[1†], Shruti Kayastha[1], Lihua Tan[1], Heng Zhang[1], Jingwen Tan[2], Linyun Li[3], Jinghua Mao[4] and Yi Sun[5*]*

[1]Yangtze University, Jingzhou, China, [2]Department of Medical Mycology, Shanghai Skin Disease Hospital, Tongji University School of Medicine, Shanghai, China, [3]Clinical Lab, Jingzhou Hospital, Yangtze University, Jingzhou, China, [4]Department of Cardiology, Jingzhou Hospital, Yangtze University, Jingzhou, China, [5]Department of Dermatology, Jingzhou Hospital, Yangtze University, Candidate Branch of National Clinical Research Center for Skin and Immune Diseases, Jingzhou, China

OPEN ACCESS

Edited by:
Miguel Cacho Teixeira, University of Lisbon, Portugal

Reviewed by:
Yinggai Song, Peking University, China
Vandbergue Santos Pereira, Federal University of Ceará, Brazil

***Correspondence:**
Jinghua Mao
jzzxyymjh@163.com
Yi Sun
jzzxyysy@163.com

[†]These authors have contributed equally to this work and share first authorship

Specialty section:
This article was submitted to Antimicrobials, Resistance and Chemotherapy, a section of the journal Frontiers in Microbiology

Received: *30 November 2021*
Accepted: *20 June 2022*
Published: *07 July 2022*

Citation:
Liu L, Zhang X, Kayastha S, Tan L, Zhang H, Tan J, Li L, Mao J and Sun Y (2022) A Preliminary in vitro and in vivo Evaluation of the Effect and Action Mechanism of 17-AAG Combined With Azoles Against Azole-Resistant Candida spp. Front. Microbiol. 13:825745. doi: 10.3389/fmicb.2022.825745

Invasive candidiasis is the primary reason for the increased cases of mortality in a medical environment. The resistance spectra of *Candida* species to antifungal drugs have gradually expanded. Particularly, the resistance spectra of *Candida auris* are the most prominent. Hsp90 plays a protective role in the stress response of fungi and facilitates their virulence. In contrast, Hsp90 inhibitors can improve the resistance of fungi to antifungal drugs by regulating the heat resistance of Hsp90, which destroys the integrity of the fungal cell walls. Hsp90 inhibitors thus offer a great potential to reduce or address fungal drug resistance. The drugs tested for the resistance include itraconazole, voriconazole, posaconazole, fluconazole, and 17-AAG. A total of 20 clinical strains of *Candida* were investigated. The broth microdilution checkerboard technique, as adapted from the CLSI M27-A4 method, was applied in this study. We found that 17-AAG alone exerted limited antifungal activity against all tested strains. The MIC range of 17-AAG was 8 to >32 μg/ml. A synergy was observed among 17-AAG and itraconazole, voriconazole, and posaconazole against 10 (50%), 7 (35%), and 13 (65%) of all isolates, respectively. Moreover, the synergy between 17-AAG and fluconazole was observed against 5 (50%) strains of azole-resistant *Candida*. However, no antagonism was recorded overall. Our result adequately verifies the influence of 17-AAG on the formation of *Candida* spp. biofilm. Moreover, we determined that with the use of rhodamine 6G to detect drug efflux and that of dihydrorhodamine-123 to detect intracellular reactive oxygen species (ROS), treatment with 17-AAG combined with azole drugs could inhibit the efflux pump of fungi and promote the accumulation of ROS in the fungal cells, thereby inducing fungal cell apoptosis. Thus, the mechanism of 17-AAG combined with azoles can kill fungi. Our results thus provide a new idea to further explore drugs against drug-resistant *Candida* spp.

Keywords: 17-AAG, *Candida auris*, azole-resistant *Candida*, synergy, Hsp90 inhibitor

INTRODUCTION

Candida is a symbiont of the normal skin and intestinal microbiota, inhabiting 30–70% of healthy individuals without causing any disease (Pappas et al., 2018). Invasive candidiasis (IC) is caused by increased fungal load and the rupture of the skin and mucosal membrane, which promotes fungal translocation or transmission into the bloodstream or cause damage to the host immune function. The mortality rate after *Candida* infection can be as high as 30–60% (Bugli et al., 2013; Arendrup and Patterson, 2017). In recent years, in parallel with the increasing use of endovascular prosthesis devices for heart diseases, the number of *Candida* patients with endocarditis prosthesis valve has also increased. The implantation of prosthetic valves and the subsequent biofilm formation in these patients has led to the development of resistance to antifungal drugs in them (Venditti, 2009). Clinical and *in vitro* resistance of *Candida* to commonly used azoles has significantly increased at present, especially that of *Candida auris* (Pristov and Ghannoum, 2019). As a type of iatrogenic pathogen, *C. auris* is widely distributed and considered highly contagious worldwide (Gonzalez-Lara and Ostrosky-Zeichner, 2020). In 2009, *C. auris* was isolated from the external auditory canal of a woman in a Tokyo hospital. However, as early as 1996, a Korean girl was reported to be infected with it (ElBaradei, 2020). Since then, *C. auris* infection has been reported throughout the world, excluding Antarctica (ElBaradei, 2020). Across the historical timeline, several outbreaks of *C. auris* infection have been reported across different parts of the world (ElBaradei, 2020). In addition, *C. auris* has reportedly demonstrated strong multi-drug resistance (MDR) and extensive drug resistance (XDR; Arendrup and Patterson, 2017). Several reports have provided evidence that most isolates (93%) are resistant to FLU, 35% to amphotericin B (AMB), and 7% to echinocandin. Echinocandins and AMB can be used as a drug for infection by *C. auris* (Bugli et al., 2013; Arendrup and Patterson, 2017; Pappas et al., 2018; Aruanno et al., 2019; ElBaradei, 2020); however, the cost of echinocandin and AMB substitutes is relatively higher. Specifically, in countries with limited resources, it is not easily available. Moreover, AMB has proven side-effects (Bugli et al., 2013; Arendrup and Patterson, 2017; Pappas et al., 2018; Aruanno et al., 2019; ElBaradei, 2020). Presently, there are only limited options of antifungal agents that can be used for the treatment of this infection. Cases of fungal resistance is increasing in parallel with the cost of developing new antifungal agents, especially in the past decades. Hence, there is an urgent need for establishing new combination therapy in this direction.

Heat shock proteins 90 (Hsp90), a group of highly conserved chaperones, stabilizes several proteins involved in basic metabolic reactions, accounting for 1–2% of all cytosolic proteins (McClellan et al., 2007; Scieglinska et al., 2019; Crunden and Diezmann, 2021). In the fungal stress response, Hsp90 protects fungi by activating important signaling pathways; this mechanism is considered beneficial for fungi to fungal volatilization (Mellatyar et al., 2018). Adenosine triphosphate is the main functional region of Hsp90 (Lamoth et al., 2012; Mellatyar et al., 2018; Aruanno et al., 2019), as has been confirmed with the use of internal and external models of *C. albicans* and *Cryptococcus* (McClellan et al., 2007; Refos et al., 2017; Aruanno et al., 2019). For instance, in *C. albicans* models, Hsp90 also controls temperature-dependent morphogenesis (Kim et al., 2019), while Hsp90 inhibitors can reduce drug resistance of fungi by destroying the integrity of fungal cell walls, inhibiting the transformation of yeast morphology to sporephore, and inhibiting the activity of ATPase at different temperatures (Lamoth et al., 2012; Aruanno et al., 2019; Li et al., 2020b). Therefore, the use of Hsp90 inhibitors combined with the existing antifungal agents for the treatment of fungal infection has broad prospects.

Geldanamycin—a member of the natural benzoquinone ansamycins family—is currently the most widely used Hsp90 inhibitor (Mellatyar et al., 2018). A synthetic variant of geldanamycin, 17-Allylamino-17-demethoxygeldamycin (17-AAG), exhibits similar biological activity and can competitively bind the ATP/ADP binding sites on Hsp90, thereby inhibiting its inherent ATPase activity (Lamoth et al., 2016; Li et al., 2020b) and reducing the resistance of fungi. Currently, it was applied at clinical stages II or III in multiple human tumor treatments and demonstrated satisfactory outcomes (McClellan et al., 2007). In the present study, we investigated the anti-*Candida* activity of 17-AAG, an Hsp90 inhibitor, alone or in combination with azoles under *in vitro* settings.

MATERIALS AND METHODS

Fungal Isolates

A total of 20 clinical isolates of *Candida* spp., including 10 strains of *C. auris* and 10 strains of drug-resistant *Candida* were included in this study. All these strains were clinical isolates, and their identity was confirmed based on their microscopic morphology and molecular sequencing results (Tan et al., 2021). *C. auris* strains were obtained from the CDC and FDA Antibiotic Resistance Isolate Bank. *Candida parapsilosis* (ATCC22019) and *Candida krusei* (ATCC00279) was included in the study to ensure quality control.

Antifungal Agents

All tested azoles, including ITR (No. S2476), VOR (No. S1442), POS (No. S1257), FLU (No. S1131), and 17-AAG (No. S1141), were bought in the powder form from Selleck Chemicals (China) and prepared in accordance with the Clinical and Laboratory Standards Institute's (CLSI) broth microdilution method M27-A4 (Blum et al., 2013) The working concentration range of 17-AAG was 0.25–32 μg/ml, while those of ITR, VOR, and POS were 0.125–16 μg/ml for *C. auris*. For drug-resistant *Candida spp*., the working concentration ranges of ITR, VOR, POS, and FLU were 0.06–8 μg/ml, 0.06–8 μg/ml, 0.03–4 μg/ml, and 0.25–32 μg/ml.

Inoculum Preparation

Conidia were freshly collected in sterile distilled water from cultures grown for 2 days on Sabouraud's dextrose agar (SDA)

and then diluted to the right concentration of $1–5 \times 10^6$ cfu/ml. Then, the suspensions were further diluted 1,000 times in the RPMI-1640 medium to achieve the desired density or approximately $1–5 \times 10^3$ cfu/ml concentration.

Testing the *in vitro* Synergy of 17-AAG and Azoles

The combination groups with 17-AAG and azoles against all test strains were estimated through broth microdilution checkerboard technique, which was performed in accordance with the CLSI M27-A4 standards. Briefly, 50 µl of serially diluted 17-AAG and another 50 µl of serially diluted azoles were inoculated on a 96-well plate in the horizontal and vertical directions, separately. Finally, the prepared plates were inoculated with 100 µl of the prepared fungal suspension and incubated for 24 h at 35°C, followed by the interpretation of the observation. The minimum inhibitory concentrations (MICs) were visually determined by the inhibition of 50% in the control group, as established by the standardized endpoint (Blum et al., 2013). The fractional inhibitory concentration index (FICI) was applied to analyze the interactions between 17-AAG and azoles (Odds, 2003), which was calculated by the following formula: FICI = d1/(D1)p + d2/(D2)p, where d1 and d2 are the doses of tested agents in combination, while (D1)p and (D2)p are the doses of two respective compounds alone. If an interaction was scored as FICI of ≤0.5, synergy; as FICI of >0.5 to ≤4, indifference and as FICI of >4, antagonism (Van Dijck et al., 2018). All experiments were conducted in triplicate.

Evacuation of *in vivo* Drug Sensitivity of 17-AAG Alone and in Combination With Azoles

Further to the abovementioned results, we selected the sixth instar (300 mg; Sichuan, China) to evaluate the *in vivo* interaction between 17-AAG and azoles referred in our previous study (Tan et al., 2021). Accordingly, *C. auris* AR 382, *C. abicans* R2, and *C. glabrata* 05448 were tested. Before the experiment, fresh spore suspension was prepared at the concentration of 1×10^8 cfu/ml. Then, 17-AAG was diluted with azoles. The solution in the monotherapy group was diluted to 200 mg/ml with normal saline, while that in the combination group was mixed in advance and diluted to 200 mg/ml with normal saline. The larvae were randomly categorized into 11 groups, as follows: untreated, normal saline, Conidal, POS, ITR, VOR, FLU, 17-AAG + POS, 17-AAG + ITR, 17-AAG + VOR, and 17-AAG + FLU groups. Then, 10 µl of the corresponding spore suspension was injected using a Hamilton syringe (25 gauge, 50 µl) from the last left foot of each set of larvae, 5 µl (1 µg/worm) was injected at 2-h apart, and the larvae were cultured at 37°C, within 120 h of injection. The survival of the larvae was monitored every 24 h. The larval survival curve was evaluated by Kaplan–Meier method and log-rank (Mantel-Cox) test, with $p < 0.05$ set as a significance threshold.

Biofilm Drug Sensitivity Testing

Sabouraud dextrose broth (SAB; 2 ml) was added to each well of a 24-well plate, to which fresh suspension of *C. auris* AR 382 was added at the final concentration of 1×10^6 cfu/ml. Then, a predetermined concentration of the drug was added. The concentration of the drug was based on the experimental results of the broth microdilution checkerboard technique (**Table 1**). We divided the experiment into 8 groups, as follows: No drug,17-AAG (16 µg/ml), ITR (0.5 µg/ml), VOR (0.5 µg/ml), POS (1 µg/ml), 17-AAG + ITR (0.25 µg/ml + 0.125 µg/ml), 17-AAG + VOR (8 µg/ml + 0.125 µg/ml), and 17-AAG + POS (4 µg/ml + 0.125 µg/ml) groups. Finally, after incubation at 121°C for 30 min, autoclaved round slices were added to a 24-well plate, followed by their incubation at 37°C for 24–48 h. Two experimental subgroups were created for each group. At the time point of 24 h and 48 h, the round slices was removed with tweezers and placed on the slide. A drop of fluorescent staining solution Calcofluor White stain (Sigma 18,909) and another drop of 10% KOH were added to the slide, followed by the observation of biofilm under fluorescence microscope. In order to further evaluate the effect of different antifungal agents on *C. auris* AR 382, the spores above the round slices were re-suspended after observation of the biofilm at 24 h and 48 h. The CFU were counted for different groups and evaluated by paired *T* test. The experiment was repeated thrice.

Testing the Extracellular Rhodamine 6G

Fresh bacterial suspension of *C. auris* AR 382 (1×10^9 cfu/ml) was added to 6 ml of the 1× PBS solution. After twice centrifugation at 4,000 rpm, the solution was re-suspended with PBS and cultured for 2 h in a shaker. After centrifugation at 4,000 rpm, the intracellular energy was exhausted and the solution was re-suspended with 10 µm of PBS R6G (Sigma 10 µm) liquor, mixed uniformly, and placed at 37°C shaking at 200 rpm for 50 min, followed by incubation on an ice bath for 10 min and twice centrifugation at 4,000 rpm. Next, 6 ml of the PBS solution was added to the control without adding any drugs. In the sugar-free and drug-free control groups, only 6 ml of the PBS solution was added without any additional sugar, and the remaining drugs with predetermined concentration were added to each tube (**Table 1**) as follows: no drug, no glucose, 17-AAG (16 µg/ml), ITR (0.5 µg/ml), VOR (0.5 µg/ml), POS (1 µg/ml), 17-AAG + ITR (0.25 µg/ml + 0.125 µg/ml), 17-AAG + VOR (8 µg/ml + 0.125 µg/ml), and 17-AAG + POS (4 µg/ml + 0.125 µg/ml). The samples were assayed at 0 min, and glucose was added after 10 min. After each sampling, the supernatant was centrifuged and added to a 96-well plate. A spectrophotometer (Beijing Perlong DNM-9602; excitation light 527 nm) was used to measure the fluorescence in the supernatant due to efflux, once every 10 min, for 1 h. The experiment was repeated thrice on different days to evaluate the induction effect of drugs on the fungal efflux pump.

Testing the Intracellular ROS

The fresh suspension of *C. auris* AR 382 was added to 10 ml of SAB at the final concentration of $3–5 \times 10^6$ cfu/ml. Germs were treated with the azoles of predetermined concentration {No drug, 17-AAG (16 µg/ml), ITR (0.5 µg/ml), VOR (0.5 µg/ml), POS (1 µg/ml), 17-AAG + ITR (0.25 µg/ml + 0.125 µg/ml),

TABLE 1 | MICs and FICIs results with the combinations of 17-AAG and azoles against azole-resistant *Candida* spp.

Strains	Species	MIC[1] (μg/m) for						
		Agent alone				Combination[2]		
		17-AAG	ITR	VOR	POS	17-AAG/ITR	17-AAG/VOR	17-AAG/POS
AR381	*C. auris*	>32	0.5	0.125	0.125	2/0.25(0.53)	0.5/0.125(1.01)	0.5/0.125(1.01)
AR382		16	0.5	0.5	1	0.5/0.125(0.28)	8/0.125(0.75)	4/0.125(0.38)
AR383		>32	0.25	2	0.5	1/0.125(0.52)	0.5/0.125(0.07)	2/0.125(0.28)
AR384		>32	1	0.5	0.25	0.5/1(1.01)	0.5/0.5(1.01)	0.5/0.125(0.51)
AR385		>32	0.5	16	1	0.5/0.5(1.01)	16/8(0.75)	0.5/0.125(0.13)
AR386		16	0.5	16	0.5	0.5/0.125(0.28)	16/16(2)	2/0.125(0.38)
AR387		16	0.25	1	1	0.5/0.25(1.03)	0.5/0.125(0.16)	0.5/0.125(0.16)
AR388		>32	1	2	0.125	0.5/1(1.01)	0.5/1(0.51)	0.5/0.125(1.01)
AR389		8	0.25	4	0.25	0.5/0.125(0.56)	0.5/2(0.56)	1/0.25(1.13)
AR390		>32	1	4	0.5	1/0.125(0.14)	1/1(0.27)	1/0.125(0.27)
64,550	*C. albicans*	>32	2	0.25	2	32/0.25(0.63)	0.5/0.125(0.51)	16/0.25(0.38)
5,310		16	2	0.125	0.06	0.5/0.125(0.09)	0.5/0.125(1.03)	2/0.03(0.63)
R2		16	1	0.5	0.06	4/0.125(0.38)	0.5/0.125(0.28)	0.5/0.03(0.53)
R9		16	16	16	8	2/0.125(0.13)	0.5/0.125(0.04)	1/0.03(0.07)
R14		16	4	8	1	1/0.125(0.09)	0.5/4(0.53)	8/0.5(1.00)
R15		32	1	1	1	1/0.125(0.16)	0.5/0.125(0.14)	4/0.03(0.16)
5,448	*C. glabrata*	>32	8	2	2	2/2(0.28)	4/2(1.06)	1/0.5(0.27)
5,150	*C. tropicalis*	>32	0.5	0.125	0.25	0.5/0.125(0.26)	0.5/0.125(1.01)	2/0.06(0.27)
ATCC22019	*C. parapsilosis*	>32	0.5	0.125	0.125	1/0.25(0.52)	0.5/0.125(1.01)	0.5/0.125(1.01)
ATCC00279	*C. krusei*	>32	0.25	1	1	0.5/0.125(0.51)	1/0.25(0.27)	8/0.25(0.38)

[1]*The MIC is the concentration resulting in 50% growth inhibition.*

[2]*Fractional inhibitory concentration index (FICI) results are shown in parentheses. Synergy (FICI < 0.5); no interaction (indifference, 0.5 < FICI < 4).*

TABLE 2 | MICs and FICIs results with the combinations of 17-AAG and FLU against azole-resistant *Candida.*

Strains	Species	MIC (μg/ml)[1] for		
		Agent alone		Combination[2]
		17-AAG	FLU	17-AAG/FLU
5310	*C. albicans*	16	0.5	0.25/0.5(1.02)
64550		>32	16	16/4(0.50)
R2		16	2	4/0.5(0.50)
R9		16	64	2/0.5(0.13)
R14		16	16	8/8 (1.00)
R15		32	16	4/1(0.19)
5448	*C. glabrata*	>32	64	0.5/64(1.01)
5150	*C. tropicalis*	>32	2	2/0.5(0.28)
ATCC22019	*C. parapsilosis*	>32	4	4/4(1.06)
ATCC00279	*C. krusei*	>32	64	2/32(0.53)

[1]*The MIC is the concentration resulting in 50% growth inhibition.*

[2]*Fractional inhibitory concentration index (FICI) results are shown in parentheses. Synergy (FICI < 0.5); no interaction (indifference, 0.5 < FICI < 4).*

17-AAG + VOR (8 μg/ml + 0.125 μg/ml), and 17-AAG + POS (4 μg/ml + 0.125 μg/ml)} and dihydrorhodamine-123 (Sigma DHR-123 5 μg/ml), followed by incubation at 37°C for 1 h. After centrifugation and resuspension, the germlings were harvested and detected by flow cytometry (Beckman Coulter DxFLEX) at an excitation wavelength of 488–505 nm and an emission wavelength of 515–575 nm. The experiment was repeated thrice on different days, and p values were calculated using unpaired T test.

RESULTS

17-AAG and Azoles Interactions *in vitro*

The MICs ranges of each drug against all *Candida* isolates were 8 to >32 μg/ml for 17-AAG, 0.25–1 μg/ml for ITR, 0.125–4 μg/ml for VOR, 0.06–2 μg/ml for POS, and 0.5–64 μg/ml for FLU, respectively (**Tables 1**, **2**). Moreover, 17-AAG alone exhibited only a slight antifungal activity against all tested strains. However, when 17-AAG was combined with ITR, VOR, or POS, synergistic anti-*Candida* effects were detected in 10 (50.0%), 7 (35.0%), and 13 (65.0%) isolates, while, in combination with FLU, the corresponding effect was observed in 5 (50%) isolates of drug-resistant *Candida* spp. The concentrations of 17-AAG in the synergistic combinations were effective within the range of 0.5–32 μg/ml (**Tables 1**, **2**; **Figure 1**). No antagonism was recorded in the two combination groups.

Evacuation of *in vivo* Drug Sensitivity of 17-AAG Alone and in Combination With Azoles

In this experiment, we used the caterpillar mellonella for the *in vivo* test, while the growth and survival rate of each group of larvae are shown in **Figure 2**. The survival rates of *C. abicans* R2, *C. auris* AR 382, and *C. glabrate* 05448 were significantly prolonged when 17-AAG combined with POS and 17-AAG combined with ITR. Especially when 17-AAG was used in combination with POS, the survival rate of *C. abicans* R2 was significantly improved ($p < 0.05$). When 17-AAG was used in combination with VOR, only *C. auris* AR 382 had significantly longer survival ($p < 0.05$).

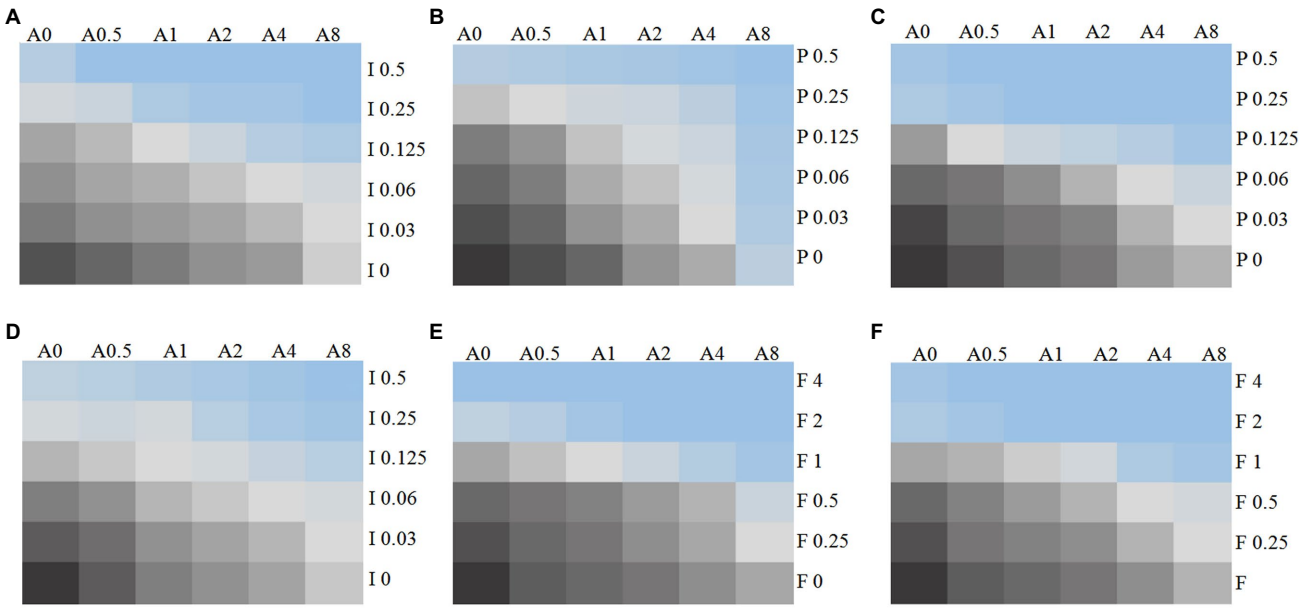

FIGURE 1 | Chromatic scale diagram of synergistic effects of partial drug sensitivity results. Several drug sensitivity diagrams with obvious synergistic effect are listed in accordance with the *in vitro* drug sensitivity test and checkerboard method, **(A)** *C. auris* AR 382 17-AAG + ITR; **(B)** *C. auris* AR 382 17-AAG + POS; **(C)** 5,150 17-AAG + POS; **(D)** R9 ITR; **(E)** R2 FLU; and **(F)** 5,150 FLU. From black to blue, indicating that the fungus growth gradually decreased, A represents 17-AAG, I represents ITR, V represents VOR, P represents POS, and the number after the letter represents concentration (μg/ml).

The 17-AAG + FLU combination can significantly prolong the survival time of larvae, especially *C. abicans* R2 ($p < 0.05$).

Biofilm Drug Sensitivity Testing

In this experiment, we performed Calcofluor White staining of the test fungus, followed by observation under a fluorescence microscope. As shown in **Figure 3**, at 24 h, the *C. auris* AR 382 biofilm was significantly reduced in the monotherapy group compared with that in the drug-free group, while the biofilm reduction was more obvious in the combination group. At 48 h, the difference was more prominent, and the biofilms in the three drug combination groups were significantly reduced (**Figure 3**). After measuring the CFU value of different groups by paired *T* test, we achieved consistent results (**Table 3**). We noted that 17-AAG could play an antifungal role by inhibiting the production of fungal biofilms when used in combination with azole drugs.

Extracellular R6G Testing

In our experiment, the fluorescent dye R6G was used, which is known to be transported in and out of several multi-drug resistant yeast cells to mammalian cells. Therefore, for the detection purpose, a spectrophotometer was used to analyze R6G for *C. auris* AR 382 under different drug treatments, followed by comparative analyses. When the cells in all groups were cultured in glucose-free PBS, the content of extracellular R6G did not increase. After the addition of glucose at 10 min, the extracellular OD value of each group began to increase to varying degrees. When all groups were compared with the sugar-free and drug-free groups, the following results were obtained: 1: in the sugar-free group, no intracellular energy was present to drive the efflux pump, which resulted in extremely low extracellular R6G content. 2: In the drug-free treatment group, significant efflux of R6G occurred when glucose was added to drive the efflux pump. The effluence of R6G in 17-AAG and azoles alone groups was less than that in the control group. However, the combination of 17-AAG with azoles drugs resulted in obviously decreased efflux of R6G (**Figure 4**). Thus, our results confirmed that 17-AAG when used in combination with an antifungal drug, possibly by inhibiting the efflux pump, decreasing the antifungal drug efflux, drug accumulation in the cells, as well as the subsequent reaction to fungal cell death.

Intracellular ROS Testing

In this study, we used the stain DHR-123—an uncharged and fluorescent-free intracellular ROS detection agent—that could actively penetrate the cell membranes. It can be oxidized to rodamine-123 by intracellular ROS that emit bright green fluorescence, which can be quantitatively detected by flow cytometry. Three repeated measurements revealed that the ROS production in *C. auris* AR 382 was higher when monotherapy was performed relative to that in the drug-free control group. However, when 17-AAG was used in combination with azole, the proportion of ROS-producing cells was significantly increased when compared with that of the control cells ($p < 0.05$; **Figure 5**). These results suggest that, when drugs accumulate in fungal cells, the subsequent accumulation of ROS induces the apoptosis of fungal cells.

DISCUSSION

Some past researches have demonstrated that 17-AAG combined with azoles or echinosporins exhibit effective synergistic antifungal

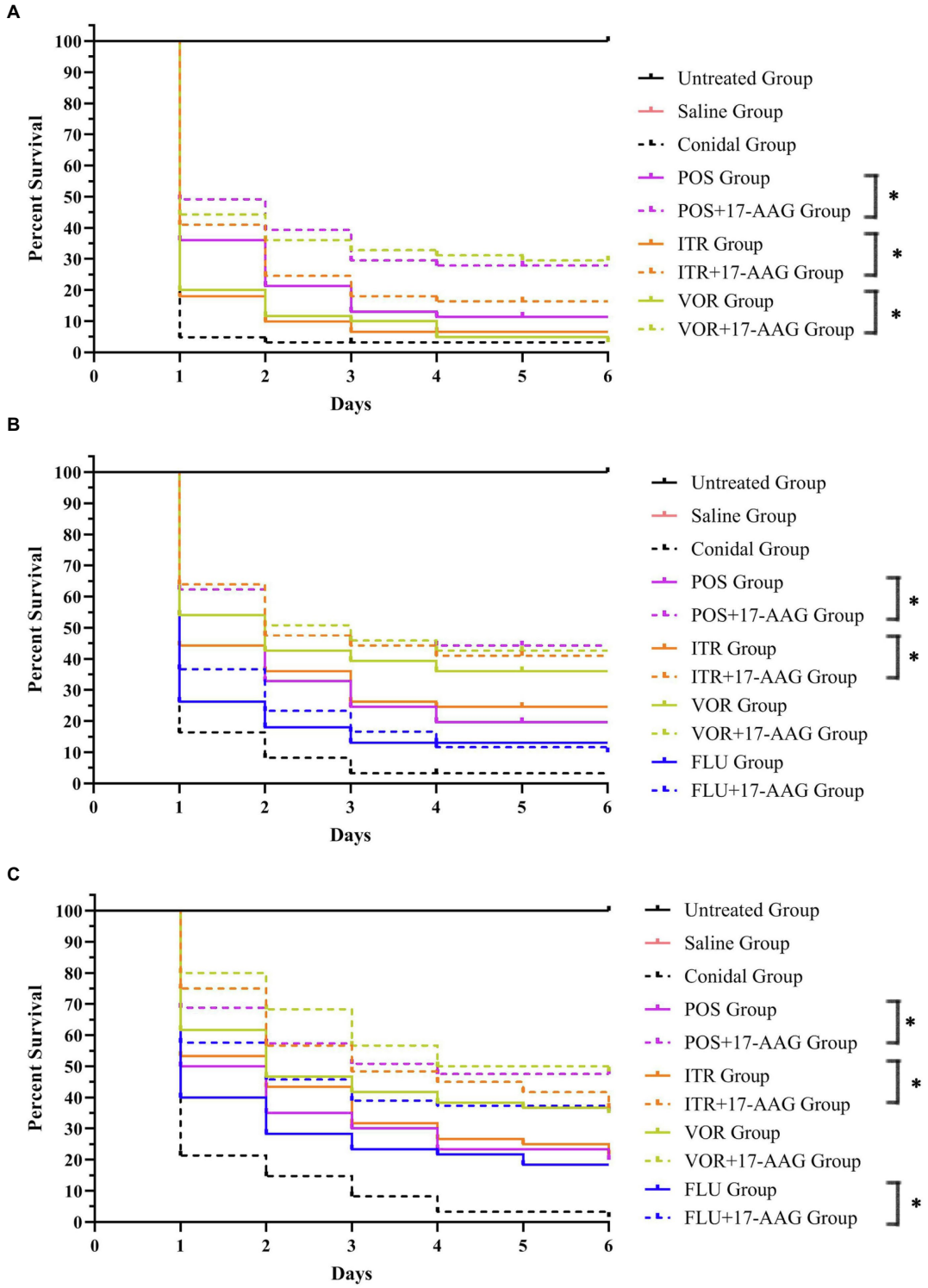

FIGURE 2 | *Galleria mellonella* survival curves following infection with *Candida* spp. **(A)** *C. auris* AR 382; **(B)** *C. glabrate* 05448; and **(C)** *C. abicans* R2. Untreated group, wild-type uninfected larvae; Saline group, wild-type larvae injected with saline; Conidial group, larvae infected with *Candida* without any treatment; itraconazole (ITC) group, *Candida*-infected larvae treated with ITC alone; voriconazole (VOR) group, *Candida*-infected larvae treated with VOR alone; posaconazole (POS) group, *Candida*-infected larvae treated with POS alone; fluconazole (FLU) group, *Candida*-infected larvae treated with FLU alone; 17-AAG + ITC group, *Candida*-infected larvae treated with 17-AAG combined with ITC; 17-AAG + VOR group, *Candida*-infected larvae treated with 17-AAG combined with VOR; 17-AAG + POS group, *Candida*-infected larvae treated with 17-AAG combined with POS. 17-AAG + FLU group, *Candida*-infected larvae treated with 17-AAG combined with FLU; $^{*}p < 0.05$.

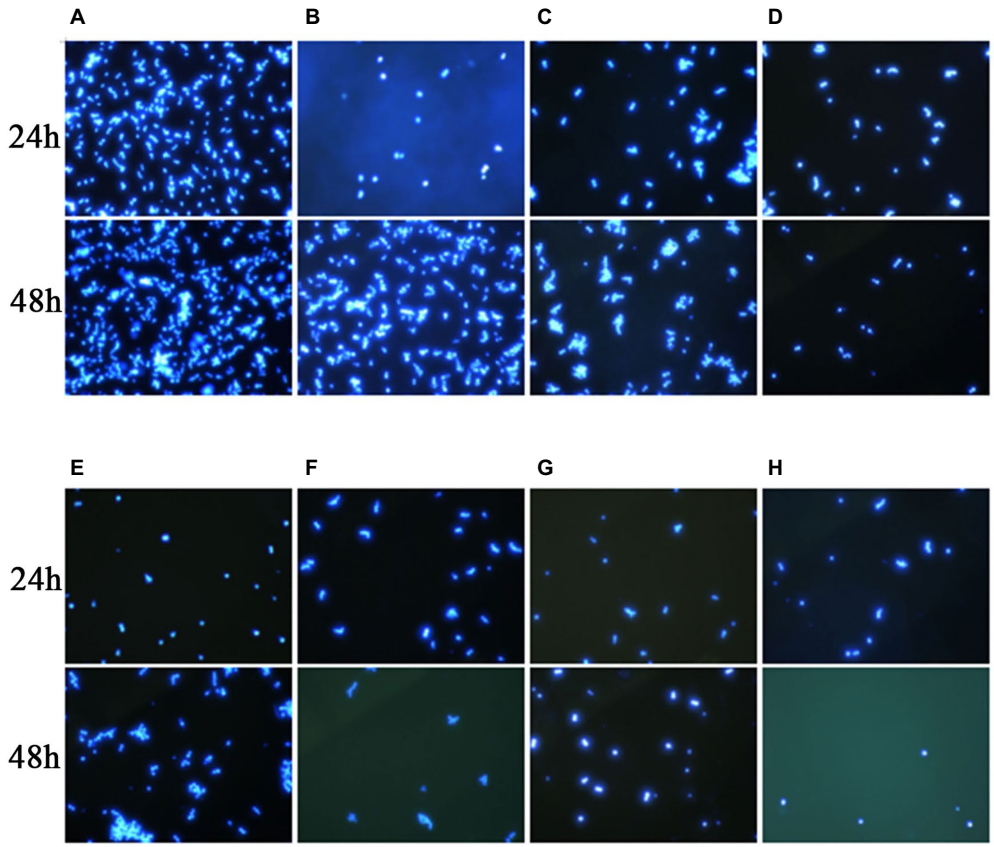

FIGURE 3 | Effects of 17-AAG and azole monotherapy and in combination on biofilm formation by *C. auris* AR 382. **(A)** No drug; **(B)** 17-AAG; **(C)** ITR; **(D)** 17-AAG + ITR; **(E)** VOR; **(F)** 17-AAG + VOR; **(G)** POS; and **(H)** 17-AAG + POS.

TABLE 3 | Concentration of spores in *C. auris* AR 382 biofilms.

Group	Spore concentration (CFU/ml)	
	24 h	48 h
No drug	3.40×10^6	5.98×10^6
17-AAG	3.22×10^6	9.35×10^6
ITR	1.48×10^6	$5.53 \times 10^{5*}$
17-AAG + ITR	1.30×10^6	$6.57 \times 10^{5*}$
VOR	7.43×10^5	$1.11 \times 10^{6*}$
17-AAG + VOR	$7.10 \times 10^{5*}$	$8.20 \times 10^{5*}$
POS	$1.15 \times 10^{6*}$	$6.53 \times 10^{5*}$
17-AAG + POS	$3.67 \times 10^{5*}$	$2.80 \times 10^{5*}$

**The CFU values of the group without antifungal drugs and the antifungal drugs group were statistically significant ($p < 0.05$).*

activity against *Aspergillus fumigatus, Aspergillus terreus, Candida rubra,* and *Candida albicans* under both *in vitro* and *in vivo* conditions (Blum et al., 2013; Jacob et al., 2015; Chatterjee and Tatu, 2017; Refos et al., 2017). In addition, some previous studies have reported that 17-AAG can significantly reduce the ATPase activity in the *in vitro* cryptococcus infection model at 37°C, which changes the effectiveness of azole drugs range from ineffective to highly effective. However, information about the effect of *C. auris* and some azole-resistant *Candida* is limited in the literature. Therefore, the application of 17-AAG combined with anti-fungal agents in the treatment of fungal infection has significant potential.

Although 17-AAG alone demonstrated non-activity against some azole-resistant *Candida* spp., for azole-resistant *Candida* spp., it demonstrated a synergistic effect with ITR, VOR, and POS, especially with POS in combination with azoles under *in vitro* conditions. For FLU-resistant *Candida* sp., it demonstrated a synergistic effect with FLU. The effective working range of 17-AAG was found to be 0.5–32 μg/ml. Our results provide strong evidence for the potential value of 17-AAG in the treatment of fungal infections caused by *C. auris* and some azole-resistance *Candida*.

We used the caterpillar mellonella as a model in our *in vivo* experiments because these larvae demonstrate similar reactions to those of mammals, making them ideal for use in our *in vivo* experiments (Tan et al., 2021). Our *in vivo* test results were nearly the same as those of our *in vitro* test results. In other words, 17-AAG demonstrated better fungicidal effect when combined with azole drugs. However, in order to validate our *in vitro* test results, further experiments with mice need to be conducted.

Some past studies have proved that 17-AAG can reduce the ATPase activity by competitively binding to the ADP/ATP site with Hsp90. For instance, the IC 50 of 37°C was lower

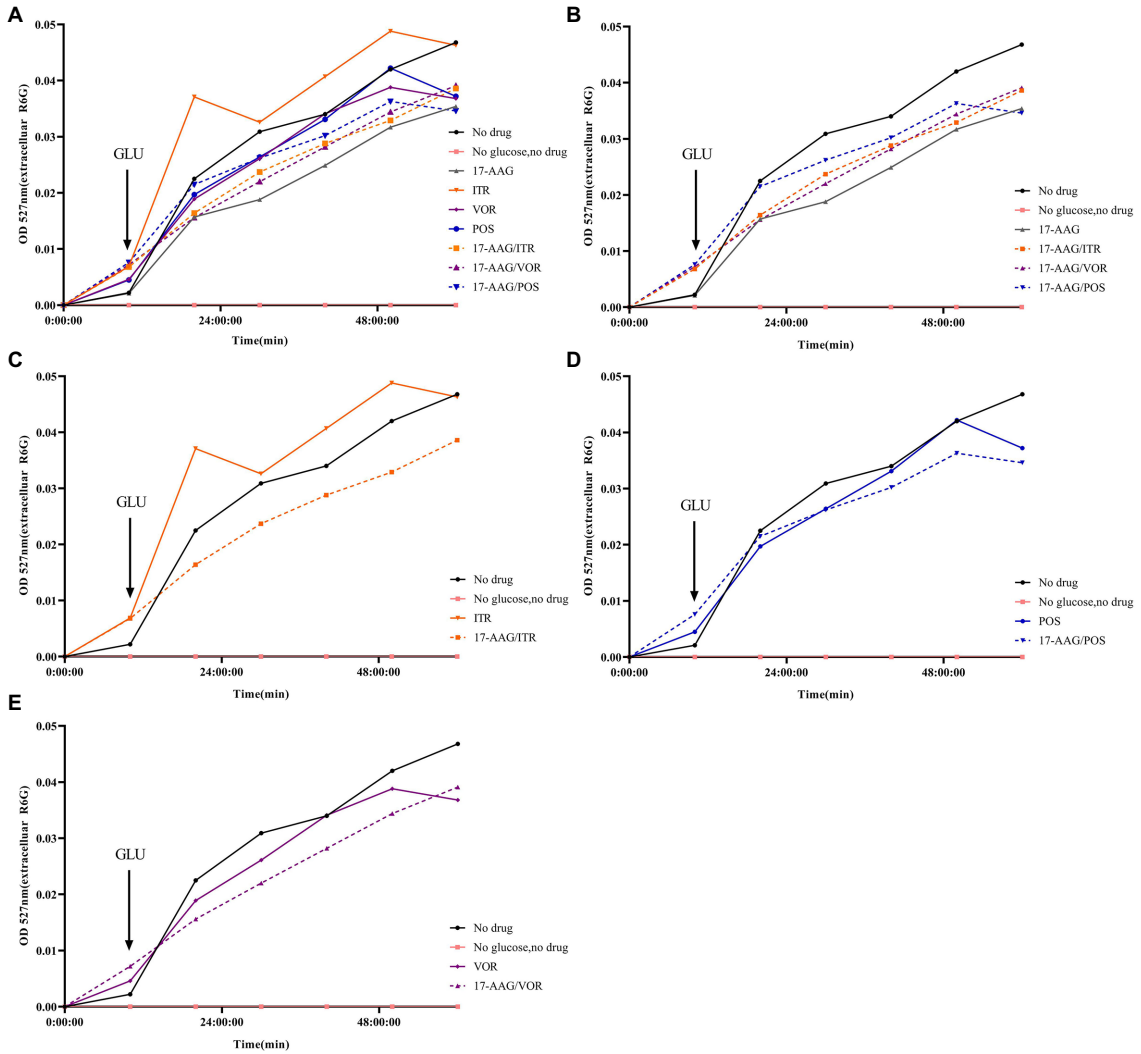

FIGURE 4 | Extracellular R6G measurements of 17-AAG and azole alone or in combination. **(A)** No drug+No glucose+17-AAG + ITR + VOR + POS + 17-AAG/ITR + 17-AAG/VOR + 17-AAG/POS; **(B)** No drug+No glucose+17-AAG + 17-AAG/ITR + 17-AAG/VOR + 17-AAG/POS; **(C)** No drug+No glucose+ITR + 17-AAG/ITR; **(D)** No drug+No glucose+VOR + 17-AAG/VOR; and **(E)** No drug+No glucose+POS + 17-AAG/POS.

than that of 25°C in a model of *Cryptococcus* infection *in vitro* (Chatterjee and Tatu, 2017). Lv has demonstrated that 17-AAG could competitively bind to the ADP/ATP site of Hsp90 in order to prevent the formation of the Hsp90 chaperone complex, which then leads to the development of unfolded substrate and further degradation (Lv et al., 2020). Further study revealed that the synergistic action target of 17-AAG and azole in anti-azole drug-resistant fungi may inhibit the drug efflux pump on fungal cell membranes, possibly caused by the inhibition of the activity of ATPase inherent in fungal cells by 17-AAG. These drugs accumulate in fungal cells. As 17-AAG stimulates the production of Ca^{2+} and endoplasmic reticulum kinase-dependent ROS in the human body (Mitchell et al., 2007), the combination of 17-AAG and azole in this study induced ROS accumulation in the fungal cells, which is consistent with the results of human experiments. Aon confirmed that ROS may exert harmful effects in either a low or a high proportion of cells. When excessive ROS accumulates in cells, the cells cannot be regulated (Aon et al., 2012). ROS has been confirmed to play the main role in the regulation of the cell cycle progression (Verbon et al., 2012), and the cells mediated by ROS over a long time are known to undergo pathological death (Zorov et al., 2014). In addition, ROS can further induce the accumulation of intracellular hydroxyl radicals, which is the key factor of cell apoptosis (Haruna et al., 2002). Therefore, when 17-AAG was used in combination with azole, the fungal cell apoptosis was negatively correlated with the drug efflux and positively correlated with the accumulation of intracellular ROS, which in turn reduced the resistance of fungi. Our study provides meaningful clues toward the elucidation of the mechanism of 17-AAG-specific antifungal activities.

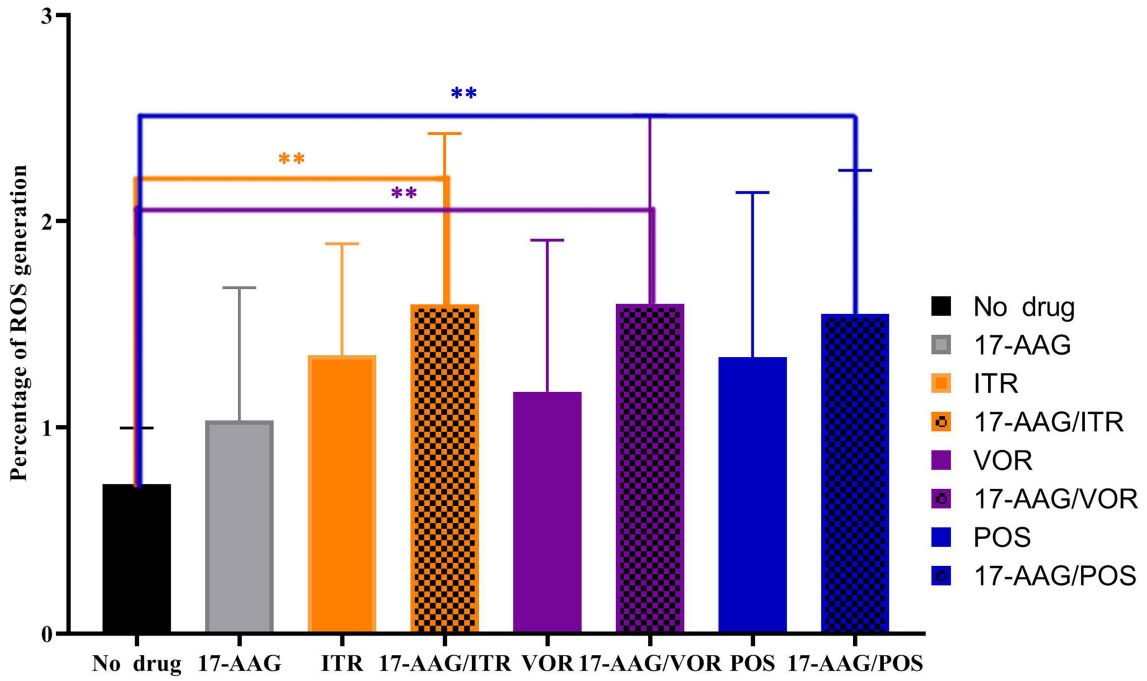

FIGURE 5 | 17-AAG and azole alone and in combination, extracellular ROS production level. $^{**}p < 0.0$.

When compared with geldanamycin, 17-AAG exhibited a higher stability, better bioavailability, and greater water solubility (Li et al., 2020b), which allows its wider distribution across animal tissues, thereby signifying its greater potential in clinical applications. Recent studies have demonstrated that low concentration of 17-AAG can inhibit the growth of breast cancer cells, induce apoptosis (Esgandari et al., 2021), and prevent myocardial dysfunction after myocardial infarction in rats (Marunouchi et al., 2021). HSP90 is a host-dependent factor of human coronaviruses MERS-CoV SARS-COV and SARS-COV-2, while HSP90 inhibitors can be used as an effective broad-spectrum antiviral agent against human coronaviruses (Li et al., 2020a). In addition, a Chinese group verified, for the first time, that the synthesis of a new 17-AAG glucoside by UDP glycosyltransferase *in vitro* can improve its water solubility and anti-tumor efficacy, thereby proving that it can be applied to clinical development through the prodrug method (Woo et al., 2017; Li et al., 2020b). Although there are more optimistic improvement programs available, the number of supporting clinical and experimental data is scarce. Presently, we need to invest more efforts toward the prevention and treatment of this type of fungal infection.

CONCLUSION

17-AAG offers great potential to reduce azoles resistance in fungi under *in vitro* conditions, which suggests that the use of Hsp90 inhibitors in combination with the existing agents for *Candida* infection is a potential therapy. Nevertheless, further investigations are warranted to clarify its potential clinical application.

DATA AVAILABILITY STATEMENT

The original contributions presented in the study are included in the article/**Supplementary Material**, further inquiries can be directed to the corresponding authors.

AUTHOR CONTRIBUTIONS

XZ carried out the *in vitro* antifungal experiment. LuL did other experiments to explore the mechanism. LuL and JT conducted *in vivo* antifungal experiments. SK and LT collection and analysis the experiment data. YS and JM designed, interpreted the experiment data, and wrote the manuscript. YS, LiL, and HZ revised the manuscript critically for important content. All authors contributed to the article and approved the submitted version.

FUNDING

This work was supported by Grant no. WJ2021M261 (YS) from Health Commission of Hubei Province Scientific Research Project and Grant no. 2019CFB567 (YS) from the Natural Science Foundation of Hubei Province. The funders had no

role in study design, data analysis, the decision to publish, or preparation of the manuscript.

ACKNOWLEDGMENTS

We thank JT and Lianjuan Yang from Department of Medical Mycology, Shanghai Skin Disease Hospital, Tongji University School of Medicine, Shanghai for kindly provided us with the isolates studied. We thank MJ Editor (www.mjeditor.com) for our linguistic assistance.

SUPPLEMENTARY MATERIAL

The Supplementary Material for this article can be found online at: https://www.frontiersin.org/articles/10.3389/fmicb.2022.825745/full#supplementary-material

REFERENCES

Aon, M. A., Stanley, B. A., Sivakumaran, V., Kembro, J. M., O'Rourke, B., Paolocci, N., et al. (2012). Glutathione/thioredoxin systems modulate mitochondrial H2O2 emission: an experimental-computational study. *J. Gen. Physiol.* 139, 479–491. doi: 10.1085/jgp.201210772

Arendrup, M. C., and Patterson, T. F. (2017). Multidrug-resistant Candida: epidemiology, molecular mechanisms, and treatment. *J. Infect. Dis.* 216, S445–S451. doi: 10.1093/infdis/jix131

Aruanno, M., Glampedakis, E., and Lamoth, F. (2019). Echinocandins for the treatment of invasive Aspergillosis: from laboratory to bedside. *Antimicrob. Agents Chemother.* 63:19. doi: 10.1128/AAC.00399-19

Blum, G., Kainzner, B., Grif, K., Dietrich, H., Zeiger, B., Sonnweber, T., et al. (2013). In vitro and in vivo role of heat shock protein 90 in amphotericin B resistance of Aspergillus terreus. *Clin. Microbiol. Infect.* 19, 50–55. doi: 10.1111/j.1469-0691.2012.03848.x

Bugli, F., Cacaci, M., Martini, C., Torelli, R., Posteraro, B., Sanguinetti, M., et al. (2013). Human monoclonal antibody-based therapy in the treatment of invasive candidiasis. *Clin. Dev. Immunol.* 2013:403121. doi: 10.1155/2013/403121

Chatterjee, S., and Tatu, U. (2017). Heat shock protein 90 localizes to the surface and augments virulence factors of *Cryptococcus neoformans*. *PLoS Negl. Trop. Dis.* 11:e0005836. doi: 10.1371/journal.pntd.0005836

Crunden, J. L., and Diezmann, S. (2021). Hsp90 interaction networks in fungi-tools and techniques. *FEMS Yeast Res.* 21:54. doi: 10.1093/femsyr/foab054

ElBaradei, A. (2020). A decade after the emergence of Candida auris: what do we know? *Eur. J. Clin. Microbiol. Infect. Dis.* 39, 1617–1627. doi: 10.1007/s10096-020-03886-9

Esgandari, K., Mohammadian, M., Zohdiaghdam, R., Rastin, S. J., Alidadi, S., and Behrouzkia, Z. (2021). Combined treatment with silver graphene quantum dot, radiation, and 17-AAG induces anticancer effects in breast cancer cells. *J. Cell. Physiol.* 236, 2817–2828. doi: 10.1002/jcp.30046

Gonzalez-Lara, M. F., and Ostrosky-Zeichner, L. (2020). Invasive Candidiasis. *Semin. Respir. Crit. Care Med.* 41, 003–012. doi: 10.1055/s-0040-1701215

Haruna, S., Kuroi, R., Kajiwara, K., Hashimoto, R., Matsugo, S., Tokumaru, S., et al. (2002). Induction of apoptosis in HL-60 cells by photochemically generated hydroxyl radicals. *Bioorg. Med. Chem. Lett.* 12, 675–676. doi: 10.1016/s0960-894x(01)00830-7

Jacob, T. R., Peres, N. T., Martins, M. P., Lang, E. A., Sanches, P. R., Rossi, A., et al. (2015). Heat shock protein 90 (Hsp90) as a molecular target for the development of novel drugs Against the Dermatophyte Trichophyton rubrum. *Front. Microbiol.* 6:1241. doi: 10.3389/fmicb.2015.01241

Kim, S. H., Iyer, K. R., Pardeshi, L., Munoz, J. F., Robbins, N., Cuomo, C. A., et al. (2019). Genetic analysis of Candida auris implicates Hsp90 in morphogenesis and azole tolerance and Cdr1 in azole resistance. *mBio* 10:18. doi: 10.1128/mBio.02529-18

Lamoth, F., Juvvadi, P. R., Fortwendel, J. R., and Steinbach, W. J. (2012). Heat shock protein 90 is required for conidiation and cell wall integrity in Aspergillus fumigatus. *Eukaryot. Cell* 11, 1324–1332. doi: 10.1128/EC.00032-12

Lamoth, F., Juvvadi, P. R., and Steinbach, W. J. (2016). Heat shock protein 90 (Hsp90): A novel antifungal target against Aspergillus fumigatus. *Crit. Rev. Microbiol.* 42, 310–321. doi: 10.3109/1040841X.2014.947239

Li, C., Chu, H., Liu, X., Chiu, M. C., Zhao, X., Wang, D., et al. (2020a). Human coronavirus dependency on host heat shock protein 90 reveals an antiviral target. *Emerg Microbes Infect* 9, 2663–2672. doi: 10.1080/22221751.2020.1850183

Li, H. M., Li, B., Sun, X., Ma, H., Zhu, M., Dai, Y., et al. (2020b). Enzymatic biosynthesis and biological evaluation of novel 17-AAG glucoside as potential anti-cancer agents. *Bioorg. Med. Chem. Lett.* 30:127282. doi: 10.1016/j.bmcl.2020.127282

Lv, J., Zhou, D., Wang, Y., Sun, W., Zhang, C., Xu, J., et al. (2020). Effects of luteolin on treatment of psoriasis by repressing HSP90. *Int. Immunopharmacol.* 79:106070. doi: 10.1016/j.intimp.2019.106070

Marunouchi, T., Ito, T., Onda, S., Kyo, L., Takahashi, K., Uchida, M., et al. (2021). Effects of 17-AAG on the RIP1/RIP3/MLKL pathway during the development of heart failure following myocardial infarction in rats. *J. Pharmacol. Sci.* 147, 192–199. doi: 10.1016/j.jphs.2021.06.009

McClellan, A. J., Xia, Y., Deutschbauer, A. M., Davis, R. W., Gerstein, M., and Frydman, J. (2007). Diverse cellular functions of the Hsp90 molecular chaperone uncovered using systems approaches. *Cell* 131, 121–135. doi: 10.1016/j.cell.2007.07.036

Mellatyar, H., Talaei, S., Pilehvar-Soltanahmadi, Y., Barzegar, A., Akbarzadeh, A., Shahabi, A., et al. (2018). Targeted cancer therapy through 17-DMAG as an Hsp90 inhibitor: overview and current state of the art. *Biomed. Pharmacother.* 102, 608–617. doi: 10.1016/j.biopha.2018.03.102

Mitchell, C., Park, M. A., Zhang, G., Han, S. I., Harada, H., Franklin, R. A., et al. (2007). 17-Allylamino-17-demethoxygeldanamycin enhances the lethality of deoxycholic acid in primary rodent hepatocytes and established cell lines. *Mol. Cancer Ther.* 6, 618–632. doi: 10.1158/1535-7163.MCT-06-0532

Odds, F. C. (2003). Synergy, antagonism, and what the chequerboard puts between them. *J. Antimicrob. Chemother.* 52:1. doi: 10.1093/jac/dkg301

Pappas, P. G., Lionakis, M. S., Arendrup, M. C., Ostrosky-Zeichner, L., and Kullberg, B. J. (2018). Invasive candidiasis. *Nat. Rev. Dis. Primers* 4:18026. doi: 10.1038/nrdp.2018.26

Pristov, K. E., and Ghannoum, M. A. (2019). Resistance of Candida to azoles and echinocandins worldwide. *Clin. Microbiol. Infect.* 25, 792–798. doi: 10.1016/j.cmi.2019.03.028

Refos, J. M., Vonk, A. G., Ten Kate, M. T., Eadie, K., Verbrugh, H. A., Bakker-Woudenberg, I., et al. (2017). Addition of 17-(allylamino)-17-demethoxygeldanamycin to a suboptimal caspofungin treatment regimen in neutropenic rats with invasive pulmonary aspergillosis delays the time to death but does not enhance the overall therapeutic efficacy. *PLoS One* 12:e0180961. doi: 10.1371/journal.pone.0180961

Scieglinska, D., Krawczyk, Z., Sojka, D. R., and Gogler-Piglowska, A. (2019). Heat shock proteins in the physiology and pathophysiology of epidermal keratinocytes. *Cell Stress Chaperones* 24, 1027–1044. doi: 10.1007/s12192-019-01044-5

Tan, J., Jiang, S., Tan, L., Shi, H., Yang, L., Sun, Y., et al. (2021). Antifungal activity of minocycline and azoles Against fluconazole-resistant Candida species. *Front. Microbiol.* 12:649026. doi: 10.3389/fmicb.2021.649026

Van Dijck, P., Sjollema, J., Cammue, B. P., Lagrou, K., Berman, J., d'Enfert, C., et al. (2018). Methodologies for in vitro and in vivo evaluation of efficacy of antifungal and antibiofilm agents and surface coatings against fungal biofilms. *Microb Cell* 5, 300–326. doi: 10.15698/mic2018.07.638

Venditti, M. (2009). Clinical aspects of invasive candidiasis: endocarditis and other localized infections. *Drugs* 69, 39–43. doi: 10.2165/11315610-000000000-00000

Verbon, E. H., Post, J. A., and Boonstra, J. (2012). The influence of reactive oxygen species on cell cycle progression in mammalian cells. *Gene* 511, 1–6. doi: 10.1016/j.gene.2012.08.038

Woo, J. K., Jang, J. E., Kang, J. H., Seong, J. K., Yoon, Y. S., Kim, H. C., et al. (2017). Lectin, Galactoside-binding soluble 3 binding protein promotes 17-N-Allylamino-17-demethoxygeldanamycin resistance through PI3K/Akt pathway in lung Cancer cell line. *Mol. Cancer Ther.* 16, 1355–1365. doi: 10.1158/1535-7163.MCT-16-0574

Zorov, D. B., Juhaszova, M., and Sollott, S. J. (2014). Mitochondrial reactive oxygen species (ROS) and ROS-induced ROS release. *Physiol. Rev.* 94, 909–950. doi: 10.1152/physrev.00026.2013

Conflict of Interest: The authors declare that the research was conducted in the absence of any commercial or financial relationships that could be construed as a potential conflict of interest.

Publisher's Note: All claims expressed in this article are solely those of the authors and do not necessarily represent those of their affiliated organizations, or those of the publisher, the editors and the reviewers. Any product that may be evaluated in this article, or claim that may be made by its manufacturer, is not guaranteed or endorsed by the publisher.

frontiers | Frontiers in Microbiology

TYPE Original Research
PUBLISHED 04 August 2022
DOI 10.3389/fmicb.2022.970146

OPEN ACCESS

EDITED BY
Rustam Aminov,
University of Aberdeen,
United Kingdom

REVIEWED BY
Vladimir Gostev,
Children's Scientific Clinical Centre for Infectious Diseases, Russia
Hosny El-Adawy,
Friedrich Loeffler Institut, Germany

*CORRESPONDENCE
Henry Lam
kehlam@ust.hk

SPECIALTY SECTION
This article was submitted to Antimicrobials, Resistance and Chemotherapy, a section of the journal Frontiers in Microbiology

RECEIVED 15 June 2022
ACCEPTED 13 July 2022
PUBLISHED 04 August 2022

CITATION
Sulaiman JE, Long L, Qian P-Y and Lam H (2022) Proteome profiling of evolved methicillin-resistant *Staphylococcus aureus* strains with distinct daptomycin tolerance and resistance phenotypes.
Front. Microbiol. 13:970146.
doi: 10.3389/fmicb.2022.970146

Proteome profiling of evolved methicillin-resistant *Staphylococcus aureus* strains with distinct daptomycin tolerance and resistance phenotypes

Jordy Evan Sulaiman[1], Lexin Long[2], Pei-Yuan Qian[2,3] and Henry Lam[1]*

[1]Department of Chemical and Biological Engineering, The Hong Kong University of Science and Technology, Kowloon, Hong Kong SAR, China, [2]Department of Ocean Science and Hong Kong Branch of Southern Marine Science and Engineering Guangdong Laboratory (Guangzhou), The Hong Kong University of Science and Technology, Kowloon, Hong Kong SAR, China, [3]Southern Marine Science and Engineering Guangdong Laboratory, Guangzhou, China

Methicillin-resistant *Staphylococcus aureus* (MRSA) is a highly dangerous pathogen, and daptomycin has been increasingly used to treat its infections in clinics. Recently, several groups have shown that tolerance and resistance of microbes can evolve rapidly under cyclic antibiotic exposure. We have previously shown that the same tolerance and resistance development occurs in MRSA treated with daptomycin in an adaptive laboratory evolution (ALE) experiment. In the present study, we performed proteomic analysis to compare six daptomycin-tolerant and resistant MRSA strains that were evolved from the same ancestral strain. The strain with a higher tolerance level than the others had the most different proteome and response to antibiotic treatment, resembling those observed in persister cells, which are small subpopulations of bacteria that survive lethal antibiotics treatment. By comparing the proteome changes across strains with similar phenotypes, we identified the key proteins that play important roles in daptomycin tolerance and resistance in MRSA. We selected two candidates to be confirmed by gene overexpression analysis. Overexpression of EcsA1 and FabG, which were up-regulated in all of the tolerant evolved strains, led to increased daptomycin tolerance in wild-type MRSA. The proteomics data also suggested that cell wall modulations were implicated in both resistance and tolerance, but in different ways. While the resistant strains had peptidoglycan changes and a more positive surface charge to directly repel daptomycin, the tolerant strains possessed different cell wall changes that do not involve the peptidoglycan nor alterations of the surface charge. Overall, our study showed the differential proteome profiles among multiple tolerant and resistant strains, pinpointed the key proteins for the two phenotypes and revealed the differences in cell wall modulations between the daptomycin-tolerant/resistant strains.

KEYWORDS

MRSA, antibiotics, daptomycin, evolution, tolerance, resistance, proteomics

Introduction

In the past 20 years, *Staphylococcus aureus* infections have become more dangerous and expensive to treat owing to the increased prevalence of antimicrobial resistance (Neyra et al. 2014). Methicillin-resistant *S. aureus* (MRSA) is one of the most dangerous pathogens to date, causing infections in both high-risk patients in hospitals (hospital-associated MRSA) and in healthy, non-hospitalized individuals without risk factors (community-associated MRSA). Since 2001, the increase in MRSA exposures and infections in the United States was largely attributed to the community-associated strains because they cannot be controlled solely based on measures implemented within the health care settings (Como-Sabetti et al., 2009; Stefani et al., 2012). Several studies have reported that MRSA was the most common cause of skin and soft tissue infections in hospitals (King et al., 2006; Moran et al., 2006). In Europe, approximately 20% of *S. aureus* isolates were methicillin-resistant, whereas in the United States, the prevalence of MRSA was more than 50% (System, 2004). MRSA infections are harder to treat than ordinary *S. aureus* infections because they are resistant to many types of *antibiotics*. Two of the most frequently used last-resort antibiotics to treat MRSA infections are vancomycin and daptomycin, with the former being the first choice. However, due to the excessive use of vancomycin, there have been multiple reports of MRSA isolates with increased vancomycin minimum inhibitory concentration (MIC), hence making daptomycin a more attractive treatment option (Murray et al., 2013).

Bacterial populations can adapt to stresses and a wide range of treatment conditions, including antibiotic therapy. Through *in vitro* laboratory evolution, several groups have shown that tolerance and resistance evolved rapidly under frequent, cyclic antibiotic treatment (Fridman et al., 2014; Mechler et al., 2015; Van den Bergh et al., 2016; Khare and Tavazoie, 2020; Sulaiman and Lam, 2020a,b, 2021b; Sulaiman et al., 2021). More recently, Liu et al. showed that this development of tolerance and resistance also occurs in patients with MRSA infection receiving drug combinations of daptomycin and rifampin (Liu et al., 2020). Resistance and tolerance are two different bacterial adaptation strategies against antibiotics. While resistance allows bacteria to grow at an elevated antibiotic concentration, tolerance describes the ability of a population to survive, but not grow, under lethal antibiotic concentrations for an extended period. Recently, it was suggested that tolerance facilitates the development of resistance (Levin-Reisman et al., 2017, 2019; Santi et al., 2021; Sulaiman and Lam, 2021a). Therefore, combatting tolerance is key to stopping the development of resistance (Windels et al., 2019), and a more in-depth investigation of the key players and pathways responsible for various tolerance phenotypes (the "tolerome") is necessary (Brauner et al., 2016; Sulaiman and Lam, 2021a). Unlike resistance that directly counteracts the action mechanism of the antibiotic, tolerance is thought to arise from a perturbed biological network of multiple pathways. Thus, proteomics is the most suitable tool to inspect the mechanisms of tolerance and to highlight the key players responsible for the phenotype (Sulaiman and Lam, 2019; Zhang et al., 2020). Proteomics has been proven to be useful in revealing the key players in *E. coli* persistence and tolerance to various antibiotics (Hu et al., 2015; Sulaiman et al., 2018; Sulaiman and Lam, 2020a,b), and has also been used to investigate persistence and tolerance phenotypes in *S. aureus* (Chatterjee et al., 2009; Overton et al., 2011; Conlon et al., 2013; Conlon et al., 2016; Zalis et al., 2019; Huemer et al., 2021; Sulaiman et al., 2021, 2022). Persistence is a phenotype similar to tolerance, but unlike tolerance where most of the cells within the population are tolerant to the drug, persistence describes a situation where the tolerant cells only occur in a small subpopulation, called "persisters" (Sulaiman and Lam, 2021a, 2022).

Recently, our group performed adaptive laboratory evolution (ALE) experiments on MRSA using daptomycin and generated strains with distinct tolerance and resistance phenotypes (Sulaiman and Lam, 2021b). All of the daptomycin-resistant mutants have a single point mutation in the *mprF* gene but in different locations. Various mutations in the *mprF* gene, as well as in the *walKR* and *dlt* operon genes, have been frequently observed in clinical isolates of MRSA and extensively studied (Tran et al., 2015). Mainly, small nucleotide polymorphisms (SNPs) in the *mprF* gene were thought to increase either the LysPG synthase activity, the flippase activity, or both, leading to an increased level of LysPG in the outer membrane leaflet, which could increase the electrostatic repulsion of daptomycin and other cationic antimicrobial peptides (CAMPs; Ernst and Peschel, 2011; Bayer et al., 2013). Ernst et al. have recently reviewed the current knowledge of MprF-mediated daptomycin resistance in *S. aureus* (Ernst and Peschel, 2019). In contrast, the newly discovered tolerant mutants bear single point mutations in genes unrelated to resistance and have not been previously reported to cause decreased susceptibility to antibiotics. Interestingly, these mutations led to different levels of tolerance toward daptomycin, with one strain (TOL6) exhibiting a much higher survival than the other strains (over 100-fold increase in survival after 3 h of daptomycin treatment). In the present study, we compared the proteomes of multiple daptomycin-tolerant and resistant MRSA strains that were evolved from the same ancestral strain and thus bearing minimal changes in the genotype. Using this strategy, we searched for any commonalities in terms of up-regulated and down-regulated processes or pathways between multiple resistant and tolerant strains. Then, we verified the importance of two DEPs common in the tolerant strains through gene overexpression analysis. Moreover, through various assays that assess cell wall properties, we revealed that the tolerant and resistant strains had distinct modifications in their cell wall. Although it was known that daptomycin did not directly inhibit cell wall synthesis, our study showed that changes in the cell wall properties were commonly observed in daptomycin-tolerant and resistant strains, and provided evidence that such changes may affect *S. aureus* susceptibility toward daptomycin (Gray and Wenzel, 2020).

Materials and methods

Bacterial strains and growth conditions

Bacterial strains used in this study are methicillin-resistant *S. aureus* (MRSA) ATCC 43300 and daptomycin-tolerant (TOL2, TOL5, TOL6) and resistant (RES1, RES2, RES3) MRSA strains. For our experiments, exponential phase cultures were prepared by incubating a 1:200 diluted overnight culture in cation-adjusted Mueller-Hinton (MH) broth until OD_{600} reached ~0.1 at 37°C with shaking. MH broth used in this study is supplemented with Ca^{2+} to a final concentration of 50 mg/l to mimic the physiological levels of calcium ions, which is important for the concentration-dependent bactericidal activity of daptomycin (Silverman et al., 2003; Safdar et al., 2004; Steenbergen et al., 2005). MH agar was used for colony counts.

The tolerant and resistant MRSA strains were obtained from a recent adaptive laboratory evolution (ALE) experiment using daptomycin antibiotic (Sulaiman and Lam, 2021b). Briefly, to generate the evolved strains, MRSA ATCC 43300 is used as the ancestral strain for the evolution experiment. Either exponential or stationary phase culture was exposed to 10 mg/l daptomycin (1 h for the exponential phase culture and 3 h for the stationary phase culture), and the antibiotic-containing medium was removed by washing three times in MH broth. Finally, the cells were resuspended in 1 ml fresh MH and grown overnight at 37°C. The next day, 3 µl of the overnight culture was resuspended in 1 ml fresh MH and grown to either exponential or stationary phase, and the antibiotic treatment was repeated. The evolved strains (TOL2, TOL5, TOL6, RES1, RES2, and RES3) were isolates collected from different lineages at different time points during the evolution experiments. The list of single point mutations in the evolved strains is summarized in Supplementary Table S1. Whole-genome sequence data of the evolved strains is available in the BioProject database (NCBI) under the accession number PRJNA724993.

Tolerance and resistance assay

To measure the tolerance level of the different strains, we measured the time-kill curve under daptomycin treatment (10 mg/l). For susceptibility assay toward vancomycin, the concentration used for treatment is 30 mg/l. To assess cell viability after antibiotic treatment, the number of survivors were counted by serially diluting cultures in MH broth, plating 100 µl on MH agar and spread plates.

The MICs of the population were recorded by the broth macrodilution method (Wiegand et al., 2008). The MIC was determined by incubating ~ $5 \cdot 10^5$ exponential phase culture in MH medium for 16 h with various concentrations of antibiotics (daptomycin or vancomycin), and inhibition of growth was observed based on the lack of turbidity. The MIC value was determined as the lowest concentration without growth, according to EUCAST guidelines. Experiments were performed with three independent cultures.

Lysostaphin lysis assay

Lysostaphin lysis assay was performed following protocols described in literature with a slight modification (Gründling et al., 2006; Barros et al., 2019). Cells were grown to an OD_{600} ~ 0.6 and harvested by centrifugation. Cells were washed with water and resuspended in PBS supplemented with 5 mg/l lysostaphin (Sigma Aldrich). Cells were then incubated at 37°C and the decrease in OD_{600} was monitored over time.

Cytochrome C binding assay

The relative positive surface charge of *S. aureus* strains was determined by quantifying the association of the positively charged cytochrome *c* (Sigma) to the staphylococcal surface (Berti et al., 2015). The cytochrome *c* binding assay was performed following protocols from previous literature (Mehta et al., 2012; Gasch et al., 2013). Briefly, 1:1000 of overnight cultures was grown in fresh medium to logarithmic phase. Cells were harvested, washed twice with MOPS (morpholinepropanesulfonic acid) buffer (20 mM, pH 7.0), and the bacterial suspension was adjusted to an OD_{600} of ~1. Aliquots of 1 ml were centrifuged, and the cell pellets were resuspended in 200 µl MOPS buffer and 50 µl of cytochrome *c* solution was added (equine heart, 2.5 mg/ml in MOPS buffer; Sigma). Samples were incubated for 10 min at room temperature, separated by centrifugation, and the supernatants were recovered. The amount of cytochrome *c* remaining in the supernatant after a 10-min binding interaction with *S. aureus* cells was quantified spectrophotometrically at an optical density at 530 nm (OD_{530}). The more unbound cytochrome *c* is detected in the supernatant suggest that the surface charge is more positive.

Sample preparation for proteomics

For proteomics analysis, exponential phase ancestral strain, tolerant (TOL2, TOL5, TOL6) and resistant strains (RES1, RES2, RES3) were treated with sub-MIC doses of daptomycin (0.25 mg/l) for 1 h, which should enable the populations to elicit an antibiotic response (Liu et al., 2014, 2016; Sulaiman et al., 2021). Exponential phase cells before antibiotic treatment were also collected. Similar to our previous work (Sulaiman et al., 2021), two different strategies are used for the proteomics analysis: (i) First, the proteome profile of the evolved strains was compared to the ancestral strain as a control to reveal the effect of the point mutations on the phenotype of the tolerant/resistant strains. (ii) Next, we compared the proteome profile of each strain before and after antibiotic treatment to obtain strain-specific antibiotic response toward sub-inhibitory daptomycin exposure. For all proteomics experiments, three biological replicates were performed for each sample including the control sample.

The cell pellet was suspended in 300 µl of lysis buffer (8 M Urea, 50 mM Tris–HCl pH 8.0), frozen in liquid nitrogen, and sonicated for 10 min. The sample was centrifuged (16,000 × *g* for 10 min) to remove cell debris and insoluble materials. An aliquot of the sample was taken for BCA protein assay (Pierce™ BCA Protein Assay Kit). After protein quantification, the sample was reduced by dithiothreitol (DTT; 0.1 M final concentration) at 37°C for 1 h. For shotgun proteomics, 150 µg of proteins were mixed with up to 250 µl of the exchange buffer (6 M Urea, 50 mM Tris–HCl pH 8.0, 600 mM guanidine HCl), transferred to Amicon® filter device (Millipore, Darmstadt, Germany), and centrifuged (14,000 × *g* for 20 min). The proteins in the filter device were alkylated with iodoacetamide (IAA, 50 mM in exchange buffer) in dark for 20 min, and then centrifuged (14,000 × *g* for 20 min). To reduce the urea concentration, 250 µl of 50 mM ammonium bicarbonate was added to the filter device and centrifuged (14,000 × *g* for 20 min). This step was repeated once. Proteins were digested by sequencing-grade modified trypsin (1:50 w/w, Promega, Madison, WI) for 12 h at 37°C. Then, the sample was acidified with 10% formic acid to a final concentration of 0.1% (v/v) and centrifuged for 16,000 × *g* for 5 min. Finally, the samples were desalted by C18 reverse-phase ZipTip (Millipore, Darmstadt, Germany) and dried with SpeedVac (Eppendorf, Hamburg, Germany) for 30 min.

Liquid chromatography

The samples were reconstituted in 25 µl water/acetonitrile/formic acid in a 97.9:2:0.1 ratio (v/v/v), and processed through Bruker nanoElute Ultra-High-Performance Liquid Chromatography (UHPLC; Bruker Daltonics, Bremen, Germany) coupled to a hybrid trapped ion mobility-quadrupole time-of-flight mass spectrometer (TimsTOF Pro, Bruker Daltonics, Bremen, Germany) *via* a nano-electrospray ion source (Captive Spray, Bruker Daltonics). A volume of 1 µl (approximately 200 ng of the protein digest) was injected into the UHPLC system and separated on an IonOpticks 25 cm Aurora Series Emitter column with Captive Spray Insert (250 mm × 75 µm internal diameter, 120 Å pore size, 1.6 µm particle size C18) at a flow rate of 0.3 µl/min. The mobile phase composition is 0.1% formic acid in water for solvent A, and 0.1% formic acid in acetonitrile for solvent B. The gradient was applied from 2 to 5% of solvent B for 0.5 min, from 5 to 30% of solvent B for 26.5 min, and then from 30 to 95% of solvent B for 0.5 min. In the end, the mobile phase was kept at 95% of solvent B for 0.5 min, and then decreased to 2% of solvent B for 0.1 min. 2 min equilibration with 2% of solvent B was applied before the next injection.

Mass spectrometry

A detailed description of the Bruker TimsTOF Pro mass spectrometer used in this work can be found in the literature (Meier et al., 2015, 2018). We set the accumulation and ramp time to 100 ms each and recorded mass spectra in the range from m/z 100–1700 using the positive electrospray mode. The ion mobility was scanned from 0.85 to 1.30 Vs/cm^2. The quadrupole isolation width was set to 2 Th for m/z < 700 and 3 Th for m/z > 700, and the collision energy was linearly increased from 27 eV to 45 eV as a function of increasing ion mobility. The overall acquisition cycle of 0.53 s comprised one full TIMS-MS scan and four Parallel Accumulation-Serial Fragmentation (PASEF) MS/ MS scans. Low-abundance precursor ions with an intensity above a threshold of 2,500 counts but below a target value of 20,000 counts were repeatedly scheduled and otherwise dynamically excluded for 0.4 min. The TIMS dimension was calibrated linearly using three selected ions from the Agilent ESI LC/MS tuning mix [m/z, 1/K0: (622.0289, 0.9848 $Vs\ cm^{-2}$), (922.0097, 1.1895 $Vs\ cm^{-2}$), (1221,9906, 1.3820 $Vs\ cm^{-2}$)] in positive mode.

Sequence database searching of proteomics data

The raw data were converted to mgf files by Bruker Compass DataAnalysis (version 5.2), and subsequently converted to mzML files by msconvert of the ProteoWizard (version 3.0.20229 64-bit; Kessner et al., 2008). The mzML files were searched using Comet (version 2016.01 rev.2; Eng et al., 2013) with a custom database. Briefly, the genome sequence of *S. aureus* ATCC 43300 was converted into a protein database using the gene prediction tool GeneMark (version 3.25; Lukashin and Borodovsky, 1998). The proteins were then annotated using BLASTp (version 2.7.1) from NCBI using *S. aureus* NCTC 8325 as the protein database. The sequences of common contaminants, such as trypsin and human keratins, and decoy sequences generated by shuffling amino acid sequences between tryptic cleavage sites were added to the database. The decoy sequences in the database are used for the false discovery rate (FDR) estimation of the identified peptides. The search parameters criteria were set as follows: 40 ppm peptide mass tolerance, monoisotopic mass type, fully digested enzyme termini, 0.05 amu fragment bin tolerance, 0 amu fragment bin offset, carbamidomethylated cysteine, and oxidated methionine as the fixed and variable modifications, respectively. The search results from Comet were processed by PeptideProphet (Keller et al., 2002), iProphet, and ProteinProphet of the Trans-Proteomics Pipeline (TPP; Deutsch et al., 2010) in the decoy-assisted non-parametric mode. Every mzML run was analyzed independently. Protein identifications were filtered at a false discovery rate of 0.01 as predicted by ProteinProphet. The mass spectrometry proteomics data have been deposited to ProteomeXchange via the PRIDE repository with the dataset identifier PXD026741.

Label-free quantification of proteomics data by spectral counting

The proteins identified in at least two out of three biological replicates were used for label-free quantification by spectral counting. The quantification of proteins was given by the normalized spectral abundance factor (NSAF; Paoletti et al., 2006), where the number of peptide-spectrum matches (PSMs)

for each protein divided by the length of the corresponding protein is normalized to the total number of PSMs divided by the lengths of protein for all identified proteins. The differentially expressed proteins were filtered by the following cutoff: average spectral counts of at least three, the *p* value for Student's *t*-test on the NSAF values were lower than 0.05, and the fold changes were higher or lower than ±1.5-folds.

Bioinformatics analysis

We visualize our proteomic data using principal component analysis (PCA) of the log NSAF values using the PCA function from the sklearn package with centering and scaling in python. We added 95% confidence intervals by calculating correlation matrices for the three replicates of each sample and then adding these intervals to our plot using the matplotlib package in python. To compare the protein expression profiles between different populations, we generated a heat map of fold changes of the differentially expressed proteins identified across the ancestral strain and evolved strains using the in-house scripts. To highlight potentially important proteins among the differentially expressed proteins, STRING version 11.0 (Szklarczyk et al., 2016) was used to predict the protein–protein interactions and to visualize the interactions. DAVID (Database for Annotation, Visualization and Integrated Discovery) version 6.8 (Sherman and Lempicki, 2009) was used for gene ontology (GO) and pathway analysis.

Gene overexpression of the differentially expressed proteins

Gene overexpression was accomplished using a tetracycline-inducible expression vector pRMC2. The bacterial strains, plasmids, and primers used in this study are listed in Supplementary Table S6. The plasmid pRMC2 was obtained from Tim Foster (Corrigan and Foster, 2009; Addgene plasmid #68940[1] 68,940).

Briefly, competent cells were first prepared as previously described and stored at −80°C (Chen et al., 2017). Then, the constructed plasmid was electroporated into the wild-type MRSA ATCC 43300 strain by thawing 50 µl of competent cells on ice for 10 min, mixing it with 1–2 µg of the plasmid, and transferring them into a 1 mm electroporation cuvette (Bio-Rad, Hercules, CA, USA). Cells were pulsed at 2.5 kV, 100 Ω, and 25 µF, incubated in 1 ml of tryptic soy broth (TSB) at 30°C for 1 h, and followed by plating on a TSB agar plate containing 7.5 µg/ml chloramphenicol for screening. Mutant strains were then subjected to relevant tolerance and resistance assays.

Real-time quantitative PCR

Real-time Quantitative PCR (RT-qPCR) was performed to confirm the overexpression of the selected genes. The primers for real-time PCR are listed in Supplementary Table S6. Briefly, a 3 ml overnight culture of mutant MRSA strains (with the addition of 0.2 µg/ml anhydrotetracycline) was harvested, stabilized with RNAprotect Bacteria Reagent (Qiagen, Hilden, German), and total RNA was extracted with RNeasy PowerBiofilm Kit (Qiagen, Hilden, German) according to the manufacturer's instruction. The RNA was first reverse transcribed to cDNA with RevertAid H Minus First-Strand cDNA Synthesis Kit after the removal of genomic DNA using DNase I (Thermo Fisher Scientific Inc., Waltham, MA, USA), followed by quantification on a Roche Diagnostics GmbH LightCycler 480 Instrument II Realtime PCR System using SYBR Green RT-PCR Reagents Kit (Applied Biosystems) with the following procedures: (i) polymerase activation at 95°C for 10 min, and (ii) annealing and extension at 53°C for 1 min with a total of 40 cycles. The specificity of primer pairs for the PCR amplification was checked by the melting curve analysis which was performed immediately after amplification. Two biological replicates and two technical replicates were performed for each sample, and the relative gene expression level was calculated based on the $2^{-\Delta\Delta Ct}$ method using *gyrA* as the internal-reference gene (Livak and Schmittgen, 2001). The RT-qPCR validation results is shown in Supplementary Figure S3.

Results and discussion

Proteome profiling of MRSA with distinct daptomycin tolerance and resistance phenotypes

The daptomycin-tolerant and resistant strains used in this study were generated from a recent adaptive laboratory evolution (ALE) experiment that mimics clinical conditions (Sulaiman and Lam, 2021b). The tolerant strains were TOL2, TOL5, and TOL6, which have increased survival upon prolonged daptomycin treatment without a change in the MIC, while the resistant strains were RES1, RES2, and RES3, which have elevated MIC toward daptomycin by 3-to 4-fold. Each of these evolved strains bears single point mutations that govern their phenotypes (Supplementary Table S1). While the tolerant strains have mutations in different genes conferring different levels of tolerance toward daptomycin (TOL2 and TOL5 have a mild-tolerance phenotype with ~5-fold increase in survival % after 3 h of treatment, and TOL6 has a high-tolerance phenotype with an over 100-fold increase in survival % after 3 h of treatment), the three resistant strains (RES1, RES2, and RES3) have a single point mutation in the same gene, *mprF*, but in different locations. Figure 1A shows the time-kill curves of the tolerant and resistant strains.

To reveal the alterations in terms of protein expression owing to the single point mutations in the tolerant/resistant strains, we compared the proteome profile of the evolved strains to that of the ancestral strain (the control) in normal growth conditions, without any treatment. Combining all replicates, 1,646, 1,499,

1 http://n2t.net/addgene:68940

1,451, 1,544, 1,587, 1,489, and 1,302 distinct proteins were identified for ancestral, RES1, RES2, RES3, TOL2, TOL5, and TOL6 strain, respectively (Figure 1B), covering around 60% of the total ~ 2,600 proteins in the proteome of common *S. aureus* strains. Using the protein expression data, we performed a principal component analysis (PCA) to determine possible features that distinguish the ancestral and the tolerant/resistant strains. We observed that all strains except TOL6 were positioned closely, with the 95% confidence interval (CI) ellipse overlapping each other (Figure 1C). TOL6 was positioned uniquely and was separated from the other six strains, indicating that it has the most distinct proteome profile from the rest. Figure 1D shows the volcano plots of fold changes against *p* values (two-tailed *t*-test), highlighting the proteins with different expression levels between the evolved strains and the ancestral strain. The list of DEPs is available in Supplementary Table S2. From the number of DEPs, we observed that the high-tolerance strain TOL6 had the most different protein expression profile from the ancestral strain (354 DEPs). This was consistent with a previous study that reported that a daptomycin-tolerant strain bearing a mutation upstream *pgsA* gene (with a similar survival level to TOL6, >100-fold survival % after 3 h of daptomycin treatment) had significant variations in the proteome profile compared to the ancestral strain (Sulaiman et al., 2021).

The expression level of the mutated genes in the tolerant and resistant strains

Using the normalized spectral abundance factor (NSAF) values from our proteomics data, we estimated the relative expression level of the proteins encoded by the mutated genes in the evolved strains (Figures 1E,F; Supplementary Table S1). First, all of the resistant strains (RES1, RES2, and RES3) increased the expression of phosphatidylglycerol lysyltransferase, which is the protein encoded by the *mprF* gene, suggesting that the daptomycin resistance phenotype is associated with MprF gain-of-function, consistent with previous reports (Yang et al., 2009; Ernst et al., 2018). In TOL2, proteins for which the genes were mutated, ribose-phosphate pyrophosphokinase (Prs) and ATP-dependent helicase/deoxyribonuclease subunit B (AddB), had significantly lower expression compared to the ancestral and other strains. Interestingly, the expression level of AddB was also lower in another tolerant strain TOL6, indicating that this protein might play a role in daptomycin tolerance. The expression levels of protein serine/threonine-protein kinase (PrkC), which was mutated in TOL5, were similar in all of the strains including TOL5. Although the mutation did not alter the expression level of protein, it might alter the protein function. Finally, the expression level of 30S ribosomal protein S18 (RpsR) was lower in the tolerant TOL6 strain than in the ancestral strain. Interestingly, the expression level of RpsR was also lower in the other resistant/tolerant strains than in the ancestral strain, implying that the down-regulation of RpsR might be a common trend associated with decreased daptomycin susceptibility. The protein of the other mutated gene in TOL6, ProP, was not detected in all of our samples, perhaps because of its low abundance. While the mutations in RES1, RES2, RES3, TOL2, and TOL5 did not alter their growth profile, TOL6 had a significantly higher doubling time than the ancestral strain (Supplementary Figure S1).

The high-tolerance TOL6 strain has the most alterations in biological processes among the tolerant/resistant strains

The PCA and volcano plots showed that the high-tolerance TOL6 strain had the most different proteome and the highest number of DEPs among the tolerant/resistant strains. Therefore, we were interested in the affected processes due to the mutations it possessed. The protein–protein interaction network of the DEPs in TOL6 is visualized in Figure 2A. There was a wide array of processes that were expressed higher in TOL6 than in the ancestral strain including protein folding, coenzyme A biosynthesis, ribosomal proteins, and chromosome condensation. Those that were expressed lower included DNA recombination, thiamine biosynthesis, response to oxidative stress, SOS response and DNA repair, amino acid biosynthesis, glycine cleavage system, purine and pyrimidine metabolism, and also cell wall organization. The down-regulation of some anabolic processes might be due to the slower growth of the mutant strain (Supplementary Figure S1). For certain processes, such as pathogenesis, response to antibiotic and the two-component system, lipoteichoic acid and peptidoglycan biosynthesis, lipid and glucose metabolism, transmembrane transport, and phosphotransferase system, there was an equal number of proteins that were expressed higher in TOL6 than in the ancestral strain.

Similarly, from the gene ontology (GO) analysis and pathway enrichment study (KEGG) on the DEPs (Figure 2B), we observed that some of the most notable up-regulated processes were protein folding and the expression of ribosomal proteins, while the down-regulated ones were glycine cleavage system, *de novo* inosine monophosphate (IMP) metabolic process, protein repair, lipid metabolism, D-glutamine and D-glutamate metabolism, and glyoxylate and dicarboxylate metabolism. This shutdown of major metabolic processes and the increased expression of ribosomal proteins on TOL6 were not observed in the other tolerant/resistant strains. Instead, it was previously observed in the proteome of *E. coli* (Sulaiman et al., 2018) and *S. aureus* (Huemer et al., 2021) persisters, which are slow-growing cells naturally present in bacterial populations in small quantities and could evade lethal antibiotic treatments. Indeed, *S. aureus* knockouts in glutamate dehydrogenase and other tricarboxylic acid (TCA) cycle enzymes (e.g., 2-oxoketoglutarate dehydrogenase, succinyl coenzyme A synthetase, and fumarase) were previously shown to cause an increased proportion of persister cells and tolerance to different antibiotics (Zalis et al., 2019). More generally, metabolic changes were linked to the formation of persisters by modulating the

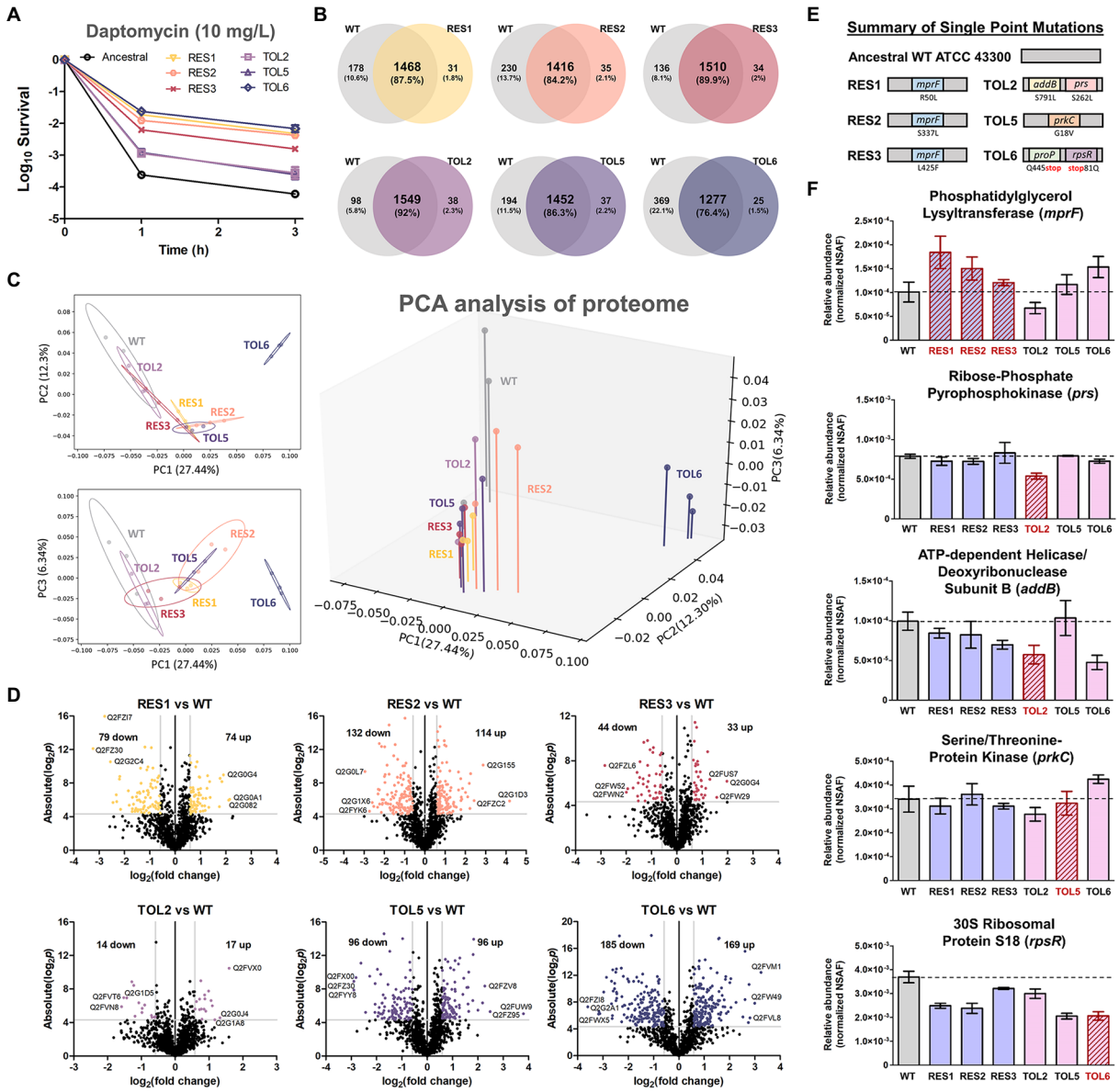

FIGURE 1
Proteome profile comparison between the tolerant/resistant strains and the ancestral strain. **(A)** Time-kill curve of the ancestral strain, resistant strains (RES1, RES2, RES3), and tolerant strains (TOL2, TOL5, TOL6) upon daptomycin treatment (10mg/l) for 3h (mean±s.e.m., *n*=3). **(B)** Venn diagrams for proteome comparison of the resistant strains (RES1, RES2, RES3) and tolerant strains (TOL2, TOL5, TOL6) with the ancestral strain. **(C)** Principal Component Analysis (PCA) of proteomes of the tolerant/resistant strains and the ancestral strain. Projections of PC1 versus PC2, PC1 versus PC3, and a three-dimensional projection of PC1, PC2, and PC3 are shown. Shaded circles represent 95% confidence intervals based on correlation matrices of the three replicates of each sample. **(D)** Volcano plots of the resistant strains (RES1, RES2, RES3) and tolerant strains (TOL2, TOL5, TOL6) compared to the ancestral strain. Differentially expressed proteins (DEPs) are defined to be those with *p* values below 0.05, and absolute fold change greater than 1.5, corresponding to the colored dots. The protein IDs of the most down-regulated and up-regulated proteins are shown. **(E)** Summary of single point mutations identified in the resistant and tolerant strains, with the respective gene and amino acid substitution. Details about the mutations can be found in Supplementary Table S1. **(F)** The expression level of the genes that are mutated in the evolved strains. Relative abundance of the proteins phosphatidylglycerol lysyltransferase (MprF), ribose-phosphate pyrophosphokinase (Prs), ATP-dependent helicase/deoxyribonuclease subunit B (AddB), serine/threonine protein kinase (PrkC), and 30S ribosomal protein S18 (RpsR) among the ancestral strain and evolved strains, measured by label-free quantitative proteomics using spectral counting, where the *y*-axis is the normalized spectral abundance factor (NSAF) values (mean±s.e.m., *n*=3). Strains that express the mutated proteins were marked with red outlines.

intracellular level of ATP in *S. aureus* (Conlon et al., 2016). Since TOL6 also had a slow-growing phenotype just like the persisters (Supplementary Figure S1), their similar proteome profile indicated that they might employ a similar approach in surviving antibiotic treatment. Moreover, the higher expression of proteins involved in protein folding in TOL6 was also observed in filamentous *E. coli* persisters from ampicillin treatment (Sulaiman and Lam, 2020b). Stresses such as antibiotic treatment were known to induce protein

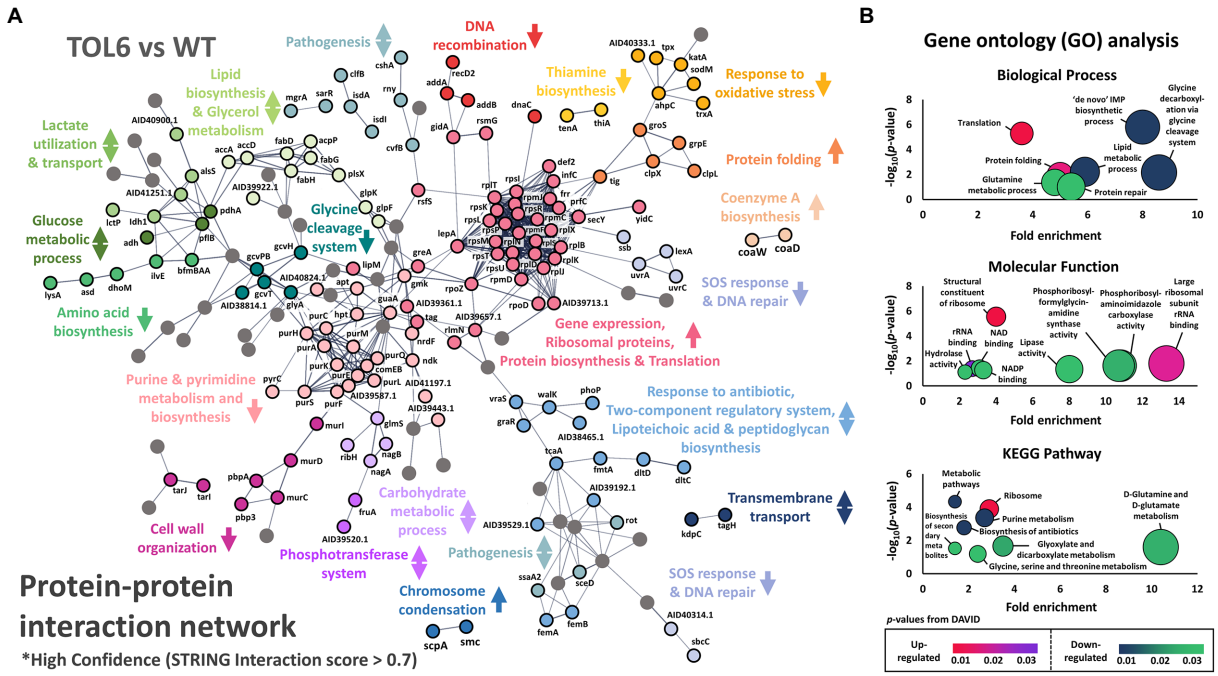

FIGURE 2
Differentially expressed proteins in the TOL6 strain compared to the ancestral strain. **(A)** Protein–protein interaction network of the DEPs of TOL6 strain compared to the ancestral strain, as predicted by STRING v11.0. The lines represent protein interaction (thicker lines mean higher confidence), and the dots in different colors represent different protein functions. Only high confidence protein–protein interactions are shown (STRING interaction score above 0.7). The arrows beside the protein function indicate the direction of expression of the process (the arrows pointing upwards mean that the process is expressed higher in TOL6, the arrows pointing downwards mean the process is expressed higher in ancestral strain, while arrows pointing both upwards and downwards mean that in a specific process, some proteins are expressed higher in TOL6 and some that are expressed higher in the ancestral strain). Nodes without function enrichment are colored gray. **(B)** Gene Ontology (GO) analysis, classified by the biological process (top) and molecular function (middle), and pathway enrichment study (KEGG; bottom) by DAVID of the DEPs of TOL6 compared to the ancestral strain. Fold enrichment is defined as the ratio of the proportion of the input information to the background information.

aggregation. Thus, it was recently postulated that the antibiotic-tolerant persister state is tightly linked to or even driven by protein aggregation (Bollen et al., 2021; Dewachter et al., 2021).

Affected processes and pathways in the tolerant and resistant strains upon antibiotic treatment

Next, we treated the tolerant/resistant strains with a sub-inhibitory concentration of daptomycin to see the effect of antibiotic treatment on the proteomes of the mutant strains. The numbers of protein identified in the treatment groups were similar to the untreated ones (~1,600–1,700 proteins; Supplementary Figure S2a). The number of DEPs in the ancestral strain was the lowest with 79 DEPs, followed by the other resistant/tolerant strains (123, 239, 165, 186, and 122 DEPs for TOL2, TOL5, RES1, RES2, and RES3, respectively), and the highest one was TOL6 with 370 DEPs (Supplementary Figure S2b). Interestingly, the high-tolerance TOL6 strain not only had the most different base-line proteome profile compared to the ancestral strain, but it also had the most significant changes in terms of antibiotic response toward daptomycin. The list of DEPs is available in Supplementary Table S3. From the heat map of the fold changes of all DEPs of the ancestral and evolved strains (Figure 3A), we observed that the DEPs in the TOL2, TOL5, and the resistant strains (RES1, RES2, and RES3) were clustered together, while the DEPs in the ancestral strain and the high-tolerance TOL6 strain were different from the other groups. These suggested that (i) the tolerant/resistant strains have a different antibiotic response compared to the ancestral strain upon daptomycin exposure, but they do share some similarities, and (ii) the high-tolerance TOL6 strain had a different antibiotic response from the ancestral strain and the rest of the tolerant/resistant strains. The latter might also be due to the fact that the proteome of TOL6 was already very different from the rest of the strains even without the addition of antibiotics (Figures 1C,D, 2), and therefore it should adapt differently to antibiotic treatment. Similarly, principal component analysis (PCA) showed that the proteome of the antibiotic-treated samples was positioned similarly, except for TOL6 which was separated from the rest of the groups, especially along PC2 (Figure 3B).

The affected processes and pathways upon antibiotic treatment are shown in Figures 3C,D for the tolerant and

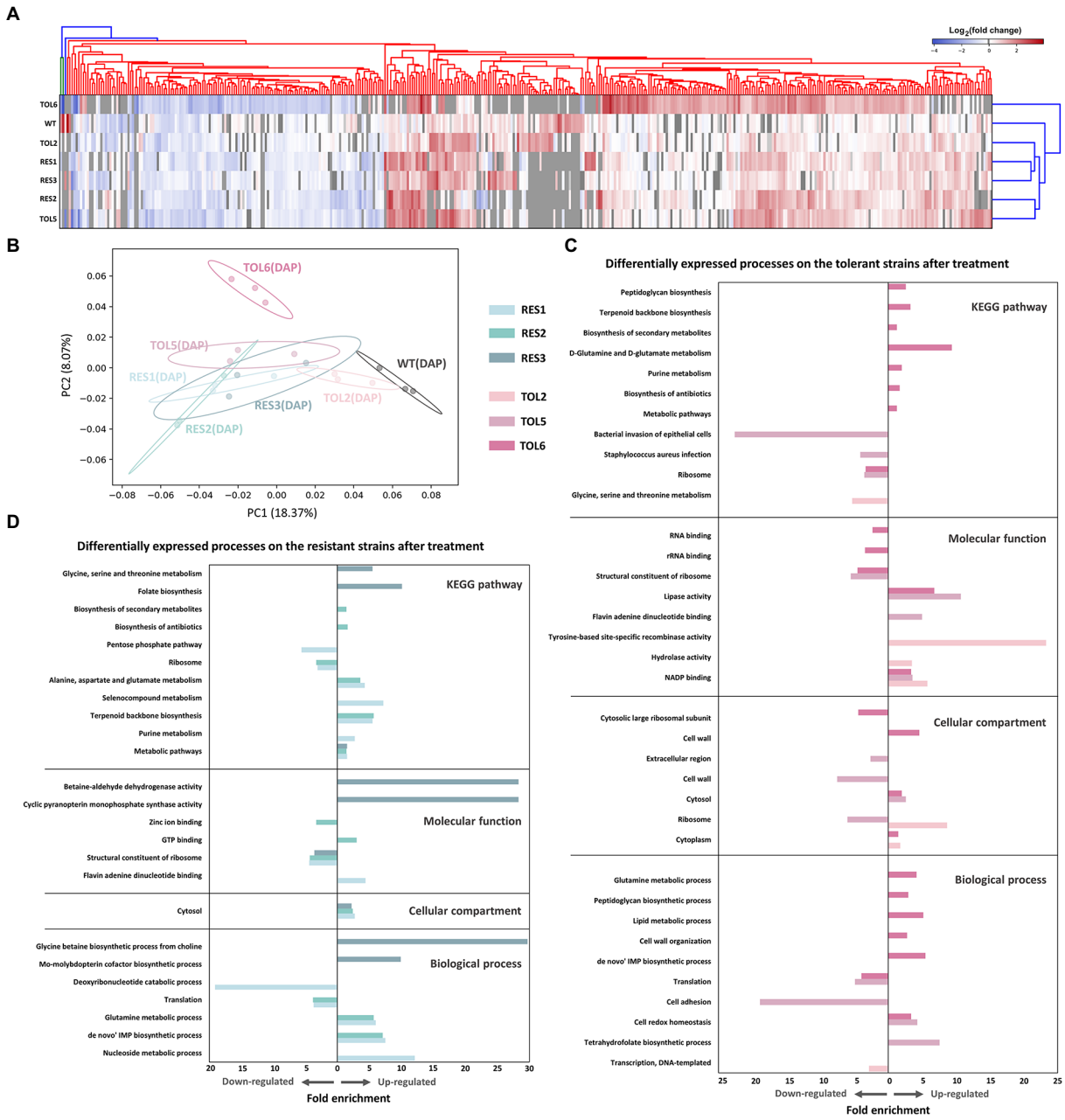

FIGURE 3
Proteomic response of the tolerant/resistant strains and the ancestral strain upon daptomycin treatment. **(A)** Heatmap of the DEPs across the ancestral strain, resistant strains (RES1, RES2, RES3), and tolerant strains (TOL2, TOL5, TOL6) upon daptomycin treatment compared to the untreated populations. The heatmap is clustered using average linkage hierarchical clustering based on Euclidean distances. The y-axis indicates different strains, and the x-axis represents the DEPs identified across all strains. DEPs that were undetected in specific samples are marked with gray color. **(B)** Principal Component Analysis (PCA) of proteomes of the tolerant/resistant strains and the ancestral strain after daptomycin treatment. Shaded circles represent 95% confidence intervals based on correlation matrices of the three replicates of each sample. **(C,D)** Gene Ontology (GO) analysis and pathway enrichment study (KEGG) by DAVID of the DEPs of the tolerant strains **(C)** and the resistant strains **(D)** after daptomycin treatment compared to those before treatment. Fold enrichment is defined as the ratio of the proportion of the input information to the background information.

resistant strains, respectively. For the tolerant strains, we could see that TOL6 had significant changes. Up-regulated processes include cell redox homeostasis, cell wall organization and peptidoglycan biosynthesis, lipid metabolism, D-glutamine and D-glutamate metabolism, and *de novo* IMP metabolism. Interestingly, all of these processes were expressed lower in TOL6 than in the ancestral strain in the absence of antibiotic (Figure 2). Moreover, we observed that upon antibiotic treatment, TOL5 down-regulated several processes, such as cell adhesion, *S. aureus* infection, and bacterial invasion of

epithelial cells, which were related to bacterial virulence and pathogenesis. Ribosomal proteins and protein translation were down-regulated not only in the TOL5 and TOL6 upon antibiotic treatment (Figure 3C), but also in the resistant strains (Figure 3D). This might be related to the fact that daptomycin posed a certain degree of inhibition against protein synthesis (Heidary et al., 2018). In the resistant strain RES3, one of the most apparent up-regulated processes was the glycine betaine biosynthesis process. An increased level of glycine betaine has been shown to be associated with daptomycin resistance (Song et al., 2013). A study examining the transcriptome of a daptomycin-resistant MRSA strain revealed an accumulation of glycine betaine within the cells, coupled with the up-regulation of choline transporter (*cudT*), choline dehydrogenase (*betA*), glycine betaine aldehyde dehydrogenase (*gbsA*), *opuD2*, and *proP* genes (Song et al., 2013). From our proteomics data, choline dehydrogenase was up-regulated by 2.0-, 2.5-, and 1.7-folds in RES1, RES2, and RES3, respectively, betaine aldehyde dehydrogenase was up-regulated by 2.1-and 2.0-folds in RES2 and RES3, respectively, and probable glycine dehydrogenase subunit 1 was up-regulated by 1.5-folds in both RES1 and RES3. Moreover, cell wall and membrane-active antibiotics such as daptomycin was known to cause oxidative stress and protein aggregation and misfolding, as revealed by the induction of molecular chaperones (Utaida et al., 2003; Wilkinson et al., 2005; Kohanski et al., 2008; Sulaiman and Lam, 2021b). Glycine betaine was reported to promote normal protein folding in stressed cells, and its accumulation helped bacteria to survive antibiotic assault (Arakawa and Timasheff, 1991; Record et al., 1998). It is worth noting that the *proP* gene that expresses proline/betaine transporter was also mutated in TOL6, leading to a truncation of 22 amino acids in the corresponding protein and a reduced sensitivity toward daptomycin (Supplementary Table S1).

Cross-comparison of multiple mutants highlighted key proteins that might be important for their phenotypes

Besides looking at the DEPs in individual strains, we sought to determine if there were any common DEPs across the tolerant/resistant strains that may act as the key players of the tolerance/resistance phenotype. This cross-comparison strategy of the proteome profile has been previously employed in *E. coli* tolerant strains and was proven to be effective in highlighting the key proteins for tolerance (Sulaiman and Lam, 2020a). By comparing each of the evolved tolerant/resistant strains to the ancestral strain, we identified 4 and 26 DEPs that were shared among the three tolerant strains (TOL2, TOL5, TOL6) and among the three resistant strains (RES1, RES2, RES3), respectively (Figures 4A,B). The common DEPs with the corresponding expression level (in terms of fold changes) are shown in Figures 4E,F for the tolerant and resistant strains, respectively. In the resistant strains, we found that most of the common DEPs were cell division and cell wall-related proteins. The up-regulated proteins were: autolysin glycyl-glycine endopeptidase LytM (known to cleave the polyglycine interpeptide bridges of the cell wall peptidoglycan), protein DltD (involved in the D-alanylation of lipoteichoic acid which influences the net charge of the cell wall), cell division protein DivIB (involved in stabilizing or promoting the assembly of the division complex). The down-regulated proteins were: cell wall-related protein ScdA (involved in the repair of iron–sulfur clusters damaged by oxidative and nitrosative stress conditions), ribitol-5-phosphate cytidylyltransferase 2 (TarI), aminoacyltransferase FemA (FmhA), lipid II isoglutaminyl synthase subunit GatD, staphylococcal secretory antigen SsaA2, adenine phosphoribosyltransferase (Apt, involved in purine metabolism), and proteins PurA, PurK, and PurN which are all part of the purine biosynthetic pathway. For the common DEPs among the tolerant strains, all of them had a higher expression of the ABC transporter domain-containing protein (EcsA1) and a lower expression of protein RbsD, which catalyzes the interconversion of beta-pyran and beta-furan forms of D-ribose.

By comparing each of the antibiotic-treated evolved tolerant/resistant strains to the untreated cultures of the same strain, we identified 22 and 19 DEPs that were shared among the three tolerant strains and among the three resistant strains, respectively (Figures 4C,D). Figures 4G,H shows the common DEPs with the corresponding expression level (in terms of fold changes) for the tolerant and resistant strains, respectively. Several proteins that we previously observed to have a lower expression in the resistant strains (Figure 4F, right) became up-regulated after antibiotic treatment, such as lipid II isoglutaminyl synthase subunit GatD, CMP/dCMP-type deaminase domain-containing protein (TadA2), and putative aluminum resistance protein (SAOUHSC_01284). In addition, we also observed that mannitol-specific phosphotransferase enzyme IIA component (MtlF, part of the phosphotransferase system), and oxygen-dependent choline dehydrogenase (BetA, involved in the biosynthesis of the osmoprotectant glycine betaine) were commonly up-regulated among the resistant strains. This reinforced the notion that glycine betaine is important for resistance against daptomycin stress as previously discussed. In the tolerant strains, we observed that another ABC transporter domain-containing protein (EcsA3) was commonly up-regulated, similar to what we observed from the tolerant strains compared to the ancestral strain in the absence of antibiotic (Figure 4E), suggesting that transporters might play a role in daptomycin tolerance. Other up-regulated proteins include superoxide dismutase [Mn/Fe] 2 (SodM) that destroys superoxide anion radicals and maintains cell viability during the late-exponential and stationary phase, 3-oxoacyl-[acyl-carrier-protein] reductase (FabG) that catalyzes the first reductive step in the elongation cycle of fatty acid biosynthesis, ribulose-5-phosphate reductase 1 (TarJ) which takes part in cell wall biogenesis, and

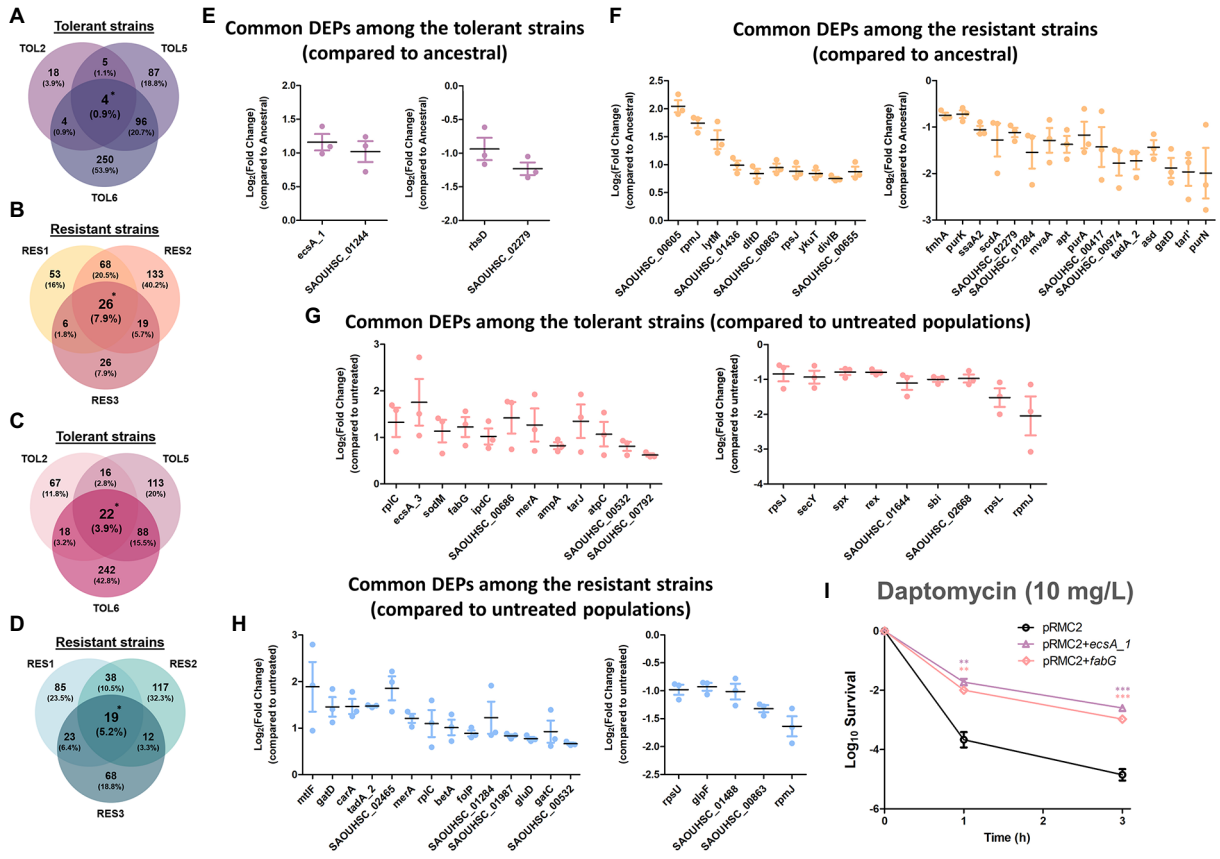

FIGURE 4
Commonly expressed DEPs among the tolerant and resistant strains. **(A–D)** Venn diagrams of the DEPs in the three tolerant strains compared to the ancestral strain **(A)**, the three resistant strains compared to the ancestral strain **(B)**, the three tolerant strains compared to the untreated populations **(C)**, the three resistant strains compared to the untreated populations **(D)**. DEPs shared between all three strains were marked with asterisks. **(E-H)** Fold changes in the overlapped DEPs among the three tolerant strains compared to the ancestral strain **(E)**, the three resistant strains compared to the ancestral strain **(F)**, the three tolerant strains compared to the untreated populations **(G)**, the three resistant strains compared to the untreated populations (**H**; mean±s.e.m., *n*=3). The left figures show up-regulated proteins, and the right figures show down-regulated proteins. **(I)** Gene overexpression of the commonly expressed DEPs among the tolerant strains. Mutants of MRSA strain harboring empty pRMC2 plasmid, pRMC2+*ecsA1* plasmid, and pRMC2+*fabG* plasmid were constructed and subjected to tolerance assay. Survival of the overexpressed mutants under daptomycin treatment (10mg/l) is shown (mean±s.e.m., *n*=3). Significance of difference from the wild-type bearing empty pRMC2 plasmid: ns, not significant, ***P*<0.01, ****P*<0.001 (two-tailed *t*-test with unequal variances). For strains bearing pRMC2 plasmids, 0.2μg/ml anhydrotetracycline was added to induce the expression of overexpressed genes.

ATP synthase epsilon chain (AtpC) that produces ATP from ADP in the presence of a proton gradient across the membrane.

For the commonly down-regulated proteins among the tolerant strains, they were protein translocase subunit SecY (involved in protein transport), global transcriptional regulator Spx (a master regulator involved in stress response), redox-sensing transcriptional regulator Rex (known to modulate transcription in response to changes in cellular NADH/NAD^+ redox state), lactamase B domain-containing protein (SAOUHSC_01644), and immunoglobulin-binding protein Sbi. Interestingly, the last two proteins were also down-regulated in two other daptomycin-tolerant strains in our previous study (one with a high-tolerance level like TOL6 and one with a mild-tolerance level like TOL2 and TOL5) in the absence and presence of daptomycin (Sulaiman et al., 2021). Combining our two studies, we were struck by the finding that these two proteins had the same trend of lower expression in five different daptomycin-tolerant strains bearing completely different point mutations, and therefore might serve as tolerance markers of MRSA. Lactamase B domain-containing protein has a homologous sequence to β-lactamases, enzymes conferring resistance to β-lactams, whereas Sbi is anchored to the cell envelope by binding to the lipoteichoic acid (LTA). Since an LTA-defective mutant of *S. aureus* reduces Sbi levels (Smith et al., 2012), it is possible that daptomycin-tolerant strains, in general, have a reduced number of LTA molecules anchored in the cell wall.

Impact of *ecsA1* and *fabG* overexpression on the daptomycin tolerance phenotype

From the list of commonly expressed DEPs that serve as potential key players of tolerance (Figure 4), we selected EcsA1

and FabG for a follow-up study in gene overexpression analysis using the expression vector pRMC2. The fold change of EcsA1 in the tolerant strains compared to the ancestral strain are 1.99, 2.13, and 2.63 for TOL2, TOL5, and TOL6, respectively (Supplementary Table S2), and the fold change of FabG in the tolerant strains upon daptomycin treatment compared to the untreated ones are 1.77, 2.95, and 2.43 for TOL2, TOL5, and TOL6, respectively (Supplementary Table S3). Verification of the gene overexpression was performed using RT-qPCR, as shown in Supplementary Figure S3.

EcsA1 is an ABC transporter domain-containing protein that was up-regulated in all of our untreated tolerant strains, whereas FabG (3-oxoacyl-[acyl-carrier-protein] reductase) was up-regulated in all of the tolerant strains upon treatment with daptomycin, suggesting that this protein might be important for the adaptation of the tolerant cells toward daptomycin. Indeed, overexpression of EcsA1 and FabG led to increased daptomycin tolerance in MRSA with ~150-and ~ 60-fold increase in survival after 3 h of treatment compared to the wild-type bearing empty pRMC2 plasmid (Figure 4I), without any increase in the MIC (Supplementary Table S4). Although the ABC transporter system plays a role in transporting toxic compounds such as toxins, drugs, and detergents (Li et al., 2016), the function of EcsA1 in *S. aureus* antibiotic tolerance remained largely uncharacterized and requires further investigation. Certainly, the significant increase in survival to daptomycin upon the overexpression of this gene testifies to its importance for the cells' tolerance phenotype. On the other hand, up-regulation of FabG, a key enzyme in fatty acid biosynthesis, is expected to alter lipid metabolism in the cells, which was also previously linked to decreased susceptibility toward daptomycin (Hofer, 2016; Hines et al., 2017; Lee et al., 2019). For instance, *S. aureus* inactivates daptomycin by releasing membrane phospholipids into the extracellular space, thereby sequestering daptomycin and preventing it from inserting into the bacterial membrane (Pader et al., 2016). Strains with different genetic backgrounds may exhibit different contributions of phospholipid shedding and hence have different tolerance levels to daptomycin (Shen et al., 2021). Indeed, in our previous study, we found that reduced daptomycin tolerance in MRSA was associated with a reduced lipid metabolic process (Sulaiman et al., 2021). Besides, through integrated multi-omics, virtual screening, and molecular docking analysis, Rahman et al. suggested several potential drug targets against *S. aureus,* including several *fab* genes which are responsible for fatty acid synthesis, such as malonyl CoA-acyl carrier protein transacylase FabD, 3-oxoacyl-[acyl-carrier-protein] synthase 3 FabH, and enoyl-[acyl-carrier-protein] reductase [NADPH] FabI.

Overall, we showed that overexpression of *ecsA1* and *fabG* increased daptomycin tolerance by 150-and 60-fold, respectively, suggesting that ABC transporter system and fatty acid metabolism play key roles in modulating daptomycin tolerance. These experiments also demonstrated the utility of our strategy of cross comparing the proteomes of distinct resistant/tolerant mutants in identifying novel gene and protein candidates relevant to these phenotypes.

The daptomycin-resistant and tolerant MRSA strains modulate their cell wall differently

Lastly, we wanted to investigate whether the tolerant and resistant strains possessed modifications in their cell wall properties, motivated by our observation that many common DEPs among the resistant strains were related to the cell wall, such as LytM, DltD, GatD, DivIB, FmhA, ScdA, and tarI (Figure 4). In addition, the expression of the MprF protein which was mutated in the resistant strains (coding for an enzyme related to cell wall modifications) was also increased in the resistant strains (Figure 1F). We exposed the resistant strains to lysostaphin, which is an endopeptidase that cleaves the cross-linking pentaglycine bridges on the peptidoglycan layer, and found that all of the resistant strains had higher survival than the ancestral strain (Figure 5A). This indicated that the resistant strains had modifications in the cell wall peptidoglycan. Interestingly, TOL5, which possessed a mutation in the *prkC* gene, also had an increased survival toward lysostaphin. This was consistent with a previous study that shows an *S. aureus* Δ*prkC* mutant has cell wall modifications and increased resistance to Triton-X100 and fosfomycin (Débarbouillé et al., 2009). Besides, several lines of indirect evidence have also suggested that *prkC* contributes to *S. aureus* cell wall synthesis. In *S. aureus, prkC* phosphorylated the response regulator GraR of the two-component system GraRS, and the phosphorylated GraR increased the expression of the *dlt* operon, thus triggering modifications of cell wall teichoic acids (Manuse et al., 2016). The other two tolerant strains, TOL2 and TOL6, had similar survival profiles to the ancestral strain under lysostaphin treatment.

Next, we tested whether alteration of cell surface charge played a role in repelling daptomycin by quantifying the association of the highly cationic cytochrome *c* molecule to the cell's surface (Figure 5B). We observed that all of the resistant strains had a higher percentage of unbound cytochrome *c* than the ancestral strain, suggesting that their surface charge was more positive. This is likely because the nonsynonymous gain-of-function mutations in *mprF* on the resistant strains increased the production of positively charged lysyl-phosphatidylglycerol (LysPG), enhanced the net positive surface charge, and ultimately reduced daptomycin binding (Yang et al., 2009). On the other hand, the increased tolerance of TOL2, TOL5 and TOL6 was not linked to surface charge alteration, as no significant difference in cytochrome *c* binding was observed for these strains relative to the ancestral strain.

Besides daptomycin, another commonly used antibiotic in clinics to treat MRSA is vancomycin, which inhibits cell wall synthesis by binding to the D-Ala-D-Ala terminal of growing

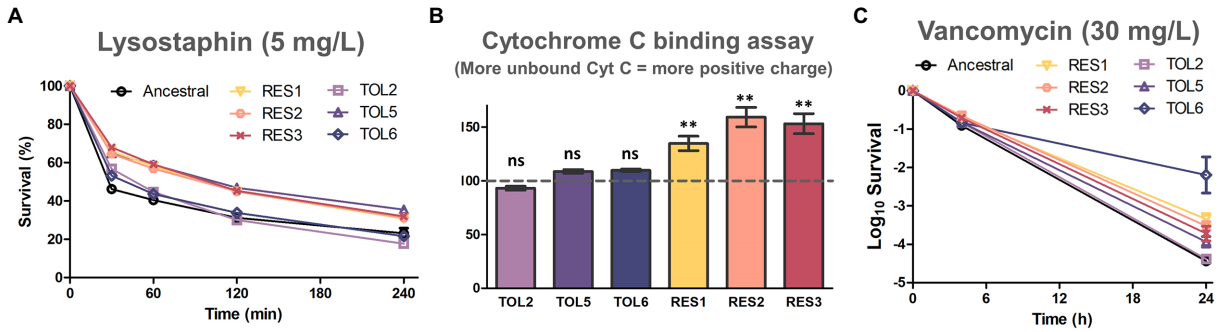

FIGURE 5
Assays to assess cell wall modifications on the evolved strains. **(A)** Lysostaphin lysis assay in the ancestral strain and evolved strains. Cells were treated with 5mg/l of lysostaphin, incubated at 37°C, and the decrease in OD_{600} was monitored over time (mean±s.e.m., n=3). **(B)** Binding of positively charged cytochrome c to the ancestral and evolved strains. The y-axis shows the percentage of unbound cytochrome c in comparison with the ancestral strain (marked with the horizontal dashed line; mean±s.e.m., n=3). Significance of difference from the ancestral strain: ns, not significant, $^{**}P<0.01$ (two-tailed t-test with unequal variances). **(C)** Time-kill curve of exponential phase ancestral strain and evolved strains with 30mg/l of vancomycin (mean±s.e.m., n=3).

peptide chains. We observed that all of the tolerant strains TOL2, TOL5, and TOL6 had a slight increase in the MIC toward vancomycin, whereas the resistant strains RES1, RES2, and RES3 had elevated MICs toward vancomycin (Supplementary Table S5). Under a prolonged treatment with a lethal concentration of vancomycin, all of the evolved strains except TOL2 had a higher survival after 24 h (Figure 5C), indicating that while the resistant strains had modifications in their peptidoglycan and a more positive cell surface charge, the tolerant strains possessed other cell wall changes that might also reduce the effectiveness of vancomycin, but the peptidoglycan does not seem to be involved. Also, while TOL5, RES1, RES2, and RES3 had a mild increase in survival to vancomycin (3.5-to 14-fold) compared to the ancestral strain, the survival of the high-tolerance strain TOL6 was 467-fold higher. This extreme cross-tolerance observed in TOL6 might also be due to their slower growth (Supplementary Figure S1), reminiscent of the characteristic of persister cells that evade antibiotics by inactivating their targets (Lewis, 2007). In this case, TOL6 had a much lower expression of proteins involved in cell wall synthesis than the ancestral and other strains (Figure 2; Supplementary Table S2), which explains why it had a much higher survival toward vancomycin.

Daptomycin disrupts multiple aspects of the cell membrane and inhibits DNA, RNA, and protein synthesis, eventually leading to cell death (Gray and Wenzel, 2020). Although there was evidence that daptomycin did not directly inhibit cell wall synthesis, other studies continued to find cell wall-related phenotypes and induction of cell wall stress stimulons upon daptomycin treatment. Studies have reported that daptomycin acted synergistically with beta-lactam antibiotics (Rand and Houck, 2004; Renzoni et al., 2017; Ye et al., 2019), and proteomics studies similar to ours have indicated that daptomycin induces cell wall stress response proteins in *S. aureus* (Ma et al., 2017) and other organisms such as *B. subtilis* (Wecke et al., 2009; Wenzel et al., 2012; Müller et al., 2016). Consistent with previous studies, we also found that the tolerant and resistant strains possessed alterations in their cell wall properties (Figure 5; Supplementary Table S5), although it remains unclear how exactly these cell wall phenotypes led to decreased daptomycin susceptibility.

Conclusion

In conclusion, we performed a deep proteome profiling of different daptomycin-tolerant and resistant MRSA strains and compared their protein expression profiles. Overall, we revealed proteome alterations associated with the specific tolerance/resistant mutations, showed how the different strains responded to antibiotic treatment and highlighted the unique processes associated with each of the phenotypes, and pointed out key proteins for daptomycin tolerance and resistance in MRSA. Through different cell wall assays, we showed that the tolerant and resistant strains modulated their cell wall differently. While the resistant strains have modifications in their cell wall peptidoglycan and have a more positive surface charge to repel daptomycin binding, tolerant strains possessed other cell wall modifications that do not involve peptidoglycan or surface charge alterations. We believe that our work is a clear step forward into understanding the different daptomycin tolerance and resistance phenotypes in MRSA, and the data generated from our proteomics study would be useful for other researchers in the field.

Data availability statement

The mass spectrometry proteomics data have been deposited to ProteomeXchange via the PRIDE repository with the dataset identifier PXD026741. Whole-genome sequence data of the evolved strains is available in the BioProject database (NCBI) under the accession number PRJNA724993.

Author contributions

JS: conceptualization, methodology, and formal analysis. JS and LL: investigation. JS and HL: writing—original draft. JS, HL, LL, and P-YQ: writing—review and editing. HL: funding acquisition. HL and P-YQ: supervision. All authors contributed to the article and approved the submitted version.

Funding

The authors acknowledge the support from Hong Kong Branch of Southern Marine Science and Engineering Guangdong Laboratory (Guangzhou; SMSEGL20SC01), Ministry of Science and Technology (MOST19SC06), and Research Grant Council (Grant Nos. 16102821, 16307620, R5013-19, and C6026-19G-A), of the Hong Kong Special Administrative Region, China.

Acknowledgments

JS want to thank the Hong Kong PhD Fellowship Scheme for the scholarship. The authors also want to thank the Biosciences Central Research Facility of the Hong Kong University of Science and Technology for access to the TimsTOF Pro mass spectrometer.

Conflict of interest

The authors declare that the research was conducted in the absence of any commercial or financial relationships that could be construed as a potential conflict of interest.

Publisher's note

Supplementary material

The Supplementary material for this article can be found online at: https://www.frontiersin.org/articles/10.3389/fmicb.2022.970146/full#supplementary-material

SUPPLEMENTARY FIGURE S1
Doubling times of the ancestral strain and TOL6. The values were extracted from the fit to the exponential growth phase (mean ± s.e.m., $n = 3$). Significance of difference with the ancestral: $^{***}P < 0.001$, (two-tailed Student's *t*-test).

SUPPLEMENTARY FIGURE S2
Proteome comparison of the strains before and after daptomycin treatment. **(a)** Venn diagrams for proteome comparison of the ancestral strain, resistant strains (RES1, RES2, RES3), and tolerant strains (TOL2, TOL5, TOL6) upon daptomycin treatment with those before treatment. **(b)** Volcano plots of the ancestral strain, resistant strains (RES1, RES2, RES3), and tolerant strains (TOL2, TOL5, TOL6) upon daptomycin treatment compared to those before treatment. Differentially expressed proteins (DEPs) are defined to be those with *p*-values below 0.05, and absolute fold change greater than 1.5, corresponding to the colored dots. The protein IDs of the most down-regulated and up-regulated proteins are shown.

SUPPLEMENTARY FIGURE S3
Quantitative real-time PCR validation of the gene overexpression using the expression vector pRMC2. Relative expression levels of *fabG* and *ecsA1* genes on the overexpressed mutants and strain bearing empty pRMC2 plasmid were normalized to that of the reference gene *gyrA* (mean ± s.e.m., $n = 4$).

SUPPLEMENTARY TABLE S1
List of single point mutations on the evolved strains.

SUPPLEMENTARY TABLE S2
List of the differentially expressed proteins in the tolerant (TOL2, TOL5, TOL6) and resistant strains (RES1, RES2, RES3) compared to the ancestral strain.

SUPPLEMENTARY TABLE S3
List of the differentially expressed proteins in the ancestral strain, tolerant (TOL2, TOL5, TOL6), and resistant strains (RES1, RES2, RES3) upon daptomycin treatment compared to the untreated ones.

SUPPLEMENTARY TABLE S4
MIC values of mutants of MRSA strain harboring empty pRMC2 plasmid, pRMC2+*ecsA1* plasmid, and pRMC2+*fabG* plasmid.

SUPPLEMENTARY TABLE S5
MIC values of the ancestral strain and evolved strains to daptomycin and vancomycin.

SUPPLEMENTARY TABLE S6
Bacterial strains, plasmids, and primers used in this study.

References

Arakawa, T., and Timasheff, S. (1991). "The interactions of proteins with salts, amino acids, and sugars at high concentration," in *Advances in Comparative and Environmental Physiology*. eds. R. Gilles, E. K. Hoffmann and L. Bolis (Berlin: Springer), 226–245.

Barros, E. M., Martin, M. J., Selleck, E. M., Lebreton, F., Sampaio, J. L. M., and Gilmore, M. S. (2019). Daptomycin resistance and tolerance due to loss of function in *Staphylococcus aureus* dsp1 and asp23. *Antimicrob. Agents Chemother.* 63, e01542–e01518. doi: 10.1128/AAC.01542-18

Bayer, A. S., Schneider, T., and Sahl, H. G. (2013). Mechanisms of daptomycin resistance in *Staphylococcus aureus*: role of the cell membrane and cell wall. *Ann. N. Y. Acad. Sci.* 1277, 139–158. doi: 10.1111/j.1749-6632.2012.06819.x

Berti, A. D., Baines, S. L., Howden, B. P., Sakoulas, G., Nizet, V., Proctor, R. A., et al. (2015). Heterogeneity of genetic pathways toward daptomycin nonsusceptibility in *Staphylococcus aureus* determined by adjunctive antibiotics. *Antimicrob. Agents Chemother.* 59, 2799–2806. doi: 10.1128/AAC.04990-14

Bollen, C., Dewachter, L., and Michiels, J. (2021). Protein aggregation as a bacterial strategy to survive antibiotic treatment. *Front. Mol. Biosci.* 8:669664. doi: 10.3389/fmolb.2021.669664

Brauner, A., Fridman, O., Gefen, O., and Balaban, N. Q. (2016). Distinguishing between resistance, tolerance and persistence to antibiotic treatment. *Nat. Rev. Microbiol.* 14, 320–330. doi: 10.1038/nrmicro.2016.34

Chatterjee, I., Schmitt, S., Batzilla, C. F., Engelmann, S., Keller, A., Ring, M. W., et al. (2009). *Staphylococcus aureus* ClpC ATPase is a late growth phase effector of metabolism and persistence. *Proteomics* 9, 1152–1176. doi: 10.1002/pmic.200800586

Chen, W., Zhang, Y., Yeo, W.-S., Bae, T., and Ji, Q. (2017). Rapid and efficient genome editing in *Staphylococcus aureus* by using an engineered CRISPR/Cas9 system. *J. Am. Chem. Soc.* 139, 3790–3795. doi: 10.1021/jacs.6b13317

Como-Sabetti, K., Harriman, K. H., Buck, J. M., Glennen, A., Boxrud, D. J., and Lynfield, R. (2009). Community-associated methicillin-resistant *Staphylococcus aureus*: trends in case and isolate characteristics from six years of prospective surveillance. *Public Health Rep.* 124, 427–435. doi: 10.1177/003335490912400312

Conlon, B. P., Nakayasu, E. S., Fleck, L. E., LaFleur, M. D., Isabella, V. M., Coleman, K., et al. (2013). Activated ClpP kills persisters and eradicates a chronic biofilm infection. *Nature* 503, 365–370. doi: 10.1038/nature12790

Conlon, B. P., Rowe, S. E., Gandt, A. B., Nuxoll, A. S., Donegan, N. P., Zalis, E. A., et al. (2016). Persister formation in *Staphylococcus aureus* is associated with ATP depletion. *Nat. Microbiol.* 1, 1–7. doi: 10.1038/nmicrobiol.2016.51

Corrigan, R. M., and Foster, T. J. (2009). An improved tetracycline-inducible expression vector for *Staphylococcus aureus*. *Plasmid* 61, 126–129. doi: 10.1016/j.plasmid.2008.10.001

Débarbouillé, M., Dramsi, S., Dussurget, O., Nahori, M.-A., Vaganay, E., Jouvion, G., et al. (2009). Characterization of a serine/threonine kinase involved in virulence of *Staphylococcus aureus*. *J. Bacteriol.* 191, 4070–4081. doi: 10.1128/JB.01813-08

Deutsch, E. W., Mendoza, L., Shteynberg, D., Farrah, T., Lam, H., Tasman, N., et al. (2010). A guided tour of the trans-proteomic pipeline. *Proteomics* 10, 1150–1159. doi: 10.1002/pmic.200900375

Dewachter, L., Bollen, C., Wilmaerts, D., Louwagie, E., Herpels, P., Matthay, P., et al. (2021). The dynamic transition of persistence toward the viable but nonculturable state during stationary phase is driven by protein aggregation. *MBio* 12, e00703–e00721. doi: 10.1128/mBio.00703-21

Eng, J. K., Jahan, T. A., and Hoopmann, M. R. (2013). Comet: an open-source MS/MS sequence database search tool. *Proteomics* 13, 22–24. doi: 10.1002/pmic.201200439

Ernst, C. M., and Peschel, A. (2011). Broad-spectrum antimicrobial peptide resistance by MprF-mediated aminoacylation and flipping of phospholipids. *Mol. Microbiol.* 80, 290–299. doi: 10.1111/j.1365-2958.2011.07576.x

Ernst, C. M., and Peschel, A. (2019). MprF-mediated daptomycin resistance. *Int. J. Med. Microbiol.* 309, 359–363. doi: 10.1016/j.ijmm.2019.05.010

Ernst, C. M., Slavetinsky, C. J., Kuhn, S., Hauser, J. N., Nega, M., Mishra, N. N., et al. (2018). Gain-of-function mutations in the phospholipid flippase MprF confer specific daptomycin resistance. *MBio* 9, e01659–e01618. doi: 10.1128/mBio.01659-18

Fridman, O., Goldberg, A., Ronin, I., Shoresh, N., and Balaban, N. Q. (2014). Optimization of lag time underlies antibiotic tolerance in evolved bacterial populations. *Nature* 513, 418–421. doi: 10.1038/nature13469

Gasch, O., Pillai, S., Dakos, J., Miyakis, S., Moellering, R. Jr., and Eliopoulos, G. (2013). Daptomycin in vitro activity against methicillin-resistant *Staphylococcus aureus* is enhanced by d-cycloserine in a mechanism associated with a decrease in cell surface charge. *Antimicrob. Agents Chemother.* 57, 4537–4539. doi: 10.1128/AAC.00799-13

Gray, D. A., and Wenzel, M. (2020). More than a pore: a current perspective on the in vivo mode of action of the lipopeptide antibiotic daptomycin. *Antibiotics* 9:17. doi: 10.3390/antibiotics9010017

Gründling, A., Missiakas, D. M., and Schneewind, O. (2006). *Staphylococcus aureus* mutants with increased lysostaphin resistance. *J. Bacteriol.* 188, 6286–6297. doi: 10.1128/JB.00457-06

Heidary, M., Khosravi, A. D., Khoshnood, S., Nasiri, M. J., Soleimani, S., and Goudarzi, M. (2018). Daptomycin. *J. Antimicrob. Chemother.* 73, 1–11. doi: 10.1093/jac/dkx349

Hines, K. M., Waalkes, A., Penewit, K., Holmes, E. A., Salipante, S. J., Werth, B. J., et al. (2017). Characterization of the mechanisms of daptomycin resistance among gram-positive bacterial pathogens by multidimensional lipidomics. *mSphere* 2, e00492–e00417. doi: 10.1128/mSphere.00492-17

Hofer, U. (2016). The central role of lipids in daptomycin action. *Nat. Rev. Microbiol.* 14:729. doi: 10.1038/nrmicro.2016.173

Hu, Y., Kwan, B. W., Osbourne, D. O., Benedik, M. J., and Wood, T. K. (2015). Toxin YafQ increases persister cell formation by reducing indole signalling. *Environ. Microbiol.* 17, 1275–1285. doi: 10.1111/1462-2920.12567

Huemer, M., Shambat, S. M., Bergada-Pijuan, J., Söderholm, S., Boumasmoud, M., Vulin, C., et al. (2021). Molecular reprogramming and phenotype switching in *Staphylococcus aureus* lead to high antibiotic persistence and affect therapy success. *Proc. Natl. Acad. Sci. U. S. A.* 118:e2014920118. doi: 10.1073/pnas.2014920118

Keller, A., Nesvizhskii, A. I., Kolker, E., and Aebersold, R. (2002). Empirical statistical model to estimate the accuracy of peptide identifications made by MS/MS and database search. *Anal. Chem.* 74, 5383–5392. doi: 10.1021/ac025747h

Kessner, D., Chambers, M., Burke, R., Agus, D., and Mallick, P. (2008). ProteoWizard: open source software for rapid proteomics tools development. *Bioinformatics* 24, 2534–2536. doi: 10.1093/bioinformatics/btn323

Khare, A., and Tavazoie, S. (2020). Extreme antibiotic persistence via heterogeneity-generating mutations targeting translation. *Msystems* 5, e00847–e00819. doi: 10.1128/mSystems.00847-19

King, M. D., Humphrey, B. J., Wang, Y. F., Kourbatova, E. V., Ray, S. M., and Blumberg, H. M. (2006). Emergence of community-acquired methicillin-resistant *Staphylococcus aureus* USA 300 clone as the predominant cause of skin and soft-tissue infections. *Ann. Intern. Med.* 144, 309–317. doi: 10.7326/0003-4819-144-5-200603070-00005

Kohanski, M. A., Dwyer, D. J., Wierzbowski, J., Cottarel, G., and Collins, J. J. (2008). Mistranslation of membrane proteins and two-component system activation trigger antibiotic-mediated cell death. *Cell* 135, 679–690. doi: 10.1016/j.cell.2008.09.038

Lee, T.-H., Hofferek, V., Separovic, F., Reid, G. E., and Aguilar, M.-I. (2019). The role of bacterial lipid diversity and membrane properties in modulating antimicrobial peptide activity and drug resistance. *Curr. Opin. Chem. Biol.* 52, 85–92. doi: 10.1016/j.cbpa.2019.05.025

Levin-Reisman, I., Brauner, A., Ronin, I., and Balaban, N. Q. (2019). Epistasis between antibiotic tolerance, persistence, and resistance mutations. *Proc. Natl. Acad. Sci.* 116, 14734–14739. doi: 10.1073/pnas.1906169116

Levin-Reisman, I., Ronin, I., Gefen, O., Braniss, I., Shoresh, N., and Balaban, N. Q. (2017). Antibiotic tolerance facilitates the evolution of resistance. *Science* 355, 826–830. doi: 10.1126/science.aaj2191

Lewis, K. (2007). Persister cells, dormancy and infectious disease. *Nat. Rev. Microbiol.* 5, 48–56. doi: 10.1038/nrmicro1557

Li, W., Zhang, H., Assaraf, Y. G., Zhao, K., Xu, X., Xie, J., et al. (2016). Overcoming ABC transporter-mediated multidrug resistance: molecular mechanisms and novel therapeutic drug strategies. *Drug Resist. Updat.* 27, 14–29. doi: 10.1016/j.drup.2016.05.001

Liu, J., Gefen, O., Ronin, I., Bar-Meir, M., and Balaban, N. Q. (2020). Effect of tolerance on the evolution of antibiotic resistance under drug combinations. *Science* 367, 200–204. doi: 10.1126/science.aay3041

Liu, X., Hu, Y., Pai, P.-J., Chen, D., and Lam, H. (2014). Label-free quantitative proteomics analysis of antibiotic response in *Staphylococcus aureus* to oxacillin. *J. Proteome Res.* 13, 1223–1233. doi: 10.1021/pr400669d

Liu, X., Pai, P.-J., Zhang, W., Hu, Y., Dong, X., Qian, P.-Y., et al. (2016). Proteomic response of methicillin-resistant *S. aureus* to a synergistic antibacterial drug combination: a novel erythromycin derivative and oxacillin. *Sci. Rep.* 6, 1–12. doi: 10.1038/srep19841

Livak, K. J., and Schmittgen, T. D. (2001). Analysis of relative gene expression data using real-time quantitative PCR and the $2-\Delta\Delta CT$ method. *Methods* 25, 402–408. doi: 10.1006/meth.2001.1262

Lukashin, A. V., and Borodovsky, M. (1998). GeneMark. hmm: new solutions for gene finding. *Nucleic Acids Res.* 26, 1107–1115. doi: 10.1093/nar/26.4.1107

Ma, W., Zhang, D., Li, G., Liu, J., He, G., Zhang, P., et al. (2017). Antibacterial mechanism of daptomycin antibiotic against *Staphylococcus aureus* based on a quantitative bacterial proteome analysis. *J. Proteome* 150, 242–251. doi: 10.1016/j.jprot.2016.09.014

Manuse, S., Fleurie, A., Zucchini, L., Lesterlin, C., and Grangeasse, C. (2016). Role of eukaryotic-like serine/threonine kinases in bacterial cell division and morphogenesis. *FEMS Microbiol. Rev.* 40, 41–56. doi: 10.1093/femsre/fuv041

Mechler, L., Herbig, A., Paprotka, K., Fraunholz, M., Nieselt, K., and Bertram, R. (2015). A novel point mutation promotes growth phase-dependent daptomycin tolerance in *Staphylococcus aureus*. *Antimicrob. Agents Chemother.* 59, 5366–5376. doi: 10.1128/AAC.00643-15

Mehta, S., Singh, C., Plata, K. B., Chanda, P. K., Paul, A., Riosa, S., et al. (2012). β-Lactams increase the antibacterial activity of daptomycin against clinical methicillin-resistant *Staphylococcus aureus* strains and prevent selection of daptomycin-resistant derivatives. *Antimicrob. Agents Chemother.* 56, 6192–6200. doi: 10.1128/AAC.01525-12

Meier, F., Beck, S., Grassl, N., Lubeck, M., Park, M. A., Raether, O., et al. (2015). Parallel accumulation–serial fragmentation (PASEF): multiplying sequencing speed and sensitivity by synchronized scans in a trapped ion mobility device. *J. Proteome Res.* 14, 5378–5387. doi: 10.1021/acs.jproteome.5b00932

Meier, F., Brunner, A.-D., Koch, S., Koch, H., Lubeck, M., Krause, M., et al. (2018). Online parallel accumulation–serial fragmentation (PASEF) with a novel trapped ion mobility mass spectrometer. *Mol. Cell. Proteomics* 17, 2534–2545. doi: 10.1074/mcp.TIR118.000900

Moran, G. J., Krishnadasan, A., Gorwitz, R. J., Fosheim, G. E., McDougal, L. K., Carey, R. B., et al. (2006). Methicillin-resistant *S. aureus* infections among patients in the emergency department. *N. Engl. J. Med.* 355, 666–674. doi: 10.1056/NEJMoa055356

Müller, A., Wenzel, M., Strahl, H., Grein, F., Saaki, T. N., Kohl, B., et al. (2016). Daptomycin inhibits cell envelope synthesis by interfering with fluid membrane microdomains. *Proc. Natl. Acad. Sci. U. S. A.* 113, E7077–E7086. doi: 10.1073/pnas.1611173113

Murray, K. P., Zhao, J. J., Davis, S. L., Kullar, R., Kaye, K. S., Lephart, P., et al. (2013). Early use of daptomycin versus vancomycin for methicillin-resistant *Staphylococcus aureus* bacteremia with vancomycin minimum inhibitory concentration >1 mg/L: a matched cohort study. *Clin. Infect. Dis.* 56, 1562–1569. doi: 10.1093/cid/cit112

Neyra, R. C., Frisancho, J. A., Rinsky, J. L., Resnick, C., Carroll, K. C., Rule, A. M., et al. (2014). Multidrug-resistant and methicillin-resistant *Staphylococcus aureus* (MRSA) in hog slaughter and processing plant workers and their community in North Carolina (USA). *Environ. Health Perspect.* 122, 471–477. doi: 10.1289/ehp.1306741

Overton, I. M., Graham, S., Gould, K. A., Hinds, J., Botting, C. H., Shirran, S., et al. (2011). Global network analysis of drug tolerance, mode of action and virulence in methicillin-resistant *S. aureus*. *BMC Syst. Biol.* 5, 68–16. doi: 10.1186/1752-0509-5-68

Pader, V., Hakim, S., Painter, K. L., Wigneshweraraj, S., Clarke, T. B., and Edwards, A. M. (2016). *Staphylococcus aureus* inactivates daptomycin by releasing membrane phospholipids. *Nat. Microbiol.* 2, 1–8. doi: 10.1038/nmicrobiol.2016.194

Paoletti, A. C., Parmely, T. J., Tomomori-Sato, C., Sato, S., Zhu, D., Conaway, R. C., et al. (2006). Quantitative proteomic analysis of distinct mammalian mediator complexes using normalized spectral abundance factors. *Proc. Natl. Acad. Sci. U. S. A.* 103, 18928–18933. doi: 10.1073/pnas.0606379103

Rand, K. H., and Houck, H. (2004). Daptomycin synergy with rifampicin and ampicillin against vancomycin-resistant enterococci. *J. Antimicrob. Chemother.* 53, 530–532. doi: 10.1093/jac/dkh104

Record, M. T. Jr., Courtenay, E. S., Cayley, D. S., and Guttman, H. J. (1998). Responses of *E. coli* to osmotic stress: large changes in amounts of cytoplasmic solutes and water. *Trends Biochem. Sci.* 23, 143–148. doi: 10.1016/S0968-0004(98)01196-7

Renzoni, A., Kelley, W. L., Rosato, R. R., Martinez, M. P., Roch, M., Fatouraei, M., et al. (2017). Molecular bases determining daptomycin resistance-mediated resensitization to β-lactams (seesaw effect) in methicillin-resistant *Staphylococcus aureus*. *Antimicrob. Agents Chemother.* 61, e01634–e01616. doi: 10.1128/AAC.01634-16

Safdar, N., Andes, D., and Craig, W. (2004). In vivo pharmacodynamic activity of daptomycin. *Antimicrob. Agents Chemother.* 48, 63–68. doi: 10.1128/AAC.48.1.63-68.2004

Santi, I., Manfredi, P., Maffei, E., Egli, A., and Jenal, U. (2021). Evolution of antibiotic tolerance shapes resistance development in chronic *Pseudomonas aeruginosa* infections. *mBio*. 12:e02348-20. doi: 10.1128/mBio.03482-20

Shen, T., Hines, K. M., Ashford, N. K., Werth, B. J., and Xu, L. (2021). Varied contribution of phospholipid shedding from membrane to Daptomycin tolerance in *Staphylococcus aureus*. *Front. Mol. Biosci.* 8:679949. doi: 10.3389/fmolb.2021.679949

Sherman, B. T., and Lempicki, R. A. (2009). Systematic and integrative analysis of large gene lists using DAVID bioinformatics resources. *Nat. Protoc.* 4, 44–57. doi: 10.1038/nprot.2008.211

Silverman, J. A., Perlmutter, N. G., and Shapiro, H. M. (2003). Correlation of daptomycin bactericidal activity and membrane depolarization in *Staphylococcus aureus*. *Antimicrob. Agents Chemother.* 47, 2538–2544. doi: 10.1128/AAC.47.8.2538-2544.2003

Smith, E. J., Corrigan, R. M., van der Sluis, T., Gründling, A., Speziale, P., Geoghegan, J. A., et al. (2012). The immune evasion protein Sbi of *Staphylococcus aureus* occurs both extracellularly and anchored to the cell envelope by binding lipoteichoic acid. *Mol. Microbiol.* 83, 789–804. doi: 10.1111/j.1365-2958.2011.07966.x

Song, Y., Rubio, A., Jayaswal, R. K., Silverman, J. A., and Wilkinson, B. J. (2013). Additional routes to *Staphylococcus aureus* daptomycin resistance as revealed by comparative genome sequencing, transcriptional profiling, and phenotypic studies. *PLoS One* 8:e58469. doi: 10.1371/journal.pone.0058469

Steenbergen, J. N., Alder, J., Thorne, G. M., and Tally, F. P. (2005). Daptomycin: a lipopeptide antibiotic for the treatment of serious gram-positive infections. *J. Antimicrob. Chemother.* 55, 283–288. doi: 10.1093/jac/dkh546

Stefani, S., Chung, D. R., Lindsay, J. A., Friedrich, A. W., Kearns, A. M., Westh, H., et al. (2012). Meticillin-resistant *Staphylococcus aureus* (MRSA): global epidemiology and harmonisation of typing methods. *Int. J. Antimicrob. Agents* 39, 273–282. doi: 10.1016/j.ijantimicag.2011.09.030

Sulaiman, J. E., Hao, C., and Lam, H. (2018). Specific enrichment and proteomics analysis of *Escherichia coli* persisters from rifampin pretreatment. *J. Proteome Res.* 17, 3984–3996. doi: 10.1021/acs.jproteome.8b00625

Sulaiman, J. E., and Lam, H. (2019). Application of proteomics in studying bacterial persistence. *Expert Rev. Proteomics* 16, 227–239. doi: 10.1080/14789450.2019.1575207

Sulaiman, J. E., and Lam, H. (2020a). Proteomic investigation of tolerant *Escherichia coli* populations from cyclic antibiotic treatment. *J. Proteome Res.* 19, 900–913. doi: 10.1021/acs.jproteome.9b00687

Sulaiman, J. E., and Lam, H. (2020b). Proteomic study of the survival and resuscitation mechanisms of filamentous persisters in an evolved *Escherichia coli* population from cyclic ampicillin treatment. *Msystems* 5, e00462–e00420. doi: 10.1128/mSystems.00462-20

Sulaiman, J. E., and Lam, H. (2021a). Evolution of bacterial tolerance under antibiotic treatment and its implications on the development of resistance. *Front. Microbiol.* 12:617412. doi: 10.3389/fmicb.2021.617412

Sulaiman, J. E., and Lam, H. (2021b). Novel daptomycin tolerance and resistance mutations in methicillin-resistant *staphylococcus aureus* from adaptive laboratory evolution. *mSphere* 6, e00692–e00621. doi: 10.1128/mSphere.00692-21

Sulaiman, J. E., and Lam, H. (2022). Proteomics in antibiotic resistance and tolerance research: mapping the resistome and the tolerome of bacterial pathogens. *Proteomics* 22:2100409. doi: 10.1002/pmic.202100409

Sulaiman, J. E., Long, L., Qian, P.-Y., and Lam, H. (2022). Proteomics and transcriptomics uncover key processes for elasnin tolerance in methicillin-resistant *Staphylococcus aureus*. *Msystems* 7, e01393–e01321. doi: 10.1128/msystems.01393-21

Sulaiman, J. E., Long, L., Wu, L., Qian, P.-Y., and Lam, H. (2021). Comparative proteomic investigation of multiple methicillin-resistant *Staphylococcus aureus* strains generated through adaptive laboratory evolution. *iScience* 24:102950. doi: 10.1016/j.isci.2021.102950

System, N. N. I. S. (2004). National Nosocomial Infections Surveillance (NNIS) system report, data summary from January 1992 through June 2004, issued October 2004. *Am. J. Infect. Control* 32, 470–485. doi: 10.1016/j.ajic.2004.10.001

Szklarczyk, D., Morris, J. H., Cook, H., Kuhn, M., Wyder, S., Simonovic, M., et al. (2016). The STRING database in 2017: quality-controlled protein–protein association networks, made broadly accessible. *Nucleic Acids Res.* 45, D362–D368. doi: 10.1093/nar/gkw937

Tran, T. T., Munita, J. M., and Arias, C. A. (2015). Mechanisms of drug resistance: daptomycin resistance. *Ann. N. Y. Acad. Sci.* 1354, 32–53. doi: 10.1111/nyas.12948

Utaida, S., Dunman, P., Macapagal, D., Murphy, E., Projan, S., Singh, V., et al. (2003). Genome-wide transcriptional profiling of the response of *Staphylococcus aureus* to cell-wall-active antibiotics reveals a cell-wall-stress stimulon. *Microbiology* 149, 2719–2732. doi: 10.1099/mic.0.26426-0

Van den Bergh, B., Michiels, J. E., Wenseleers, T., Windels, E. M., Boer, P. V., Kestemont, D., et al. (2016). Frequency of antibiotic application drives rapid evolutionary adaptation of *Escherichia coli* persistence. *Nat. Microbiol.* 1, 1–7. doi: 10.1038/nmicrobiol.2016.20

Wecke, T., Zühlke, D., Mäder, U., Jordan, S., Voigt, B., Pelzer, S., et al. (2009). Daptomycin versus friulimicin B: in-depth profiling of *Bacillus subtilis* cell envelope stress responses. *Antimicrob. Agents Chemother.* 53, 1619–1623. doi: 10.1128/AAC.01046-08

Wenzel, M., Kohl, B., Münch, D., Raatschen, N., Albada, H. B., Hamoen, L., et al. (2012). Proteomic response of *Bacillus subtilis* to lantibiotics reflects differences in interaction with the cytoplasmic membrane. *Antimicrob. Agents Chemother.* 56, 5749–5757. doi: 10.1128/AAC.01380-12

Wiegand, I., Hilpert, K., and Hancock, R. E. (2008). Agar and broth dilution methods to determine the minimal inhibitory concentration (MIC) of antimicrobial substances. *Nat. Protoc.* 3, 163–175. doi: 10.1038/nprot.2007.521

Wilkinson, B. J., Muthaiyan, A., and Jayaswal, R. K. (2005). The cell wall stress stimulon of Staphylococcus aureus and other gram-positive bacteria. *Curr. Med. Chem.Anti-Infect. Agents* 4, 259–276. doi: 10.2174/1568012054368119

Windels, E. M., Michiels, J. E., Van den Bergh, B., Fauvart, M., and Michiels, J. (2019). Antibiotics: combatting tolerance to stop resistance. *MBio* 10, e02095–e02019. doi: 10.1128/mBio.02095-19

Yang, S.-J., Xiong, Y. Q., Dunman, P. M., Schrenzel, J., François, P., Peschel, A., et al. (2009). Regulation of mprF in daptomycin-nonsusceptible *Staphylococcus aureus* strains. *Antimicrob. Agents Chemother.* 53, 2636–2637. doi: 10.1128/AAC.01415-08

Ye, Y., Xia, Z., Zhang, D., Sheng, Z., Zhang, P., Zhu, H., et al. (2019). Multifunctional pharmaceutical effects of the antibiotic daptomycin. *BioMed Res. Int* 2019, 1–9. doi: 10.1155/2019/8609218

Zalis, E. A., Nuxoll, A. S., Manuse, S., Clair, G., Radlinski, L. C., Conlon, B. P., et al. (2019). Stochastic variation in expression of the tricarboxylic acid cycle produces persister cells. *MBio* 10, e01930–e01919. doi: 10.1128/mBio.01930-19

Zhang, D., Hu, Y., Zhu, Q., Huang, J., and Chen, Y. (2020). Proteomic interrogation of antibiotic resistance and persistence in *Escherichia coli*–progress and potential for medical research. *Expert Rev. Proteomics* 17, 393–409. doi: 10.1080/14789450.2020.1784731

frontiers | Frontiers in Microbiology

TYPE Perspective
PUBLISHED 08 September 2022
DOI 10.3389/fmicb.2022.988725

OPEN ACCESS

EDITED BY
Rustam Aminov,
University of Aberdeen,
United Kingdom

REVIEWED BY
George Grant,
University of Aberdeen,
United Kingdom
Alessandra Bragonzi,
San Raffaele Scientific Institute
(IRCCS), Italy

*CORRESPONDENCE
Isabelle Bekeredjian-Ding
isabelle.bekeredjian-ding@pei.de

SPECIALTY SECTION
This article was submitted to
Antimicrobials, Resistance
and Chemotherapy,
a section of the journal
Frontiers in Microbiology

RECEIVED 07 July 2022
ACCEPTED 22 August 2022
PUBLISHED 08 September 2022

CITATION
Arrazuria R, Kerscher B, Huber KE, Hoover JL, Lundberg CV, Hansen JU, Sordello S, Renard S, Aranzana-Climent V, Hughes D, Gribbon P, Friberg LE and Bekeredjian-Ding I (2022) Expert workshop summary: Advancing toward a standardized murine model to evaluate treatments for antimicrobial resistance lung infections.
Front. Microbiol. 13:988725.
doi: 10.3389/fmicb.2022.988725

Expert workshop summary: Advancing toward a standardized murine model to evaluate treatments for antimicrobial resistance lung infections

Rakel Arrazuria[1], Bernhard Kerscher[1], Karen E. Huber[1], Jennifer L. Hoover[2], Carina Vingsbo Lundberg[3], Jon Ulf Hansen[3], Sylvie Sordello[4], Stephane Renard[4], Vincent Aranzana-Climent[5], Diarmaid Hughes[6], Philip Gribbon[7], Lena E. Friberg[5] and Isabelle Bekeredjian-Ding[1,8]*

[1]Division of Microbiology, Paul-Ehrlich-Institut, Langen, Germany, [2]Infectious Diseases Research Unit, GlaxoSmithKline Pharmaceuticals, Collegeville, PA, United States, [3]Department of Bacteria, Parasites & Fungi, Statens Serum Institut, Copenhagen, Denmark, [4]Infectious Diseases, Evotec, Toulouse, France, [5]Department of Pharmacy, Uppsala University, Uppsala, Sweden, [6]Department of Medical Biochemistry and Microbiology, Uppsala University, Uppsala, Sweden, [7]Fraunhofer Institute for Translational Medicine and Pharmacology ITMP, Discovery Research ScreeningPort, Hamburg, Germany, [8]Institute of Medical Microbiology, Immunology and Parasitology, University Hospital Bonn, Bonn, Germany

The rise in antimicrobial resistance (AMR), and increase in treatment-refractory AMR infections, generates an urgent need to accelerate the discovery and development of novel anti-infectives. Preclinical animal models play a crucial role in assessing the efficacy of novel drugs, informing human dosing regimens and progressing drug candidates into the clinic. The Innovative Medicines Initiative-funded "Collaboration for prevention and treatment of MDR bacterial infections" (COMBINE) consortium is establishing a validated and globally harmonized preclinical model to increase reproducibility and more reliably translate results from animals to humans. Toward this goal, in April 2021, COMBINE organized the expert workshop "Advancing toward a standardized murine model to evaluate treatments for AMR lung infections". This workshop explored the conduct and interpretation of mouse infection models, with presentations on PK/PD and efficacy studies of small molecule antibiotics, combination treatments (β-lactam/β-lactamase inhibitor), bacteriophage therapy, monoclonal antibodies and iron sequestering molecules, with a focus on the major Gram-negative AMR respiratory pathogens *Pseudomonas aeruginosa, Klebsiella pneumoniae* and *Acinetobacter baumannii*. Here we summarize the factors of variability that we identified in murine lung infection

models used for antimicrobial efficacy testing, as well as the workshop presentations, panel discussions and the survey results for the harmonization of key experimental parameters. The resulting recommendations for standard design parameters are presented in this document and will provide the basis for the development of a harmonized and bench-marked efficacy studies in preclinical murine pneumonia model.

KEYWORDS

murine pneumonia model, antimicrobial, lung infection, Gram-negative, PK/PD, antimicrobial efficacy studies

Introduction

The loss of antibiotics as an effective tool to treat infections due to increasing antimicrobial resistance (AMR) is a serious threat to global health (Shallcross et al., 2015). For many patients suffering from these resistant infections, the danger of a post-antibiotic era has already become a devastating reality (Pourmand et al., 2017; Murray et al., 2022). Hence, there is a need for the accelerated development of new agents to treat and prevent infections caused by AMR pathogens (WHO, 2021). Despite increasing interest in the development of new or alternative therapies, there is a high attrition rate, and new therapies that often fail to reach the market (Hughes and Karlén, 2014; Bekeredjian-Ding, 2020).

The "Collaboration for prevention and treatment of MDR bacterial infections" (COMBINE) project is part of the European Innovative Medicines Initiative (IMI) Antimicrobial Resistance (AMR) Accelerator. The goal of the Accelerator is to progress the development of new medicines to treat or even prevent resistant bacterial infections. Preclinical efficacy models play a crucial role in the proof-of-concept efficacy investigations and provide the basis for selection of dosing regimens in clinical applications (Tängdén et al., 2020; Friberg, 2021). Differences in the commonly used preclinical models are extensive (Andes and Craig, 2002; Bulitta et al., 2019; Waack et al., 2020), limiting the results' comparability and reproducibility and possibly impeding successful translation to the clinic. The pathogenesis of mouse pneumonia may have characteristics with those of human pneumonia despite anatomical and physiological differences (Mizgerd and Skerrett, 2008; Metersky and Waterer, 2020). However, pathogen-specific characteristics of virulence, infection route, infectious dose, and additional factors such animal genetic background all play a significant role in the pathology that is observed in mice (Mizgerd and Skerrett, 2008; Bielen et al., 2017; Dietert et al., 2017). To facilitate bench-to-bedside translation, and to accelerate and support the development of new antibiotics, it is necessary to establish reliable and globally harmonized preclinical models. Therefore, one of the scientific aims of COMBINE is the development of a standardized, validated murine model for the preclinical efficacy testing of novel anti-infective candidates.

We organized an expert workshop on April 27th and 28th, 2021 to discuss critical parameters of lung infection models conducted with the major Gram-negative AMR pathogens- *Pseudomonas aeruginosa, Klebsiella pneumoniae* and *Acinetobacter baumannii*. On the first day of the workshop, we shared our findings from a literature review of such models (accompanying review article: Variability of murine bacterial pneumonia models used to evaluate antimicrobial agents), presented a list of key variables and proposed standards to harmonize. Following discussion of the proposals in an expert panel forum and a survey of the workshop participants, we develop recommendations for efficacy studies (**Table 1**). The **supplementary material** contains an overview of the second day of the workshop, we explored further applications of murine lung model such us bacteriophage therapy, monoclonal antibodies and iron sequestering molecules (**Supplementary Figure 1** and Text).

Panel discussion on standardization of the acute murine pneumonia model for PK-PD and efficacy studies of small molecule antibiotics

A panel discussion with experts from academia, government and the pharmaceutical industry was held on the first day of the workshop (**Supplementary Figure 1**). This was organized into four different sections: (1) the animal, (2) the inoculum, (3) the infection procedure, and (4) the treatment and endpoints (**Figure 1**). The COMBINE experts presented a list of previously identified factors of variability and provided a proposed standard for each variable. This was followed by an open panel discussion, with the aim of reaching consensus on the parameters for inclusion in our standardized preclinical murine pneumonia model for efficacy studies of

small-molecule antibiotics. The following summarize the panel's and participants discussion.

Animal variables

Mouse strain: CD1 outbred mice are commonly used in PK/PD testing (Bulitta et al., 2019); therefore, this was proposed as the standard. The three bacterial species of primary interest (*P. aeruginosa, K. pneumoniae* and *A. baumannii*) have all been shown to have good infectivity in this mouse strain. In addition, CD1 mice are outbred and thus less expensive than many inbred strains. CD1 mice are also the strain of choice for the thigh infection model and use of the same mouse strain allows for a better comparison between these two commonly used murine models. The panel recognized that the use of inbred mice may be advantageous under some circumstances, including for bacterial strains that are

TABLE 1 Summary of standard variables proposed by COMBINE experts, panel discussion and survey outcome.

Variable	Proposed parameter	Outcome of the expert discussion	Survey outcome	Comments and suggestions
Animals				
Mouse strain	CD-1 (outbred mice)	CD-1 (outbred mice)	CD-1 (outbred mice)	
Sex	Female	Female	Animals of both sexes	Confirmation of the results in the other gender may be necessary
Age or weight	6 weeks old	6 weeks old	6 weeks old	Further agreement in using 6-8 weeks mice at the start of any intervention
Number of animals per treatment	5-6 mice per treatment group	5-6 mice per treatment group	5-6 mice per treatment group	Adjust to the power analysis if necessary
Other		Create a best practice guideline		Animals from the same vendor. A minimum of acclimatization period. Randomization and blinding
Inoculum				
Source of strains	Include one *in vivo* validated strain from an accessible strain bank	Include one *in vivo* validated strain from an accessible strain bank	Include one strain from an accessible strain bank	
Culture media	Not standardized	Not standardized	Fresh bacterial culture media	Ensure inoculum viability and growth consistency
Growth stage	Log. Phase	Log. phase	Log. phase	
Inoculum preparation	Not standardized, but should ensure viability	Not standardized	Perform a washing step and use cold PBS as vehicle.	Minimize time between inoculum preparation and infection procedure
Infection Procedure				
Immunosuppression	Yes	Yes	Yes	
Cyclophosphamide protocol	150 mg/kg at -4 d and 100 mg/kg at -1 d	150 mg/kg at -4 d and 100 mg/kg at -1 d	150 mg/kg at -4 d and 100 mg/kg at -1 d	
Anesthesia	Not standardized	Not standardized	NA	Deep enough to allow the inoculum to settle in the lungs.
Infection route	IN	IN	IN	IT route may be considered for less pathogenic strains in mice
Infection volume	50 μL	20-50 μL	50 μL	
Inoculum	Not standardized	Not standardized	Not standardized	Not standardized considering baseline levels are standardized
Treatment and Endpoints				
Time to start of treatment	2 h p.i.	2 h p.i.	2 h p.i.	
Baseline CFU[1]	6.5-7.0 $\log_{10}$ CFU	6-7 $\log_{10}$ CFU	6.5-7.0 $\log_{10}$ CFU	
Min. CFU growth in untreated mice	1 $\log_{10}$ CFU/lung	1 $\log_{10}$ CFU/lung	1 $\log_{10}$ CFU/lung	
Length of study	26 h p.i.	26 h p.i.	26 h p.i.	Take several time points including 26 h p.i. if needed
Primary endpoint	CFU/lung	CFU/lung	CFU/lung	
Sample processing methods	Not standardized	Not standardized	Not standardized	Handle all samples from a study the same

NA: Not available, d: day, p.i.: post infection, IN: Intranasal, [1]: Baseline CFU at the start of treatment, Min.: Minimum.

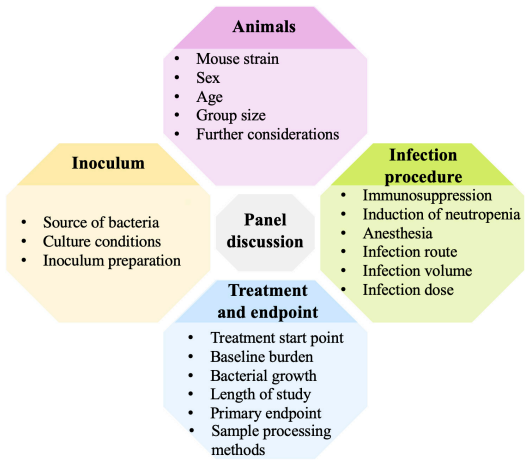

FIGURE 1
Murine pneumonia model variables addressed in the panel discussion.

less virulent and show greater consistency in establishing infection.

Sex: Female mice are predominantly used in murine pneumonia models, most likely because their behavior is generally more amenable to group housing (Jennings et al., 1998). Some studies describe sex differences in the susceptibility to infection, for example with *A. baumannii* (Pires et al., 2020), and sex differences have also been described in PK (Soldin and Mattison, 2009; Madla et al., 2021). Our recommendation is to use female mice, consistent with the overall preference, accepting that this may neglect putative sex differences. A rationale for conducting studies in a single sex of mice (instead of both males and females) may be needed since regulatory agencies may encourage studies in both sexes. If confirmation of results in the other sex is deemed necessary, the extent of duplicative work should be balanced against the ethical considerations of using additional animals for preclinical experimentation. In these cases, only bridging studies should be considered.

Age: We propose the use of young or juvenile outbred animals of at least 6 weeks of age at the time of any intervention start. This is the most common age used based on a literature analysis. When working with inbred mice, eight weeks of age or older is preferred due to their slower growth and to ensure animals display a mature immune system. The experts noted that a random allocation based on the body weight should be applied to have consistent groups if smaller- or larger-than-average animals of the same age are included in the same group.

Group size: The number of animals per group used in preclinical studies are based on the power analysis for a given effect size. Acute lung infection models, typically use five to six animals per group, thus these numbers were proposed as the standard for 24-h efficacy studies with small molecule antibiotics. However, the number of animals may need to be adjusted based on the results of a statistical power analysis. Additionally, for survival studies and/or chronic infection models with high expected variability, no less than 10 mice per group are usually required.

Further considerations: Additional animal-related variables may impact the study outcome (vendor, acclimatization, randomization, enrichment in the cage, microbiota), but their standardization was not considered feasible due to differences in the established or approved practices at individual institutions or the regional location of the facilities. To capture these important considerations, the creation of a recommended best practices guideline along with the standard murine pneumonia protocol was suggested.

Inoculum variables

Bacterial strains

It is well known that dose-response relationships can vary by bacterial strain, and this should be considered carefully when designing and conducting antimicrobial efficacy studies. Clinical strains differ in terms of the source, maintenance, number of passages, etc. For benchmarking or comparison of the results, which can be a powerful means of demonstrating the validity of the data, it was recommended to include at least one *in vivo* validated isolate (previously tested in mice and with at least 1 $\log_{10}$ growth in lung between 2h to 26 h p.i.), per bacterial species that is easily and globally accessible. While some labs routinely passage isolates in animals to boost virulence, this is not a common practice. Due to the possibility of genetic drift, we do not advocate clinical strains being passed on to animals.

Culture media

Different solid and liquid culture media may be used to grow the bacterial inoculum prior to infection of the mice. Although the majority of the institutions use broth culture, some groups use agar culture, subculturing the stocks overnight on agar media and suspending the bacteria in saline for inoculation. Each institution has their own standard procedures for bacterial culture; the consensus opinion was that the standardization of the type of media used was not necessary, as long as the bacteria are in log-phase growth, bacteria load baseline requirements are met and there is a consistent growth pattern.

Inoculum preparation

Similar to the culture media, the methods used for inoculum preparation are well established within each research group and vary depending on the institution. Standardizing the preparation of the inoculum was not considered necessary as long as reproducible bacterial viability is ensured. All the experts agreed that having consistency in the baseline count from the animal (discussed in treatment and endpoint

variables section) is key for model reproducibility. In order to achieve this, consistent methodology must be used within each laboratory. However, there is a lack of information whether the methodology itself could impact the infection outcome or antibiotic efficacy.

The use of frozen stocks to infect mice is a practice that has shown, for some labs, more stable CFU counts in murine pneumonia models. However, this approach is not recommended when working with Gram-negative bacteria since they may not tolerate freeze-thaw cycles well.

Infection procedure variables

Immunosuppression

Most studies used immunocompromised mice to test antimicrobial efficacy of small molecule antibiotics. The use of the neutropenic model aims to achieve a robust bacterial infectivity in mice and reflect the bacterial growth or replication observed in patients (Andes and Lepak, 2017), but it does not aim to mimic immunocompromised or neutropenic patients. Although the use of neutropenic versus naïve animals could have an effect on PK/PD target, most clinical dose predictions have been based on the neutropenic model (Andes and Lepak, 2017).

Induction of neutropenia

The most common protocol to achieve neutropenia in mice is intraperitoneal administration of cyclophosphamide (150 mg/kg) four days before the infection and again one day (100 mg/kg) before the infection. The use of neutropenic animals, generated with this cyclophosphamide protocol, was proposed as the standard. Some research groups use a slight variation in the cyclophosphamide protocol increasing the dose to 250 mg/kg at day minus four when working with more difficult pathogens such as *A. baumannii;* however, other groups confirmed that the proposed standard cyclophosphamide protocol allows researchers to achieve consistent and robust infectivity even when working with these bacteria.

Anaesthesia

Although most of the institutions employ inhalational anesthetics, it was considered that this variable should not be standardized because institutions typically already have their own approved methods for anesthetizing mice. While standardization of the type of anesthesia was not considered necessary by the panel, the depth and duration of anesthesia is an important parameter to consider. The anesthetic plane should be deep enough to enable full inhalation of the inoculum without sneezing or 'bubbling' on the nares, yet not so deep that respiration is slow and/or shallow. The proper depth of anesthesia will enable as much of the inoculum as possible to reach the lungs. This parameter is also important for the animal's survival. If the anesthesia is too deep, animals may have difficulty recovering after inoculation.

Infection route

IT and IN are the most commonly used routes of infection. Considering that the IN route is less invasive and less technically challenging, it was proposed as the standard. The IT route requires more skill to master, but it may provide more reproducible results, particularly if it enables a greater volume of the inoculum to reach the lungs. Thus, the IT route could be considered a reasonable alternative when working with strains of low pathogenicity in mice and when sufficiently skilled personnel are available.

Infection volume

There is a range of inoculum volume, typically 20-50 μL, reported in the literature. The initial recommendation from COMBINE was for a standard of 50 μL for inoculation of mice. However, further discussion among the panelists raised some important points for consideration. The panel noted that this volume may be too high for inbred mice of similar age as they are often considerably smaller, which may lead to lung inflammation. In addition, some institutions have restrictions on the volume that can be administered via the IN route. Lower inoculum volumes, according to some researchers, may cause the inoculum to concentrate in a single lung lobe rather than being dispersed throughout the lungs, resulting in a highly focal infection. To address these concerns, it was decided to recommend a volume range of 20-50 L rather than a specific standard volume.

Infection dose

Bacterial pathogenicity studies in mice are necessary prior to choosing the bacterial strains and infectious dosage. The infectious dose required for different bacterial strains can vary widely depending on virulence and growth characteristics for a given strain. While the inoculum concentration can have a significant impact on the outcome of the study, standardization was deemed not necessary since the baseline bacterial levels in the lung will be standardized instead.

Treatment and endpoint variables

Treatment starting point

In most protocols, antibiotic treatment begins 2 h post infection (p.i.) Thus, this was the standard proposed by and agreed upon by the panel experts.

Baseline burden

The number of bacteria present in the infected tissue at the time treatment starts (2 h p.i.) was seen as an important variable to standardize. As noted above, bacterial culture and inoculum

preparation variables do not need to be standardized as long as the study achieves a consistent and harmonized level of CFU in the lungs at the start of the treatment. A standard of 6.0-6.5 $\log_{10}$ CFU at the start of the treatment was initially proposed. Several panelists expressed their concern that this range was too narrow and potentially infeasible to reliably attain, especially for large bacterial collections. Broadening the range, however, led to concerns about increased variability in study outcomes. After further discussion, a consensus was reached to use a standard range of 6-7 $\log_{10}$ CFU as the average for the group at the start of treatment.

Bacterial growth

This variable is important to consider, as little or no growth indicates that there is spontaneous bacterial clearance, which can make a compound appear more efficacious. Although it was suggested that 1.5-2 $\log_{10}$ CFU growth in untreated mice after 26 h.p.i may be better for efficacy studies, this can be difficult to obtain with some strains. Overall, a minimum of 1 $\log_{10}$ CFU growth was considered necessary, and this was proposed as the standard. If growth in untreated (or vehicle-treated) mice is less than 1 $\log_{10}$ CFU, then results from that study should be flagged and potentially excluded from the analysis.

Length of study

Most of the studies employing an acute murine pneumonia model used an endpoint of 26 h p.i., which corresponds to 24 h post initiation of treatment, and this was agreed as the consensus standard. The inclusion of more than one time point could be valuable, but it is not practical to recommend as a standard practice. When performing longer studies, i.e., over several days, the panel recommended including 26 h p.i. as one of the time points in order to be able to compare the results among studies.

Primary endpoint

The primary outcome most commonly used and widely accepted as an important assessment for efficacy is the bacterial burden in the lung. Therefore, CFU per lung was proposed as the standard outcome measure for small molecule antibiotic efficacy studies. Additional study outcomes such as survival, immune response, etc. may be relevant for other types of molecules or experiments; typically, these would be considered secondary endpoints.

Sample processing methods

There was considerable variability in the methods used for sample processing. The following was proposed as the standard: collection of whole lungs without perfusion or weighing, homogenization in saline via method and volume of choice and adjustment of readouts to report CFU per lung. The weight of the lungs does not influence the results if data are normalized.

In the reported studies, a plethora of media were used, independent of the organism isolated. It was agreed that standardizing the lung sample culturing methods was not necessary, as long as a methodology is consistently applied and samples within a study are treated the same. Comparison of growth and antimicrobial resistance patterns pre- and post-infection was not discussed during the workshop; however it could help to better characterize bacterial strains.

Workshop survey

At the conclusion of the panel discussion, we conducted an online survey to collect the participants' opinions on the proposed and debated standards for the murine model. The survey output is given in the **Supplementary Document** and summarized in **Table 1**. Except for the sex of the animals, most of the participants agreed with all the proposed standard variables.

Conclusion

The use of standard protocols avoids the lengthy process of *in vivo* protocol development and reduces the variability of the results. It therefore complies with the 3R principle, reducing the number of animals required in the preclinical studies. In this report we identified variables that may have a significant impact on the results obtained and recommend harmonized standards for these variables. A single, standard protocol for conducting all murine lung infection models is not feasible, as models should always be adapted to best suit the particular question being answered. Thus, while the standard protocol proposed here is suitable for antimicrobial efficacy characterization of small molecule antibiotics against *P. aeruginosa, K. pneumoniae,* and *A. baumannii*, it may not be suitable for testing other type of molecules or other bacterial species. However, this standard protocol can serve as a "starting point" for further modification to support other types of testing. Having considered all comments and suggestions received during the workshop, the COMBINE team is developing a standard murine lung infection protocol that includes the parameters described in this report. This protocol will be used within the COMBINE project to assess preclinical efficacy of small molecule antibiotics. The aim of this future work is two-fold: 1) determine reproducibility of results from lab-to-lab using the standard protocol; and 2) improve preclinical-to-clinical translation by comparing PK/PD and efficacy results obtained using this standard protocol with clinical trial data for these benchmark antibiotics.

Data availability statement

The original contributions presented in this study are included in the article/**Supplementary material**, further inquiries can be directed to the corresponding author.

Author contributions

RA: writing—original draft. RA, BK, KH, JLH, CL, JUH, SS, SR, VA-C, DH, PG, LF, and IB-D: conceptualization, manuscript review, and editing. All authors read and approved the final manuscript.

Funding

COMBINE has received funding from the Innovative Medicines Initiative 2 Joint Undertaking under grant agreement No. 853967. This Joint Undertaking receives support from the European Union's Horizon 2020 Research and Innovation Programme and EFPIA companies' in kind contribution. https://www.imi.europa.eu/.

Acknowledgments

We thank all the speakers and panelists for contributing their expertise to the workshop and the attendees for participation in the survey. Moreover, we would like to thank the COMBINE consortium members for their support and in particular Linda Marchioro for her assistance in executing the event.

Conflict of interest

JLH was employed by GlaxoSmithKline Pharmaceuticals. SS and SR were employed by Evotec.

The remaining authors declare that the research was conducted in the absence of any commercial or financial relationships that could be construed as a potential conflict of interest.

Publisher's note

All claims expressed in this article are solely those of the authors and do not necessarily represent those of their affiliated organizations, or those of the publisher, the editors and the reviewers. Any product that may be evaluated in this article, or claim that may be made by its manufacturer, is not guaranteed or endorsed by the publisher.

Author disclaimer

This communication reflects the personal views of the speakers and authors from the COMBINE consortium and does not necessarily reflect the position of IMI, the European Union, EFPIA partners or regulatory agencies.

Supplementary material

The Supplementary Material for this article can be found online at: https://www.frontiersin.org/articles/10.3389/fmicb.2022.988725/full#supplementary-material

References

Andes, D. R., and Lepak, A. J. (2017). In vivo infection models in the pre-clinical pharmacokinetic/pharmacodynamic evaluation of antimicrobial agents. *Curr. Opin. Pharmacol.* 36, 94–99. doi: 10.1016/j.coph.2017.09.004

Andes, D., and Craig, W. A. (2002). Animal model pharmacokinetics and pharmacodynamics: A critical review. *Int J Antimicrob Agents* 19, 261–268. doi: 10.1016/S0924-8579(02)00022-5

Bekeredjian-Ding, I. (2020). Challenges for clinical development of vaccines for prevention of hospital-acquired bacterial infections. *Front. Immunol.* 11:1755. doi: 10.3389/fimmu.2020.01755

Bielen, K., Bart'S, J., Malhotra-Kumar, S., Jorens, P.G., Goossens, H. and Kumar-Singh, S., (2017). Animal models of hospital-acquired pneumonia: current practices and future perspectives. *Ann. Transl. Med.* 5:132

Bulitta, J. B., Hope, W. W., Eakin, A. E., Guina, T., Tam, V. H., Louie, A., et al. (2019). Generating robust and informative nonclinical in vitro and in vivo bacterial infection model efficacy data to support translation to humans. *Antimicrob. Agents Chemother.* 63, e2307–e2318. doi: 10.1128/AAC.02307-18

Dietert, K., Gutbier, B., Wienhold, S. M., Reppe, K., Jiang, X., Yao, L., et al. (2017). Spectrum of pathogen-and model-specific histopathologies in mouse models of acute pneumonia. *PLoS One* 12:e0188251. doi: 10.1371/journal.pone.0188251

Friberg, L. E. (2021). Pivotal Role of Translation in Anti-Infective Development. *Clin. Pharmacol. Ther.* 109, 856–866. doi: 10.1002/cpt.2182

Hughes, D., and Karlén, A. (2014). Discovery and preclinical development of new antibiotics. *Ups. J. Med. Sci.* 119, 162–169. doi: 10.3109/03009734.2014.896437

Jennings, M., Batchelor, G. R., Brain, P. F., Dick, A., Elliott, H., Francis, R. J., et al. (1998). Refining rodent husbandry: The mouse. *Lab. Anim.* 32, 233–259. doi: 10.1258/002367798780559301

Madla, C. M., Gavins, F. K. H., Merchant, H. A., Orlu, M., Murdan, S., and Basit, A. W. (2021). Let's talk about sex: Differences in drug therapy in males and females. *Adv. Drug Deliv. Rev.* 175:113804. doi: 10.1016/j.addr.2021.05.014

Metersky, M. and Waterer, G. (2020). Can animal models really teach us anything about pneumonia? *Con. Eur. Respir. J.* 55:1901525.

Mizgerd, J. P. and Skerrett, S. J. (2008). Animal models of human pneumonia. *Am. J. Physiol. Lung Cell. Mol. Physiol.* 294, L387–L398.

Murray, C. J., Ikuta, K. S., Sharara, F., Swetschinski, L., Robles Aguilar, G., Gray, A., et al. (2022). Global burden of bacterial antimicrobial resistance in 2019: a systematic analysis. *Lancet* 399, 629–655. doi: 10.1016/s0140-6736(21)02724-0

Pires, S., Peignier, A., Seto, J., Smyth, D. S., and Parker, D. (2020). Biological sex influences susceptibility to *Acinetobacter baumannii* pneumonia in mice. *JCI Insight* 5:e132223. doi: 10.1172/JCI.INSIGHT.132223

Pourmand, A., Mazer-Amirshahi, M., Jasani, G., and May, L. (2017). Emerging trends in antibiotic resistance: Implications for emergency medicine. *Am. J. Emerg. Med.* 35, 1172–1176. doi: 10.1016/j.ajem.2017.03.010

Shallcross, L. J., Howard, S. J., Fowler, T., and Davies, S. C. (2015). Tackling the threat of antimicrobial resistance: From policy to sustainable action. *Philos. Trans. R. Soc. B Biol. Sci.* 370:1670. doi: 10.1098/rstb.2014.0082

Soldin, O. P., and Mattison, D. R. (2009). Sex differences in pharmacokinetics and pharmacodynamics. *Clin. Pharmacokinet.* 48, 143–157. doi: 10.2165/00003088-200948030-00001

Tängdén, T., Lundberg, C. V., Friberg, L. E., and Huttner, A. (2020). How preclinical infection models help define antibiotic doses in the clinic. *Int. J. Antimicrob. Agents* 56:106008. doi: 10.1016/j.ijantimicag.2020.106008

Waack, U., Weinstein, E. A., and Farley, J. J. (2020). Assessing animal models of bacterial pneumonia used in investigational new drug applications for the treatment of bacterial pneumonia. *Antimicrob. Agents Chemother.* 64, e2242–e2219. doi: 10.1128/AAC.02242-19

WHO (2021). *2020 Antibacterial agents in clinical and preclinical development: an overview and analysis*. Geneva: World Health Organization.

frontiers | Frontiers in Microbiology

TYPE Review
PUBLISHED 08 September 2022
DOI 10.3389/fmicb.2022.988728

OPEN ACCESS

EDITED BY
Rustam Aminov,
University of Aberdeen,
United Kingdom

REVIEWED BY
Juan Carlos Vázquez-Ucha,
Institute of Biomedical Research of A Coruña (INIBIC), Spain
George Grant,
University of Aberdeen,
United Kingdom
Xenia Kostoulias,
Monash University, Australia

*CORRESPONDENCE
Isabelle Bekeredjian-Ding
isabelle.bekeredjian-ding@pei.de

SPECIALTY SECTION
This article was submitted to Antimicrobials, Resistance and Chemotherapy, a section of the journal Frontiers in Microbiology

RECEIVED 07 July 2022
ACCEPTED 15 August 2022
PUBLISHED 08 September 2022

CITATION
Arrazuria R, Kerscher B, Huber KE, Hoover JL, Lundberg CV, Hansen JU, Sordello S, Renard S, Aranzana-Climent V, Hughes D, Gribbon P, Friberg LE and Bekeredjian-Ding I (2022) Variability of murine bacterial pneumonia models used to evaluate antimicrobial agents. *Front. Microbiol.* 13:988728. doi: 10.3389/fmicb.2022.988728

Variability of murine bacterial pneumonia models used to evaluate antimicrobial agents

Rakel Arrazuria[1], Bernhard Kerscher[1], Karen E. Huber[1], Jennifer L. Hoover[2], Carina Vingsbo Lundberg[3], Jon Ulf Hansen[3], Sylvie Sordello[4], Stephane Renard[4], Vincent Aranzana-Climent[5], Diarmaid Hughes[6], Philip Gribbon[7], Lena E. Friberg[5] and Isabelle Bekeredjian-Ding[1,8]*

[1]Division of Microbiology, Paul-Ehrlich-Institut, Langen, Germany, [2]Infectious Diseases Research Unit, GlaxoSmithKline Pharmaceuticals, Collegeville, PA, United States, [3]Department of Bacteria, Parasites & Fungi, Statens Serum Institut, Copenhagen, Denmark, [4]Infectious Diseases, Evotec, Toulouse, France, [5]Department of Pharmacy, Uppsala University, Uppsala, Sweden, [6]Department of Medical Biochemistry and Microbiology, Uppsala University, Uppsala, Sweden, [7]Fraunhofer Institute for Translational Medicine and Pharmacology ITMP, Discovery Research ScreeningPort, Hamburg, Germany, [8]Institute of Medical Microbiology, Immunology and Parasitology, University Hospital Bonn, Bonn, Germany

Antimicrobial resistance has become one of the greatest threats to human health, and new antibacterial treatments are urgently needed. As a tool to develop novel therapies, animal models are essential to bridge the gap between preclinical and clinical research. However, despite common usage of *in vivo* models that mimic clinical infection, translational challenges remain high. Standardization of *in vivo* models is deemed necessary to improve the robustness and reproducibility of preclinical studies and thus translational research. The European Innovative Medicines Initiative (IMI)-funded "Collaboration for prevention and treatment of MDR bacterial infections" (COMBINE) consortium, aims to develop a standardized, quality-controlled murine pneumonia model for preclinical efficacy testing of novel anti-infective candidates and to improve tools for the translation of preclinical data to the clinic. In this review of murine pneumonia model data published in the last 10 years, we present our findings of considerable variability in the protocols employed for testing the efficacy of antimicrobial compounds using this *in vivo* model. Based on specific inclusion criteria, fifty-three studies focusing on antimicrobial assessment against *Pseudomonas aeruginosa, Klebsiella pneumoniae* and *Acinetobacter baumannii* were reviewed in detail. The data revealed marked differences in the experimental design of the murine pneumonia models employed in the literature. Notably, several differences were observed in variables that are expected to impact the obtained results, such as the immune status of the animals, the age, infection route and sample processing, highlighting the necessity of a standardized model.

KEYWORDS

murine pneumonia model, antimicrobial, lung infection, Gram-negative, PK/PD, antimicrobial efficacy studies

Introduction

Antimicrobial resistance is recognized as one of the greatest threats to human health (World Health Organization [WHO], 2017; Morehead and Scarbrough, 2018; Murray et al., 2022). Thus, new antimicrobial therapies are urgently needed, although few are currently being developed (Hughes and Karlén, 2014; Bekeredjian-Ding, 2020; Theuretzbacher et al., 2020). Due to numerous challenges, including long research timelines and limited financial reward, most large pharmaceutical companies are no longer investing in research and development of new antibiotics. To ensure a sustainable pipeline of novel therapies, improving the efficiency and attractiveness of antibiotic drug development is crucial.

Animal models are essential to bridge the translational gap between preclinical and clinical research (Denayer et al., 2014; Friberg, 2021). They provide an infection environment and anatomical barriers that are difficult to reproduce *in vitro*, and they can be very useful in predicting potentially efficacious dosing regimens (Bulitta et al., 2019; Tängdén et al., 2020). Several different mammalian species have been used to model human pneumonia including piglets (Li Bassi et al., 2014), rodents (Mizgerd and Skerrett, 2008), non-human primates (Kraft et al., 2014), sheep (Malachowa et al., 2019), and rabbits (Nguyen et al., 2021). Although these models have proven helpful in studies of disease mechanisms and in antibiotic testing, murine models have been the preferred choice in investigational new drug applications for the treatment of bacterial pneumonia (Waack et al., 2020). Despite anatomical and physiological differences, the immune system of mice mimics that of humans and pathology of murine pneumonia resemble features of human pneumonia (Mizgerd and Skerrett, 2008; Metersky and Waterer, 2020). However, the observed pathology in mice strongly depends on pathogen-specific features of virulence, route of infection, infectious dose and other factors such as animal genetic background (Mizgerd and Skerrett, 2008; Bielen et al., 2017; Dietert et al., 2017). The features and measurements of experimental acute lung injury in animals depend on the experimental question to be addressed and it has been discussed elsewhere (Matute-Bello et al., 2011). The advantages of using murine models include ease of handling and cost effectiveness. Standardization of the mouse pneumonia model is deemed necessary to improve the robustness and reproducibility in preclinical studies and therefore improve translational research (Peers et al., 2012; Begley and Ioannidis, 2015). In order to improve the reproducibility of results and to facilitate comparisons between studies, it is important to report any data that could potentially influence the outcome. Despite the development of specific guidelines such as TOP (Transparency and Openness Promotion; Nosek et al., 2015), ARRIVE (Animal Research: Reporting of In Vivo Experiments; Kilkenny et al., 2010; Percie du Sert et al., 2020) or PREPARE (Planning Research and Experimental Procedures on Animals: Recommendations for Excellence; Smith et al., 2018), there are still considerable gaps and discrepancies in the experimental information reported in the scientific literature. Establishing a standard method that includes key information can help researchers to navigate through essential variables and ensure that described study protocols are both complete and adequately detailed as well as reported in a consistent and standardized manner. The use of standardized animal model avoids the time-consuming process of developing *in vivo* protocols and reduces the variability of the results. Therefore, it adheres to the 3R principle, reducing the number of animals required in preclinical studies. In addition, the development of a standardized murine pneumonia model validated with at least one reference compound will enable antibiotic benchmarking and serve as a quality control mechanism of the results obtained between laboratories.

The European Innovative Medicines Initiative (IMI) Antimicrobial Resistance (AMR) Accelerator was created with the main goal of advancing the development of new medicines to treat or prevent resistant bacterial infections worldwide. Within the AMR Accelerator, the "Collaboration for prevention and treatment of MDR bacterial infections" (COMBINE) consortium aims to develop a standardized, quality-controlled murine pneumonia model for preclinical efficacy testing of novel anti-infective candidates and to improve tools for the translation of preclinical data to the clinic. Success in translational medicine heavily depends on the selected animal models and the experimental set up of the animal model (Hooijmans and Ritskes-Hoitinga, 2013; Denayer et al., 2014). In addition, the success of characterizing pharmacokinetics and pharmacodynamic (PK/PD) targets in animal models relies largely on host and microbial study design features and the ability to control variance (Andes and Craig, 2002; Andes and Lepak, 2017; Bulitta et al., 2019). Although recommendations for *in vivo* PK/PD studies have been published (Andes and Lepak, 2017; Bulitta et al., 2019), there is still a need for globally harmonized preclinical models.

This focused literature review aims to describe the variability in study methods and experimental protocols for the mouse lung infection model used to test antimicrobial efficacy. This is an essential preliminary step to advance the development of standardized preclinical animal models. Our review focused on murine lung infection models of the most relevant MDR Gram-negative pathogens, *Pseudomonas aeruginosa, Klebsiella pneumoniae* and *Acinetobacter baumannii,* used in proof-of-concept and/or primary pharmacology studies for small molecule antibiotics. The findings were further shared and discussed by a panel of experts at an online workshop organized by the COMBINE consortium. The resulting recommendations for standard design parameters are presented in the following joint article: "Expert Workshop Summary: Advancing toward

a standardized murine model to evaluate treatments for AMR lung infections" and they will provide the basis for the development of a harmonized and bench-marked murine lung PK/PD model.

Literature search strategy, study selection and publication characteristics

Established protocols for murine pneumonia models were collected from industrial, academic, and governmental institutions. A total of sixteen protocols from ten different institutions were reviewed and compared to create a list of parameters that varied between protocols. Furthermore, a scientific literature search was performed to investigate the variability of mouse pneumonia model protocols in published studies. Parameters from the established institutional protocols were excluded from the data analysis of the literature findings.

Study selection followed SYstematic Review Center for Laboratory animal Experimentation (SYRCLE) guidelines (Leenaars et al., 2012). The search strategy consisted of the identification and definition of three search components: mouse model, pneumonia caused by *P. aeruginosa, K. pneumoniae* and/or *A. baumannii*, and drug therapy. A total of 25 Mesh terms and 13 free text terms limited to the title and abstract were used for a literature search in PubMed (**Supplementary Table 1**). The studies selection process is summarized in **Figure 1**. A total of 601 preliminary studies were retrieved, of which 358 studies were published within the last decade in the English language. Of these, 192 publications were excluded following a title and abstract review due to not being primary studies, the disease of interest (murine pneumonia model), or not being focused on the desired intervention; thus, 166 publications were considered to be initially relevant. Following the exclusion of additional studies that focused on interventions or therapies other than small molecule antibiotics (monoclonal antibodies, bacteriophages, metal chelators, plant extracts, *Lactobacillus*, etc.), 53 studies remained (López-Rojas et al., 2011; Pachón-Ibáñez et al., 2011; Docobo-Pérez et al., 2012; Tang et al., 2012; Wang et al., 2012; Yamada et al., 2012, 2013a,b; He et al., 2013; Hirsch et al., 2013; Jacqueline et al., 2013; Louie et al., 2013, 2015; Harada et al., 2014; Hengzhuang et al., 2014; Yokoyama et al., 2014; Bowers et al., 2015; Cheah et al., 2015; Berkhout et al., 2016; Brunetti et al., 2016; Cigana et al., 2016; Lepak and Andes, 2016; Mardirossian et al., 2016; McCaughey et al., 2016; Parra Millán et al., 2016; Thabit et al., 2016; Yang et al., 2016; Kaku et al., 2017a,b; Li Y. T. et al., 2017, Li Y. et al., 2017; Lin et al., 2017a,b, 2018; Oshima et al., 2017; Sakoulas et al., 2017; Zhou J. et al., 2017, Zhou Y. F. et al., 2017; Avery et al., 2018; Chen et al., 2018; de Paula et al., 2018; Geller et al., 2018; Lou et al., 2018; Monogue et al., 2018; Kirby et al., 2019; Ku et al., 2019; Nakamura et al., 2019; Ren et al., 2019; Sanderink et al., 2019; Zhao et al., 2019; Johnson et al., 2020; Tan et al., 2020; Ma X. L. et al., 2020; **Supplementary Table 2**). Murine model variables were extracted from these articles to generate a data set for further analyses of experimental conditions. The data set contained studies from 14 different countries published from 2011 to 2020 (**Supplementary Table 2**).

Review of key variables in murine bacterial pneumonia models used to evaluate antimicrobial agents

Bacterial and intervention-related variables

Pseudomonas aeruginosa, *Klebsiella pneumoniae* and *Acinetobacter baumannii* are among the most common and difficult to treat opportunistic pathogens in nosocomial infections such as ventilator-associated pneumonia in immunocompromised patients (Ma Y. et al., 2020). We observed that antibiotic efficacy was most commonly evaluated against *P. aeruginosa* with 22 of the 53 studies reviewed including this pathogen. This pathogen is commonly involved in pneumonia of cystic fibrosis patients (Oliver et al., 2000). Although antimicrobial agents may be efficacious against more than one of these Gram-negative pathogens (Paterson et al., 2020), only a few of the published studies included the *in vivo* efficacy against two or three of the pathogens in separate experiments (termed "combination of bacteria," **Table 1** and **Figure 2**). Evaluation of antibacterial monotherapy was the most common study objective in the studies reviewed, although studies with *A. baumannii* focused mostly on the evaluation of a combination of therapies (18.9% of studies). Despite the increased attention given to drug delivery methods (Li et al., 2019), few studies have focused on the evaluation of alternative routes of drug administration (**Table 1**). This consisted mainly of aerosolization or liposomes for pulmonary administration of colistin and polymyxin B (He et al., 2013; Li Y. et al., 2017; Lin et al., 2017a,b, 2018). *P. aeruginosa* was the pathogen of choice for these investigations (7.5% of all studies, **Table 1**).

There are no firm requirements for the number of bacterial strains to be included in preclinical studies for the evaluation of novel antimicrobials *in vivo*. However, regulatory guidance (European Medicines Agency, 2016) and scientific recommendations (Bulik et al., 2017; Bulitta et al., 2019) suggest to include at least four strains of each target pathogen species for establishing PK/PD targets. Ideally, these should include a reference strain and be representative of contemporary, relevant resistance profiles and mechanisms (European Medicines Agency, 2016; Bulik et al., 2017; Bulitta et al., 2019). We observed that most of the studies included only one or two

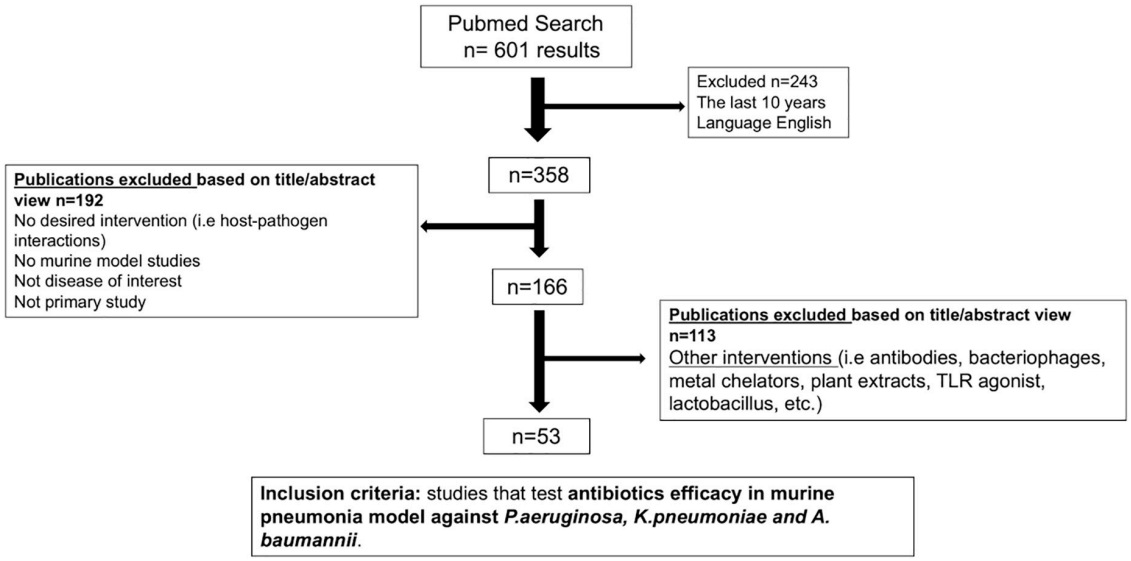

FIGURE 1
Flow diagram for the study selection process.

bacterial strains, especially those focusing on *P. aeruginosa* (35.8% of all studies). Less than one third of the studies tested three or more strains of the same species (Table 1). The value of testing several strains is that it accounts for genetic and biological variation within the target species which may affect strain fitness and susceptibility and therefore the overall efficacy assessment of the investigated drug (Andes and Lepak, 2017).

The source of the bacterial strain was reported in 67.9% of reviewed studies (Table 1). Private clinical isolates were the most common source of bacteria for *A. baumannii* and *P. aeruginosa*. The lack of globally accessible reference strains with corresponding *in vivo* benchmark data may partially explain why some studies used a strain obtained from another researcher (Table 1). Therefore, it would be highly recommended to deposit *in vivo* pathogenic strains (and associated data) in biorepositories to make them accessible to other researchers.

Another variable expected to impact bacterial fitness and infectivity is the preparation of the bacterial inoculum. However, the details related to the inoculum preparation procedure were rarely included. Only 28.3% of studies reported the bacterial growth stage at the time of infection. Of these, a fresh bacterial subculture in logarithmic phase of growth was generally employed for the infection and the use of frozen stocks was limited (Table 1). Some virulence factors are differentially expressed between logarithmic and stationary phase. Their expression often increases in stationary phase, when the cell density is high and bacteria are subjected to higher biological stress (Carter et al., 2007; Bravo et al., 2008; Choi et al., 2011). *P. aeruginosa* quorum sensing signal increases at late stationary phase (Choi et al., 2011). In *Salmonella* and *Shigella,* the production of the lipopolysaccharide long-chain O-antigen increases in the late exponential and stationary growth phases, which affects serum resistance (Carter et al., 2007; Bravo et al., 2008). Despite this, bacteria in logarithmic phase are overwhelmingly employed for *in vivo* infection for a number of reasons. First, the ability of logarithmic phase bacteria to survive and establish a robust infection in the lung is consistently reproducible. Second, logarithmic phase bacteria can be more accurately quantified in the inoculum. It is technically challenging if not impossible to produce a stationary phase culture containing no dead cells. The effects, of employing bacterial cultures in different growth stages or bacteria cultured on liquid vs solid media is currently unknown. Bacterial growth stage is rarely reported; and very few studies reported the specific stage of the log phase (Table 1). However, to be able to increase the reproducibility of the preclinical studies, it is recommended to describe the culture conditions precisely and occasionally to monitor the expression of virulence factors.

Animal-related variables

The selection of mouse strain is a choice that should be carefully considered. Outbred mice were used more frequently than inbred mice. Swiss Webster mice were the most common outbred stock, followed by ICR mice. With regard to inbred mice, C57BL/6 and BALB/c mice were used most frequently (Table 2). The preference for inbred vs. outbred mice varied depending on the bacterial species under investigation. Studies performed with *P. aeruginosa* mainly used outbred mice, while for *A. baumannii* inbred mice slightly predominated

TABLE 1 Bacterial and intervention variables in the reviewed studies.

		Number of studies	Percentage (%)
Bacteria			
P. aeruginosa		22	41.5
K. pneumoniae		12	22.6
A. baumannii		15	28.3
Combination of bacteria		4	7.5
Main objective of the study			
Evaluation of drug monotherapy		25	47.2
	P. aeruginosa	12	22.6
	K. pneumoniae	6	11.3
	A. baumannii	4	7.5
	Combination of bacteria	3	5.7
Evaluation of drug combination therapy		22	41.5
	P. aeruginosa	6	11.3
	K. pneumoniae	6	11.3
	A. baumannii	10	18.9
	Combination of bacteria	0	0.0
Evaluation of alternative drug delivery		6	11.3
	P. aeruginosa	4	7.5
	K. pneumoniae	0	0.0
	A. baumannii	1	1.9
	Combination of bacteria	1	1.9
Number of strains			
1 or 2 strains		38	71.7
	P. aeruginosa	19	35.8
	K. pneumoniae	8	15.1
	A. baumannii	11	20.8
	Combination of bacteria	0	0.0
3 or 4 strains		11	20.8
	P. aeruginosa	3	5.7
	K. pneumoniae	3	5.7
	A. baumannii	2	3.8
	Combination of bacteria	3	5.7
More than 5 strains		4	7.5
	P. aeruginosa	0	0.0
	K. pneumoniae	1	1.9
	A. baumannii	2	3.8
	Combination of bacteria	1	1.9
Bacterial source			
Own clinical isolate		25	47.2
	P. aeruginosa	11	20.8
	K. pneumoniae	4	7.5
	A. baumannii	10	18.9
Collaborator		5	9.4
	P. aeruginosa	3	5.7
	K. pneumoniae	1	1.9
	A. baumannii	1	1.9
Strains Bank		6	11.3
	P. aeruginosa	1	1.9
	K. pneumoniae	4	7.5
	A. baumannii	1	1.9
Not reported		17	32.1
Bacteria growth stage			
Frozen log. phase stock		2	3.8
Subcultured to log. phase		13	24.5
	Early log. phase	4	7.5
	Mid-log. phase	1	1.9
	Not reported	8	15.1
Not reported		38	71.7

Percentages over 53 total studies reviewed.

(**Figure 2**). When working with *K. pneumoniae,* inbred and outbred mice were used to a similar extent (**Figure 2**). Outbred mice are generally selected for PK/PD studies in murine lung and thigh models (Andes and Lepak, 2017; Bulitta et al., 2019). It has been described that *Pseudomonas* infection led to higher mortality in BALB/c mice (classified as a Th2 responder strain) compared to C3H/HeN mice (Th1 responders; Moser et al., 1997) and C57BL/6 mice are more susceptible to *Klebsiella* infection of the lung than are 129/Sv mice (Schurr et al., 2005). Inbred mice are presumed to be more uniform (thus decreasing the number of animals needed to detect a specific response) and more repeatable (a result of being genetically defined and less prone to genetic change; Festing, 2014). However, to date there is no evidence of greater trait stability in inbred mice. This suggests that the advantages of inbred mice may not be as great as previously supposed and that the use of outbred mice in biomedical research may provide an important advantage in reaching conclusions that are generalizable across conditions and populations (Tuttle et al., 2018).

The sex of experimental animals is known to impact host-pathogen interactions (García-Gómez et al., 2013). We observed that the vast majority of the studies were carried out in female mice regardless of the bacteria used for infection (**Table 2**). Interestingly, only one study used both female and male mice in separate experiments with different readouts (Kirby et al., 2019; **Table 2**). Female C57BL/6J mice have been shown to be more susceptible to *A. baumannii* lung infection than their male counterparts (Pires et al., 2020). However, an increased susceptibility of male C3HeB/FeJ mice has been reported in the oral aspiration pneumonia model (Luna et al., 2019). In humans, women with cystic fibrosis and *P. aeruginosa* infection have worse outcomes than men (Demko et al., 1995), which has been partly attributed to estrogen effects (Vidaillac et al., 2020). In the case of *K. pneumoniae* infection, female mice have showed higher survival rates than males although exposure to ozone

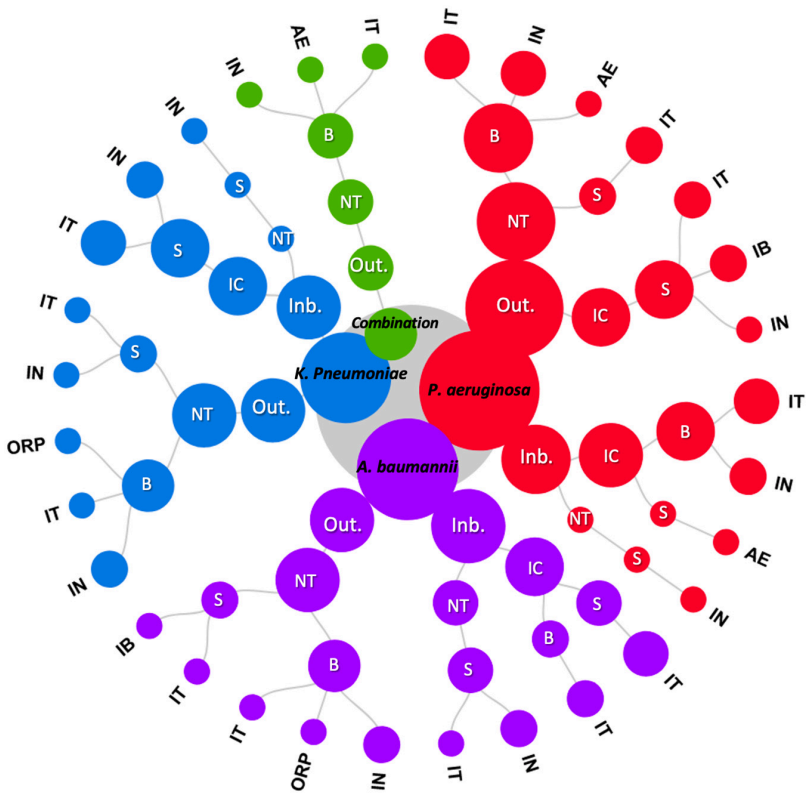

FIGURE 2
Circular dendrogram representing hierarchically structured variables. The area of the nodes represents the number of studies. Hierarchy from inside to outside: bacteria, mouse strain (Inb.: Inbred, Out.: Outbred), mouse immune status (NT: neutropenic, IC: Immunocompetent), study main readout (S: mice survival, B: bacterial load) and infection route (IT: intratracheal, IN: intranasal, ORP: oropharyngeal, IB: intrabronchial, AE: aerosolization).

reversed the trend and resulted in female mice surviving less than males (Mikerov et al., 2011). The sex of the test animal can also have implications in drug PK/PD (Soldin and Mattison, 2009; Madla et al., 2021). Therefore, the selection of male or female mice in an antimicrobial efficacy study is a variable that should be carefully considered and taken into account when interpreting the results.

The age of mice used in the study could substantially affect the immune response and thus the infection outcome (Cai et al., 2016; Jackson et al., 2017). Older mice have a more mature immune response. It has been shown in mice that B-cells have an immature phenotype until 4 weeks of age (Ghia et al., 1998) and T-cell responses mature around 8 weeks of age (Holladay and Smialowicz, 2000). In addition, drug metabolism by the liver is affected by the age of mice and has a critical impact on systemically administered compounds (Pibiri et al., 2015). This variable is also related to the weight of the animal and in some cases this parameter is reported instead of the age. For data analysis, we transformed the weight of the mice (if it was the only data provided) to age in weeks according to the vendor's growth data provided for the mouse strain of interest. The age of mice ranged from 4 to 10 weeks and animals with an average age of 6 weeks were most common. Outbred mice tended to be younger than inbred mice, and no inbred mice younger than 6 weeks were used (**Table 2**). Although outbred mice grow faster than inbred mice, their immune system may not be fully developed at the selected age (Ghia et al., 1998; Holladay and Smialowicz, 2000). This may be less of a problem for studies using outbred animals, as they are often rendered neutropenic or used at older ages in immunocompetent models. Several guidelines such as ARRIVE have strongly encouraged reporting the age of animals used in an experiment (Kilkenny et al., 2010; Percie du Sert et al., 2020). However, it is not clear if the age reported in the studies refers to the age of an animal upon arrival at the facility (before the acclimatization period), the age when the experimental infection is performed or the age when the first intervention in the animals is executed (i.e., cyclophosphamide treatment). This could lead to even greater variation in age than immediately apparent. The host microbiota correlates with animal age and affects host response and lung infection resistance (McMahan et al., 2022). The mouse microbiome varies based on a number of factors, including the animal's origin, nutrition, housing, bedding, and care during

TABLE 2 Characteristics of mice in the reviewed studies.

		Number of studies	Percentage (%)
Mouse strain			
Inbred		22	41.5
	C3H/HeN	1	1.9
	BALB/c	8	15.1
	C57BL/6	12	22.6
	DBA/2	1	1.9
Outbred		29	54.7
	NMRI	2	3.8
	Swiss Webster	12	22.6
	CD-1	3	5.7
	ddY	5	9.4
	ICR	6	11.3
	Kunming	1	1.9
Not reported		2	3.8
Sex			
Female		34	64.2
Male		9	17.0
Female and male		1	1.9
Not reported		9	17.0
Age average			
Inbred			
	4–5 weeks	0	0.0
	6–7 weeks	11	21.6
	≥8 weeks	10	19.6
	Not reported	1	2.0
Outbred			
	4–5 weeks	6	11.8
	6–7 weeks	15	29.4
	≥8 weeks	6	11.8
	Not reported	2	3.9
Number of animals per group			
Bacterial load[1]			
	2–3	12	23.5
	4–6	27	52.9
	7–10	9	17.6
	11–15	3	5.9
Survival[2]			
	2–3	0	0.0
	4–6	5	20.8
	7–10	12	50.0
	11–15	7	29.2

[1]Number of animals per group employed when bacterial load was the main readout.
[2]Number of animals per group employed when survival was the main readout.

infancy (Ericsson and Franklin, 2021). Around 6 weeks of age, the lung's microbial diversity significantly increases and is maintained throughout time (Singh et al., 2017). Researchers should make an effort to minimize the effects of this factor on the host's susceptibility to infection in order to improve the reproducibility of the studies.

The number of animals per group should be selected based on a power analysis considering expected data dispersion (Festing, 2018; Bulitta et al., 2019). We observed broad variation in the number of animals included per group. In studies with bacterial burden as the main endpoint, a range of two to fifteen animals was used, with four to six animals per group in most of the studies. In studies with survival as the study endpoint, the most common group size was 7–10 animals per group, reflecting that survival data typically present higher variability than bacterial burden (**Table 2**).

Infection procedure-related variables

Induced neutropenia is a variable that can have a significant impact on the study outcomes (Andes and Craig, 2002; Andes and Lepak, 2017). In general, a higher PK/PD index magnitude is required in neutropenic animals although it varies among drug classes and bacterial species (Andes and Craig, 2002; Andes and Lepak, 2017). We observed that neutropenic mice were used more often than immunocompetent mice (**Table 3**). Immunocompetent mice were preferred when working with inbred mouse strains, while the use of neutropenic animals prevails when outbred mice were used. This confirms the results of a previous literature review that evaluated different animal models for antibiotic efficacy testing, which found that neutropenic models slightly predominate over immunocompetent ones (Waack et al., 2020). Our analysis showed that the immune status of the mice varied by the study outcome measured. Survival was most frequently evaluated in immunocompetent animals. *P. aeruginosa* studies employed mostly immunocompetent lung models whereas *A. baumannii* and *K. pneumoniae* infections were mostly conducted in neutropenic models (**Figure 2**). Neutropenic animals were found to have increased bacterial growth over the study period in untreated animals (**Table 4**). Despite a common misconception, use of immunocompromised mice is not generally intended to mimic any particular patient population (Zhao et al., 2016; Andes and Lepak, 2017). Neutropenia promotes better growth of bacteria in mice, thus minimizing spontaneous resolution of infection (which complicates interpretation of treatment effects) and enabling more strains to be studied in mice than otherwise might be possible.

Neutropenia can be induced by different methods, including the use of drugs such as cyclophosphamide or vinblastine and neutrophil depleting antibodies (Stackowicz et al., 2020). Cyclophosphamide has a relative low cost and produce depletion of hematopoietic stem cells associated with an almost complete disappearance of blood neutrophils as early as 3–4 days after injection (Van't Wout et al., 1989; Zuluaga et al., 2006). Cyclophosphamide has the greatest effect on neutrophil numbers, but also markedly reduces numbers of circulating

TABLE 3 Inoculation and procedural parameters in the reviewed studies.

		Number of studies	Percentage (%)
Immune status			
Inbred		22	43.1
	Immnunocompetent	16	31.4
	Neutropenic	5	9.8
	Immnunocompetent and neutropenic	1	2.0
Outbred		29	56.9
	Immnunocompetent	5	9.8
	Neutropenic	24	47.1
Infectious route			
Immunocompetent		22	42.3
	Aerosolization	1	1.9
	Intrabronchial	2	3.8
	Intranasal	5	9.6
	Intratracheal	14	26.9
Neutropenic		30	57.7
	Aerosolization	2	3.8
	Intrabronchial	1	1.9
	Intranasal	14	26.9
	Intratracheal	11	21.2
	Oropharyngeal	2	3.8
Infectious volume			
	10 µl	2	4.3
	20 µl	4	8.5
	25 µl	9	19.1
	30 µl	4	8.5
	40 µl	3	6.4
	50 µl	23	48.9
	70 µl	2	4.3
Infectious dose			
<5 $\log_{10}$ CFU		4	8.3
	P. aeruginosa	3	6.3
	K. pneumoniae	1	2.1
	A. baumannii	0	0.0
5–6 $\log_{10}$ CFU		8	16.7
	P. aeruginosa	2	4.2
	K. pneumoniae	2	4.2
	A. baumannii	4	8.3
6–7 $\log_{10}$ CFU		16	33.3
	P. aeruginosa	9	18.8
	K. pneumoniae	4	8.3
	A. baumannii	3	6.3
7–8 $\log_{10}$ CFU		19	39.6
	P. aeruginosa	7	14.6
	K. pneumoniae	5	10.4
	A. baumannii	7	14.6
>8 $\log_{10}$ CFU		1	2.1
	P. aeruginosa	0	0.0
	K. pneumoniae	0	0.0
	A. baumannii	1	2.1

monocytes, B and T cells (Van't Wout et al., 1989; Zuluaga et al., 2006). Cyclophosphamide was the only methodology employed in the reviewed studies to render animals neutropenic. More than half of the studies with immunocompromised mice used a protocol of administering cyclophosphamide 4 days (150 mg/kg) and one day (100 mg/kg) before infection. The remaining studies used slight variations, such as increasing the administered dose or varying the days of administration.

The route of infection has been shown to impact host-pathogen interactions (Martins et al., 2013). In the reviewed studies, intratracheal (IT) and intranasal (IN) routes of infection were the most common, followed by aerosolization, the intrabronchial route and oropharyngeal infection route. Infections with *A. baumannii* and *P. aeruginosa* were mostly achieved through IT bacterial inoculation, while *K. pneumoniae* infection protocols mostly used IN bacterial administration (**Figure 2**). Moreover, we observed that the selection of the infection route was related to the immune status of the animal. IN infection was mostly employed when working with neutropenic animals, while for immunocompetent animals, IT infection was most common (**Table 3**). The predominance of the IN route when using neutropenic animals and the IT when employing immunocompetent animals was also observed in a previous report that summarized studies of antibiotic efficacy against seven gram-negative and two gram-positive pneumonia-causing bacterial species (Waack et al., 2020). This variation may reflect the challenge of establishing lung infections in immunocompetent mice, where a more direct inoculation method such as IT route can lead to a greater success. In our reviewed studies using three gram-negative bacteria, we observed a higher percentage of immunocompetent animals infected *via* IT route than previously reported using a higher number of pneumonia-producing bacteria (17), suggesting that the infection with these three selected gram-negative bacteria may be more difficult to achieve.

The infection volume is closely related to both the employed route of infection and the infectious dose. The administered volume ranged from 10 to 70 µl and most of the studies used a volume of 50 µl (**Table 3**). The lowest volume of 10 µl was only used for IT bacterial delivery (He et al., 2013; Hirsch et al., 2013).

It has previously been shown in a murine model of tularemia that intranasal instillation of a volume of 10 µl routinely resulted in infection of the upper airways but failed to initiate infection of the pulmonary compartment. For efficient delivery of the bacteria into the lungs, a dose volume of 50 µl or more was required (Miller et al., 2012). Similarly, studies with the azo dye Evans blue have revealed that intranasal administration of a dye volume of 40–50 µl, in comparison to 10–20 µl, led to increased dye retention in the lungs (Visweswaraiah et al., 2002; Smith et al., 2019). These data suggest that infecting volumes of at least 50 µl IN are preferred for establishing robust pulmonary infection.

Before selecting bacterial strains and infectious dose to perform antimicrobial efficacy studies, bacterial pathogenicity studies in mice are required. The infectious inoculum varied greatly between the reviewed studies. Most indicated that 7–8 $\log_{10}$ CFU were administered to initiate the infection (**Table 3**). Studies working with *P. aeruginosa* and *K. pneumoniae* used lower infectious dose than the studies working with *A. baumannii* (**Table 3**). Considering that the neutropenic model already prevails when working with this pathogen (**Figure 2**), these data may suggest greater difficulty in establishing a robust *A. baumannii* lung infection, requiring higher infectious dose.

Treatment and readout-related variables

In antibacterial research, the length of the study varies between animal species. Murine pneumonia models are mostly used for short term studies, while larger animals usually employ later endpoints (Waack et al., 2020). The vast majority of the studies reviewed here initiated antibiotic therapy at 2 h post infection (h.p.i.). However, the timing of the experimental endpoint varied according to the main study readout. Studies to determine bacterial burden were mostly terminated at 24 or 26 h.p.i., or at multiple time points between 2 and 72 h.p.i. Survival studies were most commonly terminated after 3–4 days (**Table 4**). A previous review of new drug application dossiers found that an endpoint of 24–29 h.p.i. was most commonly employed when antibacterial activity against *P. aeruginosa*, *K. pneumoniae* and *A. baumannii* was investigated. Notably, these studies followed a bimodal distribution, having 24- or 48-h endpoints (Waack et al., 2020). The endpoint used for measuring antimicrobial activity could influence the results (Andes and Craig, 2002; Cigana et al., 2020); however, the evaluation of antimicrobial treatments for chronic infection requires longer experimental time points (Cigana et al., 2020). Additionally, there might be variations in how researchers analyze animal care and humane endpoints in survival studies. Clinical disease severity scoring can be subjective, with various researchers scoring severity differently.

Unfortunately, the lung bacterial burden at the start of therapy was only reported in 28.3% of the reviewed studies. Baseline burdens fluctuated from 4.7 to 8 $\log_{10}$ CFU per lung, with the majority falling into a range of 6–7 $\log_{10}$ CFU per lung (**Table 4**). A lower burden at the start of therapy may reduce the PK/PD index magnitude, thus reducing the dose required for treatment effect, although the degree of influence can vary depending on the bacterial species and the drug class (Andes and Lepak, 2017). Importantly, the majority of results from PK/PD animal models that have been correlated with clinical outcomes reached 6–7 $\log_{10}$ CFU in the target tissue at the time therapy was initiated (Andes and Lepak, 2017). Baseline burdens further affect the bacterial growth over the study period. Bacterial growth was reported in 34 of the 53 studies reviewed, and an increase of at least 1 $\log_{10}$ CFU/lung over

TABLE 4 Treatment and procedural parameters in the reviewed studies.

	Number of studies	Percentage (%)
Treatment start point (p.i.)		
≤1 h	8	15.1
2 h	22	41.5
3–4 h	12	22.6
5–6 h	3	5.7
>6 h	8	15.1
Experimental endpoint (p.i.)		
Bacterial load[1]		
12–18 h	2	3.8
24–26 h	25	48.1
27–30 h	5	9.6
>36 h	7	13.5
Several time points (between 2 and 72 h)	13	25.0
Survival[2]		
≤2 d	3	10.7
3–4 d	12	42.9
5–6 d	5	17.9
7–9 d	6	21.4
10–11 d	2	7.1
Baseline bacterial burden (CFU per lung)		
4.7–6	1	1.89
6–7	9	16.98
7–8	5	9.4
Not reported	38	71.7
Average bacterial growth in lung (CFU per lung)		
Neutropenic mice		
≤1	2	5.9
1–2	7	20.6
2–3	9	26.5
>3	5	14.7
Immunocompetent mice		
≤1	6	17.6
1–2	2	5.9
2–3	3	8.8
>3	0	0.0
Study readouts		
Survival	26	49.1
Bacterial load	50	94.3
Blood or spleen or liver CFU	11	20.8
Histopathology	16	30.2
Immune response	11	20.8
Others[3]	5	9.4

[1]Experimental endpoint in hours (h) when bacterial load was the main readout.
[2]Experimental endpoint in days (d) when survival was the main readout.
[3]Other readouts measured: clinical score, body temperature, protein expression and lung endothelial permeability.

the experimental period (ranged from 2 and 72 h.p.i, median 26 h.p.i) was achieved in most of the studies. There were no marked differences among the three different bacterial species. However, bacterial growth over the study period was indeed related to immune status, with neutropenic mice showing higher bacterial growth than immunocompetent mice (**Table 4**). Robust infections are a prerequisite to adequately assess the antimicrobial effect of drugs. Therefore, bacterial burdens in untreated animals should not decline over the course of the study, or it becomes difficult to separate treatment effect from spontaneous resolution of infection. Depending on the selected efficacy endpoint, the effect of treatment may also be overestimated if bacterial growth is poor. The recommended specific efficacy endpoints range from 0 (stasis) to 2 $\log_{10}$ reductions in CFU calculated relative to the bacterial density at the start of treatment (Drusano, 2004; European Medicines Agency, 2016; Bulitta et al., 2019) and there remains some debate over which should be used. Stasis may be adequate for less severe infections or those involving concomitant non-drug treatments (e.g., surgical intervention such as debridement of infected tissue). For infections involving skin, soft tissue or the urinary tract, a 1 $\log_{10}$ reduction has been recommended, whereas 2 $\log_{10}$ reductions have been recommended for severe and/or high bacterial burden infections such as pneumonia (Drusano et al., 2018; Bulitta et al., 2019). In the control group (untreated or vehicle-treated), an increase in bacterial burden of 2–3 $\log_{10}$ CFU over the course of the study has been recommended (Bulitta et al., 2019). While this may be a feasible target for the standard neutropenic thigh infection model, studies reviewed suggest that it may be more difficult to achieve in the lung model especially with some pathogens (e.g., *A. baumannii*) or bacterial strains.

In the studies reviewed, specific information on sample processing was scarce. The method of lung homogenization was only reported in 15% of the studies. Stomacher, mini bead beater and ultra-turrax were the most common methodologies for processing samples. The media used for lung tissue culture and CFU count varied widely, with Mueller-Hinton (I and II) as the preferred media (47.6% of the studies) followed by Luria-Bertani (LB) agar (14.3%). Agar plates were usually cultured at 37°C, although several studies reported an incubation temperature of 35°C for *P. aeruginosa*. It is important to optimize the culture conditions for inoculation and bacterial recovery from the lung. Different sample processing techniques and media may have an impact on the study results, and it is recommended that all study samples are processed using the same methodology. Working with blinded samples is strongly encouraged, as it may reduce the potential for bias and increase the robustness of the study (Ioannidis, 2012; Bespalov et al., 2020).

Monoparametric models employing a single indicator of antibiotic efficacy represented 39.6% of the studies reviewed. Lung bacterial burden was the most common study readout (**Table 4**). While some studies reported the data as CFU/lung, others reported the data as CFU/ml of homogenized lung. CFU/ml requires additional data (lung weight) for normalization and comparison of results between studies, but lung weight was not generally reported. Regardless of the reporting units, the reduction of bacterial burden at the site of infection provides a relatively reproducible measure of antibiotic action that has been shown to forecast drug efficacy in patients (Zak and O'Reilly, 1991; Andes and Lepak, 2017). Bacterial burden is generally the preferred endpoint because it is a direct measurement of the drug's ability to kill or halt growth of the infecting pathogen. However, mortality can also be a useful endpoint and, in our review, survival of the mice was the second most common readout. The relationship between bacterial burden and survival has been previously noted, and the magnitude of drug exposure required for bacteriological cure and survival has been shown in some studies to be similar (Craig and Dalhoff, 1998; Andes and Craig, 2002). However, it should be noted that survival studies which monitor the animal's health for prolonged periods of time after the end of therapy may allow organisms that have not been eradicated to regrow and cause mortality, especially in neutropenic animals. This could substantially impact the relationship between bacterial counts and survival (Andes and Craig, 2002). In addition to survival and bacterial burden in the lungs, other outcomes in the studies reviewed included lung histopathology, bacterial load in other tissues (e.g., blood, liver or spleen), assessment of immune responses (e.g., cytokines) in BAL, serum, or lung homogenate, clinical scoring based on animal observation, body temperature, protein expression, and pulmonary endothelial permeability.

Conclusion

Standardization of the murine pneumonia model would allow better translation to the clinic and reduce animal use by providing more useful and relevant data. This literature review revealed marked differences in methodology for the murine pneumonia model used to test efficacy of small molecule antibiotics. Several parameters were relatively consistent across most of the models reviewed. These included animal sex, stage of bacterial growth for the inoculum, the starting point for treatment and the primary study outcome. Other variables differed widely, such as the immune status and age of the mice, the infection route and sample processing methodologies. Some variables, such as immune status and infectious dose, are expected to impact the study outcome more than others and can affect the PK/PD magnitude measured for a given endpoint. Although there is little direct evidence to indicate what effect, if any, a particular variable has on the outcome of a study, the myriad combinations of variables that any particular investigator uses is likely to impact the observed results. This can complicate preclinical-to-clinical translation, makes it difficult to compare drugs and/or bacterial isolates tested in different laboratories, and highlights the need for development of a standardized murine pneumonia model that has been

benchmarked appropriately. Overall, standardization of animal infection models is expected to strengthen the reproducibility and comparability of data generated during the evaluation of novel antibiotics. Furthermore, the combination of standardized protocols with quality controls, such as bacterial reference strains and benchmark control compounds with specified potency, should increase the robustness of preclinical data and improve our ability to translate from animals to humans.

Author contributions

RA: data curation, analysis, and writing—original draft. All authors: conceptualization, manuscript review and editing, and read and approved the final manuscript.

Funding

COMBINE project has received funding from the Innovative Medicines Initiative 2 Joint Undertaking under grant agreement No. 853967. This Joint Undertaking receives support from the European Union's Horizon 2020 Research and Innovation Programme and EFPIA companies' in-kind contribution. https://www.imi.europa.eu/.

Acknowledgments

We thank Evotec, GlaxoSmithKline, Statens Serum Institut, Erasmus University Medical Center, University of Poitiers, University of Liverpool, Monash University, Pharmacology Discovery Services, the University of North Texas, and the University of Florida for kindly sharing their established institutional protocols with COMBINE.

Conflict of interest

JLH was employed by GlaxoSmithKline Pharmaceuticals. SS and SR were employed by Evotec.

The remaining authors declare that the research was conducted in the absence of any commercial or financial relationships that could be construed as a potential conflict of interest.

Publisher's note

All claims expressed in this article are solely those of the authors and do not necessarily represent those of their affiliated organizations, or those of the publisher, the editors and the reviewers. Any product that may be evaluated in this article, or claim that may be made by its manufacturer, is not guaranteed or endorsed by the publisher.

Author disclaimer

This communication reflects the views only of the authors from the COMBINE consortium and does not necessarily reflect the position of IMI, the European Union, EFPIA partners or regulatory agencies.

Supplementary material

The Supplementary Material for this article can be found online at: https://www.frontiersin.org/articles/10.3389/fmicb.2022.988728/full#supplementary-material

References

Andes, D., and Craig, W. A. (2002). Animal model pharmacokinetics and pharmacodynamics: A critical review. *Int. J. Antimicrob. Agents* 19, 261–268. doi: 10.1016/S0924-8579(02)00022-5

Andes, D. R., and Lepak, A. J. (2017). *In vivo* infection models in the pre-clinical pharmacokinetic/pharmacodynamic evaluation of antimicrobial agents. *Curr. Opin. Pharmacol.* 36, 94–99. doi: 10.1016/j.coph.2017.09.004

Avery, L. M., Abdelraouf, K., and Nicolau, D. P. (2018). Assessment of the *in vivo* efficacy of WCK 5222 (Cefepime-Zidebactam) against carbapenem-resistant *Acinetobacter baumannii* in the neutropenic murine lung infection model. *Antimicrob. Agents Chemother.* 62:e00948-18. doi: 10.1128/AAC.00948-18

Begley, C. G., and Ioannidis, J. P. A. (2015). Reproducibility in science: Improving the standard for basic and preclinical research. *Circ. Res.* 116, 116–126. doi: 10.1161/CIRCRESAHA.114.303819

Bekeredjian-Ding, I. (2020). Challenges for clinical development of vaccines for prevention of hospital-acquired bacterial infections. *Front. Immunol.* 11:1755. doi: 10.3389/fimmu.2020.01755

Berkhout, J., Melchers, M. J., Van Mil, A. C., Seyedmousavi, S., Lagarde, C. M., Schuck, V. J., et al. (2016). Pharmacodynamics of ceftazidime and avibactam in neutropenic mice with thigh or lung infection. *Antimicrob. Agents Chemother.* 60, 368–375. doi: 10.1128/AAC.01269-15

Bespalov, A., Wicke, K., and Castagné, V. (2020). Blinding and randomization. *Handb. Exp. Pharmacol.* 257, 81–100. doi: 10.1007/164_2019_279

Bielen, K., Jongers, B., Malhotra-Kumar, S., Jorens, P. G., Goossens, H., and Kumar-Singh, S. (2017). Animal models of hospital-acquired pneumonia: Current practices and future perspectives. *Ann. Transl. Med.* 5:132. doi: 10.21037/atm.2017.03.72

Bowers, D. R., Cao, H., Zhou, J., Ledesma, K. R., Sun, D., Lomovskaya, O., et al. (2015). Assessment of minocycline and polymyxin B combination against *Acinetobacter baumannii*. *Antimicrob. Agents Chemother.* 59, 2720–2725. doi: 10.1128/AAC.04110-14

Bravo, D., Silva, C., Carter, J. A., Hoare, A., Álvarez, S. A., Blondel, C. J., et al. (2008). Growth-phase regulation of lipopolysaccharide O-antigen chain length influences serum resistance in serovars of *Salmonella*. *J. Med. Microbiol.* 57, 938–946. doi: 10.1099/jmm.0.47848-0

Brunetti, J., Falciani, C., Roscia, G., Pollini, S., Bindi, S., Scali, S., et al. (2016). *In vitro* and *in vivo* efficacy, toxicity, bio-distribution and resistance selection of a novel antibacterial drug candidate. *Sci. Rep.* 6:26077. doi: 10.1038/srep26077

Bulik, C. C., Okusanya, Ó. O., Lakota, E. A., Forrest, A., Bhavnani, S. M., Hoover, J. L., et al. (2017). Pharmacokinetic-pharmacodynamic evaluation of gepotidacin against gram-positive organisms using data from murine infection models. *Antimicrob. Agents Chemother.* 61:e00115-16. doi: 10.1128/AAC.00115-16

Bulitta, J. B., Hope, W. W., Eakin, A. E., Guina, T., Tam, V. H., Louie, A., et al. (2019). Generating robust and informative nonclinical *in vitro* and *in vivo* bacterial infection model efficacy data to support translation to humans. *Antimicrob. Agents Chemother.* 63:e02307-18. doi: 10.1128/AAC.02307-18

Cai, K. C., van Mil, S., Murray, E., Mallet, J. F., Matar, C., and Ismail, N. (2016). Age and sex differences in immune response following LPS treatment in mice. *Brain Behav. Immun.* 58, 327–337. doi: 10.1016/j.bbi.2016.08.002

Carter, J. A., Blondel, C. J., Zaldívar, M., Álvarez, S. A., Marolda, C. L., Valvano, M. A., et al. (2007). O-antigen modal chain length in *Shigella flexneri* 2a is growth-regulated through RfaH-mediated transcriptional control of the wzy gene. *Microbiology* 153, 3499–3507. doi: 10.1099/mic.0.2007/010066-0

Cheah, S. E., Wang, J., Nguyen, V. T. H. T., Turnidge, J. D., Li, J., and Nation, R. L. (2015). New pharmacokinetic/pharmacodynamic studies of systemically administered colistin against *Pseudomonas aeruginosa* and *Acinetobacter baumannii* in mouse thigh and lung infection models: Smaller response in lung infection. *J. Antimicrob. Chemother.* 70, 3291–3297. doi: 10.1093/jac/dkv267

Chen, C., Deslouches, B., Montelaro, R. C., and Di, Y. P. (2018). Enhanced efficacy of the engineered antimicrobial peptide WLBU2 *via* direct airway delivery in a murine model of *Pseudomonas aeruginosa* pneumonia. *Clin. Microbiol. Infect.* 24, 547.e1–547.e8. doi: 10.1016/j.cmi.2017.08.029

Choi, Y., Park, H. Y., Park, S. J., Park, S. J., Kim, S. K., Ha, C., et al. (2011). Growth phase-differential quorum sensing regulation of anthranilate metabolism in *Pseudomonas aeruginosa*. *Mol. Cells* 32, 57–65. doi: 10.1007/s10059-011-2322-6

Cigana, C., Bernardini, F., Facchini, M., Alcalá-Franco, B., Riva, C., De Fino, I., et al. (2016). Efficacy of the novel antibiotic POL7001 in preclinical models of *Pseudomonas aeruginosa* pneumonia. *Antimicrob. Agents Chemother.* 60, 4991–5000. doi: 10.1128/AAC.00390-16

Cigana, C., Ranucci, S., Rossi, A., De Fino, I., Melessike, M., and Bragonzi, A. (2020). Antibiotic efficacy varies based on the infection model and treatment regimen for *Pseudomonas aeruginosa*. *Eur. Respir. J.* 55:1802456. doi: 10.1183/13993003.02456-2018

Craig, W., and Dalhoff, A. (1998). "Pharmacodynamics of fluoroquinolones in experimental animals," in *Quinolone antibacterials. handbook of experimental pharmacology*, Vol. 127, eds J. Kuhlmann, A. Dalhoff, and H. J. Zeiler (Berlin: Springer), 207–232. doi: 10.1007/978-3-642-80364-2_7

de Paula, T. P., Santos, P. C., do Nascimento Arifa, R. D., Vieira, A. T., de Matos Baltazar, L., Ávila, T. V., et al. (2018). Treatment with atorvastatin provides additional benefits to imipenem in a model of gram-negative pneumonia induced by *Klebsiella pneumoniae* in mice. *Antimicrob. Agents Chemother.* 62:e00764-17. doi: 10.1128/AAC.00764-17

Demko, C. A., Byard, P. J., and Davis, P. B. (1995). Gender differences in cystic fibrosis: *Pseudomonas aeruginosa* infection. *J. Clin. Epidemiol.* 48, 1041–1049. doi: 10.1016/0895-4356(94)00230-N

Denayer, T., Stöhrn, T., and Van Roy, M. (2014). Animal models in translational medicine: Validation and prediction. *New Horiz. Transl. Med.* 2, 5–11. doi: 10.1016/j.nhtm.2014.08.001

Dietert, K., Gutbier, B., Wienhold, S. M., Reppe, K., Jiang, X., Yao, L., et al. (2017). Spectrum of pathogen- and model-specific histopathologies in mouse models of acute pneumonia. *PLoS One* 12:e0188251. doi: 10.1371/journal.pone.0188251

Docobo-Pérez, F., Nordmann, P., Domínguez-Herrera, J., López-Rojas, R., Smani, Y., Poirel, L., et al. (2012). Efficacies of colistin and tigecycline in mice with experimental pneumonia due to NDM-1-producing strains of *Klebsiella pneumoniae* and *Escherichia coli*. *Int. J. Antimicrob. Agents* 39, 251–254. doi: 10.1016/j.ijantimicag.2011.10.012

Drusano, G. L. (2004). Antimicrobial pharmacodynamics: Critical interactions of "bug and drug.". *Nat. Rev. Microbiol.* 2, 289–300. doi: 10.1038/nrmicro862

Drusano, G. L., Corrado, M. L., Girardi, G., Ellis-Grosse, E. J., Wunderink, R. G., Donnelly, H., et al. (2018). Dilution factor of quantitative bacterial cultures obtained by bronchoalveolar lavage in patients with ventilator-associated bacterial pneumonia. *Antimicrob. Agents Chemother.* 62:e01323-17. doi: 10.1128/AAC.01323-17

Ericsson, A. C., and Franklin, C. L. (2021). The gut microbiome of laboratory mice: Considerations and best practices for translational research. *Mamm. Genome* 32, 239–250. doi: 10.1007/s00335-021-09863-7

European Medicines Agency (2016). *Guideline on the use of pharmacokinetics and pharmacodynamics in the development of antimicrobial medicinal products*. Doc. EMA/CHMP/594085/2015. London: European Medicines Agency.

Festing, M. F. W. (2014). Evidence should trump intuition by preferring inbred strains to outbred stocks in preclinical research. *ILAR J.* 55, 399–404. doi: 10.1093/ilar/ilu036

Festing, M. F. W. (2018). On determining sample size in experiments involving laboratory animals. *Lab. Anim.* 52, 341–350. doi: 10.1177/0023677217738268

Friberg, L. E. (2021). Pivotal role of translation in anti-infective development. *Clin. Pharmacol. Ther.* 109, 856–866. doi: 10.1002/cpt.2182

García-Gómez, E., González-Pedrajo, B., and Camacho-Arroyo, I. (2013). Role of sex steroid hormones in bacterial-host interactions. *Biomed Res. Int.* 2013:928290. doi: 10.1155/2013/928290

Geller, B. L., Li, L., Martinez, F., Sully, E., Sturge, C. R., Daly, S. M., et al. (2018). Morpholino oligomers tested in vitro, in biofilm and *in vivo* against multidrug-resistant *Klebsiella pneumoniae*. *J. Antimicrob. Chemother.* 73, 1611–1619. doi: 10.1093/jac/dky058

Ghia, P., Ten Boekel, E., Rolink, A. G., and Melchers, F. (1998). B-cell development: A comparison between mouse and man. *Immunol. Today* 19, 480–485. doi: 10.1016/S0167-5699(98)01330-9

Harada, Y., Morinaga, Y., Kaku, N., Nakamura, S., Uno, N., Hasegawa, H., et al. (2014). In vitro and *in vivo* activities of piperacillin-tazobactam and meropenem at different inoculum sizes of ESBL-producing *Klebsiella pneumoniae*. *Clin. Microbiol. Infect.* 20, O831–O839. doi: 10.1111/1469-0691.12677

He, J., Abdelraouf, K., Ledesma, K. R., Chow, D. S. L., and Tam, V. H. (2013). Pharmacokinetics and efficacy of liposomal polymyxin B in a murine pneumonia model. *Int. J. Antimicrob. Agents* 42, 559–564. doi: 10.1016/j.ijantimicag.2013.07.009

Hengzhuang, W., Høiby, N., and Ciofu, O. (2014). Pharmacokinetics and pharmacodynamics of antibiotics in biofilm infections of *Pseudomonas aeruginosa* in vitro and *in vivo*. *Methods Mol. Biol.* 1147, 239–254. doi: 10.1007/978-1-4939-0467-9_17

Hirsch, E. B., Guo, B., Chang, K. T., Cao, H., Ledesma, K. R., Singh, M., et al. (2013). Assessment of antimicrobial combinations for *Klebsiella pneumoniae* carbapenemase-producing *K. pneumoniae*. *J. Infect. Dis.* 207, 786–793. doi: 10.1093/infdis/jis766

Holladay, S. D., and Smialowicz, R. J. (2000). Development of the murine and human immune system: Differential effects of immunotoxicants depend on time of exposure. *Environ. Health Perspect.* 108, 463–473. doi: 10.1289/ehp.00108s3463

Hooijmans, C. R., and Ritskes-Hoitinga, M. (2013). Progress in using systematic reviews of animal studies to improve translational research. *PLoS Med.* 10:e1001482. doi: 10.1371/journal.pmed.1001482

Hughes, D., and Karlén, A. (2014). Discovery and preclinical development of new antibiotics. *Ups. J. Med. Sci.* 119, 162–169. doi: 10.3109/03009734.2014.896437

Ioannidis, J. P. A. (2012). Extrapolating from animals to humans. *Sci. Transl. Med.* 4, s15–s151. doi: 10.1126/scitranslmed.3004631

Jackson, S. J., Andrews, N., Ball, D., Bellantuono, I., Gray, J., Hachoumi, L., et al. (2017). Does age matter? The impact of rodent age on study outcomes. *Lab. Anim.* 51, 160–169. doi: 10.1177/0023677216653984

Jacqueline, C., Roquilly, A., Desessard, C., Boutoille, D., Broquet, A., Le Mabecque, V., et al. (2013). Efficacy of ceftolozane in a murine model of *Pseudomonas aeruginosa* acute pneumonia: *In vivo* antimicrobial activity and impact on host inflammatory response. *J. Antimicrob. Chemother.* 68, 177–183. doi: 10.1093/jac/dks343

Johnson, A., McEntee, L., Farrington, N., Kolamunnage-Dona, R., Franzoni, S., Vezzelli, A., et al. (2020). Pharmacodynamics of cefepime combined with the novel extended-spectrum-lactamase (ESBL) inhibitor enmetazobactam for murine pneumonia caused by ESBLproducing *Klebsiella pneumonia*. *Antimicrob. Agents Chemother.* 64:e00180-20. doi: 10.1128/AAC.00180-20

Kaku, N., Kosai, K., Takeda, K., Uno, N., Morinaga, Y., Hasegawa, H., et al. (2017a). Efficacy and pharmacokinetics of the combination of OP0595 and cefepime in a mouse model of pneumonia caused by extended-spectrum-beta-lactamase-producing *Klebsiella pneumoniae*. *Antimicrob. Agents Chemother.* 61:e00828-17. doi: 10.1128/AAC.00828-17

Kaku, N., Morinaga, Y., Takeda, K., Kosai, K., Uno, N., Hasegawa, H., et al. (2017b). Efficacy and pharmacokinetics of ME1100, a novel optimized formulation of arbekacin for inhalation, compared with amikacin in a murine model of ventilator-associated pneumonia caused by *Pseudomonas aeruginosa*. *J. Antimicrob. Chemother.* 72, 1123–1128. doi: 10.1093/jac/dkw517

Kilkenny, C., Browne, W., Cuthill, I. C., Emerson, M., and Altman, D. G. (2010). Animal research: Reporting *in vivo* experiments: The ARRIVE guidelines. *Br. J. Pharmacol.* 160, 1577–1579. doi: 10.1111/j.1476-5381.2010.00872.x

Kirby, B. D., Al Ahmar, R., Ryan Withers, T., Valentine, M. E., Valentovic, M., Long, T. E., et al. (2019). Efficacy of aerosolized rifaximin versus tobramycin for treatment of *Pseudomonas aeruginosa* pneumonia in mice. *Antimicrob. Agents Chemother.* 63:e02341-18. doi: 10.1128/AAC.02341-18

Kraft, B. D., Piantadosi, C. A., Benjamin, A. M., Lucas, J. E., Zaas, A. K., Betancourt-Quiroz, M., et al. (2014). Development of a novel preclinical model of pneumococcal pneumonia in nonhuman primates. *Am. J. Respir. Cell Mol. Biol.* 50, 995–1004. doi: 10.1165/rcmb.2013-0340OC

Ku, N. S., Lee, S. H., Lim, Y. S., Choi, H., Ahn, J. Y., Jeong, S. J., et al. (2019). *In vivo* efficacy of combination of colistin with fosfomycin or minocycline in a mouse model of multidrug-resistant *Acinetobacter baumannii* pneumonia. *Sci. Rep.* 9:17127. doi: 10.1038/s41598-019-53714-0

Leenaars, M., Hooijmans, C. R., van Veggel, N., ter Riet, G., Leeflang, M., Hooft, L., et al. (2012). A step-by-step guide to systematically identify all relevant animal studies. *Lab. Anim.* 46, 24–31. doi: 10.1258/la.2011.011087

Lepak, A. J., and Andes, D. R. (2016). *In vivo* pharmacodynamic target assessment of delafloxacin against *Staphylococcus aureus*, *Streptococcus pneumoniae*, and *Klebsiella pneumoniae* in a murine lung infection model. *Antimicrob. Agents Chemother.* 60, 4764–4769. doi: 10.1128/AAC.00647-16

Li, C., Wang, J., Wang, Y., Gao, H., Wei, G., Huang, Y., et al. (2019). Recent progress in drug delivery. *Acta Pharm. Sin. B* 9, 1145–1162. doi: 10.1016/j.apsb.2019.08.003

Li, Y., Tang, C., Zhang, E., and Yang, L. (2017). Electrostatically entrapped colistin liposomes for the treatment of *Pseudomonas aeruginosa* infection. *Pharm. Dev. Technol.* 22, 436–444. doi: 10.1080/10837450.2016.1228666

Li, Y. T., Huang, J. R., Li, L. J., and Liu, L. S. (2017). Synergistic activity of berberine with azithromycin against *Pseudomonas aeruginosa* isolated from patients with cystic fibrosis of lung in vitro and vn vivo. *Cell. Physiol. Biochem.* 42, 1657–1669. doi: 10.1159/000479411

Li Bassi, G., Rigol, M., Marti, J. D., Saucedo, L., Ranzani, O. T., Roca, I., et al. (2014). A novel porcine model of ventilator-associated pneumonia caused by oropharyngeal challenge with *Pseudomonas aeruginosa*. *Anesthesiology* 120, 1205–1215. doi: 10.1097/ALN.0000000000000222

Lin, Y. W., Zhou, Q., Onufrak, N. J., Wirth, V., Chen, K., Wang, J., et al. (2017a). Aerosolized polymyxin B for treatment of respiratory tract infections: Determination of pharmacokinetic-pharmacodynamic indices for aerosolized polymyxin B against *Pseudomonas aeruginosa* in a mouse lung infection model. *Antimicrob. Agents Chemother.* 61:e00211-17. doi: 10.1128/AAC.00211-17

Lin, Y. W., Zhou, Q. T., Cheah, S. E., Zhao, J., Chen, K., Wang, J., et al. (2017b). Pharmacokinetics/pharmacodynamics of pulmonary delivery of colistin against *Pseudomonas aeruginosa* in a mouse lung infection model. *Antimicrob. Agents Chemother.* 61:e02025-16. doi: 10.1128/AAC.02025-16

Lin, Y. W., Zhou, Q. T., Han, M. L., Chen, K., Onufrak, N. J., Wang, J., et al. (2018). Elucidating the pharmacokinetics/pharmacodynamics of aerosolized colistin against multidrug-resistant *Acinetobacter baumannii* and *Klebsiella pneumoniae* in a mouse lung infection model. *Antimicrob. Agents Chemother.* 62:e01790-17. doi: 10.1128/AAC.01790-17

López-Rojas, R., Sánchez-Céspedes, J., Docobo-Pérez, F., Domínguez-Herrera, J., Vila, J., and Pachón, J. (2011). Pre-clinical studies of a new quinolone (UB-8902) against *Acinetobacter baumannii* resistant to ciprofloxacin. *Int. J. Antimicrob. Agents* 38, 355–359. doi: 10.1016/j.ijantimicag.2011.06.006

Lou, W., Venkataraman, S., Zhong, G., Ding, B., Tan, J. P. K., Xu, L., et al. (2018). Antimicrobial polymers as therapeutics for treatment of multidrug-resistant *Klebsiella pneumoniae* lung infection. *Acta Biomater.* 78, 78–88. doi: 10.1016/j.actbio.2018.07.038

Louie, A., Liu, W., Fikes, S., Brown, D., and Drusano, G. L. (2013). Impact of meropenem in combination with tobramycin in a murine model of *Pseudomonas aeruginosa* pneumonia. *Antimicrob. Agents Chemother.* 57, 2788–2792. doi: 10.1128/AAC.02624-12

Louie, A., Liu, W., Vanguilder, M., Neely, M. N., Schumitzky, A., Jelliffe, R., et al. (2015). Combination treatment with meropenem plus levofloxacin is synergistic against *Pseudomonas aeruginosa* infection in a murine model of pneumonia. *J. Infect. Dis.* 211, 1326–1333. doi: 10.1093/infdis/jiu603

Luna, B. M., Yan, J., Reyna, Z., Moon, E., Nielsen, T. B., Reza, H., et al. (2019). Natural history of *Acinetobacter baumannii* infection in mice. *PLoS One* 14:e0219824. doi: 10.1371/journal.pone.0219824

Ma, X. L., Guo, Y. Z., Wu, Y. M., Gong, W. T., Sun, J., and Huang, Z. (2020). *In vivo* bactericidal effect of colistin–linezolid combination in a murine model of MDR and XDR *Acinetobacter baumannii* pneumonia. *Sci. Rep.* 10:17518. doi: 10.1038/s41598-020-74503-0

Ma, Y., Wang, C., Li, Y., Li, J., Wan, Q., Chen, J., et al. (2020). Considerations and caveats in combating ESKAPE pathogens against nosocomial infections. *Adv. Sci.* 7:1901872. doi: 10.1002/advs.201901872

Madla, C. M., Gavins, F. K. H., Merchant, H. A., Orlu, M., Murdan, S., and Basit, A. W. (2021). Let's talk about sex: Differences in drug therapy in males and females. *Adv. Drug Deliv. Rev.* 175:113804. doi: 10.1016/j.addr.2021.05.014

Malachowa, N., Kobayashi, S. D., Porter, A. R., Freedman, B., Hanley, P. W., Lovaglio, J., et al. (2019). Vaccine protection against multidrug-resistant *Klebsiella pneumoniae* in a nonhuman primate model of severe lower respiratory tract infection. *mBio* 10:e2994-19. doi: 10.1128/mBio.02994-19

Mardirossian, M., Pompilio, A., Crocetta, V., De Nicola, S., Guida, F., Degasperi, M., et al. (2016). In vitro and *in vivo* evaluation of BMAP-derived peptides for the treatment of cystic fibrosis-related pulmonary infections. *Amino Acids* 48, 2253–2260. doi: 10.1007/s00726-016-2266-4

Martins, N. E., Faria, V. G., Teixeira, L., Magalhães, S., and Sucena, É. (2013). Host adaptation is contingent upon the infection route taken by pathogens. *PLoS Pathog.* 9:e1003601. doi: 10.1371/journal.ppat.1003601

Matute-Bello, G., Downey, G., Moore, B. B., Groshong, S. D., Matthay, M. A., Slutsky, A. S., et al. (2011). An official american thoracic society workshop report: Features and measurements of experimental acute lung injury in animals. *Am. J. Respir. Cell Mol. Biol.* 44, 725–738. doi: 10.1165/rcmb.2009-0210ST

McCaughey, L. C., Ritchie, N. D., Douce, G. R., Evans, T. J., and Walker, D. (2016). Efficacy of species-specific protein antibiotics in a murine model of acute *Pseudomonas aeruginosa* lung infection. *Sci. Rep.* 6:30201. doi: 10.1038/srep30201

McMahan, R. H., Hulsebus, H. J., Najarro, K. M., Giesy, L. E., Frank, D. N., Orlicky, D. J., et al. (2022). Age-related intestinal dysbiosis and enrichment of gut-specific bacteria in the lung are associated with increased susceptibility to *Streptococcus pneumoniae* infection in mice. *Front. Aging* 3:859991. doi: 10.3389/fragi.2022.859991

Metersky, M., and Waterer, G. (2020). Can animal models really teach us anything about pneumonia? Con. *Eur. Respir. J.* 55:1901525. doi: 10.1183/13993003.01525-2019

Mikerov, A. N., Cooper, T. K., Wang, G., Hu, S., Umstead, T. M., Phelps, D. S., et al. (2011). Histopathologic evaluation of lung and extrapulmonary tissues show sex differences in *Klebsiella pneumoniae* - infected mice under different exposure conditions. *Int. J. Physiol. Pathophysiol. Pharmacol.* 3, 176–190.

Miller, M. A., Stabenow, J. M., Parvathareddy, J., Wodowski, A. J., Fabrizio, T. P., Bina, X. R., et al. (2012). Visualization of murine intranasal dosing efficiency using luminescent *Francisella tularensis*: Effect of instillation volume and form of anesthesia. *PLoS One* 7:e31359. doi: 10.1371/journal.pone.0031359

Mizgerd, J. P., and Skerrett, S. J. (2008). Animal models of human pneumonia. *Am. J. Physiol. Lung Cell. Mol. Physiol.* 294, L387–L398. doi: 10.1152/ajplung.00330.2007

Monogue, M. L., Sakoulas, G., Nizet, V., and Nicolau, D. P. (2018). Humanized exposures of a β-Lactam-β-lactamase inhibitor, tazobactam, versus non-β-lactam-β-lactamase inhibitor, avibactam, with or without colistin, against *Acinetobacter baumannii* in murine thigh and lung infection models. *Pharmacology* 101, 255–261. doi: 10.1159/000486445

Morehead, M. S., and Scarbrough, C. (2018). Emergence of global antibiotic resistance. *Prim. Care* 45, 467–484. doi: 10.1016/j.pop.2018.05.006

Moser, C., Johansen, H. K., Song, Z., Hougen, H. P., Rygaard, J., and Høiby, N. (1997). Chronic *Pseudomonas aeruginosa* lung infection is more severe in Th2 responding BALB/c mice compared to Th1 responding C3H/HeN mice. *Apmis* 105, 838–842. doi: 10.1111/j.1699-0463.1997.tb05092.x

Murray, C. J., Ikuta, K. S., Sharara, F., Swetschinski, L., Robles Aguilar, G., Gray, A., et al. (2022). Global burden of bacterial antimicrobial resistance in 2019: A systematic analysis. *Lancet* 399, 629–655. doi: 10.1016/s0140-6736(21)02724-0

Nakamura, R., Ito-Horiyama, T., Takemura, M., Toba, S., Matsumoto, S., Ikehara, T., et al. (2019). *In vivo* pharmacodynamic study of cefiderocol, a novel parenteral siderophore cephalosporin, in murine thigh and lung infection models. *Antimicrob. Agents Chemother.* 63:e02031-18. doi: 10.1128/AAC.02031-18

Nguyen, N. T. Q., Gras, E., Tran, N. D., Nguyen, N. N. Y., Lam, H. T. H., Weiss, W. J., et al. (2021). *Pseudomonas aeruginosa* ventilator-associated pneumonia rabbit model for preclinical drug development. *Antimicrob. Agents Chemother.* 65:e0272420. doi: 10.1128/AAC.02724-20

Nosek, B. A., Alter, G., Banks, G. C., Borsboom, D., Bowman, S. D., Breckler, S. J., et al. (2015). Promoting an open research culture. *Science* 348, 1422–1425. doi: 10.1126/science.aab2374

Oliver, A., Cantón, R., Campo, P., Baquero, F., and Blázquez, J. (2000). High frequency of hypermutable *Pseudomonas aeruginosa* in cystic fibrosis lung infection. *Science* 288, 1251–1253. doi: 10.1126/science.288.5469.1251

Oshima, K., Nakamura, S., Iwanaga, N., Takemoto, K., Miyazaki, T., Yanagihara, K., et al. (2017). Efficacy of high-dose meropenem (six grams per day) in treatment of experimental murine pneumonia induced by meropenem-resistant *Pseudomonas aeruginosa*. *Antimicrob. Agents Chemother.* 61:e02056-16. doi: 10.1128/AAC.02056-16

Pachón-Ibáñez, M. E., Docobo-Pérez, F., Jiménez-Mejias, M. E., Ibáñez-Martínez, J., García-Curiel, A., Pichardo, C., et al. (2011). Efficacy of rifampin, in monotherapy and in combinations, in an experimental murine pneumonia model caused by panresistant *Acinetobacter baumannii* strains. *Eur. J. Clin. Microbiol. Infect. Dis.* 30, 895–901. doi: 10.1007/s10096-011-1173-6

Parra Millán, R., Jiménez Mejías, M. E., Sánchez Encinales, V., Ayerbe Algaba, R., Gutiérrez Valencia, A., Pachón Ibáñez, M. E., et al. (2016). Efficacy of lysophosphatidylcholine in combination with antimicrobial agents against *Acinetobacter baumannii* in experimental murine peritoneal sepsis and pneumonia models. *Antimicrob. Agents Chemother.* 60, 4464–4470. doi: 10.1128/AAC.02708-15

Paterson, D. L., Isler, B., and Stewart, A. (2020). New treatment options for multiresistant gram negatives. *Curr. Opin. Infect. Dis.* 33, 214–223. doi: 10.1097/QCO.0000000000000627

Peers, I. S., Ceuppens, P. R., and Harbron, C. (2012). In search of preclinical robustness. *Nat. Rev. Drug Discov.* 11, 733–734. doi: 10.1038/nrd3849

Percie du Sert, N., Hurst, V., Ahluwalia, A., Alam, S., Avey, M. T., Baker, M., et al. (2020). The ARRIVE guidelines 2.0: Updated guidelines for reporting animal research. *PLoS Biol.* 18:e3000410. doi: 10.1371/journal.pbio.3000410

Pibiri, M., Sulas, P., Leoni, V. P., Perra, A., Kowalik, M. A., Cordella, A., et al. (2015). Global gene expression profile of normal and regenerating liver in young and old mice. *Age* 37:9796. doi: 10.1007/s11357-015-9796-7

Pires, S., Peignier, A., Seto, J., Smyth, D. S., and Parker, D. (2020). Biological sex influences susceptibility to *Acinetobacter baumannii* pneumonia in mice. *JCI Insight* 5:e132223. doi: 10.1172/JCI.INSIGHT.132223

Ren, H., Liu, Y., Zhou, J., Long, Y., Liu, C., Xia, B., et al. (2019). Combination of azithromycin and gentamicin for efficient ereatment of *Pseudomonas aeruginosa* infections. *J. Infect. Dis.* 220, 1667–1678. doi: 10.1093/infdis/jiz341

Sakoulas, G., Rose, W., Berti, A., Olson, J., Munguia, J., Nonejuie, P., et al. (2017). Classical β-lactamase inhibitors potentiate the activity of daptomycin against methicillin-resistant *Staphylococcus aureus* and colistin against *Acinetobacter baumannii*. *Antimicrob. Agents Chemother.* 61:e01745-16. doi: 10.1128/AAC.01745-16

Sanderink, D., Cassisa, V., Chenouard, R., Mahieu, R., Kempf, M., Dubée, V., et al. (2019). Colistin-glycopeptide combinations against multidrug-resistant *Acinetobacter baumannii* in a mouse model of pneumonia. *Future Microbiol.* 14, 581–586. doi: 10.2217/fmb-2019-0022

Schurr, J. R., Young, E., Byrne, P., Steele, C., Shellito, J. E., and Kolls, J. K. (2005). Central role of toll-like receptor 4 signaling and host defense in experimental pneumonia caused by gram-negative bacteria. *Infect. Immun.* 73, 532–545. doi: 10.1128/IAI.73.1.532-545.2005

Singh, N., Vats, A., Sharma, A., Arora, A., and Kumar, A. (2017). The development of lower respiratory tract microbiome in mice. *Microbiome* 5:61. doi: 10.1186/s40168-017-0277-3

Smith, A. J., Clutton, R. E., Lilley, E., Hansen, K. E. A., and Brattelid, T. (2018). PREPARE: Guidelines for planning animal research and testing. *Lab. Anim.* 52, 135–141. doi: 10.1177/0023677217724823

Smith, C. A., Kulkarni, U., Chen, J., and Goldstein, D. R. (2019). Influenza virus inoculum volume is critical to elucidate age-dependent mortality in mice. *Aging Cell* 18:e12893. doi: 10.1111/acel.12893

Soldin, O. P., and Mattison, D. R. (2009). Sex differences in pharmacokinetics and pharmacodynamics. *Clin. Pharmacokinet.* 48, 143–157.

Stackowicz, J., Jönsson, F., and Reber, L. L. (2020). Mouse models and tools for the *in vivo* study of neutrophils. *Front. Immunol.* 10:3130. doi: 10.3389/fimmu.2019.03130

Tan, S., Gao, J., Li, Q., Guo, T., Dong, X., Bai, X., et al. (2020). Synergistic effect of chlorogenic acid and levofloxacin against *Klebsiella pneumoniae* infection in vitro and *in vivo*. *Sci. Rep.* 10:20013. doi: 10.1038/s41598-020-76895-5

Tang, H. J., Chuang, Y. C., Ko, W. C., Chen, C. C., Shieh, J. M., Chen, C. H., et al. (2012). Comparative evaluation of intratracheal colistimethate sodium, imipenem, and meropenem in BALB/c mice with carbapenem-resistant *Acinetobacter baumannii* pneumonia. *Int. J. Infect. Dis.* 16, e34–e40. doi: 10.1016/j.ijid.2011.09.015

Tängdén, T., Lundberg, C. V., Friberg, L. E., and Huttner, A. (2020). How preclinical infection models help define antibiotic doses in the clinic. *Int. J. Antimicrob. Agents* 56:106008. doi: 10.1016/j.ijantimicag.2020.106008

Thabit, A. K., Crandon, J. L., and Nicolau, D. P. (2016). Pharmacodynamic and pharmacokinetic profiling of delafloxacin in a murine lung model against community-acquired respiratory tract pathogens. *Int. J. Antimicrob. Agents* 48, 535–541. doi: 10.1016/j.ijantimicag.2016.08.012

Theuretzbacher, U., Outterson, K., Engel, A., and Karlén, A. (2020). The global preclinical antibacterial pipeline. *Nat. Rev. Microbiol.* 18, 275–285. doi: 10.1038/s41579-019-0288-0

Tuttle, A. H., Philip, V. M., Chesler, E. J., and Mogil, J. S. (2018). Comparing phenotypic variation between inbred and outbred mice. *Nat. Methods* 15, 994–996. doi: 10.1038/s41592-018-0224-7

Van't Wout, J. W., Linde, I., Leijh, P. C. J., and Van Furth, R. (1989). Effect of irradiation,cyclophospahmide, and etoposide (VP-16) on number of peripheral blood and peritoneal leukocytes in mice under normal conditions and during acute inflammatory reaction. *Inflammation* 13, 1–14. doi: 10.1007/BF00918959

Vidaillac, C., Yong, V. F. L., Aschtgen, M.-S., Qu, J., Yang, S., Xu, G., et al. (2020). Sex steroids induce membrane stress responses and virulence properties in *Pseudomonas aeruginosa*. *mBio* 11:e01774-20. doi: 10.1128/mbio.01774-20

Visweswaraiah, A., Novotny, L. A., Hjemdahl-Monsen, E. J., Bakaletz, L. O., and Thanavala, Y. (2002). Tracking the tissue distribution of marker dye following intranasal delivery in mice and chinchillas: A multifactorial analysis of parameters affecting nasal retention. *Vaccine* 20, 3209–3220. doi: 10.1016/S0264-410X(02)00247-5

Waack, U., Weinstein, E. A., and Farley, J. J. (2020). Assessing animal models of bacterial pneumonia used in investigational new drug applications for the treatment of bacterial pneumonia. *Antimicrob. Agents Chemother.* 64:e02242-19. doi: 10.1128/AAC.02242-19

Wang, H., Wu, H., Ciofu, O., Song, Z., and Høibya, N. (2012). *In vivo* pharmacokinetics/pharmacodynamics of colistin and imipenem in *Pseudomonas aeruginosa* biofilm infection. *Antimicrob. Agents Chemother.* 56, 2683–2690. doi: 10.1128/AAC.06486-11

World Health Organization [WHO] (2017). *Global Priority List of Antibiotic-Resistant Bacteria to Guide Research, Discovery, and Development of New Antibiotics*. Geneva: WHO, 1–7.

Yamada, K., Yamamoto, Y., Yanagihara, K., Araki, N., Harada, Y., Morinaga, Y., et al. (2012). *In vivo* efficacy and pharmacokinetics of biapenem in a murine model of ventilator-associated pneumonia with *Pseudomonas aeruginosa*. *J. Infect. Chemother.* 18, 472–478. doi: 10.1007/s10156-011-0359-2

Yamada, K., Yanagihara, K., Kaku, N., Harada, Y., Migiyama, Y., Nagaoka, K., et al. (2013a). Azithromycin attenuates lung inflammation in a mouse model of ventilator-associated pneumonia by multidrug-resistant *Acinetobacter baumannii*. *Antimicrob. Agents Chemother.* 57, 3883–3888. doi: 10.1128/AAC.00457-13

Yamada, K., Yanagihara, K., Kaku, N., Harada, Y., Migiyama, Y., Nagaoka, K., et al. (2013b). *In vivo* efficacy of biapenem with ME1071, a novel metallo-β-lactamase (MBL) inhibitor, in a murine model mimicking ventilator-associated pneumonia caused by MBL-producing *Pseudomonas aeruginosa*. *Int. J. Antimicrob. Agents* 42, 238–243. doi: 10.1016/j.ijantimicag.2013.05.016

Yang, Y. S., Lee, Y., Tseng, K. C., Huang, W. C., Chuang, M. F., Kuo, S. C., et al. (2016). *In vivo* and in vitro efficacy of minocycline-based combination therapy for minocycline-resistant *Acinetobacter baumannii*. *Antimicrob. Agents Chemother.* 60, 4047–4054. doi: 10.1128/AAC.02994-15

Yokoyama, Y., Matsumoto, K., Ikawa, K., Watanabe, E., Shigemi, A., Umezaki, Y., et al. (2014). Pharmacokinetic/pharmacodynamic evaluation of sulbactam against *Acinetobacter baumannii* in in vitro and murine thigh and lung infection models. *Int. J. Antimicrob. Agents* 43, 547–552. doi: 10.1016/j.ijantimicag.2014.02.012

Zak, O., and O'Reilly, T. (1991). Animal models in the evaluation of antimicrobial agents. *Antimicrob. Agents Chemother.* 35, 1527–1531. doi: 10.1128/AAC.35.8.1527

Zhao, M., Lepak, A. J., and Andes, D. R. (2016). Animal models in the pharmacokinetic/pharmacodynamic evaluation of antimicrobial agents. *Bioorg. Med. Chem.* 24, 6390–6400. doi: 10.1016/j.bmc.2016.11.008

Zhao, M., Lepak, A. J., Marchillo, K., and Andesa, D. R. (2019). *In vivo* pharmacodynamic target determination for delafloxacin against *Klebsiella pneumoniae* and *Pseudomonas aeruginosa* in the neutropenic murine pneumonia model. *Antimicrob. Agents Chemother.* 63:e01131-19. doi: 10.1128/AAC.01131-19

Zhou, J., Ledesma, K. R., Chang, K. T., Abodakpi, H., Gao, S., and Tama, V. H. (2017). Pharmacokinetics and pharmacodynamics of minocycline against *Acinetobacter baumannii* in a neutropenic murine pneumonia model. *Antimicrob. Agents Chemother.* 61:e02371-16. doi: 10.1128/AAC.02371-16

Zhou, Y. F., Tao, M. T., Huo, W., Liao, X. P., Sun, J., and Liu, Y. H. (2017). *In vivo* pharmacokinetic and pharmacodynamic profiles of antofloxacin against *Klebsiella pneumoniae* in a neutropenic murine lung infection model. *Antimicrob. Agents Chemother.* 61:e02691-16. doi: 10.1128/AAC.02691-16

Zuluaga, A. F., Salazar, B. E., Rodriguez, C. A., Zapata, A. X., Agudelo, M., and Vesga, O. (2006). Neutropenia induced in outbred mice by a simplified low-dose cyclophosphamide regimen: Characterization and applicability to diverse experimental models of infectious diseases. *BMC Infect. Dis.* 6:55. doi: 10.1186/1471-2334-6-55

Advantages of publishing in Frontiers

OPEN ACCESS
Articles are free to read for greatest visibility and readership

FAST PUBLICATION
Around 90 days from submission to decision

HIGH QUALITY PEER-REVIEW
Rigorous, collaborative, and constructive peer-review

TRANSPARENT PEER-REVIEW
Editors and reviewers acknowledged by name on published articles

Frontiers
Avenue du Tribunal-Fédéral 34
1005 Lausanne | Switzerland

Visit us: www.frontiersin.org
Contact us: frontiersin.org/about/contact

REPRODUCIBILITY OF RESEARCH
Support open data and methods to enhance research reproducibility

DIGITAL PUBLISHING
Articles designed for optimal readership across devices

FOLLOW US
@frontiersin

IMPACT METRICS
Advanced article metrics track visibility across digital media

EXTENSIVE PROMOTION
Marketing and promotion of impactful research

LOOP RESEARCH NETWORK
Our network increases your article's readership